

Jacketed and Functionalized Poly(paraphenyleneethynylene)s:
Nonaggregating Conjugated Polymers and Materials
Functionalized Through Click-Chemistry

A Dissertation
Presented to
The Academic Faculty

By

Brian Carl Englert

In Partial Fulfillment
Of the Requirements for the Degree
Doctor of Philosophy in Chemistry

Georgia Institute of Technology

Jacketed and Functionalized Poly(paraphenyleneethynylene)s:
Nonaggregating Conjugated Polymers and Materials
Functionalized Through Click-Chemistry

Approved by:

Dr. Uwe H. F. Bunz, Advisor
School of Chemistry & Biochemistry
Georgia Institute of Technology

Dr. Laren Tolbert
School of Chemistry & Biochemistry *Georgia*
Institute of Technology

Dr. Anselm Griffin
School of Polymer, Textile and Fiber Engineering
Georgia Institute of Technology

Dr. David Collard
School of Chemistry & Biochemistry
Georgia Institute of Technology

Dr. Joseph Perry
School of Chemistry & Biochemistry
Georgia Institute of Technology

Dr. Thomas Orlando
School of Chemistry & Biochemistry
Georgia Institute of Technology

Approval Date: April 1, 2005

Acknowledgement

I would like to thank Uwe for his inspiration, patience, and the freedom to implement. Carlito, Sandra, Selma, Glen, Wong, James, Ik-bum, Park and Jake have been the best lab mates a researcher could ask for. Together we have produced fantastic results which have allowed us make significant contributions to the field of conjugated polymers. You have all been an essential key to my research.

Jeanine has been integral to everything I have done for the past year and a half. Much thanks goes to the Burns family for warm holidays in Georgia as well as my own family for their support. As well I must extend thanks to all of those who will gather to hear my thesis defense; my committee.

Table of Contents:

ACKNOWLEDGEMENT	iii
LIST OF TABLES	vii
LIST OF FIGURES	viii
LIST OF SCHEMES	xi
LIST OF ABBREVIATIONS	xiii
SUMMARY POLY(<i>P</i> -PHENYLENEETHYNYLENE)S: “JACKETED” AND FUNCTIONALIZED SYSTEMS.	xv
CHAPTER 1: JACKETED AND FUNCTIONALIZED PPES: BACKGROUND AND PROPOSED	2
1.1 Introduction	2
1.2 Synthesis of PPEs	3
1.3 Optical properties of PPEs	5
1.4 Nonaggregating PPEs	6
1.5 Functionalization of PPE and Click Chemistry	7
1.6 PPEs as Precursor Materials for Permanent Microstructures	9
1.7 Conclusion	11
1.8 References	12
CHAPTER 2: CARBON RICH JACKETED POLY(<i>P</i> -PHENYLENEETHYNYLENE)S.	16
2.1 Introduction	16
2.2 Results and Discussion	17
2.3 Conclusion	37
2.4 Experimental	38
2.5 References	48
CHAPTER 3: CARBON RICH JACKETED POLY(<i>P</i> -PHENYLENEETHYNYLENE)S.	53
3.1 Introduction	53
3.2 Results and Discussion	54
3.3 Conclusion	60
3.4 Experimental	61
3.5 References	66

CHAPTER 4: PRECURSOR MATERIALS AND FUNCTIONALIZED POLY(P-PHENYLENEETHYNYLENE)S.	67
4.1 Introduction	67
4.2 Results and Discussion	70
4.3 Conclusion	80
4.4 Experimental	81
4.5 References	98
CHAPTER 5: SELECTIVE CLICK CHEMISTRY VIA MICROWAVE AS AN APPROACH TO NEW SMALL MOLECULES.	100
5.1 Introduction	100
5.2 Results and Discussion	103
5.3 Conclusion	110
5.4 Experimental	110
5.5 References	127
CHAPTER 6: CLICK CHEMISTRY AS A POWERFUL TOOL FOR THE CONSTRUCTION OF FUNCTIONALIZED POLY(P-PHENYLENEETHYNYLENE)S: COMPARISON OF PRE- AND POST FUNCTIONALIZATION SCHEMES.	129
6.1 Introduction	129
6.2 Results and Discussion	130
6.3 Conclusion	148
6.4 Experimental	149
6.5 References	167
CHAPTER 7: TEMPLATED CERAMIC MICROSTRUCTURES BY THE BREATH FIGURE METHOD.	170
7.1 Introduction	170
7.2 Results and Discussion	172
7.3 Conclusion	181
7.4 Experimental	181
7.5 References	187
CHAPTER 8: PYROLYSIS OF DICOLBALTHEXACARBONYL-FUNCTIONALIZED POLY(P-PHENYLENEETHYNYLENE)S.	192
8.1 Introduction	192
8.2 Results and Discussion	193
8.3 Conclusion	203
8.4 Experimental	204
8.5 References	207

CHAPTER 9: CONCLUSIONS AND FINAL REMARKS.	210
12.1 Discussion	210
12.2 References	212
APPENDIX A: CRYSTALLOGRAPHIC DATA.	213
A.1 Crystallographic Data and Figures	213
A.2 References	428

List of Tables

Table 2.1.	Crystal Data and Unit Cell Parameters.	24
Table 2.2.	Optical Properties and Molecular Weight Properties.	26
Table 4.1	Conditions explored to couple 4.4a, 4.4b, and 4.4c.	86
Table 6.1.	Degree of Polymerization and Functionalization.	145
Table A1.	Crystallographic data	214
Table A2.	Crystallographic data	223
Table A3.	Crystallographic data	230
Table A4.	Crystallographic data	241
Table A5.	Crystallographic data	253
Table A6.	Crystallographic data	262
Table A7.	Crystallographic data	272
Table A8.	Crystallographic data	281
Table A9.	Crystallographic data	301
Table A10.	Crystallographic data	321
Table A11.	Crystallographic data	334
Table A12.	Crystallographic data	344
Table A13.	Crystallographic data	352
Table A14.	Crystallographic data	362
Table A15.	Crystallographic data	384
Table A16.	Crystallographic data	401

List of Figures

Figure 1.1.	The basic structure of the PPE.	3
Figure 1.2.	Solution to Solid State Red-Shift in EthylhexyloxyPPE.	6
Figure 1.3.	Jacketing of PPEs.	7
Figure 1.4.	Pre vs. post-polymerization functionalization of PPEs.	9
Figure 1.6	Formation of bubble arrays.	10
Figure 1.7	The structure of an azide functionalized polymer.	10
Figure 1.8	Laser scanning confocal micrographs of bubble arrays.	11
Figure 2.1.	ADP representations of 2.2.	20
Figure 2.2.	ADP (50%) (top, left) representations of 2.3a.	22
Figure 2.3.	ADP (50%) (top) representations of 2.5	23
Figure 2.4.	X-ray crystal structure of 2.3b.	28
Figure 2.5.	Absorption of polymers 2.9-2.11 in chloroform.	29
Figure 2.6.	Absorption of the polymers 2.9-2.11.	29
Figure 2.7.	Absorption of model polymer 2.12.	30
Figure 2.8.	MM2 calculations of polymer 2.9.	31
Figure 2.9.	Rotational profile of a dimeric repeat unit of 2.9.	33
Figure 2.10.	PPE 2.9 remains nonplanar.	34
Figure 2.11.	2.11 in chloroform, THF THF/H ₂ O.	36
Figure 2.11.	Φ_{FL} of polymer 2.9, 2.10, 2.11, and 2.12.	37
Figure 3.1.	Single molecules of 3.15	57
Figure 3.2.	¹ HNMR and ¹³ CNMR of 3.20.	60
Figure 4.1	Molecular wire behavior in conjugated polymers.	68

Figure 4.2	Monomer X	68
Figure 4.3.	ORTEP diagram of 5a.	71
Figure 4.4.	Absorption and emission of 4.15.	74
Figure 4.5.	Emission of polymer 4.15 as a function of the % methanol.	75
Figure 4.6.	Microstructured bubbles formed from polymer 4.27.	78
Figure 4.7.	Absorbance of polymer 4.27 in solution.	79
Figure 4.8.	Emission of polymer 4.27 % methanol.	79
Figure 4.9.	Decreasing fluorescence of polymer 4.30.	80
Figure 5.1.	Series of silane substituted triazoles.	104
Figure 5.2.	ORTEP plots of compounds 5.6, 5.7.	105
Figure 5.3.	Optical properties of compound 5.33.	107
Figure 5.4.	Single crystal X-ray analysis of 5.33.	107
Figure 5.5.	Series of stannane substituted triazoles.	108
Figure 6.1.	Post and prepolymerization strategies.	131
Figure 6.2.	UV-vis and emission spectra of polymer 5.	134
Figure 6.3.	¹ HNMR of polymers 5, 6, 8a (post), and 8a (pre).	138
Figure 6.4.	¹³ CNMR of polymers 5, 6, 8a (post), and 8a (pre).	139
Figure 6.5.	IR of polymers 5, 6, 8a (post), and 8a (pre).	140
Figure 6.6.	¹³ CNMR of monomer 10a.	141
Figure 6.7.	¹³ CNMR chemical shift of functionalized polymers.	142
Figure 6.8.	UV-vis and emission spectra of polymer 8b.	146
Figure 7.1.	Bubble arrays formed from polymer 7.8.	173

Figure 7.2.	SEM-image of a bubble array from of polymer 7.3.	174
Figure 7.3.	Optical micrograph of the bubble arrays of 7.8	175
Figure 7.4.	SEM-picture of bubble array of polymer 7.8	175
Figure 7.5.	Termogravimetric analysis (TGA) of 7.8	176
Figure 7.6.	SEM-micrograph of bubble array of polymer 7.8.	176
Figure 7.7.	SEM-micrograph of bubble array of polymer 7.8	178
Figure 7.8.	Material from the pyrolysis of polymer 7.8 under air.	180
Figure 7.9.	EDX mapping of polymer 7.8 pyrolyzed under air.	180
Figure 8.1.	Tetrabenzohexadehydro[20]annulene 8.1	193
Figure 8.2.	Visible changes in the IR spectra of 8.6a	195
Figure 8.3.	Pyrolysis of 8.7a	197
Figure 8.4.	Pyrolysis of 8.7e 50% complexed	198
Figure 8.5.	Fibrous material from pyrolysis of 8.8a	198
Figure 8.6.	Size distribution of the spheres from pyrolysis of 8.7a.	199
Figure 8.7.	Transmission electron micrograph.	200
Figure 8.8.	On the left (a) a scanning electron micrograph	201
Figure 7.9.	XRD on pyrolysis of 8.7e.	202
Figure 8.10.	Size distribution of the particles from 8.7e.	203
Figure 9.1.	Basic structure of jacketed and functionalized PPEs.	211

List of Schemes

Scheme 1.1.	HCSH synthesis of PPEs	4
Scheme 1.2.	Alkyne Metathesis	5
Scheme 1.3.	1,3-dipolar cycloaddition.	8
Scheme 2.1.	Synthesis of tetraphenylbenzene units.	17
Scheme 2.2.	Synthesis of 2.3a, 2.3b, 2.5, and 2.8.	19
Scheme 2.3.	Synthesis of Polymers 2.9-2.12.	25
Scheme 3.1.	Synthesis of Müllen dendrons.	53
Scheme 3.2.	Synthesis of dibromo monomer 3.3.	55
Scheme 3.3.	Substituted tetraphenylcyclopentadienones.	56
Scheme 3.4.	Synthesis of 3.15.	56
Scheme 3.5.	Tetraphenylbenzene substituted monomers.	59
Scheme 4.1	Possible scheme to prepare functionalized PPEs.	69
Scheme 4.2	Iodination to yield 4a-c.	70
Scheme 4.3	Arbuzov reactions to yield monomers 4.5a-c.	71
Scheme 4.4	Proposed synthesis of polymer 4.7.	72
Scheme 4.5	Synthesis of sugar-phosphonate PPE.	73
Scheme 4.6	Synthesis of polymer 4.15.	74
Scheme 4.7	Synthesis of thio monomer 4.14.	76
Scheme 4.8	Synthesis of monomer 4.26.	77
Scheme 4.9	Synthesis of polymer 4.27.	78
Scheme 5.1.	Thermal formation of 1,4 and 1,5 triazoles.	102
Scheme 5.2.	Copper catalyzed synthesis of 1,4-triazoles.	103

Scheme 5.3.	Synthesis of iodine substituted 1,4-triazoles.	106
Scheme 5.4.	Use of 5.31 to yield conjugated molecules.	106
Scheme 5.5.	Synthesis of stannane substituted 1,4-triazoles.	109
Scheme 5.6.	No iodination of the aromatic rings.	110
Scheme 6.1.	Synthesis of the polymer platform 6.	132
Scheme 6.2.	In situ generation of 6.6.	134
Scheme 6.3.	Synthesis of polymer 8b.	137
Scheme 7.1.	Synthesis of polymers 7.3, 7.8, and 7.10.	172
Scheme 8.1.	The PPEs 8.6a-c reacted with dicobalt octacarbonyl.	195

List of Abbreviations

Cracac	Chromium(III)acetylacetonate
DSC	differential scanning calorimetry
GPC	Gel Permeation Chromatography
HOMO	highest occupied molecular orbital
IR	infra-red
LUMO	lowest unoccupied molecular orbital
M _n	number average molecular weight
Mp	melting point
MS	mass spectrum
M _w	weight average molecular weight
NBS	N-bromosuccinimide
NMR	nuclear magnetic resonance
OLED	organic light emitting diode
PAE	poly(aryleneethynylene)
PDI	polydispersity index
PPE	poly(<i>para</i> phenyleneethylene)
SEM	scanning electron microscope
TCE	tetrachloroethane
T _g	glass transistion
T _m	melting point
TLC	thin layer chromatography
UV-vis	ultraviolet-visible

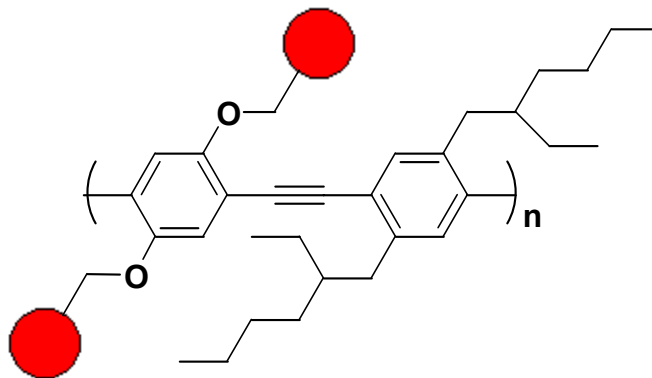
XRD	X-ray diffraction
Φ	quantum yield

Summary

The synthesis and investigation of new types of poly(*paraphenyleneethynylene*)s, PPEs, is presented. PPEs which are Jacketed are there by shielded from electronic and plararization effects in the solid state. Other PPEs contain pendent groups which may functionalized before or after polymerization to afford two versatile routes to newly functionalized polymeric materials. Based on the PPE structure, metals may be introduced and these polymers may be used as precursors for other types of materials such as ceramics.

CHAPTER 1

AND FUNCTIONALIZED PPES: BACKGROUND AND PROPOSED RESEARCH



1.1 Introduction

Conjugated polymers have been intensely studied since the Nobel prize-winning discovery by Heeger, MacDiarmid, and Shirakawa that doped polyacetylene is conducting.^{1,2,3} Poly(*paraphenyleneethynylene*)s PPEs are a more novel class of conjugated material which exhibit desirable optical properties and processability (Figure 1.1).⁴ While these materials are interesting because of their intriguing structure and electronic properties, there has been more recent work regarding the diversity of their potential applications.³ In order to further exploit these materials, the next logical step is to integrate functionality into them. The ease or difficulty with which these materials are functionalized is related directly to how they are synthesized.

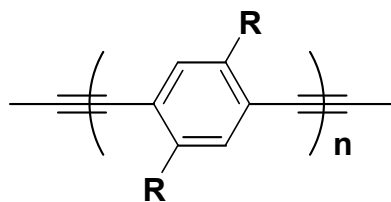
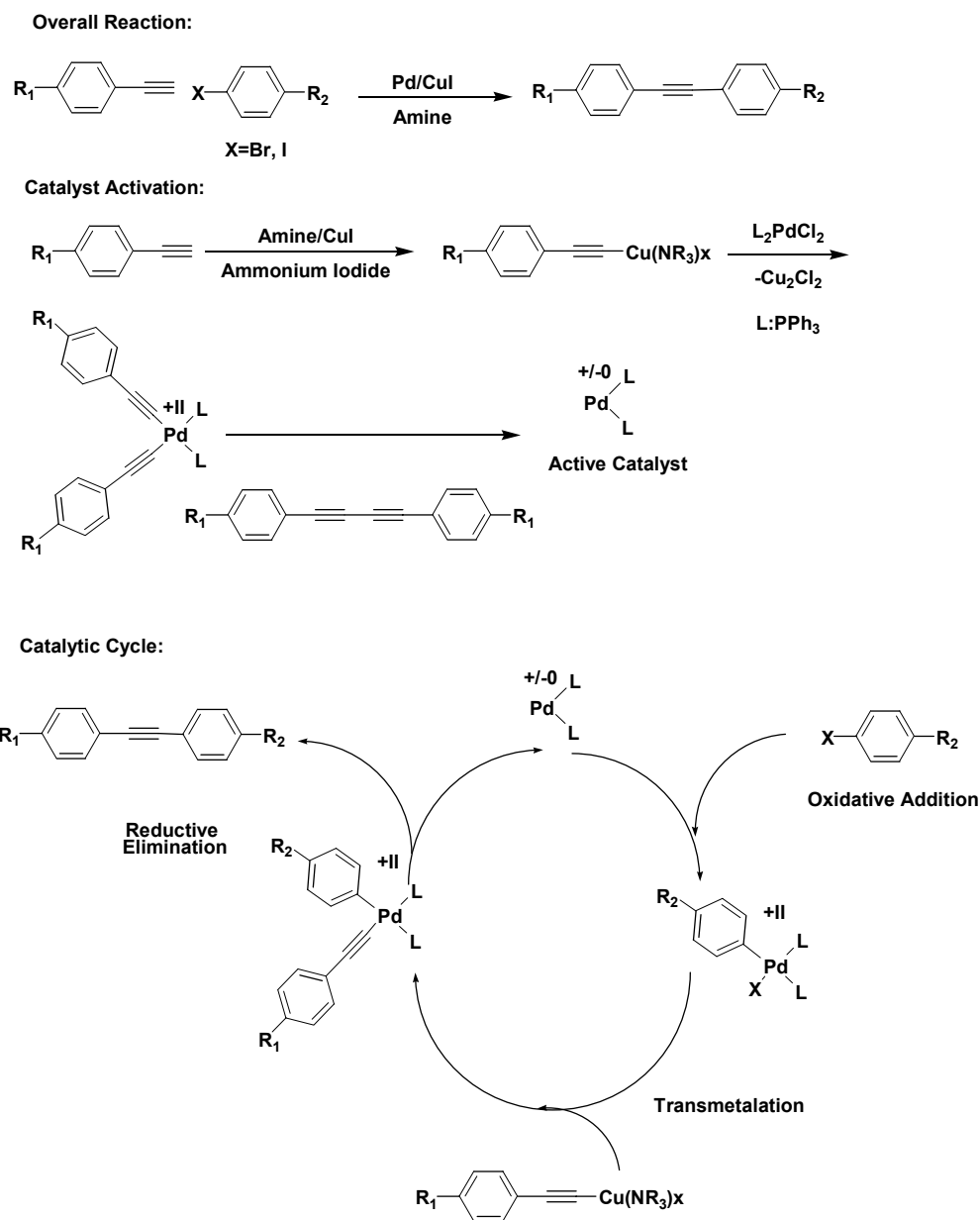


Figure 1.1. The basic structure of the PPE.

1.2 Synthesis of PPEs

PPEs are typically synthesized by one of two methods. The Heck-Cassar-Sonogashira-Hagihara (HCSH) reaction conditions employ a palladium catalyzed process to generate moderate to high molecular weight PPEs.^{5,6,7} The advantages of this method are its tolerance to a variety of monomers and functionalities. This catalytic process is a valuable tool for the formation of C-C single bonds between sp - and sp^2 - hybridized carbon centers.

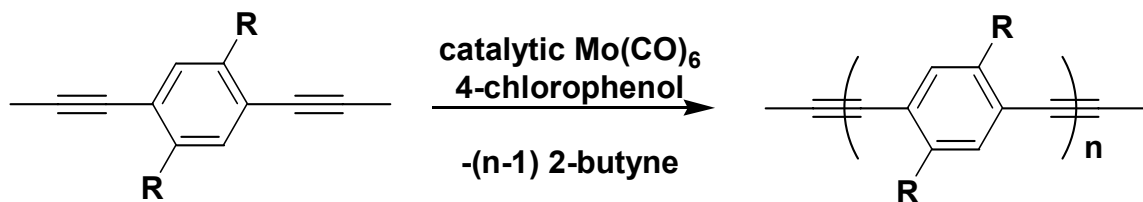
Commercially available $(Ph_3P)_2PdCl_2$ serves as the catalytic source of Pd. It is reduced to Pd^0 which is the active catalyst. Typically CuI is used as a co-catalyst. The first step (Scheme 1.1) of the reaction is transmetalation between the catalyst and two molecules of cuprated alkyne. The formed organometallic species is not stable and reductively eliminates a symmetrical butadiyne and generates the active catalyst species. The active catalyst undergoes oxidative addition with aryl bromide or iodide. Transmetalation with a cuprated alkyne followed by reductive elimination generates the product and regenerates the catalytic species.



Scheme 1.1. HCSH synthesis of PPEs

Alkyne metathesis has emerged as a promising route to high molecular weight PPEs (Scheme 1.2). Traditionally this involved use of a variety of systems such as Schrock's tungsten-carbyne.⁸ Kloppenburg, Pschirer, and Bunz optimized the reaction conditions of alkyne metathesis utilizing $\text{Mo}(\text{CO})_6$ and 4-chlorophenol, increasing the

reaction temperature from 105 to 130-150°C, and purging with nitrogen to remove the formed 2-butyne.^{9, 10} The process has worked with some alkoxy substituted monomers but has primarily been used as an effective process for the generation of alkyl PPEs.¹¹



Scheme 1.2. Alkyne Metathesis

1.3 Optical Properties of PPEs

PPEs exhibit red-shifts in absorption and fluorescence when going from solution to thin-films (Figure 1.2). PPEs also display thermochromicity and solvatochromicity.¹²⁻
¹⁴ This interesting optical behavior can result from two possible situations. The first being the formation of ground state aggregates in thin-films, which consists of many PPE chains. In this situation, electronic communication of the π -systems occurs via tight packing of polymer chains. Here a π - π -stacking effect produces the observed bathochromic shift.³ The second possible explanation would be that this is a single molecule effect that results from planarization of the benzene rings in the polymer backbone. A similar situation has been observed in polythiophenes.¹⁵ Forced planarization leads to an increased conjugation and hence a lower band gap. Rotation around the triple bond of the alkyne in solution is relatively facile and has a barrier of less than 1 kcal/mol.³

At the moment it is not clear which explanation holds. Upon “Jacketing” of PPEs into a cocoon of dendrimers it should be possible to suppress aggregate formation completely.

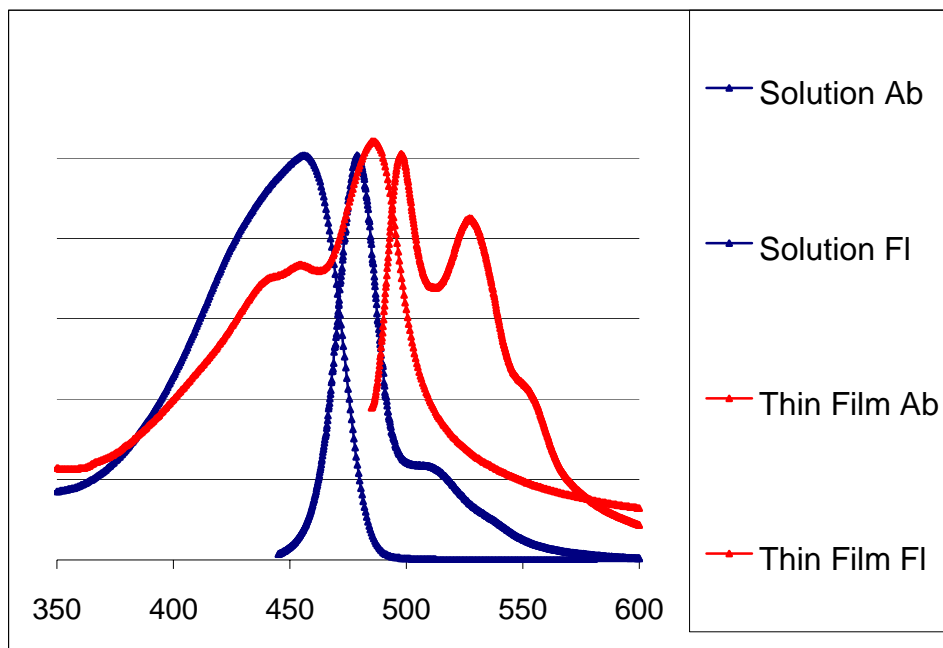


Figure 1.2. Solution to Solid State Red-Shift in Ethylhexyloxy PPE.

1.4 Non-Aggregating PPEs

Jacketing of conjugated polymers with dendrimers is of great interest as it presents the ability to isolate polymers from one another in solution as well as in the solid state (Figure 1.3). Single polymer chains which are isolated from one another would not form excimers and aggregates in the solid state.¹⁶⁻²⁰ Jacketing of polymers is typically accomplished with dendrimers.¹⁶⁻²⁰ Jacketed PPEs would be interesting for exploration of their shielded and single chain optical properties.

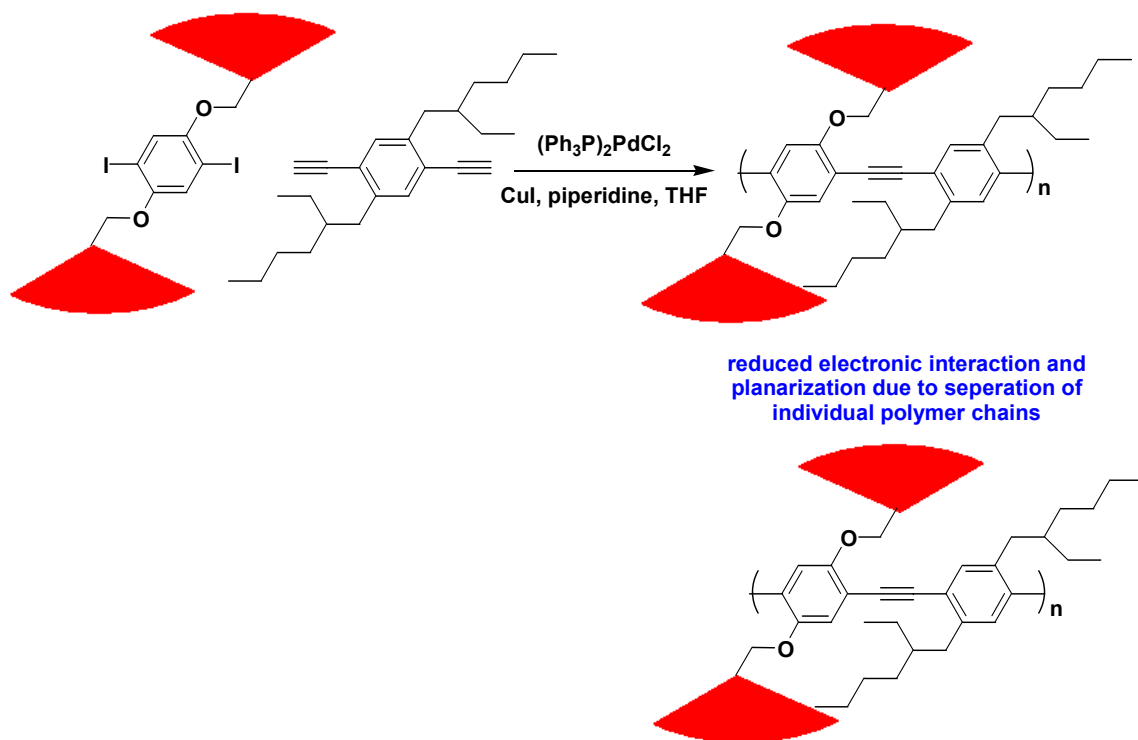
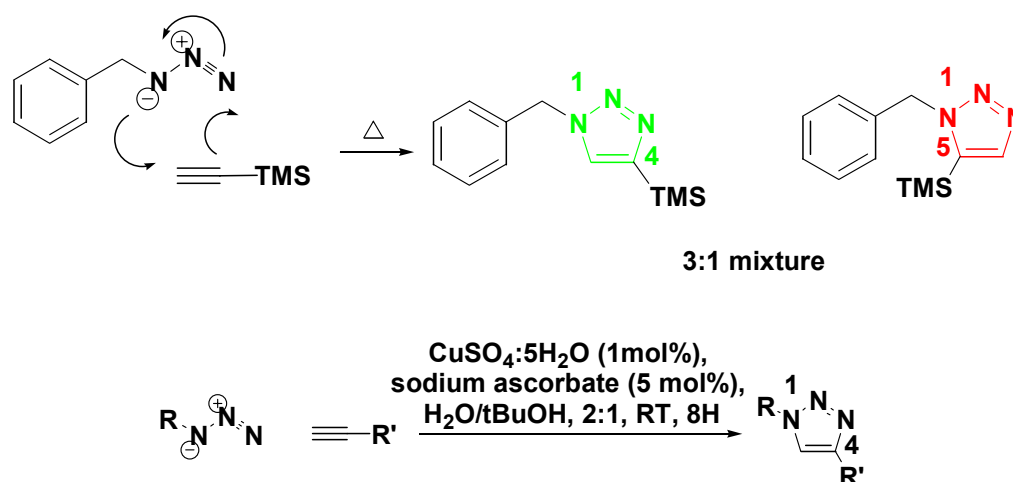


Figure 1.3. Jacketing of PPEs Leads to the Isolation of Individual Polymer Chains.

1.5 Functionalization of PPEs and Click Chemistry

The 1,3-dipolar cycloaddition of azides to alkynes is a useful route to 1,2,3-triazoles (Scheme 1.3).²⁵ Under thermal conditions, this reaction proceeds to completion and in some cases can be moderately regioselective. This process can also occur by a Cu^{I} -catalyzed process. While the thermal conditions are useful, under the Cu^{I} -catalyzed conditions there is moderate to complete selectivity for the 1,4-substituted triazole. The selectivity of the Cu^{I} -catalyzed process has proved to be less than effective when applied to non-conjugated polymeric systems.^{26b} Even with moderate regioselectivity, a reaction which would proceed to completion under mild temperatures would be valuable for the functionalization of PPEs.



Scheme 1.3. 1,3-dipolar cycloaddition of azides to alkynes under thermal and Cu^{I} catalyzed conditions.

Click chemistry has no doubt proven useful in the past, and use of this powerful tool in the future should as well prove lucrative.²⁴⁻²⁶ With its ability to proceed to completion, and its moderate to complete regioselectivity, the products of this reaction should be easily purified and characterized. Reactions such as this might prove useful in polymer chemistry for post-polymerization modification. With this in mind we began synthesis of polymers with silane masked acetylenes in the side chains. Polymerization and subsequent deprotection could afford a polymer which could be easily modified.

In the functionalization of PPEs, one can imagine several methods which could be used effectively (Figure 1.4). The most obvious route to functionalization would be the synthesis of functionalized monomers in a pre-polymerization functionalization route (Figure 1.4 top). While this has been employed effectively, it often requires purification of various monomers which can be rigorous.^{21,22} A second, and perhaps more desirable route, is a post-polymerization route (Figure 1.4 bottom). This would entail large scale production of a monomer which after polymerization could be modified. Requisites for

this monomer would be the inclusion of a reactive group which is either protected or non-reactive under polymerization conditions. Several groups have adopted this approach with success using polythiophenes and other polymeric systems.^{23,24} While these are interesting examples, more effective and versatile means for postpolymerization modification are needed. Tolerance to a wide variety of functional groups and polymeric systems are the driving force for this of research. This would require the use of reactions which go to completion and occur under mild conditions to allow for tolerance of various functional groups. Both of the above mentioned routes are useful and shall be employed.

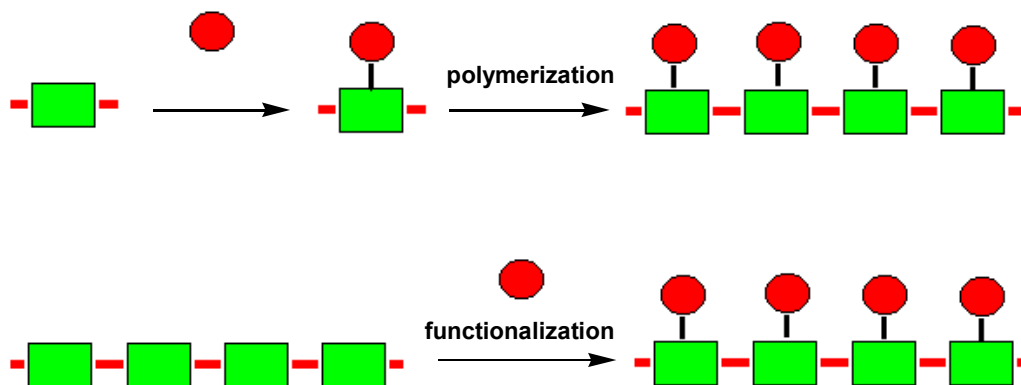


Figure 1.4. Pre vs. post-polymerization functionalization of PPEs.

1.6 PPEs as Precursor Materials for Permanent Microstructures and Nanomaterials

The microstructuring of PPEs into bubble arrays has been reported by Bunz and coworkers (Figure 1.5).²⁷ The mechanism of bubble array formation utilizing the breath figure method is illustrated in Figure 1.5. First, moist air leads to evaporative cooling of the solvent carbon disulfide (a). Next, water droplets form by condensation of the warm moist air onto the cold surface of the liquid (b). The water droplets organize into a 2D

hexagonal array (c). The water droplets sink into the solution and further evaporation leaves the polymer matrix that has formed with the imprinting of the bubbles as a fossil (d).

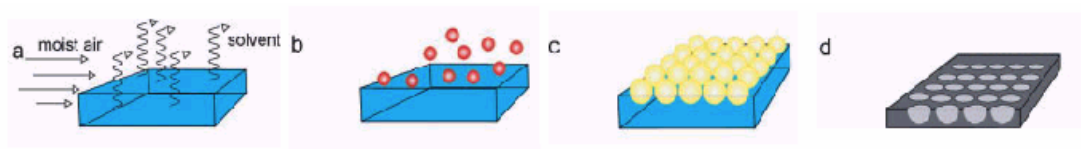


Figure 1.5 Formation of bubble arrays.

More recently these bubble arrays have been made permanent by employing the use of azide functionalized polymers and click chemistry (Figure 1.6-1.7).²⁸ When heating these self-assembled bubble arrays to 300°C picoliter beakers were obtained. Figure 1.9 shows this polymer before and after heating. Visible is the flattening of the sample due to shrinking by softening and cross-linking.

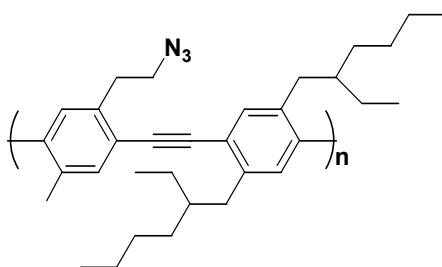


Figure 1.6 The structure of an azide functionalized polymer recently used to create permanent bubble arrays.

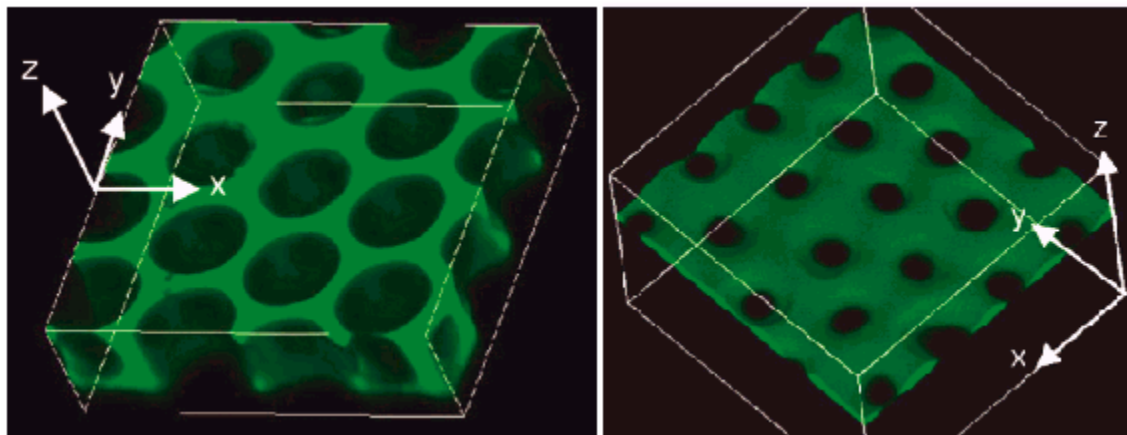


Figure 1.7 Laser scanning confocal micrographs of bubble arrays. Left: Bubble arrays formed from the azide PPE in carbon disulfide. Image dimensions are $15.2\ \mu\text{m} \times 15.2\ \mu\text{m} \times 4.7\ \mu\text{m}$. Right: Same bubble arrays after heating of the sample for 60 min to 300°C . Image dimensions are $21.3\ \mu\text{m} \times 21.3\ \mu\text{m} \times 6.5\ \mu\text{m}$.

This is interesting and it would be valuable to produce other types of materials from microstructured PPEs. Organometallic PPEs would be interesting as precursor materials for these systems. Employing methods similar to those used above, different types of novel materials could be obtained.

1.9 Conclusion

PPEs are excellent candidates for functionalized materials. They can be produced on a large scale and various monomers are easily prepared. Alkynes can easily be masked with various protecting groups. Functionalization of PPEs could be useful for various applications such as biological and metal sensing. Functionalization could also offer the ability to tailor the optical properties of PPEs. Introduction of bulky spacer groups, such as dendrons, could lead to non-aggregating PPEs. Azides can be easily prepared which makes functionalization of PPEs useful for many imagined applications;

such as integration into sensory and electronic devices. With the above in mind, we shall move through the following steps:

1. Integration of spacer groups that allow for the modification of the optical properties of PPEs
2. Synthesis of monomers which allow access to functionalized PPEs
3. Synthesis of polymers which can be modified through post-polymerization functionalization
4. Functionalization of these polymers and investigation of their properties
5. Use of functionalized PPEs as precursor polymers

In the completion of these goals we will have made significant progress toward the implementation of PPEs as sensory materials and non-aggregating molecular wires.

1.10 References

1. Chiang, C. K.; Fincher, C. R.; Park, Y. W.; Heeger, A. J.; Shirakawa, H.; Louis, E. J.; Gau, S. C.; MacKiarmid, A. G. *Phys. Rev. Lett.* **1977**, 39, 1098.
2. Shirakawa, H.; Louis, E. J.; MacKiarmid, A. G.; Chiang, C. K.; Heeger, A. J. *J. Chem. Soc.; Chem. Commun.* **1977**, 578.
3. Collis, G. E. and Burrell, A. K. *J. Org. Chem.* **2003**, 68, 8974-8983.
4. Bunz, U. H. F. *Chem. Rev.* **2000**, 100, 1605-1644.
5. Kieck, H. A.; Heck, R. F. *J. Organomet. Chem.* **1975**, 93, 259.
6. Cassar, I. *J. Organomet. Chem.* **1975**, 93, 253.
7. Sonogashira, K; Tohda, Y.; Hagihara, N. *Tetrahedron Lett.* **1975**, 16, 4467.

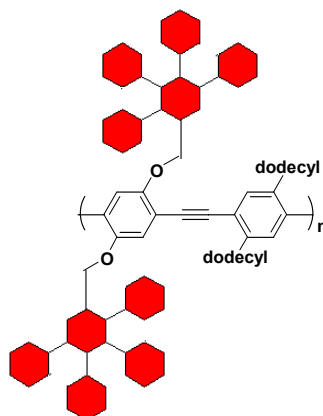
8. Schrock, R. R.; Clark, D. N.; Sancho, J.; Wengrovius, J. H.; Pederson, S. F. *Organometallics* **1982**, 1, 1645.
9. Kloppenburg, L.; Song, D.; Bunz, U. H. F. *J. Am. Chem. Soc.* **1998**, 120, 7973.
10. Pschirer, N. G.; Bunz, U. H. F. *Tetrahedron Lett.* **1999**, 40, 2481.
11. Fürstner, A. and Seidel, G. *Angew. Chem. Int. Ed.* **1998**, 37, 1734-1736.
12. Halkyard, C. E.; Rampey, M. E.; Kloppenburg, L.; Studer-Martinez, S. L.; Bunz, U. H. F. *Macromolecules* **1998**, 31, 8655.
13. Fiesel, R.; Halkyard, C. E.; Rampey, M. E.; Kloppenburg, L.; Studer-Martinez, S. L.; Scherf, U.; Bunz, U. H. F. *Macromol. Rapid Commun.* **1999**, 20, 107.
14. Miteva, T.; Palmer, L.; Kloppenburg, L.; Neher, D.; Bunz, U. H. F. *Macromolecules* **2000**, 33, 652.
15. Rughooputh, S. D. D. V.; Hotta, S.; Heeger, A. J.; Wudl, F. *J. Polym. Sci., Part B; Polym. Phys.* **1987**, 25, 1071.
16. (a) Lupton, J. M.; Schouwink, P.; Keivanidis, P. E.; Grimsdale, A. C.; Müllen, K. *Adv. Funct. Mater.* **2003**, 13, 154-158. (b) Pogantsch, A.; Wenzl, F. P.; List, E. J. W.; Leising, G.; Grimsdale, A. C.; Müllen, K. *Adv. Mater.* **2002**, 14, 1061-1064. (c)
17. (a) Schlüter, A. D.; Rabe, J. P. *Angew. Chem.* **2000**, 39, 864-883. (b) Karakaya, B.; Claussen, W.; Gessler, K.; Saenger, W.; Schlüter A. D. *J. Am. Chem. Soc.* **1997**, 119, 3296-3301. (c) Stocker, W.; Karakaya, B.; Schürmann, B. L.; Rabe, J. P.; Schlüter A. D. *J. Am. Chem. Soc.* **1998**, 120, 7691-7695.
18. (a) Masuo, S.; Yoshikawa, H.; Asahi, T.; Masuhara, H.; Sato, T.; Jiang, D. L.; Aida, T. *J. Phys. Chem. B.* **2003**, 107, 2471-2479. (b) Masuo, S.; Yoshikawa, H.; Asahi, T.; Masuhara, H.; Sato, T.; Jiang, D. L.; Aida, T. *J. Phys. Chem. B.* **2002**, 106, 905-909.

- (c) Masuo, S.; Yoshikawa, H.; Asahi, T.; Masuhara, H.; Sato, T.; Jiang, D. L.; Aida, T. *J. Phys. Chem. B.* **2002**, *105*, 2885-2889. (d) Sato, T.; Jiang, D. L.; Aida, T. *J. Am. Chem. Soc.* **1999**, *121*, 10658-10659.
19. Setayesh, S.; Grimsdale, A. C.; Weil, T.; Enkelmann, V.; Müllen, K.; Meghdadi, List, E. J. W.; Leising, G. *J. Am. Chem. Soc.* **2001**, *123*, 946-953.
20. Other dendronized conjugated polymers: (a) Bao, Z.; Amundson, K. R.; Lovinger, A. *Macromolecules* **1998**, *31*, 8647-8649. (b) Malefant, P. R. L.; Frechet, J. M. J. *Macromolecules* **2000**, *33*, 3634-3640. (c) Schenning, A. P. H. J.; Martin, R. E.; Ito, M.; Diederich, F.; Boudon, C.; Gisselbrecht, J. P.; Gross, M. *Chem. Commun.* **1998**, 1013-1014.
21. Erdogan, B.; Wilson, J. N.; and Bunz, U. H. F. *Macromolecules*, **2002**, *35*, 7863-7864.
22. Wang, Y.; Wilson, J. N.; Smith, M. D.; Bunz, U. H. F. *Macromolecules*; **2004**; *37*(26); 9701-9708.
23. Zhai, L.; Pilston, R. L.; Zaiger, K. L.; Stokes, K. K.; and McCullough, R. D. *Macromolecules* **2003**, *36*, 61-64.
24. a) Huisgen, R.; Szeimies, G.; Moebius, L. *Chem. Ber.* **1967**, *100*, 2494. b) Huisgen, R.; Knorr, R.; Moebius, L.; Szeimies, G. *Chem. Ber.* **1965**, *98*, 4014. c) Rostovtsev, V. V.; Green, L. G.; Fokin, V. V. and Sharpless, B. *Angew. Chem. Int. Ed.* **2002**, *41*, 2596-2599.
25. Lewis, W. G.; Green, L. G.; Grynszpan, F.; Radic, Z.; Garlier, P. R.; Taylor, P.; Finn, M. G.; and Sharpless, B. K. *Angew. Chem. Int. Ed.* **2002**, *41*, 1053-1057.

26. a) Tornøe, C. W.; Christensen, C.; and Meldal, M. *J. Org. Chem.* **2002**, 67, 3057-3064. b) Wu, P.; Feldman, A. K.; Nugen, A. K.; Hawker, C. J.; Scheel, A.; Voit, B.; Pyun, J.; Frechet, J. M. J.; Sharpless, B. K.; Fokin, V. V. *Angew. Chem. Int. Ed.*
27. Song, L.; Bly R. K.; Wilson, J. N.; Bakbak, S.; Park, J. O.; Srinivasarao, M.; and Bunz, U. H. F. *Adv. Mater.* **2004**, 16, 115-118.
28. Erdogan, B.; Song, L.; Wison, J. N.; Park, J. O.; Srinivasarao, M.; and Bunz, U. H. F. *J. Am. Chem. Soc.* **2004**, 126, 3678-3679.

CHAPTER 2

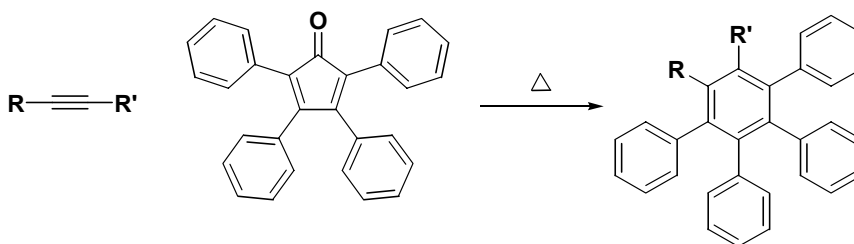
JACKETED POLY(*P*-PHENYLENEETHYNYLENE)S: NONAGGREGATING CONJUGATED POLYMERS AS BLUE-EMITTING RODS.



2.1 Introduction:

Jacketing of conjugated polymers with dendrimers is of great interest as it presents the ability to isolate polymers from one another in solution as well as solid state.¹⁻⁵ Single polymer chains which are isolated from one another do not form excimers and aggregates in the solid state. Such a strong tendency to aggregate is a major drawback of “naked” conjugated polymers. Aggregation results in collisional deactivation of photoexcited states and hinders potential application of these materials.^{1, 4} Isolation of chromophores might lead to colorfast active materials for light-emitting diodes and potentially for polymer lasers. Issues which must be dealt with before this can be realized are stability, electron transport, and charge carrier injection.

Polyfluorenes grafted by Müllen dendrimers¹⁰ have been synthesized.^{1, 4} There are no Poly(p-phenyleneethynylene)s (PPEs) known that are covered with these types of dendrimers. Müllen dendrimers are attractive when compared to Frechet dendrimers¹¹ because they are more thermally stable and easier to produce synthetically (Scheme 2.1). They are also not hydrolytically sensitive like Frechet dendrimers.



Scheme 2.1. Synthesis of tetraphenylbenzene units.

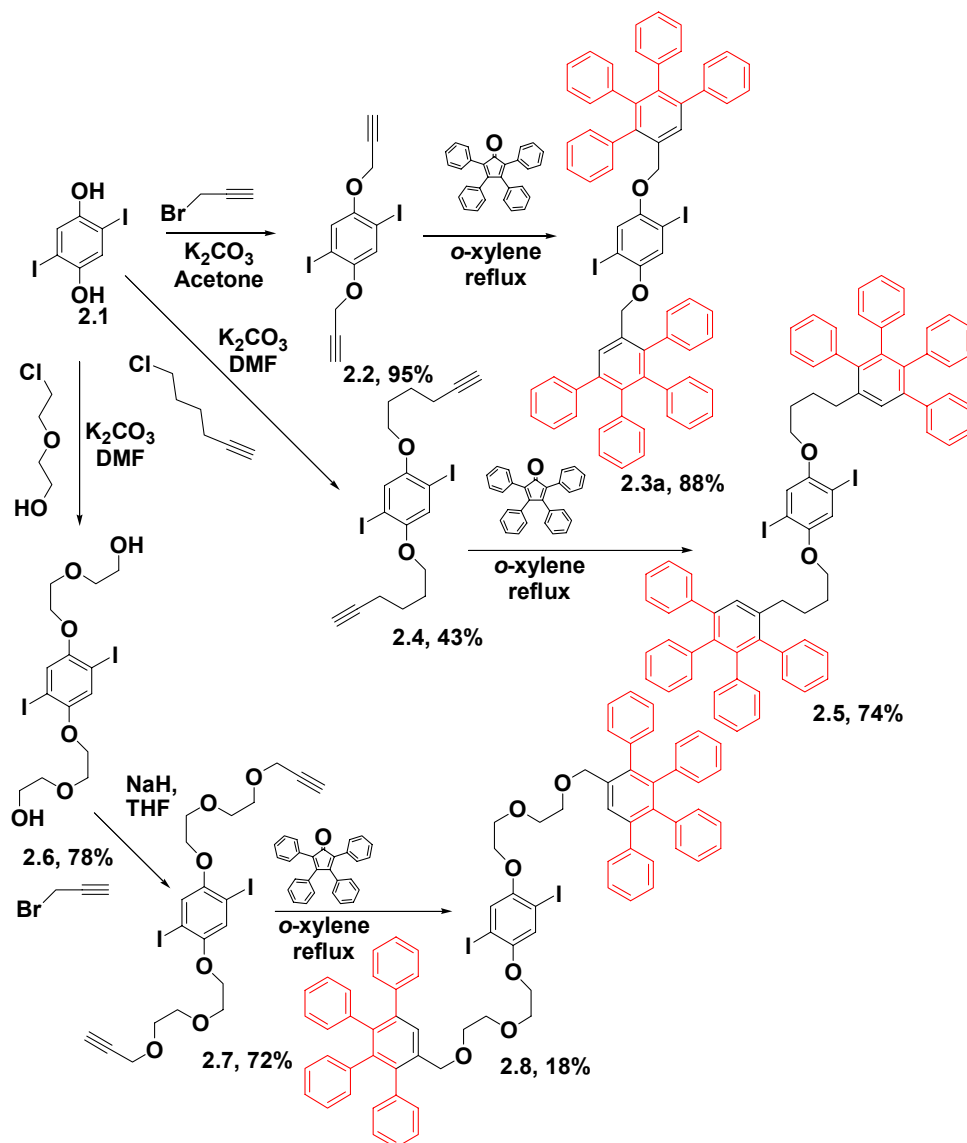
PPEs have been reported which were jacketed with Frechet's benzyl ether dendrons.³ These densely dendronized PPEs show unity fluorescence quantum yields even in relatively concentrated solution where interchain interactions inhibit unity fluorescence quantum yields on nondendronized PPEs. The reason for unity fluorescence quantum yields is that the dendronization/jacketing of PPEs efficiently suppresses collisional deactivation of the excited state of the PPE.

2.2 Results and Discussion:

2.2.1 Synthesis of monomers 2.3a, 2.5, and 2.8.

With this in mind, we set out to synthesize PPEs jacketed with Müllen dendrimers. Synthesis begins starting from diiodide **2.1**, which can be reacted with

propargyl bromide in the presence of potassium carbonate to yield **2.2** in 95%. Reaction of **2.2** with tetraphenylcyclopentadienone afforded **2.3a**. The same methodology was applied starting from **2.1** using 6-chloro hexyne in the presence of potassium carbonate to furnish **2.4** in 43% yield prior to reaction with tetraphenylcyclopentadienone to yield **2.5** in 74% yield. The synthesis of monomers with different length chains leading to the dendrimer unit allows the production of polymers where the effect of the proximity of the dendrimer unit with respect to the polymer backbone can be investigated. Diiodide **2.1** can be reacted with 2-(2-chloroethoxy)-ethanol in the presence of potassium carbonate to yield **2.6** in 78% yield.^{9c} Subsequent reaction of **2.6** with 3-bromopropyne gave **2.7** in 72%. Reaction with tetraphenylcyclopentadienone yielded **2.8** in 18% yield. In order to afford a model system, **2.3a** was coupled under Pd catalysis to an excess of 2-methylphenylacetylene to give **2.3b** in 88% yield.



Scheme 2.2. Synthesis of **2.3a**, **2.3b**, **2.5**, and **2.8** Starting from 2,5-Diiodohydroquinone (**2.1**).

Crystalline specimens of **2.2**, **2.4**, and **2.7** were grown from solutions of the corresponding diiodide in chloroform or dichloromethane. Figure 2.1 and Table 2.1 show the molecular structures and data from structure analysis of the diynes in the solid state. The propargylic substituents in **2.2** are pointing in two different hemispheres, trans to each other. In both **2.4** and **2.7**, a flat packing of the side chains is observed. In **2.4**,

the alkane chain takes up a perfect transconformation, similar to that observed for methylene groups in polyethylene.¹² In **2.7**, the triethylene glycol chains adopt a more helical conformation. This is more than likely due to the oxygen atoms in the linker chain.

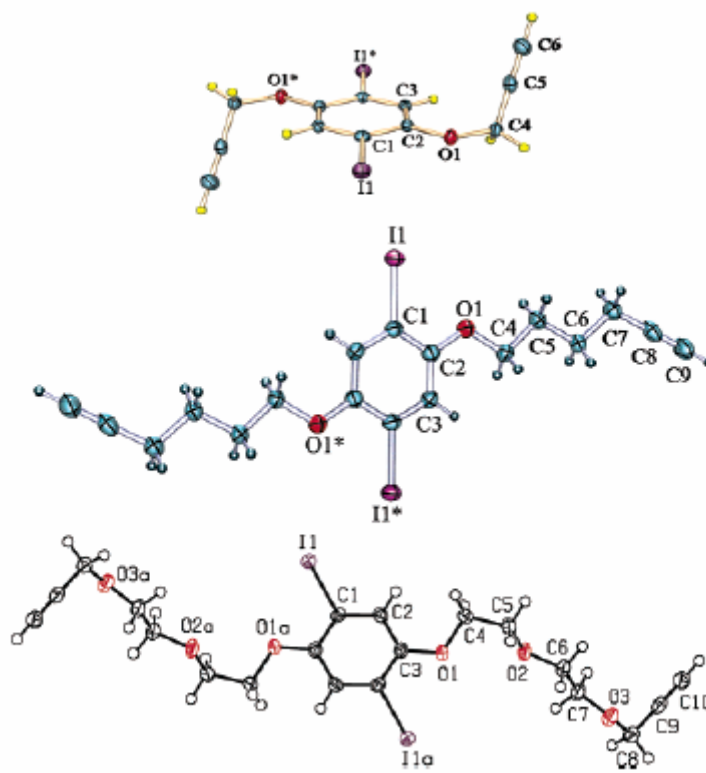


Figure 2.1. Anisotropic displacement parameter (ADP) representations (50%) of the diynes **2.2** (top), **2.4** (middle), and **2.7** (bottom) in the solid state. Diyne **2.2** shows a perpendicular trans orientation of the two propargylic units with respect to the flat arene ring. In diyne **2.4**, the side chains are coplanar to the arene ring and show a trans orientation of the methylene units as found in polyethylene. Monomer **2.7** shows a coplanar but helical arrangement of the side chains.

Growth of single crystalline specimens was attempted for **2.3a**, **2.5**, and **2.8** for structure analysis. Only **2.3a** and **2.5** afforded acceptable specimens. The structure of **2.3a** and **2.5** are shown in Figure 2.2. The pertinent crystallographic data are contained in Table 1. Single molecules of **2.3a** are Z-shaped; this conformation leads to a solid-state arrangement in which the molecules are packed in an interdigitated zigzag motif (Figure 2.2, middle). Rotation of the view by 90°C reveals that the molecules are stacked on top of each other and tilted with the tetraphenylbenzene side chains interlocking (Figure 2.2, bottom). The central diiodoarenes are far removed from each other due to the bulky side chains and do not show any intermolecular contacts with other diiodoarenes. All bond lengths and angles are in agreement with the expected values.

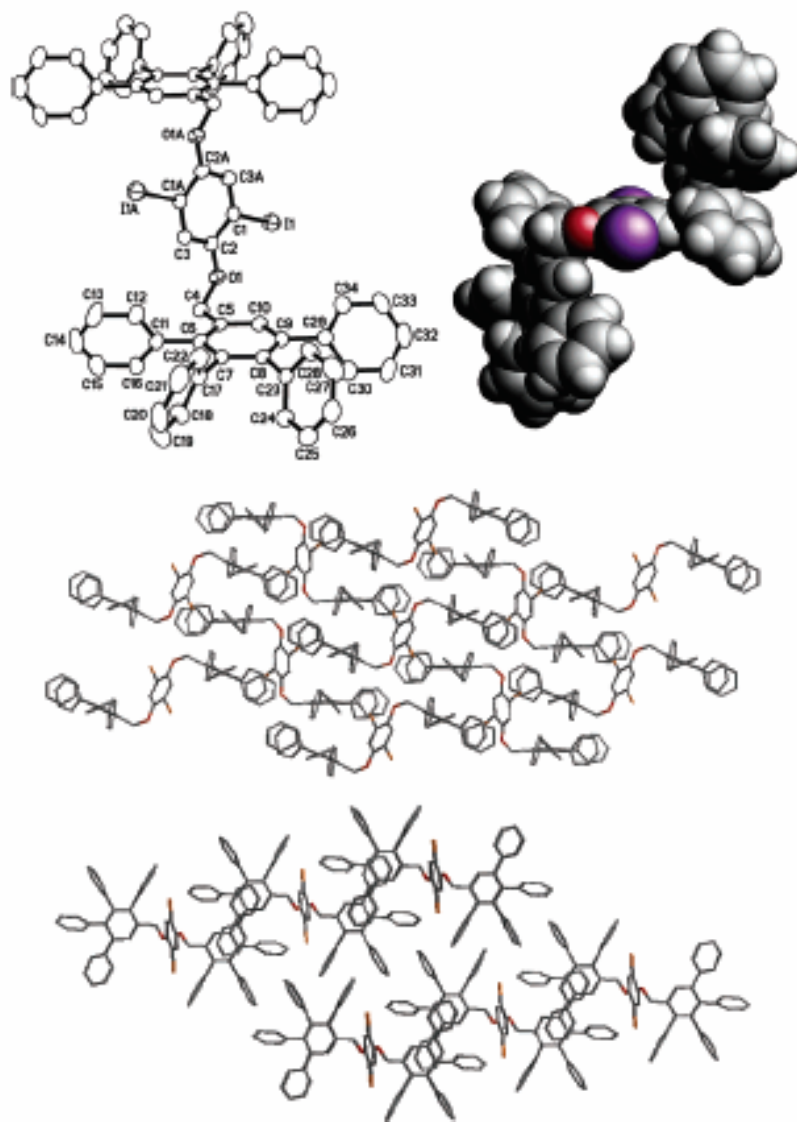


Figure 2.2. ADP (50%) (top, left) representations of **2.3a**. The monomer has a step conformation (top right, Van Der Waals representation) that leads to an interesting (middle and bottom) solid-state arrangement, in which the phenyl rings of one tetraphenylbenzene substituent are interlaced with the ones from the molecules of **2.3a** above and below.

The single-crystal structure of **2.5** is shown in Figure 2.3. The three benzene rings are almost coplanar, and the four phenyl substituents are oriented perpendicularly

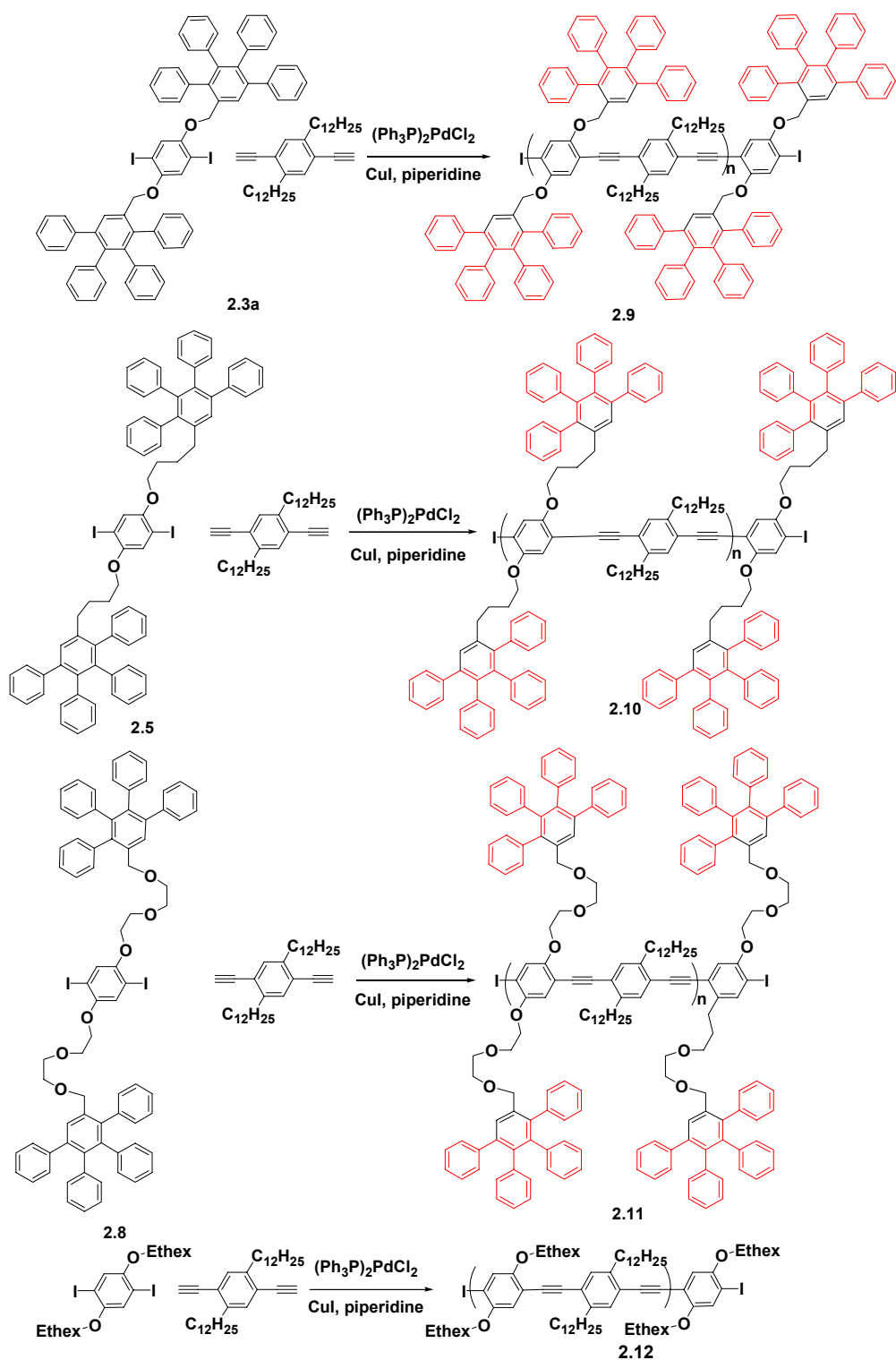
23

Table 1. Crystal Data and Unit Cell Parameters for the Compounds 2.2-5 and 2.7.

Identification code	2.2	2.3a	2.4	2.5	2.7
Empirical formula	C ₁₂ H ₈ I ₂ O ₂	C ₆₈ H ₄₈ I ₂ O ₂	C ₁₈ H ₂₀ I ₂ O ₂	C ₇₄ H ₆₀ I ₂ O ₂	C ₂₀ H ₂₄ I ₂ O ₆
Formula weight	437.98	1150.86	522.14	1378.55	614.19
Space group	P-1	P2 ₁ /n	Pbca	P-1	P2 ₁ /c
Unit cell dimensions	a = 4.2569(4) Å b = 8.9180(8) Å c = 8.9454(8) Å a = 67.777(2)° b = 79.244(2)° g = 82.963(2)°	a = 15.6063(10) Å b = 8.9275(6) Å c = 19.2262(13) Å a = 90° b = 98.979(2)° g = 90°	a = 8.0944(4) Å b = 13.7017(6) Å c = 16.9431(8) Å a = 90° b = 90° g = 90°	a = 12.5600(16) Å b = 12.9515(17) Å c = 23.031(3) Å a = 84.628(3)° b = 81.298(2)° g = 76.837(2)°	a = 15.8462(9) Å b = 7.6297(4) Å c = 9.3907(6) Å a = 90° b = 105.9060(10)° g = 90°
Volume	308.34(5) Å ³	2645.9(3) Å ³	1879.11(15) Å ³	3599.2(8) Å ³	1091.88(11) Å ³
Z	1	2	4	2	2
Density (calculated)	2.359 Mg/m ³	1.445 Mg/m ³	1.846 Mg/m ³	1.272 Mg/m ³	1.868 Mg/m ³
Absorption coefficient	5.081 mm ⁻¹	1.235 mm ⁻¹	3.351 mm ⁻¹	1.041 mm ⁻¹	2.912 mm ⁻¹
Reflections collected	2788	16828	11439	33301	7165
Independent reflections	1253 [R(int) = 0.0195]	3485 [R(int) = 0.0514]	2073 [R(int) = 0.0279]	10700 [R(int) = 0.0693]	1924 [R(int) = 0.0292]
Final R indices [I>2sigma(I)]	R1 = 0.0165, wR2 = 0.0412	R1 = 0.0541, wR2 = 0.1256	R1 = 0.0201, wR2 = 0.0524	R1 = 0.1695, wR2 = 0.3945	R1 = 0.0189, wR2 = 0.0474
R indices (all data)	R1 = 0.0170, wR2 = 0.0415	R1 = 0.0705, wR2 = 0.1348	R1 = 0.0209, wR2 = 0.0530	R1 = 0.1866, wR2 = 0.4056	R1 = 0.0196, wR2 = 0.0479
Largest diff. peak and hole	0.582 and -0.410 e.Å ⁻³	1.645 and -0.256 e.Å ⁻³	0.566 and -0.745 e.Å ⁻³	4.512 and -1.591 e.Å ⁻³	0.556 and -0.546 e.Å ⁻³
Wavelength	0.71073 Å	0.71073 Å	0.71073 Å	0.71073 Å	0.71073 Å
Temperature	150(2) K	293(2) K	150(2) K	173(2) K	150(2) K

2.2.2 Synthesis and Characterization of the Polymers.

With monomers **2.3a**, **2.5**, and **2.8** in hand, the synthesis of their polymers was realized. A preliminary experiment with **2.3a** under acetylene gas in the presence of a Pd catalyst yielded a completely insoluble polymer. Copolymerization of **2.3a**, **2.5**, and **2.8** with a 2,5-didodecyl-1,4-diethynylbenzene gave rise to the formation of soluble jacketed PPE derivatives **2.9**, **2.10**, and **2.11** in good yields with molecular weights ranging from 3×10^4 to 13×10^4 amu. Polymers **2.9-2.11** were amorphous according to powder diffraction experiments, but they showed a halo at approximately 20° , which is typical for π - π stacking interactions. The polymers did not show reversible phase transitions upon heating to above 150°C due to slow decomposition which is common for dialkoxy-PPEs. Polymer **2.12** was synthesized with an M_n of 56×10^3 and a PDI of 4.5 in order to have a nonjacketed PPE for comparison purposes (Scheme 2.3). Table 2 shows the pertinent molecular weight information for **2.9-2.12**.



Scheme 2.3. Synthesis of Polymers **2.9-2.12** by Pd-Catalyzed Coupling.

Table 2.2. Optical Properties and Molecular Weight Properties of Polymers **2.9-2.12**.

	M_n	P_n^a	PDI	absorption [nm]		emission [nm]	
				λ_{max} solution	λ_{max} film	λ_{max} solution	λ_{max} film
2.9	29×10^3	42	2.5	418	417; $\Delta = 1$ nm	453, 481	460, 480; $\Delta = 7$ nm
2.10	13×10^4	179	4.3	437	445; $\Delta = 12$ nm	456, 483	466, 492; $\Delta = 10$ nm
2.11	74×10^3	98	9.9	421	432; $\Delta = 11$ nm	449, 478	464, 472, 487; $\Delta = 15$ nm
2.12	56×10^3	142	4.5	434	448; $\Delta = 14$ nm	456, 483	469, 493, 516; $\Delta = 13$ nm

2.2.3 Optical Properties of the Polymers in Solution and in the Solid State.

In Table 2.2 and Figures 2.5-7, the optical properties of **2.9-2.12** in solution and in the solid state are shown. Polymer **2.12** is the standard to which the other polymers are compared. Its absorption maximum in solution (Table 2.2) is 434 nm, typical^{6a} for this substitution pattern. Its emission maximum in solution is at 456 nm. In the solid state, the absorption and the emission are red-shifted by 14 and 13 nm, respectively. Polymer **2.10** shows optical properties that are by and large very similar to those for **2.12**. The changes in emission and absorption when going from dilute solution into the solid state are almost identical. The remote tetraphenylbenzene, with respect to the backbone of **2.10**, does not interfere with the conformational freedom of the polymer chains; i.e., the twist angle between neighboring aryl rings is variable in solution like in **2.12**, and the polymer chains are planarized in the solid state in both **2.10** and **2.12**. Polymers **2.9** and **2.11** show very different spectroscopic behavior; their absorption maximum in solution is somewhat blue-shifted from 434 to 418 or 421 nm respectively. A blue-shifted absorption in solution is unusual because it suggests that the rotational freedom of the chains might be restricted toward a greater twist angle between neighboring phenyl rings.¹⁵⁻¹⁷

In order to investigate this rarely observed behavior, trimer **2.3b** was synthesized as a model system. Suitable single crystals of **2.3b** were grown from hexafluorobenzene.

Figure 2.4 shows an atomic displacement parameter (ADP) plot of **2.3b**. The bisphenylethynylbenzene unit is not planar in this structure, but one benzene ring is twisted by 34° (Figure 2.4) perhaps by the steric demand of the two bulky side groups. All of the hitherto reported bisphenylethynylbenzenes¹³ are strictly planar in the solid state, regardless of their substitution pattern. Figure 4 shows the packing of **2.3b** in the solid state. The conformation of the tetraphenylbenzene unit seems to dictate the packing of **2.3b** in the crystal. The molecules are stacked parallel in layers but shifted with respect to each other. In analogous polymers, the side chains could influence the conformation of the main chain, and lead to a permanently enforced twist. In this situation, close contacts between the central bisphenylethynylbenzene chromophores of different molecules do not exist. A similar situation has been observed by Müllen, Setayesh, and Enkelmann for dendronized fluorenes.⁴

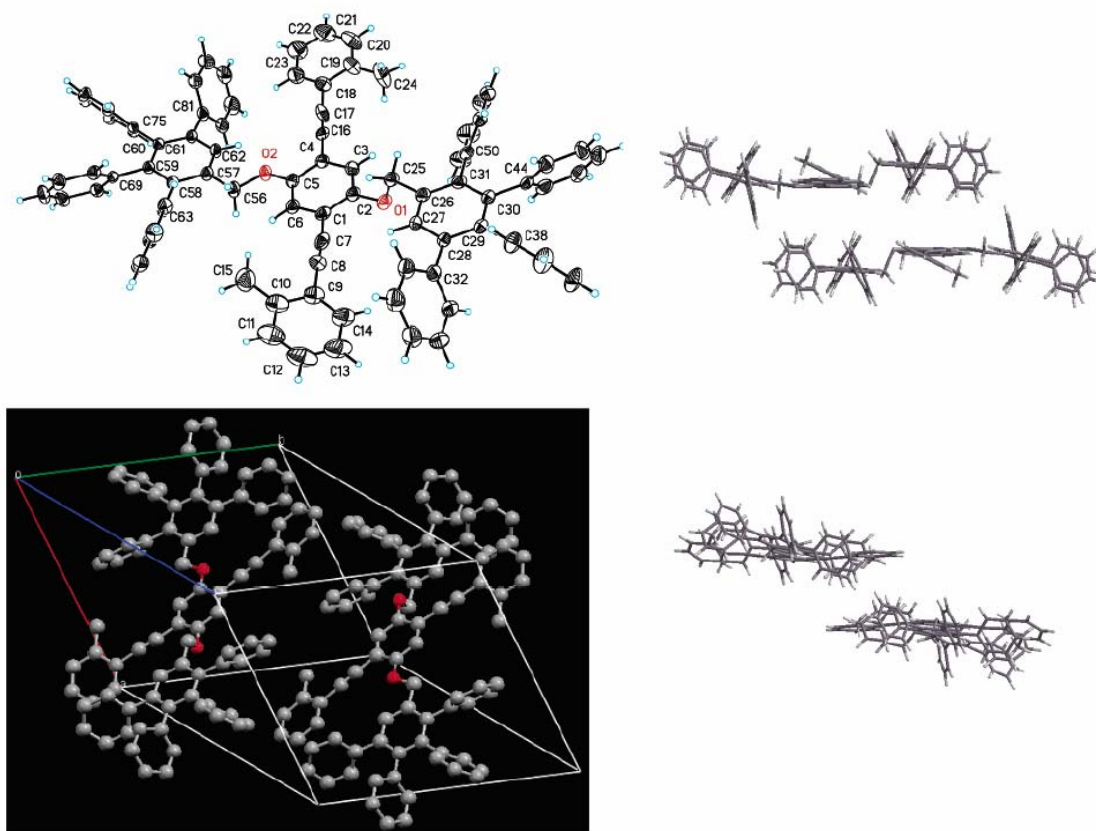


Figure 2.4. X-ray crystal structure of **2.3b**. Top left: ADP (50%) representation of a single molecules of **2.3b**. Top right: view along the conjugated diphenylalkynylbenzene axis. Visible is the twist of one external phenylethynyl unit by 34° with respect to the ventral benzene ring. Bottom: packing of **2.3b** in the solid state. The phenyl groups of one molecule are in close contact to the tolyl group of the second one. The distance of the H atom of the phenyl ring to the center of the tolylethynyl ring is 3.12 \AA .

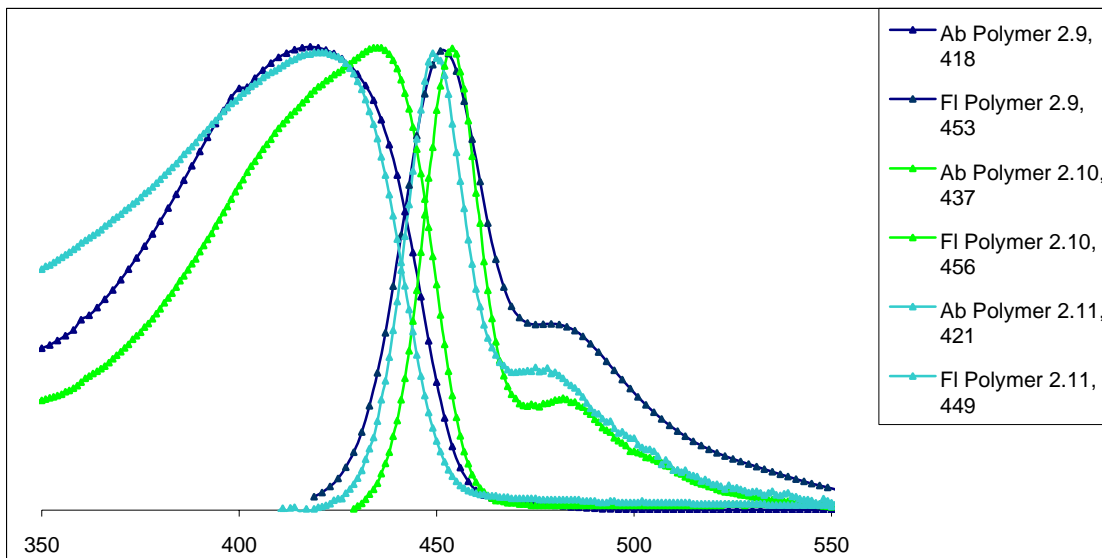


Figure 2.5. Absorption and emission of the polymers **2.9-2.11** in chloroform.

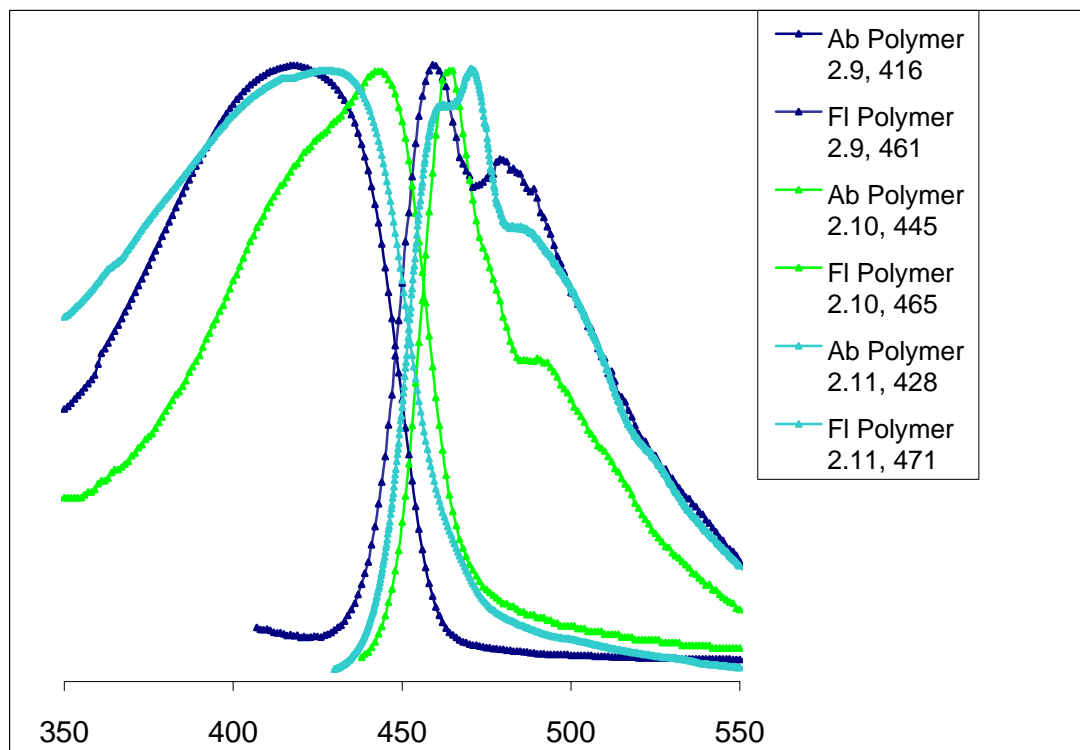


Figure 2.6. Absorption and emission of the polymers **2.9-2.11** in spin-cast films. The red-shifted shoulders are Raman-active states that are coupled to the excited state. The observed shifts are 905 cm^{-1} for **2.9**, 1227 cm^{-1} for **2.10**, and 1111 cm^{-1} for **2.11**.

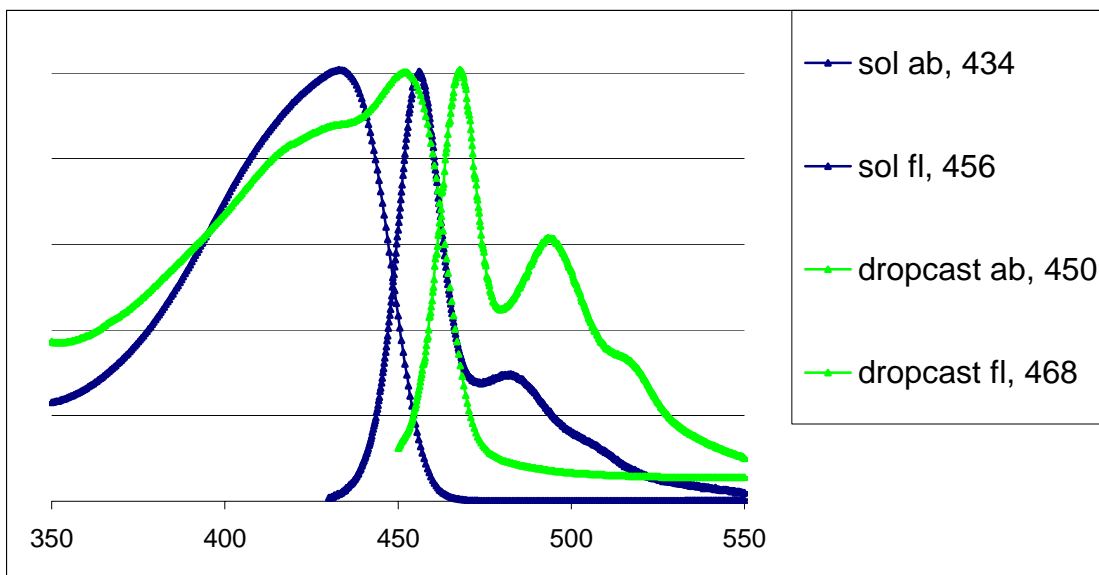


Figure 2.7. Absorption and emission spectra of model polymer **2.12** in solution and in the solid state.

The absence of diffraction patterns in powders of **2.9-2.11** suggest that all are amorphous. In **2.9** the chains of the polymers are probably well separated by the bulky tetraphenylbenzene groups. An MM2 simulation (Figure 2.8) shows a space-filling view of an octameric polymer chain of **2.9**. Two interesting features are visible. In the minimized ground state, the polymer backbone is not planar but twisted (top). The space-filling model (middle) demonstrates the sterically congested surrounding that will make a board like lamellar packing of the polymer chains difficult. The bottom of Figure 2.8 shows an end-on view, demonstrating that the main chain is buried deeply beneath the substituents.

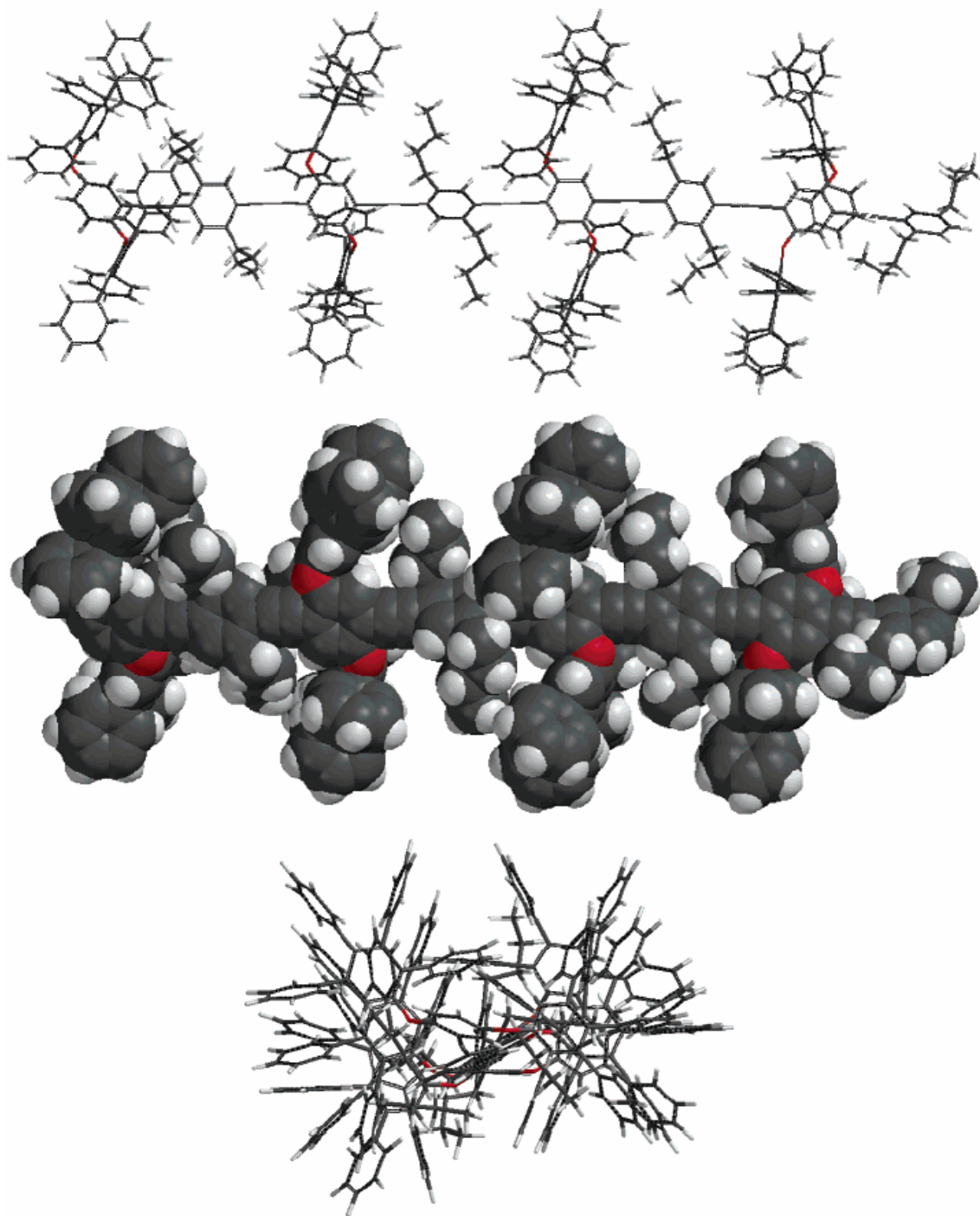


Figure 2.8. MM2 calculations of an octameric model compound of polymer **2.9**.

Quantum chemical analysis of the rotational energy potential around the two benzene rings was performed for the model dimer of polymer **2.9** (Figure 2.9). Because

of the size of the dimeric unit, it was only possible to perform analysis on a semiempirical (AM1) level. The use of AM1 can underestimate the barrier of rotation but tends to give satisfying qualitative results for carbon-based systems.¹² With AM1 a rotational barrier of only 0.2 kcal/mol is obtained for tolane, while Tour and Seminario determined a rotational barrier of 0.8 kcal/mol utilizing a sophisticated ab initio technique for the same molecule; AM1 results seem to err toward lower values.^{12b} Investigation of the model dimer by AM1 shows a complex rotational behavior. Unlike diphenylacetylene, the dimer displays several maxima and minima (Figure 2.9). This rotational profile is a representative rotational profile but probably not the global minimum, despite the routine utilized to minimize all of the rotamers. Only a costly molecular dynamics calculation would give a complete picture of all low-energy rotational profiles accessible to this complete system. However, even with this relatively simple theoretical approach, the 90° conformation does not seem to be an energy maximum anymore, contrary to the case of tolane. The AM1 calculation of the dimer shows a complex rotational profile around the CC triple bond, suggesting that polymer **2.9** is also very “un-PPE-like” with respect to its conformational behavior.^{6c,12a} PPE **2.9** probably attains nonplanar conformations in both solution as well as in the solid state. The blue shift in absorption of **2.9** in solution is due to the presence of nonplanar lowest ground states, and the similar solid state absorption wavelength is due to the nonplanarization of the backbone in the solid state. In polymer **2.9** “PPE-like” behavior is inhibited (Figure 2.10).

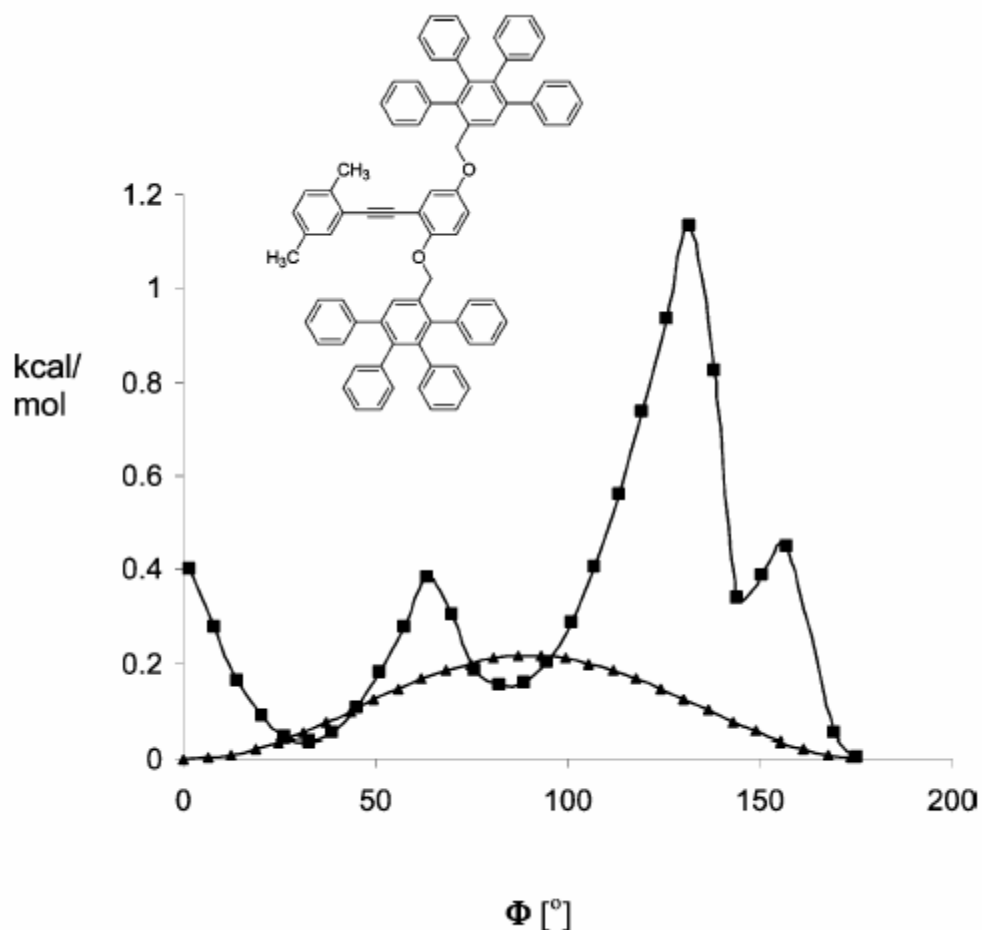


Figure 2.9. Rotational profile of a dimeric repeat unit of **2.9** (black squares) and of diphenylacetylene (blue triangles) as a model compound. The conformational analysis was performed utilizing SPARTAN with the AM1 basis set implemented on a windows platform. The X-axis represents the twist angle between the two arene rings, and the y-axis represents the relative energy (kcal mol⁻¹).

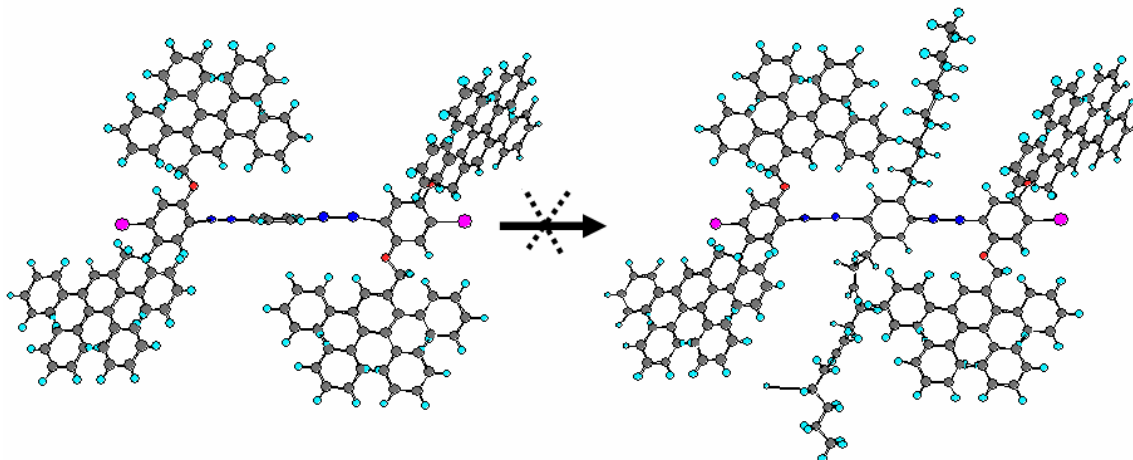


Figure 2.10. PPE **2.9** is unable to planarize in the solid state.

The solution emission spectra of all of the polymers **2.9-2.12**, on the other hand, are very similar. That can be understood because Sluch and Berg¹³ and others^{14,15} have demonstrated that after excitation of an octameric phenyleneethynylene model compound planarization of the backbone occurs to relax the first excited singlet state into its lowest, planar state. The driving force for the planarization is considerably larger in the excited state than in the ground state due to the allenic resonance structures involved, leading to almost super-imposable emission spectra for **2.9-2.12**. The excited-state geometries of **2.9** and of **2.12** will resemble each other closely, despite their different rotational preference in the ground state. The observed shoulders in the fluorescence spectra of **2.9-2.12** in solution and in the solid state are due to the participation of Raman coupled states.¹⁸

Polymer **2.11** resembles **2.9**, while **2.10** has similar properties to model polymer **2.12**. In the solid state, **2.9** is attractive as its absorption shifts only by 1 nm from solution. For the other polymers, a shift of 11-14 nm is observed when transitioning from

solution into the solid state. Polymer **2.11** shows unusual optical properties. Its bulky substituent is farthest away from the PPE backbone, but its optical properties resemble that of **2.9**. We have attempted to perform polarizing microscopy and SEM on **2.11**, but both methods only show the formation of smooth films. In addition, **2.11** is amorphous, so we could not obtain any meaningful powder X-ray diffraction data. As a consequence we are limited in our interpretation of the spectroscopic properties of **2.11**. The explanation in polymer **2.11**'s behavior might be gleaned from the packing of **2.7**, which shows a helical coiling of the ethylene glycol side chains in the solid state. This would bring the tetraphenylbenzene units closer to the polymer backbone as in **2.9**. A second possibility is the obvious difference in the hydrophobicity/hydrophilicity of the connector compared to the tetraphenylbenzene "head." This might lead to a conformational distortion of the main chain in the solid state to best accommodate the packing of the whole substituent. To test these theories, UV-vis and fluorescence spectra of **2.11** were recorded in a series of different solvents. In going from chloroform to THF the absorption maxima blue-shift from 421 to 430 nm for polymer **2.11**. This is still seven nanometers blue-shifted from that of polymer **2.10**. Perhaps even in THF the tetraphenylbenzene units are oriented in close proximity to the polymer backbone.

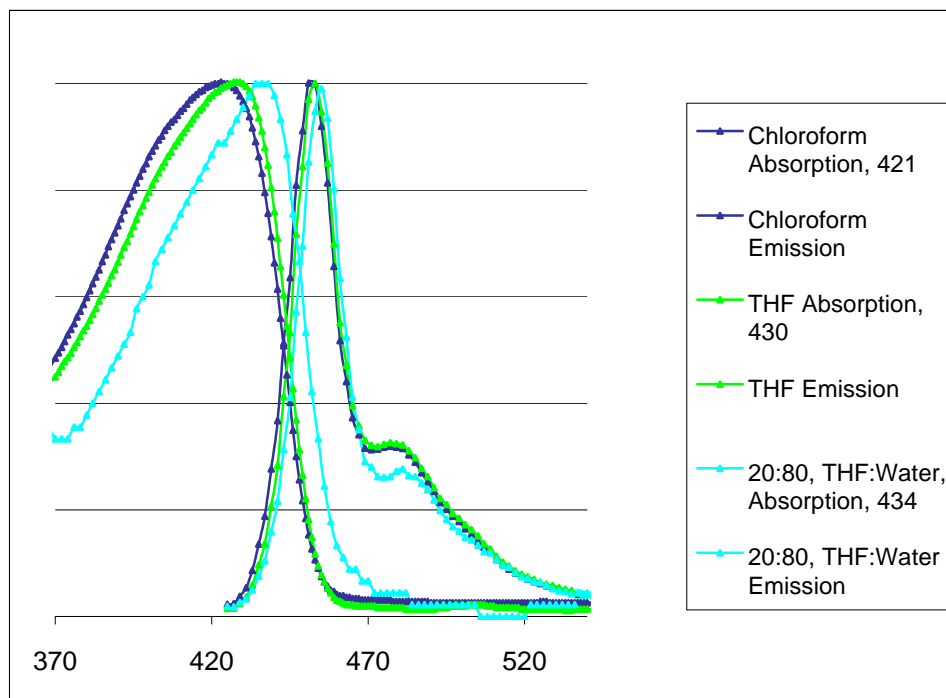


Figure 2.11. Absorption and emission of polymer **2.11** in chloroform, THF THF/H₂O.

Aida has recently demonstrated that the quantum yields of jacketed PPEs are shielded with respect to naked PPEs.^{3d} This experiment relies on the principle that as concentration decreases; so does, collisional deactivation. A phenomenon such as collisional deactivation should decrease more dramatically for shielded PPEs and fluorescence quantum yields should decrease less with reduction in concentration. Results do indicate that jacketed PPEs are shielded from collisional deactivation/quenching which would lower the fluorescence quantum yield of naked PPEs (Figure 2.12).

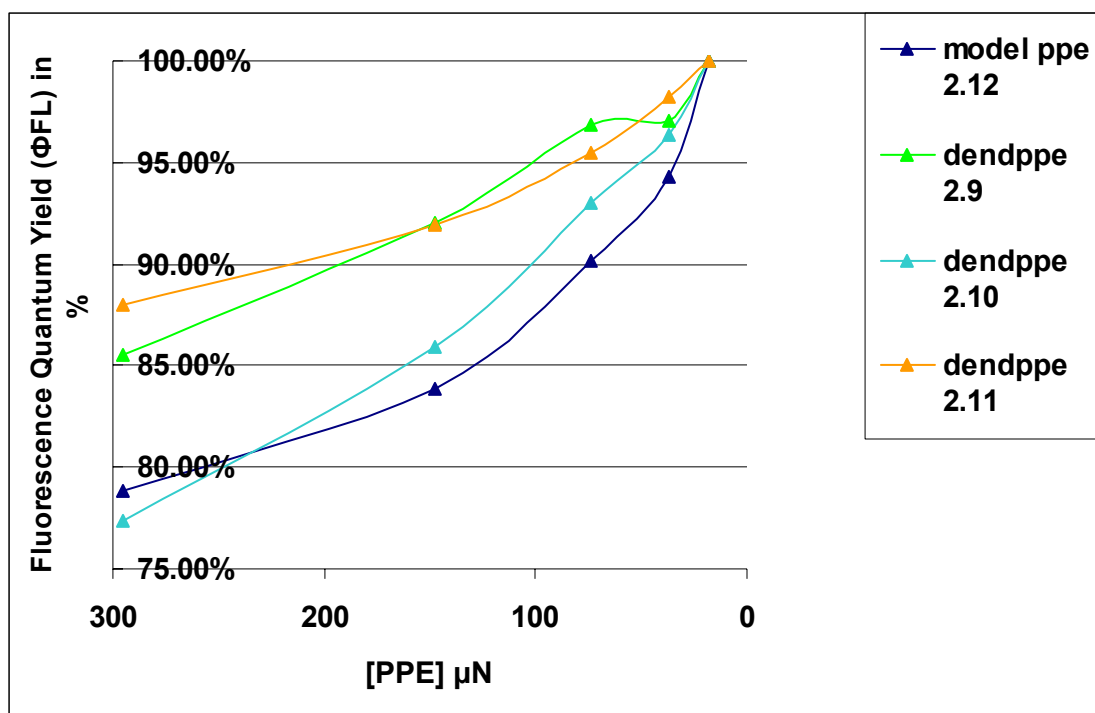


Figure 2.12. Φ_{FL} of polymer **2.9**, **2.10**, **2.11**, and **2.12** upon excitation of the conjugated backbone in chloroform with absorbances at the excitation wavelength of 0.01-0.1.

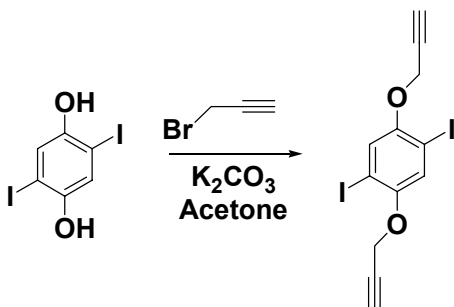
2.3 Conclusion:

The novel dialkyl-co-dialkoxy-PPEs **2.9-2.12** were prepared. Polymers **2.9-2.11** carry tetraphenylbenzene substituents. If the bulky substituents are close to the main chain, as shown in polymer **2.9** or attached by a hydrophilic linker as in polymer **2.11**, the optical properties of the PPE main chain are heavily influenced. The absorption and emission of **2.9** are blue-shifted in comparison to that of the model PPE **2.12**. The reason for the blue shift is an increased twist of the main chain both in solution and solid state and an insulation of the polymer chains from each other. This observation was corroborated by crystallographic studies on a tetraphenylbenzene-substituted

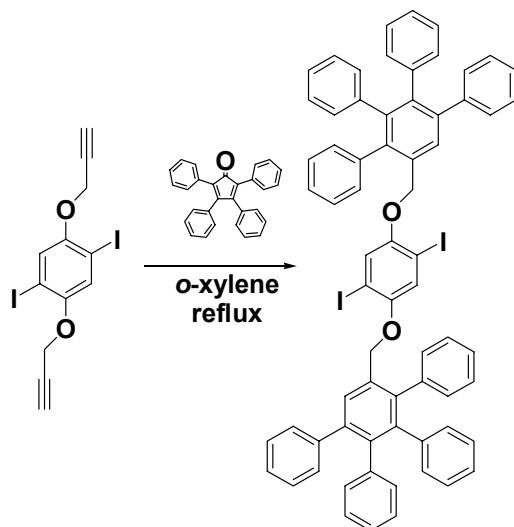
bisphenylethynylbenzene derivative (**2.3b**) that showed a significant twist of a phenyleneethynylene group. Giving an overall self-consistent picture, quantum chemical calculations suggest that polymers like **2.9** are not planar but have multiple conformational minima with respect to the rotation of two neighboring benzene rings in the conjugated main chain. Planarization of the backbone and electronic interaction between separate polymer chains is therefore difficult to attain for **2.9** as well as **2.11**.

2.4 Experimental

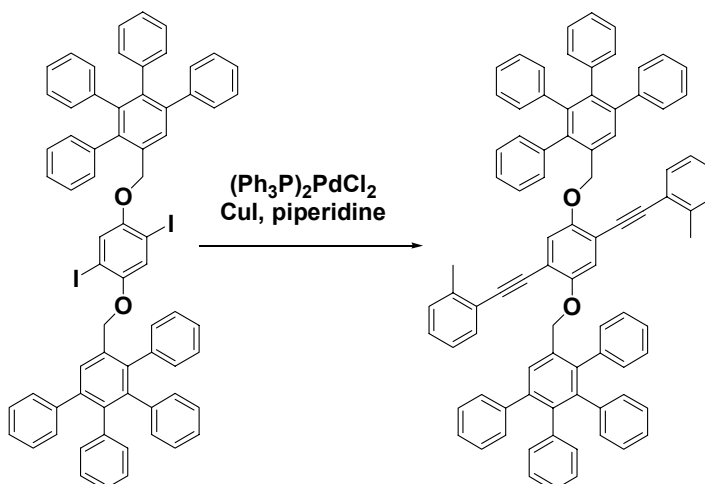
Instrumentation. The ^1H and ^{13}C NMR spectra were taken on a Varian 300 MHz or a Bruker 400 MHz spectrometer using broadband probe. The ^1H chemical shifts are referenced to the residual proton peaks of CDCl_3 at δ 7.24 (vs. TMS). The ^{13}C resonances are referenced to the central peak of CDCl_3 at δ 77.0 and $\text{CDCl}_2\text{CDCl}_2$ at δ 74.0 (vs. TMS). Tetrachloroethane and chromium(III) acetylacetonate were used when obtaining ^{13}C NMR data for all polymers. UV-VIS measurements were made with a Shimadzu UV-2401PC recording spectrophotometer. Fluorescence data was obtained with a Shimadzu RF-5301PC spectrofluorophotometer. In the case of quantum yield shielding experiments the best of twenty runs were used. A Headway Research Model PWM32 instrument was used to spin-coat dilute chloroform solutions of polymers onto quartz slides for thin film experiments. 1,4-Diiodo-2,5-dihydroquinone,^{9c} 2,5-didodecyl-1,4-diehtynylbenzene,¹⁹ **2.6**,^{9c} 1,4-diiodo-2,5-bisethylhexyloxybenzene,^{20, 21} and 2-ethynyltoluene²² were prepared in accordance to published procedures.



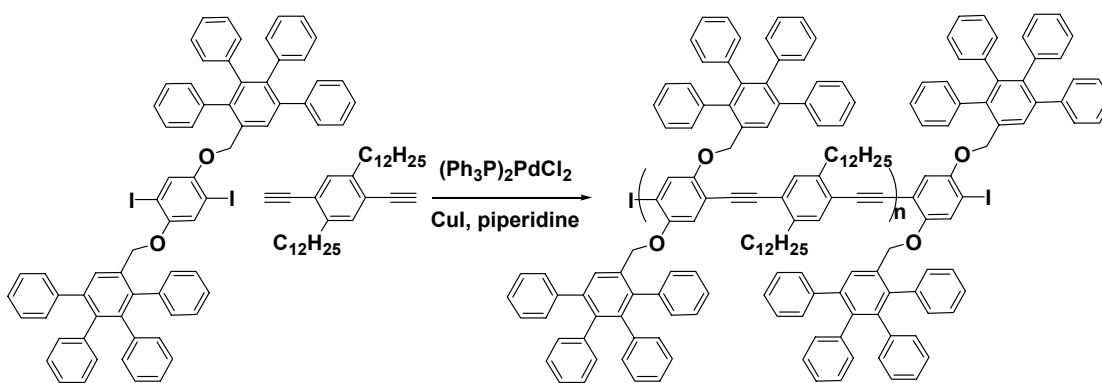
Synthesis of 2.2: 1,4-Diiodo-2,5-dihydroquinone (20.3 g, 5.61 mmol), dimethylformamide (150 mL), potassium carbonate (9.31g, 67.4 mmol), and propargyl bromide (18.7 g, 157 mmol) were placed in a 500 mL round bottom flask and heated to reflux for 48 h. The mixture was allowed to cool to room temperature and the solvent was removed. The crude product was dissolved in dichloromethane and washed with 1N HCl and water. The organic layer was dried, the solvent removed and the crude solid was purified by chromatography on silica gel (3:7, ethylacetate: hexane) to yield **2.2** as a colorless solid (23.3 g, 95%). ^1H NMR (CDCl_3): δ 7.37 (s, 2H), 4.69 (s, 4H), 2.55 (s, 2H). ^{13}C NMR (CDCl_3): δ 151.6, 123.5, 85.8, 77.1, 76.1, 57.5. IR: ν 616, 621, 627., 648, 662.50, 666, 678, 683, 689, 730, 736, 845, 851, 916, 921, 994, 1004, 1009, 1062, 1180, 1193, 1200, 1219, 1233, 1238, 1244, 1248, 1254, 1272, 1276, 1308, 1311, 1318, 1326.93, 1333, 1343, 1377, 1429, 1435, 1442, 1445, 1469, 2118, 2926, 2968, 3270, 3286, 3289.85. ES^+ MS (EI) calcd. for $[\text{C}_{12} \text{H}_8\text{I}_2\text{O}_2]$, 437.086, found 437.9; C, 32.91; H, 1.84; MP: 155 $^\circ\text{C}$.



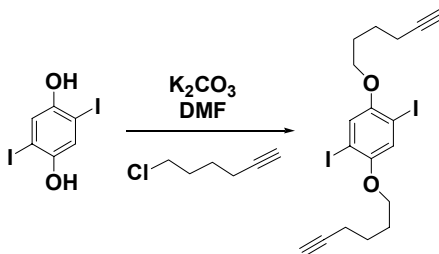
Synthesis of 2.3a: The diiodo-dialkyne compound **2.2** (6.47g, 14.8 mmol) *o*-xylene (20 mL) and tetraphenylcyclopentadienone (17.0 g, 44.2 mmol) were heated at reflux for 24 h. The solvent was removed under reduced pressure and the mixture purified by chromatography on silica gel (1:9, ethylacetate:hexane) to yield **2.3a** as a colorless solid (14.6 g, 86%). ^1H NMR (CDCl_3): δ 7.8 (s, 2H), 7.1 (m, 24H), 6.7 (m, 16H), 4.8 (s, 4H). ^{13}C NMR (CDCl_3): δ 152.8, 141.3, 140.5, 139.7, 139.6, 139.4, 138.5, 132.9, 131.1, 130.9, 129.982, 129.6, 129.2, 127.1, 127.0, 126.3, 126.2, 126.1, 125.7, 125.4, 125.1, 86.7, 70.8. IR: ν 744, 756, 831, 852, 893, 1029, 1062, 1200, 1214, 1349, 1381, 1439, 1462, 1549, 2902.19, 3023, 3044, 3056. MS (EI) calcd. [$\text{C}_{68}\text{H}_{48}\text{I}_2\text{O}_2$], 1150.17; found 1150.4; MP: 298 °C.



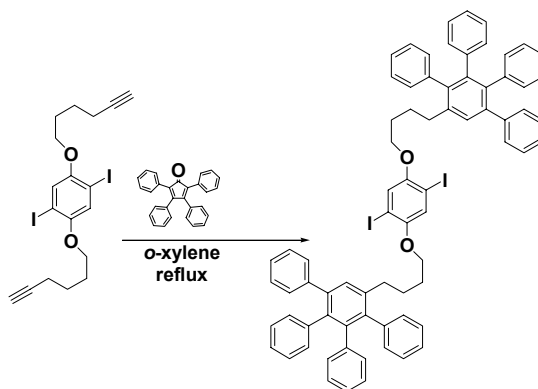
Synthesis of 2.3b: Diiodo monomer **2.3a** (2.36 g, 2.05 mmol) and 1-ethynyl-2-methylbenzene (0.500 g, 4.30 mmol) were dissolved in dichloromethane (8 mL) and piperidine (8 mL) in an oven dried Schlenk flask. The flask was flushed with nitrogen and frozen and evacuated three times after which $(\text{Ph}_3\text{P})_2\text{PdCl}_2$ (71 mg, 0.102 mmol), and CuI (20 mg, 0.105 mmol) were added. The mixture was allowed to stir at room temperature for 48 h. The solvent was removed and the mixture dissolved in dichloromethane, washed with 1N HCl, 1N NH_4OH , and water. The organic layer was dried over MgSO_4 and the solvent removed. The resulting crude product was crystallized from a 1:1 mixture of dichloromethane and methanol to yield pure **2.3b** (2.04 g, 88%). ^1H NMR (CDCl_3): δ 7.89 (s, 2H), 7.12 (m, 24H), 6.90 (m, 16H), 4.93 (s, 4H), 2.33 (s, 6H). ^{13}C NMR (TCE): δ 153.6, 141.6, 140.9, 140.3, 140.0, 139.9, 138.9, 133.9, 131.987, 131.8, 131.5, 131.2, 130.3, 129.9, 129.4, 128.3, 128.2, 127.3, 126.7, 126.4, 126.0, 125.4, 125.2, 123.4, 123.2, 118.5, 115.1, 115.0, 94.2, 90.0, 70.1, 20.4. IR: ν 698, 757, 894, 975, 1195, 1217, 1272, 1371, 1504, 1598, 1801, 1947, 2206, 2318, 2335, 2858, 2920, 3022.25, 3055. MS (FAB) Calculated for, $[\text{C}_{86}\text{H}_{62}\text{O}_2]$, 1126.47; found 1126.3; MP: 235°C.



Synthesis of Polymer 2.9: Monomer **2.3a** (0.280 g, 0.200 mmol 0.244 mmol) and 2,5-didodecyl-1,4-diehtynylbenzene (0.119 g, 0.200 mmol 0.257 mmol) were dissolved in dichloromethane (0.5 mL) and piperidine (0.5 mL) in an oven dried Schlenk flask. The flask was flushed with nitrogen and frozen and evacuated three times after which $(\text{Ph}_3\text{P})_2\text{PdCl}_2$ (1.4 mg, 2 mmol), and CuI (0.4 mg, 2 mmol) were added. The mixture was allowed to stir at room temperature for 48 h. The solvent was removed and the mixture dissolved in dichloromethane, washed with 1N HCl, 1N NH_4OH , and water. The organic layer was dried over MgSO_4 and the solvent removed. The resulting polymer was dissolved in dichloromethane and precipitated out of methanol three times to yield **2.9** (0.284 g, 86%). ^1H NMR (CDCl_3): δ 7.86 (m 2H), 7.09 (m, 24H), 6.75 (m, 16H), 4.83 (m, 4H), 1.54 (m, 8H), 1.14 (m, 28H), 0.82 (m, 6H). ^{13}C NMR (TCE): δ 152.9, 141.520, 140.8, 139.8, 138.8, 133.7, 132.0, 131.3, 130.2, 129.7, 129.2, 127.2, 126.6, 126.3, 125.9, 125.3, 125.1, 118.6, 115.0, 94.0, 90.9, 71.1, 34.1, 33.8, 31.6, 30.2, 29.0, 26.6, 22.9, 22.4, 13.8. IR: ν 693, 698, 701, 742, 756, 766, 890, 999, 1012, 1025, 1027, 1054, 1069, 1195, 1198, 1340, 1374, 1429, 1439, 1447, 1451, 1469, 1496, 1599, 2848, 2902, 2912, 2918, 2952. GPC (polystyrene standards) $M_n=29350$, $\text{PDI}=2.462$. ES^+ calcd. for $[\text{C}_{102}\text{H}_{100}\text{O}_2]$; C, 90.22; H, 7.42; found; C, 80.53; H, 6.15.

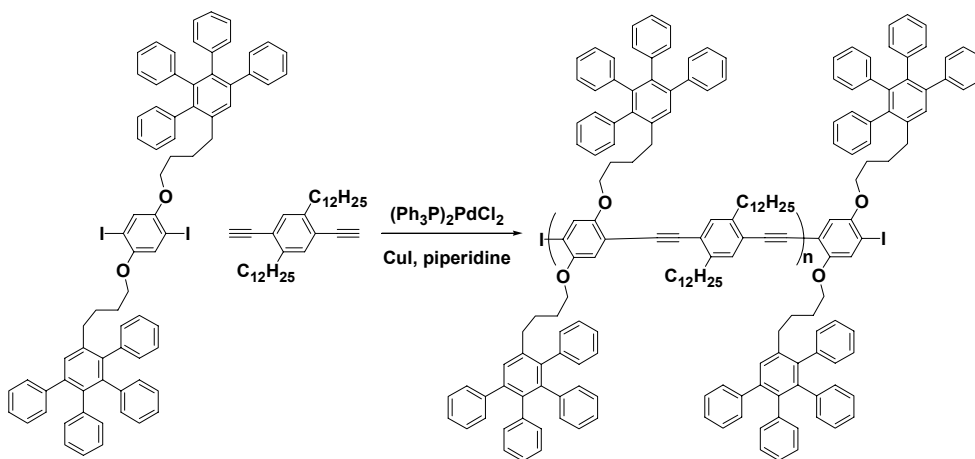


Synthesis of 2.4: 1,4-Hydroxy-2,5-diiodo benzene (18.0 g, 49.7 mmol), potassium carbonate (41.8 g, 0.302 mol), and 6-chlorohexyne (24.2 g, 0.208 mol) were dissolved in dimethylformamide (200 mL). The mixture was heated to reflux for 48h and allowed to cool to room temperature. The mixture was diluted with dichloromethane and washed with 1N HCl (2 x 150 mL). The solvent was removed under vacuum and the crude solid was purified by chromatography on silica gel (1:1, dichloromethane:hexane) to yield **2.4** as a colorless crystalline solid (11.2 g, 43%). ^1H NMR (CDCl_3): δ 7.15 (s, 2H), 3.92 (t, 4H), 2.25 (m, 4H), 1.89 (m, 6H), 1.72 (m, 4H). ^{13}C NMR (CDCl_3): δ 152.50, 122.50, 86.16, 83.98, 69.50, 68.72, 28.10, 25.04, 18.15. IR: ν 731, 999, 1001, 1032, 1207, 1349, 1398, 2110, 2800, 3089, 3263. MS (EI) calcd. [$\text{C}_{18}\text{H}_{20}\text{I}_2\text{O}_2$], 521.96; found 522.1; MP: 101 °C.



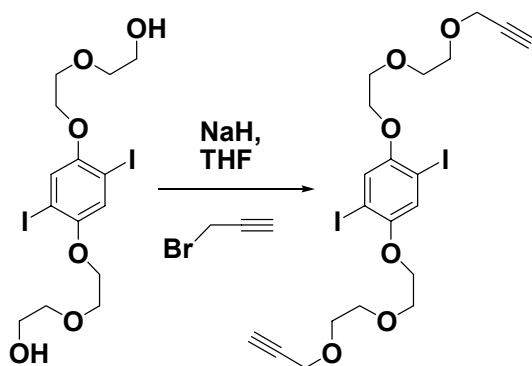
Synthesis of 2.5: Diyne **2.4** (0.826 g, 1.58 mmol) was dissolved in o-xylene (5 mL) and tetraphenylcyclopentadienone (5.00 g, 13.0 mmol) was added. The mixture was heated to reflux for 24 h, cooled to room temperature and the solvent was removed. The crude

solid was purified by chromatography on silica gel (2:8, ethyl acetate:hexane) to yield **2.5** (1.45 g, 74 %) as a colorless oil that solidified under high vacuum. ^1H NMR (CDCl_3): δ 7.43 (s, 2H), 7.02 (m, 24H), 6.72 (m, 16H), 3.71 (t, 4H), 2.57 (m, 6H), 1.73 (m, 4H). ^{13}C NMR (CDCl_3): δ 152.4, 141.8, 141.3, 140.4, 140.2, 139.9, 139.8, 139.2, 137.5, 131.431, 131.0, 130.2, 129.8, 129.8, 127.3, 127.2, 126.6, 126.3, 125.9, 125.2, 125.0, 122.2, 86.001, 69.6, 33.2, 28.8, 27.7. IR: ν 761, 1027, 1057, 1210, 1455, 1491, 1609, 1878, 1945, 2864, 2935, 3045. MS (EI) calcd. $[\text{C}_{74}\text{H}_{60}\text{I}_2\text{O}_2]$, 1234.27; found 1234.7; MP: 86 °C.



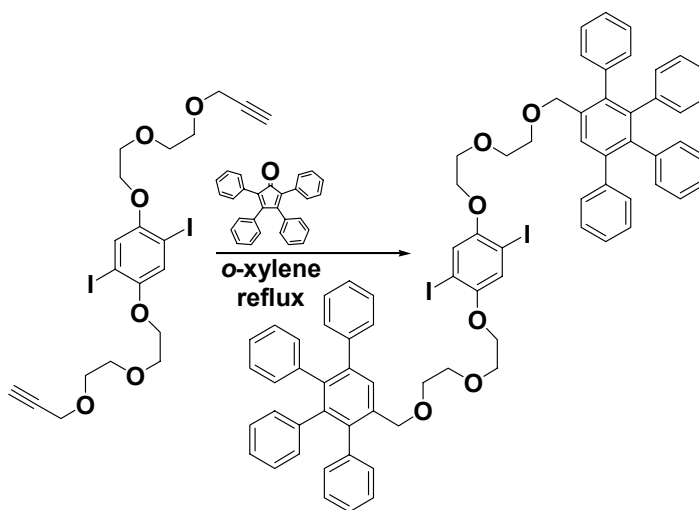
Synthesis of Polymer 2.10: Diiodo compound **2.5** (0.101 g, 81.8 μmol) and 2,5-didodecyl-1,4-diehtynylbenzene (0.0380 g, 82.1 μmol) were dissolved in tetrahydrofuran (0.2 mL) and piperidine (0.2 mL) in an oven dried Schlenk flask. The flask was flushed with nitrogen and frozen and evacuated three times after which $(\text{Ph}_3\text{P})_2\text{PdCl}_2$ (6.3 mg, 9.0 μmol), and CuI (1.7 mg, 8.9 μmol) was added. The mixture was allowed to stir at room temperature for 48 h. The solvent was removed the mixture dissolved in dichloromethane and washed with 1N HCl, 1N NH_4OH , and water. The organic layer was dried and the solvent removed. The resulting polymer **2.10** was dissolved in dichloromethane and precipitated out of methanol three times and hexane three times to yield **2.10** (74 mg, 63%). ^1H NMR (CDCl_3): δ 7.43 (m, 2H), 7.11 (m, 24H), 6.78 (m,

16H), 3.82 (m, 4H), 2.76 (m, 4H), 2.59 (m, 4H), 1.75 (m, 4H), 1.54, (m, 8H), 1.19 (m, 28H), 0.84 (m, 6H). ^{13}C NMR (TCE): δ 153.7, 143.6, 142.2, 141.6, 140.5, 140.3, 139.16, 137.8, 133.2, 132.2, 131.6, 131.3, 129.5, 127.3, 127.2, 126.6, 126.3, 125.9, 125.2, 124.95, 123.7, 123.0, 120.3, 117.6, 114.9, 94.0, 90.8, 69.7, 44.7, 33.9, 33.4, 31.8, 30.4, 29.5, 29.2, 27.51, 22.5, 13.9. IR: ν 667, 694, 697, 794, 799, 1002, 1015, 1021, 1027, 1045, 1054, 1057, 1071, 1078, 1082, 1095, 1111, 1219, 1261, 2357, 2942, 3432. GPC (polystyrene standards), $M_n=1.3 \times 10^7$, PDI = 4.3. ES^+ calcd. for $[\text{C}_{108}\text{H}_{112}\text{O}_2]$; C, 89.95; H, 7.83; found; C, 88.27; H, 12.99.



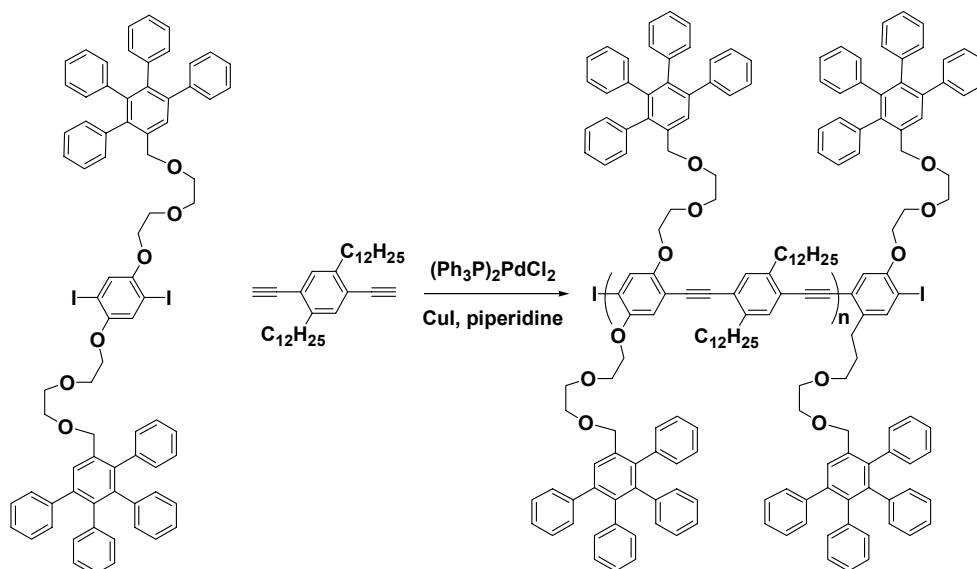
Synthesis of 2.7: Diiodo compound **2.6** (4.40 g, 8.18 mmol) was dissolved in dry tetrahydrofuran (25 mL) and under nitrogen purge NaH (0.665 g, 27.7 mmol) (80% in mineral oil) was added. Propargyl bromide (1.19 g, 10.0 mmol) was added and the mixture was allowed to stir at room temperature for 24 h. The mixture was slowly poured onto water and the precipitated solid was taken up in dichloromethane. The organic solution was washed with 0.5 N HCl (150 mL) and then with water. The organic layer was separated and dried. The solvent was removed and the crude solid purified by chromatography over silica gel (4:6, ethyl acetate:hexane) to yield **2.7** as a colorless solid (3.62 g, 72%). ^1H NMR (CDCl_3): δ 7.21 (s, 2H), 4.21 (m, 4H), 4.07 (t, 4H), 3.85 (t, 4H),

3.77 (m, 4H), 3.69 (m, 4H), 2.40 (t, 2H). ^{13}C NMR (CDCl_3): δ 152.9, 123.3, 86.3, 79.5, 74.5, 70.8, 70.2, 69.5, 69.1, 58.3. IR: ν 652, 656, 661, 666, 669, 678, 684, 694, 697, 700, 721, 725, 730, 799, 833, 841, 859, 877, 887, 918, 1000, 1015, 1025, 1033, 1051, 1066.08, 1086, 1087, 1101, 1121, 1136, 1219, 1232, 1243, 1265, 1286, 1330, 1353, 1355, 1427.71, 1435, 1437, 1445, 1450, 1455, 1463, 1466, 1486, 1492, 2830, 2837, 2849, 2861, 2879, 2884, 2895, 2920, 2929, 2935, 2944, 3272. ES^+ MS (EI) calcd. $[\text{C}_{20}\text{H}_{24}\text{I}_2\text{O}_6]$, 613.97; C, 39.11; H, 3.94; found 614.1; found C, 39.11; H, 4.02; MP: 82 $^\circ\text{C}$.



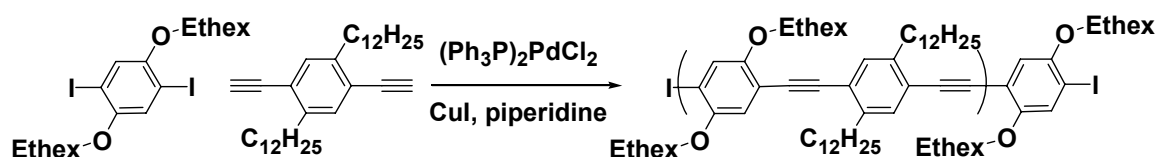
Synthesis of 2.8: Diiododiyne **2.7** (0.361 g, 0.588 mmol) was dissolved in *o*-xylene (10 mL) and tetraphenylcyclopentadienone (8.00 g, 20.8 mmol) was added. The mixture was heated to reflux for 48 h, cooled to room temperature and the solvent was removed. The crude solid was purified by chromatography over silica gel (4:6, ethyl acetate:hexane) to yield **2.8** (0.140 g, 18 %) as an oil which solidified under high vacuum. ^1H NMR (CDCl_3): δ 7.6 (s, 2H), 7.0 (m, 24H), 6.7 (m, 16H), 4.3 (s, 4H), 4.0 (t, 4H), 3.8 (t, 4H), 3.7 (m, 4H), 3.5 (m, 4H). ^{13}C NMR (CDCl_3): δ 153.0, 141.8, 141.4, 140.0, 139.9, 139.3, 139.1, 135.4, 131.4, 131.2, 130.2, 129.9, 129.4, 127.5, 127.3, 126.8, 126.5, 126.2, 126.1, 125.5, 125.2, 123.3, 86.4, 77.3, 77.2, 77.0, 76.6, 71.4, 76.6, 71.4, 71.0, 70.2, 70.0, 69.5.

IR: ν 696, 701, 744, 763, 800, 1009, 1027, 1059, 1156, 1197, 1345, 1432, 1441, 1447, 1456, 1480, 1495, 1575, 1598, 1709, 2846, 2926, 3019, 3051. ES⁺ MS (EI) calcd. [C₇₆H₆₄I₂O₆], 1326.28; C, 68.78; H, 4.86; found fragmentation: 552.2, 408, 262.9; found C, 68.72; H, 5.06; MP: 126 °C.



Synthesis of Polymer 2.11: Diiodo compound **2.8** (0.134 g, 101 μ mol) and 2,5-didodecyl-1,4-diehtynylbenzene (47.0 mg, 0.101 mmol) were dissolved in tetrahydrofuran (0.1 mL) and piperidine (0.1 mL) in an oven dried Schlenk flask. The flask was flushed with nitrogen and frozen and evacuated three times after which (Ph₃P)₂PdCl₂ (0.7 mg, 1 μ mol), and CuI (0.2 mg, 1 μ mol) were added. The mixture was allowed to stir at room temperature for 48 h. The solvent was removed and the mixture dissolved in dichloromethane and washed with 1N HCl, 1N NH₄OH, and water. The organic layer was dried over MgSO₄ and the solvent was removed. The crude polymer was dissolved in dichloromethane and precipitated out of hexane and then acetone to yield **2.11** (93 mg, 60 %) as a dark yellow solid. ¹H NMR (CDCl₃): δ 7.64 (m, 2H), 7.04 (m, 24H), 6.72 (m, 16H), 4.33 (m, 4H), 3.37 (m, 16H), 2.44 (m, 4H), 1.63 (m, 4H), 1.52

(m, 8H), 1.19 (m, 28H), 0.82 (m, 6H). ^{13}C NMR (TCE): δ 153.8, 142.0, 141.6, 140.703, 140.2, 140.1, 140.1, 139.5, 139.3, 135.4, 132.3, 131.6, 131.3, 130.5, 130.0, 129.4, 127.4, 127.2, 126.7, 126.4, 126.2, 126.0, 125.4, 125.1, 94.8, 90.5, 71.5, 71.5, 70.9, 70.5, 70.058, 69.8, 69.7, 44.7, 34.0, 31., 30.5, 29.6, 29.4, 29.2, 22.6, 22.4, 22.2, 14.0. IR: ν 617, 667, 694, 697, 718, 751, 897, 1053, 1061, 1094, 1117, 1125, 1142, 1258, 1439, 1460, 2363.60, 2943, 3402, 3537. GPC (polystyrene standards) M_n =73780, PDI = 9.9. ES^+ calcd. for $[\text{C}_{110}\text{H}_{116}\text{O}_6]$; C, 86.12; H, 7.62; found; C, 76.21; H, 12.29.



Synthesis of polymer 2.12: 2,5-Bisethylhexyloxy-1,4-diiodobenzene (0.400 g, 0.682 mmol) and 1,4-diethynyl-2,5-didodecylbenzene (0.319 g, 0.689 mmol) was dissolved in tetrahydrofuran (1.5 mL) and piperidine (1.5 mL) in an oven dried Schlenk flask. The flask was flushed with nitrogen and frozen and evacuated three times after which $(\text{Ph}_3\text{P})_2\text{PdCl}_2$ (4.8 mg, 6.8 μmol), and CuI (1.3 mg, 6.8 μmol) were added. The mixture was allowed to stir at room temperature for 48 h. The solvent was removed and the mixture dissolved in dichloromethane and washed with 1N HCl , 1N NH_4OH , and water. The organic layer was dried over MgSO_4 and the solvent removed. The resulting polymer was dissolved in dichloromethane and precipitated out of hexane and then acetone to yield **2.12** (0.449 g, 83 %) as a dark yellow solid. ^1H NMR (CDCl_3): δ 7.36 (m, 2H), 6.97 (m, 2H), 3.88 (m, 4H), 3.17 (m, 4H), 1.90 (m, 4H), 1.50 (m, 2H), 1.22 (m, 52H), 0.84 (m, 18H). ^{13}C NMR (CDCl_3): δ 153.6, 141.9, 132.2, 122.8, 116.6, 114.1, 94.0, 90.7, 71.9, 39.5, 30.5, 29.6, 29.6, 29.5, 29.3, 29.1, 23.9, 23.0, 22.6, 14.0, 11.1. IR: ν

679, 717, 858, 883, 989, 1050, 1210, 1277, 1464, 1516, 2163, 2854, 2940, 3841. GPC (polystyrene standards) M_n = 56434, PDI = 4.461. ES⁺ calcd. for [C₅₆H₈₈O₂]; C, 84.79; H, 11.18; found; C, 80.48; H, 11.11.

Differential scanning calorimetry measurements. DSC measurements were taken on a Mettler Toledo DSC 822. The samples were weighed into a 40 μ L aluminum crucible and the lid was punctured. Each sample was heated from 25-250°C at a rate of 25°C/min under N₂.

X-ray powder diffraction measurements. The X-ray powder diffraction data were collected on a Rigaku powder X-ray diffractometer using a Bragg-Brentano geometry with CuK α radiation. The step-scan covered the angular range 5-50 degrees 2 θ in steps of 0.02 degrees.

2.5 References:

1. (a) Lupton, J. M.; Schouwink, P.; Keivanidis, P. E.; Grimsdale, A. C.; Müllen, K. *Adv. Funct. Mater.* **2003**, *13*, 154-158. (b) Pogantsch, A.; Wenzl, F. P.; List, E. J. W.; Leising, G.; Grimsdale, A. C.; Müllen, K. *Adv. Mater.* **2002**, *14*, 1061-1064. (c)
2. (a) Schlüter, A. D.; Rabe, J. P. *Angew. Chem.* **2000**, *39*, 864-883. (b) Karakaya, B.; Claussen, W.; Gessler, K.; Saenger, W.; Schlüter A. D. *J. Am. Chem. Soc.* **1997**, *119*, 3296-3301. (c) Stocker, W.; Karakaya, B.; Schürmann, B. L.; Rabe, J. P.; Schlüter A. D. *J. Am. Chem. Soc.* **1998**, *120*, 7691-7695.
3. (a) Masuo, S.; Yoshikawa, H.; Asahi, T.; Masuhara, H.; Sato, T.; Jiang, D. L.; Aida, T. *J. Phys. Chem. B.* **2003**, *107*, 2471-2479. (b) Masuo, S.; Yoshikawa, H.; Asahi, T.; Masuhara, H.; Sato, T.; Jiang, D. L.; Aida, T. *J. Phys. Chem. B.* **2002**, *106*,

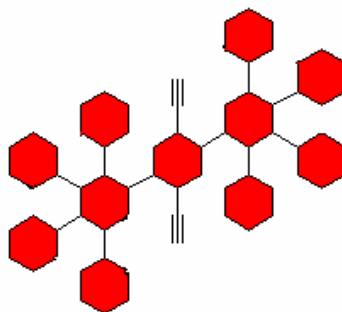
- 905-909. (c) Masuo, S.; Yoshikawa, H.; Asahi, T.; Masuhara, H.; Sato, T.; Jiang, D. L.; Aida, T. *J. Phys. Chem. B* **2002**, *105*, 2885-2889. (d) Sato, T.; Jiang, D. L.; Aida, T. *J. Am. Chem. Soc.* **1999**, *121*, 10658-10659.
4. Setayesh, S.; Grimsdale, A. C.; Weil, T.; Enkelmann, V.; Müllen, K.; Meghdadi, List, E. J. W.; Leising, G. *J. Am. Chem. Soc.* **2001**, *123*, 946-953.
 5. Other dendronized conjugated polymers: (a) Bao, Z.; Amundson, K. R.; Lovinger, A. *Macromolecules* **1998**, *31*, 8647-8649. (b) Malefant, P. R. L.; Frechet, J. M. J. *Macromolecules* **2000**, *33*, 3634-3640. (c) Schenning, A. P. H. J.; Martin, R. E.; Ito, M.; Diederich, F.; Boudon, C.; Gisselbrecht, J. P.; Gross, M. *Chem. Commun.* **1998**, 1013-1014.
 6. (a) Bunz, U. H. F. *Chem. Rev.* **2000**, *100*, 1605-1644. (b) Halkyard, C. E.; Rampey, M. E.; Kloppenburg, L.; Studer-Martinez, S. L.; Bunz, U. H. F. *Macromolecules* **1998**, *31*, 8655-8659. (c) Miteva, T.; Palmer, L.; Kloppenburg, L.; Neher, D.; Bunz, U. H. F. *Macromolecules* **2000**, *33*, 652-654.
 7. Kim, J.; Swager, T. M. *Nature* **2001**, *411*, 1030-1034.
 8. (a) Schmitz, C.; Posch, P.; Thelakkat, M.; Schmidt, H. W.; Montali, A.; Feldman, K.; Smith, P.; Weder, C. *Adv. Funct. Mater.* **2001**, *11*, 41-46. (b) Montali, A.; Smith, P.; Weder, C. *Synth. Met.* **1998**, *97*, 123-126. (c) Pschirer, N. G.; Miteva, T.; Evans, U.; Roberts, R. S.; Marshall, A. R.; Neher, D.; Myrick, M. L.; Bunz, U. H. F. *Chem. Mater.* **2001**, *13*, 2691-2696.
 9. (a) Kuroda, K.; Swager, T. M. *Makromol. Symposia* **2003**, *201*, 127-134. (b) Yang, J. S.; Swager, T. M. *J. Am. Chem. Soc.* **1998**, *120*, 11864-11873. (c) Zhou, Q.; Swager, T. M. *J. Am. Chem. Soc.* **1995**, *117*, 12593-12602.

10. (a) Berresheim, A. J.; Müller, M.; Müllen, K. *Chem. Rev.* **1999**, *99*, 1747-1785.
 (b) Watson, M. D.; Fechtenkötter, A.; Müllen, K. *Chem. Rev.* **2001**, *101*, 1267-1300.
 (c) Wiesler, U. M.; Weil, T.; Müllen, K. *Top. Curr. Chem.* **2001**, *212*, 1-40.
11. (a) Hawker, C. J.; Frechet, J. M. J. *J. Am. Chem. Soc.* **1990**, *112*, 7638-7647. (b) Furuta, P.; Brooks, J.; Thompson, M. E.; Frechet J. M. J. *J. Am. Chem. Soc.* **2003**, *125*, 13165-13172. (c) Grayson, S. K.; Frechet, J. M. J. *Chem. Rev.* **2001**, *101*, 3819-3867.
12. (a) Bunz, U. H. F.; Enkelmann, V.; Kloppenburg, L.; Jones, D.; Shimizu, K. D.; Claridge, J. B.; zur Loye, H. C.; Lieser, G. *Chem. Mater.* **1999**, *11*, 1416-1424. (b) Turner-Jones, A. *J. Polym. Sci.* **1962**, *62*, 53.
13. (a) Samori, P.; Francke, V.; Enkelmann, V.; Müllen, K.; Rabe, J. P. *Chem. Mater.* **2003**, *15*, 1032-1039. (b) Li, H.; Powell, D. R.; Firman, T. K.; West, R. *Macromolecules* **1998**, *31*, 1093-1098. (c) Smith, C. E.; Smith, P. S.; Thomas, R. L.; Robins, E. G.; Collings, J. C.; Dai, C. Y.; Scott, A. J.; Borwick, S.; Batsanov, A. S.; Watt, S. W.; Clark, S. J.; Viney, C.; Howard, J. A. K.; Clegg, W.; Marder, T. B. *J. Mater. Chem.* **2004**, 413-420. (d) Dai, C. Y.; Nguyen, P.; Marder, T. B.; Scott, A. J.; Clegg, W.; Viney, C. *Chem. Commun.* **1999**, 2493-2494.
14. (a) Brizius, G.; Billingsley, K.; Smith, M. D.; Bunz, U. H. F. *Org. Lett.* **2003**, *5*, 3951-3984. (b) The rotational barrier of tolane is calculated to 0.86 kcal/mol utilizing the B3PW91/6-311G** basis set: Seminario, J. M.; Zacarias, A. G.; Tour, J. M. *J. Am. Chem. Soc.* **1998**, *120*, 3970-3974.
15. Sluch, M. I.; Godt, A.; Bunz, U. H. F.; Berg, M. A. *J. Am. Chem. Soc.* **2001**, *123*, 6447-6448.

16. Levitus, M.; Schmieder, K.; Ricks, H.; Shimizu, K. D.; Bunz, U. H. F.; Garcia-Garibay, M. A. *J. Am. Chem. Soc.* **2001**, *123*, 4259-4265.
17. Beeby, A.; Findlay, K.; Low, P. J.; Marder, T. B. *J. Am. Chem. Soc.* **2002**, *124*, 8280-8284.
18. Electronic Materials: The Oligomer Approach; Müllen, K., Wegner, G., Eds.; Wiley-VCH: Weinheim, 1998; Chapters 6 and 7.
19. Kloppenburg, L.; Jones, D.; Bunz, U. H. F. *Macromolecules* **1999**, *32*, 4194-4203.
20. Bangcuyo, C. G.; Ellsworth, J. M.; Evans, Una; Myrick, M. L.; Bunz, U. H. F. *Macromolecules* **2003**, *36*, 546-548.
21. (a) Li, H.; Li, Y.; Zhai, J.; Cui, G.; Liu, H.; Xiao, S.; Liu, Y.; Lu, F.; Jiang, L.; Zhu, D. *Chemistry, Eur. J.* **2003**, *9*, 6031-6038. (b) see ref. 9c
22. Kishimoto, Y.; Itou, M.; Miyatake, T.; Ikariya, T.; Noyori, R. *Macromolecules* **1995**, *28*, 6662-6666.

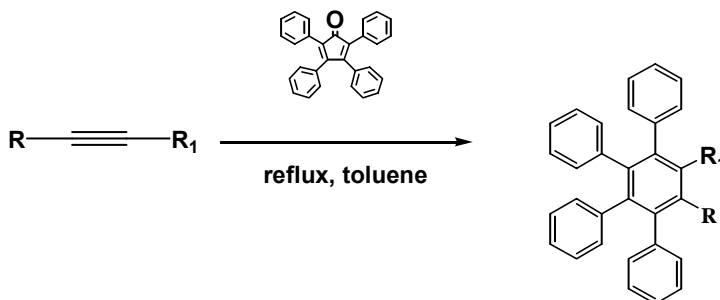
CHAPTER 3

CARBON RICH PRECURSOR MATERIALS FOR JACKETED POLY(P- PHENYLENEETHYNYLENE)S.



3.1. Introduction.

As discussed in the previous chapter, molecular wires are of increasing interest with respect to application in molecular electronics.¹ Typically these materials are composed of polymers, which do not aggregate. It is necessary in these materials for individual polymer chains to be separated from one another. This is done by employment of a spacer group, typically a large bulky group such as a dendron or dendrimer.² Müllen has produced polyfluorenes substituted with his own Müllen dendrons.³



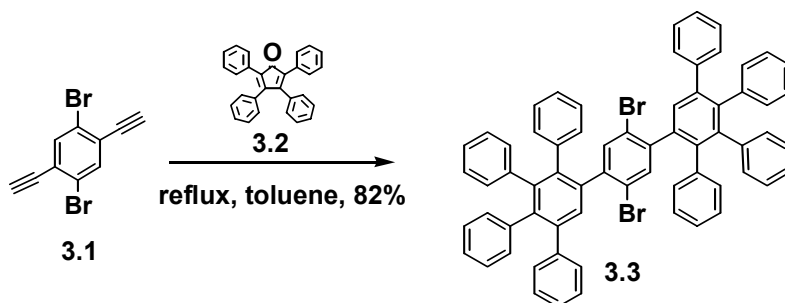
Scheme 3.1. Synthesis of Müllen dendrons.

Aida has produced these materials in the form of PPEs and more recently we have as well.^{4,5} While Aida has employed the use of Frechet dendrons, we have used Müllen dendrons as spacer groups. Compared to Frechet dendrons, Müllen dendrons are thermally and hydrolytically stable.

We were interested in producing materials bearing the spacer groups necessary to isolate polymer chains from one another; which also possessed thermal stability. While our previously produced polymers were shielded, they were not thermally stable according to DSC measurements. In PPEs which could function as molecular wires; thermal stability would be attractive for many reasons. Thermally stable polymers could potentially last longer in any device applications in which they are employed than the corresponding alkoxy PPEs, and depending on the method employed; they could be prepared more easily.

3.2. Results and Discussion.

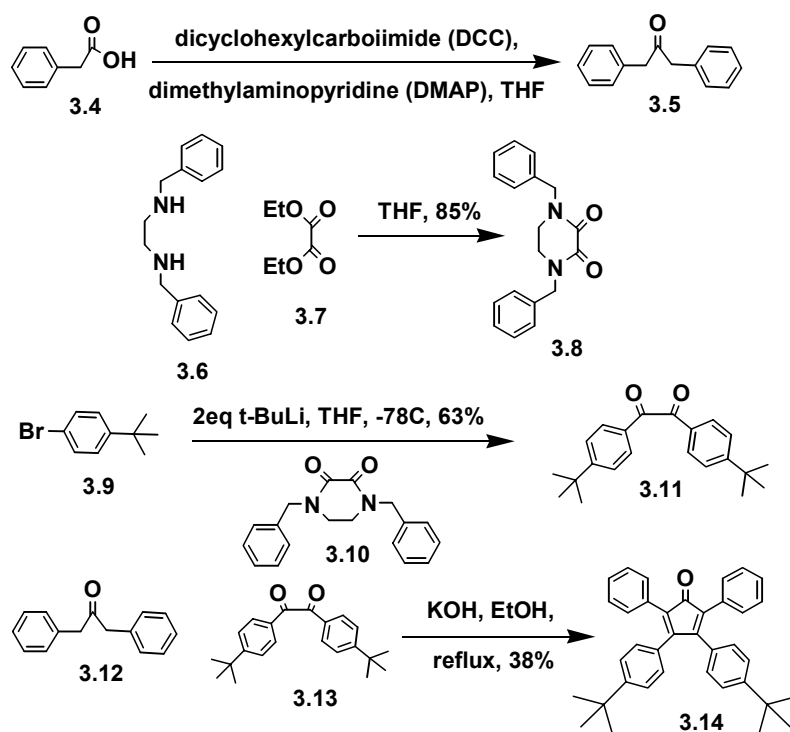
Müllen dendrons are known for their moderate to complete insolubility, but copolymerization with soluble monomers has afforded soluble polymers.^{5,6} Compound **3.1**⁷ was reacted with commercially available **3.2** (Scheme 2). Monomer **3.3** was moderately soluble. Under coupling conditions, **3.2** did not afford the corresponding silane substituted alkyne monomer. Small amounts of product and starting material were isolated as an inseparable mixture.



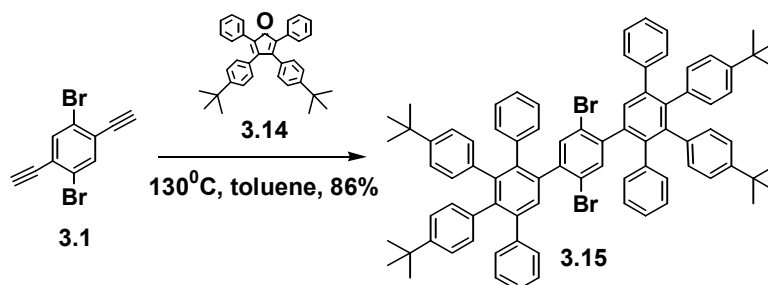
Scheme 3.2. Synthesis of dibromo monomer **3.3**.

This could be due to the limited solubility of **3.3**. These types of materials become more soluble when alkyl groups are attached to their benzene rings. The production of substituted tetraphenylcyclopentadienone is known in the literature.⁸ This synthesis requires the production of a *para*-diphenyl acetone and a di-substituted benzil. Known DCC condensation of phenylacetic acid afforded the desired *para*-diphenyl acetone **3.5**.⁹ The next portion of this synthesis requires the production of a di-substituted benzil. Friedel-Crafts acylation of the appropriately substituted benzene with oxalyl chloride results in low yields and large amounts of by-products consisting of *ortho* substituted benzils which are difficult to separate from the desired products.¹⁰

We adopted the Mueller-Westerhoff reaction to generate **3.11** (Scheme 3.5).¹¹ This reaction employs the use of 2,3-piperazinedione (**3.8**) as a keto source. Halogen-metal exchange with the appropriate substituted benzene and quenching with 2,3-piperazinedione furnishes **3.11**. Aldol condensation of **3.5** and **3.11** provided the corresponding tetraphenylcyclopentadienone (**3.14**) after thermal dehydration and column chromatography.



Scheme 3.3. Synthesis of substituted tetraphenylcyclopentadienones.



Scheme 3.4. Synthesis of **3.15**.

Reaction with bis-ethynyl-dibromobenzene (Figure 3.4) afforded monomer **3.15**. Single crystal X-ray analysis afforded structural data on single molecules of **3.15**.

The single-crystal structure of **3.15** is shown in Figure 3.1. Single molecules of **3.15** are twisted through the three central benzene rings. Of the three center benzene rings the outer two are almost coplanar; the center benzene ring is twisted and almost

perpendicular with respect to the outer two (Figure 3.1a). The four phenyl substituents are oriented perpendicularly around each of the outer phenyl rings. Rotation of the view by 90° reveals that the molecules are flat with the bromine substituents twisted into an almost perpendicular position (Figure 3.2b). Individual molecules of **3.15** are packed in an interdigitated layered fashion (Figure 3.1c, bottom left and Figure 3.1d, bottom right). The central dibromoarenes are separated from each other due to the tetraphenylbenzene units and do not show any intermolecular contacts with other dibromoarenes.

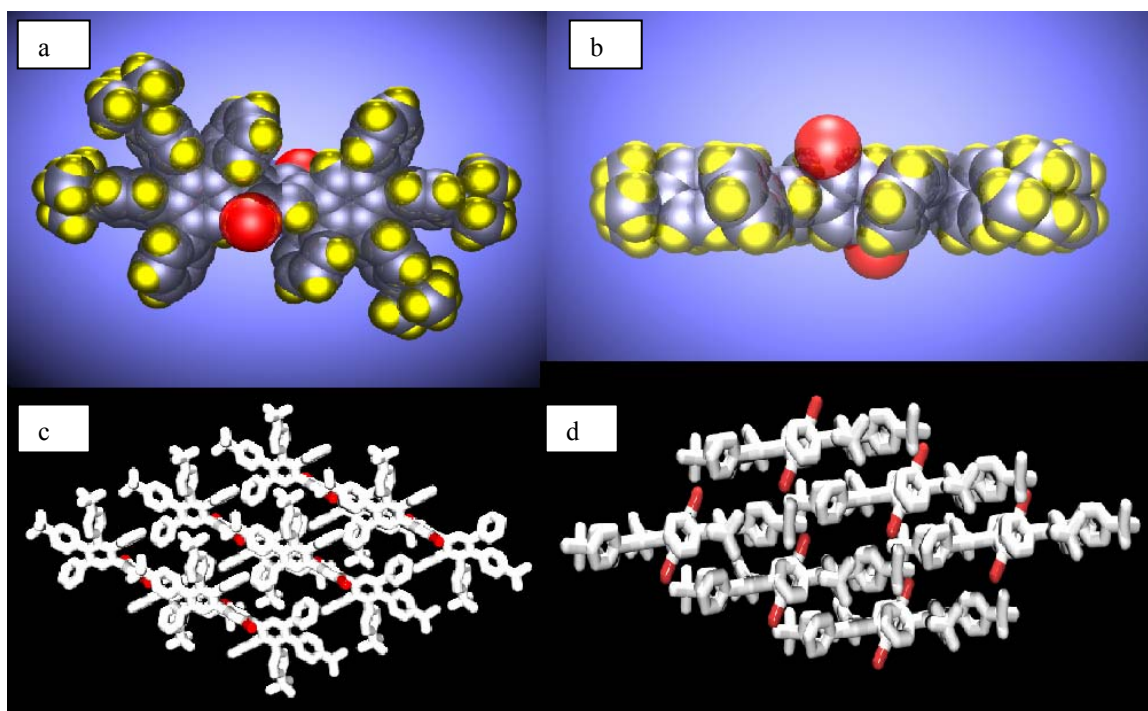


Figure 3.1. Single molecules of **3.15** are twisted through the three central benzene rings (Figure 3.1a, top left). Rotation of the view by 90° reveals that the molecules are flat (Figure 3.1b, top right). Molecules of **3.15** are packed in an interdigitated layered fashion (Figure 3.1c, bottom left and Figure 3.1d, bottom right).

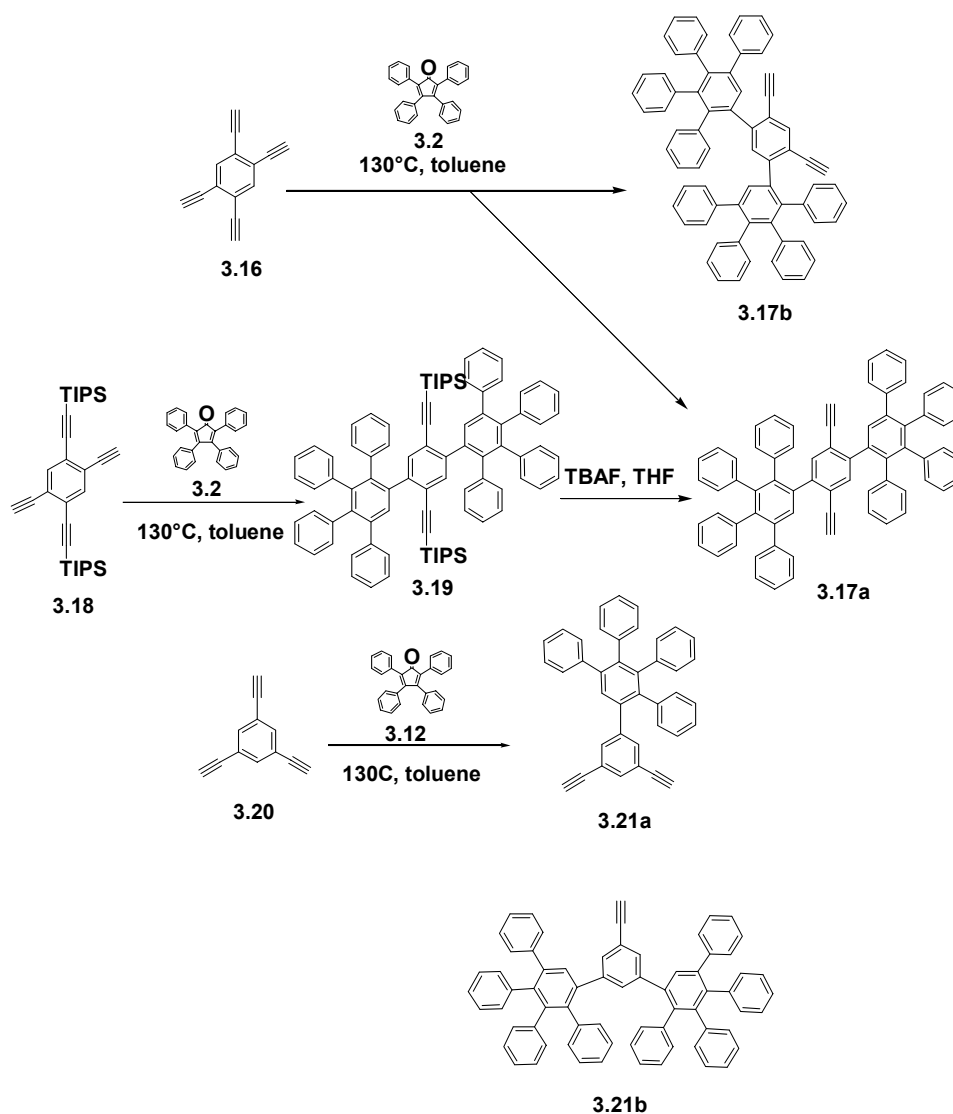
Monomer **3.15** offered no improved solubility when compared to **3.3**. Heck-Cassar-Sonogashira-Hagihara (HCSH) conditions provided only small amounts of the desired bis-alkyne derivative and **3.15** itself. This was most likely due to the sterically

congested location of the bromines and possibly the limited solubility of **3.15**. The product mixture smeared excessively when subjected to column chromatography.

It would be useful to have a method to generate a monomers which did not require coupling to the bromines as in **3.15** under sterically restricting conditions. Conceivably, this could be accomplished two ways. Compound **3.16** could be reacted with 2 eq of **3.2** (Scheme 3.5). Compound **3.17b** should not be isolated due to the steric restrictions of the tetraphenylbenzene unit.^{5a} Due to the low molecular weight of **3.16**, it should be easily sublimed to afford pure **3.17a**.

Due to the steric restrictions of tetraphenylbenzene units, it should be possible to isolate only compound **3.17a** in reasonable yield. If this does not provide **3.17a** in reasonable yield, the use of **3.18** could be employed to provide **3.19**. Subsequent deprotection should provide **3.17a**.

It would also be interesting to prepare *meta*-substituted jacketed PPEs as *meta* linkages are known to offer improved solubility.^{5b} The first of the previous two strategies offers a synthetically simple route to monomers for this purpose. Reacting **3.20** with 0.25 equivalents of tetraphenylcyclopentadienone should provide *meta*-dendronized monomers in abundance. By-product **3.21b** should not be isolated due to the steric requirements of the tetraphenylbenzene unit.



Scheme 3.5. Synthesis of tetraphenylbenzene substituted monomers.

Reacting **3.20** with 0.25 equivalents of **3.2** does indeed provide monomer **3.21a** in excellent yield (93 %) after sublimation of unreacted **3.20** and column chromatography. The presence of byproduct **3.21b** could not be confirmed by ^1H NMR or ^{13}C NMR spectra. Only **3.21a** can be seen in the ^1H NMR and ^{13}C NMR of the reaction mixture. ^1H NMR of a mixture of **3.21a** and **3.21b** should give rise to two signals between 2.5 and 3.5 ppm. Only one signal is observed (Figure 3.2, top left). The presence of a mixture of the two

regioisomers would also give four separate signals for the alkyne peaks in ^{13}C NMR analysis which is not observed (Figure 3.2, top right).

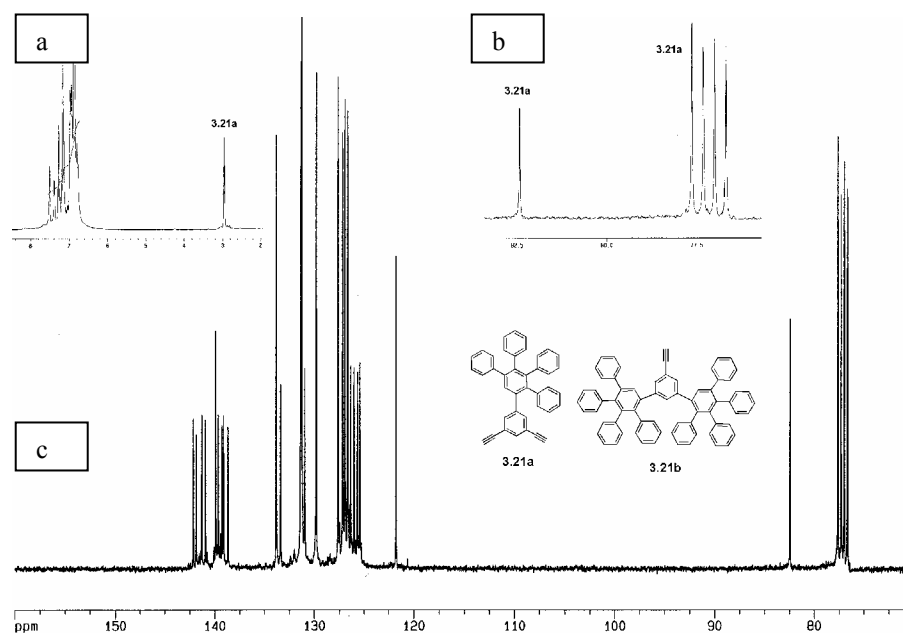


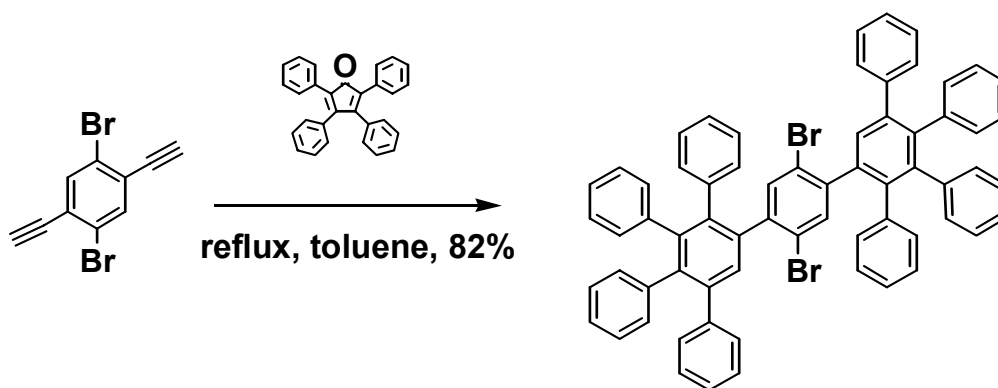
Figure 3.2. ^1H NMR and ^{13}C NMR of **3.20**. Top left, ^1H NMR (a and b); top right, ^{13}C NMR (c).

3.3. Conclusion

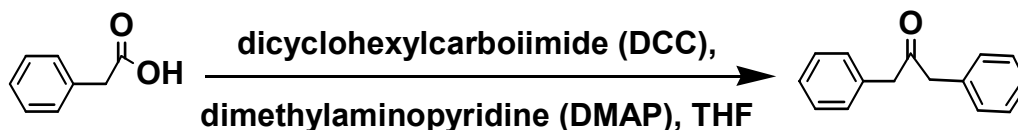
This work has introduced an important starting point for the synthesis of thermally stable dendronized poly(*paraphenyleneethynylene*)s PPEs. A simple synthesis for dendronized monomers has been realized. The corresponding polymers should be easily obtainable and well soluble provided the appropriate comonomers are used. These polymers should be effectively non-aggregating and hence shielded from planarization and electronic interaction. Carbon rich polymers may as well provide new opportunities for metal complexation followed by pyrolysis experiments and or microstructuring.

3.4. Experimental

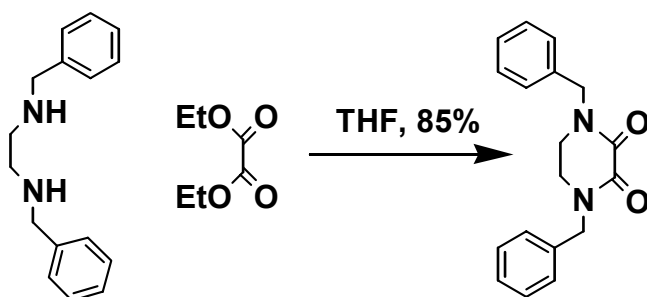
Instrumentation. The ^1H and ^{13}C NMR spectra were taken on a Varian 300 MHz or a Bruker 400 MHz spectrometer using broadband probe. The ^1H chemical shifts are referenced to the residual proton peaks of CDCl_3 at δ 7.24 (vs. TMS). The ^{13}C resonances are referenced to the central peak of CDCl_3 at δ 77.0 and $\text{CDCl}_2\text{CDCl}_2$ at δ 74.0 (vs. TMS). Compounds **3.5-3.14** were prepared in accordance to published procedures.



Synthesis of 3.3. In a flame dried 25 mL Schlenk flask **3.1** (1.5 g, 5.28 mmol) and **3.2** (6.09 g, 15.8 mmol) were dissolved in 10 mL of para-xylene. Under nitrogen, the reaction was heated to reflux for 48 h. The reaction was allowed to cool to room temperature and the solvent removed under vacuum. The crude solid was subjected to flash chromatography on silica gel (2:1 hexanes:dichloromethane) and repeated precipitation from ethanol to yield **3.3** as a colorless solid (4.32 g, 82%). ^1H NMR (CDCl_3) δ 7.24 (m, 18H), 6.92 (m, 26H). ^{13}C NMR (CDCl_3) δ 148.5, 142.7, 141.9, 137.2, 134.9, 131.3, 130.272, 128.2, 127.693, 126.340, 123.447, 118.7, 117.8. IR (KBr) cm^{-1} 2132, 1813, 1445, 1333, 1195, 1032, 812, 715, 630, 543. $T_m=240\text{-}242^\circ\text{C}$

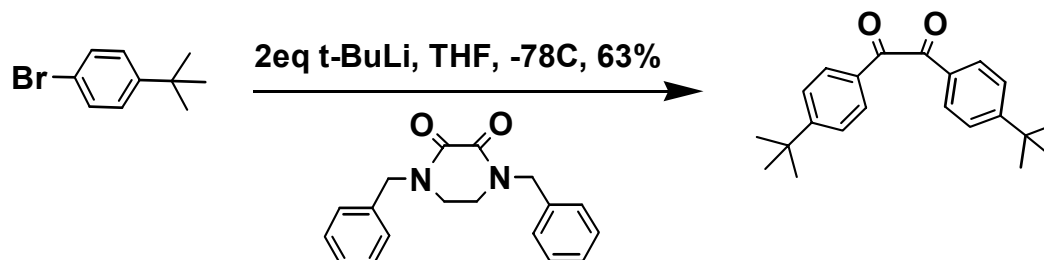


Synthesis of 3.5. In a 500 mL Schlenk flask, **3.4** (30.0 g, 115 mmol) was dissolved in 300 mL of anhydrous THF. Dicyclohexylcarbodiimide (DCC, 13.0 g, 63.0 mmol) and dimethylaminopyridine (DMAP, 3.65 g, 29.9 mmol) were added to the stirring solution under N₂. The reaction was refluxed for 1 h and gas was evolved. The solvent was evaporated and the paste was filtered through a silica plug with CH₂Cl₂ to give **3.5** (21.5 g, 46.5 mmol, 81%) as a light yellow powder. ¹H NMR (CDCl₃) δ 7.44 (m, 2H), 6.35 (d, 2H), 3.66 (s, 2H). ¹³C NMR (CDCl₃) δ 137.8, 133.2, 134.8, 131.4, 48.5. IR (KBr) cm⁻¹ 2923, 2854, 1715, 1485, 1408, 1339, 1315, 1192, 1100, 1054, 1008, 823, 808, 785, 762, 723, 669, 562, 485. T_m=85-89°C

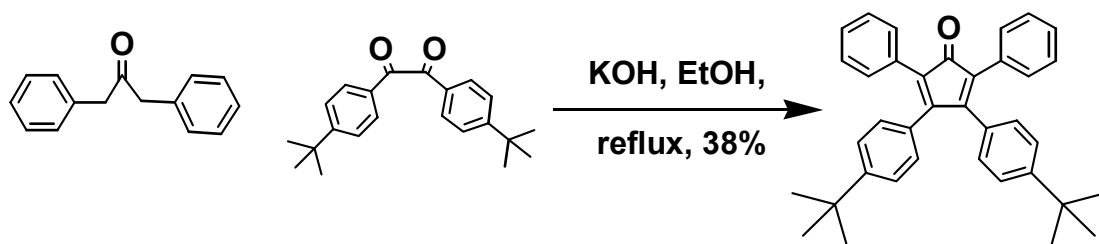


Synthesis of 3.8. In a 500 mL Schlenk flask, N,N-dibenzylethylenediamine (84.5 g, 352 mmol) and diethyl oxalate (51.4g, 352 mmol) were dissolved in 200 mL of anhydrous THF. The reaction was stirred at room temperature for 48 h upon which a white precipitate formed. The precipitate was collected by vacuum filtration and washed with cold EtOH to give **3.8** (87.8 g, 298 mmol, 85%) as a colorless powder. ¹H NMR (CDCl₃) δ 7.31-7.25 (m, 10H), 4.65 (s, 4H), 3.33 (s, 4H). ¹³C NMR (CDCl₃) δ 157.3,

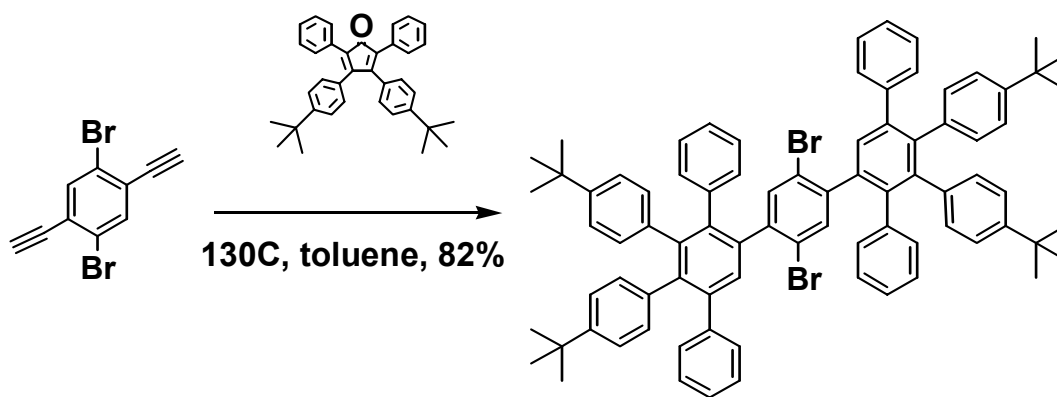
135.3, 128.7, 128.3, 83.7, 127.9, 50.4, 43.3. IR (KBr) cm^{-1} 2453, 1789, 1493, 1302, 1183, 1043, 803, 785, 762, 723, 483. $T_m=91-93^\circ\text{C}$



Synthesis of 3.11. In a 500 mL Schlenk flask, 4-bromododecylbenzene (20.0 g, 61.5 mmol) was dissolved in 300 mL of anhydrous THF and cooled to -78°C . *Tert*-BuLi (123 mmol) was added dropwise to the stirring solution. In a 1000 mL Schlenk flask, **3.9** (8.65 g, 29.4 mmol) was suspended in 200 mL of anhydrous THF and cooled to -78°C . The solution was transferred to the suspension of **3.10** via cannula. This solution was allowed to warm slowly to room temperature while stirring vigorously. After 1 h at room temperature, 500 mL of 3M HCl was poured into the solution and a yellow precipitate formed. The precipitate was collected by vacuum filtration and then filtered through a silica plug with two volumes of hexanes. The filtrate was discarded, and the silica plug was washed with two volumes of CH_2Cl_2 to collect the yellow band. The yellow filtrate was evaporated to dryness to provide **3.11** (10.2 g, 18.7 mmol, 63%) as yellow needles. ^1H NMR (CDCl_3) δ 7.89 (d, 4H), 7.53 (m, 4H), 1.37 (s, 9H). ^{13}C NMR (CDCl_3) δ 194.4, 159.9, 130.8, 130.0, 129.0, 36.2, 31.6. IR (KBr) cm^{-1} 1793, 1535, 1503, 1392, 1316, 1180, 1063, 833, 763, 656, 434. $T_m=102-106^\circ\text{C}$

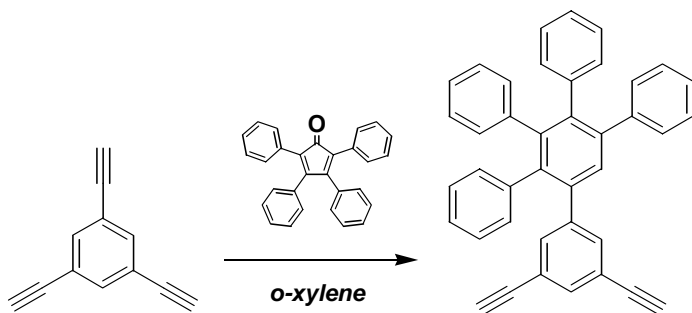


Synthesis of 3.14. **3.12** (2.30 g, 4.20 mmol) and **3.13** (1.98 g, 4.25 mmol) were dissolved in 50 mL of refluxing EtOH. NaOH (2 eq) was added and the mixture was monitored by column chromatography. After 30 min the reaction was cooled. The solvent was evaporated and the dark residue was chromatographed on silica gel with 1:4 CH₂Cl₂:Hexanes. The purple fraction was isolated and the solvent was evaporated to give **3.14** (2.13 g, 2.17 mmol, 52%) as a purple solid. ¹H NMR (CDCl₃) δ 7.23 (m, 12H), 6.88 (d, 4H), 1.23 (s, 18H). ¹³C NMR (CDCl₃) δ 154.9, 151.8, 131.3, 130.3, 130.3, 129.3, 128.1, 127.4, 125.0, 124.8, 77.6, 77.2, 76.8, 34.9, 31.4. IR (KBr) cm⁻¹ 2836, 1702, 1455, 1465, 1343, 1184, 1123, 1045, 833, 785. T_m=84-88°C



Synthesis of 3.15. In a flame dried 25 mL Schlenk flask **3.1** (0.46 g, 1.62 mmol) and **3.14** (2.00 g, 4.03 mmol) were dissolved in 10 mL of *para*-xylene. Under nitrogen, the reaction was heated to reflux for 48 h. The reaction was allowed to cool to room temperature and the solvent removed under vacuum. The crude solid was subjected to

flash chromatography on silica gel (2:1 hexanes:dichloromethane) and repeated precipitation from ethanol to yield **3.15** as a colorless solid (1.70 g, 86 %). ^1H NMR (CDCl_3) δ 7.25 (m, 18H), 6.89 (m, 26H), 1.13 (d, 36H). ^{13}C NMR (CDCl_3) δ 148.4, 137.2, 131.2, 130.2, 127.6, 126.3, 123.4, 34.3, 31.4. IR (KBr) cm^{-1} 2203, 1703, 1455, 1403, 1301, 1182, 1129, 1034, 1025, 772, 762, 723. $T_m=235\text{-}240^\circ\text{C}$.



Synthesis of 3.21a. In a flame dried 25 mL Schlenk flask **3.20** (1.00 g, 6.66 mmol) and **3.2** (0.512 g, 1.33 mmol) were dissolved in 4 mL of ortho-xylene. Under nitrogen, the reaction was heated to reflux for 48 h. The reaction was allowed to cool to room temperature and the solvent removed under vacuum. **3.20** was removed by sublimation and the crude solid was subjected to flash chromatography on silica gel (1:1 hexanes:dichloromethane) to yield **3.21a** as a colorless solid (3.23 g, 96 %). ^1H NMR (CDCl_3) 7.50-6.78 (m, 28H), 2.95 (d, 2H). ^{13}C NMR (CDCl_3) 142.1, 141.8, 141.3, 140.9, 139.9, 139.6, 139.2, 139.1, 138.6, 133.8, 133.3, 131.2, 131.2, 130.9, 129.8, 127.6, 127.1, 126.9, 126.6, 126.3, 126.0, 125.6, 125.4, 121.7, 82.4, 77.7. IR (KBr) cm^{-1} 3288, 3278, 3078, 2960, 2333, 2248, 2154, 2108, 1946, 1878, 1801, 1718, 1598, 1577, 1490, 1440, 1379, 1247, 1072, 1024, 883, 757, 698.

3.5. References

1. Masuo, S.; Yoshikawa, H.; Asahi, T.; Masuhara, H.; Sato, T.; Jiang, D.; and Aida, T. *J. Phys. Chem. B.* **2003**, 107, 2471-2479.
2. Jiang, D.; Choi, C.; Honda, K.; Li, W.; Yuzawa, T.; and Aida, T. *J. Am. Chem. Soc.* **2004**, 126, 12084-12089.
3. Setayesh, S.; Grimsdale, A. C.; Weil, T.; Enkelmann, V.; Müllen, K.; Meghdadi, F.; List, E. J. W.; and Leising, G. *J. Am. Chem. Soc.* **2001**, 123, 946-953.
4. Sato, T.; Jiang, D.; and Aida, T. *J. Am. Chem. Soc.* **1999**, 121, 10658-10659.
5. a) Brian C. Englert, Mark D. Smith, Kenneth I. Hardcastle, and Uwe H. F. Bunz. *Macromolecules*; **2004**; 37(22); 8212-8221. b) Bunz, U. H. F. *Chem. Rev.* **2000**, 100, 1605-1644.
6. Wu, J.; Watson, M. D.; and Müllen K. *Angew. Chem. Int. Ed.* **2003**, 42, 5329-5333.
7. Tovar, J. D. and Swager, T. M. *Journal of Organometallic Chemistry*, **2002**, 653, 215-222.
8. Morgenroth, F.; Reuther, E.; and Müllen, K. *Angew. Chem. Int. Ed. Engl.* **1997**, 36, 631-634.
9. Bhandari, S.; Ray, S. *Synth. Commun.* **1998**, 28, 765.
10. Mohr, B.; Enkelmann, V.; Wegner, G. *J. Org. Chem.* **1994**, 59, 635.
11. Mueller-Westerhoff, U. T.; Zhou, M. *J. Org. Chem.* **1994**, 59, 4988. b) Mueller-Westerhoff, U. T.; Zhou, M. *Synlett* **1994**, 975.

CHAPTER 4

PRECURSOR MATERIALS AND FUNCTIONALIZED POLY(PARA-PHENYLENEETHYNYLENE)S.



4.1 Introduction.

Over the past decade there have been an increasing number of papers published on the use of conjugated polymers as sensory materials water-soluble conjugated polyelectrolytes.^{1b} Some of these polymers have interesting features in aqueous solution such as the ability to interact with neutral species or electrostatically with other charged species causing quenching or enhancement of fluorescence.^{1b}

The above results from molecular wire behavior in conjugated polymers that makes them attractive for sensory applications.² Polyreceptor assemblies that are electronically connected by a conjugated polymer can present large sensitivity gains over small molecule-based fluorescent chemosensors (Figure 4.1). This is due to the fact that the quenching enhancement of a molecular wire system over an isolated fluorescent chemosensor is a simple summation of the association constants for all the receptor units in the polymer.²

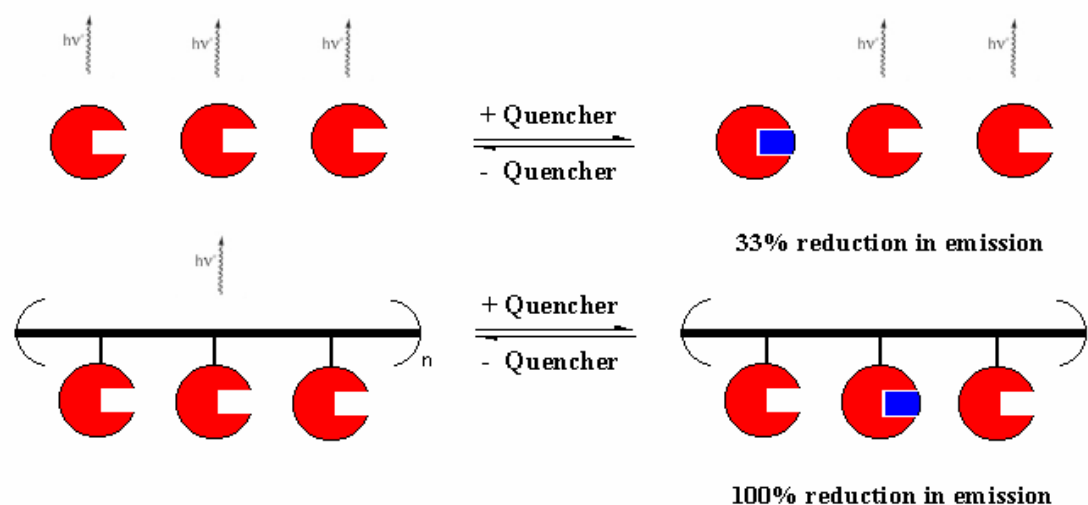


Figure 4.1 Molecular wire behavior in conjugated polymers.

PPEs with functionalized side chains could be used for sensory purposes provided their fluorescence would be altered upon binding with analyte species. With this in mind, we set out to prepare various monomers which could be easily functionalized.

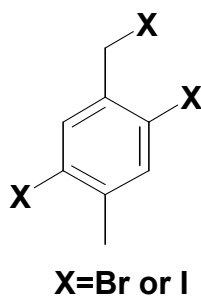


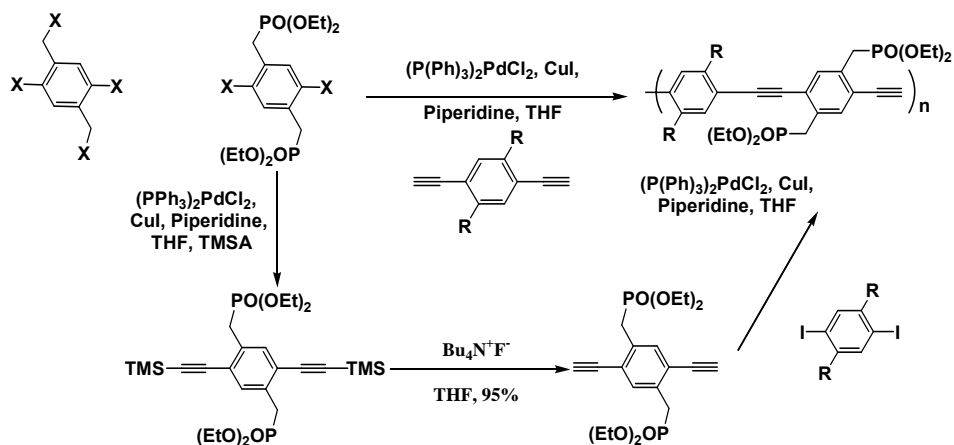
Figure 4.2

To prepare PPEs containing side chains with functional groups, it is most feasible to begin with a monomer such as the one shown in figure 4.2 and employ a scheme similar to the one shown in Scheme 4.1. Aromatic halogens allow the Heck-Cassar-Sonogashira-Hagihara (HCSH) coupling reaction to be performed.³ This reaction allows

the introduction of alkynes. Benzylic or alkyl halides can be modified to allow for the synthesis of substituted PPE polymers.

Two primary reasons for functionalization of PPEs would be for sensory purposes and water solubility; the second being a requisite for the first. Mercury contamination is widespread and occurs through anthropogenic and natural sources including oceanic, volcanic, gold mining, solid waste incineration, and the combustion of fossil fuels. After being introduced into a marine environment, bacteria convert inorganic mercury into methyl mercury, which enters the food chain and accumulates in larger organisms such as edible fish.^{4, 5} Methylmercury is neurotoxic and is implicated as a cause of prenatal brain damage,^{6, 7} various cognitive and motion disorders^{8, 9} and Minamata disease.¹¹

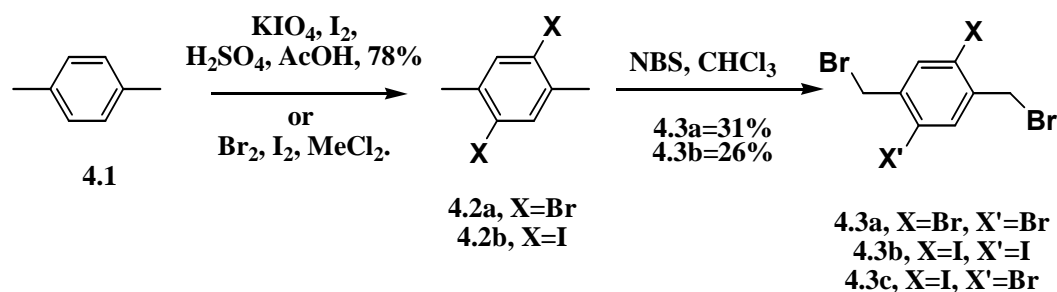
An increased understanding of the effects of mercury exposure has sparked interest in the development of new tools for detecting Hg(II) sensors that function in water and are highly selective for Hg(II) against a background of competing analytes.²² For the above reasons sugar, thio, or phosphonate functionalized PPEs might prove powerful materials in sensing applications.



Scheme 4.1 Possible scheme to prepare functionalized PPEs.

4.2 Results and Discussion

Monomer **4.3a** is known in the literature.¹² The monomer in question is synthesized by aromatic bromination¹³ of p-xylene with molecular bromine followed by benzylic bromination with N-bromosuccinimide¹⁴ to yield **4.3a** (Scheme 4.2).



Scheme 4.2 Iodination and aromatic bromination followed by radical bromination to yield **4.3a-c**.

Using phosphonate groups could impart water solubility and interesting properties to PPEs. Triethyl phosphite was used as a solvent to perform an Arbuzov type nucleophilic substitution reaction on **4.3a** to yield **4.4a** in 99% yield (Scheme 4.3).¹⁵ However under all HCSH conditions explored **4.4a** did not yield **4.5a** (Scheme 4.3). Even more active catalyst systems did not yield the desired product.¹⁶ It was then decided that monomer **4.3b** would be superior for these endeavors. Its aromatic iodines should couple more easily under HCSH conditions. Monomer **4.3b** is known in the literature.¹⁷ It was discovered that one problem encountered when using **4.3b** to prepare PPEs was the presence of a by-product **4.3c**, which occurs due to halogen exchange.¹⁸ Even with impurity **4.3c** present, **4.3b** was the better choice for use in this synthesis. Triethyl phosphite was again used as a solvent to perform an Arbuzov type nucleophilic

substitution reaction on **4.3b** to yield **4.4b**. In the final product mixture, **4.4c** was present. The phosphonate ester analogue could then be coupled to trimethylsilylacetylene under HCSH conditions to form **4.5a**.

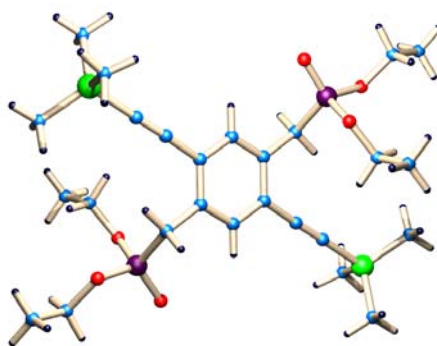
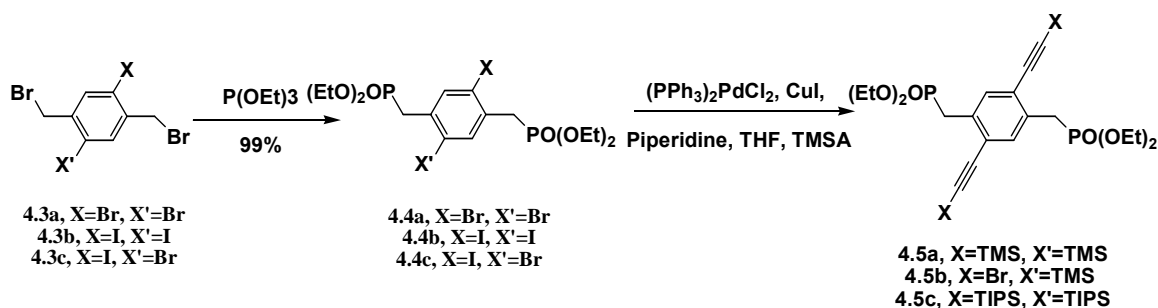


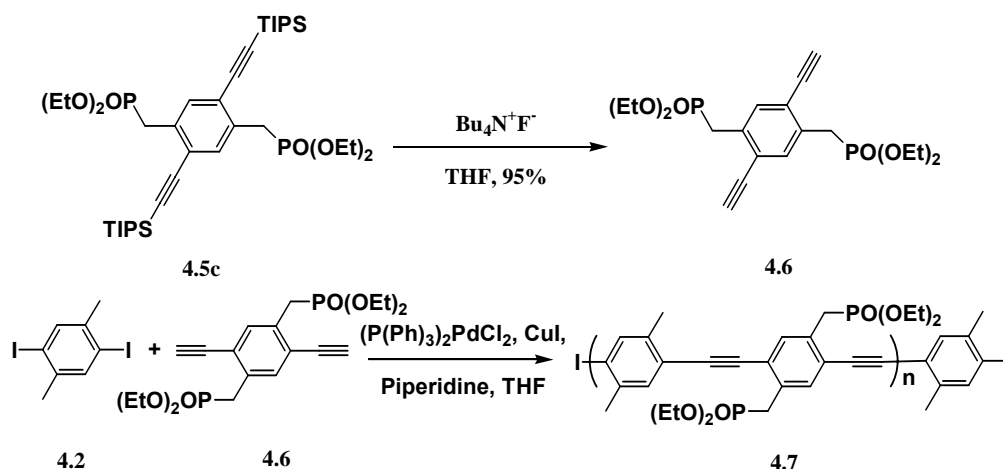
Figure 4.3. ORTEP diagram of 5a.



Scheme 4.3. Arbuzov reactions followed by HCSH conditions to yield monomers **4.5a-c**.

This coupling also did not occur under standard conditions. Various conditions had to be explored to couple **4.4b** with the appropriate silane (See Table 4.1, experimental). Monomer **4.4b** coupled (40 %) when using a 50:50 mixture of DABCO (1,4-diazabicyclo[2.2.2]octane) and piperidine as bases. Compound **4.5a** could not be easily purified due to the presence of **4.5b** and unreacted starting material. Compound **4.5b** could be accounted for by the presence of impurity **4.4c** in the starting material.

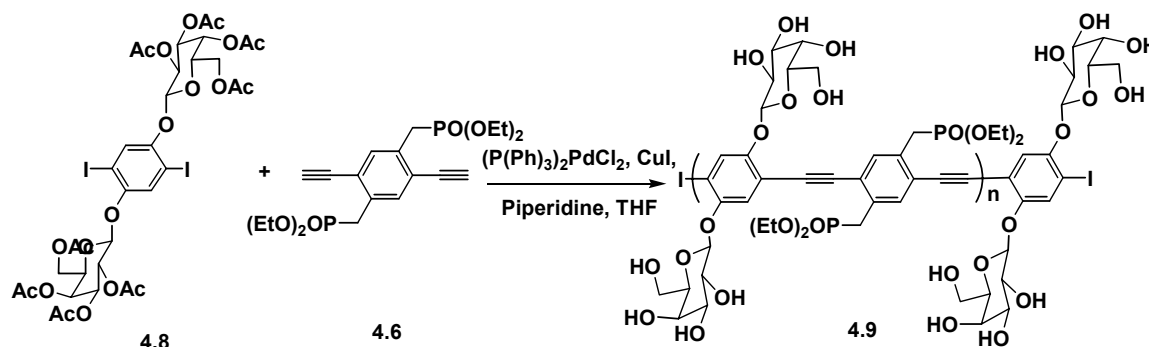
Even under bromine coupling conditions the bromine could not be displaced. It was useful to couple **4.4b** with a substituent which would provide a larger difference in polarity between the starting material and the final product. The phosphonate ester analogue **4.4b** was coupled to triisopropyl silyl acetylene (TIPS) under HCSH conditions to form **4.5c** which could be isolated in 44 % yield (Scheme 4.3). Deprotection of the TIPS group with $\text{Bu}_4\text{N}^+\text{F}^-$ afforded **4.6** in 95% yield which could be used in polymerization reaction under HCSH conditions (Scheme 4.4). The resulting PPE (**4.7**) was of an unfortunately low molecular weight, possibly due to solubility problems during polymerization.



Scheme 4.4 Proposed synthesis of polymer **4.7**.

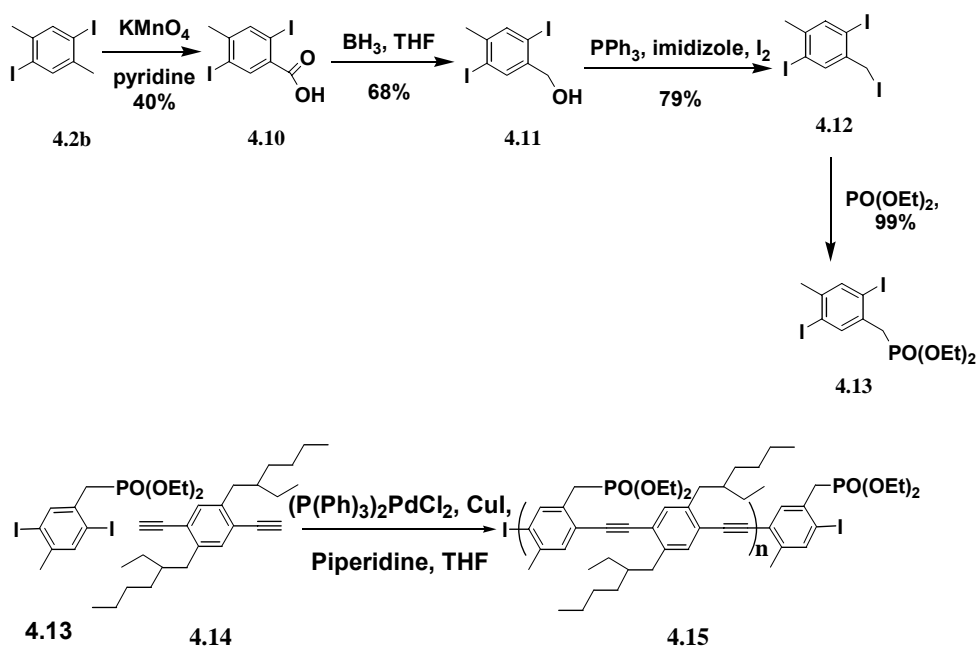
Sugar substituted PPE's have been synthesized in our lab and their properties explored.¹¹ These polymers are interesting for biological and metal sensing. In an effort to produce polymers more interesting for sensing purposes, **4.6** was coupled with **4.8**. The corresponding polymer proved to be insoluble even after reflux in various solvents. ¹³CNMR solid state NMR however indicated the presence of all initial functional groups

and that some acetate groups remained. This supported other studies done in our lab that revealed partial or complete cleavage of acetate groups during polymerizations when using piperidine.¹¹



Scheme 4.5 Synthesis of sugar-phosphonate PPE.

While **4.3b** was available on a large scale, the presence of **4.3c** made the use of this monomer troublesome. It would be useful to have a new monomer with aromatic iodines that did not contain impurities which made coupling reactions difficult. Acid monomer **4.10** is known in the literature.¹⁹ It would be useful if **4.10** could be reduced to the corresponding alcohol. This reaction proved ineffective when using LiAlH_4 as the aromatic halogens did not survive the synthetic transformation. Reductions with BH_3 in tetrahydrofuran proved to be effective and yielded alcohol **4.11** in 68% yield after column chromatography.²⁰ Triphenylphosphine and imidazole in the presence of iodine affords the corresponding iodo monomer **4.12**.²¹ This monomer can be readily transformed to phosphonate **4.13** and polymerized to yield polymer **4.15** which displays typical absorption and emission maxima for this substitution pattern in solution and the solid state.



Scheme 4.6 Synthesis of polymer **4.15**.

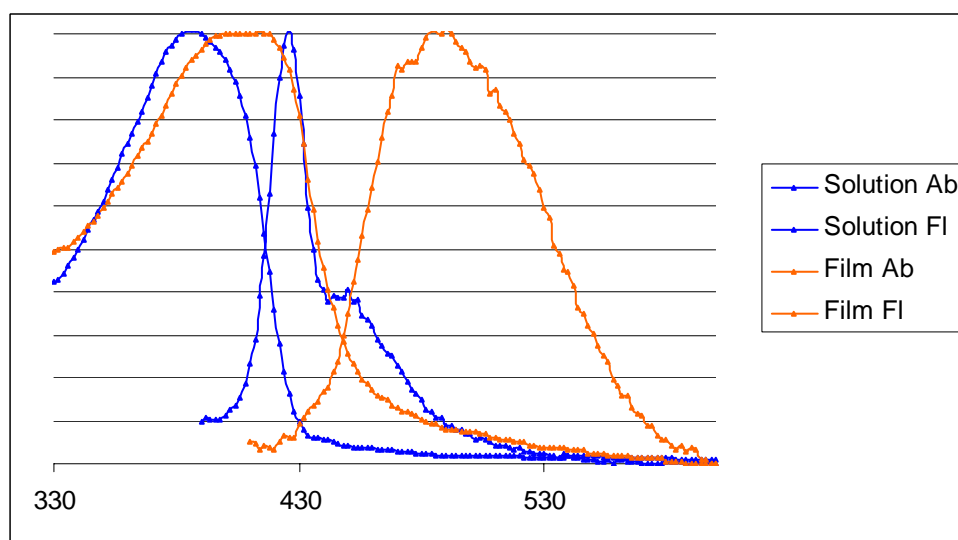


Figure 4.4. Absorption and emission of polymer **4.15** in chloroform and thin films.

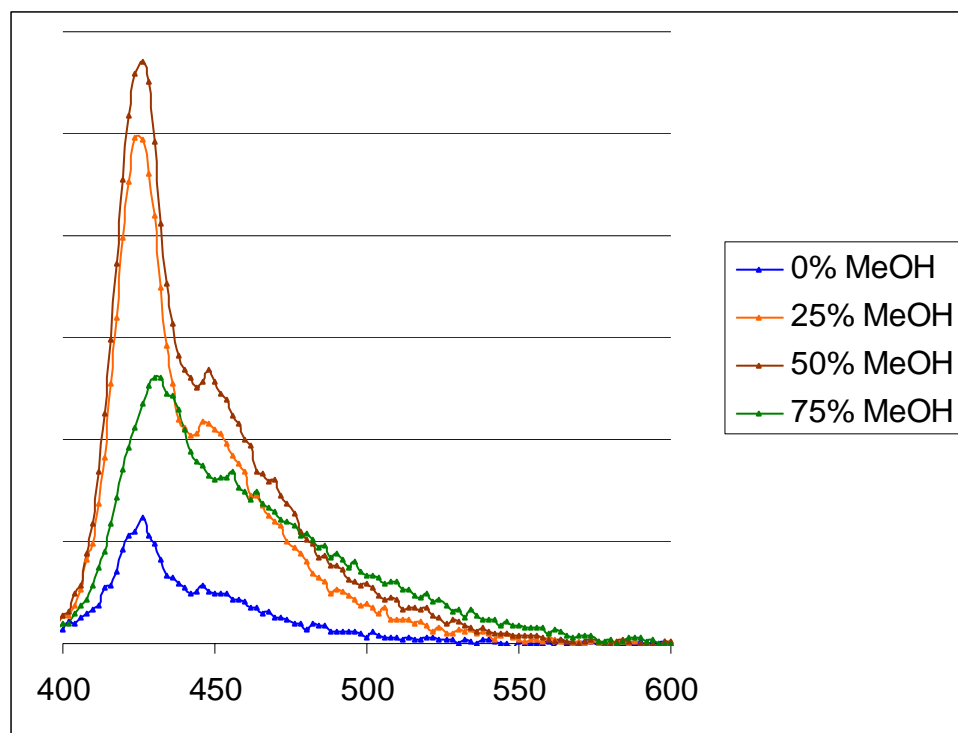
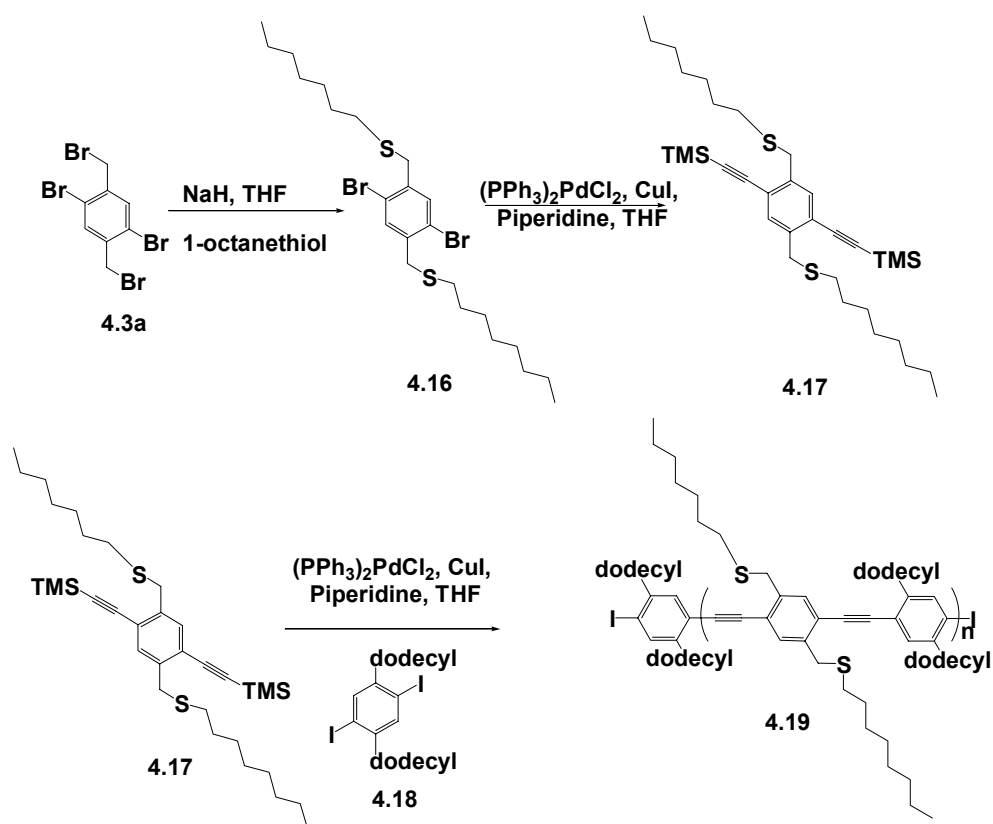


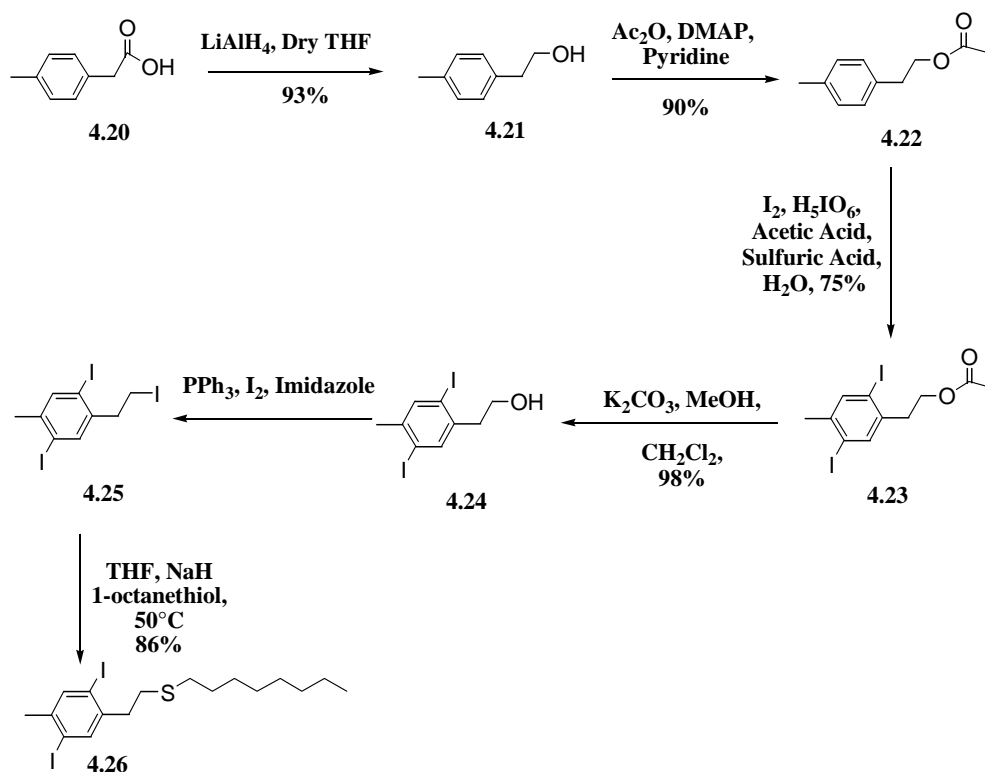
Figure 4.5. Emission of polymer **4.15** in chloroform as a function of the % methanol.

In the past thioethers have shown affinity for Hg(II).²² Monomer **4.3a** was selected for preparation of a thioether PPE with the hopes that the absence of phosphonate groups might offer improved reactivity (Scheme 4.3). Nucleophilic substitution of the halogen for the sulfide anion formed from sodium hydride and 1-octane thiol²³ yields sulfide **4.16** which could be coupled with TMS acetylene using HCSH techniques to form **4.17**. Unfortunately under standard bromine coupling conditions **4.17** could not be obtained. It is possible that the close proximity of the functional group in the present and previous molecules discussed is the reason for the limited reactivity.



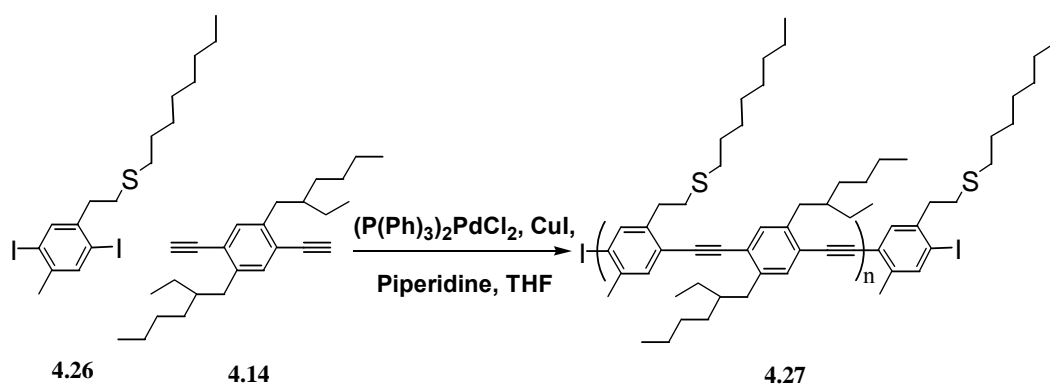
Scheme 4.7 Synthesis of thio monomer **4.14** and its proposed incorporation into PPEs.

Because the preparation of **4.10** was difficult due to over oxidation a more easily prepared monomer was sought. Acid **4.20** is commercially available and can be protected with acetic anhydride.²⁴ Iodination with periodic acid in the presence of an alcohol protected with an acetate group is known and proceeds efficiently. The corresponding monomer can be deprotected to afford **4.24** in good yield. The corresponding alcohol can be transformed to iodide **4.25** using triphenylphosphene and imidazole in the presence of iodine.¹⁴ The iodine is easily transformed in to thioether **4.26**.²³



Scheme 4.8 Synthesis of monomer **4.26**.

Polymer **4.27** can be prepared from thioether **4.26** with a degree of polymerization of fifteen which corresponds to thirty phenyleneethynylene units. The polymer is soluble in most organic solvents and can be microstructured to form bubble arrays as shown in figure 4.6.²⁴ Polymer **4.27** displays typical solution UV-vis maxima with large red-shifts in absorbance and fluorescence in thin films for PPEs with similar substitution patterns.²⁴



Scheme 4.9 Synthesis of polymer **4.27**.

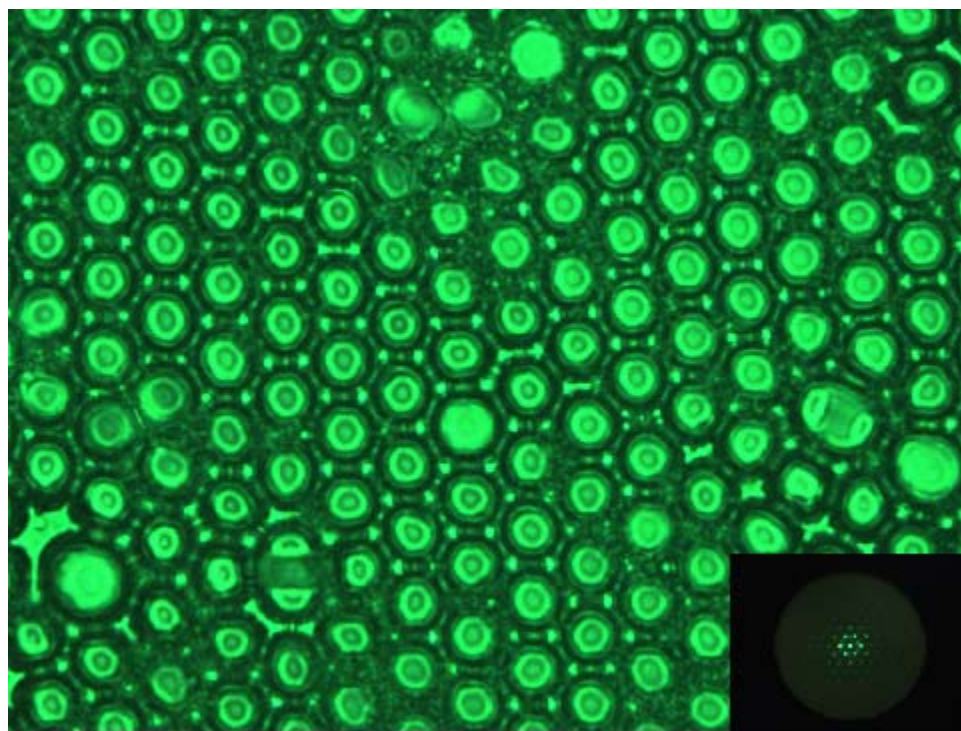


Figure 4.6. Microstructured bubbles formed from polymer **4.27**.

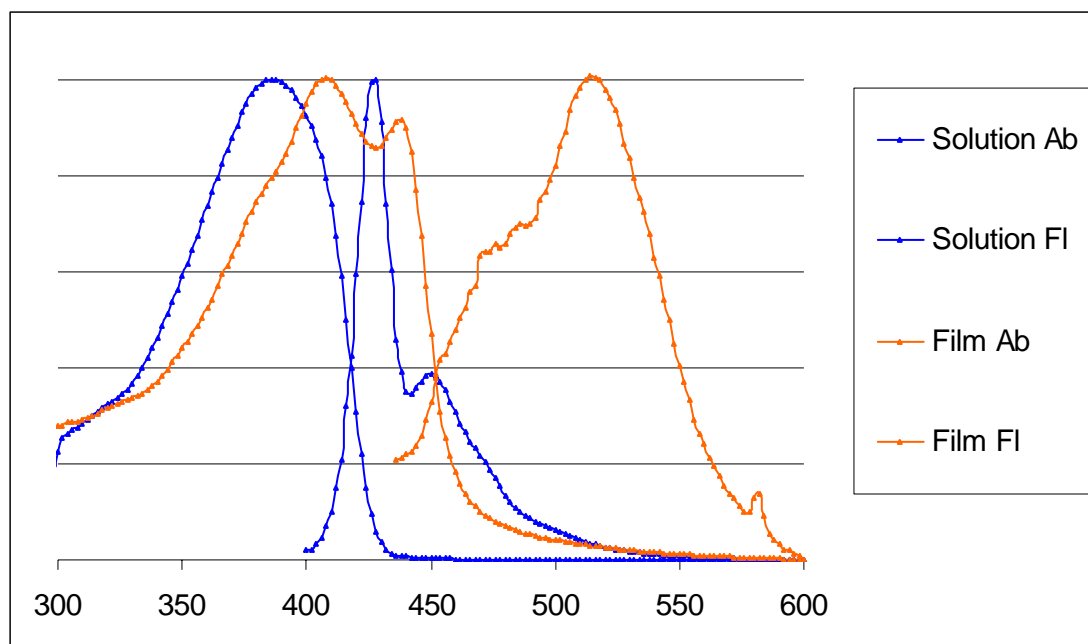


Figure 4.7. Absorbance and emission of polymer **4.27** in solution and thinfilms.

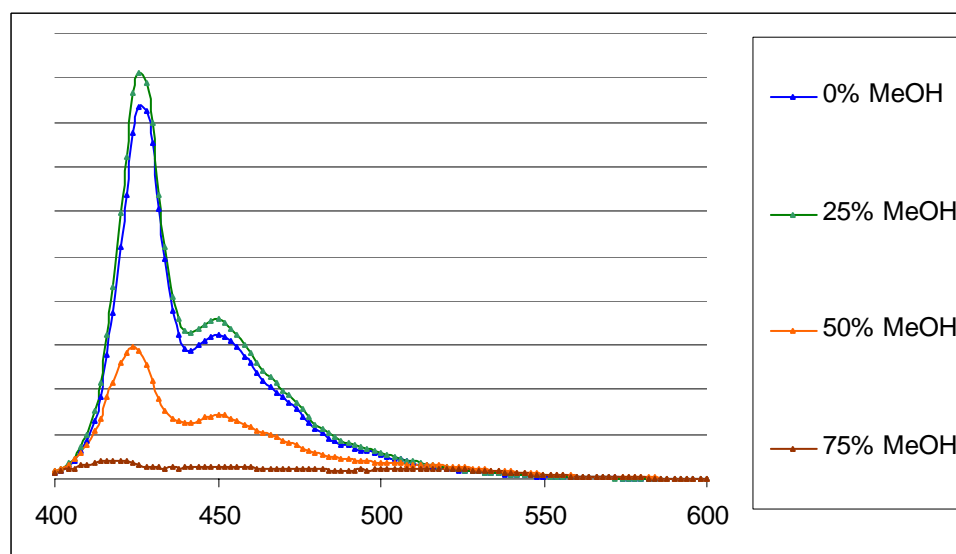


Figure 4.8. Emission of polymer **4.27** as a function of the % methanol.

Polymer **4.27** is sensitive to various Hg salts including $\text{Hg}(\text{OAc})_2$ and $\text{Hg}(\text{OTFAc})_2$, and the fluorescence decreases with the increasing additions of mercury salts in a solution of DMF. Will this is promising no quenching species tested exhibited

K_{sv} values above 4000 (Figure 4.9). While polymer **4.27** is not water soluble, the experiment works well in chloroform or THF. As a control experiment, the addition of DMF to a chloroform solution of polymer **4.27** in chloroform had no effect.

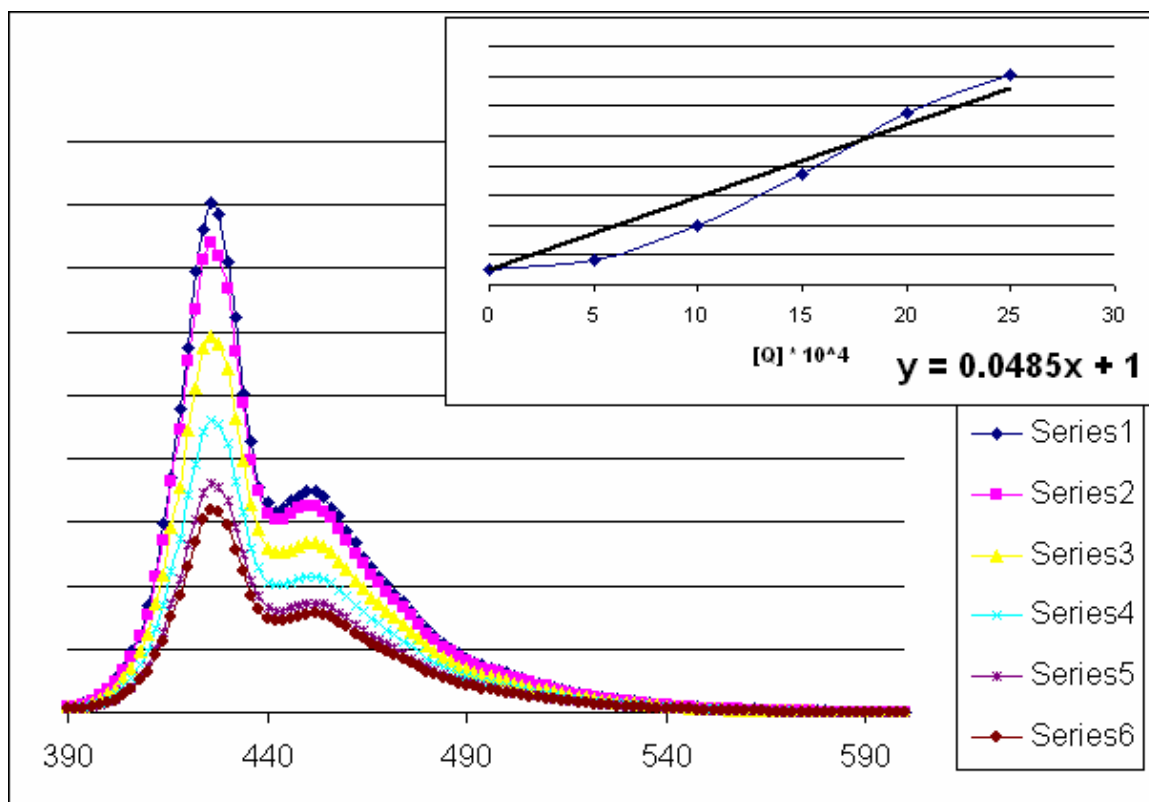


Figure 4.9. Decreasing fluorescence of polymer **4.27** with increasing $\text{Hg}(\text{OAc})_2$ and the corresponding Stern-Volmer Plot.

4.3 Conclusion

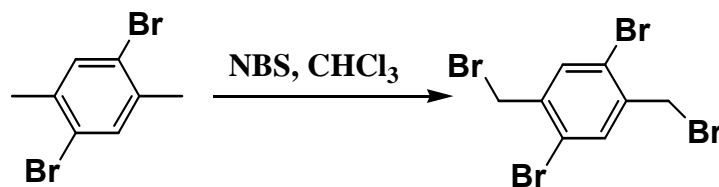
In the synthesis of any polymer the production of viable monomers is most often the greatest synthetic hurdle. The above research has laid the ground work for the synthesis of various functionalized PPEs. Some of the monomers in this chapter offer great potential for the production of functionalized PPEs. In the most promising cases the monomers have been employed to produce high quality polymers. With continued

experimentation and the appropriate choice of functional group these functionalized PPEs could be used for many important purposes such as metal or biological sensing.

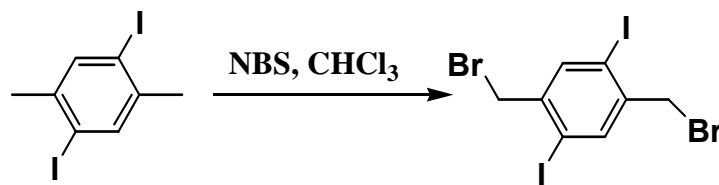
4.4 Experimental:

Instrumentation. The ^1H and ^{13}C NMR spectra were taken on a Varian 300 MHz or a Bruker 400 MHz spectrometer using a broadband probe. The ^1H chemical shifts are referenced to the residual proton peaks of CDCl_3 at δ 7.24 (vs. TMS). The ^{13}C resonances are referenced to the central peak of CDCl_3 at δ 77.0 (vs. TMS). UV-VIS measurements were taken with a Shimadzu UV-2401PC recording spectrophotometer. Fluorescence data was obtained with a Shimadzu RF-5301PC spectrofluorophotometer. A Headway Research Model PWM32 instrument was used to spin-coat dilute chloroform solutions of polymers onto quartz slides for thin film experiments. Reagents were commercial grade and were used as purchased.

Standard coupling procedure for entire procedure (for entire thesis). A round bottom flask was charged with, the corresponding arylhalide (1 eq), the corresponding acetylene (1.01 eq), and piperidine (or the corresponding base). The mixture was subjected to three freeze pump thaw cycles. Bis(triphenylphosphine)palladium(II) dichloride (0.02 eq) and copper(I) (0.01 eq) iodide were added under nitrogen and the mixture was evacuated and purged once more with nitrogen. The mixture was stirred at the appropriate temperature for the corresponding reaction time. After worked up the mixture was chromatographed on silica gel.

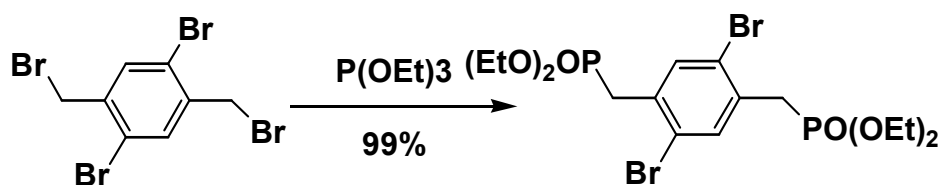


Synthesis of 4.3a: 2,5-dibromo-p-xylene (10.0 g, 37.9 mmol) was dissolved in chloroform (500 mL). NBS (14.9 g, 83.9 mol) was added to a 1000 mL one neck flask equipped with a reflux condensor and the solution was heated for 15 minutes by two 120 watt sunlamps. After 15 minutes another 14.9 g of NBS was added and the mixture was allowed to stir for 10 hours. After 10 hours the mixture was allowed to cool to room temperature and decolorized with an aqueous solution of sodium sulfite. The mixture was filtered and the solids set aside. The organic layer was separated and washed with water three times and then dried with anhydrous magnesium sulfate. The solvent was removed in vacuum and the solids were combined with the solid initially collected by filtration and recrystallized twice from toluene in the absence of light. This provides **4.3a** (3.83 g, 24%) as white crystals. ^1H NMR (300 MHz CDCl_3): δ 7.82 (s, 2H), δ 4.5 (s 4H). IR: ν 670, 773, 867, 896, 1051, 1191, 1216, 1276, 1347, 1433, 1469, 1788, 1951, 1993, 2108, 2289, 2622, 2645, 2735, 2970, 3028, 3082. MP: 198°C.



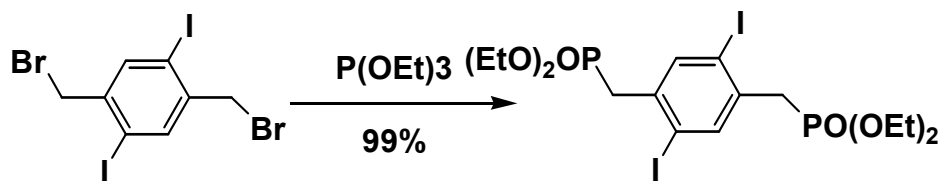
Synthesis of 4.3b: 2,5-diiodo-p-xylene (20 g, 0.056 mol) was dissolved in chloroform (500 mL). NBS (22 g, 0.124 mol) was added to a 1000 mL one neck flask equipped with a reflux condensor and the solution was heated for 15 minutes by two 120 watt sunlamps. After 15 minutes another 22 g of NBS was added and the mixture was allowed to stir for

10 hours. After 10 hours the mixture was allowed to cool to room temperature and decolorized with an aqueous solution of sodium sulfite. The mixture was filtered and the solids set aside. The organic layer was separated and washed with water three times and then dried with anhydrous magnesium sulfate. The solvent was removed in vacuum and the solids were combined with the solid initially collected by filtration and recrystallized twice from toluene in the absence of light. This provides **4.3b** (7.48 g, 26%) as white crystals. ^1H NMR (300 MHz CDCl_3): δ 7.83 (s, 2H), δ 4.48 (s 4H). ^{13}C NMR (300 MHz, CDCl_3): δ 140.7, 139.4, 100.8, 27.2. IR: ν 668, 773, 784, 810, 866, 898, 951, 1002.92, 1039, 1057, 1069, 1161, 1171, 1190, 1214, 1256, 1275, 1332, 1347, 1433, 1466, 1730, 1779, 1993, 2102, 2288, 2315, 2416, 2465, 2623, 2645, 2736, 2844, 2862, 2951, 2972, 3003, 3027, 3063, 3191, 3245, 3697, 3889, 3908. MP: 211°C.

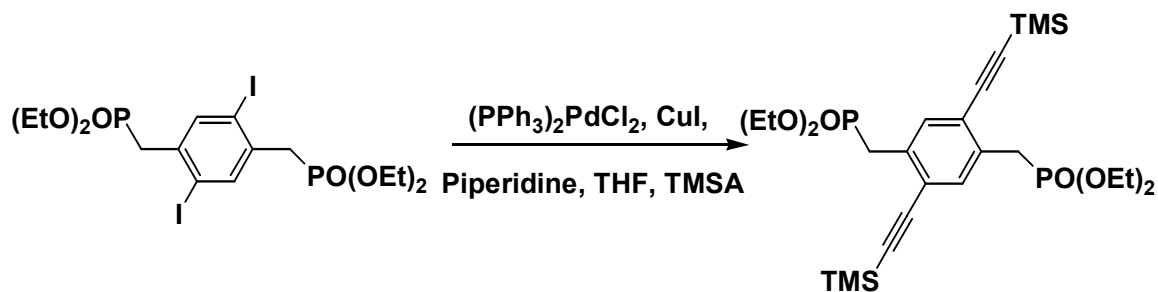


Synthesis of 4.4a: 2,5-bromo-1,4-bis(bromomethyl)benzene (5.00 g, 11.9 mmol) and triethylphosphite (59.1g, 357 mmol) was stirred for 12 hours at 125°C under reflux. After 12 hours the mixture was allowed to cool to room temperature. A white precipitate formed which was filtered and recrystallized twice from hexane. Compound **4.4a** is obtained in 99% (6.29 g) yield as a white powder. ^1H NMR (300 MHz CDCl_3): δ 7.65 (s, 2H), δ 4.02 (q, 8H), δ 3.34 (d, 4H), δ 1.24 (t, 12H). ^{13}C NMR (300 MHz, CDCl_3): δ 135.6, 133.6, 122.6, 62.6, 33.6, 32.6, 18.8. IR: ν 614, 725, 764, 788, 811, 819, 859, 892, 936, 1008, 1064, 1164, 1186, 1238, 1250, 1286, 1305, 1358, 1393, 1442, 1493, 1712, 1758, 1840, 2266, 2466, 2810, 2866, 2914, 2929, 2970, 2990, 3096, 3212, 3256, 3027,

3063, 3191, 3245, 3697, 3889, 3908. ES⁺ MS (EI) calcd. for [C₁₆ H₂₆O₆P₂], 536.13; C, 35.84; H, 4.89; found 539.1 C, 34.92; H, 4.23; MP: 118°C.

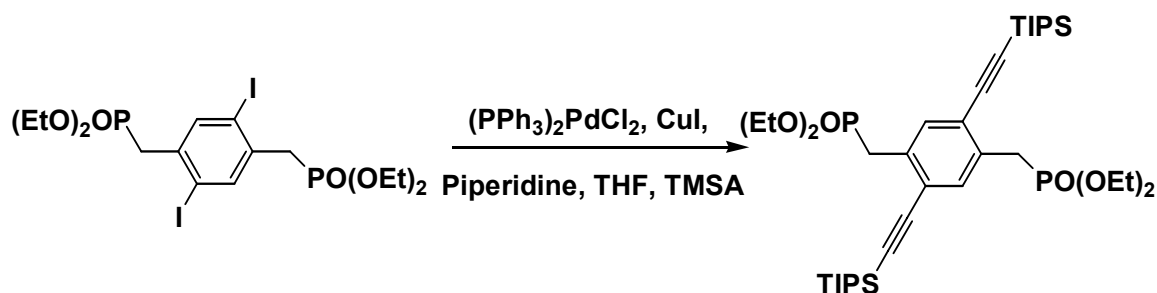


Synthesis of 4.4b: 2,5-diiodo-1,4-bis(bromomethyl)benzene (10 g, 0.019 mol) and triethylphosphite (30 mL, 0.175 mol) was stirred for 12 hours at 125°C under reflux. After 12 hours the mixture was allowed to cool to room temperature. A white precipitate formed which was filtered and recrystallized twice from hexane. **4.4b** is obtained in 97% (12.232 g) yield as a white powder. ¹H NMR (300 MHz CDCl₃): δ 7.85 (s, 2H), δ 4.03 (q, 8H), δ 3.25 (d, 4H), δ 1.24 (t, 12H). ¹³C NMR (300 MHz, CDCl₃): δ 141.9, δ 137.6, 103.3, 63.8, 37.5, 38.0, 18.6. IR: ν 614, 725, 764, 788, 811, 819, 859, 892, 936, 1017, 1046, 1064, 1163, 1186, 1237, 1251, 1286, 1305, 1358, 1392, 1413, 1479., 1769, 1835, 2267, 2494, 2741, 2773, 2866, 2914, 2929, 2968, 2992, 3094. ES⁺ MS (EI) calcd. for [C₁₆ H₂₆O₆P₂], 630.13; C, 30.50; H, 4.89; found C, 31.23; H, 4.45; MP: 133°C.



Synthesis of 4.5a: Compound **4.4b** (5.00 g, 7.93 mmol) was put in a schleck flask with $(\text{Cl})_2\text{Pd}(\text{PPh}_3)_2$ (0.05 eq), CuI (0.05 eq), and piperidine(5 mL). The flask was degassed

with nitrogen and TIPS acetylene (3.12 g, 31.8 mmol) was added. The flask was heated at 80°C for 5 days. The reaction mixture was diluted with MeCl₂ and washed with water three times. The organic layers were dried with MgSO₄ and the solvent was removed by vacuum. The resulting solid was purified by column chromatography (1:1, hexane ethylacetate), (1.58 g, 35 %, mixture of **4.5a** and **4.5b**). ¹H NMR (300 MHz CDCl₃): δ 7.57 (s, 2 H), δ 4.00 (m, 4H), δ 3.37 (m, 8H), δ 1.22 (m, 12H), δ 0.12 (s, 36H). ¹³C NMR (300 MHz, CDCl₃): δ 134.1, δ 133.0, 123.3, 106.3, 101.8, 62.3, 34.2, 33.3, 19.8, 0.3. IR: ν 635, 654, 669, 708, 727, 733, 755, 783, 801, 812, 837, 884, 901, 919, 936, 944, 954, 1003, 1010, 1051, 1163, 1221, 1244, 1249, 1365, 1383, 1442, 1453, 1461, 2149, 2715, 2864, 2887, 2812, 2832, 2945. ES⁺ MS (EI) calcd. for [C₂₆ H₄₄O₂P₂Si₂], 570.22, C, 54.71; H, 7.77; found C, 52.79; H, 8.75; MP: 124°C.

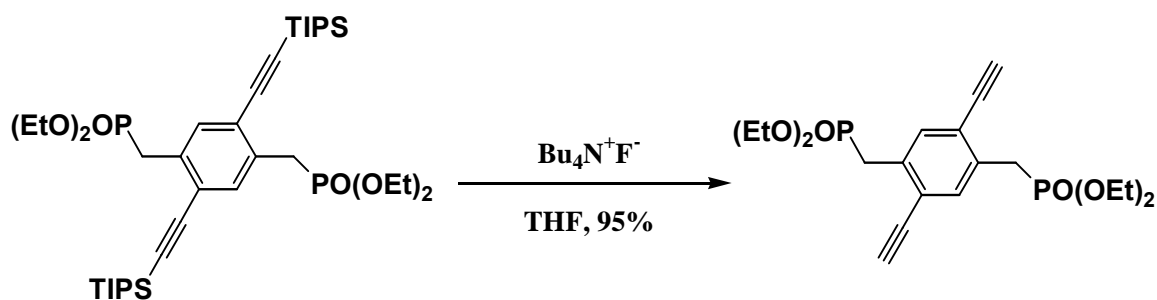


Synthesis of 4.5c: 7.01g (0.0111 mol) **4.4b** was put in a schleck flask with (Cl)₂Pd(PPh₃)₂ (0.05 eq), CuI (0.05 eq), and piperidine (5 mL). The flask was degassed with nitrogen and TIPS acetylene (9.15 mL, 0.041 mol) was added. The flask was heated at 80°C for 5 days. The reaction mixture was diluted with MeCl₂ and washed with water three times. The organic layers were dried with MgSO₄ and the solvent was removed by vacuum. The resulting solid was purified by column chromatography (1:1, hexane ethylacetate), (2.64g, 44%). ¹H NMR (300 MHz CDCl₃): δ 7.57 (s, 2 H), 4.02 (m, 8H), 3.47 (d, 4H), 1.23 (m, 18H), 1.12 (s, 36H). ¹³C NMR (300 MHz, CDCl₃): δ 134.0, 132.9, 123.9,

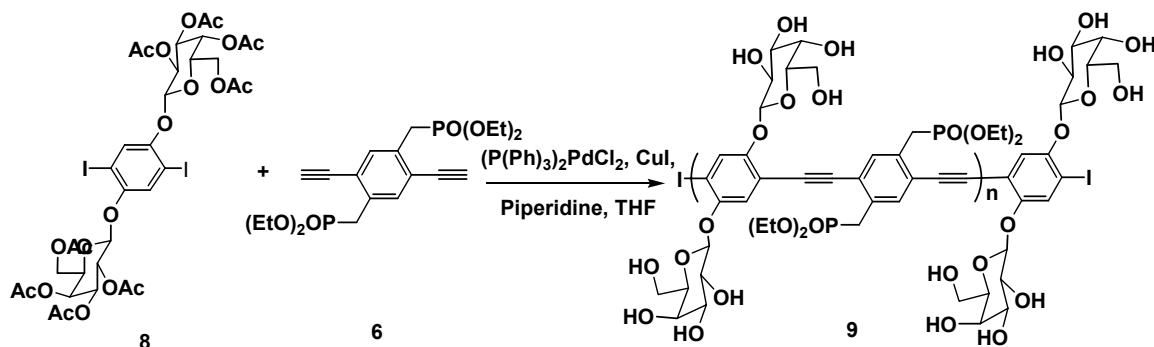
104.5, 97.1, 62.0, 31.8, 30.8, 18.6, 16.3, 11.5. IR: ν 637, 657, 671, 710, 727, 733, 755, 783, 801, 812, 837, 884, 900, 919, 935, 943, 973, 1000, 1008, 1020, 1162, 1201, 1243, 1249, 1365, 1383, 1442, 1453, 1461, 2149, 2723, 2814, 2837, 2848, 2864, 2955. ES⁺ MS (EI) calcd. for [C₃₈ H₆₈ O₆ P₂ Si₂], 739.06; C, 61.75; H, 9.27; found 738.4 C, 60.92; H, 7.25; MP: 132°C.

Table 4.1 Conditions explored to couple **4.4a**, **4.4b**, and **4.4c**. * indicates the use of a high pressure tube.

Amount	eq catalyst	eq Cul	mL base	mL of co-solvent	type of sylvane	yield	temp
iodophosphinate							
0.3241g (0.520mmol)	0.01	0.03	piperidine, 3mL	n/a	TMS 1.10mmol	<5%	RT
0.2143g (0.3401mm)	0.01	0.03	piperidine, 3mL	n/a	TMS .7mm	<5%	RT
13.121g (0.0208m)	0.01	0.03	piperidine, 15mL	THF, 15 mL	TMS, 0.0458m	<5%	RT
3.2804g	0.01	0.01	diisopropyl ethyl amine	na	TMS	<5%	RT
4.32 G	0.05	0.05	NEt ₃ , EtN(i-Pr) ₂ , 4mL	THF, 10mL	TIPSm 0.5 eq	0	RT
7.016g	0.05	0.05	NEt ₃ , EtN(i-Pr) ₂ , 6mL	THF, 3mL	TIPS 2.1	9%	80
5.555g	0.05	0.05	piperidine, 5mL	na	TIPS 4.5	44%	5 days 80*
0.5g	0.02	0.05	piperidine, 3mL	THF, 4mL	TES 2.1	in progress	RT
bromophosphinate							
7.5682g	0.03	0.03	HN(i-Pr) ₂ , 5 mL	na	TMS, 2.1 eq	0%	60
4.2969	0.01	0.03	diisoproyl amine, 3mL	na	TMS 2.2	6%	microwave
14.4	0.05	0.05	piperidine/triethylamine, 5mL	na	2.2 TMS	0	120 C
0.87	0.05	0.05	EtN(i-Pr) ₂ 2mL	THF, 2mL	.5 mL TMS	0	80 C
0.87	0.05	0.05	EtN(i-Pr) ₂ , 2mL	Dioxane, 2 mL	.5 mL TMS	0	81 C
0.87	0.05	0.05	NEt ₃ , EtN(i-Pr) ₂ , 2mL	THF, 2mL	.5 mL TMS	0	82 C
0.87	0.05	0.05	NEt ₃ , EtN(i-Pr) ₂ , 2mL	Dioxane, 2 mL	.5 mL TMS	0	83 C
0.569	0.05	0.05	NEt ₃ , EtN(i-Pr) ₂ , 12mL	THF, 6mL	TIPS, 0.5 eq	0	RT

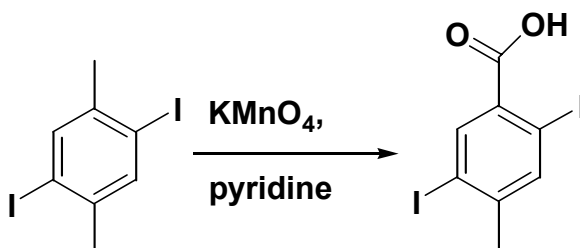


Synthesis of 4.6: Compound **4.5c** (2.708g, 3.66 mmol) was put in a 250 mL round bottom flask with THF (5 mL) and $\text{F}^-\text{N}^+(\text{Bu})_4$ (9.16 mmol, 9.2 mL 1N solution in THF). The mixture was stirred for 24 h. Hexane was added, and the mixture washed with 1 N NH_4OH and water. The organic layer was dried, and the solvent removed to afford a crude colorless solid which was purified by chromatography in ethylacetate and hexanes (1:9) to yield a colorless solid (1.53 g, 98%) ^1H NMR (300 MHz CDCl_3): δ 7.54 (s, 2H), δ 4.00 (q, 8H), δ 3.39 (m, 4H), 2.19 (s, 2H), 1.27 (t, 12H). ^{13}C NMR (300 MHz CDCl_3): δ 135.2, 133.6, 123.3, 83.4, 81.3, 62.4, 32.2, 30.3, 16.4. IR: ν 715, 844, 956, 943, 1254, 1262, 1423, 1474, 2156, 2223, 2745, 2848, 2856, 2866. ES^+ MS (EI) calcd. for $[\text{C}_{20}\text{H}_{28}\text{O}_6\text{P}_2]$, 426.38; C, 56.34; H, 6.62; O, 22.51; P, 14.53; found 426.2 C, 55.87; H, 5.64; MP: 93 $^\circ\text{C}$.

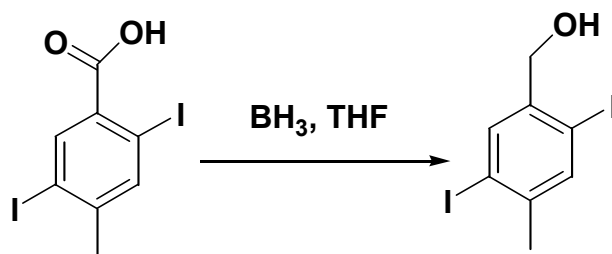


Synthesis of Polymer 4.9: Compound **4.8** (0.500 g, 0.490 mmol) and compound **4.6** (0.211 g, 0.495 mmol) were dissolved in tetrahydrofuran (2 mL) and piperidine (2 mL) in an oven dried Schlenk flask. The flask was flushed with nitrogen and frozen and

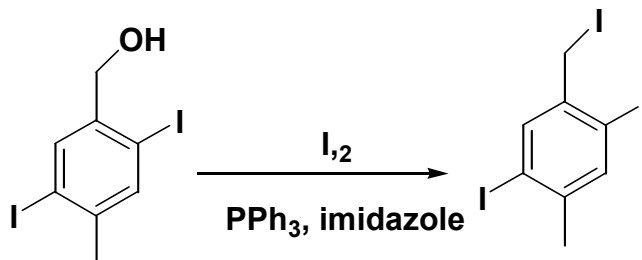
evacuated three times after which $(\text{Ph}_3\text{P})_2\text{PdCl}_2$ (3.5 mg, 4.9 mmol), and CuI (1 mg, 4.9 mmol) were added under nitrogen. The mixture was allowed to stir at room temperature for 48 h. The resulting polymer stirred in warm methanol to yield **4.27** (0.602 g, >99 %). ^{13}C NMR (Solid State): δ 168.7, 133.8, 132.8, 64.7, 63.7, 62.1, 61.6, 60.9, 49.0, 46.0, 29.0, 19.9, 16.0, 8.7, 0.2. ES^+ MS (EI) calcd. for $[\text{C}_{54}\text{H}_{66}\text{O}_{27}\text{P}_2]$; C, 53.64; H, 5.50; found C, 54.29; H, 5.31.



Synthesis of 4.10: 2,5-diiodo-p-xylene (10.0 g, 27.9 mmol), pyridine (100 mL), and water (100 mL) was heated to reflux. Potassium permanganate (42.4 g, 28.0 mmol) was added in four separate portions over three hours. After 12 h the mixture was filtered and washed with 2 N NaOH. The aqueous layer was acidified and filtered. The filtrate was dissolved in ethylacetate and washed with water. The organic layer was dried and the solvent removed to yield **4.10** as a colorless solid (3.79 g, 35 %). ^1H NMR, CDCl_3 : δ 8.43 (s, 1H), 7.96 (s, 1H), 2.47 (s, 3H). ^{13}C NMR (CDCl_3): δ 167.8, 145.9, 144.3, 141.1, 103.5, 95.4, 27.8. IR: ν 744.7, 756.5, 831.2, 852.4, 893.9, 1029.4, 1062.2, 1200.6, 1214.5, 1349.1, 1381.4, 1439.7, 1462.1, 1549.7, 2902.1, 3023.6, 3044.9, 3056.4. MS (EI) calcd. $[\text{C}_8\text{H}_6\text{I}_2\text{O}_2]$, 387.94; C, 24.77; H, 1.56; found C, 23.90; H, 2.43. MP: 140 °C.

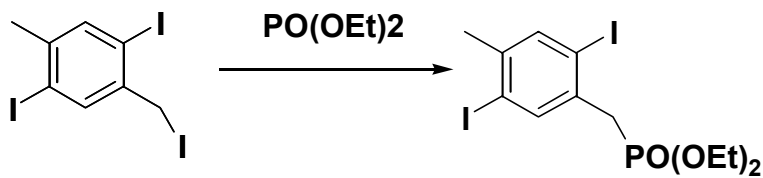


Synthesis of 4.11: Diiodo compound **4.10** (7.16 g, 18.5 mmol) was dissolved in dry tetrahydrofuran (25 mL) in an ice bath and under nitrogen hydroborane (0.665 g, 27.7 mmol) (1 N solution in THF) was added. The mixture was allowed to stir at room temperature for 24 h. The mixture was slowly poured onto water and the precipitated solid was taken up in ethylacetate. The organic solution was washed with 0.5 N HCl (150 mL) and then with water. The organic layer was separated and dried. The solvent was removed, and the crude solid was purified by chromatography over silica gel (4:6, ethyl acetate:hexane) to yield **4.11** as a colorless solid (6.14 g, 89 %). ^1H NMR (CDCl_3): δ 7.78 (s, 1H), 7.73 (s, 1H), 4.30 (s, 2H), 2.29 (s, 3H). ^{13}C NMR (CDCl_3): δ 143.1, 142.2, 139.8, 138.2, 101.9, 97.3, 68.4, 27.0. IR: ν 3343, 3201, 2962, 2849.32, 1703.43, 1692.34, 1459.23, 1372.38, 1328.32, 1292.83, 1245.54, 1184.54, 1137.34, 1063.74, 939.94. ES^+ MS (EI) calcd. $[\text{C}_8\text{H}_8\text{I}_2\text{O}]$, 373.9; C, 25.69; H, 2.16; found 373.9; found C, 24.43; H, 2.02; MP: 185-187 $^\circ\text{C}$.



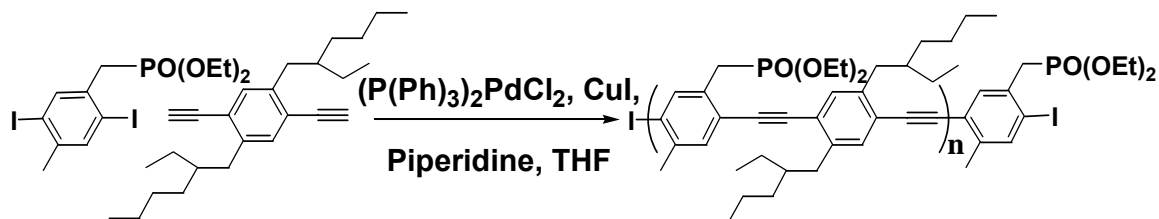
Synthesis of 4.13: 2,5-diiodo-4-methylbenzylalcohol (5.00 g, 13.4 mmol), acetonitrile (20 mL), ether (20 mL), imidazole (2.73 g, 40.1 mmol), triphenylphosphine (10.5 g, 40.1

mmol) and iodine (10.2 g, 40.1 mmol) were placed in a 500 mL round bottom flask in the listed order and stirred for 24 h. The solvent was removed. The crude product was dissolved in dichloromethane and washed with 1N HCl and water. The organic layer was dried, the solvent removed, and the crude solid was purified by chromatography on silica gel (3:7, dichloromethane: hexane) to yield **4.13** as a colorless solid (5.11 g, 79 %). ^1H NMR (CDCl_3): δ 7.82 (s, 1H), 7.69 (s, 1H), 4.43 (s, 2H), 2.27 (s, 3H). ^{13}C NMR (CDCl_3): δ 141.6, 139.5, 138.5, 135.3, 103.4, 94.6, 67.5, 27.6. IR: ν 616.7, 621.0, 627.7, 648.0, 662.5, 666.3, 678.9, 683.2, 689.0, 730.0, 736.7, 845.7, 851.5, 916.6, 921.4, 994.72, 1004.6, 1009.1, 1062.2, 1180.8, 1193.8, 1200.6, 1219.4, 1233.3, 1238.2, 1244.4, 1248.34, 1254.1, 1272.4, 1276.7, 1308.6, 1311.5, 1318.2, 1326.9, 1333.2, 1343.8, 1377.0, 1429.15, 1435.4, 1442.6, 1445.5, 1469.6, 2118.1, 2926.7, 2968.2, 3270.0, 3286.4, 3289.8. ES^+ MS (EI) calcd. for $[\text{C}_8\text{H}_7\text{I}_3]$, 483.85, found; C, 19.86; H, 1.46; found C, 22.81, H, 2.01; MP: 150-155 $^\circ\text{C}$.

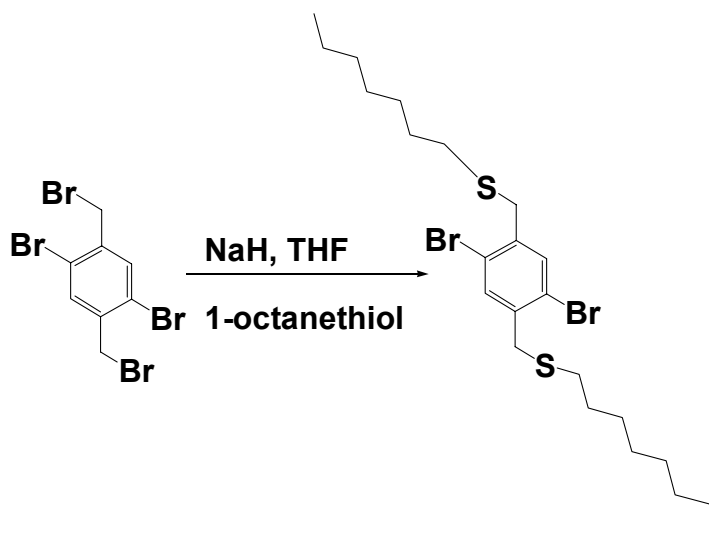


Synthesis of 4.13: 2,5-diiodo-4-methylbenzyl iodide (1.00 g, 1.03 mmol) and triethylphosphite (30 mL, 175 mmol) was stirred for 12 hours at 125 $^\circ\text{C}$ under reflux. After 12 hours the mixture was allowed to cool to room temperature. The solvent was removed and the crude solid purified by chromatography on silica gel (4:7, ethylacetate: hexane) to yield **4.13** as a colorless solid (0.490 g, 96%). ^1H NMR (300 MHz CDCl_3): δ 7.78 (s, 2H), 7.64 (s, 2H), δ 4.06 (q, 4H), δ 3.22 (d, 2H), δ 2.30 (s, 3H), 1.16 (t, 8H). ^{13}C NMR (300 MHz, CDCl_3): δ 142.1, 142.1, 140.2, 134.9, 100.9, 62.7, 38.4, 27.3, 16.8. IR:

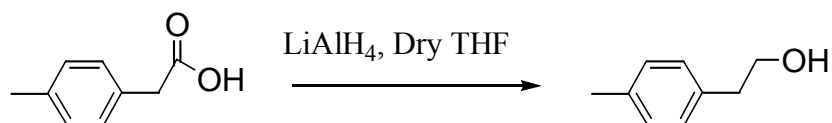
v 3056, 3015, 2969, 2943, 2911, 2885, 2843, 2801, 2730, 2553, 2456, 2305, 2063, 1164, 1748, 1496, 1445, 1433, 1417, 1372, 1331, 1314, 1258, 1246, 1190, 1118, 1077, 1029. ES⁺ MS (EI) calcd. for [C₁₂H₁₇I₂O₃P₁], 494.04; C, 29.17; H, 3.47; found C, 29.75; H, 5.45; MP: 93°C.



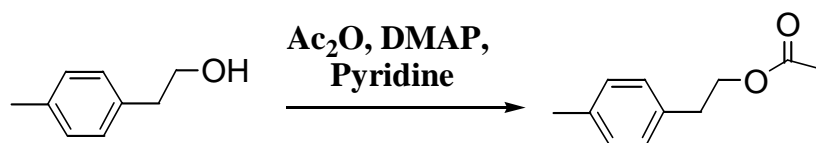
Synthesis of 4.15: Compound **4.13** (0.500 g, 1.01 mmol) and compound **4.14** (0.358 g, 1.02 mmol) were dissolved in tetrahydrofuran (1.5 mL) and piperidine (1.5 mL) in an oven dried Schlenk flask. The flask was flushed with nitrogen and frozen and evacuated three times after which $(Ph_3P)_2PdCl_2$ (2.1 mg, 2.9 mmol), and CuI (1 mg, 4.9 mmol) were added under nitrogen. The mixture was allowed to stir at room temperature for 48 h. The resulting polymer stirred in warm methanol to yield **4.15** (0.572 g, 96 %). ¹H NMR (CDCl₃): δ 7.41 (m, 2H), 7.27 (m, 2H), 4.01 (m, 4H), 3.11 (m, 2H), 2.87 (m, 6H), 2.42 (m, 5H), 2.33 (s, 3H), 1.80 (m, 2H), 1.57 (m, 2H), 1.24 (m, 26H), 1.22 (s, 6H), 0.87 (m, 9H). ¹³C NMR (TCE): δ 144.0, 133.5, 133.2, 131.3, 128.7, 129.2, 122.4, 94.3, 92.1, 61.4, 40.1, 38.6, 32.7, 32.6, 32.4, 31.8, 29.7, 29.2, 29.1, 28.9, 28.8, 25.7, 23.1, 22.6, 16.5, 13.9, 10.8. IR: v 3076, 2729, 1776, 1726, 1681, 1598, 1546, 1504, 1461, 1379, 1334, 1103, 1035, 896, 877, 763, 725, 570, 491, 428. GPC (polystyrene standards) M_n=20,014, PDI=4.3. ES⁺ MS (EI) calcd. for [C₅₄ H₆₆O₂₇P₂]; C, 53.64; H, 5.50; found C, 54.29; H, 5.31.



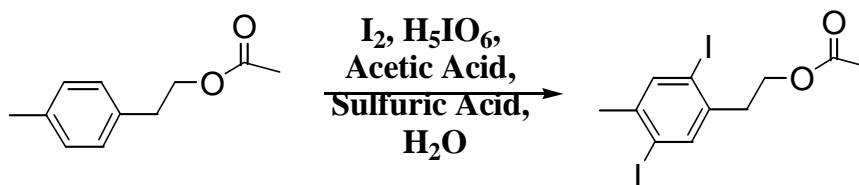
Synthesis of 4.16: Compound **4.3a** (3.00 g, 7.11 mmol) was dissolved in dry tetrahydrofuran (mL) and under nitrogen purge a mixture of 1-octanethiol (2.60g, 17.9 mmol) and NaH (0.430g, 14.9 mmol) (80% in mineral oil) in dry tetrahydrofuran was added dropwise. The mixture was allowed to stir at 40°C for 24 h. The mixture was slowly poured onto water and washed with hexane. The organic solution was washed with 0.5 N HCl (150 mL) and then with water. The organic layer was separated and dried. The solvent was removed, and the crude solid purified by chromatography over silica gel (4:6, dichloromethane:hexane) to yield **4.16** as a colorless solid (3.10 g, 81 %). ^1H NMR (CDCl_3): δ 7.7 (s, 2H), 3.6 (s, 4H), 2.4 (m, 4H), 1.2 (m, 24H), 0.8 (m, 6H). ^{13}C NMR (CDCl_3): δ 142.3, 141.2, 101.9, 41.3, 33.4, 32.9, 28.7, 27.8, 23.8, 14.8. IR: ν 2979, 2956, 2920, 2867, 2843, 2821, 2727, 2639, 2024, 1902, 1745, 1472, 1460, 1413, 1355, 1315, 1278, 1228, 1197, 1131, 1055, 1002, 926, 884, 866, 706. ES^+ MS (EI) calcd. for $[\text{C}_{24}\text{H}_{40}\text{Br}_2\text{S}_2]$, 552.51; C, 52.17; H, 7.30; found fragmentation 304.2; C, 52.79; H, 8.75; MP: °C.



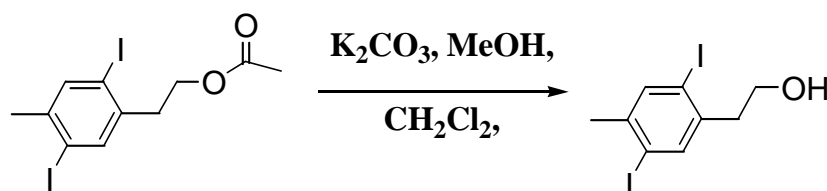
Synthesis of 4.21: Acid **4.20** (25.0 g, 0.166 mol) was dissolved in 250 mL of dry THF under nitrogen. LiAlH₄ (4.74 g, 0.125 mol) was added slowly and the mixture was stirred overnight at room temperature. The solution was slowly poured onto ice and after all the ice melted, acidified with HCl up to pH6. The resulting mixture was evaporated under vacuum and the colorless solid was washed with dichloromethane. Evaporation of the organic phase provided **4.21** as a colorless oil which was further purified by flash chromatography with ethyl acetate (21.7 g, 96%). ¹HNMR (CDCl₃): δ 7.15 (s, 4H), 3.83-3.78 (t, 2H), 2.86-2.81 (t, 2H), 2.37 (s, 3H). ¹³CNMR (CDCl₃): δ 135.6, 135.3, 129.0, 128.7, 63.5, 38.5, 20.2.



Synthesis of 4.22: To a nitrogen-purged flask; **4.21** (21.2 g, 156 mmol), acetic anhydride (79.6 g, 780 mmol), pyridine (400 mL) and 4-dimethylamino pyridine (catalytic amount) were added. The mixture was stirred at room temperature for 5-6h. The solvent and excess acetic anhydride were removed under vacuum to afford the desired product as a colorless liquid. The product was purified by column chromatography by using hexane/dichloromethane (1:3) as an eluent to yield **4.22** as a colorless oil (25.9 g, 93%). ¹HNMR (CDCl₃): δ 7.13 (s, 4H), 4.26 (t, 2H), 2.89 (t, 2H), 2.35 (s, 3H), 2.05 (s, 3H). ¹³CNMR (CDCl₃): δ 170.8, 135.8, 134.5, 129.0, 128.6, 64.9, 34.5, 20.8, 20.7. IR ν 3460, 2864, 2732, 2073, 1900, 1740, 1514, 1365, 1223, 976, 908, 812, 718, 640, 606, 550.

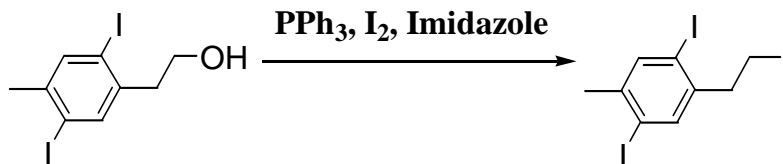


Synthesis of 4.23: To a nitrogen-purged flask, **4.22** (25.0 g, 140 mmol) iodine (39.1 g, 154 mmol), periodic acid (0.639 g, 2.81 mmol), acetic acid (500 mL), H₂O (100 mL) and H₂SO₄ (15.0 mL) were added. The mixture was heated to 80°C for 3 h under N₂. The solvent was removed under vacuum. The residue was dissolved in ethylacetate and washed with H₂O, 1N (aq) K₂CO₃ and 1N (aq) Na₂SO₃. The organic phase was dried over MgSO₄ and the solvent was evaporated. The resulting solid was purified by silica gel chromatography using hexanes/dichloroethane (1:3) to give the product **4.23** as a colorless solid (51.7 g, 78%). ¹HNMR (CDCl₃): δ 7.65 (s, 1H), 4.24-4.19 (t, 2H), 2.98-2.94 (t, 2H), 2.33 (s, 3H), 2.03 (s 3H). ¹³CNMR (CDCl₃): δ 170.7, 141.7, 139.7, 139.7, 139.6, 100.7, 100.0, 63.1, 38.4, 26.9, 20.8. IR ν 2945, 2870, 1738, 1516, 1452, 1369, 1232, 1041, 984, 878, 802, 700, 656, 606. MP=55°C.

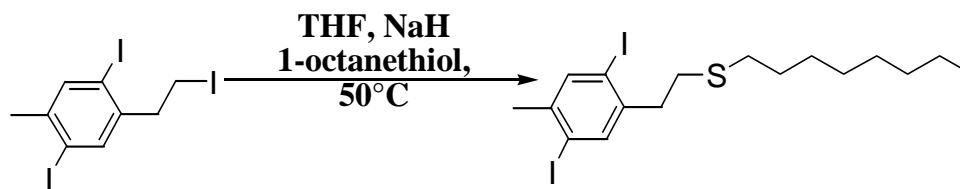


Synthesis of 4.24: Diiodo compound **4.23** (50.0g, 116 mmol) was dissolved in 65.- mL of dicholoromethane. After addition of 1.50 L of MeOH and K₂CO₃ (161 g, 1.16 mol), the mixture was stirred at room temperature overnight. The solvent was evaporated and the resultant solid was transferred into a buchner funnel and washed with H₂O to get rid of the excess K₂CO₃. The product was obtained after repeated recrystallization from

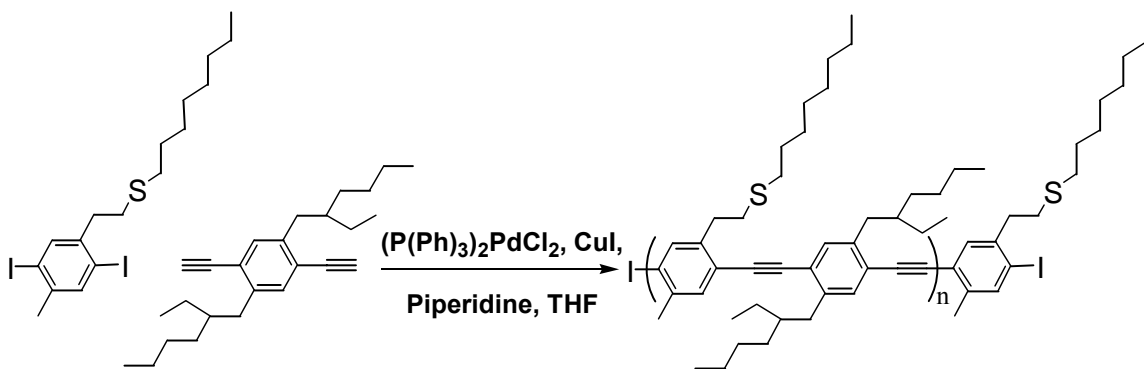
hexanes yields **4.24** as a colorless solid (41.9 g, 93%). ^1H NMR (CDCl_3): δ 7.65 (d, 2H), 3.83-3.79 (t, 2H), 2.93-2.88 (t, 2H), 2.33 (s, 3H), 1.42 (s, 1H). ^{13}C NMR (CDCl_3): δ 141.6, 140.3, 139.8, 139.7, 100.9, 100.2, 62.0, 42.4, 26.9. IR ν 3273, 2950, 2874, 1439, 1371, 1342, 1163, 1041, 1018, 995, 876, 781, 704, 654, 606. MP=120°C.



Synthesis of 4.25: Compound **4.24** (5 g, 13.1 mmol), triphenylphosphine (10.2 g, 39.2 mmol), ground iodine (9.94 g, 39.2 mmol), and imidazole (2.67 g, 39.2 mmol) were added to a solution of 50 mL ether and 50 mL acetonitrile in a round bottom flask. After 12 h the solvent was removed and the mixture dissolved in dichloromethane and stirred in aqueous sodium sulfite. The organic layer was separated and dried over MgSO_4 and filtered. The solvent was removed and the crude solid purified by chromatography on silica gel (methylenechloride:hexane, 1:10) to yield **4.25** (5.90 g, 92 %). ^1H NMR (CDCl_3): δ 7.66 (d, 2H), 3.28 (m, 2H), 3.19 (m, 2H), 2.34 (s, 3H). ^{13}C NMR (CDCl_3): δ 141.6, 140.3, 139.8, 139.7, 100.9, 100.2, 62.0, 42.4, 26.9. IR ν 3273, 2950, 2874, 1439, 1371, 1342, 1163, 1041, 1018, 995, 876, 781, 704, 654, 606. MP=115-120°C.



Synthesis of 4.26: Compound **4.25** (2.00 g, mmol) was dissolved in dry tetrahydrofuran (50 mL) and under nitrogen purge a mixture of 1-octanethiol (2.35 g, 16.1 mmol) and NaH (386 mg, 16.1 mmol) (80% in mineral oil) in dry tetrahydrofuran was added dropwise. The mixture was allowed to stir at 40°C for 24 h. The mixture was slowly poured onto water and washed with hexane. The organic solution was washed with 0.5 N HCl (150 mL) and then with water. The organic layer was separated and dried. The solvent was removed, and the crude solid purified by chromatography over silica gel (4:6, dichloromethane:hexane) to yield **4.26** as a colorless solid (1.78 g, 86 %). ^1H NMR (CDCl_3): δ 7.63 (s, 2H), 2.85 (m, 2H), 2.69 (m, 2H), 2.65 (t, 2H), 2.32 (s, 3H), 1.67 (m, 2H), 1.38 (m, 2H), 1.23 (m, 8H), 0.83 (t, 3H). ^{13}C NMR (CDCl_3): δ 142.4, 414.5, 139.8, 139.3, 100.9, 99.6, 40.3, 32.2, 31.8, 29.7, 29.2, 28.9, 26.9, 22.6, 14.1. IR: ν 2955, 2923, 2850, 2736, 1736, 1461, 1376, 1343, 1263, 1223, 1189, 1043, 1014, 872, 761, 723. ES^+ MS (EI) calcd. $[\text{C}_{17}\text{H}_{26}\text{I}_2\text{O}_1]$, 516.26; C, 39.55; H, 5.08; found fragmentation 290.2; C, 41.16; H, 5.9; MP: 86-88°C.



Synthesis of Polymer 4.27: Monomer **4.26** (1.00 g, 1.94 mmol) and 2,5-didodecyl-1,4-dichlorobenzene (0.682 g, 1.96 mmol) were dissolved in tetrahydrofuran (3 mL) and piperidine (3 mL) in an oven dried Schlenk flask. The flask was flushed with nitrogen and frozen and evacuated three times after which $(\text{P}(\text{Ph})_3)_2\text{PdCl}_2$ (13.6 mg, 19.4 mmol), and CuI (3.7 mg, 19.4 mmol) were added. The mixture was allowed to stir at room temperature for 48 h. The solvent was removed and the mixture dissolved in dichloromethane, washed with 1N HCl, 1N NH_4OH , and water. The organic layer was dried over MgSO_4 and the solvent removed. The resulting polymer was dissolved in dichloromethane and precipitated out of methanol three times to yield **4.27** (1.08 g, 91 %). ^1H NMR (CDCl_3): δ 7.40 (m, 2H), 7.26 (m, 2H), 3.10 (m, 2H), 2.85 (m, 6H), 2.40 (m, 5H), 1.80 (m, 2H), 1.57 (m, 2H), 1.24 (m, 26H) 0.86 (m, 9H). ^{13}C NMR (TCE): δ 141.0, 140.6, 140.2, 139.6, 139.4, 139.3, 137.8, 133.5, 133.0, 132.7, 132.3, 123.4, 123.0, 122.7, 94.2, 92.0, 40.2, 38.5, 32.7, 32.6, 32.6, 32.4, 31.7, 29.7, 29.1, 29.1, 28.9, 28.7, 25.6, 23.0, 22.5, 13.9, 10.8. IR: ν 3023, 2963, 2884, 2874, 2848, 2731, 2200, 1776, 1507, 1452, 1378, 1256, 1248, 1216, 1191, 1096, 1035, 932, 892, 763. GPC (polystyrene standards) $M_n=8,767$, $\text{PDI}=1.946$.

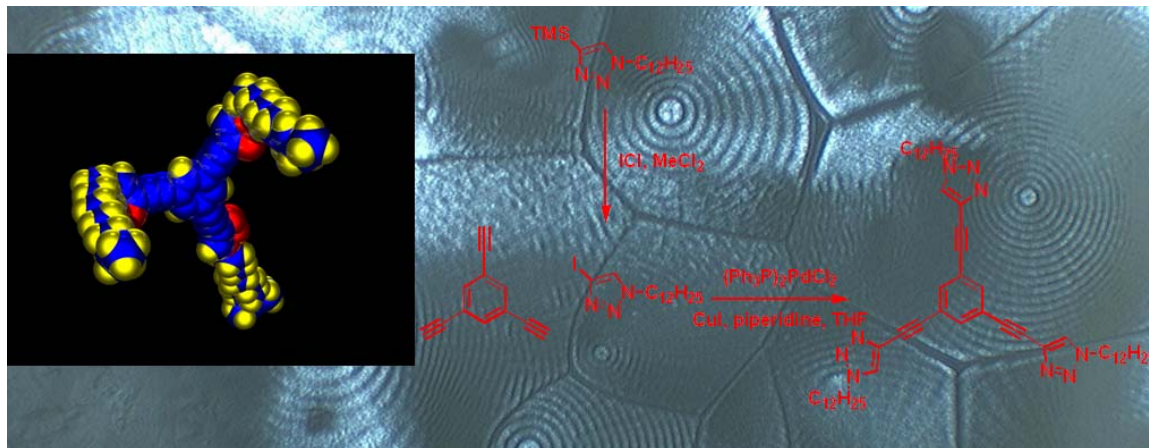
4.6 References:

1. (a) Mitschke, U.; Bauerle, P. *J. Mater. Chem.* **2000**, 10, 1471-1507. (b) Pinto, M.; Kristal, B.; & Schanze, K. *Langmuir* 2003, 19, 6523-6533.
2. Zhou, Q & Swager, T. M. *J. Am. Chem. Soc.* **1995**, 117, 12593-12602.
3. Dieck, H. A.; Heck, R. F. *J. Organomet. Chem.* **1975**, 93, 259.
4. Renzoni, A.; Zino, F.; Franchi, E. *Environ. Res.* **1998**, 77, 68-72.
5. Harris, H. H.; Pickering, I. J.; George, G. N. *Science*. **2003**, 301, 1203.
6. McKeown-Eyssen, G. E.; Ruedy, J; Neims, A. *Am. J. Epidemiol.* **1983**, 118, 470-479.
7. Prodi, L.; Bargossi, C.; Montalti, M.; Zaccheroni, N.; Su, N.; Bradshaw, J. S.; Izatt, R. M.; Savage, P. B. *J. Am. Chem. Soc.* **2000**, 122, 6769-6770.
8. Takeuchi, T.; Morikawa, N.; Matsumoto, H.; Shiraishi, Y. *Acta Neuropathol.* **1962**, 2, 40-57.
9. Matsumoto, H.; Koya, G.; Takeuchi, T.; et al. *J. Neuropathol. Exp. Neurol.* **1965**, 24, 563-574.
10. Harada, M. *Crit. Rev. Toxicol.* 1995, 25, 1-24.
11. Nolan, E. M. & Lippard, S. J. *J. Am. Chem. Soc.* **2003**, 125, 14270-14271.
12. McCoy, Ray K.; Karasz, Frank E.; Sarker, Ananda; Lahti, Paul M. *Chemistry of Materials*. **1991**, 3(5), 941-7.
13. Schwierz, Holger; Voegtler, Fritz. Kekule-Inst. Organische Chemie Biochemie, Univ. Bonn, Bonn, Germany. *Synthesis* **1999**, (2), 295-305.
14. Rozen, Shlomo; Brand, Michael; Lidor, Rami. Raymond and Beverly Sackler Fac. Exact Sci., Tel-Aviv Univ., Tel Aviv-Jaffa, Israel. *Journal of Organic Chemistry*. **1988**, 53(23), 5545-7.

15. Tan, C.; Pinto, M.& Schanze, K. *Chemical Communications*. **2002**, 10, 446.
16. Hundertmark, T.; Littke, A. F.; Buchwald, S. L.; Fu, G. C.; *Org. Lett.*; (Communication); **2000**; 2(12); 1729-1731.
17. Wheland, R. C.; Martin, E. L. *Journal of Organic Chemistry*. **1975**, 40(21), 3101-9.
18. Wilson, James N.; Windscheif, Paul M.; Evans, Una; Myrick, Michael L.; Bunz, Uwe H. F. *Macromolecules*. **2002**, 35(23), 8681-8683.
19. Erdogan, Belma; Wilson, James N.; Bunz, Uwe H. F. *Macromolecules*. **2002**, 35(21), 7863-7864.
20. Zhou, Qin; Swager, Timothy M. *Journal of the American Chemical Society*. **1995**, 117(50), 12593-602.
21. Ciufolini, Marco A.; Browne, Margaret E. *Tetrahedron Letters* **1987**, 28(2), 171-174.
22. Avery, M. A.; Gaston, M. A.; Vroman, J. A.; Wu, B.; Ager, A.; Peters, W; Robinson, B. L; and Charman, W. *J. Med. Chem.* **2002**, 45, 4321-4335.
23. Halila, Sami; Benazza, Mohammed; Demailly, Gilles. *Carbohydrate Research* **2003**, 338(2), 177-182.
24. Erdogan Belma; Song Lulu; Wilson James N; Park Jung O; Srinivasarao Mohan; Bunz Uwe H F. *Journal of the American Chemical Society* **2004**, 126(12), 3678-9.

CHAPTER 5

SELECTIVE CLICK CHEMISTRY VIA MICROWAVE AS AN APPROACH TO NEW SMALL MOLECULES.



5.1 Introduction.

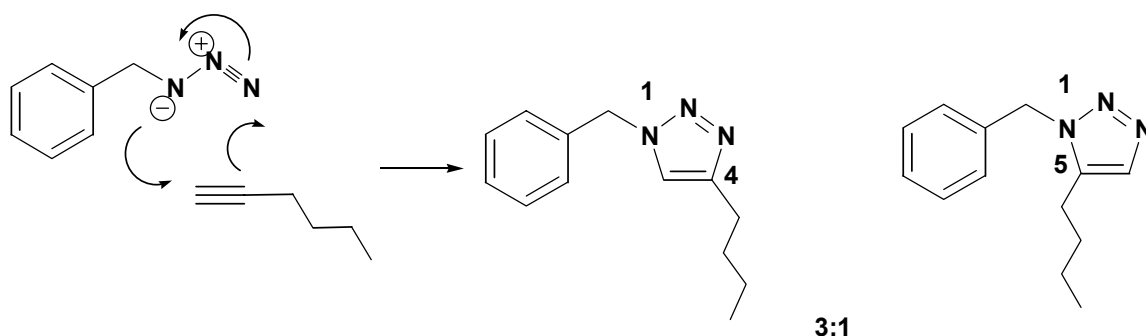
Click chemistry is a set of powerful, reliable, and selective reactions for the rapid synthesis of useful new compounds and combinatorial libraries through heteroatom links.¹ Click chemistry is enabled and defined by a handful of “spring-loaded” reactions. According to Sharpless, for a reaction to be termed “click chemistry,” that process must be modular, wide in scope, give very high yields, and generate only inoffensive byproducts that can be removed by nonchromatographic methods.¹ Required process characteristics include simple reaction conditions (insensitivity to oxygen and water), readily available starting materials and reagents, the use of benign solvents (such as water), and simple product isolation.¹ Click reactions have a high thermodynamic

driving force, usually greater than 20 kcal mol⁻¹. Processes such as these proceed rapidly to completion and also tend to be selective for a single product.¹

Carbon-heteroatom bond forming reactions are among the most common examples of click reactions, and they include the following classes of chemical transformations:

- cycloadditions of unsaturated species such as 1,3-dipolar cycloaddition reactions as well as the Diels-Alder family of transformations;
- nucleophilic substitution chemistry, particularly ring-opening reactions of strained heterocyclic electrophiles such as epoxides, aziridines, aziridinium ions, and episulfonium ions;
- carbonyl chemistry of the “non-aldol” type, such as the formation of ureas, thioureas, aromatic heterocycles, oxime ethers, hydrazones, and amides;
- additions to carbon-carbon multiple bonds, especially oxidative cases such as epoxidation, dihydroxylation, aziridination, and sulfenyl halide additions, but also Michael additions of Nu-H reactants.¹

1,3-dipolar cycloadditions or Huisgen 1,3-dipolar cycloadditions² couple two unsaturated reactants to provide fast access to five-membered heterocycles. The cycloaddition of azides and alkynes to form triazoles is a very useful member of this family. Azides and alkynes are both highly energetic functional groups with narrow distributions of reactivity.² They do not disrupt biological molecules, and are even stable toward the conditions found inside living cells.³ Typically, under thermal conditions, this reaction yields a mixture of 1,4 and 1,5 triazoles (Scheme 4.1).



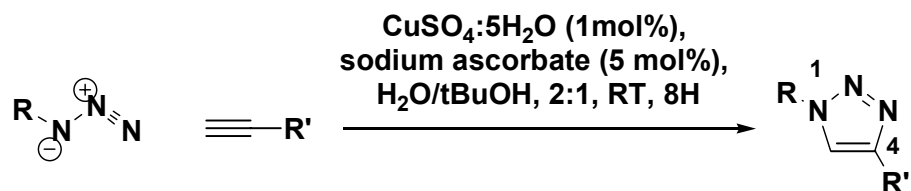
Scheme 5.1. Thermal formation of 1,4 and 1,5 triazoles.

1,4-triazoles are useful in organic synthesis and drug design.^{4a} One of the first reports of selectivity for the 1, 4-triazole was reported by Meldal using diisopropylamine and copper iodide on solid phase resins.^{4a} This approach lead to the formation of only the 1, 4 adduct. Sharpless has shown on various substrates that this reaction yields only the 1,4-triazole when using copper sulfate and sodium ascorbate (Scheme 5.2).³ Other reports have shown that the 1,3-dipolar cycloaddition even takes place within a reversibly formed, self-assembled capsule with absolute regioselectivity.^{4b}

We began to explore the regioselectivity of this reaction and found that under microwave radiation the reactions of stannanes or silanes with azides were, in most cases, regioselective. We obtained excellent regioselectivity and were able to isolate 1,4-triazoles in high yields. We have synthesized a library of substituted triazoles (Figure 5.2 & 5.4) and highlighted their use in further synthetic strategies.

Stannanes and silanes are useful in organic synthesis and can undergo a number of transformations.⁵ They can be easily transformed into iodides (Scheme 5.3).^{6, 7} In our lab we frequently couple aromatic rings substituted with iodides to alkynes using the Heck-Cassar-Sonogahira-Hagihara reaction.⁸ We were intrigued with the idea of

incorporating triazoles into larger structures. Since trimethylsilyl and stannane functionalities could easily be exchanged for iodides, the only question that remained was, which 1,4-triazoles could be prepared.



Scheme 5.2. Copper catalyzed synthesis of 1,4-triazoles.

5.2 Results and Discussion.

Using various silane and stannane substituted acetylenes, we were able to synthesize various triazoles **5.6-5.30** (Figure 5.1). In most cases the 1,4-triazole was easily isolated with no trace of the 1,5 adduct. Single crystal analysis (Figure 5.2) and NMR assured that our stereochemical assignment. This approach has the obvious advantage, that there is virtually no work up, only the removal of the solvent under vacuum resulting in products which give accurate elemental analysis.

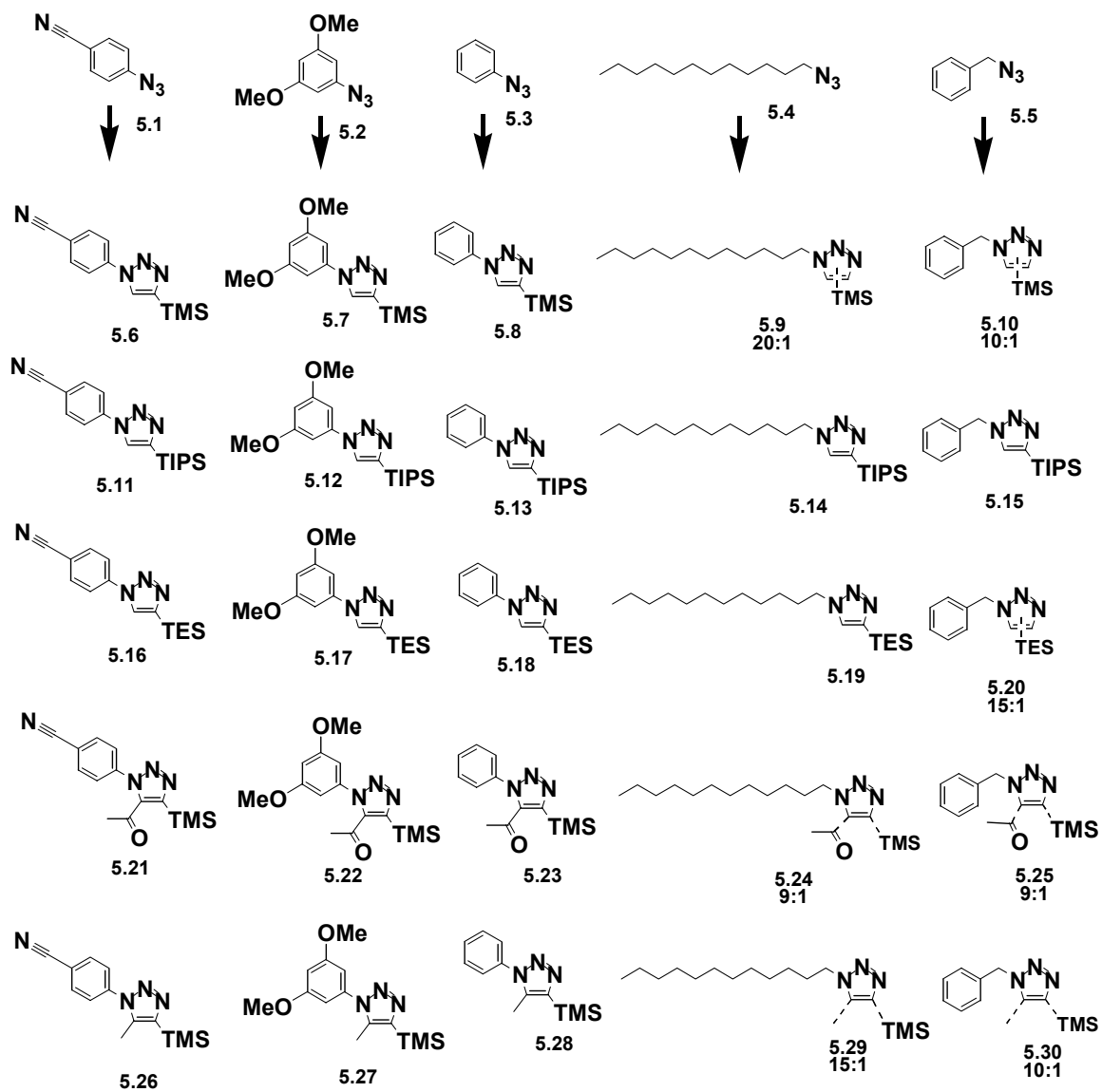


Figure 5.1. Series of silane substituted triazoles obtained under thermal conditions in a CEM discovery microwave system.

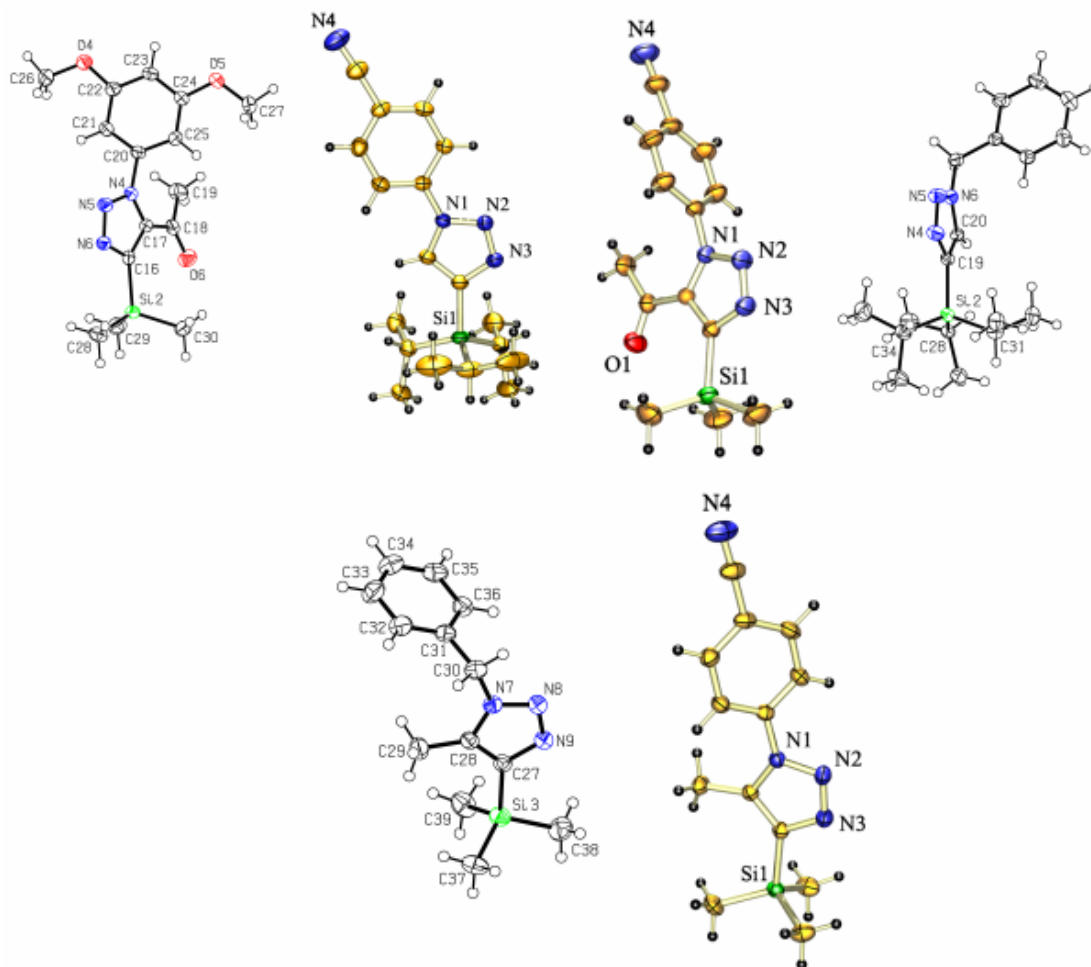
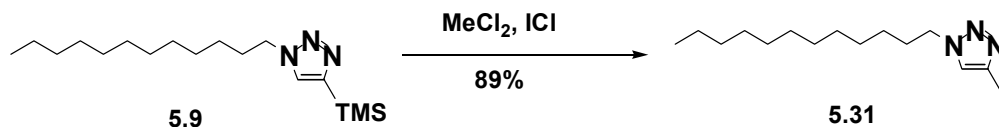


Figure 5.2. ORTEP plots of compounds **5.6**, **5.7**, **5.15**, **5.21**, **5.26**, and **5.30**.

Iodine monochloride can be used to iodinate aromatic rings.⁸ It can also be used to replace trimethylsilane groups with iodines.⁷ Due to iodine monochloride's ability to iodinate aromatic rings, we were unable to transform any triazoles containing aromatic rings in Figure 5.2 into the corresponding iodines as planned.

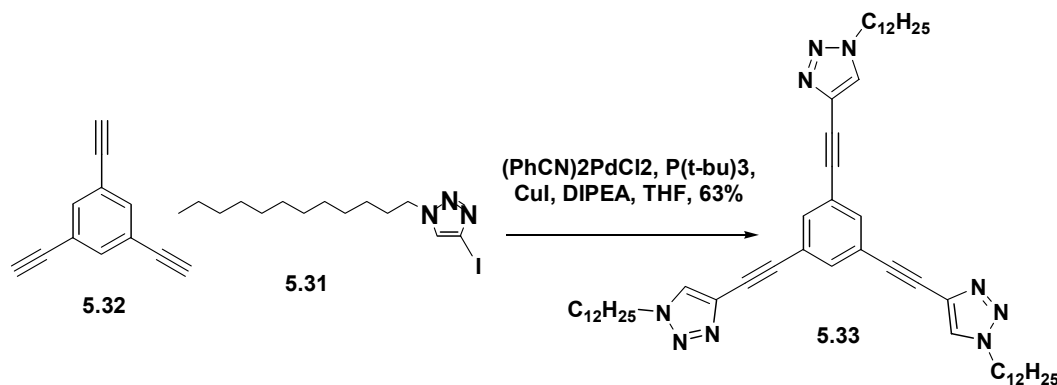
Compound **5.9** can be obtained in excellent yield. Though it is a 20:1 mixture of the 1,4 and 1,5 triazole, it can be purified. Due to the hardy nature of its precursor silane,

treatment with iodine monochloride in dichloromethane gives **5.31** in a yield of 89 % (Scheme 5.3).^{7, 8}



Scheme 5.3. Synthesis of iodine substituted 1,4-triazoles from the corresponding silanes.

Compound **5.31** could be coupled to 1,3,5-triethynyl benzene to yield **5.33** in 63% yield. Compound **5.33** crystallizes easily out of ethanol and single crystal X-ray analysis reveals that the triazole rings are slightly twisted with respect to the central benzene ring (Figure 5.4). Two of the triazole rings are oriented with nitrogens on the same side of the molecule while the third triazole's nitrogens face the opposite side of the molecule. Rubbed polyimide slides of **5.33** are shown in the chapter heading. While structure can be observed without polyimide; the image quality is much less. DSC data indicates however that **5.33** is not liquid crystalline.



Scheme 5.4. Use of iodine substituted triazole **5.31** to yield conjugated molecules.

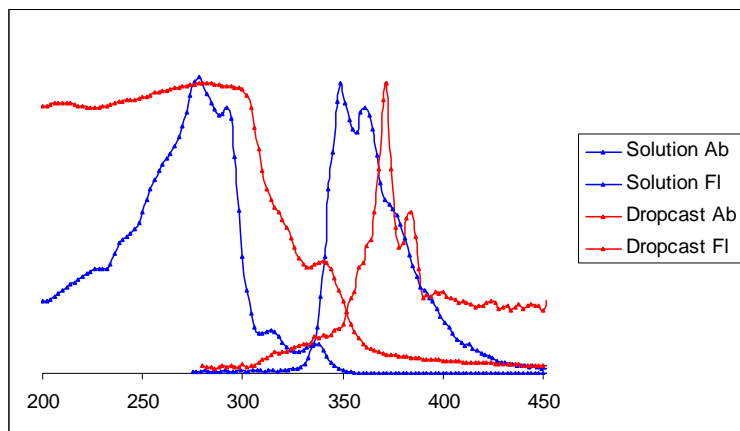


Figure 5.3. Optical properties of compound **5.33** in solution and thin-film.

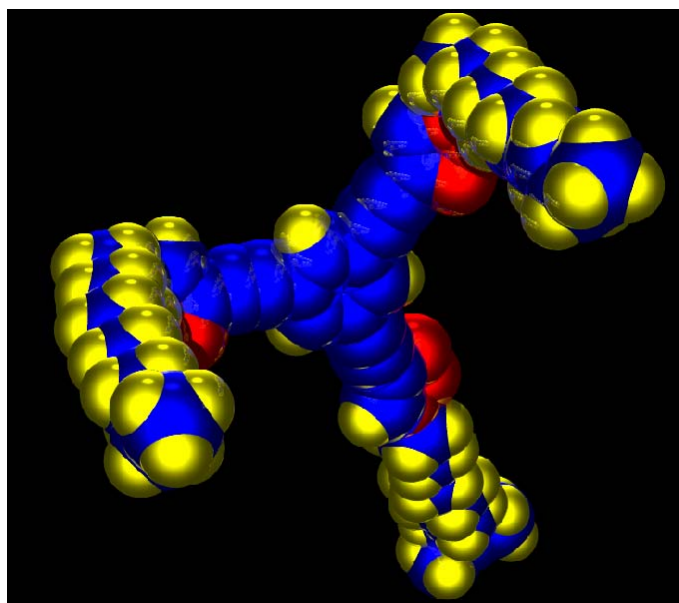


Figure 5.4. Single crystal X-ray analysis of **5.33** reveals that the triazole rings are slightly twisted with respect to the central benzene ring.

While compound **5.33** could be interesting for small molecule electronic devices, it would be more useful to have a larger selection of iodine substituted triazoles. Since

iodine monochloride did not furnish the majority of iodines desired, we opted to synthesize the corresponding triazoles from the corresponding stannane compounds (Scheme 5.4).

This offers the advantage of being able to obtain any of the desired iodo compounds without having to use iodine monochloride. Again, we synthesized a library of triazoles (Figure 5.5). Preliminary results indicate that molecular iodine can be used for the transformation, and the corresponding stannanes can be converted into the iodo compounds which we desire (Scheme 5.6 and 5.7).⁸ Compound **5.33** should be easily obtained via both synthetic routes in only slightly different overall yields (Scheme 5.5).

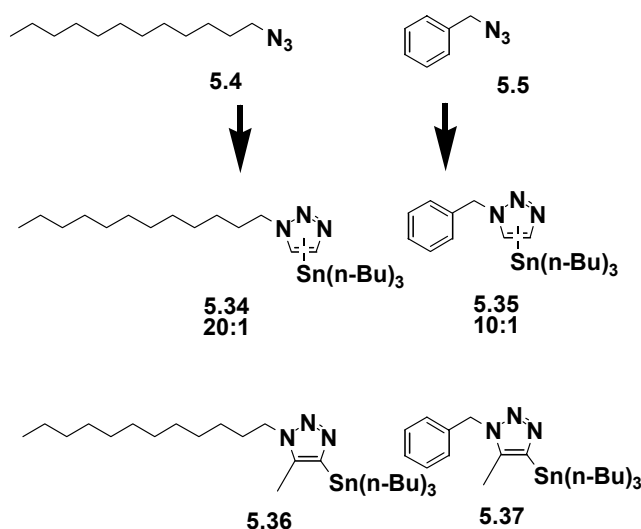
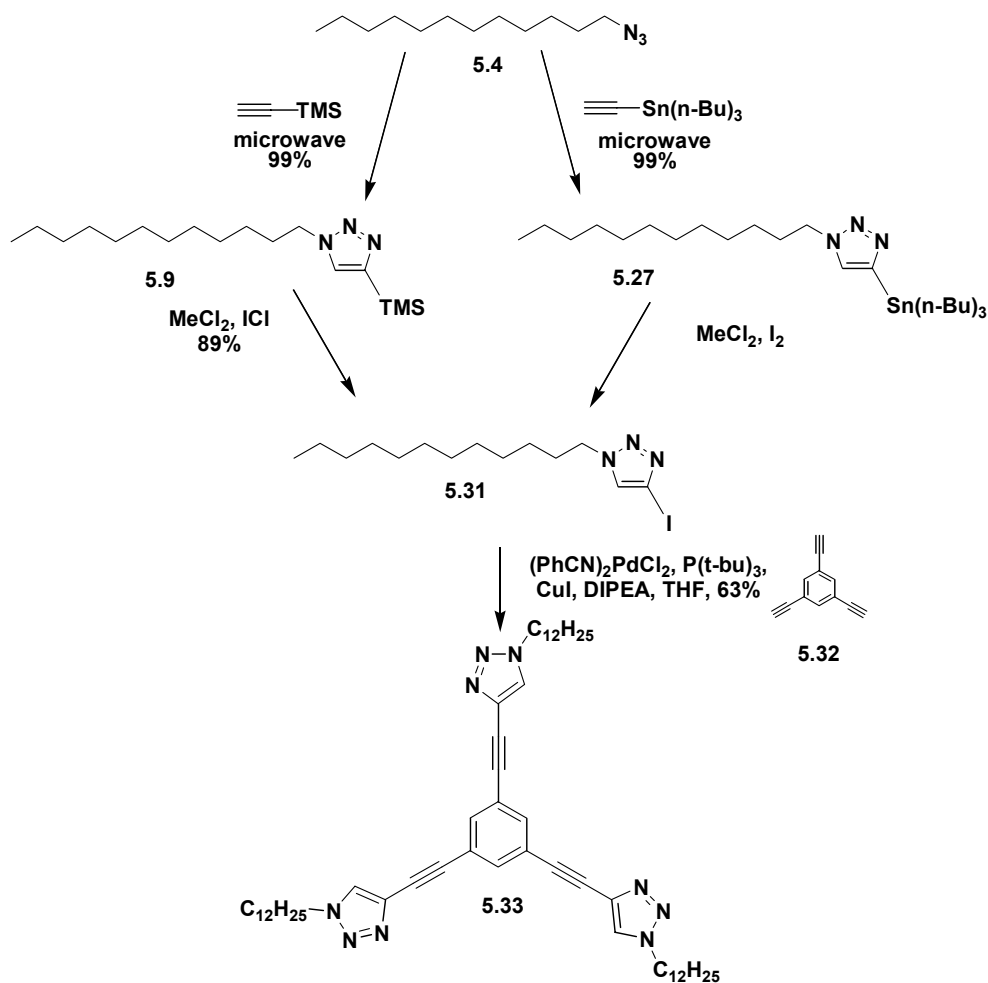
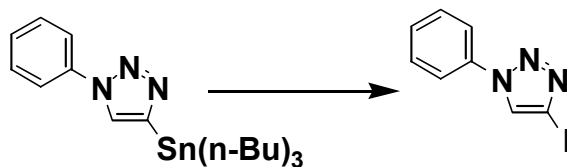


Figure 5.5. Series of stannane substituted triazoles obtained under thermal conditions in a CEM discovery microwave system.



Scheme 5.5. Synthesis of stannane substituted 1,4-triazoles and subsequent conversion to the corresponding iodine substituted 1,4-triazoles.

The next logical step is to produce more conjugated molecules like **5.33** employing the method outlined in Scheme 5.5. So far, conversion of the stannane substituted triazoles to the corresponding iodines has proceeded without any evidence of iodination of their aromatic components (Scheme 5.6). This work is currently underway in our group, and assuming the triazole functionality survives the process, many different molecules should become available.



Scheme 5.6. No iodination of the aromatic rings in 1-Phenyl-4-iodotriazole has been evidenced by preliminary ^1H NMR or ^{13}C NMR experiments.

5.3 Conclusion.

Initial work has been done detailing a promising approach to the synthesis of conjugated molecules. These methods allow incorporation of triazoles into small conjugated molecules. With further exploration, this could lead to the formation of materials useful for small molecule electronic devices or other applications. Two of the primary obstacles which must be overcome are the further conversion to the iodo substituted triazoles, as well as the ready made synthesis of a large library of these molecules and the further exploration of their properties. Due to the high yield and selectivity for one product, this chemistry would be an excellent choice for the functionalization of polymers.

5.4 Experimental

Instrumentation. The ^1H and ^{13}C NMR spectra were taken with a Varian 300 MHz or a Varian 400 MHz spectrometer using broadband probe. The ^1H chemical shifts are referenced to the residual proton peaks of CDCl_3 at δ 7.24(vs. TMS). The ^{13}C resonance is referenced to the central peak of CDCl_3 at δ 77.0 (vs. TMS). Azides 4 and 5 were prepared in accordance to published procedures. Compounds **5.1**, **5.2**, **5.3**, **5.4**, **5.5**, **5.6**, **5.7**, **5.8**, **5.11**, **5.12**, **5.13**, **5.16**, **5.17**, **5.18**, **5.21**, **5.22**, **5.23**, **5.26**, **5.27**, **5.28** were

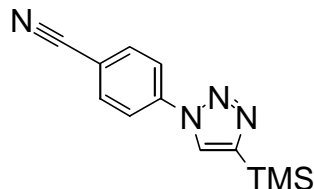
produced graciously by coworker Selma Bakbak. Compounds **5.1-5.5** were produced in accordance with literature procedures. Thanks go out to Benjamin Nehls and Selma Bakbak for their thought, work, and input on this project.

General procedure for compounds 5.6-5.30 and 5.34-5.37. The corresponding azide (1 eq) and the corresponding acetylene (3 eq) were placed in a microwavable reaction vessel. Reactions which consisted of only reactants that were liquids at room temperature were performed with no solvent. Reactions in which one or more of the starting materials were solids were performed using toluene as a solvent. Starting materials were irradiated in a CEM discovery microwave system (250 watt, 155°C, 300 psi) for 25 minutes. The reaction vessel was allowed to cool to room temperature before being opened. Solvents were removed under vacuum, and solid products were crystallized and liquid products were distilled.

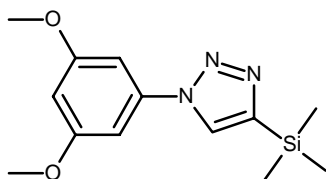
Synthesis of 5.31, iodides from silanes and stannanes. The corresponding silane or stannane and ICl (in the case of the silane) ground iodine (in the case of the stannane) (2-5 eq) were placed in a round bottom flask and stirred for 48 h. The reaction mixture was poured onto aqueous sodium sulfate and stirred until yellow. The organic layer was washed with water and dried over magnesium sulfate. The solvent was removed under vacuum and the crude product purified by recrystallization followed by chromatography over silica gel.

Visual observation of structure in 5.33 as seen in the chapter header. Rubbed polyimide is used as a substrate to aid in the visual observation of structure. One part PI 2556 (HD Microsystems) was diluted with two parts N-

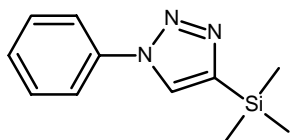
methyl-2-pyrrolidone. The dilute polyimide solution was applied on the cleaned surface, after being washed with acetone, of glass slide, and spin-coated at 2000 rpm for five min. Coated glass slides were dried at 100°C to remove solvent and baked at 180°C for 2 h. Polyimide surface was rubbed in one direction with clean tissue. Several drops of a concentrated solution of **5.33** in 1,4-Dioxane was applied, and the slide was heated up to 80°C, and then cooled down slowly to room temperature. The texture on the slide was observed using polarized optical microscope Leica DMRX.



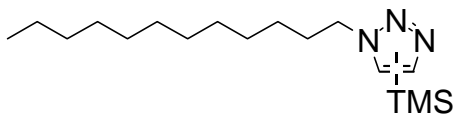
Synthesis of 5.6: Following the general procedure outlined above azide **5.1** and trimethyl silyl acetylene were reacted to yield the 1, 4-triazole. The solvent was removed under reduced pressure and the remaining solid was distilled under reduced pressure to yield **5.6** as a colorless solid (89 %). ^1H NMR (CDCl_3): δ 8.00 (s, 1 H), 7.91 (d, 2 H), 7.79 (d, 2 H), 0.35 (s, 9 H); ^{13}C NMR (CDCl_3): δ 148.2, 139.7, 133.7, 126.6, 120.6, 117.7, 111.9, -1.1; IR: ν 3747, 3126, 3100, 2955, 2899, 2805, 2399, 2226, 1944, 1878, 1605, 1511, 1482, 1426, 1393, 1291, 1247, 1204, 1198, 1147, 1110, 1040, 984, 843, 822, 761, 705, 634, 557. MP: 130 °C.



Synthesis of 5.7: Following the general procedure outlined above azide **5.2** and trimethyl silyl acetylene were reacted to yield the 1, 4-triazole. The solvent was removed under reduced pressure and the remaining solid was distilled under reduced pressure to yield **5.7** as a colorless solid (78 %). ^1H NMR (CDCl_3): δ 7.93 (s, 1 H), 6.78 (m, 2 H), 6.33 (m, 1 H), 3.67 (s, 6 H), 0.25 (s, 9 H); ^{13}C NMR (CDCl_3): δ 161.0, 146.7, 138.1, 127.0, 99.9, 98.8, 55.4, -1.3; IR: ν 3127, 2897, 2838, 1599, 1488, 1338, 1248, 1206, 1067, 988, 929, 839, 757, 680, 633. MP 84°C.

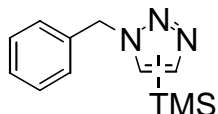


Synthesis of 5.8: Following the general procedure outlined above azide **5.3** and trimethyl silyl acetylene were reacted to yield the 1, 4-triazole. The solvent was removed under reduced pressure and the remaining solid was distilled under reduced pressure to yield **5.8** as a colorless solid (82 %). ^1H NMR (CDCl_3): δ 7.93 (s, 1 H), 7.69 (m, 2 H), 7.48 (m, 2 H), 7.38 (m, 1 H), 0.34 (s, 9 H); ^{13}C NMR (CDCl_3): δ 147.1, 136.9, 129.5, 128.3, 127.0, 120.6, -1.1; IR: ν 3740, 3137, 2953, 2894, 2247, 1957, 1878, 1747, 1600, 1505, 1464, 1207, 1156, 1044, 856, 744, 686, 632. MP: 99 °C.

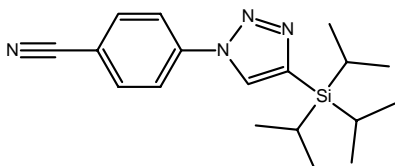


Synthesis of 5.9: Following the general procedure outlined above dodecyl azide **5.5** and trimethyl silyl acetylene were reacted to yield a 20:1 mixture of regioisomers favoring the 1, 4-triazole. The solvent was removed under reduced pressure and the remaining liquid was distilled under reduced pressure to yield **5.27** as a clear oil which solidified under reduced pressure (92%). ^1H NMR (CDCl_3): δ 0.25 (s, 9H), 0.29 (s, 0.45), 0.85 (t,

3H), 1.19 (m, 18H), 1.83 (m, 2H), 4.32 (m, 2H), 7.46 (m, 1H). ^{13}C NMR (CDCl_3): δ -0.7, 14.4, 23.0, 26.8, 27.0, 29.3, 29.6, 29.6, 29.8, 29.9, 30.8, 32.2, 49.9, 50.8, 128.8, 146.4. IR: ν 725, 816, 1193, 1248, 1465, 1488, 2851, 2952. Anal. Calculated for, $\text{C}_{17}\text{H}_{35}\text{N}_3\text{Si}$: C, 65.96; H, 11.40; N, 13.57; Si, 9.07, 309.57, found C, 65.97; H, 11.59; N, 13.4; MP: 30 $^\circ\text{C}$.

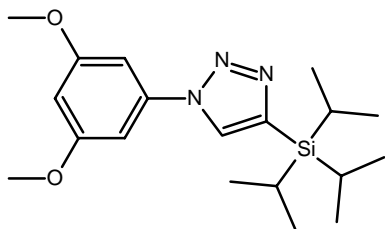


Synthesis of 5.10: Following the general procedure outlined above benzyl azide **5.4** and trimethyl silyl acetylene were reacted to yield **5.21** as a 10:1 mixture of regioisomers favoring the 1, 4-triazole. The solvent was removed under reduced pressure and the remaining solid recrystallized from ethanol to yield **5.21** as a white crystalline solid (86%). ^1H NMR (CDCl_3): δ 0.19 (s, 0.9H), 0.26 (s, 9H), 5.53 (m, 2H), 5.62 (s, 0.2H), 7.24 (m, 2H), 7.30 (m, 3H), 7.43 (m, 1H) 7.73 (s, 0.1H), ^{13}C NMR (CDCl_3): δ -0.7, 53.6, 128.2, 128.6, 129.0, 129.1, 135.2. IR: ν 1053, 1192, 1238, 1320, 1354, 1415, 1446, 1457, 1457, 1483, 1497, 2899, 2955, 3025, 3087, 3105. Anal. Calculated for, $\text{C}_{13}\text{H}_{19}\text{N}_3\text{Si}$: C, 62.29; H, 7.41; N, 18.16; Si, 12.14, found C, 62.25; H, 7.36; N, 18.11; MP: 48 $^\circ\text{C}$.

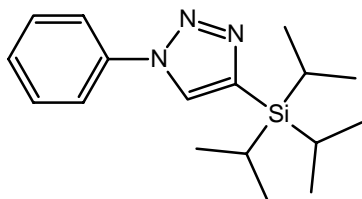


Synthesis of 5.11: Following the general procedure outlined above azide **5.1** and trimethyl silyl acetylene were reacted to yield the 1, 4-triazole. The solvent was removed under reduced pressure and the remaining solid was distilled under reduced pressure to yield **5.11** as a colorless solid (91 %). ^1H NMR (CDCl_3): δ 8.08 (s, 1 H), 7.94 (d, 2 H), 7.76 (d, 2 H), 1.32, (m, 3 H), 1.05 (d, 18 H); ^{13}C NMR (CDCl_3): δ 143.6, 139.6, 133.5,

127.5, 120.4, 117.6, 111.5, 18.4, 11.0; IR: ν 3830, 3082, 2946, 2865, 2840, 2227, 1928, 1800, 1606, 1516, 1508, 1480, 1460, 1427, 1395, 1204, 1145, 1037, 1017, 882, 845, 804, 683, 556, 519, 431. MP: 71 °C.

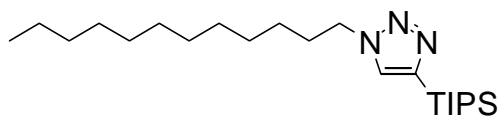


Synthesis of 5.12: Following the general procedure outlined above azide **5.2** and trimethyl silyl acetylene were reacted to yield the 1, 4-triazole. The solvent was removed under reduced pressure and the remaining solid was distilled under reduced pressure to yield **5.12** as a colorless solid (89 %). ^1H NMR (CDCl_3): δ 7.93 (s, 1 H), 6.93 (m, 2 H), 6.43 (m, 1 H), 3.85 (s, 6 H), 1.41 (m 3 H), 1.13 (d, 18 H); ^{13}C NMR (CDCl_3): δ 161.3, 142.6, 138.4, 128.0, 100.0, 99.0, 55.7, 18.6, 11.2; IR: ν 3122, 2941, 2863, 1602, 1490, 1460, 1318, 1272, 1209, 1202, 1162, 1135, 1016, 883, 8318, 681, 653, 580, 519. MP: 83 °C. MP 82°C.

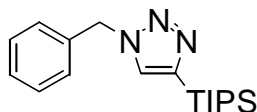


Synthesis of 5.13: Following the general procedure outlined above azide **5.1** and trimethyl silyl acetylene were reacted to yield the 1, 4-triazole. The solvent was removed under reduced pressure and the remaining solid was distilled under reduced pressure to yield **5.12** as a colorless solid (69 %). ^1H NMR (CDCl_3): δ 7.96 (s, 1 H), 7.75 (m, 2 H), 7.50 (m, 2 H), 7.40 (m, 1 H), 1.41 (m 3 H), 1.12 (d, 18 H); ^{13}C NMR (CDCl_3): δ 142.7, 137.0, 129.5, 128.2, 127.8, 120.5, 18.7, 11.2; IR: ν 3122, 3059, 2962, 2864, 2253, 1955,

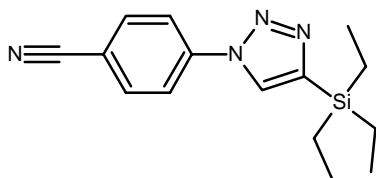
1885, 1676, 1597, 1506, 1463, 1456, 1339, 1202, 1148, 1073, 1047, 1017, 916, 883, 761, 757, 710, 693, 577. MP: 53 °C.



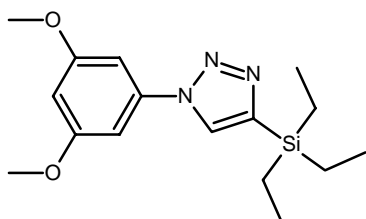
Synthesis of 5.14: Following the general procedure outlined above dodecyl azide **5.5** and trimethyl silyl acetylene were reacted. The solvent was removed under reduced pressure and the remaining liquid was distilled under reduced pressure to yield **5.29** as a clear oil (88%). ¹H NMR (CDCl₃): δ 0.839 (t, 3H), 1.03 (d, 18H), 1.19 (m, 18H), 1.34 (m, 3H), 4.33 (m, 2H), 7.48 (m, 1H). ¹³C NMR (CDCl₃): δ 11.3, 14.6, 19.2, 23.1, 27.1, 29.4, 30.0, 32.3, 50.1, 130.3, 142.1. IR: ν 649, 883, 1189, 1462, 2880, 2952. Anal. calculated for, C₂₃H₄₇N₃Si: C, 70.16; H, 12.03; N, 10.67; Si, 7.13, found C, 70.27; H, 12; N, 10.51. MP: 45°C.



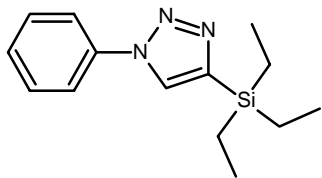
Synthesis of 5.15: Following the general procedure outlined above benzyl azide **5.4** and triisopropyl silyl acetylene were reacted. The solvent was removed under reduced pressure, and the remaining solid was recrystallized from ethanol to yield **5.22** as a white crystalline solid (92%). ¹H NMR (CDCl₃): δ 1.03 (d, 18H), 1.34 (m, 3H), 5.54 (m, 2H), 7.17 (m, 2H), 7.28 (m, 3H), 7.46 (m, 1H). ¹³C NMR (CDCl₃): δ 11.4, 18.9, 126.9, 127.8, 128.5, 129.1, 130.3, 135.4, 142.4. IR: ν 693, 780, 1455, 1496, 1662, 1689, 2895, 2989. Anal. Calculated for, C₁₈H₂₉N₃Si: C, 68.52; H, 9.26; N, 13.32, found C, 68.28; H, 9.11; N, 13.16; MP: 53 °C.



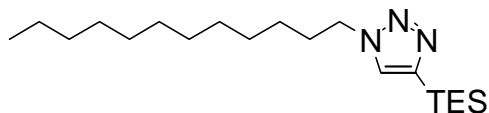
Synthesis of 5.16: Following the general procedure outlined above azide **5.1** and trimethyl silyl acetylene were reacted to yield the 1, 4-triazole. The solvent was removed under reduced pressure and the remaining solid was distilled under reduced pressure to yield **5.16** as a colorless solid (93 %). ^1H NMR (CDCl_3): δ 8.00 (s, 1 H), 7.94 (d, 2 H), 7.83 (d, 2 H), 1.03, (t, 9 H), 0.89 (q, 6 H); ^{13}C NMR (CDCl_3): δ 145.9, 140.0, 134.0, 127.3, 120.9, 118.0, 112.2, 7.7, 3.8; IR: ν 3420, 3138, 3103, 3060, 2954, 2950, 2932, 2874, 2417, 2226, 1924, 1604, 1504, 1480, 1425, 1321, 1268, 1233, 1202, 1142, 1109, 1036, 1005, 984, 842, 829, 599, 556, 476. MP: 78 °C.



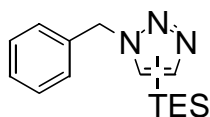
Synthesis of 5.17: Following the general procedure outlined above azide **5.2** and trimethyl silyl acetylene were reacted to yield the 1, 4-triazole. The solvent was removed under reduced pressure and the remaining solid was distilled under reduced pressure to yield **5.17** as a colorless solid (86 %). ^1H NMR (CDCl_3): δ 7.91 (s, 1 H), 6.88 (m, 2 H), 6.43 (m, 1 H), 3.79 (s, 6 H), 0.99 (t, 9 H), 0.84 (q, 6 H); ^{13}C NMR (CDCl_3): δ 161.1, 144.2, 138.3, 127.5, 99.9, 98.8, 55.5, 7.3, 3.5; IR: ν 3122, 2874, 1599, 1456, 1301, 1197, 1158, 1133, 1061, 1013, 928, 828. MP°102



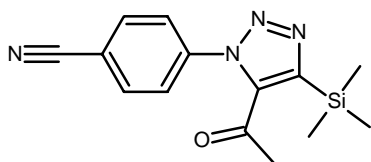
Synthesis of 5.18: Following the general procedure outlined above azide **5.3** and trimethyl silyl acetylene were reacted to yield the 1, 4-triazole. The solvent was removed under reduced pressure and the remaining solid was distilled under reduced pressure to yield **5.18** as a colorless solid (89 %). ^1H NMR (CDCl_3): δ 7.95 (s, 1 H), 7.66 (m, 2 H), 7.36 (m, 2 H), 7.26 (m, 1 H), 0.95 (t 9 H), 0.76 (q, 6 H); ^{13}C NMR (CDCl_3): δ 144.0, 136.6, 129.2, 127.9, 127.3, 120.1, 7.1, 3.3; IR: ν 3124, 3060, 2950, 2871, 2401, 2237, 1950, 1676, 1599, 1509, 1503, 1463, 1413, 1238, 1147, 1039, 984, 908, 800, 718. $T_m=108^\circ\text{C}$.



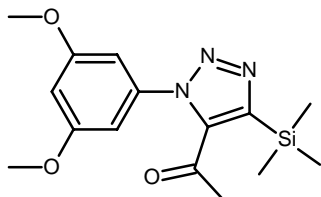
Synthesis of 5.15: Following the general procedure outlined above dodecyl azide **5.5** and trimethyl silyl acetylene were reacted. The solvent was removed under reduced pressure and the remaining liquid was distilled under reduced pressure to yield **5.26** as a clear oil (90%). ^1H NMR (CDCl_3): δ 0.76 (q, 6H), 0.94 (t, 9H) 1.17 (s, 9H), 0.83 (t, 3H), 1.23 (m, 18H), 1.80 (m, 2H), 4.30 (m, 2H), 7.46 (m, 1H). ^{13}C NMR (CDCl_3): δ 3.8, 7.6, 14.4, 23.0, 26.8, 29.2, 29.6, 29.6, 29.8, 29.9, 30.7, 32.2, 49.9, 129.5, 143.4. IR: ν 722, 1014, 1191, 1237, 1463, 1487, 2851, 2904. Anal. Calculated for, $\text{C}_{20}\text{H}_{41}\text{N}_3\text{Si}$: C, 68.31; H, 11.75; N, 11.95, found C, 68.48; H, 11.82; N, 12.05.



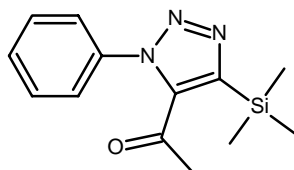
Synthesis of 5.20: Following the general procedure outlined above, benzyl azide **5.4** and triethyl silyl acetylene were reacted to yield **5.23** as a 15:1 mixture of regioisomers favoring the 1, 4-triazole. The solvent was removed under reduced pressure and the remaining solid was recrystallized from ethanol to yield **5.23** as a white crystalline solid (98%). ^1H NMR (CDCl_3): δ 0.72 (m, 6H), 0.90 (m, 9H), 5.51 (s, 2H), 5.62 (s, 0.13H), 7.20 (m, 2H), 7.30 (m, 3H), 7.45 (s, 1H), 7.60 (s, 0.06H). ^{13}C NMR (CDCl_3): δ 3.8, 8.1, 53.6, 126.9, 128.9, 129.6, 135.8, 144.6. IR: ν 994, 998, 1003, 1029, 1051, 1099, 1150.35, 1188, 1189, 1206, 1225, 1357, 1412, 1419, 1436, 1447, 1451, 1464, 1471, 1489, 1495.69, 2872, 2886, 2950. MP: 45 °C.



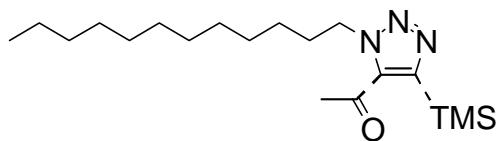
Synthesis of 5.21: Following the general procedure outlined above azide **5.3** and trimethyl silyl acetylene were reacted to yield the 1, 4-triazole. The solvent was removed under reduced pressure and the remaining solid was distilled under reduced pressure to yield **5.21** as a colorless solid (94 %). ^1H NMR (CDCl_3): δ 7.86 (d, 2 H), 7.59 (d, 2 H), 2.27 (s, 3 H), 0.44 (s, 9 H); ^{13}C NMR (CDCl_3): δ 190.7, 150.3, 142.4, 140.2, 133.8, 126.1, 117.6, 114.3, 31.4, -0.8; IR: ν 3053, 2958, 2233, 1943, 1817, 1677, 1608, 1513, 1478, 1435, 1425, 1412, 1361, 1303, 1251, 1243, 1156, 1100, 1057, 959, 848, 840, 756, 650, 570, 533. MP: 147 °C.



Synthesis of 5.22: Following the general procedure outlined above azide **5.2** and trimethyl silyl acetylene were reacted to yield the 1, 4-triazole. The solvent was removed under reduced pressure and the remaining solid was distilled under reduced pressure to yield **5.22** as a colorless solid (89 %). ^1H NMR (CDCl_3): δ 6.59 (m, 3 H), 3.82 (s, 6 H), 2.16 (s, 3 H), 0.37 (s, 9 H); ^{13}C NMR (CDCl_3): δ 191.0, 161.2, 150.0, 142.7, 137.9, 137.7, 103.8, 102.1, 55.8, 30.4, -1.3; IR: ν 3081, 2959, 2841, 1677, 1616, 1612, 1593, 1476, 1358, 1245, 1158, 1142, 1058, 1019, 970, 926, 847, 838, 768, 696, 635, 539. MP: 121 $^\circ\text{C}$.

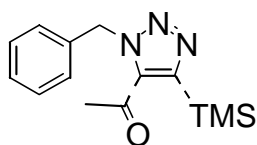


Synthesis of 5.23: Following the general procedure outlined above azide **5.3** and trimethyl silyl acetylene were reacted to yield the 1, 4-triazole. The solvent was removed under reduced pressure and the remaining solid was distilled under reduced pressure to yield **5.23** as a colorless solid (75 %). ^1H NMR (CDCl_3): δ 7.55 (m, 3 H), 7.46 (m, 2 H), 2.08 (s, 3 H), 0.35 (s, 9 H); ^{13}C NMR (CDCl_3): δ 191.0, 150.0, 143.0, 136.9, 130.5, 129.9, 125.6, 30.8, -1.0; IR: ν 3066, 2975, 2904, 1682, 1593, 1495, 1415, 1359, 1247, 1184, 1149, 1054, 1004, 963, 840, 768, 692. MP: 50 $^\circ\text{C}$.

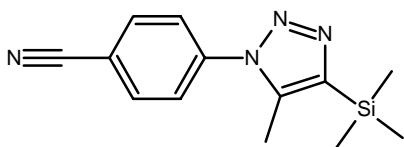


Synthesis of 5.24: Following the general procedure outlined above, dodecyl azide **5.5** and 4-trimethylsilyl-3-butyne-2-one were reacted to yield **5.28** as a 9:1 mixture of

regeoisomers favoring the 1, 4-triazole. The solvent was removed under reduced pressure, and the remaining liquid was distilled under reduced pressure to yield **5.28** as a dark oil (93%). ^1H NMR (CDCl_3): δ 0.23 (s, 1H), 0.38 (s, 9H), 0.83 (t, 3H), 1.19 (m, 18H), 1.83 (m, 2H), 4.37 (m, 2H), 7.46 (m, 1H). ^{13}C NMR (CDCl_3): δ -0.0, 14.4, 22.9, 26.8, 29.3, 29.6, 29.7, 29.8, 29.8, 30.7, 32.1, 50.7, 139.8, 149.8, 190.5. IR: ν 851, 1249, 1356, 1457, 1464, 16.79, 2849, 2947. Anal. calculated for, $\text{C}_{19}\text{H}_{37}\text{N}_3\text{OSi}$: C, 64.90; H, 10.61; N, 11.95; O, 4.55, found C, 65.98; H, 10; N, 12.32.

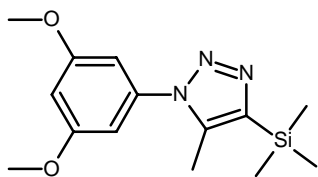


Synthesis of 5.25: Following the general procedure outlined above, benzyl azide **5.4** and 4-trimethylsilyl-3-butyne-2-one were reacted to yield a 9:1 mixture of regioisomers favoring the 1, 4-triazole. The solvent was removed under reduced pressure, and the remaining liquid was distilled under reduced pressure to yield **5.24** as a dark oil (91%). ^1H NMR (CDCl_3): δ 0.43 (s, 1H), 0.13 (s, 1H), 2.47 (s, 0.3H), 2.49 (s, 3H), 5.51 (s, 0.2H), 5.84 (s, 2H), 7.20 (m, 5H). ^{13}C NMR (CDCl_3): δ -0.0, 31.4, 53.7, 98.9, 128.0, 135.4, 190.3. IR: ν 740, 750, 801, 950, 1050, 1153, 1160, 1250, 1390, 1474, 1490, 1681, 2894, 2950, 3031. Anal. Calculated for, $\text{C}_{14}\text{H}_{19}\text{N}_3\text{OSi}$: C, 61.50; H, 7.00; N, 15.37; O, 5.85, found C, 62.33; H, 6.47; N, 14.69.

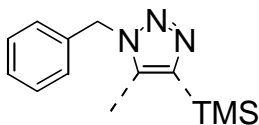


Synthesis of 5.26: Following the general procedure outlined above azide **5.1** and trimethyl silyl acetylene were reacted to yield the 1, 4-triazole. The solvent was removed

under reduced pressure and the remaining solid was distilled under reduced pressure to yield **5.26** as a colorless solid (90 %). ^1H NMR (CDCl_3): δ 7.84 (d, 2 H), 7.63 (d, 2 H), 2.40 (s, 3 H), 0.39 (s, 9 H); ^{13}C NMR (CDCl_3): δ 144.5, 139.7, 138.3, 133.3, 125.4, 117.6, 112.8, 10.4, -0.9; IR: ν 3100, 2960, 2953, 2489, 2231, 1945, 1883, 1816, 1705, 1605, 1510, 1404, 1254, 1245, 1160, 1119, 1089, 1007, 972, 836, 765, 712, 637, 567. MP: 162 °C.

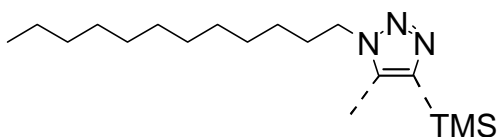


Synthesis of 5.27: Following the general procedure outlined above azide **5.2** and trimethyl silyl acetylene were reacted to yield the 1, 4-triazole. The solvent was removed under reduced pressure and the remaining solid was distilled under reduced pressure to yield **5.27** as a colorless solid (78 %). ^1H NMR (CDCl_3): δ 6.56 (s, 3 H), 3.81 (s, 6 H), 2.34 (s, 3 H), 0.38 (s, 9 H); ^{13}C NMR (CDCl_3): δ 160.9, 143.3, 138.5, 137.7, 103.7, 101.1, 55.7, 10.2, -0.8; IR: ν 3115, 2960, 2838, 2108, 1614, 1590, 1432, 1348, 1251, 1205, 1158, 1105, 1028, 928, 839, 758, 678. MP: 97 °C.

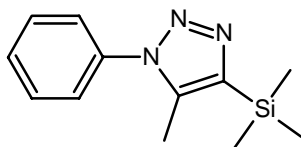


Synthesis of 5.28: Following the general procedure outlined above, benzyl azide **5.4** and 1-(trimethylsilyl)-1-propyne were reacted to yield (25) as a 10:1 mixture of regioisomers favoring the 1, 4-triazole. The solvent was removed under reduced pressure, and the remaining solid recrystallized from ethanol to yield **5.25** as a white crystalline solid (97%). ^1H NMR (CDCl_3): δ 0.13 (s, 0.9H), 0.13 (s, 9H), 2.15 (s, 3H), 2.38 (s, 0.3H),

5.42 (m, 2H), 5.62 (s, 0.2), 7.08 (m, 2H), 7.23 (m, 3H). ^{13}C NMR (CDCl_3): δ -0.5, -0.1, 9.6, 13.2, 51.4, 53.9, 127.3, 128.2, 129.0, 135.2, 138.3. IR: ν 689, 854, 1160, 1248, 1249, 1405, 1411, 1417, 1454, 1496, 2894, 2963, 3132. Anal. Calculated for, $\text{C}_{13}\text{H}_{19}\text{N}_3\text{Si}$: C, 63.63; H, 7.80; N, 17.12; Si, 11.44, found C, 63.61; H, 7.73; N, 17.02; MP: 48 °C.

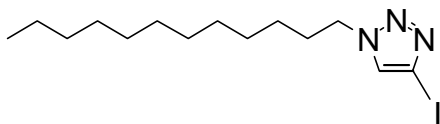


Synthesis of 5.29: Following the general procedure outlined above, dodecyl azide **5.5** and 1-(trimethylsilyl)-1-propyne were reacted to yield **5.30** as a 15:1 mixture of regioisomers favoring the 1, 4-triazole. The solvent was removed under reduced pressure, and the remaining liquid was distilled under reduced pressure to yield **5.30** as a clear oil (96%). ^1H NMR (CDCl_3): δ 0.24 (s, 9H), 0.25 (s, 0.6), 0.83 (t, 3H), 1.19 (m, 18H), 1.83 (m, 2H), 2.22 (s, 3H), 2.25 (s, 0.2H), 4.32 (m, 2H). ^{13}C NMR (CDCl_3): δ -0.5, 9.5, 14.4, 22.9, 26.9, 29.4, 29.6, 29.7, 29.8, 29.9, 30.3, 32.2, 47.5, 137.6, 143.0. IR: ν 662.98, 754.60, 1227.61, 1413.24, 1520.77, 2888.69, 2998.85. Anal. calculated for, $\text{C}_{18}\text{H}_{37}\text{N}_3\text{Si}$: C, 66.81; H, 11.52; N, 12.99, found C, 66.77; H, 11.57; N, 13.06.

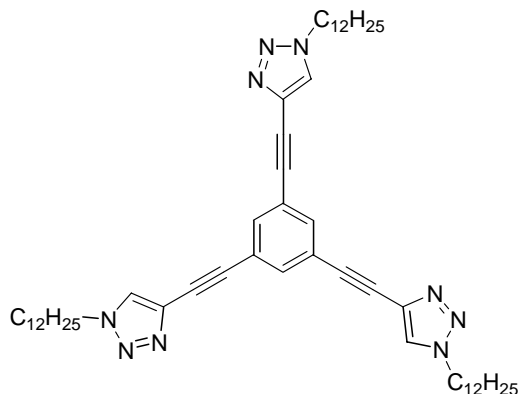


Synthesis of 5.30: Following the general procedure outlined above azide **5.3** and trimethyl silyl acetylene were reacted to yield the 1, 4-triazole. The solvent was removed under reduced pressure and the remaining solid was distilled under reduced pressure to yield **5.30** as a colorless solid (71 %). ^1H NMR (CDCl_3): δ 7.56-7.48 (m, 3 H), 7.43 (m, 2 H), 2.33 (s, 3 H), 0.38 (s, 9 H), 1.41 (d, 18 H); ^{13}C NMR (CDCl_3): δ 143.6, 138.8,

136.6, 129.6, 129.4, 125.5, 10.5, -0.54; IR: ν 3035, 2955, 2482, 1596, 1590, 1502, 1406, 1392, 1300, 1291, 1270, 1248, 1099, 1071, 918, 838, 770, 681, 634. MP: 69 °C.

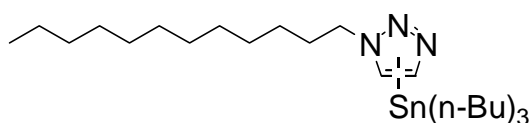


Synthesis of 5.31 from the corresponding silane: Compound **5.9** and iodine were reacted to yield the iodo substituted 1, 4-triazole. The solvent was removed under reduced pressure and the remaining solid was recrystallized from ethanol to yield **5.31** as a colorless solid (89 %). ^1H NMR (CDCl_3): δ 7.62 (s, 1 H), 4.33 (t, 2 H), 1.84 (m, 2 H), 1.23 (m, 18 H), 0.82 (t, 3 H). ^{13}C NMR (CDCl_3): δ 129.0, 87.1, 51.0, 32.2, 30.5, 29.8, 29.8, 29.6, 29.2, 26.6, 23.0, 14.4. IR: ν 3119, 2960, 2929, 2846, 1456, 1319, 1272, 1262, 1194, 1049, 720. Anal. Calcd for $\text{C}_{14}\text{H}_{26}\text{IN}_3$: 363.28. Found: fragmentation; MP: 113 °C.



Synthesis of 5.33 via the silane route: Iodo compound **5.31** (1.50 g, 4.13 mmol) and 1, 3, 6-triethynylbenzene (0.200 g, 1.33 mmol) were dissolved in dichloromethane (4 mL) and piperidine (4 mL) in an oven dried Schlenk flask. The flask was flushed with nitrogen and frozen and evacuated three times after which $(\text{Ph}_3\text{P})_2\text{PdCl}_2$ (28 mg, 41 μmol), and CuI (8 mg, 41 μmol) were added. The mixture was allowed to stir at room

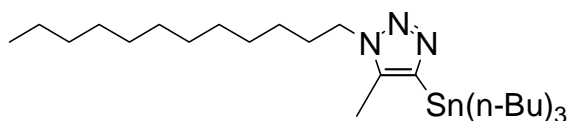
temperature for 48 h. The solvent was removed and the mixture dissolved in dichloromethane, washed with 1N HCl, 1N NH₄OH, and water. The organic layer was dried over MgSO₄ and the solvent removed. The resulting crude product was crystallized from ethanol and further purified by chromatography over silica gel (ethylacetate:hexane, 5:1) to yield pure **5.33** (722 mg, 63 %) as a pale yellow solid. ¹H NMR (CDCl₃): δ 7.89 (s, 3 H), 7.62 (s, 3H), 4.43 (t, 6H), 1.89 (m, 6H), 1.25 (m, 18 H), 0.82 (t, 3 H). ¹³C NMR (CDCl₃): δ 136.0, 130.5, 125.4, 91.5, 82.5, 51.5, 32.5, 29.3, 29.1, 26.5, 25.7, 16.8. IR: ν 685, 1223, 1160, 1247, 1248, 1411, 1413, 1418, 1423, 1496, 2856, 2953, 3654. Anal. Calcd for C₁₄H₂₆N₃: 856.28. Found: fragmentation; MP: 123 °C.



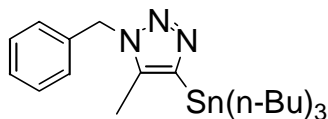
Synthesis of 5.34: Following the general procedure outlined above dodecyl azide **5.4** and the corresponding acetylene were reacted to yield a 20:1 mixture crude of the crude product favoring the 1, 4-triazole. The solvent was removed under reduced pressure and the remaining solid was crystallized from ethanol to yield **5.34** as a colorless solid (96 %). ¹H NMR (CDCl₃): δ 7.45 (s, 1H), 4.39 (q, 2H), 1.91 (m, 3H), 1.86 (m, 6H), 1.63 (m, 24H), 1.53 (m, 6H), 1.38 (m, 6H), 0.91 (m, 12H). ¹³C NMR (CDCl₃): δ 129.8, 50.0, 32.2, 30.8, 29.9, 29.8, 29.7, 29.3, 29.2, 27.9, 26.9, 23.0, 14.5, 14.0, 10.2. IR: ν 3110, 2852, 2810, 2729, 2588, 2349, 1469, 1290, 1178, 1118, 1076, 1039, 960, 794, 651. Anal. Calcd for C₂₆H₅₃N₃Sn: C, 59.32; H, 10.15. Found: C, 58.24, H 10.31 MP: 93 °C.



Synthesis of 5.35: Following the general procedure outlined above dodecyl azide **5.5** and the corresponding acetylene were reacted to yield a 10:1 mixture of regioisomers favoring the 1, 4-triazole. The solvent was removed under reduced pressure and the remaining solid was crystallized from ethanol to yield **5.35** as a colorless solid (98 %). ^1H NMR (CDCl_3): δ 7.41 (m, 3H), 7.38 (m, 2H), 7.26 (s, 1H), 5.56 (m, 2H), 1.58 (m, 6H), 1.36 (m, 6H), 1.15 (m, 6H), 1.09 (m, 6H), 0.82 (m 6H). ^{13}C NMR (CDCl_3): δ 135.5, 130.0, 129.1, 128.0, 53.6, 29.5, 29.3, 29.2, 29.1, 27.5, 14.0, 10.5, 10.3. IR: ν 3031, 2954, 2812, 2729, 2644, 2345, 1946, 1458, 1375, 1292, 1178, 1089, 1041. Anal. Calcd for $\text{C}_{21}\text{H}_{35}\text{N}_3\text{Sn}$: C, 56.27; H, 7.87. Found: C, 55.78; H, 8.28; MP: 86 °C.



Synthesis of 5.36: Following the general procedure outlined above dodecyl azide **5.4** and the corresponding acetylene were reacted to yield the crude 1, 4-triazole. The solvent was removed under reduced pressure and the remaining solid was crystallized from ethanol to yield **5.36** as a colorless solid (97 %). ^1H NMR (CDCl_3): δ 4.22 (q, 2H), 2.28 (s, 3H), 1.89 (m, 3H), 1.60 (m, 6H), 1.45 (m, 6H), 1.39 (m, 24H), 0.82 (m 12H). ^{13}C NMR (CDCl_3): δ 47.8, 32.2, 30.4, 29.9, 29.8, 29.7, 29.6, 29.4, 29.2, 27.5, 26.9, 23.0, 14.4, 14.0, 11.2, 10.0, 9.9. IR: ν 2962, 2858, 2727, 2651, 2096, 1514, 1469, 1415, 1359, 1290, 1220, 1178, 1155, 1068, 1020, 871. Anal. Calcd for $\text{C}_{26}\text{H}_{53}\text{N}_3\text{Sn}$: C, 59.32; H, 10.15; N, 7.98. Found: C, 58.2; H, 10.53 MP: 81 °C.



Synthesis of 5.37: Following the general procedure outlined above azide **5.5** and the corresponding acetylene were reacted to yield the 1, 4-triazole. The solvent was removed under reduced pressure and the remaining solid was crystallized from ethanol to yield **5.37** as a colorless solid (96 %). ¹H NMR (CDCl₃): δ 7.31 (m, 3H), 7.26 (m, 3H), 7.12 (s, 1H) 5.53 (s, 2H), 2.18 (s, 3H), 1.12 (m, 9H), 0.82 (m, 3H). ¹³C NMR (CDCl₃): δ 139.1, 135.6, 129.0, 128.1, 127.2, 51.6, 29.5, 29.4, 29.1, 28.2, 27.5, 14.0, 13.9, 10.1, 10.0. IR: ν 3064, 3031, 2952, 2850, 1519, 1463, 1417, 1217, 1151, 1074, 723. Anal. Calcd for C₂₂H₃₇N₃Sn: C, 57.16; H, 8.07; Found: C, 56.39; H, 8.42; MP: 83 °C.

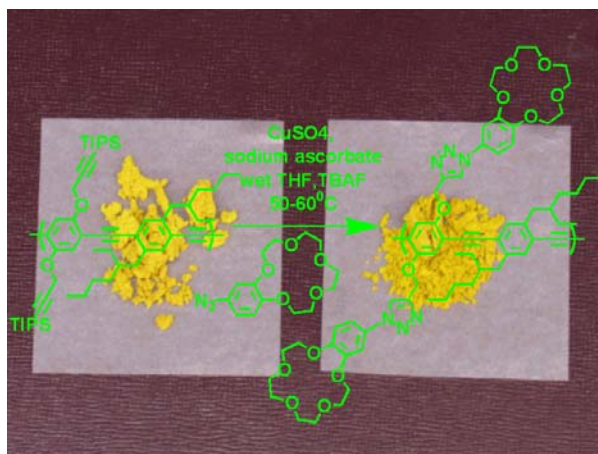
5.5 References.

1. Kolb, H. C.; Finn, M. G.; and Sharpless, B. K. *Angew. Chem. Int. Ed.* **2001**, 40, 2004-2021.
2. a) Huisgen, R; Szeimies, G.; Moebius, L. *Chem. Ber.* **1967**, 100, 2494. b) Huisgen, R.; Knorr, R.; Moebius, L.; Szeimies, G. *Chem. Ber.* **1965**, 98, 4014. c) Huisgen R., in 1,3-Dipolar Cycloaddition Chemistry (Ed. A. Padwa), Wiley, New York, **1984**, pp. 1-176.
3. Wang, Q.; Chan, T. R.; Hilgraf, R.; Fokin, V. V.; & Sharpless, B. K.; Finn, M. G. *J. Am. Chem. Soc.* **2003**, 125, 3192-3193.
4. a. Tornøe, C. W.; Christensen, C.; & Meldal, M. *J. Org. Chem.* **2002**, 67, 3057-3064. b. Chen, J.; & Rebek, J. *Org. Lett.* **2002**, 4, 327-329.
5. Rostovtsev, V. V.; Green, L. G.; Fokin, V. V.; & Sharpless, B. K. *Angew. Chem. Int. Ed.* **2002**, 41, 2596-2599.
6. Shen, Xianfeng; Ho, Douglas M.; Pascal, Robert A., Jr. *J. Am. Chem. Soc.* **2004**, 126 (18), 5798-5805.

7. Choi, Joon Hun; Choe, Yearn Seong; Lee, Kyung-Han; Choi, Yong; Kim, Sang Eun; Kim, Byung-Tae. *Carbohydrate Research*. **2003**, 338 (1), 29-34.
8. Murphy, R. A.; Kung, H.F.; Kung, M.; and Billings, J. *J. Med. Chem.* **1990**, 33, 171-178.
9. Dieck, H. A.; Heck, R. R. *J. Organomet. Chem.* **1975**, 93, 259.

CHAPTER 6

CLICK-CHEMISTRY AS A POWERFUL TOOL FOR THE CONSTRUCTION OF FUNCTIONALIZED POLY(P-PHENYLENEETHYNYLENE)S: COMPARISON OF PRE- AND POSTFUNCTIONALIZATION SCHEMES.



6.1 Introduction

The functionalization of an alkyne-appended poly(*para*-phenyleneethynylene)s (PPE) by 1,3-dipolar cycloaddition of different organic azides is described.

The post-polymerization functionalization of conjugated polymers is a useful technique in which a specific polymer backbone is post-synthetically altered. Leclerc¹ has executed this concept elegantly in the polythiophene series by polymerization of an active-ester containing thiophene monomer while Holdcroft² has developed post-polymerization

halogenation of polythiophenes. These approaches allow introduction of molecular diversity late, in the final step, of the synthetic sequence and are therefore highly efficient compared to the introduction of functional elements during the synthesis of specific monomers. Additionally, postfunctionalization schemes allow the introduction of groups that might not be compatible with the polymerization conditions. Fast assembly of libraries of polymers and introduction of different and potentially sensitive functional groups are some of the advantages of post polymerization functionalization. The caveat with postfunctionalization is the requirement of high yielding and specific reactions; errors in the functionalization of monomers can be corrected by the appropriate purification steps, while a polymer synthesized by postfunctionalization processes can not be purified further.

Huisgen and Szeimies³ investigated the 1,3-dipolar cycloaddition of azides to alkynes. Triazoles are the only product of this reaction. Sharpless recognized the potential of this transformation and retooled the dipolar cycloaddition as “Click Chemistry” for the construction of biologically active molecules.⁴ The high yield and the specificity of this transformation make it appealing, not only for synthesis of small molecules but as well for the functionalization of polymers as reported very recently by Hawker and Frechet⁵ in the attachment of dendrons to non-conjugated polymers.

6.2 Results and Discussion

PPEs are valuable due to their dramatic chromic responses.⁶⁻⁸ They have been utilized in sensory schemes and in semiconductor devices including but not restricted to light emitting diodes^{7a,b} and photodiodes.⁸ However, postfunctionalization schemes on

PPEs have only sparsely been carried out.⁶ As a consequence it is of significant interest to develop an efficient platform that could allow the manipulation of PPE's properties in a post polymerization modification approach (Figure 6.1). In this contribution a PPE scaffold, **6.6**, is introduced that allows a “click on” approach of different functional groups by a 1,3-dipolar cycloaddition. The polymers made by the postmodification approach were compared to those of the same structure but made by a conventional approach (Figure 6.1). This allows the evaluation of the click process as tool to functionalized conjugated polymers. Important (specific) questions are if the postfunctionalization process selects the alkyne appendage over the backbone alkynes, and if the conversion of the appended alkynes is complete and if it occurs with a similar regiochemical 1,4-control as reported for the copper catalyzed 1,3-dipolar cycloaddition (Figure 6.1).

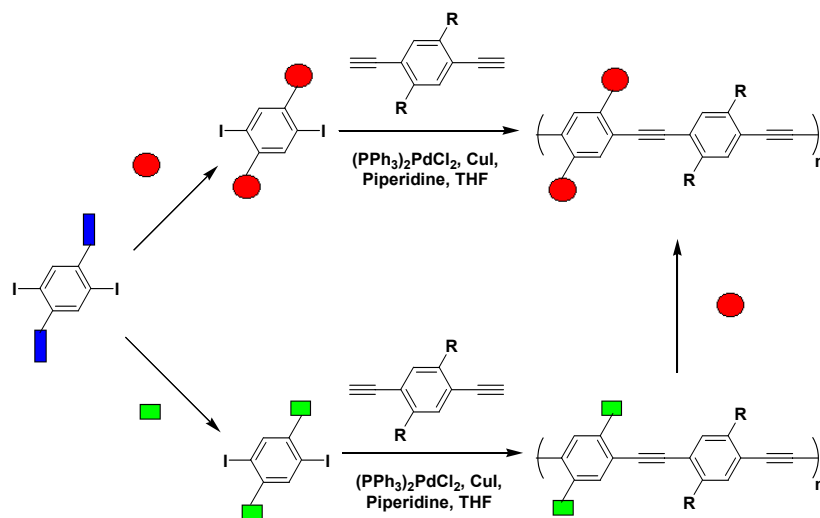
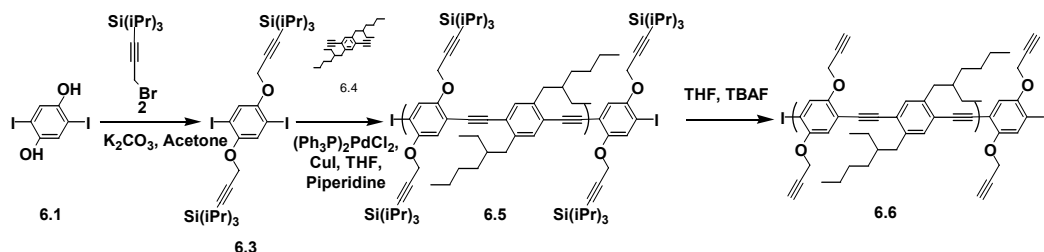


Figure 6.1. Post and prepolymerization functionalization strategies.

Synthesis and characterization of monomer **6.3**, polymer **6.5**, and polymer **6.6**

Reaction of diiodohydroquinone **6.1** with the propargylic bromide **6.2** in the presence of excess potassium carbonate furnished **6.3** in 82 % yield. The copolymerization of **6.3** with the diyne **6.4** under standard conditions with 0.7 mol% Pd-catalyst furnished polymer **6.5** in 87 % yield as a yellow, reasonably soluble, fibrous material with a degree of polymerization (P_n) of 64 (gel permeation chromatography, $M_n = 65 \times 10^3$, $M_w/M_n = \text{PDI} = 4.4$). Polymer **6.5** is characterized by its ^1H , ^{13}C and IR spectra that are in excellent agreement with the proposed structure.



Scheme 6.1. Synthesis of the polymer platform **6.6**.

Reaction of the polymer **6.5** with tetrabutylammonium fluoride furnishes a considerably less soluble polymer (**6.6**) in almost quantitative (95%) yield as a deep yellow powder. Gel permeation chromatography shows a decrease of P_n to 46 ($M_n = 24 \times 10^3$, $\text{PDI} = 1.6$). We believe that the decreased solubility of **6.6** as compared to that of **6.5** leads to a removal of higher molecular weight polymer chains during the filtration step that is necessary for the preparation of gpc samples. Aggregated and/or insoluble but very finely suspended parts of the polymer are retained by the utilized gpc ultrafilters. The yellowish appearance of the gpc ultrafilters after use supports our notion that significant amounts of **6.6** are retained.

We were able to obtain ^1H NMR and ^{13}C NMR spectra of **6.6**. The proton NMR spectrum of **6.6** resembles that of **6.5** but does a) not show a signal for the TIPS groups, b) shows an additional signal for the free alkyne groups at $\delta = 2.58$ ppm c) shows a shift in the arene protons that are now spaced and resonate at 7.17 and 7.40 ppm. The IR spectrum of **6.6** shows a strong band at 3301 cm^{-1} , which is diagnostic for the presence of a terminal alkyne. Additionally two bands at 2202 and 2122 cm^{-1} can be attributed to the $\text{C}\equiv\text{C}$ stretch band of the backbone and the free alkyne respectively. It was possible to obtain a ^{13}C NMR spectrum of **6.6** with a reasonable signal to noise ratio if chromium acetylacetonate (cracac) was added as relaxing agent.

The optical spectra of **6.5** and **6.6** are shown in Figure 6.2 and Table 6.1 and discussed. The solution spectra of **6.5** and **6.6** are typical for PPEs. The solid-state spectra of **6.5** and **6.6** are strikingly different. The removal of the TIPS groups leads to a 12 nm red shift (577 cm^{-1}) in absorption. This red shift could be either a sign of increased planarization or of inter chromophore interaction that would give testimony to the formation of weak electronic aggregates between PPE chains on top of a significant contribution of chain planarization (1475 cm^{-1}). The solid-state emission of **6.6** shows an excimer band at 533 nm that is not present in the solid-state spectrum of **6.5**, reinforcing the notion of some interchain interactions in exist in **6.6** at least in the solid state.⁹

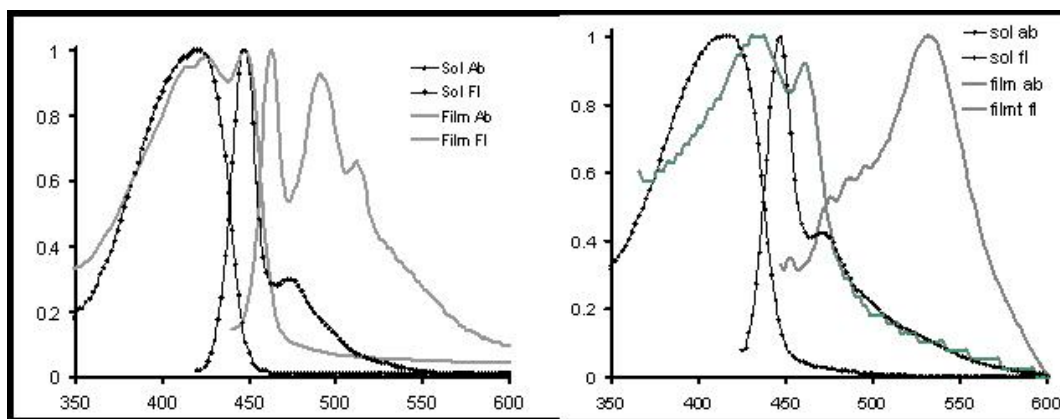
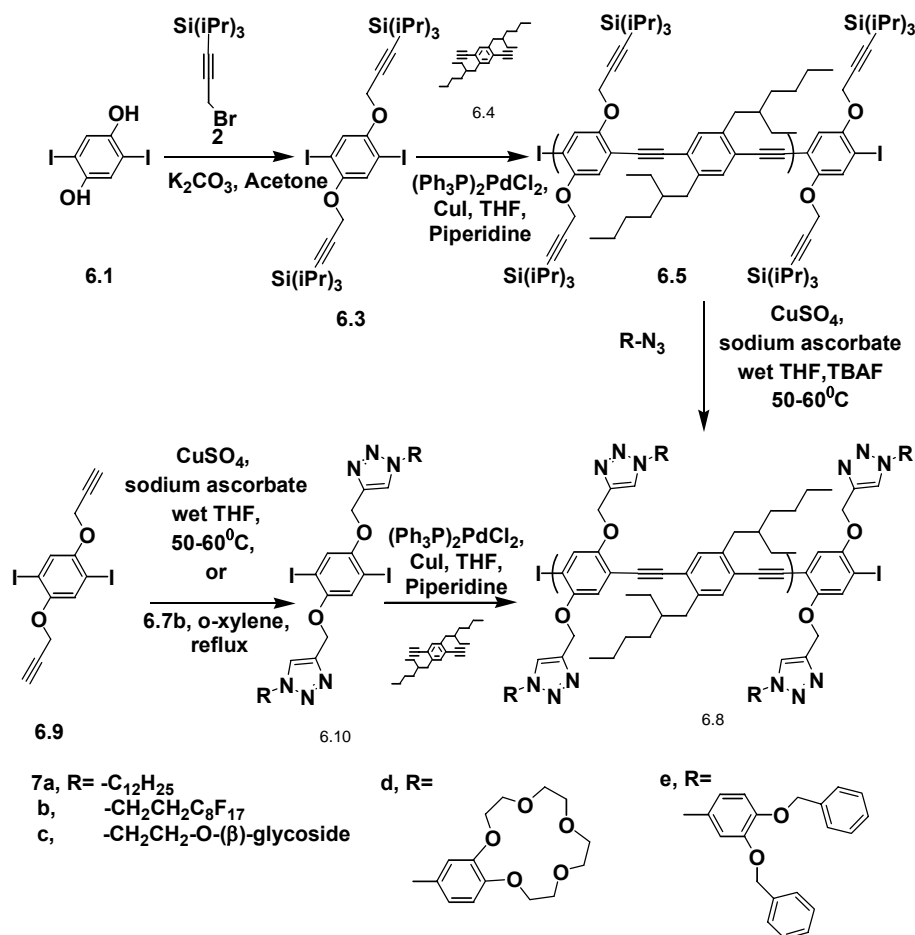


Figure 6.2. UV-vis and emission spectra of polymer **6.5** (left) and polymer **6.6** (right) in chloroform solution and in the solid state (Absorption and emission maxima see Table 1).



Scheme 2. In situ generation of **6.6** and its reaction with azides **6.7a-e** yielding **6.8a-e** and prefunctionalization approach towards **6.8a-e**.

Synthesis of functionalized polymers 8a-e

The successful formation of **6.6** allowed the investigation of its reaction with different azides. In a first experiment direct reaction of **6.6** with dodecyl azide **6.7a** was investigated under microwave irradiation, but the low solubility of polymer **6.6** in organic solvents led to material that was only to a moderate extent triazole functionalized. It was found that an in situ deprotection with tetrabutylammoniumfluoride (TBAF) and coupling procedure was a much better way of obtaining the 1,3-dipolar cycloadducts. Reaction of **6.5** with the azides **6.7a-e** in the presence of copper sulfate, TBAF and sodium ascorbate in wet THF (5% water) as solvent gave the functionalized PPEs **6.8a-e** in yields of 75-96 % after 48h at 40-60 °C. Without the addition of copper sulfate and sodium ascorbate the reaction did not proceed as well. As a consequence postmodification reactions were performed in the presence of copper sulfate and sodium ascorbate. Workup is performed by threefold precipitation of the formed polymer into methanol to remove the starting azide reagent. The yields of the postfunctionalization reactions are high and shown in Table 6.1.

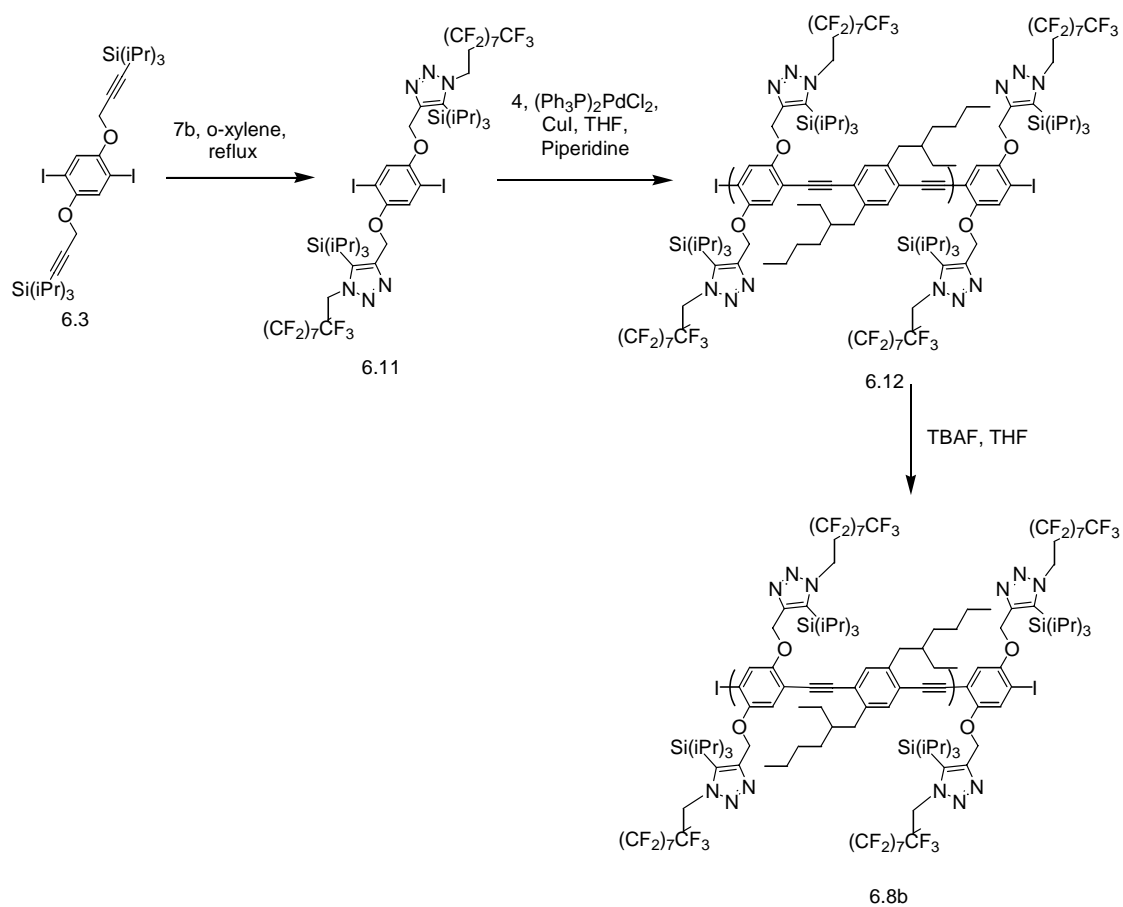
NMR and IR characterization of functionalized polymers 6.8a-e

Reactions carried out with azides **6.7a-e** afforded polymers **6.8a-e** of which **6.8a-d** were completely and **6.8e** mostly, according to ^1H , ^{13}C NMR, and IR were completely functionalized. This was confirmed by the synthesis of the same polymers **6.8a-d** by a more conventional approach (Scheme 6.2). These “premodified” polymers afforded a standard the postmodified PPEs could be compared to. In completely postmodified polymers **6.8a-d**, there were no peaks in the ^1H NMR at 2.55 ppm for the terminal alkyne (Figure 6.3). Signals for the newly formed triazoles are present at 7.5-8.0 ppm. Signals

from the triazole carbon nuclei are easily visible at 140-150 ppm and 120-130 ppm in the ^{13}C NMR spectrum of the functionalized polymers. The peak at 3294 cm^{-1} has disappeared in the postfunctionalized polymers. The excess of azide reagent **6.7** was removed completely by threefold precipitation of the polymers **6.8** into methanol, according to IR spectroscopy where the strong azide band at 2100 cm^{-1} (Figure 6.5) had disappeared.

Reaction of polymer **6.5** with azide dendron **6.7e** in a postmodification strategy afforded a polymer which contained approx. 10% of unreacted terminal alkyne according to ^1H NMR spectroscopy and comparison of its spectral data to conventionally prepared **6.8e**. Partial functionalization is not surprising, as Frechet and Hawker have observed similar results for the functionalization of non-conjugated polymeric systems.⁶

Reaction of **6.9** with azides **6.7a**, **c**, **d**, and **e** afforded monomers **6.10a**, **c**, **d**, and **e**. Reaction with diyne **6.4** under standard conditions furnished the polymers **6.8a,c-e** in excellent yields (Table 6.1). Monomer **6.10b** was obtained by this method but due to lack of solubility could neither be characterized nor purified. An alternate approach employing the reaction of **6.3** with azide **6.7b** under thermal conditions afforded monomer **6.11** (Scheme 3). Polymerization of **6.11** with **6.4** under standard conditions affords **6.12** in almost quantitative yields. The presence of the triisopropylsilyl groups can be confirmed by the presence of two signals between $\delta = 10$ and 20 ppm in the ^{13}C NMR spectrum of **6.12**. Deprotection of **6.12** with TBAF yielded polymer **6.8b** as a moderately soluble yellow solid.



Scheme 6.3. Synthesis of polymer **6.8b** via a prefunctionalized strategy starting from monomer **6.3**.

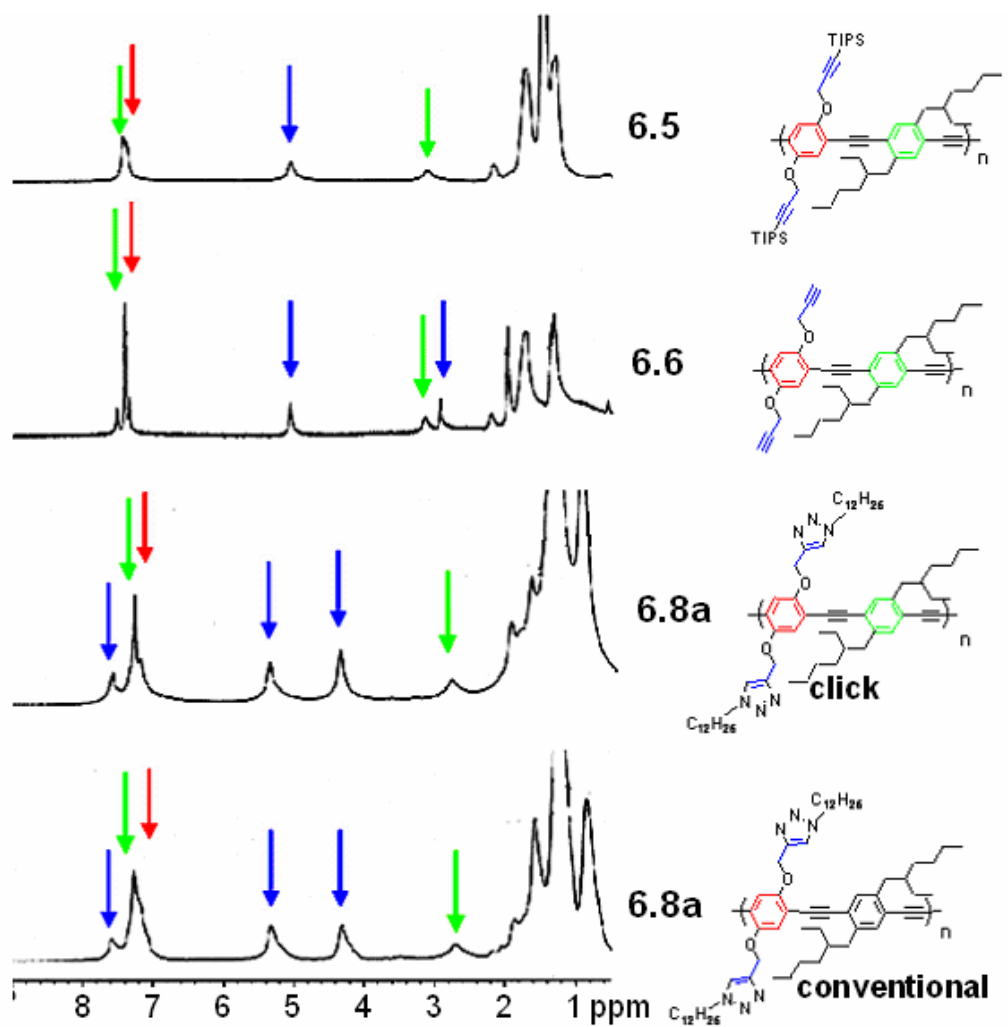


Figure 6.3. ^1H NMR of polymers **6.5**, **6.6**, **6.8a** (post), and **6.8a** (pre) (top to bottom).

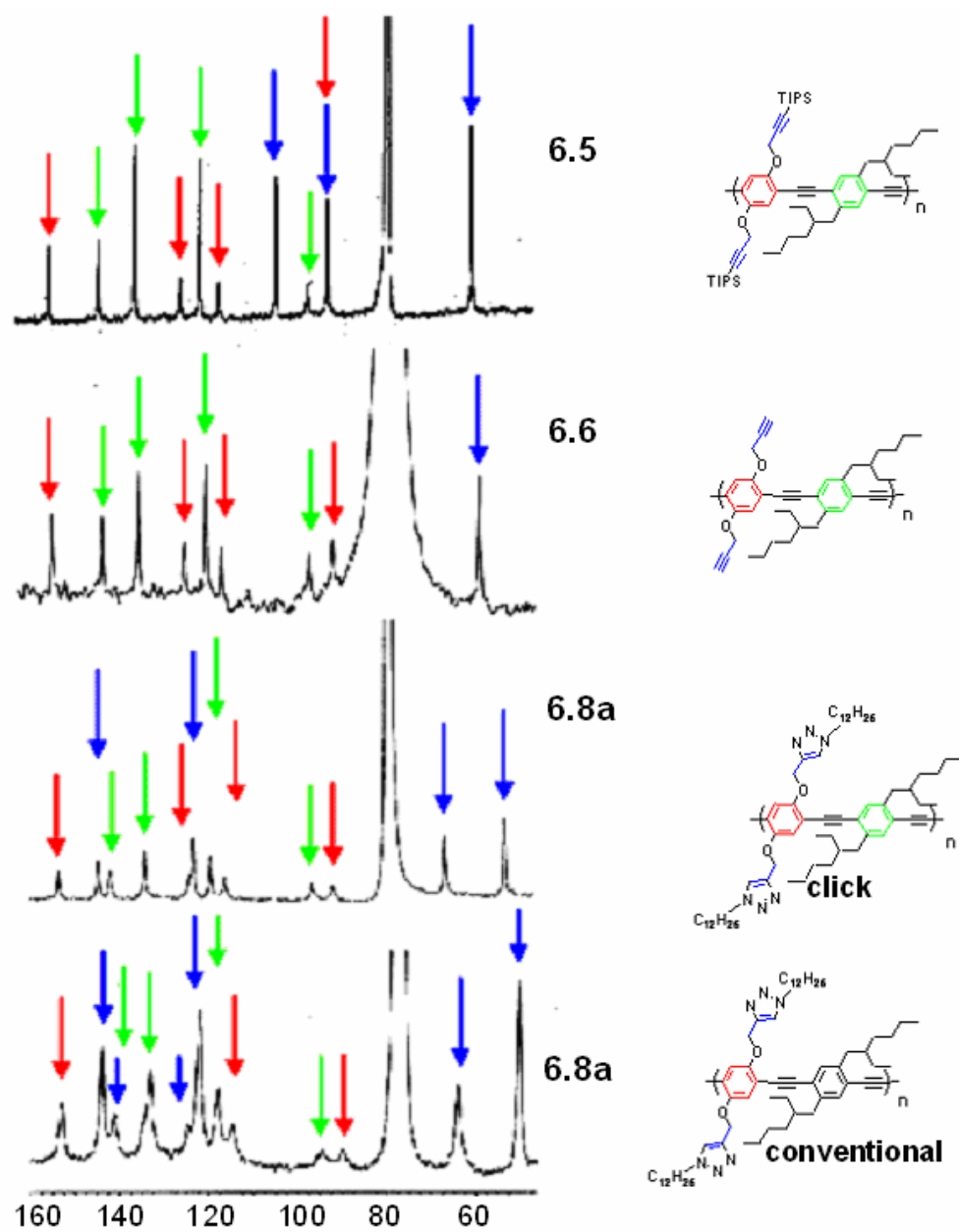


Figure 6.4. ^{13}C NMR of polymers **6.5**, **6.6**, **6.8a** (post), and **6.8a** (pre) (top to bottom).

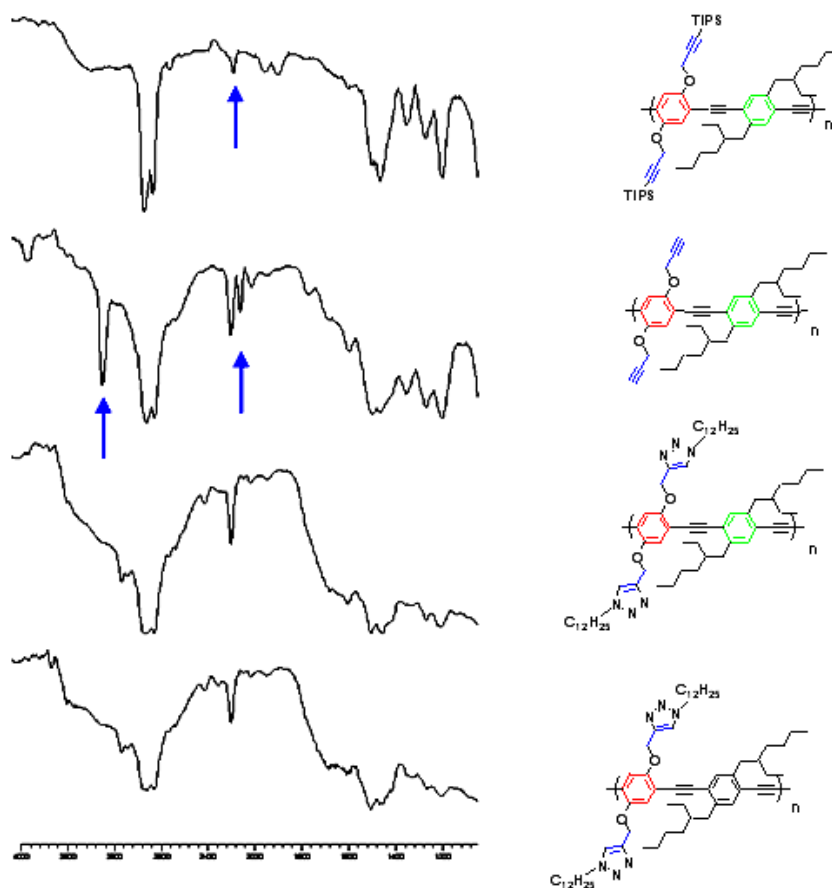


Figure 6.5. IR of polymers **6.5**, **6.6**, **6.8a** (post), and **6.8a** (pre) (top to bottom). The blue arrows point to the bands of the terminal alkynes.

Regioisomers

At room temperature, the copper catalyzed process is typically regioselective favoring the 1,4-triazole. We opted to perform these copper catalyzed reactions between 40-60°C as we observed improved yields in monomers and higher degrees of functionalization in polymeric systems. Under these conditions **6.10a**, **6.10c**, **6.10d**, **6.10e** were obtained as approximate 2:1 mixtures of the 1,4- to the 1,5-regioisomers as can be seen for the example of **6.10a**, spectroscopic data of which are shown in Figure 6. The regioisomers were not separable by flash chromatography and therefore used as

mixtures. The ^1H and ^{13}C NMR spectra of the conventionally prepared polymer **6.8a** and its cousin made by the postfunctionalization route are shown together in Figures 3. The polymers are spectroscopically indistinguishable from each other. When one inspects the NMR spectra of the polymer **6.8a** (conventional), the spectral features of the regioisomers that are well resolved in the monomer **6.10a** are not resolved at all in the spectra of the polymer **6.8a**. Due to this decrease in resolution, when going from monomer to polymer, we are not able to assess the regiochemistry of the polymers **6.8** at all by NMR spectroscopy, and therefore can not make an assessment of the regioselectivity of this process in the postfunctionalization process. Only in the formation of the sterically hindered monomer **6.11** full regioselectivity is observed, only the 1,4-product is formed.

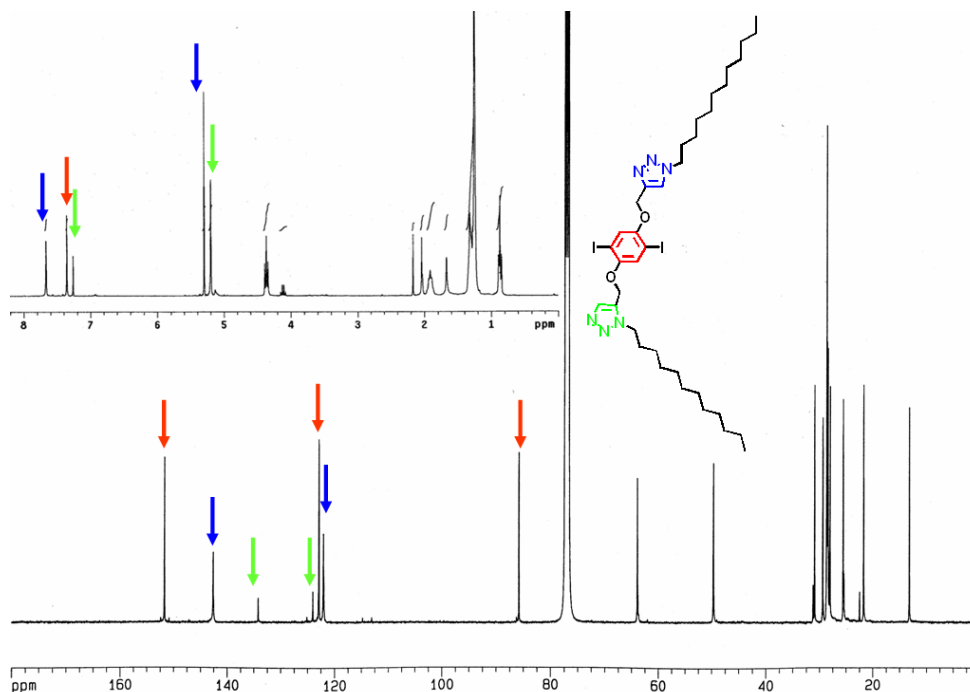


Figure 6.6. ^{13}C NMR of monomer **6.10a** showing the presence of the 1,4 (blue arrows) and 1,5 (red arrows) triazoles.

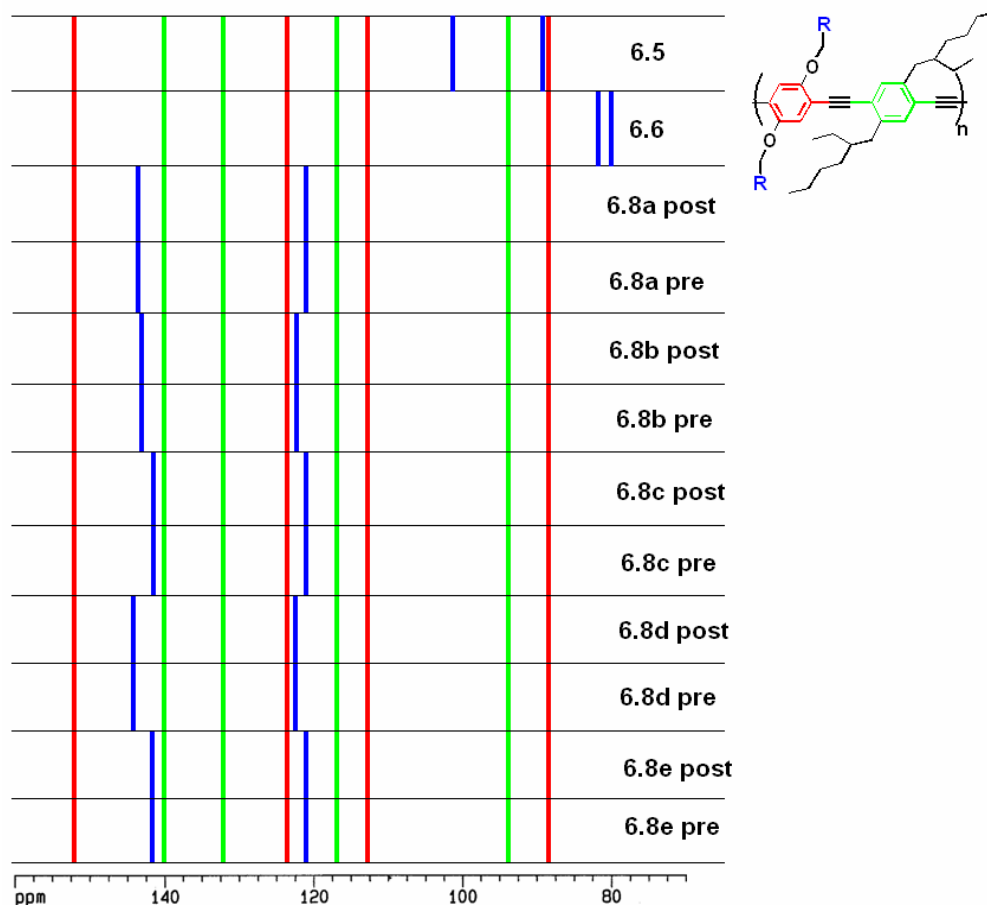


Figure 6.7. ^{13}C NMR chemical shift of precursor and functionalized polymers.

Characterization of functionalized polymers 6.8a-e

It was of interest to study the influence of postmodification on the molecular weight **6.8**. We find PPEs decreases in molecular weight when converting **6.5** into **6.8** (**6.5**: 63.6×10^3 ; $25.4 \times 10^3 > \mathbf{6.8} > 8.5 \times 10^3$) and polydispersity (**6.5**: 4.4 to between $3.2 > \mathbf{6.8} > 1.5$) with respect to platform polymer **6.5** (Table 1). This is possibly due to differences in solubility between **6.5** and the post functionalized polymers **6.8**. Material is lost during the filtration step required for GPC due to aggregated and/or insoluble parts

of **6.8** as discussed for polymer **6.6**. Gpc ultrafilters are yellowish in appearance after filtration of solutions of **6.8a-e**. The decreased polydispersity is an excellent indication for the loss of material during filtration.

To rule out the possibility of diyne formation, i.e. crosslinking, as a reason for observed insolubility, we treated polymer **6.6** with TBAF, copper sulfate and sodium ascorbate in wet THF (5% water) in the presence of air. Only after heating to reflux for 24 h we observed a material with moderate diyne linkages. Because the material was still soluble the amount of cross-linking must be moderate. The signals of the diyne linkages are however visible in the ^{13}C NMR due to their shorter relaxation time as compared to the signals attributed to the main chain. These signals that can be assigned to diyne formation were not observed in any of the postfunctionalized polymers **6.8a-e** synthesized under nitrogen with the scrupulous exclusion of oxygen.

The possibility of incorporation of triazole groups into the backbone of the PPEs as a cause for the decreased solubility was also considered. Control experiments were performed in which didodecyl-PPE was treated at 40°C for 16 h with an excess of dodecyl azide under standard postfunctionalization conditions. After precipitation into methanol only unfunctionalized PPE was isolated according to ^1H NMR, ^{13}C NMR and UV-vis spectroscopy strongly suggesting that attack on the backbone-alkynes is not favored under the current reaction conditions.

There is precedence for decreased solubility of click-functionalized polymers: Kluger et al. performed postfunctionalization of poly(oxynorbornenes)¹⁰ and noted dramatic differences in solubility between polymers functionalized with 1,4-triazoles and those not. In some cases, GPC data for these polymers could not be obtained due to

limited solubility. Matyjaszewski et al. has recently modified polymers of acrylonitrile with click-type chemistry to form tetrazoles and also noted marked differences in solubility between polymers modified by click chemistry and those not modified by click chemistry.¹¹ It is however surprising that the attachment of dodecyl chains or Frechet-type dendrons leads to a decrease in solubility. A possible explanation is that the presence/incorporation of the triazole group per se reduces the solubility of any polymer.

Table 6.1. Optical Properties, Yields, Degree of Polymerization and Degree of Functionalization of 6.5, 6.6 and 6.8

<i>Polymer</i>	Yield	M_n (PDI)	Degree of Postfunctionalization	Absorption (CHCl₃) [nm]	Absorption (Film) [nm]	Emission (CHCl₃) [nm]	Emission (Film) [nm]
6.5	87%	63.6 x 10 ³ 4.43	na	422	450,426	448	462, 490, 512
6.6	95%	24.4 x 10 ³ 1.64	>95%	420	462, 438	447	533
6.8a pre	91%	13.7 x 10 ³ 5.24	na	415	434	448	463
6.8a post	92%	8.5 x 10 ³ 3.20	>95%	413	437	448	485
6.12	91%	25.5 x 10 ⁴ 4.25	>95%	406	410	447	450
6.8b pre	82%	71.7 x 10 ³ 4.44	na	416	422	449	483
6.8b post	94%	25.4 x 10 ³ 2.56	>95%	418	435	448	479
8c pre	93%	24.5 x 10 ³ 1.01	na	421	433	454	470
6.8c post	76%	22.6 x 10 ³ 2.39	>95%	424	431	454	470, 523
6.8d pre	93%	16.2 x 10 ⁴ 7.70	na	408	416	452	470
6.8d post	82%	10.8 x 10 ⁴ 1.49	>95%	412	426	450	452, 470
6.8e pre	75%	71.8 x 10 ³ 2.10	na	416	428	450	460
6.8e post	96%	22.6 x 10 ³ 2.39	ca. 50%	412	436	450	473

Optical properties of functionalized polymers 6.8a-e

The optical properties of polymers **6.8a-e** were examined and compared with their pre-modified counterparts. In solution, absorption and fluorescence maxima of structurally identical polymers **6.8a-e** occur at similar wavelengths (± 2 nm). It is interesting to note that the largest difference in absorption is found when comparing platform polymer **6.6** to functionalized polymers. For all polymers (**6.8**), both pre and post-functionalized, blue shifts in absorption are observed when compared to **6.6** (Table 1). Polymer **6.12** with TIPS groups attached to the pendent triazole moieties is an extreme case has a solution absorption maxima of 406 nm, which is blue shifted by 6 to 24 nm of the absorption maxima of post and pre-polymers **6.8a-e** (Figure 6.8). The solid-state emission of **6.12** is almost unchanged to that obtained in solution. We assume that the increased steric demand of the TIPS groups forces the PPEs into a non-planar ground state.^{12, 13}

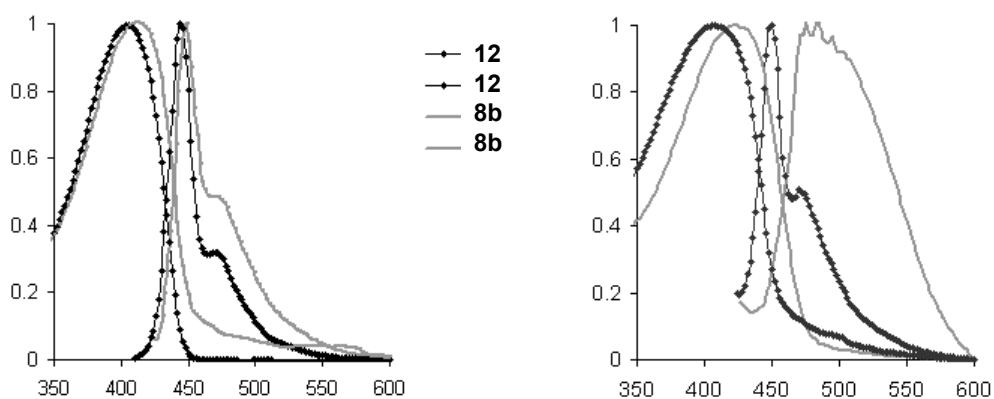


Figure 6.8. UV-vis and emission spectra of polymer **6.8b** conventional and polymer **6.12** in chloroform and in the solid state. The only difference is the TIPS group attached to the triazole units.

The solution emission spectra of polymers **6.8a-e** vary only slightly and are almost superimposable.⁹ All of the investigated polymers **6.5**, **6.6**, **6.8**, **6.12** have the same backbone. In the solid state, i.e. in thin films their absorption spectra vary considerably. The polymer **6.6** shows an absorption maximum at 462 nm, while the TIPS-substituted **12** has a solid state absorption maximum located at 410 nm. All of the other, triazole-functionalized polymers, **6.8**, show absorption maxima ranging from 416-436 nm. It is interesting to note that the red shift in the absorption spectra of **6.8a-e** when going from solution into the solid state, is quite small, only 6-17 nm. That is unusual, because the precursor polymer **6.6**, featuring the same backbone shows a shift of 42 nm when going from solution into the solid state. The differences in the thin film UV-spectra between pre- and postfunctionalized polymers **6.8a-e** of identical structure is small, and as a rule the absorption of the post-functionalized samples is 8-13 nm red shifted.

The introduction of the triazole unit into the side chains of the PPEs **6.8** and the PPE **6.12** influences their absorption insofar as a more twisted conformations of the main chain must be assumed resulting in the presence of nonplanar ground states. In the case of **6.12** the large TIPS substituent will probably lead to an additional twist of the main chain and the conformation of **6.12**'s backbone in solution and in the solid state will be very similar. The subtle differences between the absorption of the pre vs. the postfunctionalized triazole-substituted PPEs **6.8a-e** is possibly due to differences in the ratio of 1,4- and 1,5-isomers.

DSC of functionalized polymers 6.8a-e

The thermal behavior of polymers **6.8a-e** was investigated between 0-250°C by differential scanning calorimetry (DSC). Polymers **6.5**, **6.6**, **6.8b**, **6.8c**, **6.8d** and **6.8e**

show slow decomposition and no phase transitions. Polymer **6.8a**, obtained by a premodification strategy, shows an endothermic transition beginning at 66°C and ending at 126°C.^{5b} A reproducible isotropic transition at 200°C upon heating and cooling was also observed. Polymer **6.8a** synthesized by a postmodification strategy showed only slow decomposition. When comparing polymers synthesized by a post and pre-modification strategy it is important to note that the conventional and the click polymers **6.8** often have different degrees of polymerization but identical substituents and are therefore expected to behave differently. Longer polymer chains would melt at higher temperatures. As discussed above slightly differing polymer structures such as the presence of 1,5-triazoles would also be expected to cause differences in the solid state properties of these polymers.

6.3 Conclusion

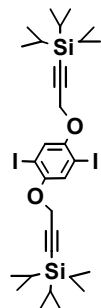
We have produced a series of PPEs (**6.8a-e**) by employing click chemistry in both pre and post-polymerization functionalization approaches. In examples where the structural repeat unit of the polymer was the same, the optical properties of these polymers in solution proved to be identical. Differing thin-film optical and thermal behavior properties result from differing degrees of polymerization and small amounts of triazole regioisomers. Click chemistry provided a means to completely functionalize PPEs via a postmodification strategy. In the case of azide **6.7e**, this approach provided a polymer **6.8e** which was to 90% functionalized. While all of these triazole-functionalized polymers aggregate, their absorption spectra are quite insensitive to the aggregation

process, which suggests that triazole-functionalized PPEs may find attractive applications in biological sensing schemes.¹⁴

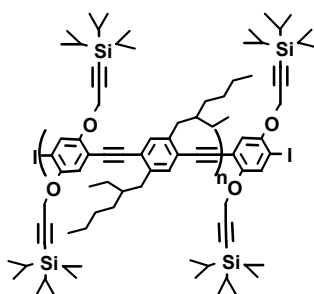
6.4 Experimental

Instrumentation. The ^1H and ^{13}C NMR spectra were taken on a Varian 300 MHz or a Bruker 400 MHz spectrometer using a broadband probe. The ^1H chemical shifts are referenced to the residual proton peaks of CDCl_3 at δ 7.24 and DMSO at δ 2.49. The ^{13}C resonances are referenced to the central peak of CDCl_3 at δ 77.0 and DMSO at δ 39.5. Chromium(III)acetylacetonate was used when obtaining ^{13}C NMR data for all polymers. UV-VIS measurements were made with a Shimadzu UV-2401PC recording spectrophotometer. Fluorescence data was obtained with a Shimadzu RF-5301PC spectrofluorophotometer. A Headway Research Model PWM32 instrument was used to spin-coat dilute chloroform solutions of polymers onto quartz slides for thin film experiments. 1,4-Diiodo-2,5-dihydroquinone,¹³ 1,4-diethynyl-2,5-bis(2-ethylhexyl)-benzene **6.4**,¹³ dodecyl azide **6.7a**,¹² and **6.9**¹³ were prepared and characterized in accordance to published procedures.

General Procedure for Conversion of Halide to Azide: In a round bottom flask the corresponding organic halide was dissolved in acetone, 10 eq of sodium azide were added, and the mixture was heated to reflux for 24 h, cooled to room temperature and the solvent was removed under vacuum. Following aqueous work up the crude products were purified by column chromatography on silica gel with dichloromethane:hexane as an eluent.

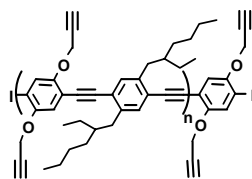


Synthesis of 6.3: 1,4-Hydroxy-2,5-diiodo benzene (4.73 g, 13.1 mmol), potassium carbonate (18.1 g, 131 mmol), and **6.2** (9.00 g, 32.7 mmol) were dissolved in acetone (150 mL). The mixture was heated to reflux for 24 h, allowed to cool to room temperature, was then diluted with dichloromethane and washed with 1N HCl (2 x 150 mL). The solvent was removed under vacuum. The crude solid was purified by chromatography on silica gel (1:1, dichloromethane:hexane) to yield **6.3** as a colorless crystalline solid (8.05 g, 82%). ^1H NMR (CDCl_3): δ 7.47 (m 2H), 4.73 (m, 4H), 1.20 (m, 6H), 1.03 (m, 36H). ^{13}C NMR (CDCl_3): δ 152.2, 124.6, 101.2, 90.8, 86.4, 59.0, 18.9, 11.4. IR: ν 2953, 2735, 2610, 2461, 2183, 2081, 1999, 1901, 1821, 1469, 1372, 1272, 1217, 1068, 1003, 915. MP: 80-82°C.



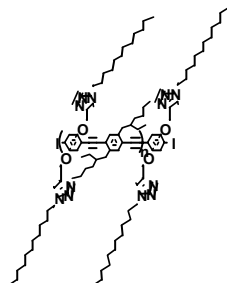
Synthesis of polymer 6.5: Monomer **6.3** (10.0 g, 13.3 mmol) and 2,5-ethylnonyl-1,4-diethynylbenzene **6.4** (4.72 g, 13.5 mmol) were dissolved in tetrahydrofuran (26 mL) and piperidine (26 mL) in an oven dried Schlenk flask. The flask was flushed with nitrogen, frozen and evacuated three times after which $(\text{Ph}_3\text{P})_2\text{PdCl}_2$ (65 mg, 93 μmol), and CuI (10

mg, 53 δ mol) were added. The mixture was allowed to stir at room temperature for 48 h, after which the solvent was removed, the mixture dissolved in dichloromethane, washed with 1N HCl, 1N NH_4OH , and water. The organic layer was dried over MgSO_4 and the solvent removed. The resulting polymer was re-dissolved in dichloromethane and precipitated out of methanol (three times 1L) to yield **6.6** (9.81 g, 87%) as a yellow solid. ^1H NMR (CDCl_3): δ 7.29 (m, 2H), 7.24 (m, 2H), 4.79 (m, 4H), 2.74 (m, 2H), 1.75 (m, 2H), 1.52 (m, 16H), 1.25 (m, 6H), 1.02 (m, 36H), 0.82 (m, 6H). ^{13}C NMR (CDCl_3): δ 152.4, 141.2, 133.2, 123.1, 118.6, 114.5, 101.7, 94.7, 90.1, 58.0, 40.3, 38.4, 32.4, 28.8, 25.6, 23.0, 22.2, 20.5, 18.4, 16.4, 13.9, 11.1, 10.7. IR: ν 2957, 2943, 2920, 2911, 2883, 2860, 2846, 2361, 2159, 1507, 1498, 1489, 1481, 1464, 1457, 1442, 1415, 1344, 1280, 1251, 1196, 1185, 1038, 1032, 1023, 1015, 1008, 983, 879, 665, 647. GPC (polystyrene standards) $M_n = 63.6 \times 10^3$, PDI = 4.42.



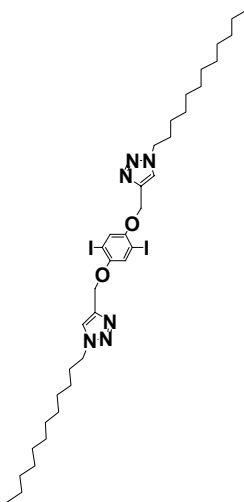
Synthesis of polymer 6.6: Polymer **6.5** (0.250 g, 0.296 mmol) was dissolved in THF (50 mL) under nitrogen purge in an oven dried Schlenk flask. Under nitrogen tetrabutylammoniumfluoride (1 mL, 1M solution in THF, containing ca. 5% water) was added slowly over 5 min. The mixture was allowed to stir at room temperature for 12 h. The solvent was removed, the mixture dissolved in dichloromethane, washed with 1N HCl, 1N NH_4OH , and water. The organic layer was dried over MgSO_4 and the solvent removed. The product was dissolved in dichloromethane and precipitated out of methanol (200 mL) to yield polymer **6.6** (0.149 g, 95%) as a deep yellow solid. ^1H NMR (CDCl_3): δ 7.38 (m, 2H), 7.19 (m, 2H), 4.80 (m, 4H), 2.75 (m, 4H), 2.55 (m, 2H), 1.76

(m, 2H), 1.55 (m, 16H), 1.28 (m, 6H), 0.84 (m, 6H). ^{13}C NMR (TCE): δ 152.8, 141.5, 133.4, 123.2, 118.3, 114.9, 95.2, 89.9, 57.4, 40.4, 38.4, 32.5, 28.8, 25.7, 23.1, 14.0, 10.8. IR: ν 3752, 3663, 3309, 2960, 2921, 2864, 2200, 2135, 1545, 1507, 1455, 1416, 1371, 1262, 1202, 1033, 924, 892, 854, 674, 632. GPC (polystyrene standards) $M_n = 24.4 \times 10^3$, PDI = 1.64.



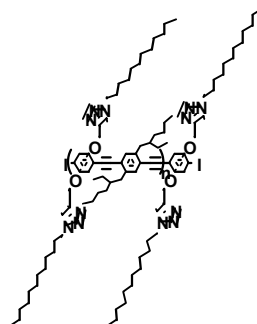
Synthesis of polymer 6.8a (post-polymerization functionalization): Polymer **6.5** (0.100 g, 0.118 mmol) and azide **6.7a** (62 mg, 0.295 mmol) were dissolved in THF (15 mL) under nitrogen purge in an oven dried Schlenk flask. The flask was flushed with nitrogen and frozen and evacuated three times after which CuSO_4 (0.5 mg, 1.9 μmol), sodium ascorbate (4 mg, 19 μmol), and tetrabutylammoniumfluoride (0.25 mL, 1M solution in THF, containing ca. 5% water) were added. The mixture was allowed to stir at 40°C for 48 h. The THF was removed under vacuum and the mixture was dissolved in dichloromethane, washed with 1N HCl, 1N NH_4OH , and water. The organic layer was dried over MgSO_4 and the solvent removed. The resulting polymer was dissolved in dichloromethane and precipitated out of methanol to yield **6.15** (0.104 g, 92%) as a yellow solid. ^1H NMR (CDCl_3): δ 7.58 (m, 2H), 7.28 (m, 4H), 5.33 (m, 4H), 4.31 (m, 4H), 2.72 (m, 4H), 1.87 (m, 12H), 1.58 (m, 46H), 0.86 (m, 18H). ^{13}C NMR (CDCl_3): δ 152.8, 143.9, 141.2, 133.2, 123.1, 122.0, 118.1, 114.9, 94.7, 89.9, 64.1, 50.2, 40.2, 38.3, 32.3, 31.7, 30.0, 29.2, 26.3, 25.5, 22.7, 13.8, 10.6. IR: ν 3136, 2948, 2851, 2729, 2673,

2418, 2201, 2094, 1599, 1507, 1461, 1446, 1418, 1378, 1334, 1277, 1212, 1007, 861, 722. GPC (polystyrene standards) M_n = 8463, PDI = 3.20.

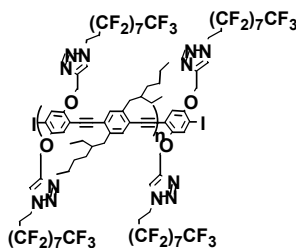


Synthesis of 6.10a: Diiodo compound **6.9** (1.00 g, 2.28 mmol) and azide **6.7a** (1.93 g, 9.13 mmol) were dissolved in THF under nitrogen purge in an oven dried Schlenk flask. The flask was flushed with nitrogen, frozen, and evacuated three times after which CuSO_4 (6 mg, 22.8 μmol) and sodium ascorbate (45 mg, 228 μmol) were added. The mixture was allowed to stir at 50°C for 48 h. The solvent was removed and the mixture dissolved in dichloromethane, washed with 1N HCl, 1N NH_4OH , and water. The organic layer was dried over MgSO_4 . The solvent was removed under vacuum and the crude product purified by chromatography on silica gel (1:1, ethylacetate:hexane) to yield **6.10a** as a light yellow crystalline solid (1.74 g, 89 %). ^1H NMR (CDCl_3): δ 7.66 (s, 2H), 7.35 (s, 2H), 5.19 (s, 4H), 4.34 (t, 8H), 3.89 (m, 4H), 1.91 (m, 4H), 1.24 (m, 36H), 0.84 (t, 6H). ^{13}C NMR (CDCl_3): δ 152.7, 143.7, 135.3, 125.1, 123.9, 122.8, 86.8, 65.0, 50.8, 32.5, 32.2, 30.6, 29.9, 29.8, 29.7, 29.6, 29.3, 26.8, 26.7, 23.7, 23.0, 14.5. IR: ν 3179, 2947, 2844, 2428, 2121, 1900, 1650, 1573, 1485, 1409, 1341, 1204, 1142, 1072, 1038,

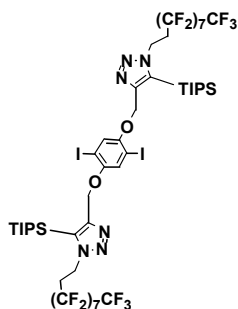
892, 840, 802, 723, 647. MS Calculated for, $[C_{36}H_{58}I_2N_6O_2]$, 860.69; found 860.3; MP: 113-115°C.



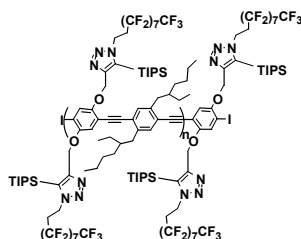
Synthesis of polymer 6.8a (pre-polymerization functionalization): Monomer **6.10a** (0.500 g, 0.581 mmol) and 2,5-ethylhexyl-1,4-diethynylbenzene **6.4** (0.205 g, 0.586 mmol) were dissolved in dichloromethane (2 mL) and piperidine (2 mL) in an oven dried Schlenk flask. The flask was flushed with nitrogen, frozen and evacuated three times after which $(Ph_3P)_2PdCl_2$ (4 mg, 6 μ mol), and CuI (1 mg, 6 μ mol) were added. The mixture was allowed to stir at room temperature for 48 h. The solvent was removed and the mixture dissolved in dichloromethane, washed with 1N HCl, 1N NH_4OH , and water. The organic layer was dried over $MgSO_4$ and the solvent removed. The resulting polymer was dissolved in dichloromethane and precipitated out of methanol three times to yield **6.8a** (0.511 g, 91 %) as a yellow solid. 1H NMR ($CDCl_3$): δ 7.57 (m, 2H), 7.26 (m, 4H), 5.31 (m, 4H), 4.30 (m, 4H), 2.72 (m, 4H), 1.85 (m, 12H), 1.56 (m, 46H), 0.82 (m, 18H). ^{13}C NMR ($CDCl_3$): δ 153.0, 143.82, 141.1, 133.0, 124.8, 121.9, 117.8, 114.5, 94.4, 89.7, 89.7, 63.9, 50.0, 40.0, 38.1, 32.0, 29.0, 26.0, 22.6, 13.6, 10.4. IR: ν 3602, 3083, 2954, 2841, 2434, 2196, 2028, 1688, 1529, 1499, 1361, 1212, 890, 824, 777, 600. GPC (polystyrene standards) $M_n = 13.7 \times 10^3$, PDI = 5.24.



Synthesis of polymer 6.8b (post-polymerization functionalization): Polymer **6.5** (0.100 g, 0.118 mmol) and azide **6.7b** (0.231 g, 0.471 mmol) were dissolved in THF (15 mL) under nitrogen purge in an oven dried Schlenk flask. The flask was flushed with nitrogen, frozen and evacuated three times after which CuSO₄ (0.5 mg, 2 μmol), L-Ascorbic acid sodium salt (4 mg, 19 μmol), and tetrabutylammoniumfluoride (0.25 mL, 1M solution in THF, containing ca. 5% water) were added. The mixture was allowed to stir at 60°C for 48 h. The solvent was removed under vacuum. The mixture was re-dissolved in dichloromethane, washed with 1N HCl, 1N NH₄OH and water. The organic layer was dried over MgSO₄ and the solvent was removed. The resulting polymer was dissolved in dichloromethane and precipitated out of methanol to yield **6.8b** (0.168 g, 94%) as a yellow solid. ¹H NMR (CDCl₃): δ 7.64 (m, 2H), 7.26 (m, 2H), 7.17 (m, 2H), 5.34 (m, 4H), 4.64 (m, 4H), 2.82 (m, 4H), 1.25 (m, 20H), 0.84 (m, 12H). ¹³C NMR (CDCl₃): δ 153.0, 144.5, 141.2, 133.2, 122.2, 118.2, 114.9, 110.6, 94.8, 90.1, 63.8, 57.9, 42.3, 40.3, 38.3, 32.3, 31.7, 29.7, 28.6, 25.5, 22.9, 18.3, 13.8, 11.0, 10.6. IR: ν 3311, 3259, 2961, 2443, 2204, 1702, 1592, 1505, 1456, 1415, 1356, 1316, 1258, 1076, 1015, 887, 799, 752, 707, 658. GPC (polystyrene standards) M_n = 25.4 × 10³, PDI = 2.56.

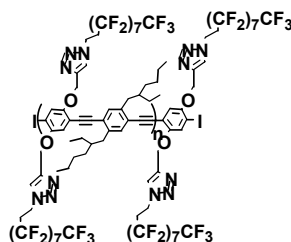


Synthesis of 6.11: Diiodo compound **6.3** (1.00 g, 1.33 mmol) and azide **6.7b** (2.93 g, 5.99 mmol) were dissolved in *o*-xylene under nitrogen purge in an oven dried Schlenk flask. The mixture was allowed to stir at reflux for 48 h. The solvent was removed under vacuum and the crude product purified by chromatography on silica gel (1:3, ethylacetate:hexane) to yield **6.10b** as a colorless solid and single regioisomer (2.01 g, 86 %). ^1H NMR (CDCl_3): δ 7.25 (s, 2H), 5.06 (s, 4H), 4.74 (t, 4H), 3.04 (m, 4H), 1.43 (m, 6H), 1.09 (m, 36H). ^{13}C NMR (CDCl_3): δ 152.4, 142.3, 137.0, 123.0, 85.8, 60.8, 40.7, 31.8, 18.8, 18.5, 11.5, 1.1. ^{19}F NMR (CDCl_3): -82.1, -115.4, -123.0, -123.2, -124.1, -124.5, -127.5. IR: ν 3090, 2947, 2867, 2725, 2464, 2363, 2105, 2002, 1692, 1467, 1458, 1375, 1352, 1233, 1207, 1150, 1055, 1000, 883, 848, 711, 647. MS Calculated for, $[\text{C}_{50}\text{H}_{56}\text{F}_{34}\text{I}_2\text{N}_6\text{O}_2\text{Si}_2]$, 1728.9; found 1729.4; MP: 146-150°C.



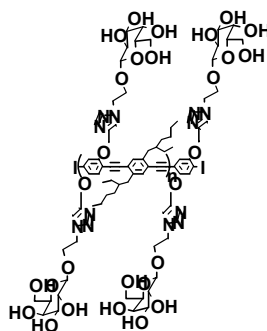
Synthesis of polymer 6.12 (pre-polymerization functionalization): Monomer **6.11** (single regioisomer) 1.00 g, 0.574 mmol) and 2,5-ethylhexyl-1,4-diethynylbenzene **6.4** (0.203 g, 0.579 mmol) were dissolved in dichloromethane (2 mL) and piperidine (2 mL) in an oven dried Schlenk flask. The flask was flushed with nitrogen, frozen and

evacuated three times after which $(\text{Ph}_3\text{P})_2\text{PdCl}_2$ (20 mg, 29 μmol), and CuI (6 mg, 29 μmol) were added. The mixture was allowed to stir at room temperature for 48 h. The solvent was removed and the mixture dissolved in dichloromethane, washed with 1N HCl , 1N NH_4OH , and water. The organic layer was dried over MgSO_4 and the solvent removed. The resulting polymer **6.12** was dissolved in dichloromethane and precipitated out of methanol three times to yield a yellow solid (1.42 g, 91 %). ^1H NMR (CDCl_3): δ 7.26 (m, 4H), 7.18 (m, 2H), 5.35 (m, 4H), 4.66 (m, 4H), 2.80 (m, 4H), 1.24 (m, 18H), 1.01 (m, 42H) 0.82 (m, 12H). ^{13}C NMR (CDCl_3): δ 152.7, 141.9, 141.4, 137.4, 133.2, 122.5, 117.3, 114.7, 113.2, 110.5, 95.6, 88.8, 60.4, 44.8, 40.4, 38.1, 32.2, 31.6, 28.6, 25.4, 22.8, 18.3, 13.7, 11.3, 10.5. IR: ν 2962, 2867, 2726, 2357, 2205, 1506, 1460, 1412, 1367, 1259, 1092, 1018, 872, 797, 658. GPC (polystyrene standards) $M_n = 25.5 \times 10^4$, PDI = 4.25.



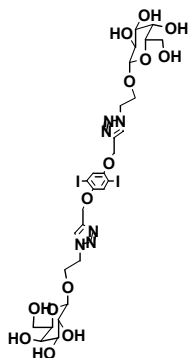
Synthesis of Polymer 6.8b (pre-polymerization functionalization): Polymer **6.12** (0.5 g, 0.331 mmol) was dissolved in THF (50 mL) under nitrogen purge in an oven dried Schlenk flask. Under nitrogen tetrabutylammoniumfluoride (3 mL, 1M solution in THF, containing ca. 5% water) was added slowly over 5 min. The mixture was stirred for 24 hours. The solvent was removed under vacuum and the resulting solid dissolved in dichloromethane and washed with water. The organic layer was dried under MgSO_4 , filtered and the solvent removed to afford **8b** as a yellow solid (0.398 g, 96 %). ^1H NMR (CDCl_3): δ 7.65-7.51 (m, 2H), 7.25 (m, 2H), 7.18 (m, 2H), 5.32 (m, 4H), 4.63 (m, 4H),

2.82 (m, 4H), 1.24 (m, 20H), 0.83 (m, 12H). ^{13}C NMR (CDCl_3): δ 152.7, 140.8, 132.9, 122.8, 117.1, 114.3, 112.7, 100.7, 94.5, 89.6, 67.5, 63.1, 42.0, 40.0, 37.8, 31.8, 28.2, 25.0, 22.5, 17.9, 13.5, 10.2. IR: ν 2959, 2863, 2206, 1691, 1614, 1463, 1223, 1027, 883, 744, 709, 652. GPC (polystyrene standards) M_n 71.7×10^3 , PDI = 4.44.

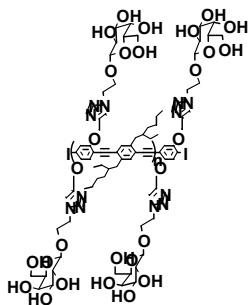


Synthesis of Polymer 6.8c (post-polymerization functionalization): Polymer **6.5** (0.100 g, 0.118 mmol) and azide **6.7c** (88.4 mg, 0.355 mmol) were dissolved in THF (15 mL) under nitrogen purge in an oven dried Schlenk flask. The flask was flushed with nitrogen and frozen and evacuated three times after which CuSO_4 (0.5 mg, 2 μmol), sodium ascorbate (4 mg, 19 μmol), and tetrabutylammoniumfluoride (0.25 mL, 1M solution in THF, containing ca. 5% water) were added. The mixture was stirred at 50°C for 48 h. The solvent was removed and the mixture dissolved in dichloromethane, washed with 1N HCl, 1N NH_4OH , and water. The organic layer was dried over MgSO_4 and the solvent removed under vacuum. The resulting polymer was dissolved in hot DMSO and precipitated out of methanol (three times) to yield **6.8c** (0.093 g, 76 %) as a yellow solid. ^1H NMR (DMSO): δ 7.56-7.50 (m, 4H), 7.41 (m, 2H), 5.73 (m, 2H), 4.92 (m, 2H), 4.59 (m, 6H), 4.01 (m, 12H), 3.18 (m, 12H), 1.91 (m, 32H), 1.73 (m, 6H), 1.55 (m, 16H), 1.25 (m, 6H), 0.84 (m, 12H). ^{13}C NMR (TCE): δ 152.6, 141.7, 132.6, 124.6, 117.5, 102.8, 93.9, 90.3, 76.4, 72.9, 69.8, 67.0, 60.8, 57.3, 48.1, 30.1, 27.8, 24.8, 22.6,

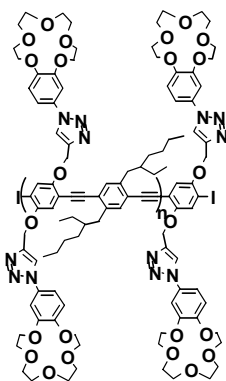
18.7, 13.2, 10.3. IR: ν 3544, 3309, 2948, 2866, 2528, 2200, 2102, 1730, 1625, 1436, 1382, 1203, 1118, 1076, 1041, 862, 740, 555, 453, 412. GPC (polystyrene standards) M_n = 22.6×10^3 , PDI = 2.39.



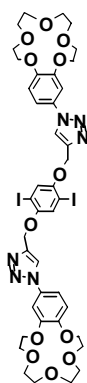
Synthesis of 6.10c: Diiodo compound **6.9** (1.00 g, 2.28 mmol) and azide **6.7c** (2.00 g, 4.79 mmol) were dissolved in THF under nitrogen purge in an oven dried Schlenk flask. The flask was flushed with nitrogen, frozen and evacuated three times after which CuSO_4 (6 mg, 22.8 μmol) and sodium ascorbate (45 mg, 228 μmol) were added. The mixture was allowed to stir at 50°C for 48 h. The solvent was removed and the mixture dissolved in dichloromethane, washed with 1N HCl, 1N NH_4OH , and water. The organic layer was dried over MgSO_4 . The solvent was removed under vacuum and the crude product purified by chromatography on silica gel (1:1, ethylacetate:dichloromethane) to yield **6.10c** as a colorless crystalline solid (1.81 g, 62 %). ^1H NMR (CDCl_3): δ 7.78 (s, 2H), 7.41 (s, 2H), 7.24 (s, 2H), 5.15 (m, 6H), 4.49 (m, 12H), 3.95 (m, 4H), 3.68 (m, 4H), 1.97 (m, 24H). ^{13}C NMR (CDCl_3): δ 170.3, 169.8, 169.1, 169.0, 152.5, 143.1, 124.2, 123.7, 100.4, 86.5, 72.3, 71.8, 70.8, 68.1, 67.6, 64.4, 61.6, 50.1, 20.7, 20.5. IR: ν 3557, 3479, 3454, 3086, 2955, 2876, 2739, 2450, 2419, 2109, 2028, 1961, 1916, 1732, 1645.17, 1482, 1320, 1172, 993, 952, 907, 854, 795, 753, 696, 649, 602. MS Calculated for, $[\text{C}_{44}\text{H}_{54}\text{I}_2\text{N}_6\text{O}_{22}]$, 1272.74; found 1273.1; MP: 156-160°C.



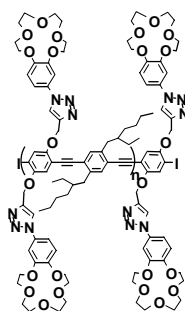
Synthesis of polymer 6.8c (pre-polymerization functionalization): Monomer **6.10c** (0.230 g, 0.251 mmol) and 2,5-ethylhexyl-1,4-diethynylbenzene **6.4** (0.088 g, 0.251 mmol) were dissolved in dichloromethane (2 mL) and piperidine (2 mL) in an oven dried Schlenk flask. The flask was flushed with nitrogen, frozen and evacuated three times after which $(\text{Ph}_3\text{P})_2\text{PdCl}_2$ (3 mg, 5 μmol), and CuI (1 mg, 5 μmol) were added. The mixture was allowed to stir at room temperature for 48 h. The solvent was removed and the mixture dissolved in dichloromethane, washed with 1N HCl, 1N NH_4OH , and water. The organic layer was dried over MgSO_4 and the solvent removed. The solvent was concentrated and the polymer precipitated out of H_2O (50:50) twice to yield **6.13** (0.241 g, 93%). ^1H NMR (DMSO): δ 7.56 (m, 2H), 7.50 (m, 2H), 7.41 (m, 2H), 5.72 (m, 2H), 4.91 (m, 2H), 4.59 (m, 6H), 4.01 (m, 12H), 3.18 (m, 12H), 1.91 (m, 32H), 1.70 (m, 6H), 1.54 (m, 16H), 1.26 (m, 6H), 0.87 (m, 6H). ^{13}C NMR (DMSO): δ 152.7, 141.9, 140.7, 132.6, 124.5, 122.3, 117.7, 113.7, 111.9, 102.7, 93.8, 85.9, 76.48, 73.0, 69.9, 66.6, 61.0, 58.1, 49.4, 31.5, 27.8, 24.9, 21.9, 13.2, 10.2. IR: ν 3577, 3454, 3258, 3126, 2956, 2924, 2806, 2710, 2201, 1960, 1644, 1598, 1513, 1466, 1401, 1279, 1213, 1163, 1023, 991, 870, 804. GPC (polystyrene standards) $M_n = 24.5 \times 10^4$, PDI = 1.01.



Synthesis of polymer 6.8d (post-polymerization functionalization): Polymer **6.5** (0.100 g, 0.188 mmol) and azide **6.7d** (0.116 g, 0.375 mmol) were dissolved in THF under nitrogen purge in an oven dried Schlenk flask. The flask was flushed with nitrogen, frozen and evacuated three times after which CuSO₄ (0.5 mg, 1.9 μmol), L-Ascorbic acid sodium salt (4 mg, 18.7 μmol), and tetrabutylammoniumfluoride (0.25 mL, 1M solution in THF, containing ca. 5% water) were added. The mixture was allowed to stir at 40°C for 48 h. The solvent was concentrated and the polymer precipitated out of methanol:H₂O (50:50) twice to yield **6.8d** (0.149 g, 82%). ¹H NMR (CDCl₃): δ 8.01 (m, 1H), 7.63 (m, 1H), 7.38 (m, 2H), 6.86 (m, 2H), 4.80 (m, 4H), 4.13 (m, 8H), 3.89 (m, 8H), 3.73 (m, 16H), 2.75 (m, 4H), 2.55 (m, 2H), 1.76 (m, 2H), 1.55 (m, 16H), 1.28 (m, 6H), 0.84 (m, 6H). ¹³C NMR (TCE): δ 153.5, 150.0, 144.9, 141.7, 133.6, 130.6, 120.7, 118.1, 114.3, 112.5, 107.1, 94.9, 90.1, 70.4, 69.6, 64.5, 53.23, 40.4, 38.5, 32.4, 28.8, 25.6, 22.6, 14.0, 10.9. IR: ν 3642, 3561, 3515, 3412, 2930, 2857, 2351, 2205, 1644, 1592, 1504, 1445, 1263, 1138, 1130. GPC (polystyrene standards) M_n = 108.4 × 10³, PDI = 1.49.

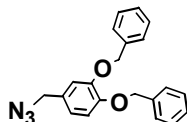


Synthesis of 6.10d: Diiodo compound **6.9** (0.500 g, 1.14 mmol) and azide **6.7d** (1.05 g, 3.39 mmol) were dissolved in THF under nitrogen purge in an oven dried Schlenk flask. The flask was flushed with nitrogen, frozen and evacuated three times after which CuSO₄ (3 mg, 11 μmol) and sodium ascorbate (23 mg, 114 μmol) were added. The mixture was allowed to stir at 50°C for 48 h. The solvent was removed and the mixture dissolved in dichloromethane, washed with 1N HCl, 1N NH₄OH, and water. The organic layer was dried over MgSO₄. The solvent was removed under vacuum and the crude product purified by chromatography on silica gel (10:1, ethylacetate:hexane) to yield **6.10d** as a colorless crystalline solid (0.651 g, 53 %). ¹H NMR (CDCl₃): δ 7.77 (m, 2H), 7.23 (m, 2H), 7.56 (m, 4H), 6.78 (t, 2H), 5.14 (m, 4H), 4.11 (m, 8H), 3.87 (m, 8H), 3.61 (m, 16H). ¹³C NMR (CDCl₃): δ 152.9, 135.5, 130.1, 124.8, 124.4, 118.5, 114.8, 111.4, 107.4, 86.8, 78.9, 71.9, 71.0, 69.9, 61.1, 58.2. IR: ν 3259, 2954, 2871, 2360, 2115, 1734, 1600, 1518, 1455, 1349, 1223, 1021, 801. MS Calculated for, [C₄₀H₄₆I₂N₆O₁₂], 1056.6; found 1057.2; MP: 162-164°C.

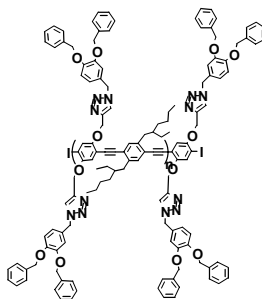


Synthesis of Polymer 6.8d (Pre-polymerization functionalization): Monomer **6.10d**

(0.301 g, 0.280 mmol) and 2,5-ethylhexyl-1,4-diethynylbenzene **6.4** (99.2 mg, 0.283 mmol) were dissolved in dichloromethane (2 mL) and piperidine (2 mL) in an oven dried Schlenk flask. The flask was flushed with nitrogen, frozen and evacuated three times after which $(\text{Ph}_3\text{P})_2\text{PdCl}_2$ (10 mg, 14 μmol), and CuI (3 mg, 14 μmol) were added. The mixture was allowed to stir at room temperature for 48 h. The solvent was removed and the mixture dissolved in dichloromethane, washed with 1N HCl, 1N NH_4OH , and water. The organic layer was dried over MgSO_4 and the solvent removed. The resulting polymer was dissolved in dichloromethane and precipitated out of methanol three times to yield **6.8d** (0.309 g, 93 %) as a yellow solid. ^1H NMR (CDCl_3): δ 8.01 (m, 2H), 7.26 (m, 10H), 5.39 (m, 4H), 4.14 (m, 16H), 3.75 (m, 16H), 2.68 (m, 4H), 1.24 (m, 16H), 0.84 (m, 12H). ^{13}C NMR (CDCl_3): δ 153.0, 144.4, 142.6, 141.2, 135.0, 133.0, 131.7, 130.3, 120.4, 117.2, 113.2, 112.0, 106.3, 95.0, 89.8, 70.7, 70.7, 68.8, 63.7, 40.1, 38.0, 32.1, 30.5, 28.4, 25.2, 22.7, 13.8, 10.5. IR: ν 2958, 2207, 1604, 1510, 1453, 1261, 1101, 1018, 933, 802. GPC (polystyrene standards) $M_n = 16.2 \times 10^4$, PDI = 7.70.

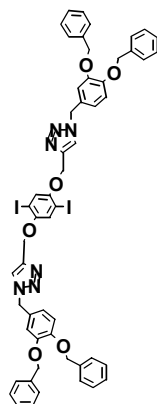


Synthesis of 6.7e: 3,4-dibenzyloxybenzyl chloride (0.500 g, 1.48 mmol) and sodium azide (0.959 g, 14.8 mmol) were dissolved in acetone in an oven dried Schlenk flask. The mixture was allowed to stir at reflux for 48 h. The solvent was removed, the mixture dissolved in dichloromethane and washed with water. The organic layer was dried over MgSO_4 . The solvent was removed under vacuum and the crude product was purified by chromatography on silica gel (2:1, dichloromethane:hexane) to yield **6.7e** as a light yellow crystalline solid (0.430 g, 84 %). ^1H NMR (CDCl_3): δ 7.39 (m, 10H), 6.85 (m, 3H), 5.19 (s, 4H), 4.23 (s, 2H). ^{13}C NMR (CDCl_3): δ 149.3, 149.2, 137.4, 134.3, 128.7, 128.1, 128.1, 127.6, 127.5, 121.8, 115., 3, 115.1, 71.6, 71.5, 54.9. IR: ν 3337, 3027, 2897, 2838, 2445, 2079, 1599, 1413, 1304, 1248, 1201, 1057, 988, 940, 839, 767, 670, 633. MS Calculated for, $[\text{C}_{21}\text{H}_{19}\text{N}_3\text{O}_2]$, 345.39; found fragmentation; MP: 82-85°C.



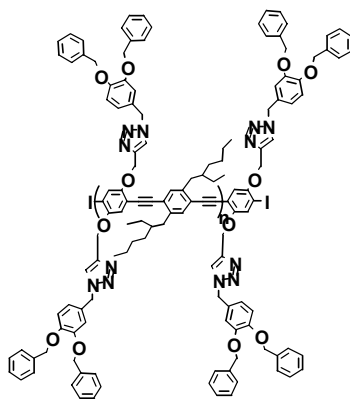
Synthesis of Polymer 6.8e (Post-polymerization functionalization). Polymer **6.5** (0.100 g, 0.118 mmol) and azide **6.7e** (163 mg, 0.471 mmol) were dissolved in THF (10 mL) under nitrogen purge in an oven dried Schlenk flask. The flask was flushed with nitrogen, frozen and evacuated three times after which CuSO_4 (0.5 mg, 2 μmol), sodium ascorbate (4 mg, 19 μmol), and tetrabutylammoniumfluoride (0.25 mL, 1M solution in

THF, containing ca. 5% water) were added. The mixture was stirred at 60°C for 48 h. The solvent was removed and the mixture dissolved in dichloromethane, washed with 1N HCl, 1N NH₄OH, and water. The organic layer was dried over MgSO₄ and the solvent removed under vacuum. The resulting polymer was dissolved in dichloromethane and precipitated out of methanol (three times) to yield **6.8e** (0.139 g, 96%) as a yellow solid. ¹H NMR (CDCl₃): δ 7.37 (m, 2H), 7.25 (m, 28H), 4.79 (m, 16H), 2.74 (m, 4H), 2.54 (m, 2H), 1.74 (m, 2H), 1.54 (m, 16H), 1.29 (m, 6H), 0.84 (m, 6H). ¹³C NMR (TCE): δ 152.3, 141.4, 133.4, 132.0, 128.4, 127.8, 127.3, 123.1, 118.2, 115.2, 94.2, 89.5, 71.3, 57.4, 40.4, 38.4, 32.4, 28.7, 25.7, 23.0, 14.0, 10.8. IR: ν 3306, 2957, 2918, 2864, 2200, 2122, 1948, 1638, 1599, 1505, 1456, 1419, 1259, 1204, 1025, 804. GPC (polystyrene standards) M_n = 22.6 x 10³, PDI = 2.39.



Synthesis of 6.10e: Diiodo compound **6.9** (0.400 g, 0.913 mmol) and azide **6.7e** (1.26 g, 3.65 mmol) were dissolved in THF under nitrogen purge in an oven dried Schlenk flask. The flask was flushed with nitrogen, frozen and evacuated three times after which CuSO₄ (2 mg, 9 μmol) and sodium ascorbate (18 mg, 97.3 μmol) was added. The mixture was allowed to stir at 50°C for 48 h. The solvent was removed and the mixture dissolved in dichloromethane, washed with 1N HCl, 1N NH₄OH, and water. The organic layer was

dried over MgSO_4 . The solvent was removed under vacuum and the crude product purified by chromatography on silica gel (1:1, ethylacetate:dichloromethane) to yield **6.10e** as a colorless solid (0.830 g, 80 %). ^1H NMR (CDCl_3): δ 7.56 (s, 2H), 7.46 (m, 22H), 7.12 (m, 6H), 5.64 (d, 4H), 5.39 (m, 4H), 5.10 (d, 8H). ^{13}C NMR (CDCl_3): δ 152.5, 149.2, 149.0, 138.7, 136.7, 136.6, 128.4, 127.8, 127.2, 127.0, 123.7, 122.5, 121.3, 114.7, 114.7, 86.6, 71.2, 64.6, 54.0. IR: ν 3060, 3031, 2927, 2867, 2088, 1953, 1753, 1728, 1595, 1513, 1348, 1263, 1217, 1135, 1054, 1021, 846, 698, 616. MS Calculated for, $[\text{C}_{52}\text{H}_{42}\text{I}_2\text{N}_6\text{O}_6]$, 1100.74; found fragmentation; MP: 155-157°C.



Synthesis of Polymer 6.8e (Pre-polymerization functionalization): Monomer **6.10e** (0.600 g, 0.532 mmol) and 2,5-ethylhexyl-1,4-diethynylbenzene **6.4** (0.188 g, 0.537 mmol) were dissolved in THF (2 mL) and piperidine (2 mL) in an oven dried Schlenk flask. The flask was flushed with nitrogen, frozen and evacuated three times after which $(\text{Ph}_3\text{P})_2\text{PdCl}_2$ (19 mg, 27 μmol), and CuI (5 mg, 27 μmol) were added. The mixture was allowed to stir at room temperature for 48 h. The solvent was removed and the mixture dissolved in dichloromethane, washed with 1N HCl, 1N NH_4OH , and water. The organic layer was dried over MgSO_4 and the solvent removed. The resulting polymer was dissolved in dichloromethane and precipitated out of methanol three times to yield **6.8a**

(0.493 g, 75 %) as a yellow solid. ^1H NMR (CDCl_3): δ 7.36 (m, 2H), 7.23 (m, 28H), 4.80 (m, 16H), 2.74 (m, 4H), 2.54 (m, 2H), 1.74 (m, 2H), 1.54 (m, 16H), 1.29 (m, 6H), 0.83 (m, 6H). ^{13}C NMR (CDCl_3): δ 160.6, 152.8, 148.8, 143.9, 141.1, 136.4, 133.0, 131.1, 128.1, 127.5, 127.0, 123.9, 122.3, 121.0, 117.5, 114.4, 94.6, 89.9, 70.8, 63.5, 53.6, 45.7, 40.0, 38.0, 31.9, 31.4, 30.6, 29.0, 28.3, 27.3, 25.1, 24.5, 23.3, 22.7, 20.3, 13.7, 10.4. IR: ν 2944, 2938, 2723, 2597, 2396, 2204, 1955, 1602, 1445, 1268, 1125, 1004, 803. GPC (polystyrene standards) $M_n = 71.8 \times 10^3$, PDI = 2.10.

6.5 References:

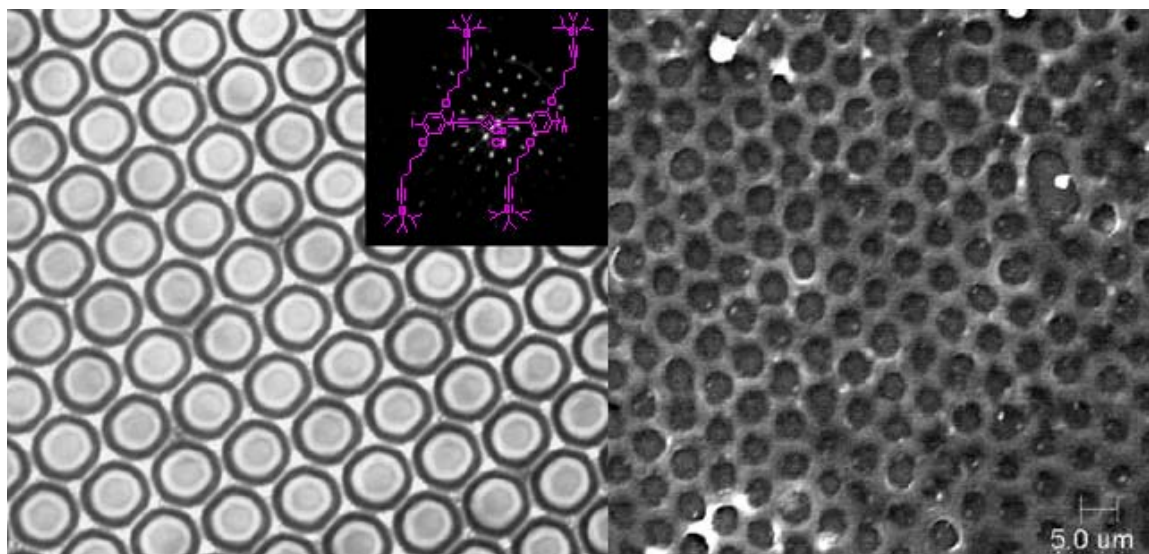
1. Bernier, S.; Garreau, S.; Bera-Aberem, M.; Gravel, C.; Leclerc, M. *J. Am. Chem. Soc.* **2002**, *124*, 12463.
2. a) Li, Y. N.; Vamvounis, G.; Holdcroft, S. *Chemistry of Materials*. **2002**, *14*, 1424.
b) Li, Y. N.; Vamvounis, G.; Yu, J. F.; Holdcroft, S. *Macromolecules* **2001**, *34*, 3130.
3. a) Huisgen, R.; Szeimies, G.; Moebius, L. *Chem. Ber.* **1967**, *100*, 2494. b) Huisgen, R.; Knorr, R.; Moebius, L.; Szeimies, G. *Chem. Ber.* **1965**, *98*, 4014.
4. a) Lewis, W. G.; Green, L. G.; Grynszpan, F.; Radic, Z.; Carlier, P. R.; Taylor, P.; Finn, M. G.; Sharpless, B. K. *Angew. Chem. Int. Ed.* **2002**, *41*, 1053. b) Rostovtsev, V. V.; Green, L. G.; Fokin, V. V.; Sharpless, B. K. *Angew. Chem. Int. Ed.* **2002**, *41*, 2596.
5. a) Wu, P.; Feldman, A. K.; Nugen, A. K.; Hawker, C. J.; Scheel, A.; Voit, B.; Pyun, J.; Frechet, J. M. J.; Sharpless, B. K.; Fokin, V. V. *Angew. Chem. Int. Ed.* **2004**, *43*,

2. b) Helms, B.; Mynar, J. L.; Hawker, C. J.; Frechet, J. M. J. *J. Am. Chem. Soc.* **2004**, *126*, 15020.
6. a) Wagner, M.; Nuyken, O. *Macromolecules* **2003**, *36*, 6716. b) Wagner, M. Nuyken, O., *J. Macromol. Sci. A* **2004**, *41*, 637. Wang, Y. Q.; Wilson, J. N.; Smith, M. D.; Bunz, U. H. F. *Macromolecules* **2004**, *37*, 970. c) Wilson, J. N., Wang, Y. Q.; Lavigne, J. J.; Bunz, U. H. F. *Chem Commun*, **2003**, 1626. d) Disney, M. D.; Zheng, J.; Swager, T. M.; Seeberger, P. H. *J. Am. Chem. Soc.* **2004**, *126*, 13343. e) Hecht S.; Khan A. *Angew. Chem.* **2003**, *42*, 6021. f) Breen, C. A.; Deng, T.; Breiner, T.; Thomas, E. L.; Swager, T. M. *J. Am. Chem. Soc.* **2003**, *125*, 9942.
7. a) Kraft, A.; Grimsdale, A. C.; Holmes, A. B. *Angew. Chem.* **1998**, *37*, 402. b) Pschirer, N. G.; Miteva, T.; Evans, U.; Roberts, R. S.; Marshall, A. R.; Neher, D.; Myrick, M. L.; Bunz, U. H. F. *Chem. Mater.* **2001**, *13*, 2691. c) Schmitz, C.; Posch, P.; Thelakkat, M.; Schmidt, H. W.; Montali, A.; Feldman, K.; Smith, P.; Weder, C. *Adv. Funct. Mater.* **2001**, *11*, 41.
8. Xu, Y.; Berger, P. R.; Wilson, J. N.; Bunz, U. H. F. *Appl. Phys. Lett.* **2004**, *85*, 4219.
9. a) Bunz, U. H. F.; Wilson, J. N.; Bangcuyo C. *ACS Symp. Ser.* **2005**, *888*, 147. b) Halkyard, C. E.; Rampey, M. E.; Kloppenburg, L.; Studer-Martinez, S. L.; Bunz, U. H. F. *Macromolecules* **1998**, *31*, 8655. c) Wilson, J. N.; Steffen, W.; McKenzie, T. G.; Lieser, G.; Oda, M.; Neher, D.; Bunz, U. H. F. *J. Am. Chem. Soc.* **2002**, *124*, 6830. d) Kim, J. S.; Swager, T. M. *Nature* **2001**, *411*, 1030. e) Miteva, T.; Palmer, L.; Kloppenburg, L.; Neher, D.; Bunz, U. H. F. *Macromolecules*, **2000**, *33*, 652.

10. Binder, W. H.; Kluger, C. *Macromolecules*, **2004**, *37*, 9321.
11. Tsarevsky, N. V.; Bernaerts, K. V.; Dugour, B.; Du Prez, F. E.; Matyjaszewski, K. *Macromolecules* **2004**, *37*, 9308.
12. a) Englert, B. C.; Smith, M. D.; Hardcastle, K. I.; Bunz, U. H. F.; *Macromolecules*; **2004**, *37*, 8212.
13. a) Bunz, U. H. F. *Chem. Rev.* **2000**, *100*, 1605. b) Wilson, J. N.; Waybright, S. M.; McAlpine, K.; Bunz, U. H. F. *Macromolecules* **2002**, *35*, 3799. c) Huang, W. Y.; Gao, W.; Kwei, T. K.; Okamoto, Y. *Macromolecules* **2001**, *34*, 1570. d) Sluch, M. I.; Godt, A.; Bunz, U. H. F.; Berg, M. A. *J. Am. Chem. Soc.* **2001**, *123*, 6447.
14. Breitkamp, R. B.; Tew, G. N. *Macromolecules* **2004**, *37*, 1163.

CHAPTER 7

TEMPLATED CERAMIC MICROSTRUCTURES BY THE BREATH FIGURE METHOD.



7.1 Introduction

Non-oxide Si-C ceramics are hard insoluble materials which are resistant to high temperatures, oxidizing, and reducing agents. These materials are often made by utilizing precursor polymers such as polysilanes and polycarbosilanes that can be cast into molds, crosslinked, and then thermolyzed.¹ Because of these properties they are of great industrial and scientific importance.

For successful preparation of such ceramics the precursor polymer must have high unsaturation and processability. Providing these polymers can be microstructured, novel device architectures could be accessed by backfilling such ceramics with organic semiconductors.

For use in photonic crystals and as potential support for biological application such as cell growth and as dirt-repellant coatings exhibiting the lotus leaf effect; these materials must be microstructured.² There has been widespread effort to utilize templating methods. One common approach is to infiltrate a colloidal crystal of polystyrene spheres with a soluble inorganic precursor. The precursor is then decomposed into a crosslinked preceramic and further heated to burn off the polystyrene and produce the ceramic.³ Silica nanospheres can also be used and then removed using hydrofluoric acid. In both of these methods the dimensions of the skeletal structures, are fixed and dependent upon the size of the templates and mesospheres.⁴

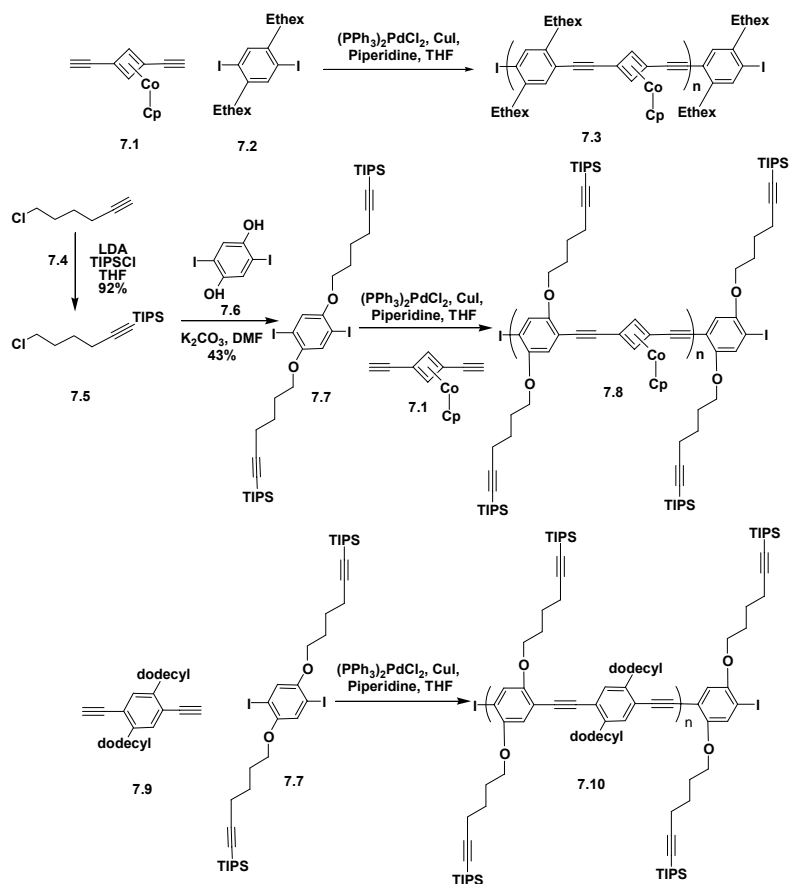
Micro- and nanostructuring of semiconducting polymers is of great importance in the fabrication of photonic bandgap materials and devices such as photovoltaic cells and thin-film transistors.⁵ There have been a variety of templating methods developed based on self-assembly. Some of these methods include using emulsion templating,⁶ templating using ordered arrays of colloidal particles,⁷⁻¹¹ and self-organized surfactants that generate mesoporous silica.¹²⁻¹⁴

Recently Bunz et al reported microstructures obtained from Poly(para-phenyleneethynylene) PPEs by using the breath figure method.¹⁵ This method enables the microstructuring of PPEs into hexagonally ordered two dimensional (2D) arrays due to the condensation of water vapor from moist air onto the polymer solution surface into small droplets. After sinking into polymer solution, further evaporation of the polymer solution leaves fossilized bubbles which are organized into a 2D hexagonal arrays which vary from 0.2 to 20 microns and are monodisperse in many cases. This has proven to be a powerful method to create permanent structures by using cross-linkable polymers as a

substrait.¹⁶ It would be interesting to use these bubble arrays to create other types of microstructured materials. With this in mind, organometallic polymer **7.8** was synthesized.

7.2 Results and Discussion

Polymer **7.8** (Scheme 7.1) can be used to fabricate permanent hexagonal microstructures which result from pyrolysis of its two-dimensional (2D) bubble arrays. The bubble arrays can be made permanent by heating them to 500°C under air or nitrogen. The interconnected bubble arrays are converted into a mesh of “picoliter”³ beakers after pyrolysis.



Scheme 7.1. Synthesis of polymers **7.3**, **7.8**, and **7.10**.

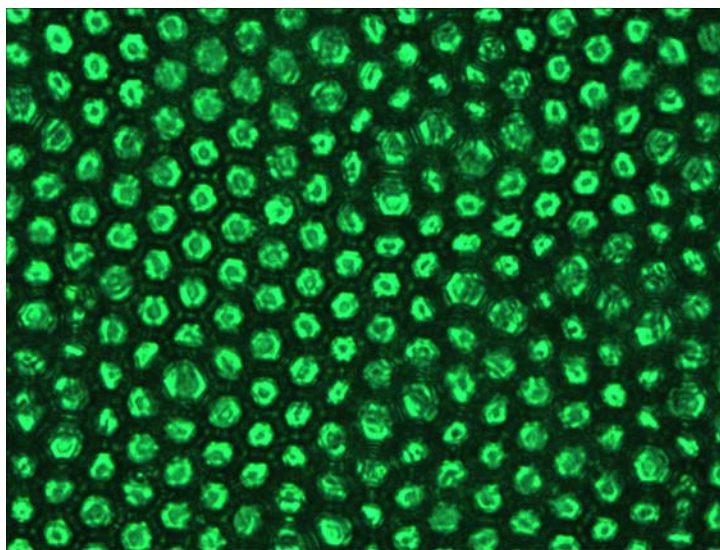


Figure 7.1. Bubble arrays formed from polymer **7.8**, each bubble is approximately 5 μm in diameter.

Polymer **7.3** was synthesized by reaction of cobaltcyclobutadiene complex **1**^{16b-e} with diiodide **7.2** under Pd/Cu-catalysis^{17, 18} (Scheme 1) in 88% with a molecular weight $M_n = 2.7 \times 10^4$ and a polydispersity (PDI) of 9.1 (bimodal). Silylated monomer **7.7** was synthesized by reaction of 6-chlorohexyne **7.4** with lithiumdiisopropylamide (LDA) and quenching the resulting anion with chlorotriisopropylsilane to give **7.5**. Silane **7.5** is the reacted with diiodohydroquinone derivative **7.6** to provide monomer **7.7** in 43% yield. Coupling of complex **7.1** with **7.7** under standard Pd-catalysis conditions yielded polymer **7.8** as a deep yellow and nonfluorescent material after standard workup and precipitation. Polymer **7.8** has a molecular weight of $M_n = 1.3 \times 10^4$ and a PDI of 1.6. Reaction of diiodide **7.7** with 1,4-diethynyl-2,5-bisdodecylbenzene **7.9** under standard Pd/Cu-catalysis affords cobalt free polymer **7.10** as a fluorescent solid that is soluble in common organic solvents. Polymer **7.10** has a molecular weight of 30.4×10^3 with a PDI of 4.54.

While polymer **7.8** forms high quality bubbles, polymers **7.3** and **7.10** form badly misshapen arrays. Upon co-dissolution of **7.3** with a 3.2-fold excess of carboxy-terminated polystyrene, well developed bubble arrays were obtained from a carbon disulfide/pentane mixture (2:1 v/v, Figure 2). While bubbles of this mixture change size from domain to domain, single domains show perfectly monodisperse patches of hexagonally arranged bubble arrays. When heating these bubbles to 530°C, most of the polymeric substance pyrolyzed off and only a small amount of material is left (Figure 6.3, right). Hexagonal ordering is still visible in the remaining ridges.

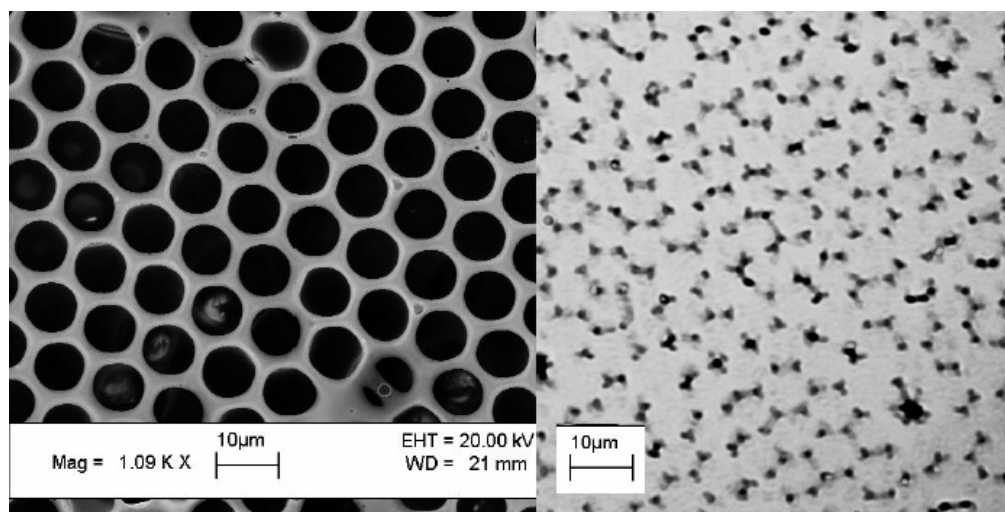


Figure 7.2. SEM-image of a bubble array formed from a mixture of polymer **7.3** and polystyrene (65%) at ambient temperature (left). Optical micrograph of the same material pyrolyzed at 530°C after all the polystyrene has been burned off (right).

While some silyl substituted PPEs form bubble arrays easily,³ polymer **7.10** or its oligomer (Pn = 5) did not. It gave only disordered arrays. When pyrolyzed at 530°C, structure was not retained. When subjected to standard conditions of the breath figure method, polymer **7.8** forms bubble arrays of excellent quality.

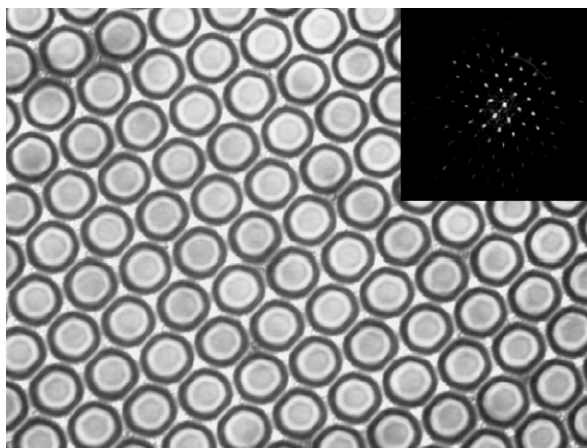


Figure 7.3. Optical micrograph of the bubble arrays of **7.8** at an ambient temperature. The bubbles are approximately 5 microns in diameter. The inset is a diffraction pattern of the bubble array taken with a Bertrand lens. The width of the picture is 65 microns.

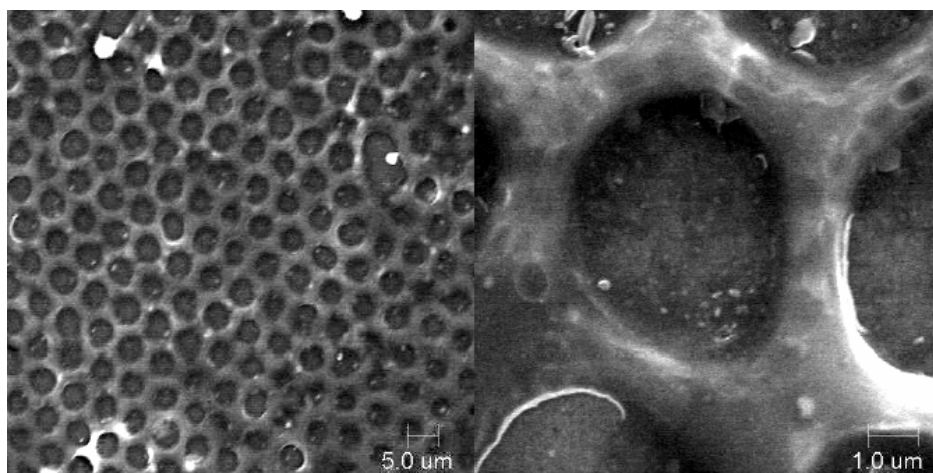


Figure 7.4. SEM-picture of bubble array of polymer **7.8** after a pyrolysis under nitrogen up to 530°C (1000-fold magnification, left). Same material at higher magnification (8000-fold, right).

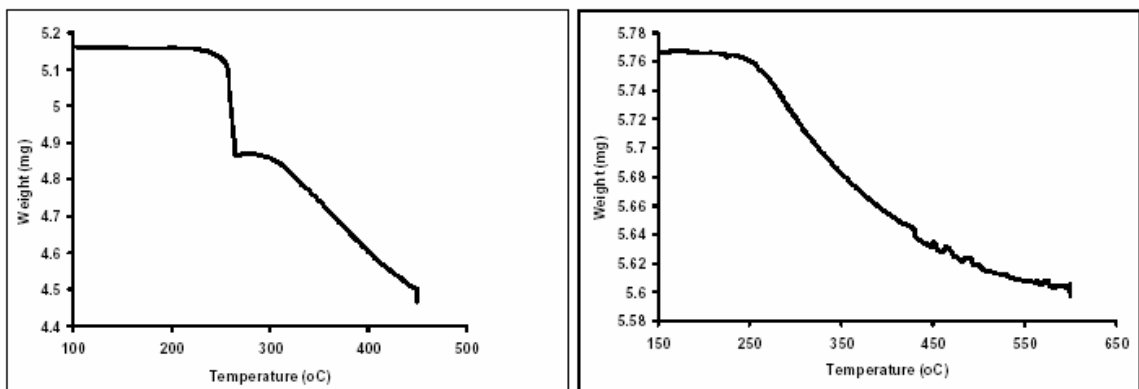


Figure 7.5. Thermogravimetric analysis (TGA) of **7.8** under nitrogen (left). There is 5.6% weight lost up to 265°C and 12.8% weight lost up to 450°C. TGA of **7.8** under air (right). There is 2.8% weight lost up to 600°C.

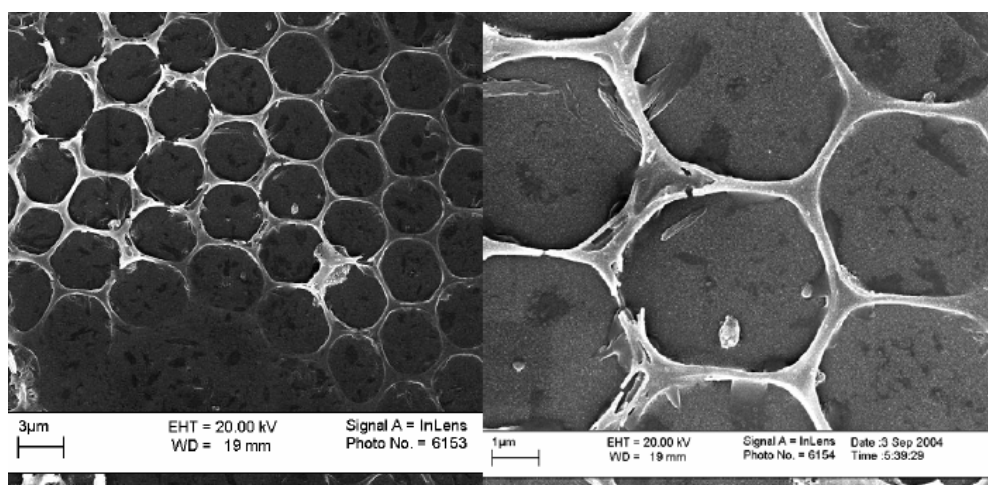


Figure 7.6. SEM-micrograph of bubble array of polymer **7.8** after a second pyrolysis under air at two different magnifications.

Figure 7.3 displays optical micrographs of bubble arrays formed from polymer **7.8**. Bubbles are uniform and approximately 5 µm in diameter. Hexagonal ordering is proven by the diffraction pattern shown in the inset taken through a Bertrand lens. Bubbles arrays of **7.8** remain intact upon heating to above 500°C. It has been shown that

polymers similar to **7.8** attained a nematic liquid crystalline phase but did not melt.¹⁹ When bubble arrays of polymer **7.8** are heated to 530°C, they collapse from open interconnected structures into more compact honeycomb-like arrays of picoliter-sized holes.

Scanning electron micrograph (SEM) of bubble arrays of **7.8** after pyrolysis (figure 4) shows that most of the material survived the conditions. This is not surprising since the degree of unsaturation in **7.8** is high. The polystyrene mixed with polymer **7.3** to form bubbles (figure 1) depolymerizes above 480°C, and this explains why mixed bubbles formed from **7.3** and polystyrene are greatly reduced upon pyrolysis.

Thermogravimetric analyses of **7.8** were performed under nitrogen and under air (Figure 7.5) to quantify mass loss. Under nitrogen there was a weight loss of 5.6% up to 264°C and a combined weight loss of 12.8% up to 450°C. According to powder X-ray diffraction, the pyrolyzed material was amorphous. There was an absence of any C-H stretching bands or organic functional group bands in the IR spectrum. This ascertains that **7.8** was converted into amorphous ceramic. SEM microscopy allows the determination of the elemental composition of the ceramic by energy dispersive X-ray microanalysis (EDX).²⁰ Arrays of polymer **7.8** pyrolyzed under N₂ contain 69.08 % carbon, 12.49 % oxygen, 8.30 % silicon, and 10.13 % cobalt.

To gain insight into which fragments might be lost upon pyrolysis, high temperature mass spectrometry was performed on grains of **7.8**. Mass spectra run at 200°C and 206°C do not show any common or specific degradation patterns. At 451°C signals at 189 and 207 amu are observed. These peaks cannot be attributed to specific fragments stemming from the original polymer structure. The combined results suggest

that mostly hydrogen is lost, and that crosslinking occurs without cleavage of any specific molecular fragments during pyrolysis. The loss of small molecules is not uncommon in the pyrolysis of carbon rich organometallic materials as shown in the pyrolysis of dicobalt octacarbonyl complexes of tolans and similar systems.^{19d-g} EDX data support a stoichiometry of approximately $C_{49}CoO_2Si_2$ (calcd. 80.0 % C, 4.36 % O, 7.63 % Si, 7.96 % Co), and this is within experimental error margins for EDX. Deviation from calculated values is common in EDX measurements of lighter elements such as carbon and oxygen, while the higher elements are determined with greater accuracy. The increased value for oxygen content might also be due to trace oxidation during pyrolysis. From these results it can be concluded that the pyrolysis of **7.8** under nitrogen leads to an amorphous ceramic containing C, Si, Co, and some oxygen. These results are suggestive, within experimental error of EDX, of the preservation of the starting stoichiometry for all elements except hydrogen.

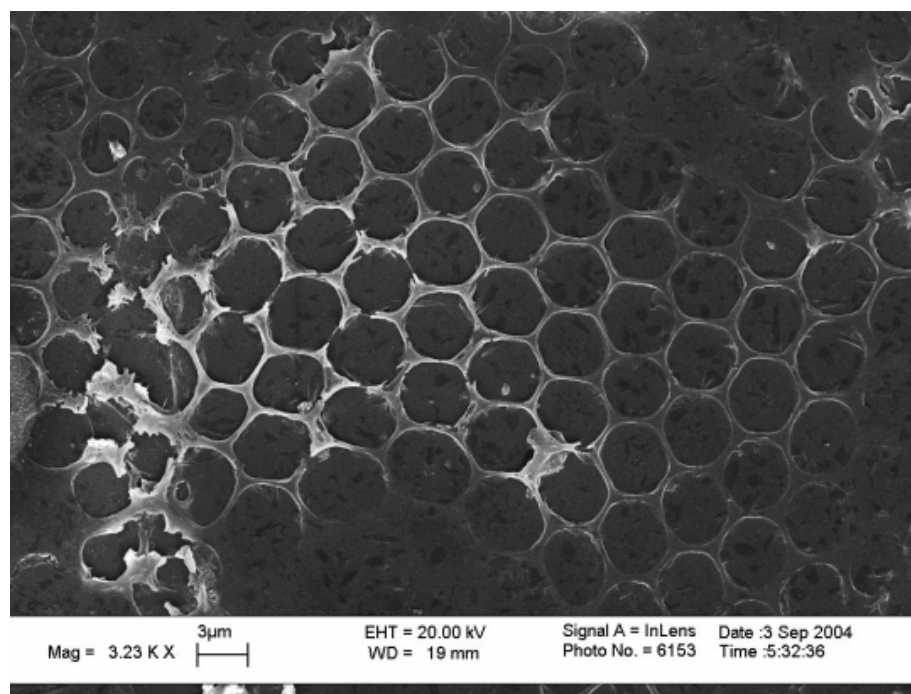


Figure 7.7. SEM-micrograph of bubble array of polymer **7.8** after pyrolysis under air.

Even in air the structure is preserved when heated to elevated temperatures. The initial material from pyrolysis under nitrogen survives after a second pyrolysis under air at 530°C (Figure 6.6). Heating of un-pyrolyzed arrays of polymer **7.8** to 530°C in air led to a slightly altered array with thinner but sharper walls (Figure 7.7). This suggests that some material is burned off in the process. The ligaments which connect the inorganic picoliter holes are reduced from 1 micron to approximately 0.5 microns, but the overall microscopic structure persists.

The TGA trace of the pyrolysis of **7.8** under air is shown in figure 7.5 (right). Upon heating to 600°C, a weight loss of only 2.8 % is observed. This was curious, and the concomitant EDX data show that there is no carbon left in the ceramic. Instead a composite of the stoichiometry $\text{Co}_2\text{Si}_4\text{O}_{11}$ (found Co 23.71 %, Si 22.13 %, O 54.18 %, calcd. Co 29.02 %, Si 27.66%, O 43.33 %; EDX) is formed. The oxygen values are off by the greatest percent, but determination of lighter elements leads to an error in EDX measurements.²⁰ The material is amorphous and does not show any X-ray diffraction pattern. EDX mapping analysis shows the material from the pyrolysis of polymer **7.8** under air contains no carbon (Figure 7.8 and 7.9). Under these conditions, we have most likely formed a cobalt silicate or a mixed $\text{SiO}_2/\text{Co}_2\text{O}_3$ ceramic.

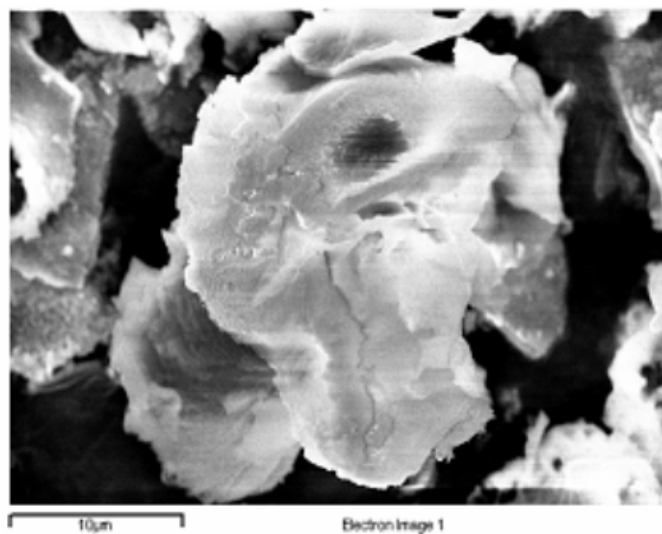


Figure 7.8. Material from the pyrolysis of polymer **7.8** under air.

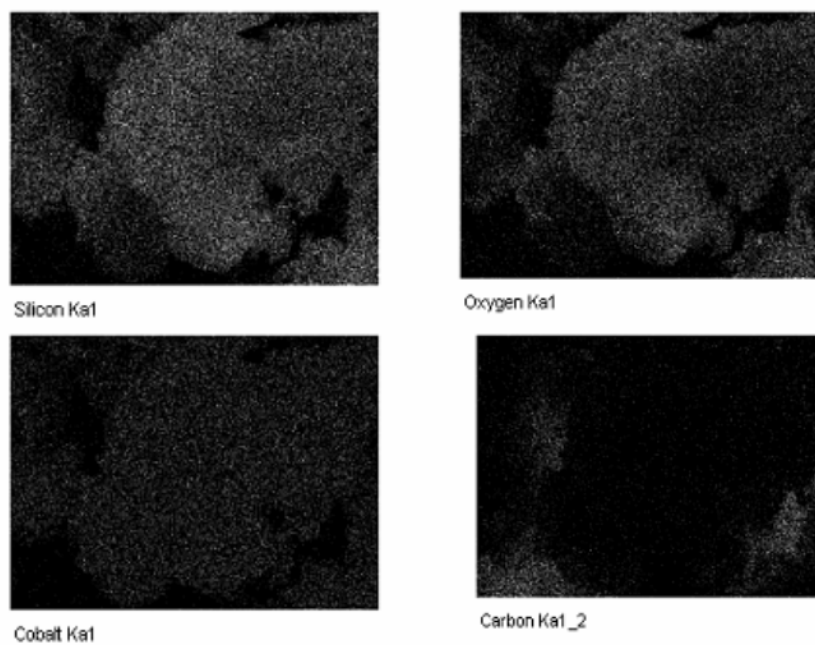


Figure 7.9. EDX mapping analysis of polymer **7.8** pyrolyzed under air.

7.3 Conclusion

It has been demonstrated that the fabrication of microstructured oxides and non-oxide ceramics is efficient when employing the breath figure method. Cobalt containing polymer **7.8** is an excellent choice for the fabrication of bubble arrays, which can be pyrolyzed to yield ceramic materials. When heating bubble arrays formed from polymer **7.8** under nitrogen or in air to temperatures above 500°C, the microscopic ordering of the bubble arrays is preserved. A Si-C-Co ceramic with low amounts of oxygen is obtainable when heating under nitrogen, and a Si-Co-O ceramic with the approximate composition of $\text{Co}_2\text{Si}_4\text{O}_{11}$ is obtained when heating under air. In the future, it might be interesting to investigate cobalt silicates for catalytic purposes.²¹ This methodology could also be expanded to ferrocene containing polymers to produce magnetite and ferrosilicate microstructures that could be utilized as magnetic and electronic materials.

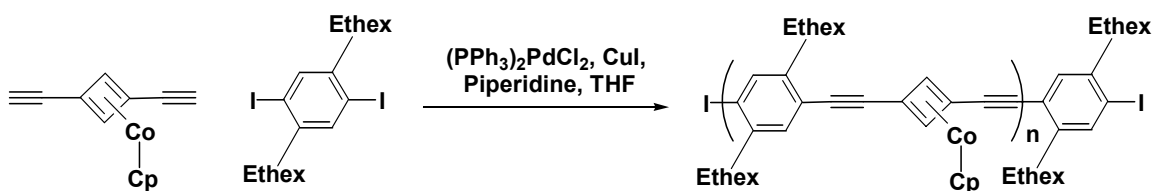
7.4 Experimental.

Instrumentation. The ^1H and ^{13}C NMR spectra were taken with a Varian 300 MHz or a Bruker 400 MHz spectrometer using a broadband probe. The ^1H chemical shifts are referenced to the residual proton peaks of CDCl_3 at δ 7.24 (vs. TMS). The ^{13}C resonances are referenced to the central peak of CDCl_3 at δ 77.0 (vs. TMS) or $\text{d}_2\text{-TCE}$ at δ = 74.0. Compound **1**¹ was prepared in accordance to published procedures. SEM images were taken and energy-dispersive X-Ray microanalysis was performed on a LEO 1530 thermally-assisted FEG SEM equipped with an EDX unit by Oxford Instruments, which does not give data on elements lighter than fluorine.² Polymer **6.3** was prepared by Dr. Stefan scholz.

Bubble preparation. The bubbles were cast from a solution of 3 mg polymer per mL of carbon disulfide and cast under a temperature of 23°C, a humidity of 84%, and an airspeed varying between 150 and 300 meters/minute.^{3, 10, 14} Bubbles of polymer 3 were cast from a solution of 1 mg polymer and 3.5 mg polystyrene (MW=25 x 10³) in a CS₂/pentane mixture (800 µL, v/v).

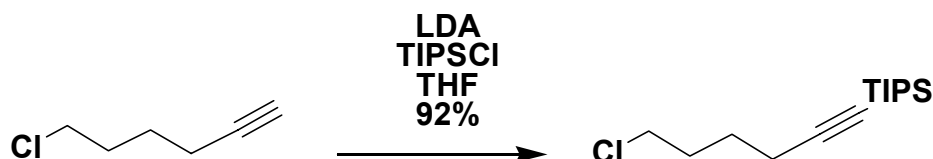
Bubble pyrolysis under nitrogen. The samples were pyrolyzed under nitrogen in a tube furnace under the following setup. First, the samples were placed in a glass tube sealed at one side with nitrogen gas flowing through it. Next, the probe container was placed into a tube furnace, equipped with a second glass tube of wider diameter, the ends of the latter tube were capped with glass fiber wool. Samples were then heated to 100°C and held for one hour, then heated to 200°C and held for another hour, and finally heated to 600°C and held for three hours. The sample remained under nitrogen during cooling 300°C. By this point, the color had changed from the original orange color to a slate gray.

Bubble pyrolysis under air. Samples subjected to pyrolysis under nitrogen were cooled to room temperature. The sample was then heated overnight at 800°C under air. Microstructures were evident even after this heating. Compound **7.1** and polymer **7.3** were synthesized by Dr. Stefan Scholz.



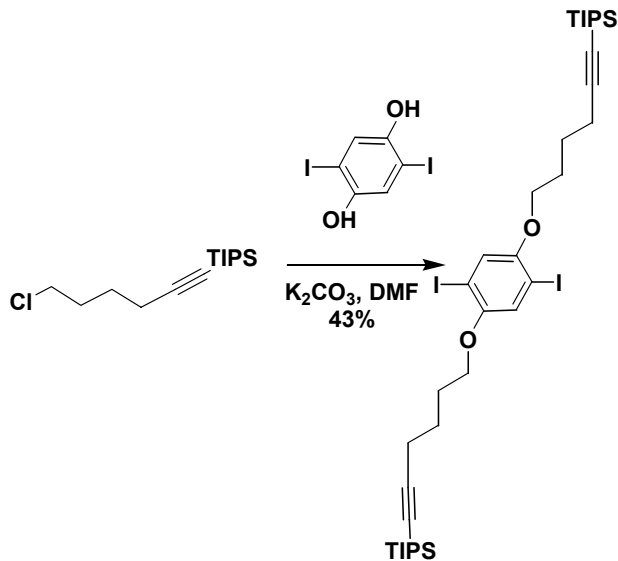
Synthesis of polymer 7.3. In a flame dried Schlenk flask (1,3-diethynylcyclobutadiene) (cyclopentadienyl) cobalt 1 (300 mg, 1.35 mmol) and 1,4-bis(2-ethyl)hexyl-2,5-diiodobenzene 2 (749 mg, 1.35 mmol) were dissolved in a mixture of piperidine (3.5 mL)

and THF (1.5 mL). The solution was degassed by three freeze pump thaw cycles. Bis(tri-phenylphosphine)palladium(II)-chloride (23.5 mg, 33.5 μ mol, 2.5 mol %) and copper (I)-iodide (6.4 mg, 34 μ mol, 2.5 mol %) were added in a stream of nitrogen. The mixture was heated up to 40°C for 48 h. The highly viscous reaction mixture was allowed to cool to room temperature, taken up in chloroform, and then washed with water (25 mL), 10% aqueous ammonia solution (25 mL), and 25% aqueous hydrochloric acid (25 mL). The chloroform solution was concentrated in vacuo to 25 mL and methanol was added (1 L). The yellow polymer, which precipitated, was filtered off, washed with methanol, and dried in oil pump vacuo (622 mg, 88%). ^1H NMR (300 MHz, CDCl_3 , 25°C): δ = 7.10 (s, 2H), 5.02 (s, 5H), 4.62 (s, 4H), 2.58 (s, 4H), 1.60 (m, 2H), 1.28 (brs, 16H), 0.89 (m, 12H). ^{13}C NMR (100 MHz, CDCl_3 , 40°C): δ = 140.6, 132.7, 122.7, 91.1, 89.6, 81.1, 68.1, 64.1, 50.6, 47.6, 32.5, 25.6, 23.0, 14.0, 9.8. IR (KBr) ν = 2954, 2927, 2920, 2911, 2892, 2869, 2856, 2178, 1455, 1434, 1412, 1378, 1107, 1001, 811 cm^{-1} . GPC (polystyrene standards): M_n = 26976, PDI=9.1 (bimodal). UV-VIS (CHCl_3): λ_{max} = 369 nm (0.507×10^6).



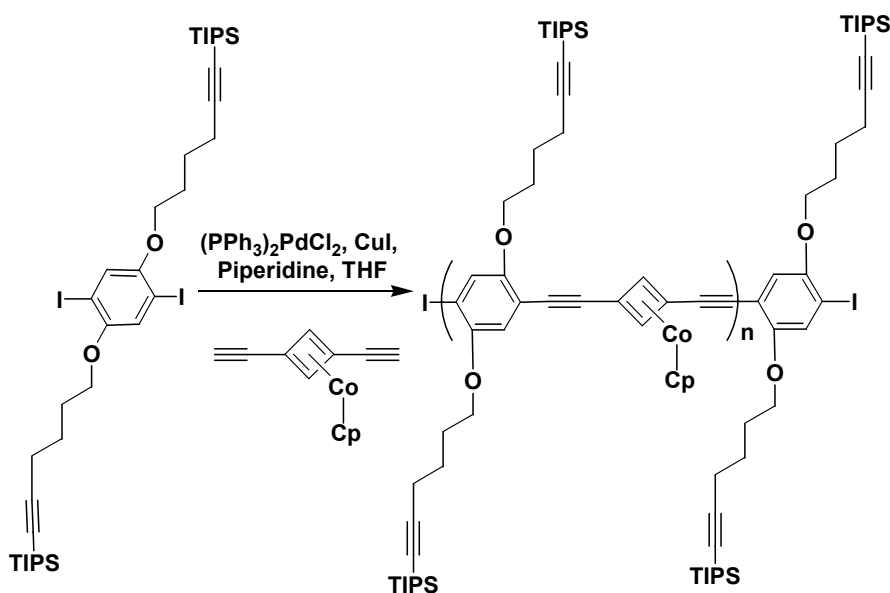
Synthesis of 7.2. Under nitrogen, 6-chlorohexyne (10 g, 85.8 mmol) was dissolved in dry tetrahydrofuran (100 mL). The mixture was cooled to -78°C . Lithium diisopropyl amide (2 N solution in THF/n-Heptane, 42.9 mL, 85.8 mmol) was added dropwise. The mixture was allowed to stir for 10 minutes, and then it was allowed to warm to -10°C and stirred for 30 minutes. The temperature was then cooled to -78°C and

triisopropylsilylchloride (16.5 g, 85.8 mmol) was added dropwise. The mixture was stirred for 24 h. Then, mixture was slowly poured onto water and extracted with chloroform. The organic solution was washed with 0.5 N HCl. The organic layer was separated and dried over MgSO₄, and the solvent removed. The remaining oil was distilled under reduced pressure to yield **7.2** as a light brown oil (21.6g, 92 %). ¹H NMR (CDCl₃): δ 3.58 (t, 2H), 2.31 (t, 2H), 1.91 (m, 2H), 1.69 (m, 2H), 1.06 (s, 21H). ¹³C NMR (CDCl₃): δ 108.1, 81.1, 44.7, 31.7, 26.2, 18.9, 11.6. IR: ν 677, 879, 968, 1015, 1250, 1297, 1445, 2131, 2168, 2243, 2521, 2562, 2622, 2683, 2715, 2721, 2804, 2834, 2852, 3024. MS and ES Calculated for, [C₁₅H₂₉ClSi], 272.93; C, 66.01; H, 10.71; found fragmentation, 270.2; C, 66.08; H, 10.86.



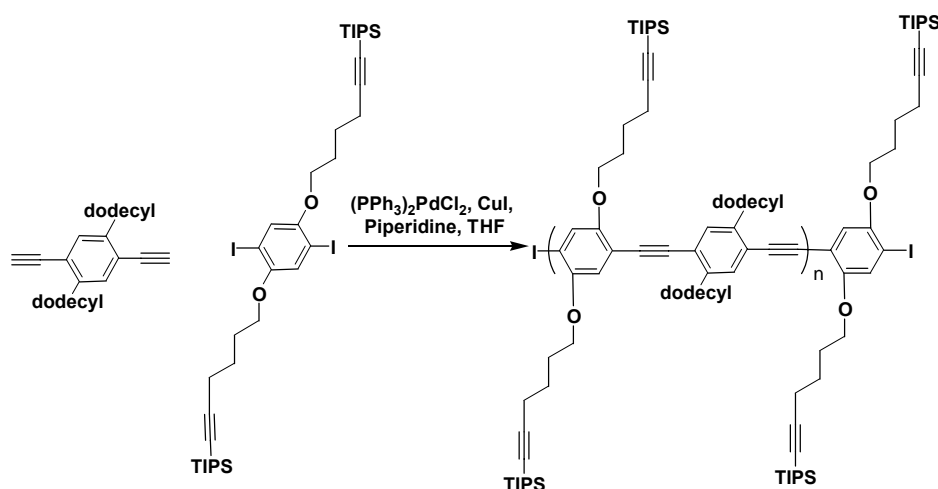
Synthesis of 7.3. 1,4-Hydroxy-2,5-diiodo benzene (3.00 g, 8.29 mmol), potassium carbonate (11.5 g, 82.9 mol), and **7.2** (9.05 g, 33.5 mmol) were dissolved in dimethylformamide (200 mL). The mixture was heated to reflux for 48h and allowed to cool to room temperature, diluted with dichloromethane, and then washed with 1N HCl (2 x 150 mL). The solvent was removed under vacuum, and the crude solid was purified

by chromatography on silica gel (1:1, dichloromethane:hexane) to yield **7.3** as a colorless crystalline solid (2.99 g, 43 %). ^1H NMR (CDCl_3): δ 7.16 (s, 2H), 3.99 (t, 2H), 2.38 (t, 2H), 1.97 (m, 2H), 1.79 (m, 2H), 1.09 (s, 42H). ^{13}C NMR (TCE): δ 152.8, 122.8, 108.6, 86.5, 80.9, 69.9, 28.5, 25.8, 19.9, 19.0, 11.6. IR: ν 657, 961, 1046, 1210, 1249, 1346, 1384, 1462, 1681, 2165, 2358, 2722, 2866, 2944, 3085. ES^+ MS (EI) Calculated for, $[\text{C}_{36}\text{H}_{60}\text{I}_2\text{O}_2\text{Si}_2]$, 834.84; C, 51.79; H, 7.24; found 834.4; C, 51.60 ; H, 7.29; MP: 48°C.



Synthesis of polymer 7.4. Diiodo monomer **7.3** (0.738 g, 0.883 mmol) and diethynyl monomer **7.1** (0.196 g, 0.875 mmol) were dissolved in THF (2 mL) and piperidine (1.5 mL) in an oven dried schlenk flask. The flask was frozen, evacuated, and flushed with nitrogen three times after which $(\text{Ph}_3\text{P})_2\text{PdCl}_2$ (6.2 mg, 8.83 μmol) and CuI (1.7 mg, 8.83 μmol) were added. The mixture was allowed to stir at room temperature for 48 h. The solvent was removed, and then the mixture was dissolved in dichloromethane and washed with 1N HCl, 1N NH_4OH , and water. The organic layer was dried over MgSO_4 , and the solvent removed. The resulting polymer was dissolved in dichloromethane and

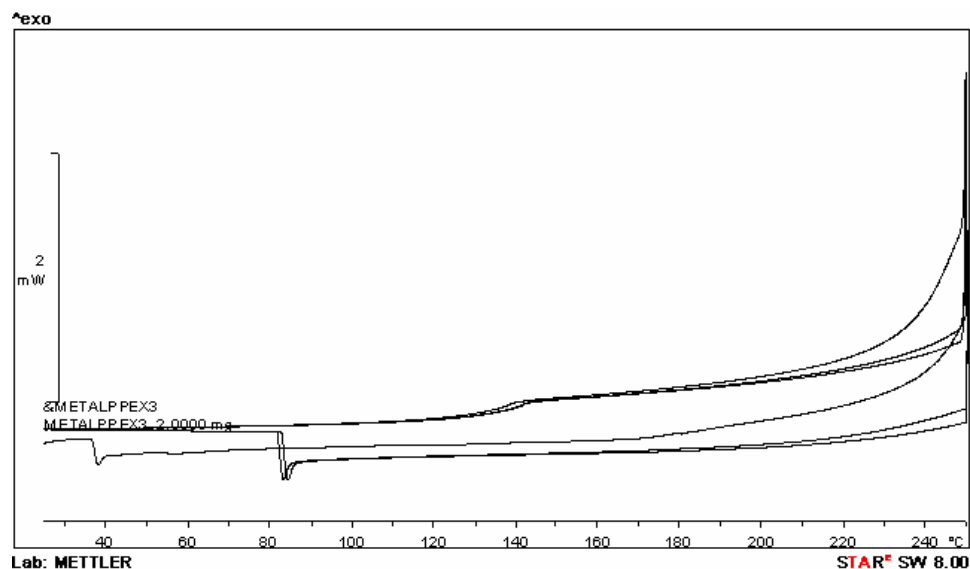
precipitated out of methanol three times to yield **7.4** (0.599 g, 84 %) as a orange solid. ^1H NMR (CDCl_3): δ 6.80 (m, 2H), 5.04 (m, 5H), 4.68 (m, 2H), 3.98 (m, 4H), 2.39 (m, 4H), 1.95 (m, 4H), 1.79 (m, 4H), 1.06 (m, 42H). ^{13}C NMR (TCE): δ 153.8, 116.7, 108.5, 92.0, 86.3, 81.2, 80.7, 69.0, 64.4, 56.1, 28.3, 25.4, 19.4, 18.6, 11.3. IR: ν 676, 790, 881, 1002, 1033, 1066, 1263, 1377, 1461, 1502, 1649, 2165, 2360, 2723, 2754, 2848, 2925, 2962, 3110, 3388. GPC (polystyrene standards) $M_n=13,377$, PDI=1.590. ES^+ Calculated for, $[\text{C}_{49}\text{H}_{62}\text{CoO}_2\text{Si}_2]$; C, 73.74; H, 7.83; found C, 65.87 ; H, 7.82.



Synthesis of polymer 7.10: Diiodo monomer **7.3** (0.500 g, 0.599 mmol) and diethynyl monomer **7.9** (0.280 g, 0.605 mmol) were dissolved in THF (2 mL) and piperidine (1.5 mL) in an oven dried Schlenk flask. The flask was frozen, evacuated, and flushed with nitrogen three times after which $(\text{Ph}_3\text{P})_2\text{PdCl}_2$ (4.2 mg, 5.9 μmol), and CuI (1.1 mg, 6.0 μmol) were added. The mixture was allowed to stir at room temperature for 48 h. Dichloromethane was added, and the solution was washed with 1N HCl , 1N NH_4OH , and water. The organic layer was dried over MgSO_4 , and the solvent was concentrated. The resulting polymer was dissolved in dichloromethane and precipitated out of methanol three times to yield **7.4** (0.556 g, 89 %) as a yellow solid. ^1H NMR (CDCl_3): δ 7.37 (m,

2H), 6.92 (m, 2H), 4.10 (m, 4H), 2.86 (m, 4H), 2.38 (m, 4H), 2.02 (m, 4H), 1.81 (m, 4H), 1.15 (m, 46H), 1.06 (m, 36H), 0.88 (m, 6H). ^{13}C NMR (TCE): δ 153.3, 141.9, 132.2, 122.7, 116.6, 114.1, 108.5, 94.0, 90.5, 80.7, 69.4, 35.1, 31.9, 30.6, 29.7, 29.6, 29.4, 29.37, 28.0, 25.3, 22.6, 19.5, 18.6, 14.1, 11.5, 11.4, 11.2. IR: ν 676, 798, 815, 858, 1012, 1265, 2171, 2331, 2358, 2866, 2925, 2958. GPC (polystyrene standards) M_n =30,436, PDI=4.538. ES $^+$ Calculated for, $[\text{C}_{70}\text{H}_{112}\text{O}_2\text{Si}_2]$; C, 80.70; H, 10.84; found C, 77.09; H, 12.35.

Differential scanning calorimetry measurements. DSC measurements were taken on a Mettler Toledo DSC 822. The samples were weighed into a 40 μL aluminum crucible, and the lid was punctured. Each sample was heated from 25-250 $^\circ\text{C}$ at a rate of 25 $^\circ\text{C}/\text{min}$ under N_2 .



7.5 References

1. a) M. Birot, J. P. Pillot, J. Dunogues, *Chem Rev.* **1995**, 95, 1443-1477. b) D. C. Bradley, *Chem Rev.* **1989**, 89, 1317-1322. c) S. Wong, V. Kitaev, G. A. Ozin, *J. Am.*

- Chem. Soc.* **2003**, 125, 15589-15598. b) A. Blanco, E. Chomski, S. Grabtchak, M. Ibisate, S. John, S. W. Leonard, C. Lopez, F. Meseguer, H. Miguez, J. P. Mondia, G. A. Ozin, O. Toader, H. M. van Driel, *Nature* **2000**, 405, 437-440. c) M. J. MacLachlan, M. Ginzburg, N. Coombs, T. W. Coyle, N. P. Raju, J. E. Greedan, G. A. Ozin, I. Manners, *Science* **2000**, 287, 1460-1463.
2. a) L. Feng, S. H. Li, Y. S. Li, H. J. Li, L. J. Zhang, J. Zhai, Y. L. Song, B. Z. Liu, L. Jiang, D. B. Zhu, *Adv. Mater.* **2002**, 14, 1857-1860. b) L. Feng, Y. L. Song, J. Zhai, B. Q. Liu, J. Xu, L. Jiang, D. B. Zhu, *Angew. Chem.* **2003**, 115, 824-926; *Angew. Chem. Int. Ed. Engl.* **2003**, 42, 800-802. c) J. Y. Shiu, C. W. Kuo, P. L. Chen, C. Y. Mou, *Chem. Mater.* **2004**, 16, 561-564. d) A. Lafuma, D. Quere, *Nature Mater.* **2003**, 2, 457-460.
3. Brian C. Englert, Stefan Scholz, Peter J. Leech, Mohan Srinivasarao, and Uwe H. F. Bunz. *European Journal of Chemistry* **2004**, Accepted and In Press.
4. a) C. B. Murray, C. R. Kagan, M. G. Bawendi, *Ann. Rev. Mater. Science* **2000**, 30, 545-610. b) O. D. Velev, E. W. Kaler, *Adv. Mater.* **2000**, 12, 531-534. c) O. D. Velev, T. A. Jede, R. F. Lobo, A. M. Lenhoff, *Chem. Mater.* **1999**, 10, 3597-3602. d) P. Jiang, J. F. Bertone, V. L. Colvin, *Science* **2000**, 291, 453-457. e) A. Stein, Micropor. Mater. **2001**, 44, 227-239. f) Y. Wang, V. Salgueirino-Maceira, L. W. Liz-Marzn, F. Caruso, *Adv. Mater.* **2002**, 14, 908-912.
5. a) Kietzke, T.; Neher, D.; Landfester, K.; Montenegro, R.; Guntner, R.; Scherf, U. *Nat. Mater.* **2003**, 2, 406. b) Piok, T.; Gamerith, S.; Gadermaier, C.; Plank, H.; Wenzl, F. P.; Patil, S. Montenegro, R.; Kietzke, T.; Neher, D.; Scherf, U.; Landfester, K.; List, E. J. W. *Adv. Mater.* **2003**, 15, 800. c) Landfester, K.;

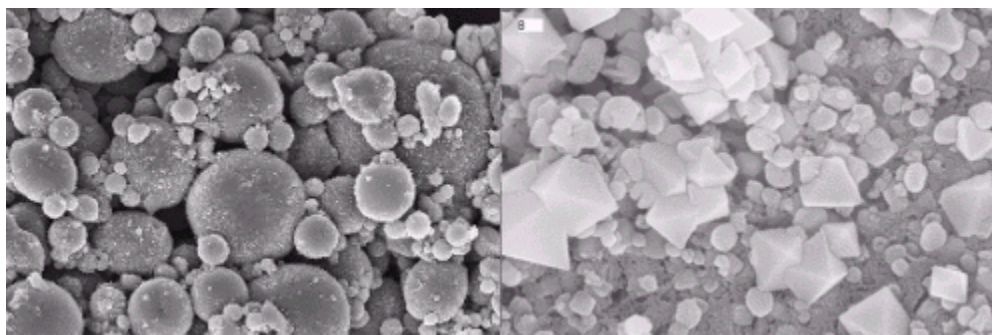
- Montenegro, R.; Scherf, U.; Guntner, R.; Asawapirom, U.; Patil, S.; Neher, D.; Kietzke, T. *Adv. Mater.*, **2002**, 14, 651. d) Jenekhe, S. A.; Chen, X. L. *Science* **1999**, 283, 372. e) Jenekhe, S. A.; Chen, X. L. *Science* **1998**, 279, 1903. f) Müller, M.; Zentel, R.; Maka, T.; Romanov, S. G.; Torres, C. M. S. *Adv. Mater.* **2000**, 12, 1499. g) Müller, M.; Zentel, R.; Maka, T.; Romanov, S. G.; Torres, C. M. S. *Chem. Mater.* **2000**, 2, 2508.
6. Imhof, A.; Pine, D. J. *Nature*, **1997**, 389, 948.
 7. Holland, B. T.; Stein, A. *Science* **1998**, 281, 538.
 8. Yan, H. W.; Blanford, C. F.; Holland, B. T.; Parent, M.; Smyrl, W. H.; Stein, A. *Adv. Mater.* **1999**, 11, 1003.
 9. Kulinowski, K. M.; Jiang, P.; Vaswani, H.; Colvin, V. L. *Adv. Mater.* **2000**, 12, 833.
 10. Velez, O. D.; Jede, T. A.; Lobo, R. F.; Lenhoff, A. M. *Nature* **1997**, 389, 447.
 11. Imhof, A.; Pine, D. J., *Nature* **1997**, 389, 948.
 12. Monnier, A.; Schüth, F.; Huo, Q.; Kumar, D.; Margolese, D.; Maxwell, R. S.; Stucky, G. D.; Krishnamurty, M.; Petroff, P.; Firouzi, A.; Janicke, M.; Chmelka, B. F. *Science* **1993**, 261, 1299.
 13. Beck, J. S.; Vartulli, J. C.; Roth, W. J.; Leonowicz, M. E.; Kresge, C. T.; Schmitt, K. D.; Chu, C. T. W.; Olson, D. H.; Sheppard, S. B.; McCullen, J. B.; Higgins, J. L.; Schlenker, J. *Am. Chem. Soc.* **1992**, 114, 10834.
 14. Kresge, C. T.; Leonowicz, M. E.; Roth, W. J.; Vartuli, J. C.; Bech, J. S. *Nature* **1992**, 359, 710.

15. Song, L. Bly, R. K. Wilson, J. N. Bakbak, S. Park. J. O. Srinivasarao, M. Bunz, U. H. F. *Adv. Mater.* **2004**, 16, 115-118.
16. a) Erdogan, B.; Song, L.; Wilson, J. N.; Park, J. O.; Srinivasarao, M.; and Bunz, U. H. F. *J. Am. Chem. Soc.* **2004**, 126, 3678-3679. b) M. Laskoski, J. G. Morton, M. D. Smith, U. H. F. Bunz, *J. Organomet. Chem.* **2002**, 652, 21-30. c) M. Altmann, PhD, Gutenberg Universität, Mainz, **1997**, 103. d) J. R. Fritch, K. P. C. Vollhardt, *J. Am. Chem. Soc.* **1978**, 100, 3643-3645. e) J. R. Fritch, K. P. C. Vollhardt, *Organometallics* **1982**, 1, 590-602.
17. U. H. F. Bunz, *Chem. Rev.* **2000**, 100, 1605-1644.
18. a) E. Negishi, L. Anastasia, *Chem. Rev.* **2003**, 103, 1979-2017. b) K. Sonogashira, *J. Organomet. Chem.* **2002**, 653, 46-49.
19. a) M. Altmann, U. H. F. Bunz, *Angew. Chem.* **1995**, 107, 603-605. *Angew. Chem. Int. Ed. Engl.* **1995**, 34, 569-571. b) M. Altmann, V. Enkelmann, G. Lieser, U. H. F. Bunz, *Adv. Mater.* **1995**, 7, 726-728. c) Zur Loye, U. H. F. Bunz, *Chem. – Eur. J.* **2001**, 7, 117-126. d) R. Boese, A. J. Matzger, K. P. C. Vollhardt, *J. Am. Chem. Soc.* **1997**, 119, 2052-2053. e) K. P. Baldwin, A. J. Matzger, D. A. Scheiman, C. A. Tessier, K. P. C. Vollhardt, W. J. Youngs, *Synlett* **1995**, 1215-1218. f) P. I. Dosa, C. Erben, V. S. Iyer, K. P. C. Vollhardt, I. M. Wasser, *J. Am. Chem. Soc.* **1999**, 121, 10430-10431. g) V. S. Iyer, K. P. C. Vollhardt, R. Wilhelm, *Angew. Chem.* **2003**, 115, 4515-4519; *Angew. Chem. Int. Ed. Engl.* **2003**, 42, 4379-4383.
20. Energy-Dispersive X-Ray Microanalysis, Ed. D. Vanghan, Kevex Corporation, Foster City CA, **1983**.

21. a) E. vanSteen, G. S. Sewell, R. A. Makhothe, C. Micklethwaite, H. Manstein, M. diLange, C. T. O'Connor, *J. Catalysis* **1996**, 162, 220-229. b) B. Ernst, S. Libs, P. Chaumette, A. Kiennemann, *Appl. Catal. A*. **1999**, 186, 145-168.

CHAPTER 8

PYROLYSIS OF DICOBALTHEXACARBONYL- FUNCTIONALIZED POLY(*P*- PHENYLENEETHYNYLENE)S.



8.1 Introduction

Micron-sized, spherical, non-fullerene carbon is found in meteorites.¹ Similar spheres are prepared in the laboratory by pyrolysis of polyethylene/PVC mixtures under high pressure, methane over an (undisclosed) mixed metal oxide catalyst, aqueous acidic solutions of glucose, polytetrafluoroethylene in supercritical water, ferrocene, hexachlorobenzene with sodium metal in an autoclave, and tetrachloromethane with sodium amide.²⁻⁷ In cases where transition metals are involved in the process, metal kernels were observed in the center of the spheres that seemed to function either as a catalyst and/or as a nucleation site.⁴ Spheres in which the metal is distributed evenly and homogeneously (either as an alloy or as a carbide/ceramic type) are unknown.²⁻⁷ The high yield formation of homogeneous cobalt/carbon spheres by pyrolysis of a metalated poly(*paraphenyleneethynylene*)(PPE **8.7a**) is reported.

Tetrabenzohexadehydro[20]annulene (**8.1**) explodes to form carbon nanotubes and onions.⁸ Tris-dicobalt hexacarbonyl complex **8.2**, the dicobalthexacarbonyl complex of tolane (**8.3**) and a multinuclear cobalt complex of a hexaalkynylated hexabenzocoronene derivative (**8.4**) do likewise but only under conflagration or even without visible heat evolution.⁹⁻¹¹ The pyrolytic approach works for the ferrocene-ligated dehydroannulene **8.5**, that deflagrates into bagel-shaped, tube-like all-carbon objects (Figure 8.1).¹² Synthesis and investigation of the thermal decomposition of metalated PPEs **8.7** was a natural yet promising extension of these reports (Scheme 8.1).

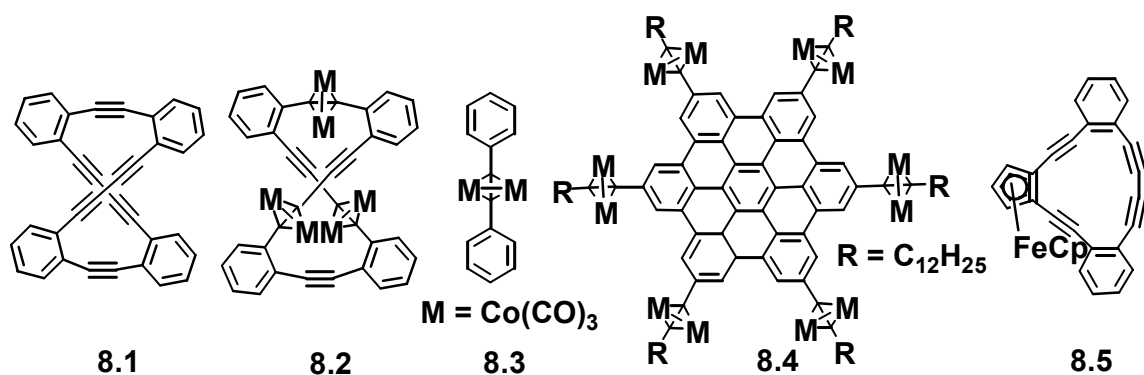
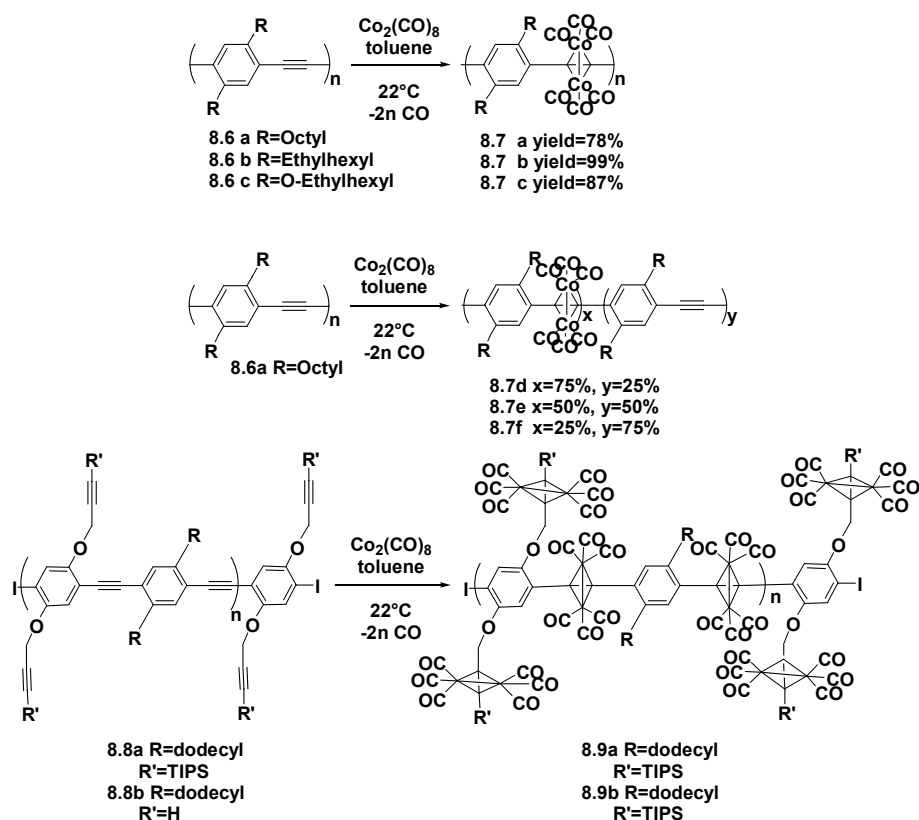


Figure 8.1. Tetrabenzohexadehydro[20]annulene **8.1**, tris-dicobalt hexacarbonyl complex **8.2**, the dicobalthexacarbonyl complex of tolane **8.3**, multinuclear cobalt complex of a hexaalkynylated hexabenzocoronene derivative (**8.4**), and ferrocene-ligated dehydroannulene, **8.5** form all-carbon objects under the appropriate conditions.

8.2 Results and Discussion

Post-functionalization of PPEs¹³ is difficult but reduction¹⁴ or appendage of organo-palladium and platinum fragments¹⁵ have been described. PPEs **8.6a-c**¹³ reacted in good-to-excellent yields (Scheme 8.1) with dicobalt octacarbonyl in toluene and dichloromethane (room temperature) to form metalated species **8.7a-c** after precipitation into methanol.¹⁶ Both IR and NMR spectroscopy indicate complete occupancy of the

alkyne sites by dicobalt hexacarbonyl fragments. The organometallic PPE **8.7a** is intrinsically less soluble than its precursor, **8.6a**. A highly soluble sample of **8.7a** was produced when PPE **8.6a** of low molecular weight ($P_n = 15$) was reacted with dicobalt octacarbonyl. The diagnostic signals in the ^{13}C NMR spectrum of **8.6a** ($\delta = 93.0$, alkyne; 122.7, 132.3, 141.8 arene)¹³ changed upon complexation, and signals of **8.7a** were recorded at $\delta = 95.9$ (complexed alkyne), 132.6, 136.9, 139.4 (arene) and 199.3 (Co-C \equiv O). The IR spectrum of **8.7a** differs from that of **8.6a** (2200 cm^{-1} weak, alkyne stretch; 1722, 1701 cm^{-1} , strong). The alkyne stretch has disappeared, and a new set of intense IR bands has appeared for **8.7a** at 2081, 2050, 2025, and 2004 cm^{-1} representing the C-O stretch vibrations of the carbonyl ligands (Figure 8.2). These CO-stretch vibrations have shifted with respect to those of $\text{Co}_2(\text{CO})_8$ ¹⁷ assuring that no unreacted cobalt octacarbonyl was left in the product. The reaction of **8.7a** with HCl in chloroform leads to full demetallation and the re-isolation of intact **8.6a**, as expected for a carbonyl complex. Attempts to make **8.7a** more lipophilic by a ligand exchange reaction with triphenylphosphine furnished a material with low solubility.



Scheme 8.1. The PPEs **8.6a-c** reacted in good-to-excellent yields with dicobalt octacarbonyl in toluene and dichloromethane (room temperature) into the metalated species **8.7a-c** after precipitation into methanol.

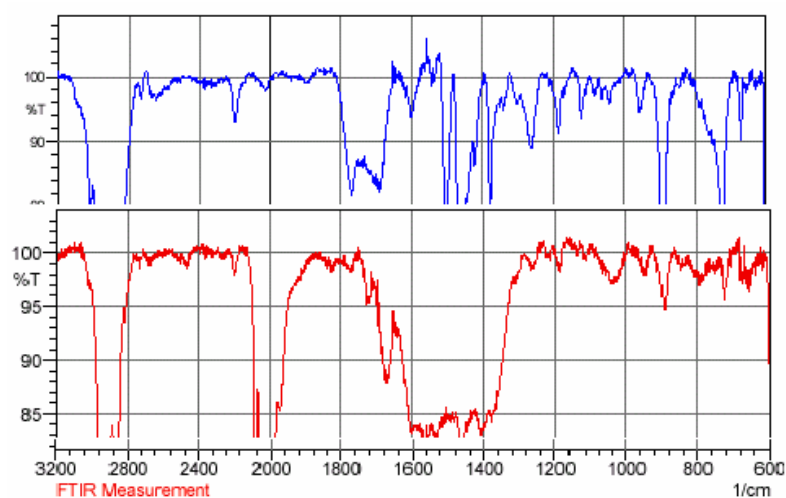


Figure 8.2. Visible changes in the IR spectra of **8.6a** upon complexation (non-complexed=blue, complexed=red).

The metallation of **8.6b** and the alkoxy-PPE **8.6c** is likewise facile and furnished the polycomplexes **8.7b** and **8.7c** in excellent yields as greenish-black materials (Scheme 1). Their structures are in accord with their obtained spectroscopic data. The clean reaction of PPEs **8.6** with dicobalt octacarbonyl is gratifying and in agreement with recent results by Manners regarding the complexation of side-chain alkynyl-appended polyferrocenylsilanes by dicobalt octacarbonyl.¹⁶

Pyrolysis of **8.7a** with a heat gun, or more controlled conditions for 1 h in a tube furnace at 650 °C under nitrogen, formed microscopic spheres (Figure 8.3a) as a sole product. Upon pyrolysis of **8.7b**, however, misshapen small tubes form (Figure 8.3b). An inset shows the stubby tubes at larger magnification. Upon pyrolysis of **8.7c**, scaly, carbonaceous matter was isolated. Neither tubes nor spheres were detected. The formation of the micro- and nanostructures was due to cobalt complexation. PPE **8.6a** was pyrolyzed by itself under identical conditions to give a smooth film featuring small pores (Figure 8.4). The pyrolysis of dicobalt octacarbonyl leads to micron-sized, ill-defined flakes according to scanning electron microscopy.

Reaction of **8.6a** with the appropriate amounts of dicobalt octacarbonyl leads to the formation of **8.7d**, **8.7e**, and **8.7f** corresponding to 75%, 50%, and 25% complexation of the PPE backbone respectively (Scheme 8.1). Scaly, carbonaceous matter is isolated after pyrolysis and purification of **8.7d**. Pyrolysis of **8.7e** and **8.7f** leads to octahedral shaped particles and misshapen particles respectively (Figure 8.4a, b, and c).

Previous endeavors in our lab involving polymers containing silica and cobalt generated interesting results.^{16c} We thought similar materials might offer interesting results if pyrolyzed. With this in mind, polymers **8.8a** and **8.8b** were reacted with

dicobalt octacarbonyl and the subsequent insoluble organometallic polymers were isolated and pyrolyzed (Scheme 8.1). While the pyrolysis of **8.8a** yielded only fibrous material, **8.8b** produced fused spheres (Figure 8.5). Further attempted pyrolysis experiments with **8.8b** have only yielded similar results. Washing these materials with aqueous acid solution might remove any excess material but in this case has offered no improvement over these results.

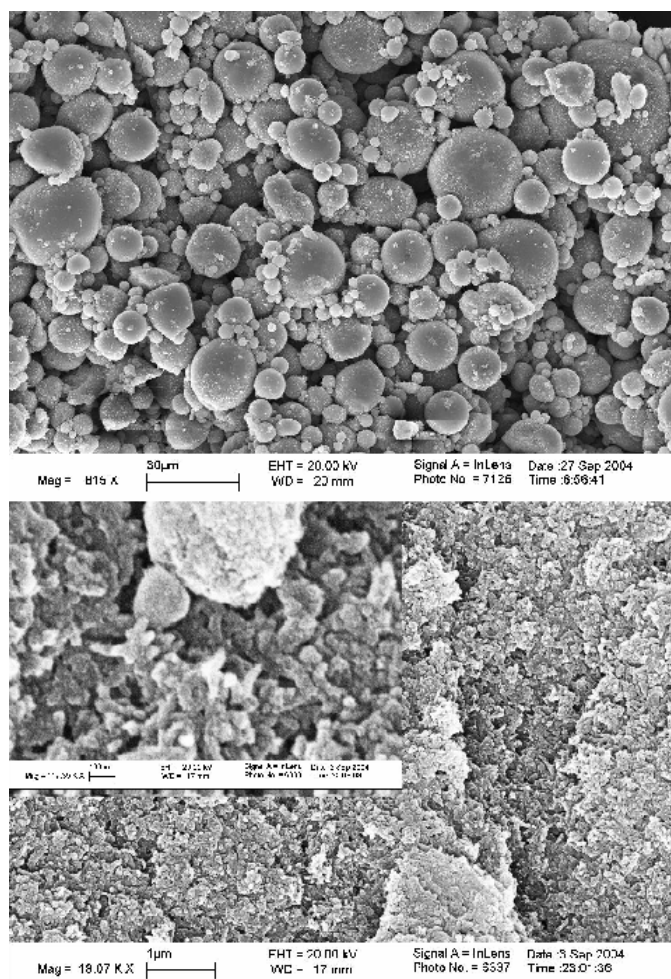


Figure 8.3a (top) and b (bottom). Pyrolysis of **8.7a** (top) with a heat gun, or under more controlled conditions, for 1 h in a tube furnace at 650 °C under nitrogen formed microscopic spheres as a sole product. Upon pyrolysis of **8.7b** (bottom), however, misshapen small tubes formed.

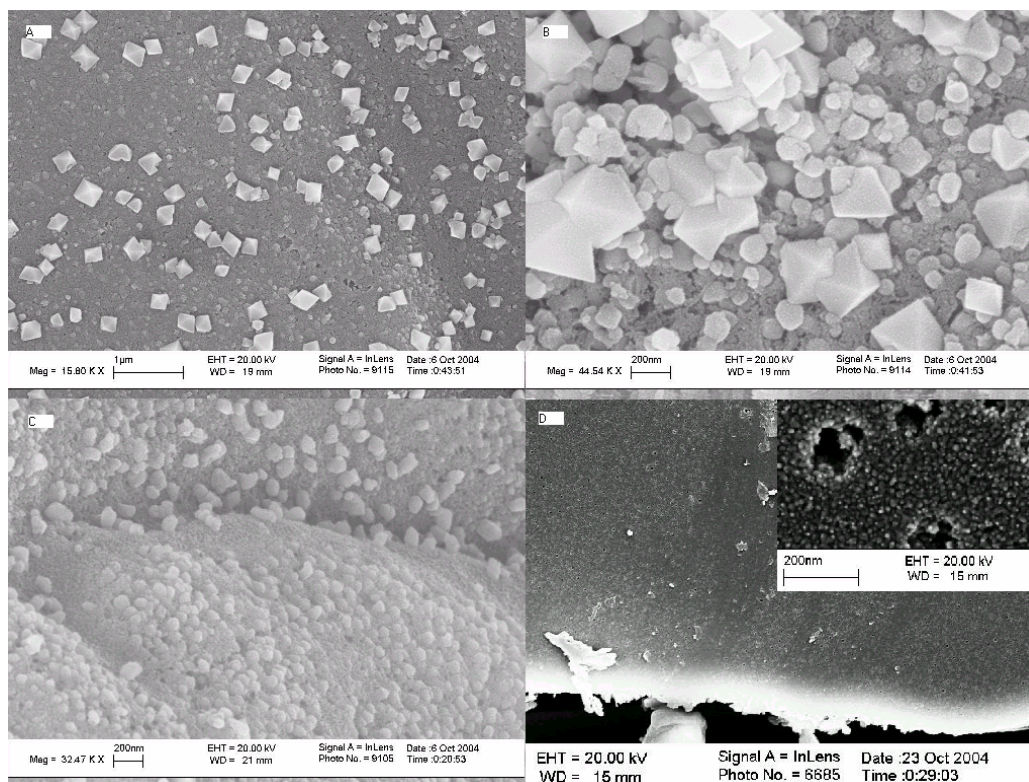


Figure 8.4a-d. Pyrolysis of **8.7e** 50% complexed (8.4a and b, top left and top right) and **8.7f** 25% complexed (bottom left) leads to octahedral shaped particles and misshapen particles respectively. PPE **8.6a** 0% complexed (bottom right) was pyrolyzed by itself under conditions identical to that of **8.7a** to give a smooth film featuring small pores.

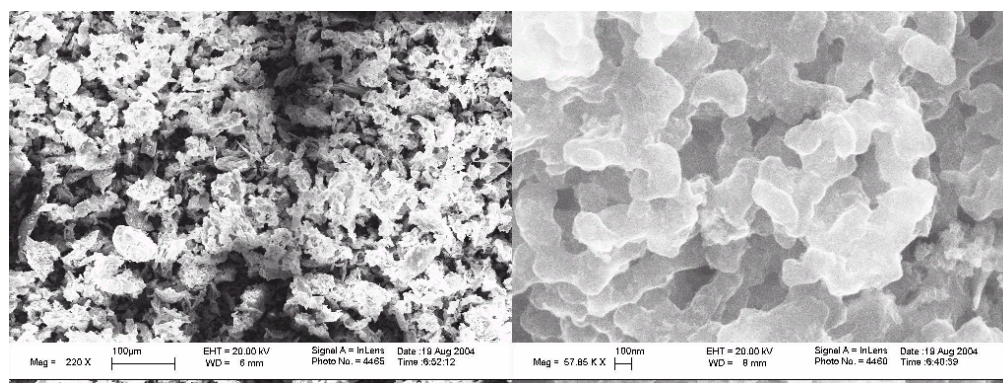


Figure 8.5. Fibrous material from pyrolysis of **8.8a** and fused spheres from pyrolysis of **8.8b**.

While all pyrolysis products are interesting, the spheres and octahedral crystals interested us the most. The size distribution of the spheres obtained from pyrolysis of **8.7a** was analyzed (Figure 8.6) by evaluating a blow-up of Figure 8.3a; 668 spheres were counted. While the size distribution is statistical, there seem to be sizes 1.8, 4.8, 7.2, 12, 15, 18, and 20 microns. Spheres of these diameters form in a somewhat higher yield. The largest sphere was 0.03 mm in diameter. The most commonly observed sphere size was $1.8 (\pm 0.2)$ microns.

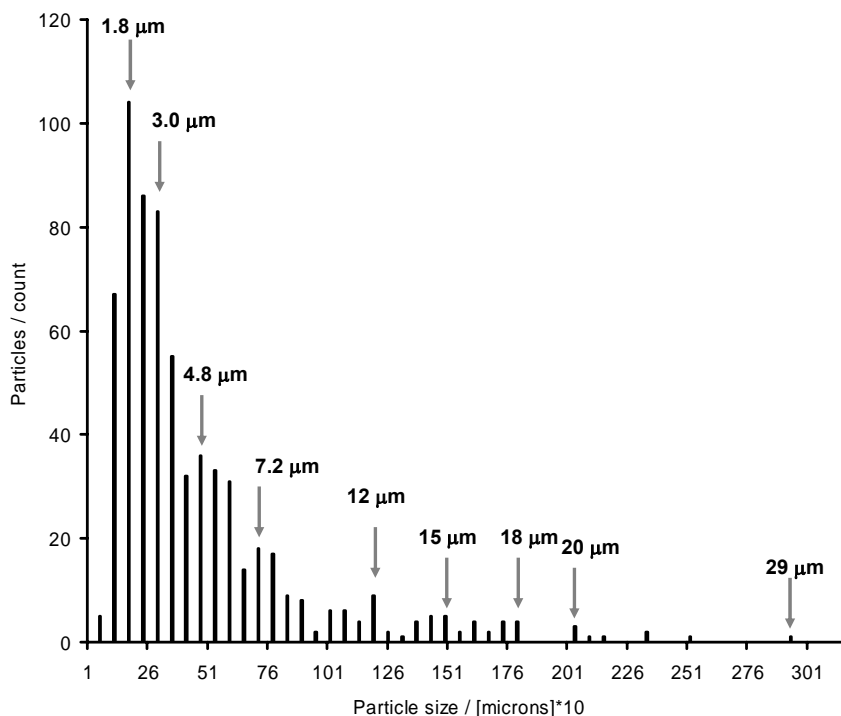


Figure 8.6. Size distribution of the spheres obtained from pyrolysis of **8.7a**.

Figure **8.7a** shows a transmission electron micrograph of several representative 1.8 micron large spheres; they are solid, clean, isotropic and do not have a discernable interior structure. Electron diffraction indicates that the spheres are amorphous and do not contain a metal seed. What is the elemental composition of these spheres? Are they

carbon-only or do they contain cobalt? Electron dispersive X-ray analysis (EDX)¹⁸ of a representative 5 micron large sphere is shown in Figure 8.8. On the left (a) a scanning electron micrograph is presented while the right hand side pictures map the relative concentration of cobalt (b) and carbon (c). The elemental distribution of carbon and cobalt is homogeneous according to the contrast observed. The spheres consist of 56.1 wt % carbon, 30.3 wt % Co, and 10.7 wt% of oxygen (EDX). The residual 2.9 wt % is due to silicon (1.3 %), iodine (0.8%) and aluminum (0.4 %). The presence of iodine is perhaps due to the iodine end groups in the starting polymer **8.6a**. Silicon, aluminum, and an undetermined amount of the oxygen signal are background due to the Si-wafer that is utilized for the EDX-measurements. The EDX data fit quite well to a proposed material of the composition $C_{18}Co_2O_4$ (calculated: C, 56.59; Co, 30.85; O, 12.56). The oxygen containing material could form from **8.7a** (composition: $C_{30}H_{36}Co_2O_6$) by loss of two CO units and several molecules of low boiling alkanes by fragmentation and disproportionation of the side chains.

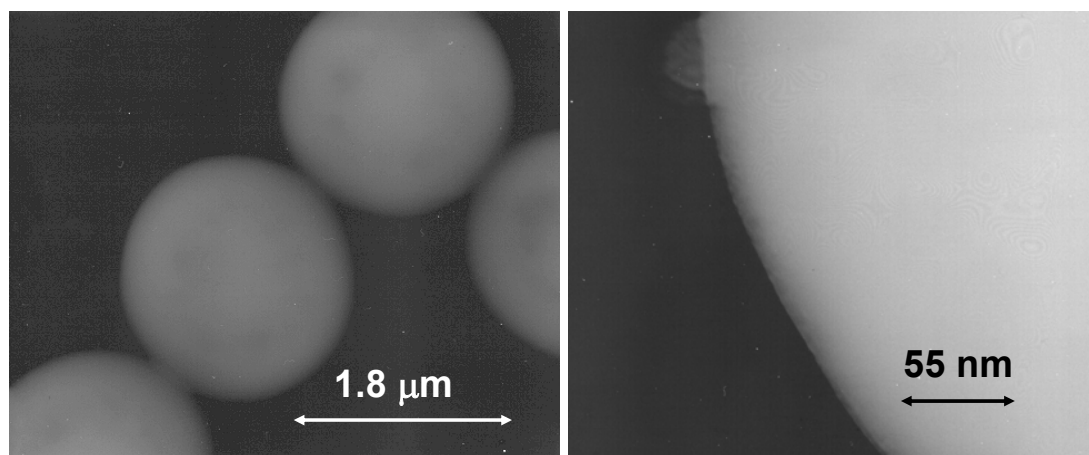


Figure 8.7a (left) and b (right). Transmission electron micrograph of several representative 1.8 micron large spheres.

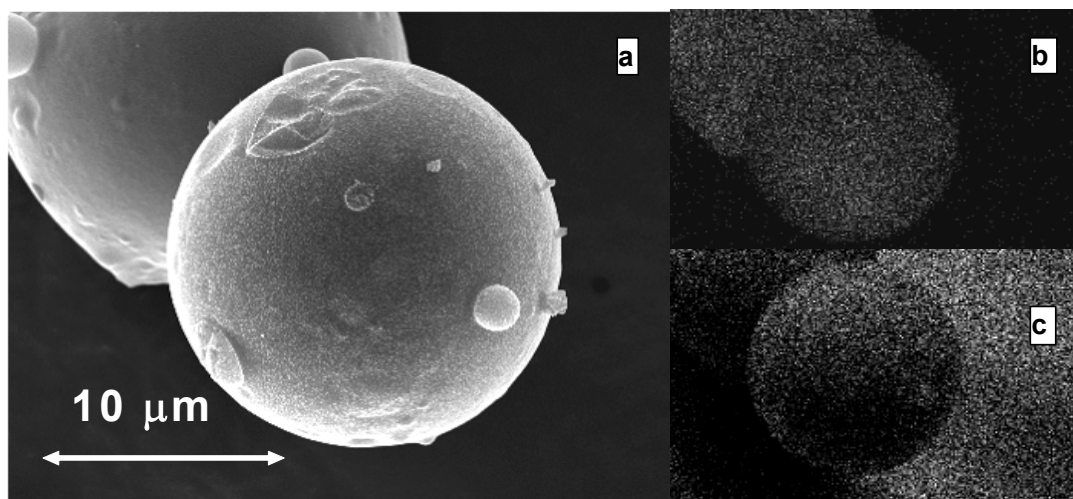


Figure 8.8. On the left (a) a scanning electron micrograph of a representative 5 micron large sphere is presented while the right hand side electron dispersive X-ray analysis (EDX) pictures map the relative concentration of cobalt (b) and carbon (c).

The determination of second row elements by EDX is afflicted by inaccuracies, and the observed oxygen content might be a) entirely due to the substrate and/or b) significantly different than measured.¹⁸ If we assume that the spheres contain cobalt and carbon only, i.e. no oxygen, a ratio of 64.9 % C and 35.1 % Co is extracted from the EDX measurement, which fits to a composition of C_9Co (calcd. C, 64.72 %; Co, 35.28 %). This “carbide,” C_9Co , could form from **8.7a** by loss of 6 molecules each of methane, CO and hydrogen respectively. Such a loss of small molecules is likely under pyrolytic conditions as demonstrated by Vollhardt^{8a} observing the evolution of hydrogen and methane during the explosive thermolysis of **8.1**. The most common cobalt carbide is Co_2C .¹⁹ We assume that the formed microspheres are homogeneous mixtures of carbon and Co_2C or might represent a new cobalt carbide.

Pyrolysis of **8.7e** leads to octahedral shaped particles with an upper size limit of 200-300 nm (Figure 8.4a and b). XRD analysis indicates that these particles are

composed primarily of cobalt with small amounts of carbon and oxygen (Figure 8.9). While formation of monodisperse cobalt nanocrystals from cobalt complexed PPEs is unknown, it is not unknown with regards to cobalt. Murray and co-workers have employed solution phase reduction of cobalt chloride in the presence of stabilizing agents to produce magnetic colloids (ferrofluids) of cobalt nanocrystals.²⁰ They were able to isolate nearly monodisperse nanocrystal samples ranging in size from 2 to 11 nm.

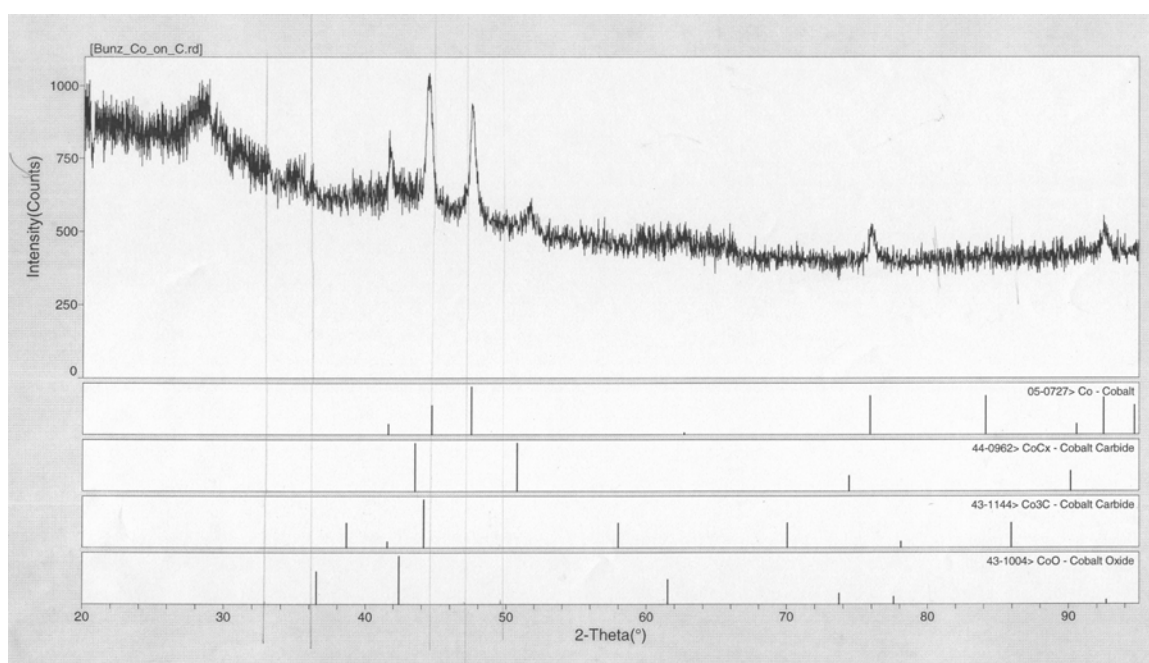


Figure 7.9. XRD data on octahedral shaped particles formed from pyrolysis of **8.7e**.

The size distribution of the particles obtained from pyrolysis of **8.7e** was analyzed (Figure 8.10) by counting 181 particles. Particles with a cross length of 10 to 15 nm (across the center of the square base) form in higher yields than particles above 50 nm. The largest particles formed were ~200-300 nm.

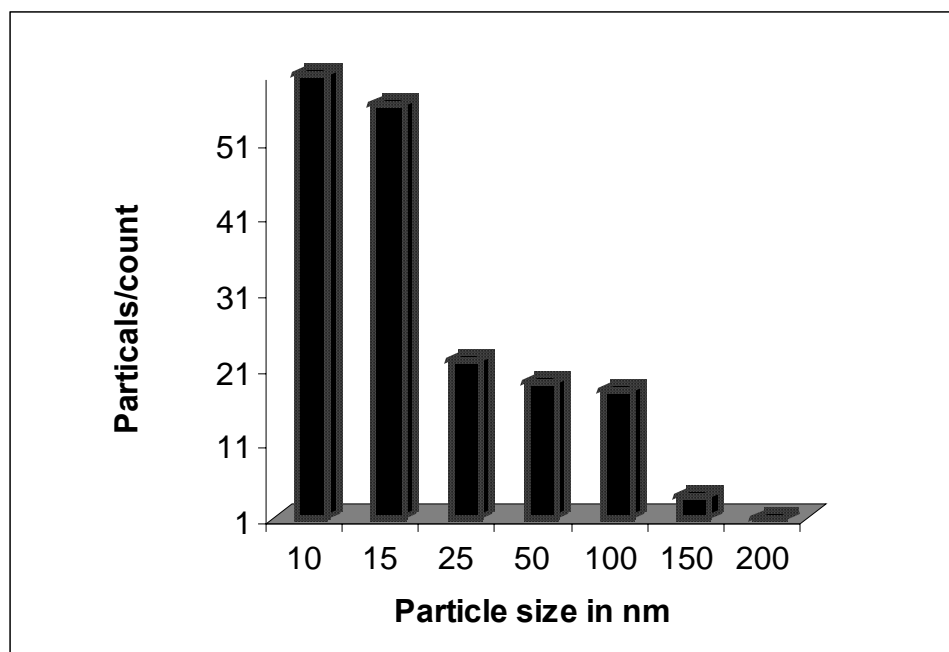


Figure 8.10. Size distribution of the particles obtained from pyrolysis of **8.7e**.

8.3 Conclusion

In conclusion, the above PPEs are easily complexed by dicobalt octacarbonyl. Completely Cobalt-complexed PPEs **8.7a** does not form all carbon materials but gives rise to novel microscopic cobalt-carbon spheres upon pyrolysis at 650°C. **8.7e** forms tetrahedral shaped particles. Despite the high reaction temperatures employed in these pyrolysis experiments, the structures of the precursors play a significant role in the elemental composition and the final shape (tubes, spheres, rods) of the product of the pyrolysis.⁸⁻¹² There is not much insight into the gestation processes of the spheres or octahedral crystals and investigation of the intriguing mechanism is planned.

8.4 Experimental:

Instrumentation. The ^1H and ^{13}C NMR spectra were taken on a Varian 300 MHz or a Bruker 400 MHz spectrometer using broadband probe. The ^1H chemical shifts are referenced to the residual proton peaks of CDCl_3 at δ 7.24 (vs. TMS). The ^{13}C resonances are referenced to the central peak of CDCl_3 at δ 77.0 (vs. TMS). Compounds **8.6a-c**, **8.7a-c** were prepared by Dr. Stefan Scholz and co-workers.

Reaction of 8.6a with diobalt octacarbonyl in toluene: **8.6a** (250 mg, 0.77 mmol rep. units) and dicobalt octacarbonyl (530 mg, 1.55 mmol) were placed in a Schlenk flask (100 mL) and toluene (50 mL) was added under inert gas. The flask was closed with a rubber septum and a bubbler mounted to the valve. The mixture was stirred until no more gas was liberated yielding a deep green/ black solution. The solvent and excess cobalt carbonyl were condensed off in oil pump vacuum. The remaining residue was taken up in chloroform, filtered, concentrated under reduced pressure, and methanol (1 L) was added. A dark greenish-black material precipitated which was filtered, washed with methanol, and dried in oil pump vacuum to yield 367 mg (78 %) of **7a**. ^1H NMR (300 MHz, C_6D_{12}): δ = 0.89, 1.40, 2.46, 7.62; $^{13}\text{C}\{^1\text{H}\}$ NMR (100 MHz, C_6D_{12}): δ = 14.2, 23.3, 29.0, 30.3, 32.5, 95.9, 132.6, 136.9, 139.4; 199.3; IR (KBr): $\tilde{\nu}$ = 2954, 2924, 2854, 2081, 2050, 2025, 2004, 1466, 1377, 1096, 902, 795.

Reaction of 8.6a with dicobalt octacarbonyl in toluene to yield 8.7d-f (125 mg, 0.39 mmol) and dicobalt octacarbonyl (0.25, 0.50, or 0.75 eq) were placed in a Schlenk flask (100 mL) and toluene (25 mL) was added under nitrogen. The flask was capped with a rubber septum and a bubbler mounted to the valve. The mixture was stirred until no more gas was liberated yielding a deep green/ black solution. The solvent was condensed off

under oil pump vacuum. The remaining residue was taken up in chloroform, filtered, concentrated under reduced pressure added to methanol (x 2) (200 mL) was added. A dark greenish-black material precipitated which was filtered, washed with methanol, and dried under oil pump vacuum to yield **8.7d-f** (50, 68, and 72%) as moderately soluble powders. **8.7d** IR: ν = 3968, 3956, 3924, 3904, 3886, 3870, 3856, 3838, 3821, 3802, 3771, 3751, 3714, 2961, 2851, 2196, 2083, 2050, 2024, 2003, 1771, 1563, 1259, 1115, 1057, 886, 722. **8.7e** IR: ν = 3987, 3970, 3931, 3914, 3891, 3884, 3865, 3845, 3830, 3812, 3792, 3761, 3737, 3724, 3702, 3662, 3640, 3612, 2924, 2858, 2197, 2083, 2051, 2027, 2003, 1770, 1676, 1487, 1449, 1411, 1075, 889. **8.7f** IR ν =3977, 3962, 3948, 3930, 3904, 3887, 3869, 3855, 3840, 3821, 3802, 3785, 3774, 2946, 2850, 2196, 2083, 2013, 1774, 1652, 1528, 1477, 1455, 1257, 1058, 949, 888, 762, 723, 678.

Synthesis of Polymer 8.8a: Monomer **6.3** (8.50 g, 11.3 mmol) and 2,5-dodecyl-1,4-diehtynylbenzene (5.29 g, 11.4 mmol) were dissolved in tetrahydrofuran (26 mL) and piperidine (26 mL) in an oven dried Schlenk flask. The flask was flushed with nitrogen, frozen and evacuated three times after which $(\text{Ph}_3\text{P})_2\text{PdCl}_2$ (57 mg, 81 mmol), and CuI (9 mg, 46 mmol) were added. The mixture was allowed to stir at room temperature for 48 h. The solvent was removed, the mixture dissolved in dichloromethane, washed with 1N HCl, 1N NH_4OH , and water. The organic layer was dried over MgSO_4 and the solvent removed. The resulting polymer was dissolved in dichloromethane and precipitated out of methanol four times to yield **8.8a** (9.11 g, 84 %) as a yellow solid. ^1H NMR (CDCl_3): δ 7.29 (m, 2H), 7.23 (m, 2H), 4.8 (m, 4H), 1.53 (m, 8H), 1.15 (m, 28H), 0.82 (m, 6H). ^{13}C NMR (CDCl_3): δ 152.4, 141.2 133.2, 123.1, 118.6, 114.5, 101.7, 94.7, 90.1, 58.2, 34.2, 33.8, 31.7, 30.2, 29.1, 26.7, 23.0, 22.4, 13.8. IR: ν 2943, 2923, 2873, 2865, 2832,

2358, 2154, 1514, 1492, 1492, 1462, 1458, 1445, 1424, 1348, 1273, 1183, 1029, 1001, 978, 672, 638. GPC (polystyrene standards) $M_n = 42.1 \times 10^3$, PDI = 2.45.

Synthesis of Polymer 8.8b: Polymer **8.8a** (0.5 g, 0.522 mmol) was dissolved in THF (20 mL) under nitrogen purge in an oven dried Schlenk flask. Under nitrogen tetrabutylammoniumfluoride (2 mL, 1M solution in THF, containing ca. 5% water) was added slowly over 5 min. The mixture was allowed to stir at room temperature for 12 h. The solvent was removed and the mixture dissolved in dichloromethane, washed with 1N HCl, 1N NH_4OH , and water. The organic layer was dried over MgSO_4 and the solvent removed. The resulting product was dissolved in dichloromethane and precipitated out of methanol to yield polymer **8.8b** (0.310 g, 92%) as a deep yellow solid. ^1H NMR (CDCl_3): δ 7.38 (m, 2H), 7.19 (m, 2H), 4.82 (m, 4H), 1.54 (m, 8H), 1.15 (m, 28H), 0.82 (m, 6H). ^{13}C NMR (TCE): δ 152.7, 141.4, 133.3, 123.2, 118.2, 114.8, 95.2, 89.7, 58.3, 34.2, 33.8, 31.7, 30.2, 29.1, 26.7, 23.0, 22.4, 13.7. IR: ν 3753, 3665, 3312, 2959, 2920, 2863, 2204, 2132, 1547, 1505, 1414, 1262, 1203, 1036, 934, 902, 834, 664, 432. GPC (polystyrene standards) $M_n = 36.2 \times 10^3$, PDI = 3.52.

Reaction of 8.8a and 8.8b with dicobalt octacarbonyl in toluene to yield 8.9a and 8.9b (0.50 mmol) and dicobalt octacarbonyl (2 eq/triple bond) were placed in a Schlenk flask (100 mL) and toluene (30 mL) was added under nitrogen. The flask was capped with a rubber septum and a bubbler mounted to the valve. The mixture was stirred for 24 h. The solvent was condensed off under oil pump vacuum. The remaining residue was taken up in chloroform, filtered, concentrated under reduced pressure added to methanol (x 2) (200 mL) was added. A dark greenish-black material precipitated which was

filtered, washed with methanol, and dried under oil pump vacuum to yield **8.9a** and **8.9b** (81 and 92 %) as insoluble powders. **8.9a** IR: ν =2927, 2850, 2334, 2178, 2085, 2052, 2026, 2002, 1859, 1672, 1187, 1039, 881, 831. **8.9b** IR: ν =2921, 2852, 2336, 2183, 2096, 2083, 2053, 2023, 1983, 1350, 1194, 823.

Sample pyrolysis: A quartz tube (35 mm outer diameter, 500 mm long) was closed up on one end with a rubber stopper that had a gas inlet. The tube was placed for 1 h in a tube furnace and heated to 650 °C. A slow stream of nitrogen was blown through the tube, and a sample was placed in an alumina boat and introduced into the heated tube under a constant gentle stream of nitrogen. The second end of the tube was closed with a perforated rubber stopper that was connected to an oil bubbler to allow a slow nitrogen flow. The sample was held at 650 °C for 1 h and cooled down to ambient temperature. The pyrolysis of the polymers proceeded without deflagration. The grain like material was transferred to a SEM sample stud or a TEM grid and examined.

8.5 References

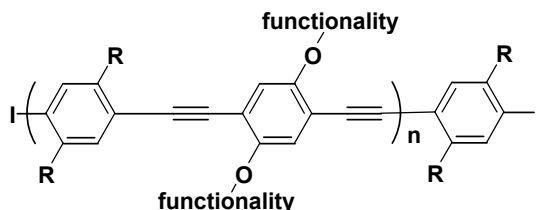
1. a) P. Fraundorf, M. Wackenhut, *Astrophys. J.* **2002**, 578, L153. b) S. Amari, E. Zinner, R. S. Lewis, *Meteoritics* **1995**, 30, 679.
2. M. Inagaki, K. Kuroda, M. Sakai, *Carbon* **1983**, 21, 231.
3. a) Z. C. Kang, Z. L. Wang, *Phil. Mag. B.* **1996**, 73, 905. b) Z. L. Wang, Z. C. Kang, *J. Phys. Chem.* **1996**, 100, 17725.
4. X. Sun, Y. Li, *Angew. Chem. Int. Ed.* **2004**, 43, 597.
5. X. Yang, C. Li, W. Wang, B. Yang, S. Zhang, Y. Qian, *J. Chem. Soc., Chem. Commun.* **2004**, 342.
6. H. Hou, A. K. Schaper, F. Weller, A. Greiner, *Chem. Mater.* **2002**, 14, 3990.

7. a) G. Hu, D. Ma, M. Cheng, L. Liu, X. Bao, *J. Chem. Soc., Chem. Commun.* **2002**, 1948. b) Y. Xiong, Y. Xie, Z. Li, C. Wu, R. Zhang, *J. Chem. Soc., Chem. Commun.* **2003**, 904.
8. a) R. Boese, A. J. Matzger, K. P. C. Vollhardt, *J. Am. Chem. Soc.* **1997**, 119, 2052. b) R. Faust, *Angew. Chem. Int. Ed.* **1998**, 37, 2825. c) For a review on onion like graphite particles see: D. Ugarte, *Carbon* **1995**, 33, 989. d) C. N. Rao, B. C. Satishkumar, A. Govindaraj, M. Nath, *Chem. Phys. Chem.* **2001**, 2, 78.
9. P. I. Dosa, C. Erben, V. S. Iyer, K. P. C. Vollhardt, I. M. Wasser, *J. Am. Chem. Soc.* **1999**, 121, 10430.
10. V. S. Iyer, K. P. C. Vollhardt, R. Wilhelm, *Angew. Chem. Int. Ed.* **2003**, 42, 4379.
11. J. Wu, B. El Hamaoui, J. Li, L. Zhi, U. Kolb, K. Müllen, *Small* **2005**, 1, 210.
12. a) M. Laskoski, W. Steffen, J. G. M. Morton, M. D. Smith, U. H. F. Bunz, *J. Am. Chem. Soc.* **2002**, 124, 13814. b) R. D. Adams, U. H. F. Bunz, W. Fu, L. Nguyen, *J. Organomet. Chem.* **1999**, 578, 91.
13. a) U. H. F. Bunz, *Chem. Rev.* **2000**, 100, 1605. b) J. N. Wilson, S. M. Waybright, K. McAlpine, U. H. F. Bunz, *Macromolecules* **2002**, 35, 3799. c) L. Kloppenburg, D. Jones, U. H. F. Bunz, *Macromolecules* **1999**, 32, 4194.
14. a) A. R. Marshall, U. H. F. Bunz, *Macromolecules* **2001**, 34, 4688. b) J. B. Beck, A. Kokil, D. Ray, S. J. Rowan, C. Weder, *Macromolecules* **2002**, 35, 590.
15. a) A. Kokil, I. Shiyonovskaya, K. D. Singer, C. Weder, *J. Am. Chem. Soc.* **2002**, 124, 9978. b) C. Huber, F. Bangerter, W. R. Caseri, C. Weder, *J. Am. Chem. Soc.* **2001**, 123, 3857.
16. a) S. B. Clendenning, S. Aouba, M. S. Rayat, D. Grozea, J. B. Sorge, P. M. Brodersen, R. N. S. Sodhi, Z.-H. Lu, C. M. Yip, M. R. Freedman, H. E. Ruda, I. Manners, *Adv. Mater.* **2004**, 16, 215. b) S. B. Clendenning, S. Fournier-Bidoz, A. Pietrangelo, G. C. Yang, S. J. Han, P. M. Brodersen, C. M. Yip, Z. H. Lu, G. A. Ozin, I. Manners, *J. Mater. Chem.* **2004**, 14, 1686. c) for the reaction of polydiacetylene with dicobalt octacarbonyl see: P. Magnus, D. P. Becker, *J. Chem. Soc., Chem. Commun.* **1985**, 640. c) Brian C. Englert, Stefan Scholz, Peter J. Leech, Mohan Srinivasarao, and Uwe H. F. Bunz. *European Journal of Chemistry*, In Press.
17. C. Elschenbroich, *Organometallchemie*, 4th Edition, Teubner Verlag, Stuttgart, **2004**, p 332.
18. *Energy-Dispersive X-Ray Microanalysis*, Ed. D. Vanghan, Kevex Corporation, Foster City CA, **1983**.

19. Gmelins Handbuch der Anorganischen Chemie, Kobalt, Teil A, Ergänzungsband Syst. Nr. 58, 8th Edition, Verlag Chemie, Weinheim **1961**, pp 671-676.
20. Shouheng, S. and Murray, C. B. *Journal of Applied Physics*. **1999**, 85, 4325-4330.

CHAPTER 9

CONCLUSIONS AND FINAL REMARKS.



12.1. Discussion

We have demonstrated the ability to produce molecular wires through the pre-functionalization of PPEs.¹ Production of carbon rich non-aggregating PPEs should yield thermally stable molecular wires. This produces non-aggregating rigid rods. These materials exhibit properties in the solid state which are in some cases quite similar to those in solution. This is the result of a polymer, which has been tailored to exist in an independent environment. These polymers have been shown to be electronically and dynamically shielded from separate polymer chains.² These polymers have exhibited the ability to resist collisional deactivation in dilute solution. Some of these materials are effectively “jacketed” molecular wires. We are further tailoring these materials to be thermally stable using a series of simple yet regioselective reactions. This has produced polymers which will prove useful in future applications.

We have successfully made steps towards the functionalization PPEs. These include approaches to pre-functionalized and post-functionalized PPEs which have introduced a number of functional groups that could be used in bio/metal-sensing applications.

The above implementations have called for the use of reactions which are complete and selective. These reactions have afforded the desired products with superior yield and selectivity. We have determined click chemistry to be a valuable methodology in this quest. It has not only supplied us with a route to functionalized PPEs but has as well yielded a direct route to conjugated small molecules. This easily moves PPEs to their next plateau. This next plateau supports the examination of post-functionalized PPEs and their comparison to pre-functionalized PPEs. These materials should and do exhibit the same properties regardless of their method of production.

We have also shown that PPEs which contain metals may be used as precursors in the synthesis of other types of materials. The ability to microstructure PPEs can be used advantageously to produce microstructured ceramic materials.³ This is an interesting alternative to templating approaches. These types of materials may be useful for photonic bandgap applications. Metal complexed PPEs have been pyrolyzed and transformed various nano-structures.⁴

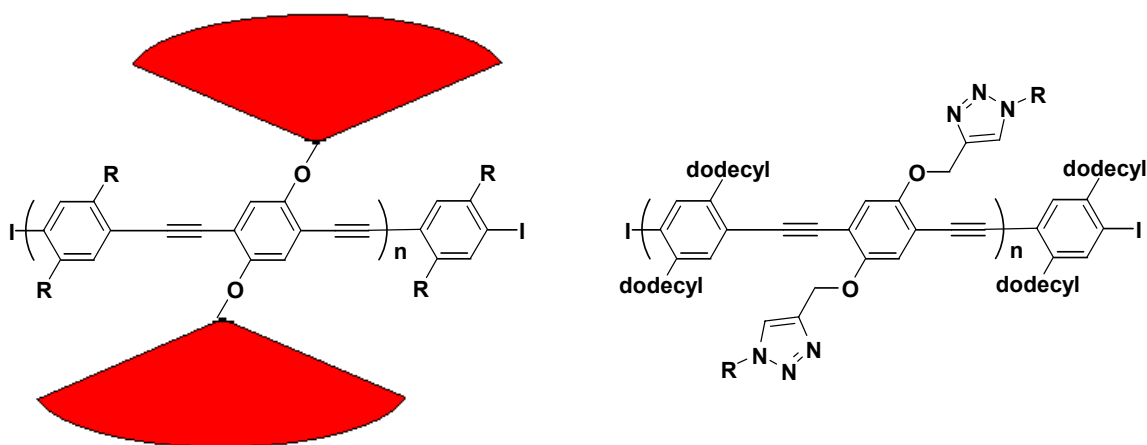


Figure 9.1. Basic structure of jacketed and functionalized PPEs.

Most important in the work presented is the introduction of a variety of sensitive functional/spacer groups to PPEs under various conditions. This has afforded polymers which could be deemed useful in a wide variety of applications (Figure 9.1). Considering the above achievements, we have moved through the following steps:

1. Integration of spacer groups which allow for the modification of the optical properties of PPEs
2. Synthesis of monomers which allow access to functionalized PPEs
3. Synthesis of polymers which can be modified through post-polymerization functionalization
4. Functionalization of these polymers and investigation of their properties
5. Use of functionalized PPEs as precursor polymers

We have effectively made significant progress towards the implementation PPEs as sensory materials, “jacketed” nonaggregating rigid rods, and precursors in route to other types of materials.

12.2. References:

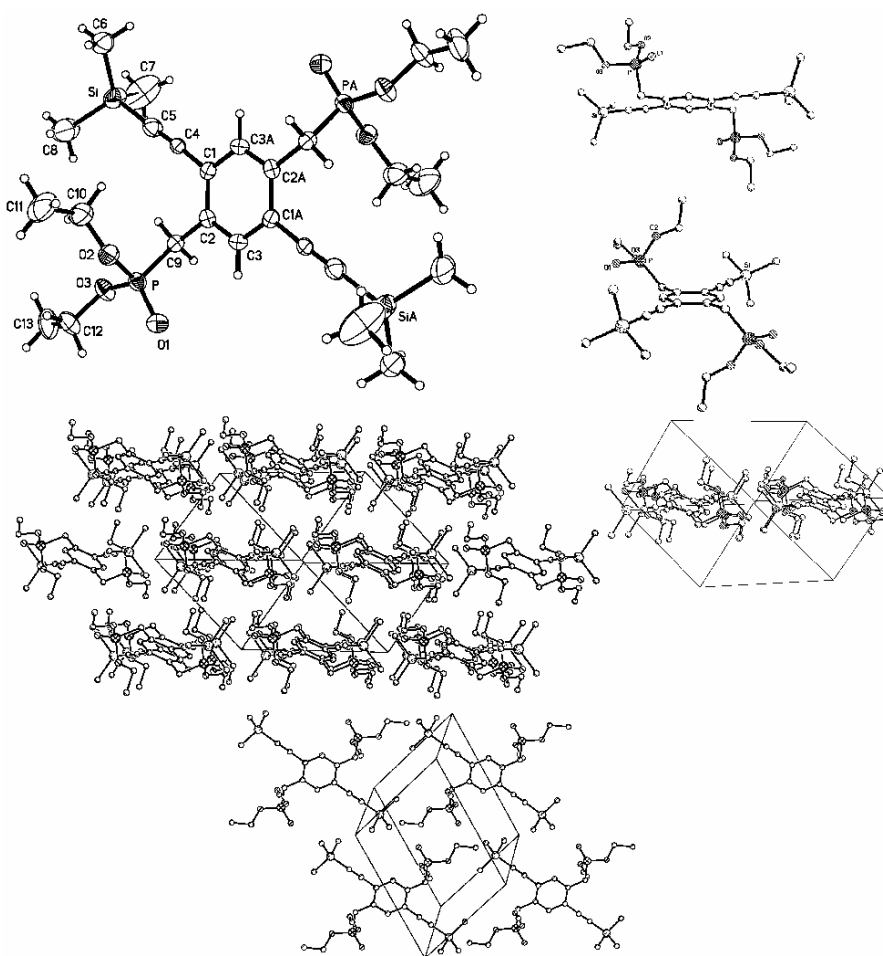
1. Brian C. Englert, Mark D. Smith, Kenneth I. Hardcastle, and Uwe H. F. Bunz. *Macromolecules*; **2004**; 37(22); 8212-8221.
2. Sato, T.; Jiang, D.; and Aida, T. *J. Am. Chem. Soc.* **1999**, 121, 10658-10659.
3. Brian C. Englert, Stefan Scholz, Peter J. Leech, Mohan Srinivasarao, and Uwe H. F. Bunz. *European Journal of Chemistry. Accepted and In Press.*
4. Prof. U. Bunz, Dr. S. Scholz, P. Leech, B. Englert, Prof. M. Wech, W. Sommer. *Advanced Materials. Accepted and In Press.*

APPENDIX A

ADDITIONAL CRYSTALLOGRAPHIC DATA AND STRUCTURES.

A.1 Crystallographic Data and Figures

X-Ray Structure Determination, $C_{26}H_{44}O_6P_2Si_2$



A yellow-brown plate was mounted onto the end of a thin glass fiber using inert oil. X-ray intensity data covering the entire sphere of reciprocal space were measured at 150(1) K on a Bruker SMART APEX CCD-based diffractometer (Mo K α radiation, $\lambda = 0.71073$ Å).¹ The raw data frames were integrated with SAINT+,¹ which also applied corrections for Lorentz and polarization effects. The final unit cell parameters are based on the least-squares refinement of 3621 reflections with $I > 5\sigma(I)$ from the data set. Analysis of the data showed negligible crystal decay during collection. An empirical absorption correction based on the multiple measurement of equivalent reflections was applied with the program SADABS.¹

C₂₆H₄₄O₆P₂Si₂ crystallizes in the triclinic system. The structure was solved in the space group P-1 by a combination of direct methods and difference Fourier syntheses, and refined by full-matrix least-squares against F², using the SHELXTL software package.² The asymmetric unit contains half of the centrosymmetric molecule. Non-hydrogen atoms were refined with anisotropic displacement parameters; hydrogen atoms were placed in geometrically idealized positions and refined as standard riding atoms.

(1) SMART Version 5.625, SAINT+ Version 6.02a and SADABS. Bruker Analytical X-ray Systems, Inc., Madison, Wisconsin, USA, 1998.

(2) Sheldrick, G. M. SHELXTL Version 5.1; Bruker Analytical X-ray Systems, Inc., Madison, Wisconsin, USA, 1997.

Table A1. Crystal data and structure refinement for bu01s.

Identification code	bu01s	
Empirical formula	C ₂₆ H ₄₄ O ₆ P ₂ Si ₂	
Formula weight	570.73	
Temperature	150(1) K	
Wavelength	0.71073 Å	
Crystal system	Triclinic	
Space group	P-1	
Unit cell dimensions	a = 8.5624(6) Å	$\alpha = 72.6960(10)^\circ$.
	b = 8.8972(6) Å	$\beta = 84.972(2)^\circ$.
	c = 11.2157(8) Å	$\gamma = 84.0890(10)^\circ$.
Volume	809.96(10) Å ³	
Z	1	
Density (calculated)	1.170 Mg/m ³	
Absorption coefficient	0.242 mm ⁻¹	
F(000)	306	
Crystal size	0.20 x 0.16 x 0.06 mm ³	
Theta range for data collection	1.91 to 23.25°.	

Index ranges	-9<=h<=9, -9<=k<=9, -12<=l<=12
Reflections collected	5735
Independent reflections	2333 [R(int) = 0.0379]
Completeness to theta = 23.25°	100.0 %
Absorption correction	Semi-empirical from equivalents
Max. and min. transmission	0.9829 and 0.7256
Refinement method	Full-matrix least-squares on F ²
Data / restraints / parameters	2333 / 0 / 168
Goodness-of-fit on F ²	1.052
Final R indices [I>2sigma(I)]	R1 = 0.0519, wR2 = 0.1269
R indices (all data)	R1 = 0.0641, wR2 = 0.1333
Largest diff. peak and hole	0.301 and -0.266 e.Å ⁻³

Atomic coordinates ($\times 10^4$) and equivalent isotropic displacement parameters ($\text{\AA}^2 \times 10^3$) for bu01s. U(eq) is defined as one third of the trace of the orthogonalized U^{ij} tensor.

	x	y	z	U(eq)
C(1)	360(3)	589(3)	3721(3)	27(1)
C(2)	373(3)	1585(3)	4483(3)	25(1)
C(3)	19(3)	969(3)	5748(3)	28(1)
C(4)	711(3)	1176(3)	2369(3)	27(1)
C(5)	1078(4)	1651(4)	1298(3)	38(1)
C(6)	2483(5)	672(4)	-936(4)	57(1)
C(7)	-185(7)	3204(6)	-1204(4)	108(2)
C(8)	3070(8)	3848(6)	-634(5)	126(3)
C(9)	745(3)	3280(3)	3932(3)	28(1)
C(10)	4454(4)	2441(5)	3209(4)	55(1)
C(11)	6137(5)	1813(6)	3294(4)	81(2)
C(12)	3838(4)	6399(4)	3751(4)	50(1)
C(13)	3804(5)	7895(4)	2708(4)	66(1)
O(1)	2182(3)	3815(3)	5857(2)	40(1)
O(2)	3855(2)	2619(2)	4409(2)	39(1)
O(3)	2676(3)	5423(2)	3561(2)	41(1)
P	2392(1)	3793(1)	4552(1)	30(1)
Si	1627(1)	2355(1)	-392(1)	51(1)

Bond lengths [Å] and angles [°] for bu01s.

C(1)-C(3)#1	1.396(4)
C(1)-C(2)	1.403(4)
C(1)-C(4)	1.464(4)
C(2)-C(3)	1.379(4)
C(2)-C(9)	1.506(4)
C(3)-C(1)#1	1.396(4)
C(4)-C(5)	1.175(4)
C(5)-Si	1.845(4)
C(6)-Si	1.842(4)
C(7)-Si	1.845(5)
C(8)-Si	1.852(5)
C(9)-P	1.782(3)
C(10)-O(2)	1.445(4)
C(10)-C(11)	1.491(5)
C(12)-O(3)	1.454(4)
C(12)-C(13)	1.488(5)
O(1)-P	1.464(2)
O(2)-P	1.575(2)
O(3)-P	1.570(2)
C(3)#1-C(1)-C(2)	119.8(3)
C(3)#1-C(1)-C(4)	119.6(3)
C(2)-C(1)-C(4)	120.6(3)
C(3)-C(2)-C(1)	118.0(3)
C(3)-C(2)-C(9)	121.1(3)
C(1)-C(2)-C(9)	121.0(2)
C(2)-C(3)-C(1)#1	122.2(3)
C(5)-C(4)-C(1)	176.3(3)
C(4)-C(5)-Si	178.5(3)
C(2)-C(9)-P	114.5(2)
O(2)-C(10)-C(11)	109.0(3)
O(3)-C(12)-C(13)	108.6(3)
C(10)-O(2)-P	122.4(2)
C(12)-O(3)-P	120.1(2)

O(1)-P-O(3)	115.66(13)
O(1)-P-O(2)	109.02(12)
O(3)-P-O(2)	106.93(12)
O(1)-P-C(9)	115.90(13)
O(3)-P-C(9)	99.87(13)
O(2)-P-C(9)	108.81(13)
C(6)-Si-C(7)	109.3(2)
C(6)-Si-C(5)	109.26(16)
C(7)-Si-C(5)	107.63(19)
C(6)-Si-C(8)	110.8(2)
C(7)-Si-C(8)	111.7(3)
C(5)-Si-C(8)	108.0(2)

Symmetry transformations used to generate equivalent atoms:

#1 -x,-y,-z+1

Anisotropic displacement parameters ($\text{\AA}^2 \times 10^3$) for bu01s. The anisotropic displacement factor exponent takes the form: $-2\pi^2 [h^2 a^{*2} U^{11} + \dots + 2 h k a^* b^* U^{12}]$

	U^{11}	U^{22}	U^{33}	U^{23}	U^{13}	U^{12}
C(1)	24(2)	31(2)	24(2)	-7(1)	0(1)	-2(1)
C(2)	23(2)	24(2)	26(2)	-3(1)	-4(1)	-3(1)
C(3)	32(2)	27(2)	29(2)	-13(1)	-3(1)	-3(1)
C(4)	32(2)	19(2)	31(2)	-9(1)	6(1)	-7(1)
C(5)	47(2)	31(2)	36(2)	-8(2)	-2(2)	-9(2)
C(6)	69(3)	54(2)	51(2)	-21(2)	12(2)	-15(2)
C(7)	142(5)	112(4)	41(3)	5(3)	-12(3)	49(4)
C(8)	192(6)	88(4)	116(5)	-64(3)	101(4)	-90(4)
C(9)	28(2)	28(2)	26(2)	-8(1)	0(1)	-1(1)
C(10)	41(2)	69(3)	64(3)	-36(2)	0(2)	-2(2)
C(11)	48(2)	113(4)	92(4)	-56(3)	1(2)	19(3)
C(12)	53(2)	39(2)	62(3)	-14(2)	-2(2)	-22(2)
C(13)	52(2)	35(2)	101(3)	-8(2)	17(2)	-14(2)
O(1)	44(1)	44(1)	36(1)	-17(1)	-3(1)	-6(1)
O(2)	31(1)	40(1)	47(1)	-19(1)	0(1)	1(1)
O(3)	45(1)	33(1)	45(1)	-5(1)	-7(1)	-15(1)
P	31(1)	25(1)	33(1)	-8(1)	-2(1)	-5(1)
Si	78(1)	39(1)	32(1)	-7(1)	15(1)	-11(1)

Hydrogen coordinates ($\times 10^4$) and isotropic displacement parameters ($\text{\AA}^2 \times 10^{-3}$)
for bu01s.

	x	y	z	U(eq)
H(3)	33	1627	6276	34
H(6A)	3403	171	-464	86
H(6B)	2803	1047	-1829	86
H(6C)	1698	-98	-806	86
H(7A)	-988	2443	-938	162
H(7B)	42	3445	-2110	162
H(7C)	-571	4176	-995	162
H(8A)	2603	4715	-314	188
H(8B)	3359	4260	-1529	188
H(8C)	4012	3358	-186	188
H(9A)	-190	3972	4076	33
H(9B)	947	3495	3016	33
H(10A)	4361	3475	2559	66
H(10B)	3834	1704	2974	66
H(11A)	6754	2578	3476	121
H(11B)	6536	1636	2496	121
H(11C)	6226	813	3964	121
H(12A)	4898	5834	3768	61
H(12B)	3595	6632	4560	61
H(13A)	4136	7663	1918	99
H(13B)	4520	8601	2860	99
H(13C)	2733	8408	2658	99

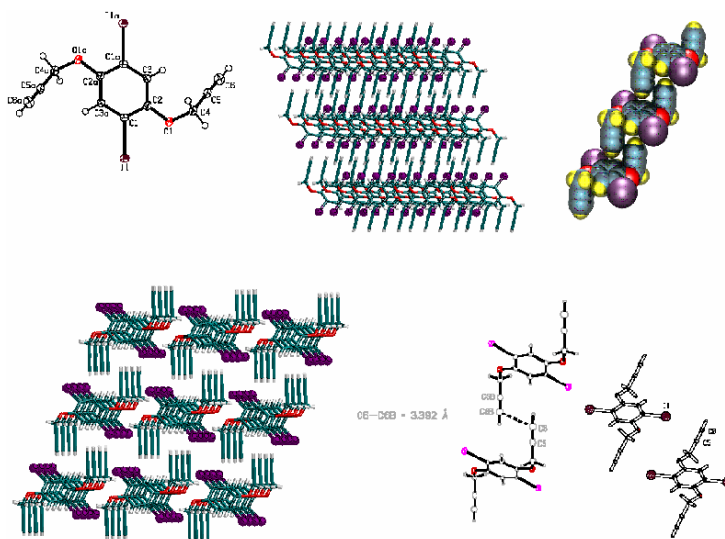
Torsion angles [°] for bu01s.

C(3)#1-C(1)-C(2)-C(3)	0.5(4)
C(4)-C(1)-C(2)-C(3)	179.4(2)
C(3)#1-C(1)-C(2)-C(9)	-178.8(3)
C(4)-C(1)-C(2)-C(9)	0.1(4)
C(1)-C(2)-C(3)-C(1)#1	-0.6(4)
C(9)-C(2)-C(3)-C(1)#1	178.7(3)
C(3)#1-C(1)-C(4)-C(5)	-111(5)
C(2)-C(1)-C(4)-C(5)	70(5)
C(1)-C(4)-C(5)-Si	133(10)
C(3)-C(2)-C(9)-P	59.3(3)
C(1)-C(2)-C(9)-P	-121.4(3)
C(11)-C(10)-O(2)-P	156.9(3)
C(13)-C(12)-O(3)-P	-177.3(2)
C(12)-O(3)-P-O(1)	48.4(3)
C(12)-O(3)-P-O(2)	-73.2(3)
C(12)-O(3)-P-C(9)	173.5(2)
C(10)-O(2)-P-O(1)	-174.4(2)
C(10)-O(2)-P-O(3)	-48.7(3)
C(10)-O(2)-P-C(9)	58.4(3)
C(2)-C(9)-P-O(1)	-68.7(2)
C(2)-C(9)-P-O(3)	166.3(2)
C(2)-C(9)-P-O(2)	54.5(2)
C(4)-C(5)-Si-C(6)	-51(12)
C(4)-C(5)-Si-C(7)	68(12)
C(4)-C(5)-Si-C(8)	-171(12)

Symmetry transformations used to generate equivalent atoms:

#1 -x,-y,-z+1

X-Ray Structure Determination, C₁₂H₈I₂O₂, 2



X-ray intensity data from a colorless block were measured at 150(1) K on a Bruker SMART APEX CCD-based diffractometer (Mo K α radiation, $\lambda = 0.71073$ Å).¹ Raw data frame integration and Lp corrections were performed with SAINT+.¹ Final unit cell parameters were determined by least-squares refinement of 2545 reflections from the data set with $I > 5(\sigma)I$. Analysis of the data showed negligible crystal decay during collection. The data were corrected for absorption with SADABS.¹ Patterson methods structure solution, difference Fourier calculations and full-matrix least-squares refinement against F^2 were performed with SHELXTL.²

C₁₂H₈I₂O₂ crystallizes in the triclinic system. The space group P-1 was assumed and confirmed by the successful solution and refinement of the data. The molecule is situated on an inversion center. Non-hydrogen atoms were refined with anisotropic displacement parameters; hydrogen atoms were placed in idealized positions and included as riding atoms with refined isotropic displacement parameters.

(1) SMART Version 5.628, SAINT+ Version 6.22 and SADABS Version 2.05. Bruker Analytical X-ray Systems, Inc., Madison, Wisconsin, USA, 2001.

(2) Sheldrick, G. M. SHELXTL Version 6.1; Bruker Analytical X-ray Systems, Inc., Madison, Wisconsin, USA, 2000.

Table A2. Crystal data and structure refinement for bce4s.

Identification code	bce4s	
Empirical formula	C ₁₂ H ₈ I ₂ O ₂	
Formula weight	437.98	
Temperature	150(2) K	
Wavelength	0.71073 Å	
Crystal system	Triclinic	
Space group	P-1	
Unit cell dimensions	a = 4.2569(4) Å b = 8.9180(8) Å c = 8.9454(8) Å	$\alpha = 67.777(2)^\circ$ $\beta = 79.244(2)^\circ$ $\gamma = 82.963(2)^\circ$
Volume	308.34(5) Å ³	
Z	1	
Density (calculated)	2.359 Mg/m ³	
Absorption coefficient	5.081 mm ⁻¹	
F(000)	202	
Crystal size	0.20 x 0.08 x 0.05 mm ³	
Theta range for data collection	2.47 to 26.35°	
Index ranges	-5 ≤ h ≤ 5, -11 ≤ k ≤ 11, -11 ≤ l ≤ 11	
Reflections collected	2788	
Independent reflections	1253 [R(int) = 0.0195]	
Completeness to theta = 26.35°	99.6 %	
Absorption correction	Semi-empirical from equivalents	
Max. and min. transmission	1.0000 and 0.7570	
Refinement method	Full-matrix least-squares on F ²	
Data / restraints / parameters	1253 / 0 / 78	
Goodness-of-fit on F ²	1.083	
Final R indices [I > 2σ(I)]	R1 = 0.0165, wR2 = 0.0412	
R indices (all data)	R1 = 0.0170, wR2 = 0.0415	
Extinction coefficient	0.0115(16)	
Largest diff. peak and hole	0.582 and -0.410 e.Å ⁻³	

Atomic coordinates ($\times 10^4$) and equivalent isotropic displacement parameters ($\text{\AA}^2 \times 10^3$) for bce4s. $U(\text{eq})$ is defined as one third of the trace of the orthogonalized U^{ij} tensor.

	x	y	z	U(eq)
I(1)	6689(1)	2287(1)	8771(1)	21(1)
O(1)	2306(4)	5443(2)	7884(2)	21(1)
C(1)	5662(6)	3925(3)	6501(3)	17(1)
C(2)	3574(6)	5278(3)	6430(3)	18(1)
C(3)	2938(6)	6356(3)	4904(3)	17(1)
C(4)	-29(6)	6752(3)	7866(3)	22(1)
C(5)	1447(7)	8319(3)	7275(3)	23(1)
C(6)	2662(8)	9560(4)	6852(4)	32(1)

Bond lengths [Å] and angles [°] for bce4s.

I(1)-C(1)	2.093(2)
O(1)-C(2)	1.367(3)
O(1)-C(4)	1.435(3)
C(1)-C(3)#1	1.385(4)
C(1)-C(2)	1.396(4)
C(2)-C(3)	1.394(4)
C(3)-C(1)#1	1.385(4)
C(3)-H(3)	0.9500
C(4)-C(5)	1.470(4)
C(4)-H(4A)	0.9900
C(4)-H(4B)	0.9900
C(5)-C(6)	1.177(4)
C(6)-H(6)	0.9500
C(2)-O(1)-C(4)	118.2(2)
C(3)#1-C(1)-C(2)	121.2(2)
C(3)#1-C(1)-I(1)	119.34(19)
C(2)-C(1)-I(1)	119.42(19)
O(1)-C(2)-C(3)	124.8(2)
O(1)-C(2)-C(1)	116.8(2)
C(3)-C(2)-C(1)	118.4(2)
C(1)#1-C(3)-C(2)	120.4(2)
C(1)#1-C(3)-H(3)	119.8
C(2)-C(3)-H(3)	119.8
O(1)-C(4)-C(5)	112.0(2)
O(1)-C(4)-H(4A)	109.2
C(5)-C(4)-H(4A)	109.2
O(1)-C(4)-H(4B)	109.2
C(5)-C(4)-H(4B)	109.2
H(4A)-C(4)-H(4B)	107.9
C(6)-C(5)-C(4)	177.8(3)
C(5)-C(6)-H(6)	180.0

Symmetry transformations used to generate equivalent atoms:

#1 -x+1,-y+1,-z+1

Anisotropic displacement parameters ($\text{\AA}^2 \times 10^3$) for bce4s. The anisotropic displacement factor exponent takes the form: $-2\pi^2 [h^2 a^{*2} U^{11} + \dots + 2 h k a^* b^* U^{12}]$

	U^{11}	U^{22}	U^{33}	U^{23}	U^{13}	U^{12}
I(1)	24(1)	21(1)	16(1)	-5(1)	-5(1)	1(1)
O(1)	26(1)	20(1)	15(1)	-8(1)	2(1)	2(1)
C(1)	18(1)	16(1)	15(1)	-4(1)	-4(1)	-3(1)
C(2)	19(1)	20(1)	17(1)	-9(1)	0(1)	-4(1)
C(3)	18(1)	15(1)	18(1)	-6(1)	-2(1)	-1(1)
C(4)	24(1)	22(1)	20(1)	-10(1)	1(1)	1(1)
C(5)	27(1)	25(1)	20(1)	-12(1)	-4(1)	4(1)
C(6)	38(2)	26(2)	32(2)	-11(1)	-5(1)	-2(1)

Hydrogen coordinates ($\times 10^4$) and isotropic displacement parameters ($\text{\AA}^2 \times 10^{-3}$)
for bce4s.

	x	y	z	U(eq)
H(3)	1537	7288	4827	20(7)
H(4A)	-1205	6537	8985	17(7)
H(4B)	-1594	6808	7153	40(10)
H(6)	3643	10561	6510	78(15)

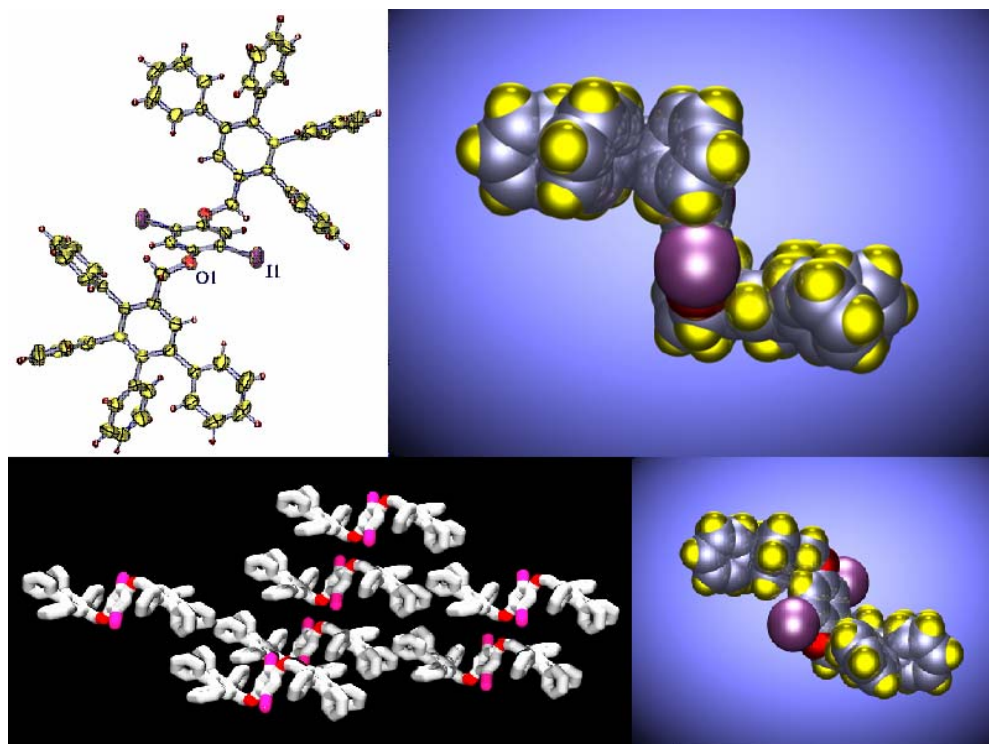
Torsion angles [°] for bce4s.

C(4)-O(1)-C(2)-C(3)	4.7(4)
C(4)-O(1)-C(2)-C(1)	-175.5(2)
C(3)#1-C(1)-C(2)-O(1)	179.7(2)
I(1)-C(1)-C(2)-O(1)	-0.1(3)
C(3)#1-C(1)-C(2)-C(3)	-0.5(4)
I(1)-C(1)-C(2)-C(3)	179.67(17)
O(1)-C(2)-C(3)-C(1)#1	-179.7(2)
C(1)-C(2)-C(3)-C(1)#1	0.4(4)
C(2)-O(1)-C(4)-C(5)	-76.1(3)

Symmetry transformations used to generate equivalent atoms:

#1 -x+1,-y+1,-z+1

X-Ray Structure Determination, $C_{68}H_{48}I_2O_2$, 3a



X-ray intensity data from a colorless plate were measured at 293(2) K on a Bruker SMART APEX CCD-based diffractometer (Mo $K\alpha$ radiation, $\lambda = 0.71073$ Å).¹ Raw data frame integration and Lp corrections were performed with SAINT+.¹ Final unit cell parameters were determined by least-squares refinement of 5239 reflections from the data set with $I > 5(\sigma)I$. Analysis of the data showed negligible crystal decay during collection. An empirical absorption correction was applied with SADABS.¹ Direct methods structure solution, difference Fourier calculations and full-matrix least-squares refinement against F^2 were performed with SHELXTL.²

$C_{68}H_{48}I_2O_2$ crystallizes in the space group $P2_1/n$ as determined by the pattern of systematic absences in the intensity data. The molecule is situated about a center of symmetry; the asymmetric unit therefore consists of half the molecule. All non-hydrogen atoms were refined with anisotropic displacement parameters; hydrogen atoms were placed in idealized positions and included as riding atoms.

(1) SMART Version 5.628, SAINT+ Version 6.22 and SADABS Version 2.05. Bruker Analytical X-ray Systems, Inc., Madison, Wisconsin, USA, 2001.

(2) Sheldrick, G. M. SHELXTL Version 6.1; Bruker Analytical X-ray Systems, Inc., Madison, Wisconsin, USA, 2000.

Table A3. Crystal data and structure refinement for bce03s.

Identification code	bce03s	
Empirical formula	C ₆₈ H ₄₈ I ₂ O ₂	
Formula weight	1150.86	
Temperature	293(2) K	
Wavelength	0.71073 Å	
Crystal system	Monoclinic	
Space group	P2 ₁ /n	
Unit cell dimensions	a = 15.6063(10) Å	α = 90°.
	b = 8.9275(6) Å	β = 98.979(2)°.
	c = 19.2262(13) Å	γ = 90°.
Volume	2645.9(3) Å ³	
Z	2	
Density (calculated)	1.445 Mg/m ³	
Absorption coefficient	1.235 mm ⁻¹	
F(000)	1156	
Crystal size	0.38 x 0.09 x 0.04 mm ³	
Theta range for data collection	1.57 to 22.54°.	
Index ranges	-16 ≤ h ≤ 16, -9 ≤ k ≤ 9, -20 ≤ l ≤ 20	
Reflections collected	16828	
Independent reflections	3485 [R(int) = 0.0514]	
Completeness to theta = 22.54°	100.0 %	
Absorption correction	Semi-empirical from equivalents	
Max. and min. transmission	1.0000 and 0.7775	
Refinement method	Full-matrix least-squares on F ²	
Data / restraints / parameters	3485 / 0 / 325	
Goodness-of-fit on F ²	1.080	
Final R indices [I > 2σ(I)]	R1 = 0.0541, wR2 = 0.1256	
R indices (all data)	R1 = 0.0705, wR2 = 0.1348	
Largest diff. peak and hole	1.645 and -0.256 e.Å ⁻³	

Atomic coordinates ($\times 10^4$) and equivalent isotropic displacement parameters ($\text{\AA}^2 \times 10^3$) for bce03s. $U(\text{eq})$ is defined as one third of the trace of the orthogonalized U^{ij} tensor.

	x	y	z	$U(\text{eq})$
I(1)	1642(1)	3124(1)	4349(1)	76(1)
O(1)	336(3)	1994(4)	5292(2)	50(1)
C(1)	650(3)	4251(6)	4750(3)	44(1)
C(2)	158(3)	3488(6)	5169(3)	39(1)
C(3)	-496(3)	4250(6)	5421(3)	44(1)
C(4)	-33(4)	1255(6)	5837(3)	46(1)
C(5)	389(4)	1705(6)	6567(3)	43(1)
C(6)	-77(3)	1921(6)	7121(3)	45(1)
C(7)	365(3)	2257(6)	7794(3)	43(1)
C(8)	1271(3)	2364(6)	7918(3)	43(1)
C(9)	1737(3)	2176(6)	7362(3)	45(1)
C(10)	1283(4)	1848(6)	6698(3)	47(1)
C(11)	-1053(4)	1847(7)	7001(3)	48(1)
C(12)	-1536(4)	3149(8)	6973(3)	62(2)
C(13)	-2444(5)	3060(11)	6858(3)	83(3)
C(14)	-2850(5)	1716(13)	6781(4)	87(3)
C(15)	-2374(5)	442(11)	6797(4)	80(2)
C(16)	-1484(4)	497(8)	6912(3)	60(2)
C(17)	-133(3)	2499(7)	8396(3)	47(1)
C(18)	-518(4)	1314(9)	8691(3)	70(2)
C(19)	-925(5)	1521(12)	9274(4)	95(3)
C(20)	-962(5)	2924(14)	9550(4)	100(3)
C(21)	-609(5)	4090(11)	9264(4)	85(2)
C(22)	-185(4)	3908(8)	8690(3)	65(2)
C(23)	1718(3)	2722(6)	8645(3)	46(1)
C(24)	1707(4)	1737(8)	9199(3)	63(2)
C(25)	2113(5)	2106(9)	9865(4)	79(2)
C(26)	2521(5)	3464(10)	9986(4)	79(2)
C(27)	2546(5)	4417(9)	9459(4)	81(2)
C(28)	2139(4)	4066(8)	8783(3)	66(2)
C(29)	2709(4)	2250(6)	7438(3)	49(2)
C(30)	3231(4)	1485(8)	7976(4)	68(2)
C(31)	4137(5)	1478(9)	8013(5)	88(2)
C(32)	4514(5)	2256(10)	7526(5)	90(3)
C(33)	4009(5)	3008(8)	7007(5)	92(3)
C(34)	3111(4)	3000(7)	6960(4)	72(2)

Bond lengths [Å] and angles [°] for bce03s.

I(1)-C(1)	2.091(5)
O(1)-C(2)	1.375(6)
O(1)-C(4)	1.433(6)
C(1)-C(2)	1.378(7)
C(1)-C(3)#1	1.390(7)
C(2)-C(3)	1.375(7)
C(3)-C(1)#1	1.390(7)
C(3)-H(3)	0.9300
C(4)-C(5)	1.509(7)
C(4)-H(4A)	0.9700
C(4)-H(4B)	0.9700
C(5)-C(10)	1.385(8)
C(5)-C(6)	1.394(8)
C(6)-C(7)	1.401(7)
C(6)-C(11)	1.505(8)
C(7)-C(8)	1.400(8)
C(7)-C(17)	1.507(8)
C(8)-C(9)	1.394(8)
C(8)-C(23)	1.496(8)
C(9)-C(10)	1.392(8)
C(9)-C(29)	1.503(8)
C(10)-H(10)	0.9300
C(11)-C(16)	1.378(8)
C(11)-C(12)	1.382(8)
C(12)-C(13)	1.402(10)
C(12)-H(12)	0.9300
C(13)-C(14)	1.354(11)
C(13)-H(13)	0.9300
C(14)-C(15)	1.356(11)
C(14)-H(14)	0.9300
C(15)-C(16)	1.373(9)
C(15)-H(15)	0.9300
C(16)-H(16)	0.9300
C(17)-C(18)	1.382(9)
C(17)-C(22)	1.386(9)
C(18)-C(19)	1.384(10)
C(18)-H(18)	0.9300
C(19)-C(20)	1.365(12)
C(19)-H(19)	0.9300
C(20)-C(21)	1.335(12)
C(20)-H(20)	0.9300
C(21)-C(22)	1.382(9)
C(21)-H(21)	0.9300
C(22)-H(22)	0.9300
C(23)-C(28)	1.374(8)
C(23)-C(24)	1.383(8)
C(24)-C(25)	1.377(9)
C(24)-H(24)	0.9300
C(25)-C(26)	1.373(10)
C(25)-H(25)	0.9300
C(26)-C(27)	1.327(10)
C(26)-H(26)	0.9300
C(27)-C(28)	1.390(8)
C(27)-H(27)	0.9300

C(28)-H(28)	0.9300
C(29)-C(34)	1.367(9)
C(29)-C(30)	1.391(9)
C(30)-C(31)	1.404(10)
C(30)-H(30)	0.9300
C(31)-C(32)	1.371(11)
C(31)-H(31)	0.9300
C(32)-C(33)	1.350(11)
C(32)-H(32)	0.9300
C(33)-C(34)	1.389(10)
C(33)-H(33)	0.9300
C(34)-H(34)	0.9300

C(2)-O(1)-C(4)	118.6(4)
C(2)-C(1)-C(3)#1	121.5(5)
C(2)-C(1)-I(1)	119.4(4)
C(3)#1-C(1)-I(1)	119.1(4)
O(1)-C(2)-C(3)	124.1(5)
O(1)-C(2)-C(1)	117.6(5)
C(3)-C(2)-C(1)	118.2(5)
C(2)-C(3)-C(1)#1	120.3(5)
C(2)-C(3)-H(3)	119.9
C(1)#1-C(3)-H(3)	119.9
O(1)-C(4)-C(5)	113.0(4)
O(1)-C(4)-H(4A)	109.0
C(5)-C(4)-H(4A)	109.0
O(1)-C(4)-H(4B)	109.0
C(5)-C(4)-H(4B)	109.0
H(4A)-C(4)-H(4B)	107.8
C(10)-C(5)-C(6)	118.7(5)
C(10)-C(5)-C(4)	118.3(5)
C(6)-C(5)-C(4)	122.9(5)
C(5)-C(6)-C(7)	119.7(5)
C(5)-C(6)-C(11)	120.9(5)
C(7)-C(6)-C(11)	119.4(5)
C(8)-C(7)-C(6)	120.7(5)
C(8)-C(7)-C(17)	119.1(5)
C(6)-C(7)-C(17)	120.2(5)
C(9)-C(8)-C(7)	119.7(5)
C(9)-C(8)-C(23)	121.2(5)
C(7)-C(8)-C(23)	119.1(5)
C(10)-C(9)-C(8)	118.5(5)
C(10)-C(9)-C(29)	117.4(5)
C(8)-C(9)-C(29)	124.1(5)
C(5)-C(10)-C(9)	122.7(5)
C(5)-C(10)-H(10)	118.6
C(9)-C(10)-H(10)	118.6
C(16)-C(11)-C(12)	118.5(6)
C(16)-C(11)-C(6)	121.4(5)
C(12)-C(11)-C(6)	120.1(5)
C(11)-C(12)-C(13)	119.4(7)
C(11)-C(12)-H(12)	120.3
C(13)-C(12)-H(12)	120.3
C(14)-C(13)-C(12)	120.8(7)
C(14)-C(13)-H(13)	119.6
C(12)-C(13)-H(13)	119.6

C(13)-C(14)-C(15)	119.7(7)
C(13)-C(14)-H(14)	120.2
C(15)-C(14)-H(14)	120.2
C(14)-C(15)-C(16)	120.7(7)
C(14)-C(15)-H(15)	119.7
C(16)-C(15)-H(15)	119.7
C(15)-C(16)-C(11)	120.9(7)
C(15)-C(16)-H(16)	119.5
C(11)-C(16)-H(16)	119.5
C(18)-C(17)-C(22)	118.1(6)
C(18)-C(17)-C(7)	120.9(6)
C(22)-C(17)-C(7)	120.9(6)
C(17)-C(18)-C(19)	120.9(7)
C(17)-C(18)-H(18)	119.5
C(19)-C(18)-H(18)	119.5
C(20)-C(19)-C(18)	119.3(8)
C(20)-C(19)-H(19)	120.3
C(18)-C(19)-H(19)	120.3
C(21)-C(20)-C(19)	120.7(8)
C(21)-C(20)-H(20)	119.6
C(19)-C(20)-H(20)	119.6
C(20)-C(21)-C(22)	121.1(8)
C(20)-C(21)-H(21)	119.5
C(22)-C(21)-H(21)	119.5
C(21)-C(22)-C(17)	119.9(7)
C(21)-C(22)-H(22)	120.1
C(17)-C(22)-H(22)	120.1
C(28)-C(23)-C(24)	118.0(5)
C(28)-C(23)-C(8)	120.4(5)
C(24)-C(23)-C(8)	121.6(5)
C(25)-C(24)-C(23)	120.3(6)
C(25)-C(24)-H(24)	119.8
C(23)-C(24)-H(24)	119.8
C(26)-C(25)-C(24)	120.2(7)
C(26)-C(25)-H(25)	119.9
C(24)-C(25)-H(25)	119.9
C(27)-C(26)-C(25)	120.3(6)
C(27)-C(26)-H(26)	119.8
C(25)-C(26)-H(26)	119.8
C(26)-C(27)-C(28)	120.3(7)
C(26)-C(27)-H(27)	119.8
C(28)-C(27)-H(27)	119.8
C(23)-C(28)-C(27)	120.8(6)
C(23)-C(28)-H(28)	119.6
C(27)-C(28)-H(28)	119.6
C(34)-C(29)-C(30)	117.6(6)
C(34)-C(29)-C(9)	121.2(5)
C(30)-C(29)-C(9)	121.1(5)
C(29)-C(30)-C(31)	120.5(7)
C(29)-C(30)-H(30)	119.7
C(31)-C(30)-H(30)	119.7
C(32)-C(31)-C(30)	120.0(7)
C(32)-C(31)-H(31)	120.0
C(30)-C(31)-H(31)	120.0
C(33)-C(32)-C(31)	119.5(7)
C(33)-C(32)-H(32)	120.3

C(31)-C(32)-H(32)	120.3
C(32)-C(33)-C(34)	120.9(8)
C(32)-C(33)-H(33)	119.5
C(34)-C(33)-H(33)	119.5
C(29)-C(34)-C(33)	121.4(7)
C(29)-C(34)-H(34)	119.3
C(33)-C(34)-H(34)	119.3

Symmetry transformations used to generate equivalent atoms:

#1 -x,-y+1,-z+1

Anisotropic displacement parameters ($\text{\AA}^2 \times 10^3$) for bce03s. The anisotropic displacement factor exponent takes the form: $-2\pi^2 [h^2 a^{*2} U^{11} + \dots + 2 h k a^* b^* U^{12}]$

	U^{11}	U^{22}	U^{33}	U^{23}	U^{13}	U^{12}
I(1)	73(1)	68(1)	97(1)	8(1)	45(1)	22(1)
O(1)	61(2)	47(2)	40(2)	0(2)	7(2)	7(2)
C(1)	36(3)	59(4)	37(3)	-3(3)	10(3)	6(3)
C(2)	45(3)	42(3)	29(3)	-6(2)	-2(3)	3(3)
C(3)	48(3)	46(3)	38(3)	3(3)	9(3)	3(3)
C(4)	52(3)	42(3)	43(3)	2(3)	6(3)	3(3)
C(5)	46(3)	42(3)	39(3)	2(3)	1(3)	4(3)
C(6)	43(3)	48(3)	39(3)	6(3)	-2(3)	4(3)
C(7)	43(3)	48(3)	34(3)	0(2)	-1(3)	0(3)
C(8)	41(3)	41(3)	46(3)	3(3)	-2(3)	0(2)
C(9)	37(3)	46(3)	50(4)	4(3)	6(3)	2(3)
C(10)	48(4)	50(3)	45(3)	-1(3)	8(3)	6(3)
C(11)	45(3)	65(4)	32(3)	-2(3)	1(3)	0(3)
C(12)	54(4)	82(5)	47(4)	-9(3)	1(3)	9(3)
C(13)	57(5)	137(8)	53(4)	-24(5)	1(4)	35(5)
C(14)	46(4)	159(9)	57(5)	-14(5)	8(4)	-21(5)
C(15)	61(5)	112(7)	64(5)	1(4)	1(4)	-24(5)
C(16)	47(4)	77(5)	52(4)	8(3)	-2(3)	-10(3)
C(17)	36(3)	74(4)	28(3)	-1(3)	0(3)	1(3)
C(18)	66(4)	93(5)	54(4)	2(4)	15(4)	-16(4)
C(19)	81(6)	137(8)	75(5)	3(5)	35(5)	-24(5)
C(20)	55(5)	186(11)	62(5)	-30(6)	16(4)	-11(6)
C(21)	62(5)	125(7)	63(5)	-36(5)	-2(4)	17(5)
C(22)	65(4)	81(5)	48(4)	-14(4)	5(3)	11(4)
C(23)	35(3)	57(4)	41(3)	4(3)	-3(3)	-2(3)
C(24)	60(4)	82(5)	41(4)	4(3)	-6(3)	-14(3)
C(25)	78(5)	105(6)	48(4)	18(4)	-8(4)	-15(5)
C(26)	62(4)	134(7)	38(4)	-12(4)	-5(3)	-15(5)
C(27)	92(5)	95(6)	53(5)	-24(4)	8(4)	-37(4)
C(28)	73(4)	71(5)	51(4)	-3(3)	2(3)	-24(4)
C(29)	46(3)	51(4)	49(4)	2(3)	7(3)	1(3)
C(30)	55(4)	74(5)	73(5)	3(4)	4(4)	-1(3)
C(31)	55(5)	105(6)	97(6)	-1(5)	-15(4)	8(4)
C(32)	43(4)	98(6)	129(8)	-14(6)	8(5)	-6(4)
C(33)	53(5)	78(5)	150(8)	16(5)	34(5)	-8(4)
C(34)	60(4)	67(4)	88(5)	13(4)	14(4)	1(3)

Hydrogen coordinates ($\times 10^4$) and isotropic displacement parameters ($\text{\AA}^2 \times 10^{-3}$)
for bce03s.

	x	y	z	U(eq)
H(3)	-836	3761	5706	53
H(4A)	25	180	5785	55
H(4B)	-647	1486	5782	55
H(10)	1593	1720	6326	57
H(12)	-1262	4075	7029	74
H(13)	-2771	3935	6834	100
H(14)	-3453	1668	6717	104
H(15)	-2654	-478	6730	96
H(16)	-1168	-389	6930	72
H(18)	-504	363	8495	84
H(19)	-1172	713	9475	114
H(20)	-1235	3070	9941	120
H(21)	-649	5040	9455	102
H(22)	65	4729	8502	78
H(24)	1423	822	9121	75
H(25)	2110	1433	10234	95
H(26)	2782	3718	10439	95
H(27)	2837	5324	9543	97
H(28)	2151	4750	8420	79
H(30)	2978	974	8313	81
H(31)	4481	947	8368	106
H(32)	5114	2265	7552	108
H(33)	4264	3538	6678	110
H(34)	2777	3517	6594	86

Torsion angles [°] for bce03s.

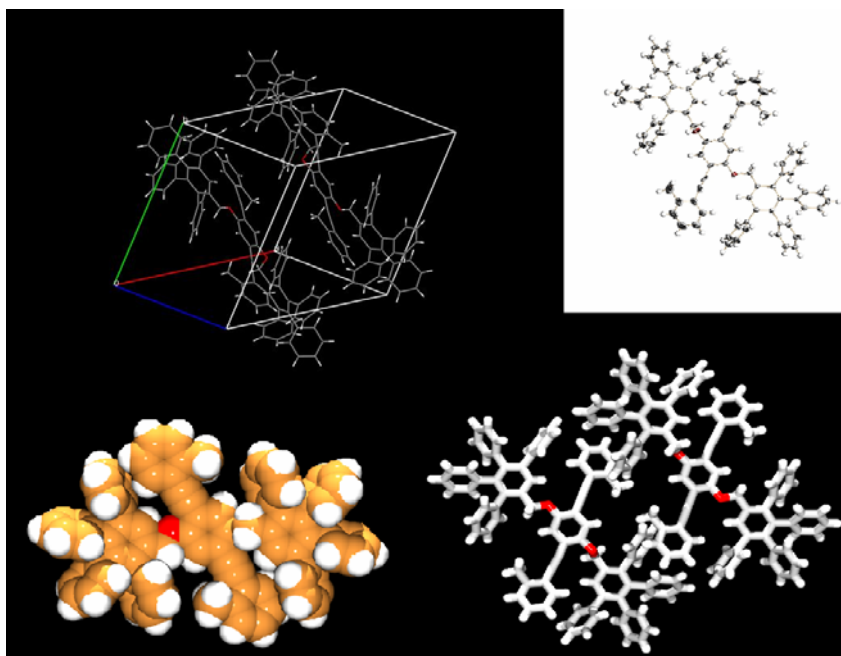
C(4)-O(1)-C(2)-C(3)	-15.0(7)
C(4)-O(1)-C(2)-C(1)	167.1(4)
C(3)#1-C(1)-C(2)-O(1)	177.8(4)
I(1)-C(1)-C(2)-O(1)	-1.3(6)
C(3)#1-C(1)-C(2)-C(3)	-0.2(8)
I(1)-C(1)-C(2)-C(3)	-179.4(4)
O(1)-C(2)-C(3)-C(1)#1	-177.7(5)
C(1)-C(2)-C(3)-C(1)#1	0.2(8)
C(2)-O(1)-C(4)-C(5)	-72.9(6)
O(1)-C(4)-C(5)-C(10)	-41.8(7)
O(1)-C(4)-C(5)-C(6)	140.9(5)
C(10)-C(5)-C(6)-C(7)	-0.8(8)
C(4)-C(5)-C(6)-C(7)	176.4(5)
C(10)-C(5)-C(6)-C(11)	177.2(5)
C(4)-C(5)-C(6)-C(11)	-5.5(8)
C(5)-C(6)-C(7)-C(8)	-0.6(8)
C(11)-C(6)-C(7)-C(8)	-178.7(5)
C(5)-C(6)-C(7)-C(17)	179.7(5)
C(11)-C(6)-C(7)-C(17)	1.6(8)
C(6)-C(7)-C(8)-C(9)	1.8(8)
C(17)-C(7)-C(8)-C(9)	-178.5(5)
C(6)-C(7)-C(8)-C(23)	-179.9(5)
C(17)-C(7)-C(8)-C(23)	-0.2(8)
C(7)-C(8)-C(9)-C(10)	-1.6(8)
C(23)-C(8)-C(9)-C(10)	-179.8(5)
C(7)-C(8)-C(9)-C(29)	-179.2(5)
C(23)-C(8)-C(9)-C(29)	2.5(8)
C(6)-C(5)-C(10)-C(9)	1.0(8)
C(4)-C(5)-C(10)-C(9)	-176.3(5)
C(8)-C(9)-C(10)-C(5)	0.2(8)
C(29)-C(9)-C(10)-C(5)	178.0(5)
C(5)-C(6)-C(11)-C(16)	75.8(7)
C(7)-C(6)-C(11)-C(16)	-106.2(6)
C(5)-C(6)-C(11)-C(12)	-103.7(6)
C(7)-C(6)-C(11)-C(12)	74.4(7)
C(16)-C(11)-C(12)-C(13)	0.3(9)
C(6)-C(11)-C(12)-C(13)	179.7(6)
C(11)-C(12)-C(13)-C(14)	0.6(10)
C(12)-C(13)-C(14)-C(15)	-1.7(11)
C(13)-C(14)-C(15)-C(16)	2.0(12)
C(14)-C(15)-C(16)-C(11)	-1.1(11)
C(12)-C(11)-C(16)-C(15)	0.0(9)
C(6)-C(11)-C(16)-C(15)	-179.4(6)
C(8)-C(7)-C(17)-C(18)	-107.5(6)
C(6)-C(7)-C(17)-C(18)	72.2(7)
C(8)-C(7)-C(17)-C(22)	69.7(7)
C(6)-C(7)-C(17)-C(22)	-110.6(6)
C(22)-C(17)-C(18)-C(19)	-1.6(9)
C(7)-C(17)-C(18)-C(19)	175.7(6)
C(17)-C(18)-C(19)-C(20)	1.5(12)
C(18)-C(19)-C(20)-C(21)	-0.1(13)
C(19)-C(20)-C(21)-C(22)	-1.1(12)
C(20)-C(21)-C(22)-C(17)	0.9(10)
C(18)-C(17)-C(22)-C(21)	0.4(8)

C(7)-C(17)-C(22)-C(21)	-176.8(5)
C(9)-C(8)-C(23)-C(28)	66.0(8)
C(7)-C(8)-C(23)-C(28)	-112.3(7)
C(9)-C(8)-C(23)-C(24)	-115.6(7)
C(7)-C(8)-C(23)-C(24)	66.2(8)
C(28)-C(23)-C(24)-C(25)	-0.5(10)
C(8)-C(23)-C(24)-C(25)	-179.0(6)
C(23)-C(24)-C(25)-C(26)	1.0(11)
C(24)-C(25)-C(26)-C(27)	-1.6(12)
C(25)-C(26)-C(27)-C(28)	1.7(12)
C(24)-C(23)-C(28)-C(27)	0.6(9)
C(8)-C(23)-C(28)-C(27)	179.1(6)
C(26)-C(27)-C(28)-C(23)	-1.2(11)
C(10)-C(9)-C(29)-C(34)	45.6(8)
C(8)-C(9)-C(29)-C(34)	-136.8(6)
C(10)-C(9)-C(29)-C(30)	-130.7(6)
C(8)-C(9)-C(29)-C(30)	46.9(8)
C(34)-C(29)-C(30)-C(31)	-0.8(10)
C(9)-C(29)-C(30)-C(31)	175.6(6)
C(29)-C(30)-C(31)-C(32)	1.4(12)
C(30)-C(31)-C(32)-C(33)	-0.8(13)
C(31)-C(32)-C(33)-C(34)	-0.3(13)
C(30)-C(29)-C(34)-C(33)	-0.3(10)
C(9)-C(29)-C(34)-C(33)	-176.7(6)
C(32)-C(33)-C(34)-C(29)	0.8(12)

Symmetry transformations used to generate equivalent atoms:

#1 -x,-y+1,-z+1

Crystal Structure Analysis for C₈₆H₆₂O₂, **3b**



A suitable crystal of **3b** was coated with Paratone N oil, suspended in a small fiber loop and placed in a cooled nitrogen gas stream at 173 K on a Bruker D8 SMART APEX CCD sealed tube diffractometer with graphite monochromated MoK α (0.71073 Å) radiation. Data were measured using a series of combinations of phi and omega scans with 10 s frame exposures and 0.3° frame widths. Data collection, indexing and initial cell refinements were all carried out using SMART¹ software. Frame integration and final cell refinements were done using SAINT² software. The final cell parameters were determined from least-squares refinement on 7091 reflections. The SADABS³ program was used to carry out absorption corrections.

The structure was solved using Direct methods and difference Fourier techniques (SHELX⁴, V6.12).⁴ Hydrogen atoms were placed their expected chemical positions using the HFIX command and were included in the final cycles of least squares with isotropic U_{ij} 's related to the atom's rriden upon. The C-H distances were fixed at 0.93 Å (aromatic and amide), 0.98 Å (methine), 0.97 Å (methylene), or 0.96 Å (methyl). All non-hydrogen atoms were refined anisotropically. Scattering factors and anomalous dispersion corrections are taken from the *International Tables for X-ray Crystallography*⁵. Structure solution, refinement, graphics and generation of publication

materials were performed by using SHELXTL, V6.12 software. Additional details of data collection and structure refinement are given in Table 1.

References

1. SMART Version 5.628, **2003**, Bruker AXS, Inc., Analytical X-ray Systems, 5465 East Cheryl Parkway, Madison WI 53711-5373.
2. SAINT Version 6.36A, **2002**, Bruker AXS, Inc., Analytical X-ray Systems, 5465 East Cheryl Parkway, Madison WI 53711-5373.
3. SADABS Version 2.10, **2003**, George Sheldrick, University of Göttingen,
4. SHELXTL V6.12, **2002**, Bruker AXS, Inc., Analytical X-ray Systems, 5465 East Cheryl Parkway, Madison WI 53711-5373.
5. A. J. C. Wilson (ed), *International Tables for X-ray Crystallography, Volume C*. Kynoch, Academic Publishers, Dordrecht, **1992**, Tables 6.1.1.4 (pp. 500-502) and 4.2.6.8 (pp. 219-222)
6. PLATON, A. L. Spek, Acta.Cryst., C34 (1990).

Details.

There were two small, interstitial regions in the lattice containing some disordered solvent that could not be identified nor modeled successfully so the program SQUEEZE⁶ was used to cancel out this residual electron density.

Table A4. Crystal data and structure refinement for bce20SQ.

Identification code	BCE20sq	
Empirical formula	C ₈₆ H ₆₂ O ₂	
Formula weight	1127.36	
Temperature	173(2) K	
Wavelength	0.71073 Å	
Crystal system	Triclinic	
Space group	P-1	
Unit cell dimensions	a = 14.2586(19) Å	α = 75.054(3)°.
	b = 15.310(2) Å	β = 78.969(3)°.
	c = 17.941(2) Å	γ = 64.198(2)°.
Volume	3392.6(8) Å ³	
Z	2	
Density (calculated)	1.104 Mg/m ³	
Absorption coefficient	0.064 mm ⁻¹	
F(000)	1188	
Crystal size	0.48 x 0.38 x 0.20 mm ³	
Theta range for data collection	1.59 to 28.51°.	
Index ranges	-19<=h<=19, -20<=k<=20, -23<=l<=23	
Reflections collected	47536	
Independent reflections	17018 [R(int) = 0.0534]	
Completeness to theta = 28.51°	98.8 %	

Absorption correction
Max. and min. transmission
Refinement method
Data / restraints / parameters
Goodness-of-fit on F^2
Final R indices [$I > 2\sigma(I)$]
R indices (all data)
Largest diff. peak and hole

Semi-empirical from equivalents
0.9872 and 0.9697
Full-matrix least-squares on F^2
17018 / 0 / 795
1.029
 $R1 = 0.0809$, $wR2 = 0.2259$
 $R1 = 0.1181$, $wR2 = 0.2496$
1.185 and -0.338 e.Å⁻³

Atomic coordinates ($\times 10^4$) and equivalent isotropic displacement parameters ($\text{\AA}^2 \times 10^3$) for bce20SQ. U(eq) is defined as one third of the trace of the orthogonalized U^{ij} tensor.

	x	y	z	U(eq)
C(1)	5835(2)	1888(2)	2624(1)	38(1)
C(2)	5661(2)	2160(2)	3341(1)	41(1)
C(3)	5032(2)	3112(2)	3422(1)	42(1)
C(4)	4549(2)	3832(2)	2803(1)	37(1)
C(5)	4744(2)	3571(1)	2074(1)	34(1)
C(6)	5379(2)	2613(2)	1990(1)	38(1)
C(7)	6467(2)	869(2)	2519(1)	47(1)
C(8)	6907(2)	154(2)	2371(1)	36(1)
C(9)	7595(2)	-844(2)	2172(2)	55(1)
C(10)	7375(2)	-1034(2)	1510(2)	66(1)
C(11)	7988(3)	-1939(3)	1305(2)	88(1)
C(12)	8799(3)	-2631(2)	1740(3)	95(1)
C(13)	9012(3)	-2436(2)	2367(2)	90(1)
C(14)	8405(2)	-1544(2)	2591(2)	70(1)
C(15)	6482(3)	-281(3)	1057(2)	89(1)
C(16)	3835(2)	4845(2)	2932(1)	40(1)
C(17)	3280(2)	5545(2)	3036(1)	47(1)
C(18)	2485(2)	6516(2)	3216(1)	49(1)
C(19)	2302(2)	6646(2)	3982(2)	63(1)
C(20)	1576(3)	7561(3)	4127(2)	82(1)
C(21)	1053(3)	8309(2)	3557(2)	86(1)
C(22)	1231(3)	8166(2)	2824(2)	82(1)
C(23)	1937(2)	7276(2)	2647(2)	62(1)
C(24)	2885(4)	5818(3)	4604(2)	101(1)
C(25)	5513(2)	1017(2)	4438(1)	44(1)
C(26)	6172(2)	129(1)	4987(1)	36(1)
C(27)	6730(2)	-734(2)	4713(1)	37(1)
C(28)	7348(2)	-1599(1)	5179(1)	34(1)
C(29)	7384(2)	-1606(1)	5952(1)	32(1)
C(30)	6825(2)	-733(1)	6239(1)	32(1)
C(31)	6225(2)	147(1)	5752(1)	34(1)
C(32)	7953(2)	-2491(2)	4826(1)	40(1)
C(33)	7435(2)	-2867(2)	4507(1)	50(1)
C(34)	7986(3)	-3690(2)	4173(2)	67(1)
C(35)	9055(3)	-4125(2)	4147(2)	76(1)
C(36)	9587(2)	-3745(2)	4449(2)	72(1)
C(37)	9037(2)	-2932(2)	4790(2)	56(1)
C(38)	8016(2)	-2547(1)	6463(1)	34(1)
C(39)	7782(2)	-3364(2)	6603(1)	47(1)
C(40)	8384(2)	-4240(2)	7057(2)	64(1)
C(41)	9238(2)	-4314(2)	7363(2)	67(1)
C(42)	9466(2)	-3508(2)	7231(2)	55(1)
C(43)	8862(2)	-2629(2)	6785(1)	41(1)
C(44)	6860(2)	-733(1)	7063(1)	35(1)
C(45)	6451(2)	-1278(2)	7654(1)	44(1)
C(46)	6472(2)	-1270(2)	8415(1)	60(1)
C(47)	6906(2)	-700(2)	8589(2)	66(1)
C(48)	7312(2)	-161(2)	8005(2)	59(1)
C(49)	7291(2)	-173(2)	7247(1)	45(1)
C(50)	5639(2)	1078(2)	6057(1)	39(1)
C(51)	4841(2)	1154(2)	6650(1)	41(1)

C(52)	4313(2)	2015(2)	6937(1)	52(1)
C(53)	4571(2)	2799(2)	6645(2)	63(1)
C(54)	5351(3)	2738(2)	6043(2)	72(1)
C(55)	5880(2)	1880(2)	5745(2)	59(1)
C(56)	4355(2)	4054(2)	768(1)	41(1)
C(57)	3650(2)	4933(1)	241(1)	35(1)
C(58)	3509(2)	4832(1)	-476(1)	31(1)
C(59)	2824(2)	5651(1)	-957(1)	29(1)
C(60)	2296(2)	6566(1)	-728(1)	31(1)
C(61)	2478(2)	6662(1)	-21(1)	33(1)
C(62)	3143(2)	5840(1)	453(1)	37(1)
C(63)	4105(2)	3872(1)	-738(1)	33(1)
C(64)	4849(2)	3805(2)	-1370(1)	40(1)
C(65)	5374(2)	2931(2)	-1639(2)	51(1)
C(66)	5170(2)	2112(2)	-1275(2)	57(1)
C(67)	4451(2)	2165(2)	-643(2)	53(1)
C(68)	3916(2)	3040(2)	-380(1)	44(1)
C(69)	2671(1)	5550(1)	-1724(1)	31(1)
C(70)	2914(2)	6133(2)	-2396(1)	35(1)
C(71)	2760(2)	6056(2)	-3104(1)	46(1)
C(72)	2362(2)	5399(2)	-3153(1)	52(1)
C(73)	2131(2)	4816(2)	-2492(1)	46(1)
C(74)	2276(2)	4889(1)	-1781(1)	36(1)
C(75)	1539(2)	7423(1)	-1229(1)	30(1)
C(76)	1683(2)	8288(1)	-1528(1)	35(1)
C(77)	995(2)	9056(2)	-2013(1)	45(1)
C(78)	146(2)	8978(2)	-2192(1)	47(1)
C(79)	-21(2)	8136(2)	-1884(1)	45(1)
C(80)	682(2)	7360(2)	-1414(1)	38(1)
C(81)	1980(2)	7615(2)	251(1)	40(1)
C(82)	909(2)	8064(2)	431(1)	53(1)
C(83)	475(2)	8944(2)	693(2)	67(1)
C(84)	1100(3)	9389(2)	757(2)	70(1)
C(85)	2161(3)	8951(2)	588(2)	67(1)
C(86)	2605(2)	8057(2)	342(1)	51(1)
O(1)	6156(1)	1466(1)	3959(1)	49(1)
O(2)	4271(1)	4313(1)	1490(1)	39(1)

Bond lengths [Å] and angles [°] for bce20SQ.

C(1)-C(2)	1.396(3)	C(47)-C(48)	1.361(4)
C(1)-C(6)	1.397(3)	C(48)-C(49)	1.370(4)
C(1)-C(7)	1.465(3)	C(50)-C(55)	1.372(3)
C(2)-C(3)	1.369(3)	C(50)-C(51)	1.389(3)
C(2)-O(1)	1.377(2)	C(51)-C(52)	1.380(3)
C(3)-C(4)	1.387(3)	C(52)-C(53)	1.355(4)
C(4)-C(5)	1.408(3)	C(53)-C(54)	1.384(5)
C(4)-C(16)	1.489(3)	C(54)-C(55)	1.388(4)
C(5)-O(2)	1.353(2)	C(56)-O(2)	1.419(2)
C(5)-C(6)	1.377(3)	C(56)-C(57)	1.499(3)
C(7)-C(8)	1.074(3)	C(57)-C(62)	1.374(3)
C(8)-C(9)	1.505(3)	C(57)-C(58)	1.396(3)
C(9)-C(14)	1.374(4)	C(58)-C(59)	1.403(2)
C(9)-C(10)	1.413(4)	C(58)-C(63)	1.490(3)
C(10)-C(11)	1.380(4)	C(59)-C(60)	1.399(3)
C(10)-C(15)	1.499(4)	C(59)-C(69)	1.489(3)
C(11)-C(12)	1.386(5)	C(60)-C(61)	1.400(3)
C(12)-C(13)	1.351(6)	C(60)-C(75)	1.492(2)
C(13)-C(14)	1.378(4)	C(61)-C(62)	1.387(3)
C(16)-C(17)	1.057(3)	C(61)-C(81)	1.483(3)
C(17)-C(18)	1.496(4)	C(63)-C(68)	1.385(3)
C(18)-C(23)	1.381(4)	C(63)-C(64)	1.388(3)
C(18)-C(19)	1.398(4)	C(64)-C(65)	1.381(3)
C(19)-C(20)	1.387(4)	C(65)-C(66)	1.381(4)
C(19)-C(24)	1.499(4)	C(66)-C(67)	1.369(4)
C(20)-C(21)	1.363(5)	C(67)-C(68)	1.377(3)
C(21)-C(22)	1.348(5)	C(69)-C(70)	1.386(3)
C(22)-C(23)	1.370(4)	C(69)-C(74)	1.388(3)
C(25)-O(1)	1.412(3)	C(70)-C(71)	1.373(3)
C(25)-C(26)	1.501(3)	C(71)-C(72)	1.379(3)
C(26)-C(27)	1.375(3)	C(72)-C(73)	1.368(3)
C(26)-C(31)	1.396(3)	C(73)-C(74)	1.371(3)
C(27)-C(28)	1.387(3)	C(75)-C(80)	1.374(3)
C(28)-C(29)	1.395(3)	C(75)-C(76)	1.383(3)
C(28)-C(32)	1.490(3)	C(76)-C(77)	1.377(3)
C(29)-C(30)	1.399(3)	C(77)-C(78)	1.369(3)
C(29)-C(38)	1.494(3)	C(78)-C(79)	1.369(3)
C(30)-C(31)	1.409(3)	C(79)-C(80)	1.377(3)
C(30)-C(44)	1.488(3)	C(81)-C(86)	1.385(3)
C(31)-C(50)	1.490(3)	C(81)-C(82)	1.386(3)
C(32)-C(33)	1.382(3)	C(82)-C(83)	1.382(3)
C(32)-C(37)	1.387(3)	C(83)-C(84)	1.371(4)
C(33)-C(34)	1.383(4)	C(84)-C(85)	1.370(4)
C(34)-C(35)	1.368(5)	C(85)-C(86)	1.384(3)
C(35)-C(36)	1.384(5)		
C(36)-C(37)	1.377(4)	C(2)-C(1)-C(6)	118.72(19)
C(38)-C(43)	1.379(3)	C(2)-C(1)-C(7)	122.22(18)
C(38)-C(39)	1.381(3)	C(6)-C(1)-C(7)	119.05(19)
C(39)-C(40)	1.379(3)	C(3)-C(2)-O(1)	120.3(2)
C(40)-C(41)	1.379(4)	C(3)-C(2)-C(1)	120.46(18)
C(41)-C(42)	1.362(4)	O(1)-C(2)-C(1)	119.21(19)
C(42)-C(43)	1.376(3)	C(2)-C(3)-C(4)	121.4(2)
C(44)-C(45)	1.375(3)	C(3)-C(4)-C(5)	118.46(19)
C(44)-C(49)	1.379(3)	C(3)-C(4)-C(16)	119.21(18)
C(45)-C(46)	1.375(3)	C(5)-C(4)-C(16)	122.32(17)
C(46)-C(47)	1.386(4)	O(2)-C(5)-C(6)	124.35(18)

O(2)-C(5)-C(4)	115.47(17)	C(39)-C(40)-C(41)	120.2(2)
C(6)-C(5)-C(4)	120.18(17)	C(42)-C(41)-C(40)	119.6(2)
C(5)-C(6)-C(1)	120.73(19)	C(41)-C(42)-C(43)	120.4(2)
C(8)-C(7)-C(1)	173.2(2)	C(42)-C(43)-C(38)	120.8(2)
C(7)-C(8)-C(9)	175.8(3)	C(45)-C(44)-C(49)	118.7(2)
C(14)-C(9)-C(10)	120.3(2)	C(45)-C(44)-C(30)	120.79(19)
C(14)-C(9)-C(8)	123.5(3)	C(49)-C(44)-C(30)	120.5(2)
C(10)-C(9)-C(8)	116.2(2)	C(46)-C(45)-C(44)	120.8(2)
C(11)-C(10)-C(9)	118.1(3)	C(45)-C(46)-C(47)	119.6(3)
C(11)-C(10)-C(15)	121.2(3)	C(48)-C(47)-C(46)	119.7(2)
C(9)-C(10)-C(15)	120.7(2)	C(47)-C(48)-C(49)	120.5(3)
C(10)-C(11)-C(12)	120.2(4)	C(48)-C(49)-C(44)	120.7(3)
C(13)-C(12)-C(11)	121.2(3)	C(55)-C(50)-C(51)	119.0(2)
C(12)-C(13)-C(14)	120.0(3)	C(55)-C(50)-C(31)	119.9(2)
C(9)-C(14)-C(13)	120.2(3)	C(51)-C(50)-C(31)	121.15(19)
C(17)-C(16)-C(4)	175.6(3)	C(52)-C(51)-C(50)	120.7(2)
C(16)-C(17)-C(18)	177.7(3)	C(53)-C(52)-C(51)	120.4(2)
C(23)-C(18)-C(19)	119.9(2)	C(52)-C(53)-C(54)	119.4(2)
C(23)-C(18)-C(17)	121.7(2)	C(53)-C(54)-C(55)	120.8(3)
C(19)-C(18)-C(17)	118.4(2)	C(50)-C(55)-C(54)	119.7(3)
C(20)-C(19)-C(18)	117.1(3)	O(2)-C(56)-C(57)	108.88(16)
C(20)-C(19)-C(24)	122.9(3)	C(62)-C(57)-C(58)	119.48(16)
C(18)-C(19)-C(24)	120.1(3)	C(62)-C(57)-C(56)	120.84(17)
C(21)-C(20)-C(19)	122.3(3)	C(58)-C(57)-C(56)	119.68(17)
C(22)-C(21)-C(20)	119.7(3)	C(57)-C(58)-C(59)	119.39(17)
C(21)-C(22)-C(23)	120.4(3)	C(57)-C(58)-C(63)	120.26(16)
C(22)-C(23)-C(18)	120.6(3)	C(59)-C(58)-C(63)	120.33(16)
O(1)-C(25)-C(26)	108.92(17)	C(60)-C(59)-C(58)	120.58(16)
C(27)-C(26)-C(31)	119.78(17)	C(60)-C(59)-C(69)	119.67(15)
C(27)-C(26)-C(25)	117.27(18)	C(58)-C(59)-C(69)	119.73(16)
C(31)-C(26)-C(25)	122.94(19)	C(59)-C(60)-C(61)	119.21(16)
C(26)-C(27)-C(28)	121.71(18)	C(59)-C(60)-C(75)	120.30(16)
C(27)-C(28)-C(29)	119.43(18)	C(61)-C(60)-C(75)	120.48(16)
C(27)-C(28)-C(32)	118.07(17)	C(62)-C(61)-C(60)	119.30(17)
C(29)-C(28)-C(32)	122.50(17)	C(62)-C(61)-C(81)	118.18(16)
C(28)-C(29)-C(30)	119.54(16)	C(60)-C(61)-C(81)	122.52(16)
C(28)-C(29)-C(38)	119.49(17)	C(57)-C(62)-C(61)	121.97(17)
C(30)-C(29)-C(38)	120.97(17)	C(68)-C(63)-C(64)	118.46(19)
C(29)-C(30)-C(31)	120.25(17)	C(68)-C(63)-C(58)	121.60(19)
C(29)-C(30)-C(44)	119.90(16)	C(64)-C(63)-C(58)	119.91(18)
C(31)-C(30)-C(44)	119.85(17)	C(65)-C(64)-C(63)	120.4(2)
C(26)-C(31)-C(30)	119.22(18)	C(64)-C(65)-C(66)	120.1(2)
C(26)-C(31)-C(50)	120.69(17)	C(67)-C(66)-C(65)	119.9(2)
C(30)-C(31)-C(50)	120.08(17)	C(66)-C(67)-C(68)	120.1(2)
C(33)-C(32)-C(37)	119.2(2)	C(67)-C(68)-C(63)	121.0(2)
C(33)-C(32)-C(28)	119.8(2)	C(70)-C(69)-C(74)	118.95(18)
C(37)-C(32)-C(28)	120.9(2)	C(70)-C(69)-C(59)	119.95(17)
C(32)-C(33)-C(34)	120.5(3)	C(74)-C(69)-C(59)	121.09(18)
C(35)-C(34)-C(33)	119.8(3)	C(71)-C(70)-C(69)	120.3(2)
C(34)-C(35)-C(36)	120.4(3)	C(70)-C(71)-C(72)	120.2(2)
C(37)-C(36)-C(35)	119.8(3)	C(73)-C(72)-C(71)	119.7(2)
C(36)-C(37)-C(32)	120.2(3)	C(72)-C(73)-C(74)	120.7(2)
C(43)-C(38)-C(39)	118.60(18)	C(73)-C(74)-C(69)	120.1(2)
C(43)-C(38)-C(29)	120.91(18)	C(80)-C(75)-C(76)	118.36(17)
C(39)-C(38)-C(29)	120.47(18)	C(80)-C(75)-C(60)	120.05(18)
C(40)-C(39)-C(38)	120.4(2)	C(76)-C(75)-C(60)	121.58(17)

C(77)-C(76)-C(75)	120.55(19)
C(78)-C(77)-C(76)	120.3(2)
C(77)-C(78)-C(79)	119.79(19)
C(78)-C(79)-C(80)	119.9(2)
C(75)-C(80)-C(79)	121.1(2)
C(86)-C(81)-C(82)	119.1(2)
C(86)-C(81)-C(61)	119.1(2)
C(82)-C(81)-C(61)	121.9(2)
C(83)-C(82)-C(81)	120.2(3)
C(84)-C(83)-C(82)	120.1(3)
C(85)-C(84)-C(83)	120.5(2)
C(84)-C(85)-C(86)	119.8(3)
C(85)-C(86)-C(81)	120.4(3)
C(2)-O(1)-C(25)	112.39(16)
C(5)-O(2)-C(56)	116.92(15)

Symmetry transformations used to generate equivalent atoms:

Anisotropic displacement parameters ($\text{\AA}^2 \times 10^3$) for bce20SQ. The anisotropic displacement factor exponent takes the form: $-2\pi^2 [h^2 a^{*2} U^{11} + \dots + 2 h k a^* b^* U^{12}]$

	U ¹¹	U ²²	U ³³	U ²³	U ¹³	U ¹²
C(1)	31(1)	30(1)	42(1)	4(1)	-7(1)	-8(1)
C(2)	35(1)	39(1)	34(1)	9(1)	-7(1)	-7(1)
C(3)	42(1)	41(1)	31(1)	0(1)	-5(1)	-8(1)
C(4)	34(1)	34(1)	31(1)	2(1)	-5(1)	-7(1)
C(5)	37(1)	29(1)	32(1)	2(1)	-10(1)	-11(1)
C(6)	40(1)	32(1)	36(1)	-2(1)	-11(1)	-10(1)
C(7)	40(1)	57(2)	39(1)	14(1)	-12(1)	-24(1)
C(8)	47(1)	27(1)	36(1)	-1(1)	2(1)	-23(1)
C(9)	56(2)	34(1)	64(2)	-4(1)	0(1)	-14(1)
C(10)	70(2)	44(1)	81(2)	-17(1)	5(2)	-22(1)
C(11)	95(3)	61(2)	106(3)	-35(2)	18(2)	-31(2)
C(12)	105(3)	41(2)	106(3)	-18(2)	30(2)	-14(2)
C(13)	79(2)	45(2)	100(3)	3(2)	11(2)	1(2)
C(14)	68(2)	43(1)	72(2)	3(1)	-4(2)	-8(1)
C(15)	98(3)	82(2)	89(2)	-29(2)	-27(2)	-25(2)
C(16)	29(1)	43(1)	26(1)	17(1)	-7(1)	-6(1)
C(17)	68(2)	56(2)	25(1)	-6(1)	0(1)	-36(1)
C(18)	49(1)	45(1)	49(1)	-16(1)	2(1)	-15(1)
C(19)	80(2)	63(2)	47(2)	-16(1)	7(1)	-32(2)
C(20)	104(3)	83(2)	66(2)	-44(2)	28(2)	-42(2)
C(21)	89(2)	56(2)	95(3)	-33(2)	11(2)	-10(2)
C(22)	79(2)	49(2)	89(2)	-19(2)	-7(2)	2(2)
C(23)	64(2)	48(1)	57(2)	-17(1)	-8(1)	-2(1)
C(24)	158(4)	97(3)	44(2)	-9(2)	-6(2)	-54(3)
C(25)	37(1)	38(1)	40(1)	5(1)	-6(1)	-7(1)
C(26)	32(1)	29(1)	35(1)	4(1)	-5(1)	-7(1)
C(27)	35(1)	38(1)	29(1)	-1(1)	-7(1)	-8(1)
C(28)	31(1)	31(1)	34(1)	-3(1)	-7(1)	-9(1)
C(29)	30(1)	28(1)	35(1)	0(1)	-10(1)	-10(1)
C(30)	31(1)	29(1)	33(1)	-1(1)	-9(1)	-11(1)
C(31)	29(1)	28(1)	36(1)	0(1)	-3(1)	-7(1)
C(32)	44(1)	31(1)	35(1)	-4(1)	-11(1)	-3(1)
C(33)	63(2)	40(1)	45(1)	-8(1)	-16(1)	-14(1)
C(34)	89(2)	47(2)	63(2)	-19(1)	-20(2)	-15(2)
C(35)	97(2)	46(2)	63(2)	-24(1)	-20(2)	5(2)
C(36)	56(2)	59(2)	71(2)	-24(2)	-14(1)	14(1)
C(37)	47(1)	51(1)	57(2)	-19(1)	-13(1)	-1(1)
C(38)	36(1)	25(1)	37(1)	-4(1)	-12(1)	-6(1)
C(39)	54(1)	35(1)	55(1)	2(1)	-21(1)	-18(1)
C(40)	87(2)	32(1)	75(2)	8(1)	-35(2)	-24(1)
C(41)	80(2)	28(1)	78(2)	4(1)	-44(2)	-1(1)
C(42)	55(2)	36(1)	66(2)	-9(1)	-36(1)	0(1)
C(43)	41(1)	30(1)	48(1)	-5(1)	-17(1)	-7(1)
C(44)	28(1)	28(1)	38(1)	-6(1)	-10(1)	-1(1)
C(45)	51(1)	34(1)	38(1)	-1(1)	-11(1)	-9(1)
C(46)	68(2)	50(1)	36(1)	1(1)	-7(1)	-3(1)
C(47)	70(2)	60(2)	50(2)	-24(1)	-25(1)	7(1)
C(48)	50(1)	54(2)	70(2)	-31(1)	-23(1)	-1(1)
C(49)	36(1)	36(1)	57(1)	-17(1)	-12(1)	-4(1)
C(50)	34(1)	27(1)	43(1)	-1(1)	-10(1)	-2(1)

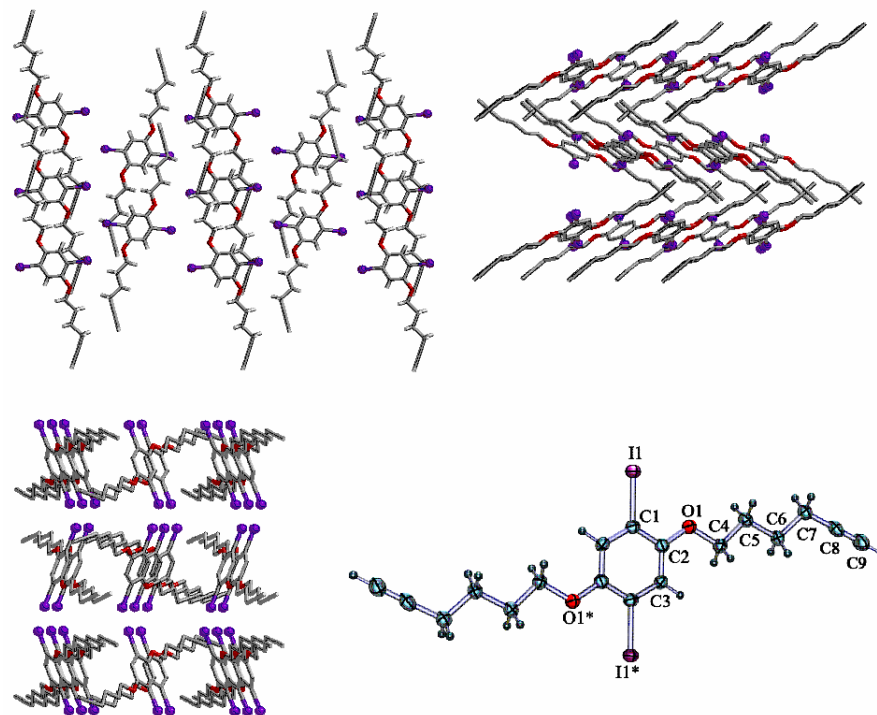
C(51)	38(1)	40(1)	37(1)	-5(1)	-9(1)	-7(1)
C(52)	48(1)	51(1)	44(1)	-13(1)	-8(1)	-4(1)
C(53)	61(2)	43(1)	73(2)	-24(1)	-17(1)	1(1)
C(54)	77(2)	35(1)	97(2)	-13(1)	-3(2)	-19(1)
C(55)	58(2)	34(1)	73(2)	-9(1)	7(1)	-14(1)
C(56)	51(1)	28(1)	35(1)	-4(1)	-18(1)	-4(1)
C(57)	39(1)	26(1)	33(1)	-1(1)	-14(1)	-5(1)
C(58)	36(1)	25(1)	29(1)	-3(1)	-7(1)	-8(1)
C(59)	32(1)	25(1)	28(1)	-3(1)	-7(1)	-8(1)
C(60)	31(1)	28(1)	28(1)	-4(1)	-6(1)	-7(1)
C(61)	35(1)	26(1)	33(1)	-6(1)	-9(1)	-4(1)
C(62)	45(1)	30(1)	31(1)	-7(1)	-15(1)	-4(1)
C(63)	36(1)	24(1)	34(1)	-4(1)	-14(1)	-3(1)
C(64)	39(1)	35(1)	41(1)	-10(1)	-10(1)	-7(1)
C(65)	42(1)	48(1)	53(1)	-22(1)	-7(1)	-4(1)
C(66)	62(2)	35(1)	67(2)	-24(1)	-22(1)	1(1)
C(67)	69(2)	26(1)	61(2)	-7(1)	-20(1)	-11(1)
C(68)	54(1)	32(1)	42(1)	-4(1)	-9(1)	-14(1)
C(69)	29(1)	25(1)	30(1)	-6(1)	-8(1)	-2(1)
C(70)	38(1)	31(1)	33(1)	-7(1)	-5(1)	-10(1)
C(71)	56(1)	45(1)	32(1)	-5(1)	-5(1)	-16(1)
C(72)	74(2)	49(1)	35(1)	-15(1)	-16(1)	-18(1)
C(73)	54(1)	37(1)	51(1)	-13(1)	-16(1)	-15(1)
C(74)	37(1)	28(1)	38(1)	-4(1)	-10(1)	-9(1)
C(75)	32(1)	27(1)	25(1)	-7(1)	-5(1)	-3(1)
C(76)	35(1)	27(1)	36(1)	-6(1)	-8(1)	-5(1)
C(77)	49(1)	26(1)	49(1)	-1(1)	-10(1)	-6(1)
C(78)	47(1)	30(1)	48(1)	-5(1)	-21(1)	4(1)
C(79)	41(1)	36(1)	52(1)	-14(1)	-21(1)	-1(1)
C(80)	39(1)	30(1)	41(1)	-7(1)	-11(1)	-7(1)
C(81)	47(1)	31(1)	31(1)	-9(1)	-14(1)	-1(1)
C(82)	49(1)	45(1)	51(1)	-20(1)	-9(1)	-1(1)
C(83)	61(2)	56(2)	60(2)	-29(1)	-9(1)	9(1)
C(84)	85(2)	45(1)	66(2)	-33(1)	-19(2)	3(1)
C(85)	85(2)	50(2)	69(2)	-31(1)	-17(2)	-17(2)
C(86)	58(2)	41(1)	52(1)	-22(1)	-13(1)	-8(1)
O(1)	41(1)	45(1)	42(1)	11(1)	-10(1)	-8(1)
O(2)	51(1)	26(1)	32(1)	-1(1)	-17(1)	-6(1)

Hydrogen coordinates ($\times 10^4$) and isotropic displacement parameters ($\text{\AA}^2 \times 10^{-3}$)
for bce20SQ.

	x	y	z	U(eq)
H(3)	4924	3284	3914	51
H(6)	5508	2444	1496	45
H(11)	7854	-2088	864	105
H(12)	9213	-3253	1596	113
H(13)	9579	-2915	2652	108
H(14)	8548	-1412	3037	83
H(15A)	5821	-182	1381	133
H(15B)	6479	-515	598	133
H(15C)	6562	347	894	133
H(20)	1439	7670	4643	99
H(21)	566	8929	3676	103
H(22)	863	8685	2427	98
H(23)	2052	7181	2129	75
H(24A)	2870	6087	5048	151
H(24B)	3612	5479	4402	151
H(24C)	2555	5348	4767	151
H(25A)	5182	812	4117	53
H(25B)	4953	1493	4732	53
H(27)	6690	-738	4192	45
H(33)	6694	-2558	4517	60
H(34)	7625	-3953	3963	81
H(35)	9433	-4693	3919	92
H(36)	10329	-4043	4421	87
H(37)	9401	-2673	5001	67
H(39)	7202	-3321	6386	57
H(40)	8210	-4795	7159	77
H(41)	9663	-4923	7665	80
H(42)	10047	-3553	7448	66
H(43)	9028	-2072	6699	49
H(45)	6149	-1664	7535	53
H(46)	6192	-1652	8819	72
H(47)	6919	-686	9113	80
H(48)	7613	227	8123	71
H(49)	7575	208	6845	54
H(51)	4656	608	6861	50
H(52)	3765	2058	7340	63
H(53)	4220	3384	6853	76
H(54)	5527	3290	5832	86
H(55)	6407	1849	5326	71
H(56A)	4151	3493	846	49
H(56B)	5087	3847	534	49
H(62)	3252	5906	938	45
H(64)	4998	4364	-1619	48
H(65)	5876	2894	-2076	61
H(66)	5529	1512	-1462	68
H(67)	4322	1598	-385	63
H(68)	3409	3073	53	53
H(70)	3187	6587	-2366	42
H(71)	2929	6456	-3563	55
H(72)	2247	5353	-3643	63

H(73)	1868	4356	-2527	55
H(74)	2105	4486	-1325	43
H(76)	2262	8353	-1398	42
H(77)	1109	9642	-2223	54
H(78)	-325	9507	-2529	57
H(79)	-619	8087	-1995	54
H(80)	571	6770	-1213	46
H(82)	472	7766	374	63
H(83)	-257	9241	829	80
H(84)	795	10006	920	83
H(85)	2591	9259	639	80
H(86)	3342	7745	236	61

X-Ray Structure Determination, C₁₈H₂₀I₂O₂, 4



X-ray intensity data from a colorless plate were measured at 150(1) K on a Bruker SMART APEX CCD-based diffractometer (Mo K α radiation, $\lambda = 0.71073$ Å).¹ Raw data frame integration and Lp corrections were performed with SAINT+.¹ Final unit cell parameters were determined by least-squares refinement of 9426 reflections from the data set with $I > 5(\sigma)I$. Analysis of the data showed negligible crystal decay during collection. The data were corrected for absorption with SADABS.¹ Patterson methods structure solution, difference Fourier calculations and full-matrix least-squares refinement against F^2 were performed with SHELXTL.²

C₁₈H₂₀I₂O₂ crystallizes in the orthorhombic space group Pbca as determined uniquely by the pattern of systematic absences in the intensity data. The molecule is situated on an inversion center. Non-hydrogen atoms were refined with anisotropic displacement parameters; hydrogen atoms were placed in idealized positions and included as riding atoms with refined isotropic displacement parameters.

(1) SMART Version 5.628, SAINT+ Version 6.22 and SADABS Version 2.05. Bruker Analytical X-ray Systems, Inc., Madison, Wisconsin, USA, 2001.

(2) Sheldrick, G. M. SHELXTL Version 6.1; Bruker Analytical X-ray Systems, Inc., Madison, Wisconsin, USA, 2000.

Table A5. Crystal data and structure refinement for bce6s.

Identification code	bce6s	
Empirical formula	C18 H20 I2 O2	
Formula weight	522.14	
Temperature	150(2) K	
Wavelength	0.71073 Å	
Crystal system	Orthorhombic	
Space group	Pbca	
Unit cell dimensions	a = 8.0944(4) Å	$\alpha = 90^\circ$.
	b = 13.7017(6) Å	$\beta = 90^\circ$.
	c = 16.9431(8) Å	$\gamma = 90^\circ$.
Volume	1879.11(15) Å ³	
Z	4	
Density (calculated)	1.846 Mg/m ³	
Absorption coefficient	3.351 mm ⁻¹	
F(000)	1000	
Crystal size	0.36 x 0.26 x 0.12 mm ³	
Theta range for data collection	2.40 to 27.13°.	
Index ranges	-8 ≤ h ≤ 10, -17 ≤ k ≤ 16, -21 ≤ l ≤ 21	
Reflections collected	11439	
Independent reflections	2073 [R(int) = 0.0279]	
Completeness to theta = 27.13°	99.7 %	
Absorption correction	Semi-empirical from equivalents	
Max. and min. transmission	1.0000 and 0.6576	
Refinement method	Full-matrix least-squares on F ²	
Data / restraints / parameters	2073 / 0 / 111	
Goodness-of-fit on F ²	1.115	
Final R indices [I > 2sigma(I)]	R1 = 0.0201, wR2 = 0.0524	
R indices (all data)	R1 = 0.0209, wR2 = 0.0530	
Extinction coefficient	0.0025(2)	
Largest diff. peak and hole	0.566 and -0.745 e.Å ⁻³	

Atomic coordinates ($\times 10^4$) and equivalent isotropic displacement parameters ($\text{\AA}^2 \times 10^3$) for bce6s. $U(\text{eq})$ is defined as one third of the trace of the orthogonalized U^{ij} tensor.

	x	y	z	U(eq)
I(1)	9763(1)	5909(1)	3088(1)	23(1)
O(1)	7253(2)	4652(1)	4068(1)	27(1)
C(1)	9882(2)	5362(2)	4240(1)	20(1)
C(2)	8593(2)	4797(1)	4541(1)	21(1)
C(3)	8728(2)	4436(1)	5307(1)	21(1)
C(4)	6013(3)	3984(2)	4345(1)	24(1)
C(5)	4676(3)	3935(2)	3725(1)	26(1)
C(6)	3253(2)	3285(2)	3995(1)	23(1)
C(7)	1988(3)	3138(2)	3333(1)	27(1)
C(8)	651(3)	2477(2)	3562(1)	28(1)
C(9)	-402(3)	1918(2)	3748(2)	38(1)

Bond lengths [Å] and angles [°] for bce6s.

I(1)-C(1)	2.094(2)
O(1)-C(2)	1.363(2)
O(1)-C(4)	1.437(2)
C(1)-C(3)#1	1.390(3)
C(1)-C(2)	1.395(3)
C(2)-C(3)	1.394(3)
C(3)-C(1)#1	1.390(3)
C(3)-H(3)	0.9500
C(4)-C(5)	1.510(3)
C(4)-H(4A)	0.9900
C(4)-H(4B)	0.9900
C(5)-C(6)	1.526(3)
C(5)-H(5A)	0.9900
C(5)-H(5B)	0.9900
C(6)-C(7)	1.532(3)
C(6)-H(6A)	0.9900
C(6)-H(6B)	0.9900
C(7)-C(8)	1.464(3)
C(7)-H(7A)	0.9900
C(7)-H(7B)	0.9900
C(8)-C(9)	1.188(4)
C(9)-H(9)	0.9500
C(2)-O(1)-C(4)	117.19(15)
C(3)#1-C(1)-C(2)	120.98(19)
C(3)#1-C(1)-I(1)	118.70(14)
C(2)-C(1)-I(1)	120.32(15)
O(1)-C(2)-C(3)	123.91(18)
O(1)-C(2)-C(1)	117.50(17)
C(3)-C(2)-C(1)	118.56(18)
C(1)#1-C(3)-C(2)	120.46(18)
C(1)#1-C(3)-H(3)	119.8
C(2)-C(3)-H(3)	119.8
O(1)-C(4)-C(5)	107.53(16)
O(1)-C(4)-H(4A)	110.2
C(5)-C(4)-H(4A)	110.2
O(1)-C(4)-H(4B)	110.2
C(5)-C(4)-H(4B)	110.2
H(4A)-C(4)-H(4B)	108.5
C(4)-C(5)-C(6)	110.96(18)
C(4)-C(5)-H(5A)	109.4
C(6)-C(5)-H(5A)	109.4
C(4)-C(5)-H(5B)	109.4
C(6)-C(5)-H(5B)	109.4
H(5A)-C(5)-H(5B)	108.0
C(5)-C(6)-C(7)	111.22(17)
C(5)-C(6)-H(6A)	109.4
C(7)-C(6)-H(6A)	109.4
C(5)-C(6)-H(6B)	109.4
C(7)-C(6)-H(6B)	109.4
H(6A)-C(6)-H(6B)	108.0
C(8)-C(7)-C(6)	112.48(18)
C(8)-C(7)-H(7A)	109.1
C(6)-C(7)-H(7A)	109.1

C(8)-C(7)-H(7B)	109.1
C(6)-C(7)-H(7B)	109.1
H(7A)-C(7)-H(7B)	107.8
C(9)-C(8)-C(7)	178.1(3)
C(8)-C(9)-H(9)	180.0

Symmetry transformations used to generate equivalent atoms:

#1 -x+2,-y+1,-z+1

Anisotropic displacement parameters ($\text{\AA}^2 \times 10^3$) for bce6s. The anisotropic displacement factor exponent takes the form: $-2\pi^2 [h^2 a^{*2} U^{11} + \dots + 2 h k a^* b^* U^{12}]$

	U^{11}	U^{22}	U^{33}	U^{23}	U^{13}	U^{12}
I(1)	25(1)	26(1)	18(1)	3(1)	-1(1)	-1(1)
O(1)	23(1)	32(1)	25(1)	8(1)	-6(1)	-8(1)
C(1)	23(1)	19(1)	19(1)	2(1)	1(1)	1(1)
C(2)	22(1)	20(1)	22(1)	0(1)	-2(1)	0(1)
C(3)	21(1)	20(1)	21(1)	2(1)	1(1)	-2(1)
C(4)	23(1)	26(1)	25(1)	4(1)	-2(1)	-5(1)
C(5)	25(1)	29(1)	23(1)	2(1)	-4(1)	-5(1)
C(6)	24(1)	23(1)	23(1)	-1(1)	-2(1)	-3(1)
C(7)	26(1)	28(1)	27(1)	1(1)	-5(1)	-3(1)
C(8)	24(1)	36(1)	25(1)	-6(1)	-6(1)	0(1)
C(9)	32(1)	52(2)	29(1)	-1(1)	-4(1)	-12(1)

Hydrogen coordinates ($\times 10^4$) and isotropic displacement parameters ($\text{\AA}^2 \times 10^{-3}$)
for bce6s.

	x	y	z	U(eq)
H(3)	7864	4049	5522	23(6)
H(4A)	5547	4216	4852	30(7)
H(4B)	6500	3330	4429	20(6)
H(5A)	5145	3674	3228	31(7)
H(5B)	4255	4601	3618	29(6)
H(6A)	2703	3588	4456	27(6)
H(6B)	3694	2643	4161	26(6)
H(7A)	1512	3778	3187	30(7)
H(7B)	2555	2871	2863	28(6)
H(9)	-1244	1472	3897	56(9)

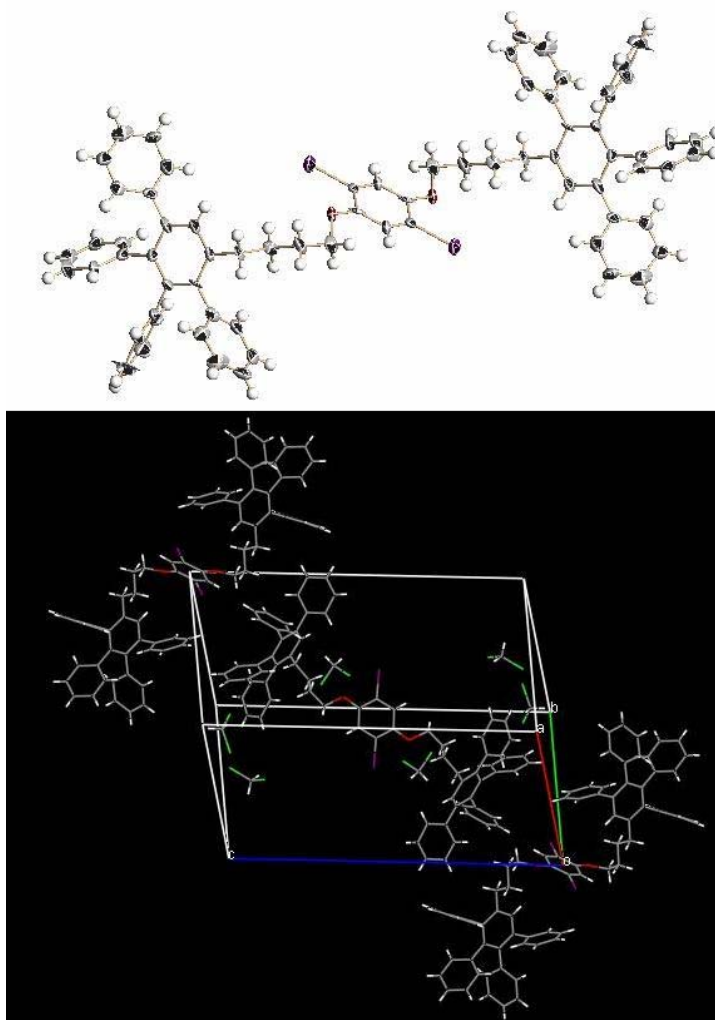
Torsion angles [°] for bce6s.

C(4)-O(1)-C(2)-C(3)	-8.3(3)
C(4)-O(1)-C(2)-C(1)	173.35(18)
C(3)#1-C(1)-C(2)-O(1)	178.37(18)
I(1)-C(1)-C(2)-O(1)	-2.3(2)
C(3)#1-C(1)-C(2)-C(3)	-0.1(3)
I(1)-C(1)-C(2)-C(3)	179.20(14)
O(1)-C(2)-C(3)-C(1)#1	-178.26(18)
C(1)-C(2)-C(3)-C(1)#1	0.1(3)
C(2)-O(1)-C(4)-C(5)	-179.38(17)
O(1)-C(4)-C(5)-C(6)	-176.62(17)
C(4)-C(5)-C(6)-C(7)	-173.50(18)
C(5)-C(6)-C(7)-C(8)	177.06(19)
C(6)-C(7)-C(8)-C(9)	-68(7)

Symmetry transformations used to generate equivalent atoms:

#1 -x+2,-y+1,-z+1

Crystal Structure Analysis for $C_{74}H_{60}I_2O_2$, **5**.



A suitable crystal of **5** was coated with Paratone N oil, suspended in a small fiber loop and placed in a cooled nitrogen gas stream at 173 K on a Bruker D8 SMART APEX CCD sealed tube diffractometer with graphite monochromated MoK_{α} (0.71073 Å) radiation. Data were measured using a series of combinations of phi and omega scans with 10 s frame exposures and 0.3° frame widths. Data collection, indexing and initial cell refinements were all carried out using SMART¹ software. Frame integration and final cell refinements were done using SAINT² software. The final cell parameters were determined from least-squares refinement on 7297 reflections. The SADABS³ program was used to carry out absorption corrections.

The structure was solved using Direct methods and difference Fourier techniques (SHELXTL, V6.12).⁴ Hydrogen atoms were placed their expected chemical positions using the HFIX command and were included in the final cycles of least squares with isotropic U_{ij} 's related to the atom's ridden upon. The C-H distances were fixed at 0.93 Å (aromatic and amide), 0.98 Å (methine), 0.97 Å (methylene), or

0.96 Å (methyl). All non-hydrogen atoms were refined anisotropically. Scattering factors and anomalous dispersion corrections are taken from the *International Tables for X-ray Crystallography*⁵. Structure solution, refinement, graphics and generation of publication materials were performed by using SHELXTL, V6.12 software. Additional details of data collection and structure refinement are given in Table 1.

References

6. SMART Version 5.628, **2003**, Bruker AXS, Inc., Analytical X-ray Systems, 5465 East Cheryl Parkway, Madison WI 53711-5373.
7. SAINT Version 6.36A, **2002**, Bruker AXS, Inc., Analytical X-ray Systems, 5465 East Cheryl Parkway, Madison WI 53711-5373.
8. SADABS Version 2.10, **2003**, George Sheldrick, University of Göttingen,
9. SHELXTL V6.12, **2002**, Bruker AXS, Inc., Analytical X-ray Systems, 5465 East Cheryl Parkway, Madison WI 53711-5373.
10. A. J. C. Wilson (ed), *International Tables for X-ray Crystallography, Volume C*. Kynoch, Academic Publishers, Dordrecht, **1992**, Tables 6.1.1.4 (pp. 500-502) and 4.2.6.8 (pp. 219-222).

Details

The only available crystals were extremely thin plates that showed some degree of twinning. the final difference Fourier maps contained residual electron density in the vicinity of the iodine atoms as a consequence of this twinning – disorder behavior.

Table A6. Crystal data and structure refinement for BCE21Rs.

Identification code	bce21rs	
Empirical formula	C75.69 H63.38 Cl3.38 I2 O2	
Formula weight	1378.55	
Temperature	173(2) K	
Wavelength	0.71073 Å	
Crystal system	Triclinic	
Space group	P-1	
Unit cell dimensions	a = 12.5600(16) Å	$\alpha = 84.628(3)^\circ$.
	b = 12.9515(17) Å	$\beta = 81.298(2)^\circ$.
	c = 23.031(3) Å	$\gamma = 76.837(2)^\circ$.
Volume	3599.2(8) Å ³	
Z	2	
Density (calculated)	1.272 Mg/m ³	
Absorption coefficient	1.041 mm ⁻¹	
F(000)	1394	
Crystal size	0.35 x 0.17 x 0.085 mm ³	
Theta range for data collection	1.62 to 23.53°.	
Index ranges	-14 ≤ h ≤ 14, -14 ≤ k ≤ 14, -25 ≤ l ≤ 25	
Reflections collected	33301	
Independent reflections	10700 [R(int) = 0.0693]	
Completeness to theta = 23.53°	100.0 %	
Absorption correction	Semi-empirical from equivalents	
Max. and min. transmission	1.00 and 0.583974	
Refinement method	Full-matrix least-squares on F ²	
Data / restraints / parameters	10700 / 2 / 772	
Goodness-of-fit on F ²	1.174	
Final R indices [I > 2σ(I)]	R1 = 0.1695, wR2 = 0.3945	
R indices (all data)	R1 = 0.1866, wR2 = 0.4056	
Largest diff. peak and hole	4.512 and -1.591 e.Å ⁻³	

Atomic coordinates ($\times 10^4$) and equivalent isotropic displacement parameters ($\text{\AA}^2 \times 10^3$) for BCE21Rs. $U(\text{eq})$ is defined as one third of the trace of the orthogonalized U^{ij} tensor.

	x	y	z	$U(\text{eq})$
I(1)	2747(1)	9126(1)	10201(1)	52(1)
I(2)	6141(2)	7227(2)	4744(1)	86(1)
O(1)	1486(8)	8761(9)	9203(5)	42(3)
O(2)	5560(11)	5888(12)	5908(5)	65(4)
C(1)	1073(11)	9642(12)	10094(7)	34(4)
C(2)	733(14)	9377(13)	9577(6)	38(4)
C(3)	-372(12)	9742(14)	9509(7)	42(4)
C(4)	1215(14)	8784(16)	8601(8)	53(5)
C(5)	2197(14)	8183(16)	8237(8)	48(4)
C(6)	3207(13)	8701(13)	8167(7)	39(4)
C(7)	4130(13)	8122(14)	7749(8)	45(4)
C(8)	5172(12)	8551(13)	7679(6)	34(4)
C(9)	5402(14)	9270(14)	7202(6)	43(4)
C(10)	6380(13)	9667(13)	7153(6)	36(4)
C(11)	7131(12)	9277(13)	7558(7)	39(4)
C(12)	6899(13)	8529(13)	8022(7)	40(4)
C(13)	5912(13)	8204(13)	8064(7)	40(4)
C(14)	4584(14)	9707(14)	6795(7)	40(4)
C(15)	3748(14)	10552(15)	6910(8)	50(5)
C(16)	2964(15)	10942(17)	6516(10)	61(6)
C(17)	3073(18)	10496(19)	5995(9)	64(6)
C(18)	3930(20)	9633(19)	5852(9)	68(6)
C(19)	4722(15)	9262(14)	6239(9)	51(5)
C(20)	6611(12)	10509(14)	6710(7)	40(4)
C(21)	6577(14)	11493(14)	6889(8)	49(4)
C(22)	6840(17)	12303(18)	6487(13)	76(7)
C(23)	7150(20)	12090(30)	5899(15)	100(11)
C(24)	7170(20)	11120(30)	5710(9)	84(8)
C(25)	6921(16)	10302(19)	6118(9)	66(6)
C(26)	8178(13)	9680(13)	7521(8)	42(4)
C(27)	8320(15)	10299(12)	7929(8)	46(4)
C(28)	9260(14)	10711(14)	7871(9)	49(4)
C(29)	10037(17)	10528(18)	7414(10)	65(6)
C(30)	9903(17)	9920(20)	7003(10)	71(6)
C(31)	8981(13)	9474(16)	7024(8)	52(5)
C(32)	7703(13)	8012(13)	8435(7)	41(4)
C(33)	8781(15)	7516(13)	8219(8)	45(4)
C(34)	9487(15)	6950(13)	8587(8)	48(4)
C(35)	9128(18)	6877(16)	9177(9)	60(5)
C(36)	8079(16)	7384(16)	9407(8)	57(5)
C(37)	7392(15)	7945(14)	9034(8)	49(4)
C(38)	5455(16)	5883(15)	4919(8)	52(5)
C(39)	5165(16)	5465(16)	4439(8)	54(5)
C(40)	5294(16)	5404(16)	5475(8)	54(5)
C(41)	5291(16)	5487(18)	6514(8)	59(5)
C(42)	5736(14)	6048(16)	6885(8)	50(5)
C(43)	7009(16)	5640(20)	6824(8)	65(6)
C(44)	7504(15)	6279(15)	7181(9)	56(5)
C(45)	8670(14)	5778(15)	7256(8)	48(4)
C(46)	9524(17)	6119(16)	6880(8)	58(5)
C(47)	10607(14)	5739(14)	6922(7)	42(4)

C(48)	10896(13)	4912(13)	7362(7)	39(4)
C(49)	10083(12)	4505(13)	7734(6)	37(4)
C(50)	8954(13)	4938(14)	7677(8)	45(4)
C(51)	11447(14)	6211(15)	6526(8)	49(5)
C(52)	11850(20)	7010(20)	6728(9)	89(8)
C(53)	12540(20)	7570(20)	6370(9)	85(8)
C(54)	12867(17)	7260(20)	5786(12)	85(9)
C(55)	12590(20)	6430(20)	5590(11)	93(9)
C(56)	11800(20)	5890(20)	5955(10)	85(8)
C(57)	12085(13)	4504(12)	7428(6)	34(4)
C(58)	12529(15)	4734(16)	7899(8)	54(5)
C(59)	13601(15)	4346(16)	7983(8)	54(5)
C(60)	14287(15)	3664(16)	7608(8)	53(5)
C(61)	13879(13)	3380(15)	7112(8)	49(5)
C(62)	12792(13)	3809(13)	7044(7)	40(4)
C(63)	10397(12)	3631(12)	8195(7)	33(3)
C(64)	11012(13)	2675(13)	8042(7)	36(4)
C(65)	11315(13)	1889(14)	8478(9)	49(5)
C(66)	10965(16)	2071(16)	9055(9)	55(5)
C(67)	10361(14)	3032(17)	9215(8)	50(5)
C(68)	10057(13)	3826(14)	8784(8)	44(4)
C(69)	8075(13)	4540(13)	8080(8)	45(4)
C(70)	7870(14)	3583(15)	8001(8)	51(5)
C(71)	6974(19)	3199(16)	8377(10)	63(6)
C(72)	6353(18)	3830(19)	8801(11)	72(7)
C(73)	6601(18)	4795(19)	8894(10)	70(6)
C(74)	7442(13)	5138(15)	8525(9)	52(5)
C(1S)	6040(30)	8320(30)	1043(14)	60(8)
C(2S)	7533(18)	3680(17)	238(10)	35(5)
C(3S)	10050(40)	4000(40)	5910(30)	90(20)
Cl(1S)	5545(6)	7938(8)	447(3)	64(2)
Cl(2S)	5049(8)	9100(7)	1502(4)	81(3)
Cl(3S)	8121(6)	4764(6)	398(3)	62(2)
Cl(4S)	6179(6)	3863(7)	577(4)	81(2)
Cl(5S)	9925(14)	2827(15)	6360(7)	75(5)
Cl(6S)	8884(14)	4357(12)	5510(7)	66(4)

Bond lengths [Å] and angles [°] for BCE21Rs.

I(1)-C(1)	2.100(14)	C(45)-C(46)	1.40(3)
I(2)-C(38)	2.093(17)	C(45)-C(50)	1.41(2)
O(1)-C(2)	1.35(2)	C(46)-C(47)	1.35(3)
O(1)-C(4)	1.47(2)	C(47)-C(48)	1.43(2)
O(2)-C(40)	1.35(2)	C(47)-C(51)	1.49(2)
O(2)-C(41)	1.46(2)	C(48)-C(49)	1.40(2)
C(1)-C(3)#1	1.35(2)	C(48)-C(57)	1.49(2)
C(1)-C(2)	1.42(2)	C(49)-C(50)	1.42(2)
C(2)-C(3)	1.39(2)	C(49)-C(63)	1.50(2)
C(3)-C(1)#1	1.35(2)	C(50)-C(69)	1.49(2)
C(4)-C(5)	1.48(3)	C(51)-C(56)	1.39(3)
C(5)-C(6)	1.55(2)	C(51)-C(52)	1.39(3)
C(6)-C(7)	1.49(2)	C(52)-C(53)	1.39(3)
C(7)-C(8)	1.52(2)	C(53)-C(54)	1.41(4)
C(8)-C(13)	1.36(2)	C(54)-C(55)	1.34(4)
C(8)-C(9)	1.41(2)	C(55)-C(56)	1.46(4)
C(9)-C(10)	1.42(2)	C(57)-C(58)	1.38(2)
C(9)-C(14)	1.48(2)	C(57)-C(62)	1.39(2)
C(10)-C(11)	1.41(2)	C(58)-C(59)	1.36(2)
C(10)-C(20)	1.47(2)	C(59)-C(60)	1.36(3)
C(11)-C(12)	1.42(2)	C(60)-C(61)	1.43(3)
C(11)-C(26)	1.51(2)	C(61)-C(62)	1.38(2)
C(12)-C(13)	1.38(2)	C(63)-C(64)	1.35(2)
C(12)-C(32)	1.50(2)	C(63)-C(68)	1.39(2)
C(14)-C(15)	1.35(3)	C(64)-C(65)	1.39(2)
C(14)-C(19)	1.42(3)	C(65)-C(66)	1.36(3)
C(15)-C(16)	1.42(3)	C(66)-C(67)	1.35(3)
C(16)-C(17)	1.35(3)	C(67)-C(68)	1.39(2)
C(17)-C(18)	1.39(3)	C(69)-C(70)	1.36(3)
C(18)-C(19)	1.41(3)	C(69)-C(74)	1.38(3)
C(20)-C(21)	1.37(3)	C(70)-C(71)	1.46(3)
C(20)-C(25)	1.39(3)	C(71)-C(72)	1.36(3)
C(21)-C(22)	1.40(3)	C(72)-C(73)	1.40(3)
C(22)-C(23)	1.39(4)	C(73)-C(74)	1.38(3)
C(23)-C(24)	1.37(4)	C(1S)-Cl(2S)	1.71(3)
C(24)-C(25)	1.40(3)	C(1S)-Cl(1S)	1.75(3)
C(26)-C(27)	1.35(2)	C(2S)-Cl(4S)	1.73(2)
C(26)-C(31)	1.41(2)	C(2S)-Cl(3S)	1.82(2)
C(27)-C(28)	1.39(2)	C(3S)-Cl(5S)	1.79(2)
C(28)-C(29)	1.32(3)	C(3S)-Cl(6S)	1.79(2)
C(29)-C(30)	1.34(3)		
C(30)-C(31)	1.40(3)	C(2)-O(1)-C(4)	115.8(12)
C(32)-C(37)	1.38(2)	C(40)-O(2)-C(41)	117.9(15)
C(32)-C(33)	1.40(2)	C(3)#1-C(1)-C(2)	122.0(14)
C(33)-C(34)	1.36(2)	C(3)#1-C(1)-I(1)	120.1(12)
C(34)-C(35)	1.37(3)	C(2)-C(1)-I(1)	117.8(12)
C(35)-C(36)	1.38(3)	O(1)-C(2)-C(3)	124.9(15)
C(36)-C(37)	1.35(2)	O(1)-C(2)-C(1)	118.1(14)
C(38)-C(40)	1.38(2)	C(3)-C(2)-C(1)	116.9(15)
C(38)-C(39)	1.40(3)	C(1)#1-C(3)-C(2)	121.1(16)
C(39)-C(40)#2	1.36(3)	O(1)-C(4)-C(5)	107.9(15)
C(40)-C(39)#2	1.36(3)	C(4)-C(5)-C(6)	113.4(15)
C(41)-C(42)	1.42(3)	C(7)-C(6)-C(5)	110.9(13)
C(42)-C(43)	1.55(3)	C(6)-C(7)-C(8)	114.1(14)
C(43)-C(44)	1.50(3)	C(13)-C(8)-C(9)	119.7(14)
C(44)-C(45)	1.49(2)	C(13)-C(8)-C(7)	119.5(14)

C(9)-C(8)-C(7)	120.7(14)	C(45)-C(44)-C(43)	112.6(16)
C(8)-C(9)-C(10)	119.3(14)	C(46)-C(45)-C(50)	118.1(15)
C(8)-C(9)-C(14)	120.9(14)	C(46)-C(45)-C(44)	119.3(16)
C(10)-C(9)-C(14)	119.5(14)	C(50)-C(45)-C(44)	122.6(17)
C(11)-C(10)-C(9)	119.0(14)	C(47)-C(46)-C(45)	124.0(17)
C(11)-C(10)-C(20)	118.7(14)	C(46)-C(47)-C(48)	117.9(16)
C(9)-C(10)-C(20)	122.3(14)	C(46)-C(47)-C(51)	119.5(16)
C(10)-C(11)-C(12)	120.6(14)	C(48)-C(47)-C(51)	122.6(14)
C(10)-C(11)-C(26)	120.6(14)	C(49)-C(48)-C(47)	120.8(14)
C(12)-C(11)-C(26)	118.8(15)	C(49)-C(48)-C(57)	120.3(13)
C(13)-C(12)-C(11)	117.9(16)	C(47)-C(48)-C(57)	118.8(14)
C(13)-C(12)-C(32)	118.7(14)	C(48)-C(49)-C(50)	119.1(14)
C(11)-C(12)-C(32)	123.2(14)	C(48)-C(49)-C(63)	120.4(13)
C(8)-C(13)-C(12)	123.4(15)	C(50)-C(49)-C(63)	120.5(14)
C(15)-C(14)-C(19)	118.2(16)	C(45)-C(50)-C(49)	119.9(15)
C(15)-C(14)-C(9)	122.9(16)	C(45)-C(50)-C(69)	120.0(14)
C(19)-C(14)-C(9)	118.7(16)	C(49)-C(50)-C(69)	119.9(15)
C(14)-C(15)-C(16)	121.7(19)	C(56)-C(51)-C(52)	120.3(19)
C(17)-C(16)-C(15)	120(2)	C(56)-C(51)-C(47)	121(2)
C(16)-C(17)-C(18)	120.4(19)	C(52)-C(51)-C(47)	118.7(17)
C(17)-C(18)-C(19)	119.4(19)	C(53)-C(52)-C(51)	123(2)
C(18)-C(19)-C(14)	119.9(19)	C(52)-C(53)-C(54)	117(2)
C(21)-C(20)-C(25)	119.9(16)	C(55)-C(54)-C(53)	123(2)
C(21)-C(20)-C(10)	119.0(15)	C(54)-C(55)-C(56)	120(2)
C(25)-C(20)-C(10)	121.0(17)	C(51)-C(56)-C(55)	117(3)
C(20)-C(21)-C(22)	121(2)	C(58)-C(57)-C(62)	115.8(15)
C(23)-C(22)-C(21)	119(2)	C(58)-C(57)-C(48)	121.8(15)
C(24)-C(23)-C(22)	121(2)	C(62)-C(57)-C(48)	122.2(14)
C(23)-C(24)-C(25)	120(2)	C(59)-C(58)-C(57)	123.3(17)
C(20)-C(25)-C(24)	120(2)	C(60)-C(59)-C(58)	120.6(17)
C(27)-C(26)-C(31)	119.5(16)	C(59)-C(60)-C(61)	119.1(16)
C(27)-C(26)-C(11)	121.4(16)	C(62)-C(61)-C(60)	117.7(17)
C(31)-C(26)-C(11)	118.9(16)	C(61)-C(62)-C(57)	123.4(16)
C(26)-C(27)-C(28)	120.6(19)	C(64)-C(63)-C(68)	120.1(14)
C(29)-C(28)-C(27)	121.8(19)	C(64)-C(63)-C(49)	120.9(14)
C(28)-C(29)-C(30)	118.2(17)	C(68)-C(63)-C(49)	119.0(15)
C(29)-C(30)-C(31)	124(2)	C(63)-C(64)-C(65)	119.8(16)
C(30)-C(31)-C(26)	116.1(19)	C(66)-C(65)-C(64)	120.3(18)
C(37)-C(32)-C(33)	117.9(15)	C(67)-C(66)-C(65)	120.7(16)
C(37)-C(32)-C(12)	121.5(15)	C(66)-C(67)-C(68)	119.5(18)
C(33)-C(32)-C(12)	120.5(15)	C(63)-C(68)-C(67)	119.6(17)
C(34)-C(33)-C(32)	121.0(17)	C(70)-C(69)-C(74)	119.3(18)
C(33)-C(34)-C(35)	118.9(18)	C(70)-C(69)-C(50)	119.5(17)
C(34)-C(35)-C(36)	121.4(18)	C(74)-C(69)-C(50)	121.2(16)
C(37)-C(36)-C(35)	118.7(18)	C(69)-C(70)-C(71)	120.3(18)
C(36)-C(37)-C(32)	122.0(17)	C(72)-C(71)-C(70)	118.4(18)
C(40)-C(38)-C(39)	120.0(16)	C(71)-C(72)-C(73)	121(2)
C(40)-C(38)-I(2)	122.8(14)	C(74)-C(73)-C(72)	119(2)
C(39)-C(38)-I(2)	117.2(12)	C(73)-C(74)-C(69)	122.1(19)
C(40)#2-C(39)-C(38)	119.9(16)	Cl(2S)-C(1S)-Cl(1S)	113.6(18)
O(2)-C(40)-C(39)#2	124.4(16)	Cl(4S)-C(2S)-Cl(3S)	109.3(12)
O(2)-C(40)-C(38)	115.5(17)	Cl(5S)-C(3S)-Cl(6S)	107.6(16)
C(39)#2-C(40)-C(38)	120.1(17)		
C(42)-C(41)-O(2)	107.8(16)		
C(41)-C(42)-C(43)	109.4(17)		
C(44)-C(43)-C(42)	110.2(18)		

Symmetry transformations used to generate equivalent atoms:

#1 -x,-y+2,-z+2 #2 -x+1,-y+1,-z+1

Anisotropic displacement parameters ($\text{\AA}^2 \times 10^3$) for BCE21Rs. The anisotropic displacement factor exponent takes the form: $-2\pi^2 [h^2 a^{*2} U^{11} + \dots + 2 h k a^* b^* U^{12}]$

	U ¹¹	U ²²	U ³³	U ²³	U ¹³	U ¹²
I(1)	29(1)	76(1)	50(1)	-2(1)	-4(1)	-11(1)
I(2)	100(1)	105(1)	60(1)	6(1)	11(1)	-59(1)
O(1)	25(5)	60(7)	36(6)	-3(5)	7(5)	-5(5)
O(2)	60(8)	100(11)	39(7)	23(7)	-11(6)	-35(8)
C(1)	23(8)	45(9)	34(8)	17(7)	-4(6)	-11(7)
C(2)	53(10)	40(9)	23(8)	22(7)	-11(7)	-19(8)
C(3)	19(7)	56(11)	39(9)	9(8)	9(7)	2(7)
C(4)	40(10)	64(12)	65(12)	-5(10)	1(9)	-37(9)
C(5)	39(9)	77(13)	36(9)	-11(9)	5(7)	-31(9)
C(6)	46(10)	36(9)	39(9)	-1(7)	-2(7)	-18(7)
C(7)	31(8)	56(11)	48(10)	9(8)	7(7)	-24(8)
C(8)	30(8)	45(9)	29(8)	-5(7)	4(6)	-14(7)
C(9)	44(9)	67(12)	17(7)	10(7)	1(7)	-18(8)
C(10)	35(8)	47(10)	24(8)	4(7)	-1(6)	-12(7)
C(11)	26(8)	39(9)	46(10)	6(7)	3(7)	-7(7)
C(12)	39(9)	45(10)	35(9)	1(7)	13(7)	-19(8)
C(13)	36(9)	51(10)	31(9)	8(7)	3(7)	-13(8)
C(14)	47(10)	50(10)	33(9)	-1(8)	-4(7)	-30(9)
C(15)	43(10)	63(12)	44(10)	8(9)	4(8)	-22(9)
C(16)	39(10)	68(13)	69(14)	22(11)	3(9)	-16(9)
C(17)	63(13)	83(16)	53(13)	27(12)	-20(10)	-34(12)
C(18)	94(17)	82(16)	52(12)	-1(11)	-41(12)	-46(14)
C(19)	46(10)	40(10)	72(13)	2(9)	-14(9)	-16(8)
C(20)	25(8)	54(11)	37(9)	7(8)	-1(7)	-11(7)
C(21)	43(10)	47(11)	48(10)	10(9)	-6(8)	5(8)
C(22)	48(12)	61(14)	110(20)	41(14)	-13(13)	-19(10)
C(23)	65(15)	130(30)	110(20)	80(20)	-27(15)	-55(16)
C(24)	95(18)	130(20)	29(11)	44(13)	-14(11)	-40(17)
C(25)	57(12)	93(16)	57(13)	32(11)	-17(10)	-46(11)
C(26)	29(8)	41(10)	56(11)	19(8)	-10(8)	-14(7)
C(27)	60(11)	30(9)	57(11)	20(8)	-21(9)	-28(8)
C(28)	42(10)	52(11)	60(12)	11(9)	-23(9)	-19(8)
C(29)	52(12)	92(16)	71(14)	19(12)	-34(11)	-48(11)
C(30)	46(11)	105(18)	63(14)	16(13)	10(10)	-37(12)
C(31)	27(9)	78(13)	50(11)	11(9)	1(8)	-18(9)
C(32)	40(9)	43(10)	42(10)	17(8)	-8(7)	-20(8)
C(33)	52(11)	45(10)	39(9)	4(8)	-5(8)	-16(8)
C(34)	50(10)	38(10)	54(11)	6(8)	-8(9)	-8(8)
C(35)	69(14)	56(12)	65(14)	8(10)	-37(11)	-24(10)
C(36)	57(12)	68(13)	43(10)	16(9)	-22(9)	-3(10)
C(37)	48(10)	40(10)	52(11)	2(8)	6(9)	-5(8)
C(38)	59(11)	56(12)	48(11)	9(9)	-5(9)	-34(9)
C(39)	64(12)	75(13)	30(9)	7(9)	-1(8)	-39(11)
C(40)	56(11)	76(14)	32(10)	3(9)	-9(8)	-22(10)
C(41)	49(11)	88(15)	38(10)	16(10)	-4(8)	-19(10)
C(42)	37(9)	73(13)	43(10)	6(9)	-7(8)	-19(9)
C(43)	54(12)	113(18)	35(10)	13(11)	-12(9)	-39(12)

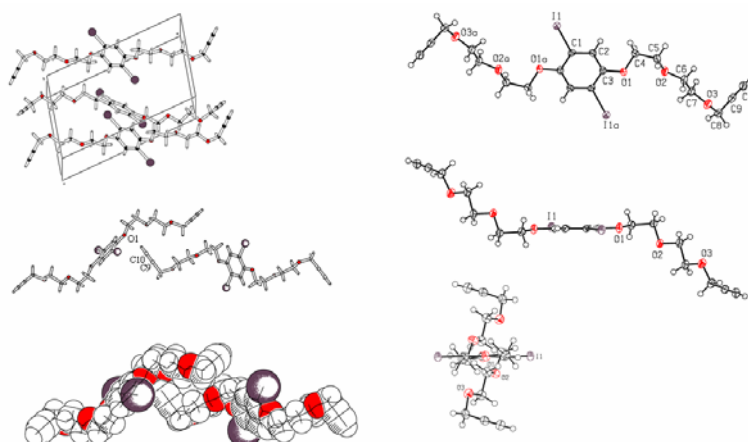
C(44)	50(11)	52(12)	63(12)	-4(9)	-5(9)	-4(9)
C(45)	40(10)	57(11)	46(10)	-1(9)	-17(8)	-4(8)
C(46)	67(13)	58(12)	43(11)	13(9)	-15(9)	-1(10)
C(47)	40(9)	52(11)	35(9)	-7(8)	-8(7)	-6(8)
C(48)	32(8)	44(10)	39(9)	14(7)	-9(7)	-9(7)
C(49)	31(8)	57(10)	25(8)	-6(7)	-9(6)	-12(7)
C(50)	25(8)	60(11)	49(10)	6(9)	-1(7)	-11(8)
C(51)	40(9)	52(11)	44(10)	33(9)	-8(8)	-3(8)
C(52)	99(18)	150(20)	29(11)	20(13)	-1(11)	-71(18)
C(53)	80(16)	150(20)	43(13)	8(13)	-4(11)	-62(16)
C(54)	43(12)	96(19)	100(20)	66(16)	-14(12)	-10(12)
C(55)	110(20)	85(19)	60(15)	31(14)	21(14)	-12(17)
C(56)	120(20)	77(16)	48(13)	9(11)	19(13)	-20(14)
C(57)	40(9)	36(9)	25(8)	-1(7)	-2(7)	-6(7)
C(58)	44(10)	65(13)	52(11)	-24(10)	-9(9)	-1(9)
C(59)	48(11)	79(14)	42(10)	5(10)	-28(9)	-17(10)
C(60)	40(10)	75(13)	39(10)	12(9)	-15(8)	-1(9)
C(61)	27(8)	67(12)	50(11)	12(9)	5(8)	-13(8)
C(62)	42(9)	54(10)	26(8)	13(7)	-7(7)	-22(8)
C(63)	27(8)	39(9)	34(9)	12(7)	-8(6)	-14(7)
C(64)	38(9)	48(10)	30(8)	12(7)	-8(7)	-29(8)
C(65)	30(9)	46(11)	76(14)	7(10)	-14(9)	-23(8)
C(66)	60(12)	53(12)	67(14)	33(10)	-42(11)	-35(10)
C(67)	42(10)	77(14)	35(9)	16(9)	-12(8)	-26(10)
C(68)	36(9)	48(10)	50(11)	4(8)	-7(8)	-18(8)
C(69)	36(9)	35(10)	65(12)	1(8)	-25(9)	1(7)
C(70)	33(9)	61(12)	56(11)	6(9)	-8(8)	-7(8)
C(71)	77(15)	45(11)	79(15)	8(11)	-37(13)	-21(11)
C(72)	50(12)	72(16)	97(18)	25(14)	-12(12)	-27(11)
C(73)	57(13)	79(16)	63(13)	4(11)	-16(11)	7(11)
C(74)	25(8)	54(11)	76(13)	2(10)	1(9)	-14(8)
Cl(1S)	36(4)	120(7)	44(4)	-18(4)	7(3)	-32(4)
Cl(2S)	95(7)	77(6)	71(6)	-42(5)	10(5)	-20(5)
Cl(3S)	56(4)	56(4)	73(5)	-4(3)	-10(3)	-10(3)
Cl(4S)	37(4)	98(6)	99(6)	-18(5)	12(4)	-6(4)
Cl(5S)	72(10)	96(12)	49(8)	12(8)	-14(7)	-6(9)
Cl(6S)	83(11)	53(9)	53(8)	0(7)	5(7)	-7(7)

Hydrogen coordinates ($\times 10^4$) and isotropic displacement parameters ($\text{\AA}^2 \times 10^{-3}$)
for BCE21Rs.

	x	y	z	U(eq)
H(3)	-639	9555	9178	50
H(4A)	578	8451	8604	63
H(4B)	1020	9526	8437	63
H(5A)	2003	8126	7842	58
H(5B)	2400	7455	8419	58
H(6A)	2993	9451	8018	47
H(6B)	3458	8691	8555	47
H(7A)	3879	8160	7359	54
H(7B)	4306	7364	7890	54
H(13)	5745	7713	8379	48
H(15)	3683	10895	7265	60
H(16)	2361	11516	6617	73
H(17)	2560	10776	5726	77
H(18)	3982	9297	5497	82
H(19)	5347	8715	6130	61
H(21)	6372	11628	7294	59
H(22)	6807	12988	6614	91
H(23)	7349	12630	5624	120
H(24)	7361	10989	5304	101
H(25)	6961	9615	5992	79
H(27)	7771	10454	8259	55
H(28)	9346	11137	8167	59
H(29)	10674	10821	7378	78
H(30)	10469	9775	6678	86
H(31)	8900	9059	6721	63
H(33)	9025	7574	7808	54
H(34)	10217	6611	8436	57
H(35)	9611	6470	9435	71
H(36)	7845	7340	9819	69
H(37)	6672	8303	9191	59
H(39)	5289	5787	4054	65
H(41A)	4481	5601	6621	71
H(41B)	5612	4717	6559	71
H(42A)	5410	5938	7299	60
H(42B)	5554	6819	6772	60
H(43A)	7188	4883	6962	78
H(43B)	7326	5706	6405	78
H(44A)	7473	6997	6985	68
H(44B)	7058	6362	7573	68
H(46)	9332	6649	6578	70
H(52)	11632	7180	7127	107
H(53)	12790	8124	6511	102
H(54)	13297	7663	5522	102
H(55)	12910	6192	5212	112
H(56)	11542	5341	5810	102
H(58)	12064	5187	8179	64
H(59)	13870	4554	8308	65
H(60)	15028	3380	7674	64
H(61)	14342	2911	6838	59
H(62)	12511	3619	6718	48

H(64)	11238	2538	7639	43
H(65)	11769	1223	8372	58
H(66)	11145	1518	9348	66
H(67)	10146	3163	9620	60
H(68)	9619	4498	8891	52
H(70)	8309	3161	7699	61
H(71)	6830	2526	8327	76
H(72)	5745	3610	9037	87
H(73)	6195	5209	9207	83
H(74)	7590	5807	8580	62
H(1S1)	6384	7678	1271	72
H(1S2)	6628	8717	891	72
H(2S1)	7556	3663	-192	42
H(2S2)	7968	2995	385	42
H(3S1)	10743	3864	5627	106
H(3S2)	10067	4583	6150	106

X-Ray Structure Determination, $C_{20}H_{24}I_2O_6$, 7



X-ray intensity data from a colorless plate were measured at 150(1) K on a Bruker SMART APEX CCD-based diffractometer (Mo $K\alpha$ radiation, $\lambda = 0.71073$ Å).¹ Raw data frame integration and Lp corrections were performed with SAINT+.¹ Final unit cell parameters were determined by least-squares refinement of 6267 reflections from the data set with $I > 5(\sigma)I$. Analysis of the data showed negligible crystal decay during collection. The data were corrected for absorption with SADABS.¹ Patterson methods structure solution, difference Fourier calculations and full-matrix least-squares refinement against F^2 were performed with SHELXTL.²

$C_{20}H_{24}I_2O_6$ crystallizes in the space group $P2_1/c$ as determined uniquely by the pattern of systematic absences in the intensity data. The molecule is situated on an inversion center. Non-hydrogen atoms were refined with anisotropic displacement parameters; hydrogen atoms were placed in idealized positions and included as riding atoms with refined isotropic displacement parameters.

(1) SMART Version 5.628, SAINT+ Version 6.22 and SADABS Version 2.05. Bruker Analytical X-ray Systems, Inc., Madison, Wisconsin, USA, 2001.

(2) Sheldrick, G. M. SHELXTL Version 6.1; Bruker Analytical X-ray Systems, Inc., Madison, Wisconsin, USA, 2000.

Table A7. Crystal data and structure refinement for bce5ss.

Identification code	bce5ss	
Empirical formula	C ₂₀ H ₂₄ I ₂ O ₆	
Formula weight	614.19	
Temperature	150(2) K	
Wavelength	0.71073 Å	
Crystal system	Monoclinic	
Space group	P2 ₁ /c	
Unit cell dimensions	a = 15.8462(9) Å	α = 90°.
	b = 7.6297(4) Å	β = 105.9060(10)°.
	c = 9.3907(6) Å	γ = 90°.
Volume	1091.88(11) Å ³	
Z	2	
Density (calculated)	1.868 Mg/m ³	
Absorption coefficient	2.912 mm ⁻¹	
F(000)	596	
Crystal size	0.36 x 0.30 x 0.16 mm ³	
Theta range for data collection	1.34 to 25.03°.	
Index ranges	-18 ≤ h ≤ 18, -9 ≤ k ≤ 9, -11 ≤ l ≤ 9	
Reflections collected	7165	
Independent reflections	1924 [R(int) = 0.0292]	
Completeness to theta = 25.03°	99.8 %	
Absorption correction	Semi-empirical from equivalents	
Max. and min. transmission	1.0000 and 0.6911	
Refinement method	Full-matrix least-squares on F ²	
Data / restraints / parameters	1924 / 0 / 140	
Goodness-of-fit on F ²	1.089	
Final R indices [I > 2σ(I)]	R1 = 0.0189, wR2 = 0.0474	
R indices (all data)	R1 = 0.0196, wR2 = 0.0479	
Extinction coefficient	0.0125(6)	
Largest diff. peak and hole	0.556 and -0.546 e.Å ⁻³	

Atomic coordinates ($\times 10^4$) and equivalent isotropic displacement parameters ($\text{\AA}^2 \times 10^3$) for bce5ss. $U(\text{eq})$ is defined as one third of the trace of the orthogonalized U^{ij} tensor.

	x	y	z	U(eq)
I(1)	6217(1)	1858(1)	8296(1)	22(1)
O(1)	3525(1)	1636(2)	3228(2)	22(1)
C(1)	5475(1)	717(3)	6324(2)	18(1)
C(2)	4733(2)	1571(3)	5491(3)	19(1)
C(3)	4250(1)	871(3)	4141(2)	19(1)
C(4)	3299(2)	3373(3)	3609(3)	21(1)
C(5)	2523(2)	3961(3)	2397(3)	23(1)
O(2)	1781(1)	2946(2)	2475(2)	24(1)
C(6)	1051(2)	3212(3)	1216(3)	25(1)
C(7)	293(2)	2185(3)	1468(3)	25(1)
O(3)	-350(1)	2071(2)	79(2)	26(1)
C(8)	-1162(2)	1417(3)	219(3)	26(1)
C(9)	-1651(2)	2762(3)	791(3)	24(1)
C(10)	-2029(2)	3904(3)	1219(3)	26(1)

Bond lengths [Å] and angles [°] for bce5ss.

I(1)-C(1)	2.092(2)
O(1)-C(3)	1.363(3)
O(1)-C(4)	1.443(2)
C(1)-C(2)	1.384(3)
C(1)-C(3)#1	1.397(3)
C(2)-C(3)	1.396(3)
C(2)-H(2)	0.9500
C(3)-C(1)#1	1.397(3)
C(4)-C(5)	1.497(3)
C(4)-H(4A)	0.9900
C(4)-H(4B)	0.9900
C(5)-O(2)	1.426(3)
C(5)-H(5A)	0.9900
C(5)-H(5B)	0.9900
O(2)-C(6)	1.424(3)
C(6)-C(7)	1.505(3)
C(6)-H(6A)	0.9900
C(6)-H(6B)	0.9900
C(7)-O(3)	1.421(3)
C(7)-H(7A)	0.9900
C(7)-H(7B)	0.9900
O(3)-C(8)	1.420(3)
C(8)-C(9)	1.473(4)
C(8)-H(8A)	0.9900
C(8)-H(8B)	0.9900
C(9)-C(10)	1.188(4)
C(10)-H(10)	0.9500
C(3)-O(1)-C(4)	117.46(18)
C(2)-C(1)-C(3)#1	121.4(2)
C(2)-C(1)-I(1)	119.24(16)
C(3)#1-C(1)-I(1)	119.34(16)
C(1)-C(2)-C(3)	120.2(2)
C(1)-C(2)-H(2)	119.9
C(3)-C(2)-H(2)	119.9
O(1)-C(3)-C(2)	124.4(2)
O(1)-C(3)-C(1)#1	117.1(2)
C(2)-C(3)-C(1)#1	118.4(2)
O(1)-C(4)-C(5)	107.14(19)
O(1)-C(4)-H(4A)	110.3
C(5)-C(4)-H(4A)	110.3
O(1)-C(4)-H(4B)	110.3
C(5)-C(4)-H(4B)	110.3
H(4A)-C(4)-H(4B)	108.5
O(2)-C(5)-C(4)	108.41(19)
O(2)-C(5)-H(5A)	110.0
C(4)-C(5)-H(5A)	110.0
O(2)-C(5)-H(5B)	110.0
C(4)-C(5)-H(5B)	110.0
H(5A)-C(5)-H(5B)	108.4
C(6)-O(2)-C(5)	111.98(18)
O(2)-C(6)-C(7)	107.3(2)
O(2)-C(6)-H(6A)	110.3
C(7)-C(6)-H(6A)	110.3

O(2)-C(6)-H(6B)	110.3
C(7)-C(6)-H(6B)	110.3
H(6A)-C(6)-H(6B)	108.5
O(3)-C(7)-C(6)	106.9(2)
O(3)-C(7)-H(7A)	110.3
C(6)-C(7)-H(7A)	110.3
O(3)-C(7)-H(7B)	110.3
C(6)-C(7)-H(7B)	110.3
H(7A)-C(7)-H(7B)	108.6
C(8)-O(3)-C(7)	112.17(19)
O(3)-C(8)-C(9)	111.7(2)
O(3)-C(8)-H(8A)	109.3
C(9)-C(8)-H(8A)	109.3
O(3)-C(8)-H(8B)	109.3
C(9)-C(8)-H(8B)	109.3
H(8A)-C(8)-H(8B)	107.9
C(10)-C(9)-C(8)	177.0(3)
C(9)-C(10)-H(10)	180.0

Symmetry transformations used to generate equivalent atoms:

#1 -x+1,-y,-z+1

Anisotropic displacement parameters ($\text{\AA}^2 \times 10^3$) for bce5ss. The anisotropic displacement factor exponent takes the form: $-2\pi^2 [h^2 a^{*2} U^{11} + \dots + 2 h k a^* b^* U^{12}]$

	U^{11}	U^{22}	U^{33}	U^{23}	U^{13}	U^{12}
I(1)	21(1)	21(1)	20(1)	-3(1)	2(1)	1(1)
O(1)	18(1)	18(1)	26(1)	-2(1)	0(1)	4(1)
C(1)	15(1)	18(1)	19(1)	0(1)	4(1)	-4(1)
C(2)	17(1)	15(1)	25(1)	0(1)	7(1)	0(1)
C(3)	14(1)	19(1)	23(1)	3(1)	5(1)	0(1)
C(4)	20(1)	16(1)	27(1)	-2(1)	5(1)	1(1)
C(5)	18(1)	19(1)	32(1)	3(1)	5(1)	1(1)
O(2)	15(1)	24(1)	31(1)	6(1)	1(1)	0(1)
C(6)	18(1)	27(1)	26(1)	2(1)	0(1)	3(1)
C(7)	18(1)	29(1)	23(1)	0(1)	1(1)	2(1)
O(3)	18(1)	34(1)	23(1)	-3(1)	2(1)	0(1)
C(8)	20(1)	26(1)	29(1)	-5(1)	3(1)	-2(1)
C(9)	18(1)	28(1)	22(1)	1(1)	1(1)	-4(1)
C(10)	24(1)	29(1)	24(1)	1(1)	4(1)	3(1)

Hydrogen coordinates ($\times 10^4$) and isotropic displacement parameters ($\text{\AA}^2 \times 10^{-3}$)
for bce5ss.

	x	y	z	U(eq)
H(2)	4552	2637	5840	15(6)
H(4A)	3799	4183	3694	17(6)
H(4B)	3152	3352	4567	11(6)
H(5A)	2409	5221	2517	30(7)
H(5B)	2639	3795	1422	24(6)
H(6A)	1191	2799	308	18(6)
H(6B)	901	4473	1099	25(7)
H(7A)	489	999	1845	21(6)
H(7B)	49	2787	2200	27(7)
H(8A)	-1052	399	898	28(7)
H(8B)	-1523	1011	-761	25(7)
H(10)	-2332	4817	1561	37(8)

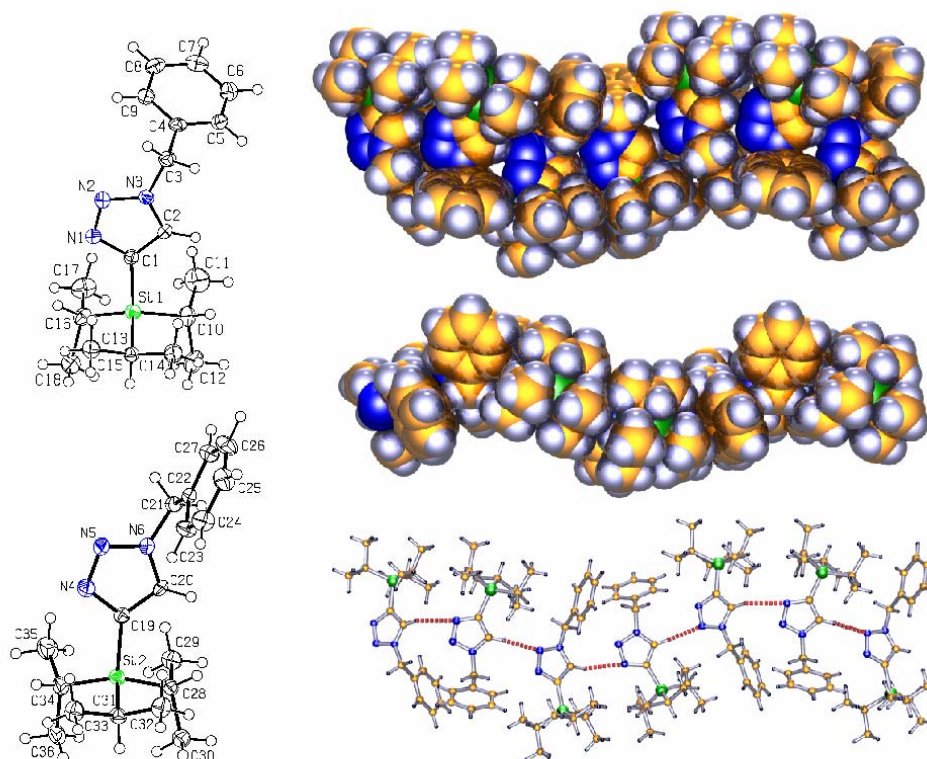
Torsion angles [°] for bce5ss.

C(3)#1-C(1)-C(2)-C(3)	-1.4(4)
I(1)-C(1)-C(2)-C(3)	177.23(16)
C(4)-O(1)-C(3)-C(2)	7.1(3)
C(4)-O(1)-C(3)-C(1)#1	-172.63(19)
C(1)-C(2)-C(3)-O(1)	-178.4(2)
C(1)-C(2)-C(3)-C(1)#1	1.3(3)
C(3)-O(1)-C(4)-C(5)	176.35(19)
O(1)-C(4)-C(5)-O(2)	69.7(2)
C(4)-C(5)-O(2)-C(6)	-170.10(19)
C(5)-O(2)-C(6)-C(7)	-176.09(19)
O(2)-C(6)-C(7)-O(3)	-164.93(18)
C(6)-C(7)-O(3)-C(8)	-169.00(19)
C(7)-O(3)-C(8)-C(9)	76.5(3)
O(3)-C(8)-C(9)-C(10)	33(5)

Symmetry transformations used to generate equivalent atoms:

#1 -x+1,-y,-z+1

X-Ray Structure Determination, C₁₈H₂₉N₃Si



X-ray crystal data on 4.15. Top left and bottom left views of the two crystallographically independent molecules, Si1 and Si2. Displacement ellipsoids drawn at the 50% probability level. Right top, middle, and left; infinite chains of CH \cdots N bonded chains:

C20-H20 \cdots N1: $d = 2.636 \text{ \AA}$, $\angle = 163.9^\circ$

C2-H2 \cdots N5: $d = 2.426 \text{ \AA}$, $\angle = 155.8^\circ$

Sum of van der Waals radii, (H+N) = 2.75 \AA

X-ray intensity data from a colorless plate were measured at 150(1) K on a Bruker SMART APEX CCD-based diffractometer (Mo K α radiation, $\lambda = 0.71073 \text{ \AA}$).¹ Raw data frame integration and Lp corrections were performed with SAINT+.¹ Final unit cell parameters were determined by least-squares refinement of 5551 reflections from the data set with $I > 5(\sigma)I$. Analysis of the data showed negligible crystal decay during collection. The data were not corrected for absorption. Direct methods structure solution, difference Fourier calculations and full-matrix least-squares refinement against F^2 were performed with SHELXTL.²

C₁₈H₂₉N₃Si crystallizes in the orthorhombic space group P2₁2₁2₁ as determined uniquely by the pattern of systematic absences in the intensity data. **The asymmetric** unit consists of two chemically identical but conformationally inequivalent molecules.

All non-hydrogen atoms were refined with anisotropic displacement parameters. Hydrogen atoms were placed in geometrically idealized positions and included as riding atoms. Initially Friedel opposites were not merged, yielding an absolute structure (Flack) parameter of 0.03(10), indicating the correct configuration. Due to the large s.u. of the Flack parameter, however, opposites were merged for the final refinement cycles.

(1) SMART Version 5.625 and SAINT+ Version 6.22. Bruker Analytical X-ray Systems, Inc., Madison, Wisconsin, USA, 2001.

(2) Sheldrick, G. M. SHELXTL Version 6.1; Bruker Analytical X-ray Systems, Inc., Madison, Wisconsin, USA, 2000.

Table A8. Crystal data and structure refinement for merg4.

Identification code	bce10	
Empirical formula	C18 H29 N3 Si	
Formula weight	315.53	
Temperature	150(2) K	
Wavelength	0.71073 Å	
Crystal system	Orthorhombic	
Space group	P2 ₁ 2 ₁ 2 ₁	
Unit cell dimensions	a = 7.7783(5) Å	α = 90°.
	b = 20.2187(12) Å	β = 90°.
	c = 23.8578(14) Å	γ = 90°.
Volume	3752.0(4) Å ³	
Z	8	
Density (calculated)	1.117 Mg/m ³	
Absorption coefficient	0.127 mm ⁻¹	
F(000)	1376	
Crystal size	0.32 x 0.26 x 0.08 mm ³	
Theta range for data collection	1.32 to 25.03°.	
Index ranges	-9 ≤ h ≤ 9, -24 ≤ k ≤ 24, -28 ≤ l ≤ 28	
Reflections collected	29274	
Independent reflections	3762 [R(int) = 0.0659]	
Completeness to theta = 25.03°	99.9 %	
Absorption correction	None	
Refinement method	Full-matrix least-squares on F ²	
Data / restraints / parameters	3762 / 0 / 409	
Goodness-of-fit on F ²	1.005	
Final R indices [I > 2σ(I)]	R1 = 0.0406, wR2 = 0.0829	
R indices (all data)	R1 = 0.0475, wR2 = 0.0854	
Absolute structure parameter	Opposites merged	
Largest diff. peak and hole	0.293 and -0.177 e.Å ⁻³	

Atomic coordinates ($\times 10^4$) and equivalent isotropic displacement parameters ($\text{\AA}^2 \times 10^3$)
for merg4. $U(\text{eq})$ is defined as one third of the trace of the orthogonalized U^{ij} tensor.

	x	y	z	U(eq)
Si(1)	4164(1)	1628(1)	1649(1)	21(1)
Si(2)	2115(1)	4682(1)	810(1)	20(1)
C(1)	2818(4)	2056(1)	2194(1)	21(1)
C(2)	1800(4)	1792(1)	2606(1)	23(1)
C(3)	-140(4)	2302(2)	3338(1)	28(1)
C(4)	865(4)	2302(1)	3877(1)	25(1)
C(5)	1168(4)	1715(2)	4164(1)	29(1)
C(6)	2139(5)	1716(2)	4649(1)	35(1)
C(7)	2835(5)	2290(2)	4855(1)	35(1)
C(8)	2545(4)	2877(2)	4574(1)	32(1)
C(9)	1570(4)	2882(2)	4091(1)	28(1)
C(10)	4831(5)	801(2)	1943(1)	32(1)
C(11)	5790(6)	822(2)	2500(1)	57(1)
C(12)	5834(5)	384(2)	1515(1)	43(1)
C(13)	2706(4)	1477(1)	1029(1)	22(1)
C(14)	1289(4)	978(2)	1166(1)	32(1)
C(15)	1946(5)	2121(1)	814(1)	29(1)
C(16)	5960(4)	2211(2)	1443(1)	28(1)
C(17)	7360(5)	2288(2)	1892(1)	44(1)
C(18)	6780(5)	2046(2)	876(1)	34(1)
C(19)	1141(4)	4803(1)	1525(1)	20(1)
C(20)	1255(4)	4392(1)	1981(1)	21(1)
C(21)	171(4)	4487(1)	2978(1)	25(1)
C(22)	-1549(4)	4167(1)	3084(1)	22(1)
C(23)	-2633(4)	3974(2)	2658(1)	29(1)
C(24)	-4157(5)	3646(2)	2769(1)	37(1)
C(25)	-4596(5)	3497(2)	3311(1)	38(1)
C(26)	-3536(5)	3698(2)	3747(1)	37(1)
C(27)	-2036(5)	4030(2)	3634(1)	29(1)
C(28)	3806(4)	4024(1)	924(1)	21(1)
C(29)	5315(4)	4257(2)	1288(1)	33(1)

C(30)	4486(4)	3709(2)	383(1)	28(1)
C(31)	416(4)	4356(1)	316(1)	24(1)
C(32)	-402(4)	3721(2)	544(1)	32(1)
C(33)	-966(5)	4873(2)	180(1)	33(1)
C(34)	2910(5)	5501(1)	535(1)	27(1)
C(35)	3912(5)	5929(2)	951(1)	44(1)
C(36)	3918(5)	5428(2)	-14(1)	37(1)
N(1)	2577(3)	2729(1)	2211(1)	25(1)
N(2)	1490(4)	2877(1)	2612(1)	28(1)
N(3)	1005(3)	2304(1)	2852(1)	23(1)
N(4)	228(3)	5351(1)	1694(1)	29(1)
N(5)	-201(4)	5285(1)	2223(1)	29(1)
N(6)	433(3)	4699(1)	2400(1)	21(1)

Bond lengths [Å] and angles [°] for merg4.

Si(1)-C(1)	1.879(3)
Si(1)-C(10)	1.886(3)
Si(1)-C(13)	1.890(3)
Si(1)-C(16)	1.892(3)
Si(2)-C(19)	1.881(3)
Si(2)-C(34)	1.886(3)
Si(2)-C(31)	1.889(3)
Si(2)-C(28)	1.890(3)
C(1)-C(2)	1.372(4)
C(1)-N(1)	1.374(3)
C(2)-N(3)	1.342(4)
C(2)-H(2)	0.9500
C(3)-N(3)	1.462(4)
C(3)-C(4)	1.504(4)
C(3)-H(3A)	0.9900
C(3)-H(3B)	0.9900
C(4)-C(9)	1.391(4)
C(4)-C(5)	1.390(4)
C(5)-C(6)	1.383(4)
C(5)-H(5)	0.9500
C(6)-C(7)	1.371(4)
C(6)-H(6)	0.9500
C(7)-C(8)	1.380(4)
C(7)-H(7)	0.9500
C(8)-C(9)	1.379(4)
C(8)-H(8)	0.9500
C(9)-H(9)	0.9500
C(10)-C(11)	1.525(4)
C(10)-C(12)	1.538(4)
C(10)-H(10)	1.0000
C(11)-H(11A)	0.9800
C(11)-H(11B)	0.9800
C(11)-H(11C)	0.9800
C(12)-H(12A)	0.9800

C(12)-H(12B)	0.9800
C(12)-H(12C)	0.9800
C(13)-C(15)	1.519(4)
C(13)-C(14)	1.530(4)
C(13)-H(13)	1.0000
C(14)-H(14A)	0.9800
C(14)-H(14B)	0.9800
C(14)-H(14C)	0.9800
C(15)-H(15A)	0.9800
C(15)-H(15B)	0.9800
C(15)-H(15C)	0.9800
C(16)-C(18)	1.532(4)
C(16)-C(17)	1.535(4)
C(16)-H(16)	1.0000
C(17)-H(17A)	0.9800
C(17)-H(17B)	0.9800
C(17)-H(17C)	0.9800
C(18)-H(18A)	0.9800
C(18)-H(18B)	0.9800
C(18)-H(18C)	0.9800
C(19)-C(20)	1.372(4)
C(19)-N(4)	1.377(4)
C(20)-N(6)	1.340(3)
C(20)-H(20)	0.9500
C(21)-N(6)	1.458(3)
C(21)-C(22)	1.508(4)
C(21)-H(21A)	0.9900
C(21)-H(21B)	0.9900
C(22)-C(23)	1.377(4)
C(22)-C(27)	1.393(4)
C(23)-C(24)	1.383(5)
C(23)-H(23)	0.9500
C(24)-C(25)	1.371(4)
C(24)-H(24)	0.9500
C(25)-C(26)	1.388(5)
C(25)-H(25)	0.9500

C(26)-C(27)	1.372(5)
C(26)-H(26)	0.9500
C(27)-H(27)	0.9500
C(28)-C(30)	1.533(4)
C(28)-C(29)	1.534(4)
C(28)-H(28)	1.0000
C(29)-H(29A)	0.9800
C(29)-H(29B)	0.9800
C(29)-H(29C)	0.9800
C(30)-H(30A)	0.9800
C(30)-H(30B)	0.9800
C(30)-H(30C)	0.9800
C(31)-C(32)	1.532(4)
C(31)-C(33)	1.535(4)
C(31)-H(31)	1.0000
C(32)-H(32A)	0.9800
C(32)-H(32B)	0.9800
C(32)-H(32C)	0.9800
C(33)-H(33A)	0.9800
C(33)-H(33B)	0.9800
C(33)-H(33C)	0.9800
C(34)-C(35)	1.532(4)
C(34)-C(36)	1.533(4)
C(34)-H(34)	1.0000
C(35)-H(35A)	0.9800
C(35)-H(35B)	0.9800
C(35)-H(35C)	0.9800
C(36)-H(36A)	0.9800
C(36)-H(36B)	0.9800
C(36)-H(36C)	0.9800
N(1)-N(2)	1.312(3)
N(2)-N(3)	1.346(3)
N(4)-N(5)	1.312(3)
N(5)-N(6)	1.351(3)
C(1)-Si(1)-C(10)	107.73(13)

C(1)-Si(1)-C(13)	106.36(13)
C(10)-Si(1)-C(13)	108.23(13)
C(1)-Si(1)-C(16)	107.74(13)
C(10)-Si(1)-C(16)	116.44(15)
C(13)-Si(1)-C(16)	109.87(13)
C(19)-Si(2)-C(34)	109.46(13)
C(19)-Si(2)-C(31)	109.20(14)
C(34)-Si(2)-C(31)	108.53(13)
C(19)-Si(2)-C(28)	104.00(12)
C(34)-Si(2)-C(28)	116.07(15)
C(31)-Si(2)-C(28)	109.37(13)
C(2)-C(1)-N(1)	106.6(2)
C(2)-C(1)-Si(1)	129.6(2)
N(1)-C(1)-Si(1)	123.5(2)
N(3)-C(2)-C(1)	106.2(2)
N(3)-C(2)-H(2)	126.9
C(1)-C(2)-H(2)	126.9
N(3)-C(3)-C(4)	111.2(3)
N(3)-C(3)-H(3A)	109.4
C(4)-C(3)-H(3A)	109.4
N(3)-C(3)-H(3B)	109.4
C(4)-C(3)-H(3B)	109.4
H(3A)-C(3)-H(3B)	108.0
C(9)-C(4)-C(5)	118.1(3)
C(9)-C(4)-C(3)	121.3(3)
C(5)-C(4)-C(3)	120.6(3)
C(6)-C(5)-C(4)	120.2(3)
C(6)-C(5)-H(5)	119.9
C(4)-C(5)-H(5)	119.9
C(7)-C(6)-C(5)	121.1(3)
C(7)-C(6)-H(6)	119.5
C(5)-C(6)-H(6)	119.5
C(6)-C(7)-C(8)	119.3(3)
C(6)-C(7)-H(7)	120.4
C(8)-C(7)-H(7)	120.4
C(7)-C(8)-C(9)	120.1(3)

C(7)-C(8)-H(8)	120.0
C(9)-C(8)-H(8)	120.0
C(8)-C(9)-C(4)	121.2(3)
C(8)-C(9)-H(9)	119.4
C(4)-C(9)-H(9)	119.4
C(11)-C(10)-C(12)	110.3(3)
C(11)-C(10)-Si(1)	115.7(2)
C(12)-C(10)-Si(1)	112.3(2)
C(11)-C(10)-H(10)	105.9
C(12)-C(10)-H(10)	105.9
Si(1)-C(10)-H(10)	105.9
C(10)-C(11)-H(11A)	109.5
C(10)-C(11)-H(11B)	109.5
H(11A)-C(11)-H(11B)	109.5
C(10)-C(11)-H(11C)	109.5
H(11A)-C(11)-H(11C)	109.5
H(11B)-C(11)-H(11C)	109.5
C(10)-C(12)-H(12A)	109.5
C(10)-C(12)-H(12B)	109.5
H(12A)-C(12)-H(12B)	109.5
C(10)-C(12)-H(12C)	109.5
H(12A)-C(12)-H(12C)	109.5
H(12B)-C(12)-H(12C)	109.5
C(15)-C(13)-C(14)	110.9(3)
C(15)-C(13)-Si(1)	111.07(19)
C(14)-C(13)-Si(1)	111.82(19)
C(15)-C(13)-H(13)	107.6
C(14)-C(13)-H(13)	107.6
Si(1)-C(13)-H(13)	107.6
C(13)-C(14)-H(14A)	109.5
C(13)-C(14)-H(14B)	109.5
H(14A)-C(14)-H(14B)	109.5
C(13)-C(14)-H(14C)	109.5
H(14A)-C(14)-H(14C)	109.5
H(14B)-C(14)-H(14C)	109.5
C(13)-C(15)-H(15A)	109.5

C(13)-C(15)-H(15B)	109.5
H(15A)-C(15)-H(15B)	109.5
C(13)-C(15)-H(15C)	109.5
H(15A)-C(15)-H(15C)	109.5
H(15B)-C(15)-H(15C)	109.5
C(18)-C(16)-C(17)	110.0(3)
C(18)-C(16)-Si(1)	113.7(2)
C(17)-C(16)-Si(1)	114.0(2)
C(18)-C(16)-H(16)	106.2
C(17)-C(16)-H(16)	106.2
Si(1)-C(16)-H(16)	106.2
C(16)-C(17)-H(17A)	109.5
C(16)-C(17)-H(17B)	109.5
H(17A)-C(17)-H(17B)	109.5
C(16)-C(17)-H(17C)	109.5
H(17A)-C(17)-H(17C)	109.5
H(17B)-C(17)-H(17C)	109.5
C(16)-C(18)-H(18A)	109.5
C(16)-C(18)-H(18B)	109.5
H(18A)-C(18)-H(18B)	109.5
C(16)-C(18)-H(18C)	109.5
H(18A)-C(18)-H(18C)	109.5
H(18B)-C(18)-H(18C)	109.5
C(20)-C(19)-N(4)	106.8(2)
C(20)-C(19)-Si(2)	127.8(2)
N(4)-C(19)-Si(2)	125.4(2)
N(6)-C(20)-C(19)	106.2(2)
N(6)-C(20)-H(20)	126.9
C(19)-C(20)-H(20)	126.9
N(6)-C(21)-C(22)	114.1(3)
N(6)-C(21)-H(21A)	108.7
C(22)-C(21)-H(21A)	108.7
N(6)-C(21)-H(21B)	108.7
C(22)-C(21)-H(21B)	108.7
H(21A)-C(21)-H(21B)	107.6
C(23)-C(22)-C(27)	118.2(3)

C(23)-C(22)-C(21)	122.8(3)
C(27)-C(22)-C(21)	118.9(3)
C(22)-C(23)-C(24)	121.3(3)
C(22)-C(23)-H(23)	119.4
C(24)-C(23)-H(23)	119.4
C(25)-C(24)-C(23)	120.0(3)
C(25)-C(24)-H(24)	120.0
C(23)-C(24)-H(24)	120.0
C(24)-C(25)-C(26)	119.6(3)
C(24)-C(25)-H(25)	120.2
C(26)-C(25)-H(25)	120.2
C(27)-C(26)-C(25)	120.1(3)
C(27)-C(26)-H(26)	120.0
C(25)-C(26)-H(26)	120.0
C(26)-C(27)-C(22)	120.9(3)
C(26)-C(27)-H(27)	119.6
C(22)-C(27)-H(27)	119.6
C(30)-C(28)-C(29)	109.9(3)
C(30)-C(28)-Si(2)	114.3(2)
C(29)-C(28)-Si(2)	113.4(2)
C(30)-C(28)-H(28)	106.2
C(29)-C(28)-H(28)	106.2
Si(2)-C(28)-H(28)	106.2
C(28)-C(29)-H(29A)	109.5
C(28)-C(29)-H(29B)	109.5
H(29A)-C(29)-H(29B)	109.5
C(28)-C(29)-H(29C)	109.5
H(29A)-C(29)-H(29C)	109.5
H(29B)-C(29)-H(29C)	109.5
C(28)-C(30)-H(30A)	109.5
C(28)-C(30)-H(30B)	109.5
H(30A)-C(30)-H(30B)	109.5
C(28)-C(30)-H(30C)	109.5
H(30A)-C(30)-H(30C)	109.5
H(30B)-C(30)-H(30C)	109.5
C(32)-C(31)-C(33)	110.8(3)

C(32)-C(31)-Si(2)	111.2(2)
C(33)-C(31)-Si(2)	112.6(2)
C(32)-C(31)-H(31)	107.3
C(33)-C(31)-H(31)	107.3
Si(2)-C(31)-H(31)	107.3
C(31)-C(32)-H(32A)	109.5
C(31)-C(32)-H(32B)	109.5
H(32A)-C(32)-H(32B)	109.5
C(31)-C(32)-H(32C)	109.5
H(32A)-C(32)-H(32C)	109.5
H(32B)-C(32)-H(32C)	109.5
C(31)-C(33)-H(33A)	109.5
C(31)-C(33)-H(33B)	109.5
H(33A)-C(33)-H(33B)	109.5
C(31)-C(33)-H(33C)	109.5
H(33A)-C(33)-H(33C)	109.5
H(33B)-C(33)-H(33C)	109.5
C(35)-C(34)-C(36)	110.4(3)
C(35)-C(34)-Si(2)	115.9(2)
C(36)-C(34)-Si(2)	112.4(2)
C(35)-C(34)-H(34)	105.7
C(36)-C(34)-H(34)	105.7
Si(2)-C(34)-H(34)	105.7
C(34)-C(35)-H(35A)	109.5
C(34)-C(35)-H(35B)	109.5
H(35A)-C(35)-H(35B)	109.5
C(34)-C(35)-H(35C)	109.5
H(35A)-C(35)-H(35C)	109.5
H(35B)-C(35)-H(35C)	109.5
C(34)-C(36)-H(36A)	109.5
C(34)-C(36)-H(36B)	109.5
H(36A)-C(36)-H(36B)	109.5
C(34)-C(36)-H(36C)	109.5
H(36A)-C(36)-H(36C)	109.5
H(36B)-C(36)-H(36C)	109.5
N(2)-N(1)-C(1)	109.6(2)

N(1)-N(2)-N(3)	107.1(2)
C(2)-N(3)-N(2)	110.5(2)
C(2)-N(3)-C(3)	128.7(2)
N(2)-N(3)-C(3)	120.6(2)
N(5)-N(4)-C(19)	109.4(2)
N(4)-N(5)-N(6)	107.3(2)
C(20)-N(6)-N(5)	110.3(2)
C(20)-N(6)-C(21)	129.5(2)
N(5)-N(6)-C(21)	120.2(2)

Symmetry transformations used to generate equivalent atoms:

Anisotropic displacement parameters ($\text{\AA}^2 \times 10^3$) for merg4. The anisotropic displacement factor exponent takes the form: $-2\pi^2 [h^2 a^{*2} U^{11} + \dots + 2 h k a^* b^* U^{12}]$

	U ¹¹	U ²²	U ³³	U ²³	U ¹³	U ¹²
Si(1)	22(1)	22(1)	20(1)	0(1)	0(1)	3(1)
Si(2)	20(1)	22(1)	19(1)	2(1)	2(1)	1(1)
C(1)	22(2)	20(2)	20(1)	-1(1)	-3(1)	0(1)
C(2)	29(2)	17(2)	23(2)	-3(1)	-1(1)	-3(1)
C(3)	25(2)	32(2)	26(2)	-3(1)	5(2)	-3(2)
C(4)	23(2)	30(2)	22(2)	-6(1)	7(1)	0(2)
C(5)	34(2)	25(2)	27(2)	-5(1)	8(2)	-4(2)
C(6)	39(2)	33(2)	32(2)	3(1)	0(2)	3(2)
C(7)	31(2)	50(2)	26(2)	-5(1)	-1(2)	5(2)
C(8)	32(2)	32(2)	33(2)	-12(1)	1(2)	-4(2)
C(9)	29(2)	28(2)	28(2)	-2(1)	6(1)	1(2)
C(10)	34(2)	26(2)	35(2)	7(1)	-3(2)	4(2)
C(11)	72(3)	55(2)	43(2)	9(2)	-19(2)	27(2)
C(12)	47(2)	27(2)	54(2)	0(2)	-2(2)	12(2)
C(13)	24(2)	23(2)	20(1)	-1(1)	0(1)	1(1)
C(14)	32(2)	32(2)	31(2)	0(1)	-2(2)	-2(2)
C(15)	30(2)	30(2)	28(2)	2(1)	-7(2)	0(2)
C(16)	23(2)	26(2)	33(2)	-3(1)	1(2)	2(2)
C(17)	30(2)	57(2)	46(2)	-14(2)	0(2)	-7(2)
C(18)	26(2)	37(2)	38(2)	-1(1)	7(2)	-2(2)
C(19)	18(2)	22(2)	22(2)	-1(1)	3(1)	0(1)
C(20)	19(2)	17(1)	26(2)	-4(1)	3(1)	2(1)
C(21)	29(2)	26(2)	20(2)	-2(1)	2(1)	-1(1)
C(22)	27(2)	18(2)	21(2)	0(1)	3(1)	3(1)
C(23)	32(2)	35(2)	21(2)	1(1)	3(2)	-7(2)
C(24)	32(2)	41(2)	37(2)	-2(2)	-2(2)	-11(2)
C(25)	30(2)	41(2)	44(2)	8(2)	8(2)	-8(2)
C(26)	36(2)	47(2)	29(2)	9(2)	10(2)	-2(2)
C(27)	30(2)	36(2)	22(2)	2(1)	0(2)	2(2)
C(28)	22(2)	22(2)	20(2)	2(1)	2(1)	1(1)
C(29)	26(2)	40(2)	31(2)	1(1)	-1(2)	7(2)

C(30)	27(2)	29(2)	27(2)	1(1)	1(2)	1(2)
C(31)	23(2)	27(2)	22(2)	0(1)	0(1)	4(1)
C(32)	27(2)	30(2)	39(2)	-1(1)	-4(2)	-3(2)
C(33)	28(2)	33(2)	38(2)	1(1)	-5(2)	2(2)
C(34)	31(2)	24(2)	27(2)	5(1)	4(2)	-1(2)
C(35)	56(3)	37(2)	40(2)	5(2)	0(2)	-14(2)
C(36)	45(2)	33(2)	34(2)	14(1)	14(2)	3(2)
N(1)	30(2)	22(1)	22(1)	-2(1)	3(1)	-2(1)
N(2)	35(2)	23(1)	26(1)	1(1)	3(1)	-1(1)
N(3)	25(2)	25(1)	18(1)	-1(1)	1(1)	-4(1)
N(4)	32(2)	27(1)	27(1)	3(1)	6(1)	3(1)
N(5)	37(2)	23(1)	28(1)	1(1)	7(1)	6(1)
N(6)	21(1)	20(1)	23(1)	2(1)	0(1)	0(1)

Hydrogen coordinates ($\times 10^4$) and isotropic displacement parameters ($\text{\AA}^2 \times 10^{-3}$)
for merg4.

	x	y	z	U(eq)
H(2)	1682	1337	2699	28
H(3A)	-885	1906	3324	33
H(3B)	-889	2698	3325	33
H(5)	706	1312	4026	34
H(6)	2327	1313	4844	41
H(7)	3510	2284	5186	42
H(8)	3017	3278	4714	39
H(9)	1377	3288	3902	34
H(10)	3740	555	2017	38
H(11A)	5871	374	2655	85
H(11B)	5167	1107	2764	85
H(11C)	6949	999	2441	85
H(12A)	6966	583	1451	64
H(12B)	5196	369	1161	64
H(12C)	5978	-66	1660	64
H(13)	3424	1285	721	26
H(14A)	667	1122	1501	48
H(14B)	1804	543	1234	48
H(14C)	489	948	849	48
H(15A)	1229	2031	485	44
H(15B)	2877	2424	710	44
H(15C)	1243	2324	1108	44
H(16)	5420	2657	1399	33
H(17A)	8037	1880	1914	66
H(17B)	6822	2376	2255	66
H(17C)	8115	2658	1792	66
H(18A)	7621	2388	779	50
H(18B)	5886	2029	587	50
H(18C)	7358	1616	899	50
H(20)	1806	3973	1996	25

H(21A)	286	4876	3227	30
H(21B)	1089	4170	3079	30
H(23)	-2329	4067	2280	35
H(24)	-4899	3524	2470	44
H(25)	-5620	3258	3388	46
H(26)	-3849	3607	4124	45
H(27)	-1320	4168	3934	35
H(28)	3232	3661	1138	25
H(29A)	6040	3878	1385	49
H(29B)	4872	4460	1632	49
H(29C)	5997	4582	1080	49
H(30A)	5083	4045	160	41
H(30B)	3522	3530	167	41
H(30C)	5287	3352	477	41
H(31)	1003	4240	-44	29
H(32A)	-907	3809	913	48
H(32B)	479	3377	578	48
H(32C)	-1303	3571	286	48
H(33A)	-1884	4667	-40	50
H(33B)	-452	5235	-36	50
H(33C)	-1446	5049	530	50
H(34)	1856	5760	438	33
H(35A)	5028	5724	1029	66
H(35B)	3258	5968	1301	66
H(35C)	4090	6370	791	66
H(36A)	4171	5867	-167	56
H(36B)	3229	5177	-285	56
H(36C)	4997	5193	58	56

Torsion angles [°] for merg4.

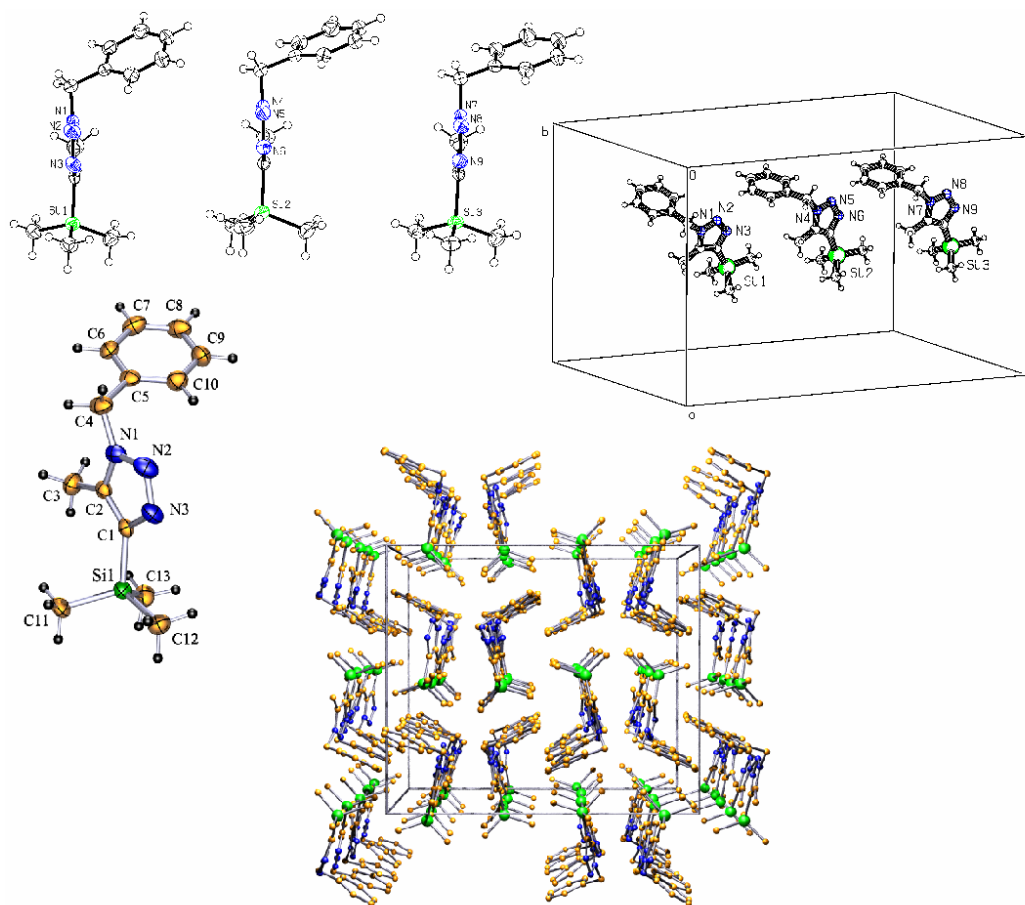
C(10)-Si(1)-C(1)-C(2)	-27.9(3)
C(13)-Si(1)-C(1)-C(2)	87.9(3)
C(16)-Si(1)-C(1)-C(2)	-154.3(3)
C(10)-Si(1)-C(1)-N(1)	158.0(2)
C(13)-Si(1)-C(1)-N(1)	-86.1(3)
C(16)-Si(1)-C(1)-N(1)	31.6(3)
N(1)-C(1)-C(2)-N(3)	-0.1(3)
Si(1)-C(1)-C(2)-N(3)	-175.0(2)
N(3)-C(3)-C(4)-C(9)	80.0(4)
N(3)-C(3)-C(4)-C(5)	-97.5(3)
C(9)-C(4)-C(5)-C(6)	0.3(5)
C(3)-C(4)-C(5)-C(6)	177.9(3)
C(4)-C(5)-C(6)-C(7)	-0.7(5)
C(5)-C(6)-C(7)-C(8)	0.7(5)
C(6)-C(7)-C(8)-C(9)	-0.3(5)
C(7)-C(8)-C(9)-C(4)	-0.1(5)
C(5)-C(4)-C(9)-C(8)	0.1(5)
C(3)-C(4)-C(9)-C(8)	-177.6(3)
C(1)-Si(1)-C(10)-C(11)	-56.4(3)
C(13)-Si(1)-C(10)-C(11)	-171.0(3)
C(16)-Si(1)-C(10)-C(11)	64.7(3)
C(1)-Si(1)-C(10)-C(12)	175.8(2)
C(13)-Si(1)-C(10)-C(12)	61.2(3)
C(16)-Si(1)-C(10)-C(12)	-63.1(3)
C(1)-Si(1)-C(13)-C(15)	57.6(2)
C(10)-Si(1)-C(13)-C(15)	173.2(2)
C(16)-Si(1)-C(13)-C(15)	-58.7(2)
C(1)-Si(1)-C(13)-C(14)	-66.9(2)
C(10)-Si(1)-C(13)-C(14)	48.6(2)
C(16)-Si(1)-C(13)-C(14)	176.8(2)
C(1)-Si(1)-C(16)-C(18)	-160.0(2)
C(10)-Si(1)-C(16)-C(18)	78.9(3)
C(13)-Si(1)-C(16)-C(18)	-44.5(3)
C(1)-Si(1)-C(16)-C(17)	72.8(2)

C(10)-Si(1)-C(16)-C(17)	-48.3(3)
C(13)-Si(1)-C(16)-C(17)	-171.7(2)
C(34)-Si(2)-C(19)-C(20)	-141.5(3)
C(31)-Si(2)-C(19)-C(20)	99.8(3)
C(28)-Si(2)-C(19)-C(20)	-16.8(3)
C(34)-Si(2)-C(19)-N(4)	35.2(3)
C(31)-Si(2)-C(19)-N(4)	-83.5(3)
C(28)-Si(2)-C(19)-N(4)	159.8(3)
N(4)-C(19)-C(20)-N(6)	-0.2(3)
Si(2)-C(19)-C(20)-N(6)	177.0(2)
N(6)-C(21)-C(22)-C(23)	12.1(4)
N(6)-C(21)-C(22)-C(27)	-171.1(3)
C(27)-C(22)-C(23)-C(24)	-0.7(5)
C(21)-C(22)-C(23)-C(24)	176.1(3)
C(22)-C(23)-C(24)-C(25)	-1.2(5)
C(23)-C(24)-C(25)-C(26)	2.4(5)
C(24)-C(25)-C(26)-C(27)	-1.6(5)
C(25)-C(26)-C(27)-C(22)	-0.3(5)
C(23)-C(22)-C(27)-C(26)	1.4(5)
C(21)-C(22)-C(27)-C(26)	-175.5(3)
C(19)-Si(2)-C(28)-C(30)	165.5(2)
C(34)-Si(2)-C(28)-C(30)	-74.2(2)
C(31)-Si(2)-C(28)-C(30)	48.9(2)
C(19)-Si(2)-C(28)-C(29)	-67.5(2)
C(34)-Si(2)-C(28)-C(29)	52.8(2)
C(31)-Si(2)-C(28)-C(29)	176.0(2)
C(19)-Si(2)-C(31)-C(32)	-55.6(2)
C(34)-Si(2)-C(31)-C(32)	-174.8(2)
C(28)-Si(2)-C(31)-C(32)	57.6(2)
C(19)-Si(2)-C(31)-C(33)	69.4(2)
C(34)-Si(2)-C(31)-C(33)	-49.8(3)
C(28)-Si(2)-C(31)-C(33)	-177.4(2)
C(19)-Si(2)-C(34)-C(35)	44.7(3)
C(31)-Si(2)-C(34)-C(35)	163.8(3)
C(28)-Si(2)-C(34)-C(35)	-72.6(3)
C(19)-Si(2)-C(34)-C(36)	173.0(2)

C(31)-Si(2)-C(34)-C(36)	-67.9(3)
C(28)-Si(2)-C(34)-C(36)	55.7(3)
C(2)-C(1)-N(1)-N(2)	0.6(3)
Si(1)-C(1)-N(1)-N(2)	175.8(2)
C(1)-N(1)-N(2)-N(3)	-0.7(3)
C(1)-C(2)-N(3)-N(2)	-0.3(3)
C(1)-C(2)-N(3)-C(3)	-175.8(3)
N(1)-N(2)-N(3)-C(2)	0.7(3)
N(1)-N(2)-N(3)-C(3)	176.6(2)
C(4)-C(3)-N(3)-C(2)	82.7(4)
C(4)-C(3)-N(3)-N(2)	-92.4(3)
C(20)-C(19)-N(4)-N(5)	0.0(3)
Si(2)-C(19)-N(4)-N(5)	-177.3(2)
C(19)-N(4)-N(5)-N(6)	0.3(3)
C(19)-C(20)-N(6)-N(5)	0.4(3)
C(19)-C(20)-N(6)-C(21)	-179.6(3)
N(4)-N(5)-N(6)-C(20)	-0.4(3)
N(4)-N(5)-N(6)-C(21)	179.6(3)
C(22)-C(21)-N(6)-C(20)	-97.3(4)
C(22)-C(21)-N(6)-N(5)	82.7(3)

Symmetry transformations used to generate equivalent atoms:

X-Ray Structure Determination, C₁₃H₁₉N₃Si



X-ray intensity data from a colorless plate were measured at 150(1) K on a Bruker SMART APEX CCD-based diffractometer (Mo K α radiation, $\lambda = 0.71073$ Å).¹ Raw data frame integration and Lp corrections were performed with SAINT+.¹ Final unit cell parameters were determined by least-squares refinement of 7543 reflections from the data set with $I > 5(\sigma)I$. Analysis of the data showed negligible crystal decay during collection. No absorption correction was applied. Direct methods structure solution, difference Fourier calculations and full-matrix least-squares refinement against F^2 were performed with SHELXTL.²

C₁₃H₁₉N₃Si crystallizes in the orthorhombic space group *Pbca* as determined uniquely by the pattern of systematic absences in the intensity data. The asymmetric unit consists of three crystallographically independent but chemically identical molecules. Non-hydrogen atoms were refined with anisotropic displacement parameters; hydrogen atoms were placed in geometrically idealized positions and included as riding atoms.

(1) SMART Version 5.625 and SAINT+ Version 6.22. Bruker Analytical X-ray Systems, Inc., Madison, Wisconsin, USA, 2001.

(2) Sheldrick, G. M. SHELXTL Version 6.1; Bruker Analytical X-ray Systems, Inc., Madison, Wisconsin, USA, 2000.

Table A9. Crystal data and structure refinement for bce11m.

Identification code	bce11m	
Empirical formula	C13 H19 N3 Si	
Formula weight	245.40	
Temperature	150(2) K	
Wavelength	0.71073 Å	
Crystal system	Orthorhombic	
Space group	Pbca	
Unit cell dimensions	a = 16.6219(9) Å	$\alpha = 90^\circ$.
	b = 19.4081(10) Å	$\beta = 90^\circ$.
	c = 26.6198(14) Å	$\gamma = 90^\circ$.
Volume	8587.5(8) Å ³	
Z	24	
Density (calculated)	1.139 Mg/m ³	
Absorption coefficient	0.148 mm ⁻¹	
F(000)	3168	
Crystal size	0.60 x 0.28 x 0.10 mm ³	
Theta range for data collection	1.53 to 26.42°.	
Index ranges	-20 ≤ h ≤ 20, -24 ≤ k ≤ 21, -33 ≤ l ≤ 31	
Reflections collected	60170	
Independent reflections	8813 [R(int) = 0.0727]	
Completeness to theta = 26.42°	99.9 %	
Absorption correction	None	
Refinement method	Full-matrix least-squares on F ²	
Data / restraints / parameters	8813 / 0 / 472	
Goodness-of-fit on F ²	1.027	
Final R indices [I > 2σ(I)]	R1 = 0.0422, wR2 = 0.0921	
R indices (all data)	R1 = 0.0681, wR2 = 0.0999	
Largest diff. peak and hole	0.266 and -0.237 e.Å ⁻³	

Atomic coordinates ($\times 10^4$) and equivalent isotropic displacement parameters ($\text{\AA}^2 \times 10^3$) for bce11m. $U(\text{eq})$ is defined as one third of the trace of the orthogonalized U^{ij} tensor.

	x	y	z	U(eq)
Si(1)	5210(1)	3722(1)	2629(1)	32(1)
Si(2)	5141(1)	3753(1)	5876(1)	32(1)
Si(3)	5173(1)	3647(1)	9171(1)	33(1)
C(1)	4312(1)	3499(1)	2237(1)	27(1)
C(2)	4222(1)	3420(1)	1725(1)	30(1)
C(3)	4772(1)	3540(1)	1293(1)	45(1)
C(4)	3044(1)	2988(1)	1200(1)	44(1)
C(5)	2634(1)	3583(1)	940(1)	34(1)
C(6)	2688(1)	3651(1)	426(1)	40(1)
C(7)	2289(1)	4179(1)	180(1)	46(1)
C(8)	1846(1)	4647(1)	450(1)	46(1)
C(9)	1791(1)	4589(1)	963(1)	46(1)
C(10)	2174(1)	4055(1)	1210(1)	40(1)
C(11)	6021(1)	3096(1)	2469(1)	44(1)
C(12)	4895(1)	3636(1)	3296(1)	46(1)
C(13)	5544(1)	4621(1)	2496(1)	47(1)
C(14)	4132(1)	3605(1)	5579(1)	26(1)
C(15)	3893(1)	3427(1)	5101(1)	28(1)
C(16)	4330(1)	3348(1)	4615(1)	40(1)
C(17)	2512(1)	3125(1)	4745(1)	34(1)
C(18)	2287(1)	3695(1)	4385(1)	33(1)
C(19)	2401(1)	3621(1)	3876(1)	44(1)
C(20)	2172(1)	4142(1)	3545(1)	55(1)
C(21)	1830(1)	4734(1)	3731(1)	55(1)
C(22)	1722(1)	4815(1)	4238(1)	50(1)
C(23)	1950(1)	4299(1)	4568(1)	40(1)
C(24)	5884(1)	3141(1)	5603(1)	42(1)
C(25)	4996(1)	3595(1)	6558(1)	51(1)
C(26)	5478(1)	4657(1)	5762(1)	46(1)
C(27)	4168(1)	3466(1)	8879(1)	27(1)
C(28)	3927(1)	3383(1)	8386(1)	27(1)

C(29)	4366(1)	3423(1)	7898(1)	39(1)
C(30)	2559(1)	3086(1)	8008(1)	34(1)
C(31)	2332(1)	3710(1)	7698(1)	31(1)
C(32)	2457(1)	3718(1)	7185(1)	41(1)
C(33)	2228(1)	4280(1)	6899(1)	48(1)
C(34)	1872(1)	4839(1)	7128(1)	45(1)
C(35)	1755(1)	4841(1)	7638(1)	43(1)
C(36)	1983(1)	4277(1)	7925(1)	36(1)
C(37)	5914(1)	3001(1)	8943(1)	46(1)
C(38)	5023(1)	3585(1)	9863(1)	49(1)
C(39)	5503(1)	4535(1)	9002(1)	50(1)
N(1)	3462(1)	3184(1)	1661(1)	34(1)
N(2)	3087(1)	3122(1)	2106(1)	42(1)
N(3)	3598(1)	3311(1)	2457(1)	37(1)
N(4)	3084(1)	3346(1)	5132(1)	28(1)
N(5)	2818(1)	3480(1)	5601(1)	33(1)
N(6)	3451(1)	3636(1)	5873(1)	31(1)
N(7)	3129(1)	3243(1)	8411(1)	28(1)
N(8)	2872(1)	3242(1)	8892(1)	33(1)
N(9)	3500(1)	3374(1)	9175(1)	32(1)

Bond lengths [Å] and angles [°] for bce11m.

Si(1)-C(12)	1.8565(18)
Si(1)-C(13)	1.8641(18)
Si(1)-C(11)	1.8642(16)
Si(1)-C(1)	1.8726(16)
Si(2)-C(25)	1.8585(19)
Si(2)-C(24)	1.8610(17)
Si(2)-C(26)	1.8667(17)
Si(2)-C(14)	1.8768(15)
Si(3)-C(37)	1.8598(17)
Si(3)-C(39)	1.8629(18)
Si(3)-C(38)	1.8635(19)
Si(3)-C(27)	1.8755(15)
C(1)-N(3)	1.3742(19)
C(1)-C(2)	1.379(2)
C(2)-N(1)	1.3542(19)
C(2)-C(3)	1.489(2)
C(3)-H(3A)	0.9800
C(3)-H(3B)	0.9800
C(3)-H(3C)	0.9800
C(4)-N(1)	1.459(2)
C(4)-C(5)	1.509(2)
C(4)-H(4A)	0.9900
C(4)-H(4B)	0.9900
C(5)-C(6)	1.377(2)
C(5)-C(10)	1.393(2)
C(6)-C(7)	1.385(2)
C(6)-H(6)	0.9500
C(7)-C(8)	1.372(3)
C(7)-H(7)	0.9500
C(8)-C(9)	1.373(3)
C(8)-H(8)	0.9500
C(9)-C(10)	1.381(2)
C(9)-H(9)	0.9500
C(10)-H(10)	0.9500

C(11)-H(11A)	0.9800
C(11)-H(11B)	0.9800
C(11)-H(11C)	0.9800
C(12)-H(12A)	0.9800
C(12)-H(12B)	0.9800
C(12)-H(12C)	0.9800
C(13)-H(13A)	0.9800
C(13)-H(13B)	0.9800
C(13)-H(13C)	0.9800
C(14)-N(6)	1.3768(19)
C(14)-C(15)	1.377(2)
C(15)-N(4)	1.3570(18)
C(15)-C(16)	1.491(2)
C(16)-H(16A)	0.9800
C(16)-H(16B)	0.9800
C(16)-H(16C)	0.9800
C(17)-N(4)	1.4667(19)
C(17)-C(18)	1.509(2)
C(17)-H(17A)	0.9900
C(17)-H(17B)	0.9900
C(18)-C(19)	1.377(3)
C(18)-C(23)	1.387(2)
C(19)-C(20)	1.393(3)
C(19)-H(19)	0.9500
C(20)-C(21)	1.373(3)
C(20)-H(20)	0.9500
C(21)-C(22)	1.370(3)
C(21)-H(21)	0.9500
C(22)-C(23)	1.385(2)
C(22)-H(22)	0.9500
C(23)-H(23)	0.9500
C(24)-H(24A)	0.9800
C(24)-H(24B)	0.9800
C(24)-H(24C)	0.9800
C(25)-H(25A)	0.9800
C(25)-H(25B)	0.9800

C(25)-H(25C)	0.9800
C(26)-H(26A)	0.9800
C(26)-H(26B)	0.9800
C(26)-H(26C)	0.9800
C(27)-N(9)	1.3739(19)
C(27)-C(28)	1.380(2)
C(28)-N(7)	1.3566(18)
C(28)-C(29)	1.491(2)
C(29)-H(29A)	0.9800
C(29)-H(29B)	0.9800
C(29)-H(29C)	0.9800
C(30)-N(7)	1.463(2)
C(30)-C(31)	1.514(2)
C(30)-H(30A)	0.9900
C(30)-H(30B)	0.9900
C(31)-C(32)	1.380(2)
C(31)-C(36)	1.385(2)
C(32)-C(33)	1.384(2)
C(32)-H(32)	0.9500
C(33)-C(34)	1.377(2)
C(33)-H(33)	0.9500
C(34)-C(35)	1.371(3)
C(34)-H(34)	0.9500
C(35)-C(36)	1.387(2)
C(35)-H(35)	0.9500
C(36)-H(36)	0.9500
C(37)-H(37A)	0.9800
C(37)-H(37B)	0.9800
C(37)-H(37C)	0.9800
C(38)-H(38A)	0.9800
C(38)-H(38B)	0.9800
C(38)-H(38C)	0.9800
C(39)-H(39A)	0.9800
C(39)-H(39B)	0.9800
C(39)-H(39C)	0.9800
N(1)-N(2)	1.345(2)

N(2)-N(3)	1.3141(19)
N(4)-N(5)	1.3489(18)
N(5)-N(6)	1.3128(18)
N(7)-N(8)	1.3484(18)
N(8)-N(9)	1.3125(18)

C(12)-Si(1)-C(13)	110.49(9)
C(12)-Si(1)-C(11)	111.35(9)
C(13)-Si(1)-C(11)	110.50(8)
C(12)-Si(1)-C(1)	106.72(8)
C(13)-Si(1)-C(1)	110.36(8)
C(11)-Si(1)-C(1)	107.32(8)
C(25)-Si(2)-C(24)	111.23(9)
C(25)-Si(2)-C(26)	110.64(9)
C(24)-Si(2)-C(26)	109.76(8)
C(25)-Si(2)-C(14)	105.63(8)
C(24)-Si(2)-C(14)	109.37(7)
C(26)-Si(2)-C(14)	110.14(8)
C(37)-Si(3)-C(39)	110.50(9)
C(37)-Si(3)-C(38)	111.59(9)
C(39)-Si(3)-C(38)	109.69(9)
C(37)-Si(3)-C(27)	109.17(7)
C(39)-Si(3)-C(27)	109.60(8)
C(38)-Si(3)-C(27)	106.19(8)
N(3)-C(1)-C(2)	107.35(14)
N(3)-C(1)-Si(1)	120.78(12)
C(2)-C(1)-Si(1)	131.61(12)
N(1)-C(2)-C(1)	105.33(14)
N(1)-C(2)-C(3)	121.88(16)
C(1)-C(2)-C(3)	132.79(15)
C(2)-C(3)-H(3A)	109.5
C(2)-C(3)-H(3B)	109.5
H(3A)-C(3)-H(3B)	109.5
C(2)-C(3)-H(3C)	109.5
H(3A)-C(3)-H(3C)	109.5
H(3B)-C(3)-H(3C)	109.5

N(1)-C(4)-C(5)	113.70(14)
N(1)-C(4)-H(4A)	108.8
C(5)-C(4)-H(4A)	108.8
N(1)-C(4)-H(4B)	108.8
C(5)-C(4)-H(4B)	108.8
H(4A)-C(4)-H(4B)	107.7
C(6)-C(5)-C(10)	118.94(16)
C(6)-C(5)-C(4)	120.00(16)
C(10)-C(5)-C(4)	121.03(17)
C(5)-C(6)-C(7)	120.69(17)
C(5)-C(6)-H(6)	119.7
C(7)-C(6)-H(6)	119.7
C(8)-C(7)-C(6)	119.87(19)
C(8)-C(7)-H(7)	120.1
C(6)-C(7)-H(7)	120.1
C(7)-C(8)-C(9)	120.12(18)
C(7)-C(8)-H(8)	119.9
C(9)-C(8)-H(8)	119.9
C(8)-C(9)-C(10)	120.28(18)
C(8)-C(9)-H(9)	119.9
C(10)-C(9)-H(9)	119.9
C(9)-C(10)-C(5)	120.08(18)
C(9)-C(10)-H(10)	120.0
C(5)-C(10)-H(10)	120.0
Si(1)-C(11)-H(11A)	109.5
Si(1)-C(11)-H(11B)	109.5
H(11A)-C(11)-H(11B)	109.5
Si(1)-C(11)-H(11C)	109.5
H(11A)-C(11)-H(11C)	109.5
H(11B)-C(11)-H(11C)	109.5
Si(1)-C(12)-H(12A)	109.5
Si(1)-C(12)-H(12B)	109.5
H(12A)-C(12)-H(12B)	109.5
Si(1)-C(12)-H(12C)	109.5
H(12A)-C(12)-H(12C)	109.5
H(12B)-C(12)-H(12C)	109.5

Si(1)-C(13)-H(13A)	109.5
Si(1)-C(13)-H(13B)	109.5
H(13A)-C(13)-H(13B)	109.5
Si(1)-C(13)-H(13C)	109.5
H(13A)-C(13)-H(13C)	109.5
H(13B)-C(13)-H(13C)	109.5
N(6)-C(14)-C(15)	107.43(13)
N(6)-C(14)-Si(2)	119.31(12)
C(15)-C(14)-Si(2)	133.19(12)
N(4)-C(15)-C(14)	104.94(14)
N(4)-C(15)-C(16)	121.64(15)
C(14)-C(15)-C(16)	133.38(14)
C(15)-C(16)-H(16A)	109.5
C(15)-C(16)-H(16B)	109.5
H(16A)-C(16)-H(16B)	109.5
C(15)-C(16)-H(16C)	109.5
H(16A)-C(16)-H(16C)	109.5
H(16B)-C(16)-H(16C)	109.5
N(4)-C(17)-C(18)	113.13(13)
N(4)-C(17)-H(17A)	109.0
C(18)-C(17)-H(17A)	109.0
N(4)-C(17)-H(17B)	109.0
C(18)-C(17)-H(17B)	109.0
H(17A)-C(17)-H(17B)	107.8
C(19)-C(18)-C(23)	119.27(17)
C(19)-C(18)-C(17)	120.91(16)
C(23)-C(18)-C(17)	119.81(17)
C(18)-C(19)-C(20)	120.53(19)
C(18)-C(19)-H(19)	119.7
C(20)-C(19)-H(19)	119.7
C(21)-C(20)-C(19)	119.5(2)
C(21)-C(20)-H(20)	120.2
C(19)-C(20)-H(20)	120.2
C(22)-C(21)-C(20)	120.32(19)
C(22)-C(21)-H(21)	119.8
C(20)-C(21)-H(21)	119.8

C(21)-C(22)-C(23)	120.36(19)
C(21)-C(22)-H(22)	119.8
C(23)-C(22)-H(22)	119.8
C(22)-C(23)-C(18)	119.96(19)
C(22)-C(23)-H(23)	120.0
C(18)-C(23)-H(23)	120.0
Si(2)-C(24)-H(24A)	109.5
Si(2)-C(24)-H(24B)	109.5
H(24A)-C(24)-H(24B)	109.5
Si(2)-C(24)-H(24C)	109.5
H(24A)-C(24)-H(24C)	109.5
H(24B)-C(24)-H(24C)	109.5
Si(2)-C(25)-H(25A)	109.5
Si(2)-C(25)-H(25B)	109.5
H(25A)-C(25)-H(25B)	109.5
Si(2)-C(25)-H(25C)	109.5
H(25A)-C(25)-H(25C)	109.5
H(25B)-C(25)-H(25C)	109.5
Si(2)-C(26)-H(26A)	109.5
Si(2)-C(26)-H(26B)	109.5
H(26A)-C(26)-H(26B)	109.5
Si(2)-C(26)-H(26C)	109.5
H(26A)-C(26)-H(26C)	109.5
H(26B)-C(26)-H(26C)	109.5
N(9)-C(27)-C(28)	107.23(13)
N(9)-C(27)-Si(3)	120.39(12)
C(28)-C(27)-Si(3)	132.37(12)
N(7)-C(28)-C(27)	105.10(14)
N(7)-C(28)-C(29)	122.12(15)
C(27)-C(28)-C(29)	132.79(14)
C(28)-C(29)-H(29A)	109.5
C(28)-C(29)-H(29B)	109.5
H(29A)-C(29)-H(29B)	109.5
C(28)-C(29)-H(29C)	109.5
H(29A)-C(29)-H(29C)	109.5
H(29B)-C(29)-H(29C)	109.5

N(7)-C(30)-C(31)	113.23(13)
N(7)-C(30)-H(30A)	108.9
C(31)-C(30)-H(30A)	108.9
N(7)-C(30)-H(30B)	108.9
C(31)-C(30)-H(30B)	108.9
H(30A)-C(30)-H(30B)	107.7
C(32)-C(31)-C(36)	119.13(16)
C(32)-C(31)-C(30)	120.75(15)
C(36)-C(31)-C(30)	120.11(16)
C(31)-C(32)-C(33)	120.77(17)
C(31)-C(32)-H(32)	119.6
C(33)-C(32)-H(32)	119.6
C(34)-C(33)-C(32)	119.64(18)
C(34)-C(33)-H(33)	120.2
C(32)-C(33)-H(33)	120.2
C(35)-C(34)-C(33)	120.16(17)
C(35)-C(34)-H(34)	119.9
C(33)-C(34)-H(34)	119.9
C(34)-C(35)-C(36)	120.30(17)
C(34)-C(35)-H(35)	119.9
C(36)-C(35)-H(35)	119.9
C(31)-C(36)-C(35)	120.00(17)
C(31)-C(36)-H(36)	120.0
C(35)-C(36)-H(36)	120.0
Si(3)-C(37)-H(37A)	109.5
Si(3)-C(37)-H(37B)	109.5
H(37A)-C(37)-H(37B)	109.5
Si(3)-C(37)-H(37C)	109.5
H(37A)-C(37)-H(37C)	109.5
H(37B)-C(37)-H(37C)	109.5
Si(3)-C(38)-H(38A)	109.5
Si(3)-C(38)-H(38B)	109.5
H(38A)-C(38)-H(38B)	109.5
Si(3)-C(38)-H(38C)	109.5
H(38A)-C(38)-H(38C)	109.5
H(38B)-C(38)-H(38C)	109.5

Si(3)-C(39)-H(39A)	109.5
Si(3)-C(39)-H(39B)	109.5
H(39A)-C(39)-H(39B)	109.5
Si(3)-C(39)-H(39C)	109.5
H(39A)-C(39)-H(39C)	109.5
H(39B)-C(39)-H(39C)	109.5
N(2)-N(1)-C(2)	110.51(14)
N(2)-N(1)-C(4)	119.78(14)
C(2)-N(1)-C(4)	129.69(16)
N(3)-N(2)-N(1)	107.63(13)
N(2)-N(3)-C(1)	109.18(14)
N(5)-N(4)-C(15)	111.04(13)
N(5)-N(4)-C(17)	119.66(13)
C(15)-N(4)-C(17)	129.27(14)
N(6)-N(5)-N(4)	107.00(12)
N(5)-N(6)-C(14)	109.57(13)
N(8)-N(7)-C(28)	110.85(13)
N(8)-N(7)-C(30)	119.38(13)
C(28)-N(7)-C(30)	129.74(14)
N(9)-N(8)-N(7)	107.09(12)
N(8)-N(9)-C(27)	109.73(13)

Symmetry transformations used to generate equivalent atoms:

Anisotropic displacement parameters ($\text{\AA}^2 \times 10^3$) for bce11m. The anisotropic displacement factor exponent takes the form: $-2\pi^2 [h^2 a^{*2} U^{11} + \dots + 2 h k a^* b^* U^{12}]$

	U ¹¹	U ²²	U ³³	U ²³	U ¹³	U ¹²
Si(1)	28(1)	34(1)	33(1)	-3(1)	-1(1)	1(1)
Si(2)	28(1)	33(1)	33(1)	-1(1)	-2(1)	-4(1)
Si(3)	28(1)	36(1)	37(1)	-3(1)	-3(1)	-3(1)
C(1)	26(1)	23(1)	32(1)	2(1)	2(1)	4(1)
C(2)	31(1)	23(1)	36(1)	1(1)	-1(1)	4(1)
C(3)	50(1)	48(1)	36(1)	-4(1)	6(1)	2(1)
C(4)	50(1)	31(1)	51(1)	-4(1)	-19(1)	-3(1)
C(5)	34(1)	27(1)	41(1)	-2(1)	-9(1)	-6(1)
C(6)	42(1)	36(1)	42(1)	-9(1)	-4(1)	-3(1)
C(7)	61(1)	43(1)	34(1)	1(1)	-8(1)	-10(1)
C(8)	54(1)	36(1)	48(1)	6(1)	-17(1)	0(1)
C(9)	45(1)	42(1)	52(1)	-2(1)	-6(1)	10(1)
C(10)	45(1)	41(1)	35(1)	3(1)	-3(1)	1(1)
C(11)	30(1)	47(1)	53(1)	-5(1)	-4(1)	7(1)
C(12)	49(1)	54(1)	34(1)	-3(1)	-4(1)	3(1)
C(13)	42(1)	41(1)	57(1)	-7(1)	2(1)	-8(1)
C(14)	27(1)	23(1)	30(1)	-1(1)	3(1)	1(1)
C(15)	27(1)	23(1)	33(1)	1(1)	1(1)	3(1)
C(16)	37(1)	51(1)	32(1)	-5(1)	3(1)	4(1)
C(17)	34(1)	29(1)	41(1)	-1(1)	-7(1)	-3(1)
C(18)	28(1)	29(1)	42(1)	1(1)	-9(1)	-5(1)
C(19)	47(1)	40(1)	46(1)	-3(1)	-10(1)	-6(1)
C(20)	64(1)	56(1)	43(1)	11(1)	-17(1)	-18(1)
C(21)	52(1)	43(1)	71(2)	23(1)	-27(1)	-13(1)
C(22)	40(1)	34(1)	75(2)	6(1)	-14(1)	2(1)
C(23)	34(1)	35(1)	51(1)	1(1)	-5(1)	0(1)
C(24)	28(1)	41(1)	57(1)	-2(1)	-4(1)	1(1)
C(25)	50(1)	67(1)	35(1)	2(1)	-9(1)	-12(1)
C(26)	41(1)	37(1)	61(1)	-5(1)	2(1)	-9(1)
C(27)	26(1)	25(1)	31(1)	1(1)	2(1)	2(1)
C(28)	27(1)	23(1)	32(1)	2(1)	2(1)	2(1)

C(29)	36(1)	48(1)	34(1)	0(1)	6(1)	-2(1)
C(30)	32(1)	31(1)	40(1)	-3(1)	-7(1)	-1(1)
C(31)	26(1)	32(1)	35(1)	-3(1)	-5(1)	0(1)
C(32)	44(1)	42(1)	36(1)	-8(1)	-6(1)	9(1)
C(33)	58(1)	51(1)	33(1)	2(1)	-6(1)	9(1)
C(34)	47(1)	40(1)	47(1)	6(1)	-10(1)	8(1)
C(35)	39(1)	37(1)	53(1)	-5(1)	-3(1)	13(1)
C(36)	34(1)	41(1)	33(1)	-2(1)	0(1)	4(1)
C(37)	27(1)	49(1)	61(1)	-10(1)	-7(1)	2(1)
C(38)	46(1)	61(1)	39(1)	-2(1)	-10(1)	-7(1)
C(39)	43(1)	43(1)	66(2)	-3(1)	7(1)	-11(1)
N(1)	37(1)	27(1)	39(1)	4(1)	-8(1)	-1(1)
N(2)	32(1)	46(1)	50(1)	13(1)	-4(1)	-6(1)
N(3)	28(1)	43(1)	40(1)	11(1)	1(1)	1(1)
N(4)	27(1)	24(1)	33(1)	2(1)	-2(1)	0(1)
N(5)	29(1)	35(1)	35(1)	3(1)	3(1)	-1(1)
N(6)	30(1)	33(1)	31(1)	0(1)	3(1)	0(1)
N(7)	28(1)	26(1)	31(1)	1(1)	-2(1)	1(1)
N(8)	28(1)	38(1)	32(1)	3(1)	2(1)	0(1)
N(9)	28(1)	36(1)	30(1)	2(1)	1(1)	1(1)

Hydrogen coordinates ($\times 10^4$) and isotropic displacement parameters ($\text{\AA}^2 \times 10^{-3}$)
for bce11m.

	x	y	z	U(eq)
H(3A)	4882	3102	1123	67
H(3B)	5279	3738	1414	67
H(3C)	4519	3860	1055	67
H(4A)	2637	2633	1282	53
H(4B)	3437	2779	966	53
H(6)	3003	3334	239	48
H(7)	2322	4217	-175	55
H(8)	1577	5012	282	56
H(9)	1489	4916	1149	55
H(10)	2124	4011	1564	48
H(11A)	6148	3132	2110	65
H(11B)	5838	2628	2545	65
H(11C)	6503	3201	2667	65
H(12A)	5352	3741	3515	68
H(12B)	4712	3164	3358	68
H(12C)	4455	3958	3365	68
H(13A)	6050	4712	2673	70
H(13B)	5132	4945	2611	70
H(13C)	5627	4677	2134	70
H(16A)	4234	2885	4480	60
H(16B)	4908	3413	4671	60
H(16C)	4136	3693	4375	60
H(17A)	2018	2952	4909	41
H(17B)	2751	2740	4552	41
H(19)	2638	3211	3748	53
H(20)	2251	4088	3194	65
H(21)	1668	5089	3507	66
H(22)	1490	5228	4363	60
H(23)	1875	4359	4919	48
H(24A)	6398	3185	5781	64

H(24B)	5963	3246	5246	64
H(24C)	5683	2668	5638	64
H(25A)	5505	3672	6735	76
H(25B)	4820	3118	6610	76
H(25C)	4587	3911	6689	76
H(26A)	5110	4976	5930	69
H(26B)	5479	4750	5400	69
H(26C)	6023	4719	5896	69
H(29A)	4317	2982	7721	59
H(29B)	4935	3522	7961	59
H(29C)	4134	3790	7692	59
H(30A)	2065	2886	8157	41
H(30B)	2799	2734	7785	41
H(32)	2703	3333	7027	49
H(33)	2315	4281	6546	57
H(34)	1708	5223	6933	54
H(35)	1516	5230	7795	52
H(36)	1899	4281	8278	43
H(37A)	6443	3098	9089	69
H(37B)	5950	3025	8576	69
H(37C)	5740	2538	9043	69
H(38A)	5536	3666	10034	73
H(38B)	4823	3125	9948	73
H(38C)	4631	3932	9970	73
H(39A)	5136	4871	9154	76
H(39B)	5496	4588	8636	76
H(39C)	6050	4612	9128	76

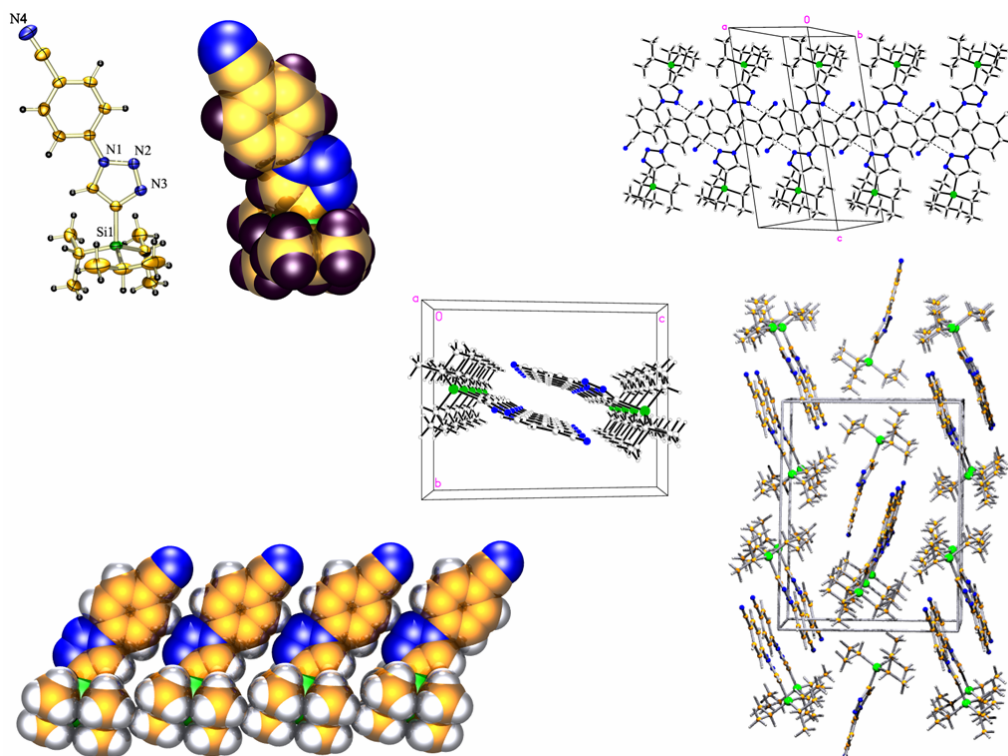
Torsion angles [°] for bce11m.

C(12)-Si(1)-C(1)-N(3)	-0.45(15)
C(13)-Si(1)-C(1)-N(3)	-120.54(13)
C(11)-Si(1)-C(1)-N(3)	119.00(13)
C(12)-Si(1)-C(1)-C(2)	-173.71(15)
C(13)-Si(1)-C(1)-C(2)	66.20(17)
C(11)-Si(1)-C(1)-C(2)	-54.25(17)
N(3)-C(1)-C(2)-N(1)	-0.51(16)
Si(1)-C(1)-C(2)-N(1)	173.43(12)
N(3)-C(1)-C(2)-C(3)	179.82(16)
Si(1)-C(1)-C(2)-C(3)	-6.3(3)
N(1)-C(4)-C(5)-C(6)	136.63(17)
N(1)-C(4)-C(5)-C(10)	-45.5(2)
C(10)-C(5)-C(6)-C(7)	-0.4(2)
C(4)-C(5)-C(6)-C(7)	177.52(16)
C(5)-C(6)-C(7)-C(8)	1.2(3)
C(6)-C(7)-C(8)-C(9)	-0.7(3)
C(7)-C(8)-C(9)-C(10)	-0.7(3)
C(8)-C(9)-C(10)-C(5)	1.5(3)
C(6)-C(5)-C(10)-C(9)	-0.9(2)
C(4)-C(5)-C(10)-C(9)	-178.84(16)
C(25)-Si(2)-C(14)-N(6)	20.48(14)
C(24)-Si(2)-C(14)-N(6)	140.28(12)
C(26)-Si(2)-C(14)-N(6)	-99.02(13)
C(25)-Si(2)-C(14)-C(15)	-155.88(16)
C(24)-Si(2)-C(14)-C(15)	-36.08(18)
C(26)-Si(2)-C(14)-C(15)	84.62(17)
N(6)-C(14)-C(15)-N(4)	-1.29(17)
Si(2)-C(14)-C(15)-N(4)	175.38(12)
N(6)-C(14)-C(15)-C(16)	176.36(16)
Si(2)-C(14)-C(15)-C(16)	-7.0(3)
N(4)-C(17)-C(18)-C(19)	123.21(16)
N(4)-C(17)-C(18)-C(23)	-57.6(2)
C(23)-C(18)-C(19)-C(20)	-0.9(2)
C(17)-C(18)-C(19)-C(20)	178.27(15)

C(18)-C(19)-C(20)-C(21)	0.1(3)
C(19)-C(20)-C(21)-C(22)	0.6(3)
C(20)-C(21)-C(22)-C(23)	-0.5(3)
C(21)-C(22)-C(23)-C(18)	-0.2(3)
C(19)-C(18)-C(23)-C(22)	0.9(2)
C(17)-C(18)-C(23)-C(22)	-178.25(15)
C(37)-Si(3)-C(27)-N(9)	125.13(13)
C(39)-Si(3)-C(27)-N(9)	-113.72(13)
C(38)-Si(3)-C(27)-N(9)	4.69(15)
C(37)-Si(3)-C(27)-C(28)	-53.22(17)
C(39)-Si(3)-C(27)-C(28)	67.93(17)
C(38)-Si(3)-C(27)-C(28)	-173.65(15)
N(9)-C(27)-C(28)-N(7)	-0.20(16)
Si(3)-C(27)-C(28)-N(7)	178.31(12)
N(9)-C(27)-C(28)-C(29)	179.67(16)
Si(3)-C(27)-C(28)-C(29)	-1.8(3)
N(7)-C(30)-C(31)-C(32)	122.38(17)
N(7)-C(30)-C(31)-C(36)	-58.6(2)
C(36)-C(31)-C(32)-C(33)	-0.9(3)
C(30)-C(31)-C(32)-C(33)	178.14(16)
C(31)-C(32)-C(33)-C(34)	0.1(3)
C(32)-C(33)-C(34)-C(35)	0.8(3)
C(33)-C(34)-C(35)-C(36)	-0.9(3)
C(32)-C(31)-C(36)-C(35)	0.8(2)
C(30)-C(31)-C(36)-C(35)	-178.26(15)
C(34)-C(35)-C(36)-C(31)	0.1(3)
C(1)-C(2)-N(1)-N(2)	0.59(17)
C(3)-C(2)-N(1)-N(2)	-179.69(14)
C(1)-C(2)-N(1)-C(4)	-177.84(15)
C(3)-C(2)-N(1)-C(4)	1.9(2)
C(5)-C(4)-N(1)-N(2)	94.58(19)
C(5)-C(4)-N(1)-C(2)	-87.1(2)
C(2)-N(1)-N(2)-N(3)	-0.44(18)
C(4)-N(1)-N(2)-N(3)	178.16(13)
N(1)-N(2)-N(3)-C(1)	0.10(18)
C(2)-C(1)-N(3)-N(2)	0.26(18)

Si(1)-C(1)-N(3)-N(2)	-174.46(11)
C(14)-C(15)-N(4)-N(5)	1.40(17)
C(16)-C(15)-N(4)-N(5)	-176.59(14)
C(14)-C(15)-N(4)-C(17)	-176.73(14)
C(16)-C(15)-N(4)-C(17)	5.3(2)
C(18)-C(17)-N(4)-N(5)	102.28(17)
C(18)-C(17)-N(4)-C(15)	-79.7(2)
C(15)-N(4)-N(5)-N(6)	-0.96(16)
C(17)-N(4)-N(5)-N(6)	177.38(12)
N(4)-N(5)-N(6)-C(14)	0.10(16)
C(15)-C(14)-N(6)-N(5)	0.77(17)
Si(2)-C(14)-N(6)-N(5)	-176.45(10)
C(27)-C(28)-N(7)-N(8)	0.46(16)
C(29)-C(28)-N(7)-N(8)	-179.43(14)
C(27)-C(28)-N(7)-C(30)	-177.71(14)
C(29)-C(28)-N(7)-C(30)	2.4(2)
C(31)-C(30)-N(7)-N(8)	107.96(16)
C(31)-C(30)-N(7)-C(28)	-74.0(2)
C(28)-N(7)-N(8)-N(9)	-0.55(17)
C(30)-N(7)-N(8)-N(9)	177.83(12)
N(7)-N(8)-N(9)-C(27)	0.41(17)
C(28)-C(27)-N(9)-N(8)	-0.13(17)
Si(3)-C(27)-N(9)-N(8)	-178.85(10)

X-Ray Structure Determination, $C_{18}H_{26}N_4Si$



X-ray intensity data from a colorless block were measured at 150(1) K on a Bruker SMART APEX CCD-based diffractometer (Mo $K\alpha$ radiation, $\lambda = 0.71073$ Å).¹ Raw data frame integration and Lp corrections were performed with SAINT+.¹ Final unit cell parameters were determined by least-squares refinement of 8234 reflections from the data set with $I > 5(\sigma)I$. Analysis of the data showed negligible crystal decay during collection. No absorption correction was applied. Direct methods structure solution, difference Fourier calculations and full-matrix least-squares refinement against F^2 were performed with SHELXTL.²

$C_{18}H_{26}N_4Si$ crystallizes in the space group $P2_1/n$ as uniquely determined by the pattern of systematic absences in the intensity data. All non-hydrogen atoms were refined with anisotropic displacement parameters. Hydrogen atoms were placed in geometrically idealized positions and included as riding atoms.

(1) SMART Version 5.625 and SAINT+ Version 6.22. Bruker Analytical X-ray Systems, Inc., Madison, Wisconsin, USA, 2001.

(2) Sheldrick, G. M. SHELXTL Version 6.1; Bruker Analytical X-ray Systems, Inc., Madison, Wisconsin, USA, 2000.

Table A10. Crystal data and structure refinement for sb187m.

Identification code	sb187m	
Empirical formula	C ₁₈ H ₂₆ N ₄ Si	
Formula weight	326.52	
Temperature	150(1) K	
Wavelength	0.71073 Å	
Crystal system	Orthorhombic	
Space group	P2 ₁ /n	
Unit cell dimensions	a = 7.4598(4) Å	α = 90°.
	b = 14.1758(7) Å	β = 99.7570(10)°.
	c = 18.1362(9) Å	γ = 90°.
Volume	1890.14(17) Å ³	
Z	4	
Density (calculated)	1.147 Mg/m ³	
Absorption coefficient	0.129 mm ⁻¹	
F(000)	704	
Crystal size	0.50 x 0.44 x 0.40 mm ³	
Theta range for data collection	1.83 to 25.05°.	
Index ranges	-8 ≤ h ≤ 8, -16 ≤ k ≤ 16, -21 ≤ l ≤ 21	
Reflections collected	13613	
Independent reflections	3334 [R(int) = 0.0421]	
Completeness to theta = 25.05°	100.0 %	
Absorption correction	None	
Refinement method	Full-matrix least-squares on F ²	
Data / restraints / parameters	3334 / 0 / 214	
Goodness-of-fit on F ²	1.055	
Final R indices [I > 2σ(I)]	R1 = 0.0532, wR2 = 0.1464	
R indices (all data)	R1 = 0.0601, wR2 = 0.1515	
Largest diff. peak and hole	0.541 and -0.273 e.Å ⁻³	

Atomic coordinates ($\times 10^4$) and equivalent isotropic displacement parameters ($\text{\AA}^2 \times 10^3$) for sb187m. $U(\text{eq})$ is defined as one third of the trace of the orthogonalized U^{ij} tensor.

	x	y	z	U(eq)
Si(1)	2047(1)	4527(1)	1718(1)	34(1)
C(1)	3063(3)	5006(2)	2665(1)	33(1)
C(2)	4848(3)	5077(2)	2993(1)	34(1)
C(3)	6376(3)	5824(1)	4192(1)	28(1)
C(4)	8098(3)	5845(2)	4007(1)	35(1)
C(5)	9571(3)	6081(2)	4547(1)	38(1)
C(6)	9314(3)	6300(2)	5266(1)	35(1)
C(7)	7574(3)	6292(2)	5445(1)	34(1)
C(8)	6098(3)	6058(2)	4908(1)	31(1)
C(9)	10895(3)	6505(2)	5823(2)	45(1)
C(10)	3900(3)	3795(2)	1396(1)	39(1)
C(11)	3401(4)	3483(2)	578(1)	57(1)
C(12)	4572(3)	2952(2)	1901(2)	48(1)
C(13)	-81(3)	3845(2)	1796(1)	45(1)
C(14)	214(4)	2952(2)	2273(2)	62(1)
C(15)	-1188(4)	3612(3)	1030(2)	66(1)
C(16)	1533(4)	5563(2)	1078(1)	56(1)
C(17)	150(6)	6224(3)	1318(2)	96(2)
C(18)	3286(5)	6103(2)	985(2)	77(1)
N(1)	4872(2)	5549(1)	3644(1)	29(1)
N(2)	3151(2)	5768(1)	3726(1)	33(1)
N(3)	2067(2)	5441(1)	3141(1)	35(1)
N(4)	12186(3)	6642(2)	6246(1)	62(1)

Bond lengths [Å] and angles [°] for sb187m.

Si(1)-C(16)	1.871(3)
Si(1)-C(1)	1.883(2)
Si(1)-C(13)	1.884(3)
Si(1)-C(10)	1.898(2)
C(1)-C(2)	1.367(3)
C(1)-N(3)	1.376(3)
C(2)-N(1)	1.354(3)
C(2)-H(2)	0.9500
C(3)-C(4)	1.383(3)
C(3)-C(8)	1.389(3)
C(3)-N(1)	1.422(3)
C(4)-C(5)	1.384(3)
C(4)-H(4)	0.9500
C(5)-C(6)	1.386(3)
C(5)-H(5)	0.9500
C(6)-C(7)	1.390(3)
C(6)-C(9)	1.446(3)
C(7)-C(8)	1.382(3)
C(7)-H(7)	0.9500
C(8)-H(8)	0.9500
C(9)-N(4)	1.141(3)
C(10)-C(11)	1.534(3)
C(10)-C(12)	1.537(3)
C(10)-H(10)	1.0000
C(11)-H(11A)	0.9800
C(11)-H(11B)	0.9800
C(11)-H(11C)	0.9800
C(12)-H(12A)	0.9800
C(12)-H(12B)	0.9800
C(12)-H(12C)	0.9800
C(13)-C(14)	1.527(4)
C(13)-C(15)	1.529(3)
C(13)-H(13)	1.0000
C(14)-H(14A)	0.9800

C(14)-H(14B)	0.9800
C(14)-H(14C)	0.9800
C(15)-H(15A)	0.9800
C(15)-H(15B)	0.9800
C(15)-H(15C)	0.9800
C(16)-C(17)	1.512(4)
C(16)-C(18)	1.549(5)
C(16)-H(16)	1.0000
C(17)-H(17A)	0.9800
C(17)-H(17B)	0.9800
C(17)-H(17C)	0.9800
C(18)-H(18A)	0.9800
C(18)-H(18B)	0.9800
C(18)-H(18C)	0.9800
N(1)-N(2)	1.353(2)
N(2)-N(3)	1.306(3)

C(16)-Si(1)-C(1)	106.93(11)
C(16)-Si(1)-C(13)	111.27(13)
C(1)-Si(1)-C(13)	109.29(10)
C(16)-Si(1)-C(10)	108.73(12)
C(1)-Si(1)-C(10)	106.01(10)
C(13)-Si(1)-C(10)	114.23(11)
C(2)-C(1)-N(3)	106.47(18)
C(2)-C(1)-Si(1)	129.47(16)
N(3)-C(1)-Si(1)	123.84(16)
N(1)-C(2)-C(1)	106.49(19)
N(1)-C(2)-H(2)	126.8
C(1)-C(2)-H(2)	126.8
C(4)-C(3)-C(8)	121.0(2)
C(4)-C(3)-N(1)	119.40(18)
C(8)-C(3)-N(1)	119.61(18)
C(3)-C(4)-C(5)	119.5(2)
C(3)-C(4)-H(4)	120.3
C(5)-C(4)-H(4)	120.3
C(4)-C(5)-C(6)	120.0(2)

C(4)-C(5)-H(5)	120.0
C(6)-C(5)-H(5)	120.0
C(5)-C(6)-C(7)	120.2(2)
C(5)-C(6)-C(9)	118.4(2)
C(7)-C(6)-C(9)	121.4(2)
C(8)-C(7)-C(6)	120.1(2)
C(8)-C(7)-H(7)	120.0
C(6)-C(7)-H(7)	120.0
C(7)-C(8)-C(3)	119.3(2)
C(7)-C(8)-H(8)	120.4
C(3)-C(8)-H(8)	120.4
N(4)-C(9)-C(6)	177.0(3)
C(11)-C(10)-C(12)	110.7(2)
C(11)-C(10)-Si(1)	112.68(17)
C(12)-C(10)-Si(1)	114.99(16)
C(11)-C(10)-H(10)	105.9
C(12)-C(10)-H(10)	105.9
Si(1)-C(10)-H(10)	105.9
C(10)-C(11)-H(11A)	109.5
C(10)-C(11)-H(11B)	109.5
H(11A)-C(11)-H(11B)	109.5
C(10)-C(11)-H(11C)	109.5
H(11A)-C(11)-H(11C)	109.5
H(11B)-C(11)-H(11C)	109.5
C(10)-C(12)-H(12A)	109.5
C(10)-C(12)-H(12B)	109.5
H(12A)-C(12)-H(12B)	109.5
C(10)-C(12)-H(12C)	109.5
H(12A)-C(12)-H(12C)	109.5
H(12B)-C(12)-H(12C)	109.5
C(14)-C(13)-C(15)	109.8(2)
C(14)-C(13)-Si(1)	115.15(18)
C(15)-C(13)-Si(1)	112.00(18)
C(14)-C(13)-H(13)	106.4
C(15)-C(13)-H(13)	106.4
Si(1)-C(13)-H(13)	106.4

C(13)-C(14)-H(14A)	109.5
C(13)-C(14)-H(14B)	109.5
H(14A)-C(14)-H(14B)	109.5
C(13)-C(14)-H(14C)	109.5
H(14A)-C(14)-H(14C)	109.5
H(14B)-C(14)-H(14C)	109.5
C(13)-C(15)-H(15A)	109.5
C(13)-C(15)-H(15B)	109.5
H(15A)-C(15)-H(15B)	109.5
C(13)-C(15)-H(15C)	109.5
H(15A)-C(15)-H(15C)	109.5
H(15B)-C(15)-H(15C)	109.5
C(17)-C(16)-C(18)	110.8(3)
C(17)-C(16)-Si(1)	112.7(2)
C(18)-C(16)-Si(1)	111.6(2)
C(17)-C(16)-H(16)	107.1
C(18)-C(16)-H(16)	107.1
Si(1)-C(16)-H(16)	107.1
C(16)-C(17)-H(17A)	109.5
C(16)-C(17)-H(17B)	109.5
H(17A)-C(17)-H(17B)	109.5
C(16)-C(17)-H(17C)	109.5
H(17A)-C(17)-H(17C)	109.5
H(17B)-C(17)-H(17C)	109.5
C(16)-C(18)-H(18A)	109.5
C(16)-C(18)-H(18B)	109.5
H(18A)-C(18)-H(18B)	109.5
C(16)-C(18)-H(18C)	109.5
H(18A)-C(18)-H(18C)	109.5
H(18B)-C(18)-H(18C)	109.5
N(2)-N(1)-C(2)	109.69(17)
N(2)-N(1)-C(3)	120.70(16)
C(2)-N(1)-C(3)	129.60(18)
N(3)-N(2)-N(1)	107.25(16)
N(2)-N(3)-C(1)	110.10(17)

Symmetry transformations used to generate equivalent atoms:

Anisotropic displacement parameters ($\text{\AA}^2 \times 10^3$) for sb187m. The anisotropic displacement factor exponent takes the form: $-2\pi^2 [h^2 a^{*2} U^{11} + \dots + 2 h k a^* b^* U^{12}]$

	U^{11}	U^{22}	U^{33}	U^{23}	U^{13}	U^{12}
Si(1)	37(1)	38(1)	24(1)	-3(1)	-1(1)	1(1)
C(1)	37(1)	34(1)	26(1)	-2(1)	2(1)	3(1)
C(2)	37(1)	38(1)	27(1)	-6(1)	4(1)	4(1)
C(3)	34(1)	23(1)	26(1)	1(1)	2(1)	0(1)
C(4)	40(1)	34(1)	30(1)	-4(1)	8(1)	-1(1)
C(5)	33(1)	35(1)	45(1)	-5(1)	7(1)	-2(1)
C(6)	37(1)	26(1)	37(1)	-2(1)	-3(1)	-1(1)
C(7)	47(1)	28(1)	26(1)	-2(1)	4(1)	-3(1)
C(8)	35(1)	30(1)	29(1)	0(1)	6(1)	-3(1)
C(9)	46(1)	35(1)	48(1)	-5(1)	-3(1)	0(1)
C(10)	38(1)	44(1)	36(1)	-5(1)	7(1)	-4(1)
C(11)	54(2)	78(2)	40(1)	-19(1)	8(1)	6(1)
C(12)	47(1)	40(1)	56(2)	-4(1)	9(1)	5(1)
C(13)	41(1)	61(2)	34(1)	-10(1)	8(1)	-4(1)
C(14)	55(2)	76(2)	57(2)	4(2)	13(1)	-17(2)
C(15)	47(2)	106(3)	44(2)	-12(2)	2(1)	-27(2)
C(16)	84(2)	41(2)	34(1)	-3(1)	-14(1)	8(1)
C(17)	137(3)	83(3)	54(2)	-16(2)	-30(2)	66(2)
C(18)	118(3)	48(2)	56(2)	12(1)	-11(2)	-20(2)
N(1)	32(1)	29(1)	25(1)	0(1)	4(1)	3(1)
N(2)	32(1)	39(1)	29(1)	-3(1)	3(1)	3(1)
N(3)	34(1)	41(1)	29(1)	-2(1)	0(1)	4(1)
N(4)	53(1)	58(2)	67(2)	-12(1)	-17(1)	-2(1)

Hydrogen coordinates ($\times 10^4$) and isotropic displacement parameters ($\text{\AA}^2 \times 10^{-3}$)
for sb187m.

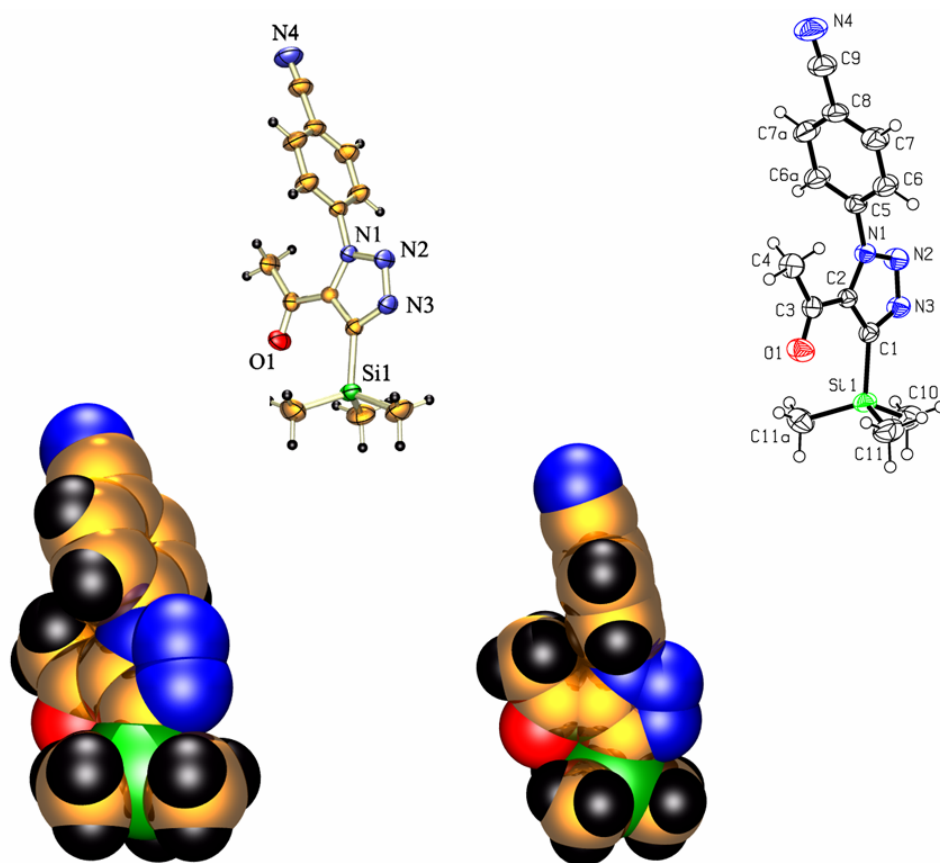
	x	y	z	U(eq)
H(2)	5871	4842	2802	41
H(4)	8269	5698	3512	42
H(5)	10760	6093	4425	45
H(7)	7400	6449	5938	41
H(8)	4905	6056	5027	37
H(10)	4970	4225	1417	47
H(11A)	4471	3206	413	86
H(11B)	2987	4030	264	86
H(11C)	2425	3012	532	86
H(12A)	3615	2472	1859	71
H(12B)	4872	3164	2422	71
H(12C)	5658	2682	1745	71
H(13)	-855	4273	2049	54
H(14A)	-962	2715	2364	93
H(14B)	989	3098	2752	93
H(14C)	805	2471	2009	93
H(15A)	-480	3193	759	99
H(15B)	-1472	4195	744	99
H(15C)	-2321	3297	1094	99
H(16)	993	5310	575	67
H(17A)	650	6502	1804	145
H(17B)	-960	5873	1359	145
H(17C)	-139	6727	945	145
H(18A)	2978	6616	624	115
H(18B)	4138	5669	804	115
H(18C)	3852	6365	1469	115

Torsion angles [°] for sb187m.

C(16)-Si(1)-C(1)-C(2)	-98.4(2)
C(13)-Si(1)-C(1)-C(2)	141.0(2)
C(10)-Si(1)-C(1)-C(2)	17.5(2)
C(16)-Si(1)-C(1)-N(3)	75.3(2)
C(13)-Si(1)-C(1)-N(3)	-45.2(2)
C(10)-Si(1)-C(1)-N(3)	-168.78(18)
N(3)-C(1)-C(2)-N(1)	-0.2(2)
Si(1)-C(1)-C(2)-N(1)	174.38(16)
C(8)-C(3)-C(4)-C(5)	1.5(3)
N(1)-C(3)-C(4)-C(5)	-177.79(19)
C(3)-C(4)-C(5)-C(6)	-0.4(3)
C(4)-C(5)-C(6)-C(7)	-0.6(3)
C(4)-C(5)-C(6)-C(9)	177.5(2)
C(5)-C(6)-C(7)-C(8)	0.6(3)
C(9)-C(6)-C(7)-C(8)	-177.5(2)
C(6)-C(7)-C(8)-C(3)	0.4(3)
C(4)-C(3)-C(8)-C(7)	-1.5(3)
N(1)-C(3)-C(8)-C(7)	177.77(18)
C(5)-C(6)-C(9)-N(4)	-29(6)
C(7)-C(6)-C(9)-N(4)	149(6)
C(16)-Si(1)-C(10)-C(11)	-56.1(2)
C(1)-Si(1)-C(10)-C(11)	-170.71(19)
C(13)-Si(1)-C(10)-C(11)	68.9(2)
C(16)-Si(1)-C(10)-C(12)	175.86(18)
C(1)-Si(1)-C(10)-C(12)	61.21(19)
C(13)-Si(1)-C(10)-C(12)	-59.2(2)
C(16)-Si(1)-C(13)-C(14)	176.68(19)
C(1)-Si(1)-C(13)-C(14)	-65.5(2)
C(10)-Si(1)-C(13)-C(14)	53.1(2)
C(16)-Si(1)-C(13)-C(15)	50.2(2)
C(1)-Si(1)-C(13)-C(15)	168.1(2)
C(10)-Si(1)-C(13)-C(15)	-73.3(2)
C(1)-Si(1)-C(16)-C(17)	-62.3(3)
C(13)-Si(1)-C(16)-C(17)	56.9(3)

C(10)-Si(1)-C(16)-C(17)	-176.4(2)
C(1)-Si(1)-C(16)-C(18)	63.1(2)
C(13)-Si(1)-C(16)-C(18)	-177.7(2)
C(10)-Si(1)-C(16)-C(18)	-51.0(2)
C(1)-C(2)-N(1)-N(2)	0.1(2)
C(1)-C(2)-N(1)-C(3)	-178.96(19)
C(4)-C(3)-N(1)-N(2)	-161.24(19)
C(8)-C(3)-N(1)-N(2)	19.5(3)
C(4)-C(3)-N(1)-C(2)	17.7(3)
C(8)-C(3)-N(1)-C(2)	-161.5(2)
C(2)-N(1)-N(2)-N(3)	0.0(2)
C(3)-N(1)-N(2)-N(3)	179.21(17)
N(1)-N(2)-N(3)-C(1)	-0.2(2)
C(2)-C(1)-N(3)-N(2)	0.3(3)
Si(1)-C(1)-N(3)-N(2)	-174.73(15)

X-Ray Structure Determination, C₁₄H₁₆N₄OSi



X-ray intensity data from a yellow plate were measured at 150(1) K on a Bruker SMART APEX CCD-based diffractometer (Mo K α radiation, $\lambda = 0.71073$ Å).¹ Raw data frame integration and Lp corrections were performed with SAINT+.¹ Final unit cell parameters were determined by least-squares refinement of 8878 reflections from the data set with $I > 5(\sigma)I$. Analysis of the data showed negligible crystal decay during collection. No absorption correction was applied. Direct methods structure solution, difference Fourier calculations and full-matrix least-squares refinement against F^2 were performed with SHELXTL.²

Systematic absences in the intensity data indicated the space groups Pna2₁ and Pnma, the latter of which was eventually confirmed. The asymmetric unit consists of half of the molecule, which resides on a crystallographic mirror plane. Non-hydrogen atoms were refined with anisotropic displacement parameters. Hydrogen atoms could be located in difference maps but were placed in idealized positions and included as riding atoms for the final refinement cycles.

(1) SMART Version 5.628 and SAINT+ Version 6.22. Bruker Analytical X-ray Systems, Inc., Madison, Wisconsin, USA, 2001.

(2) Sheldrick, G. M. SHELXTL Version 6.1; Bruker Analytical X-ray Systems, Inc., Madison, Wisconsin, USA, 2000.

Table A11. Crystal data and structure refinement for pnmam.

Identification code	pnmam	
Empirical formula	C ₁₄ H ₁₆ N ₄ O Si	
Formula weight	284.40	
Temperature	150(2) K	
Wavelength	0.71073 Å	
Crystal system	Orthorhombic	
Space group	Pnma	
Unit cell dimensions	a = 16.1527(10) Å	α = 90°.
	b = 7.0332(4) Å	β = 90°.
	c = 13.7637(9) Å	γ = 90°.
Volume	1563.63(17) Å ³	
Z	4	
Density (calculated)	1.208 Mg/m ³	
Absorption coefficient	0.151 mm ⁻¹	
F(000)	600	
Crystal size	0.54 x 0.40 x 0.12 mm ³	
Theta range for data collection	1.94 to 25.02°.	
Index ranges	-19 ≤ h ≤ 19, -8 ≤ k ≤ 7, -16 ≤ l ≤ 16	
Reflections collected	12537	
Independent reflections	1509 [R(int) = 0.0761]	
Completeness to theta = 25.02°	100.0 %	
Absorption correction	None	
Refinement method	Full-matrix least-squares on F ²	
Data / restraints / parameters	1509 / 0 / 113	
Goodness-of-fit on F ²	1.165	
Final R indices [I > 2σ(I)]	R1 = 0.0501, wR2 = 0.1242	
R indices (all data)	R1 = 0.0534, wR2 = 0.1261	
Largest diff. peak and hole	0.284 and -0.316 e.Å ⁻³	

Atomic coordinates ($\times 10^4$) and equivalent isotropic displacement parameters ($\text{\AA}^2 \times 10^3$) for pnmm. $U(\text{eq})$ is defined as one third of the trace of the orthogonalized U^{ij} tensor.

	x	y	z	U(eq)
Si(1)	5371(1)	2500	8206(1)	37(1)
C(1)	4435(2)	2500	7384(2)	31(1)
C(2)	4337(2)	2500	6386(2)	29(1)
C(3)	4992(2)	2500	5631(2)	33(1)
C(4)	4789(2)	2500	4571(2)	45(1)
C(5)	3025(2)	2500	5352(2)	33(1)
C(6)	2813(1)	790(4)	4942(2)	46(1)
C(7)	2391(2)	791(4)	4066(2)	51(1)
C(8)	2197(2)	2500	3626(2)	43(1)
C(9)	1810(2)	2500	2675(3)	53(1)
C(10)	4925(3)	2500	9461(2)	61(1)
C(11)	5979(2)	300(4)	8007(2)	60(1)
N(1)	3500(1)	2500	6235(2)	31(1)
N(2)	3098(2)	2500	7088(2)	41(1)
N(3)	3661(2)	2500	7779(2)	38(1)
N(4)	1531(2)	2500	1910(2)	68(1)
O(1)	5708(1)	2500	5912(2)	50(1)

Bond lengths [Å] and angles [°] for pnmam.

Si(1)-C(11)#1	1.853(3)
Si(1)-C(11)	1.853(3)
Si(1)-C(10)	1.872(4)
Si(1)-C(1)	1.888(3)
C(1)-N(3)	1.363(4)
C(1)-C(2)	1.383(4)
C(2)-N(1)	1.368(3)
C(2)-C(3)	1.483(4)
C(3)-O(1)	1.219(4)
C(3)-C(4)	1.495(4)
C(4)-H(4A)	0.9800
C(4)-H(4B)	0.9800
C(5)-C(6)	1.372(3)
C(5)-C(6)#1	1.372(3)
C(5)-N(1)	1.438(3)
C(6)-C(7)	1.385(3)
C(6)-H(6)	0.9500
C(7)-C(8)	1.382(3)
C(7)-H(7)	0.9500
C(8)-C(7)#1	1.382(3)
C(8)-C(9)	1.450(4)
C(9)-N(4)	1.145(4)
C(10)-H(10A)	0.9800
C(10)-H(10B)	0.9800
C(11)-H(11A)	0.9800
C(11)-H(11B)	0.9800
C(11)-H(11C)	0.9800
N(1)-N(2)	1.342(3)
N(2)-N(3)	1.316(3)
C(11)#1-Si(1)-C(11)	113.18(19)
C(11)#1-Si(1)-C(10)	109.91(11)
C(11)-Si(1)-C(10)	109.91(11)
C(11)#1-Si(1)-C(1)	109.65(9)

C(11)-Si(1)-C(1)	109.65(9)
C(10)-Si(1)-C(1)	104.17(15)
N(3)-C(1)-C(2)	107.0(2)
N(3)-C(1)-Si(1)	119.7(2)
C(2)-C(1)-Si(1)	133.3(2)
N(1)-C(2)-C(1)	105.3(2)
N(1)-C(2)-C(3)	126.7(2)
C(1)-C(2)-C(3)	128.0(2)
O(1)-C(3)-C(2)	116.9(3)
O(1)-C(3)-C(4)	121.2(3)
C(2)-C(3)-C(4)	121.8(2)
C(3)-C(4)-H(4A)	109.8
C(3)-C(4)-H(4B)	109.3
H(4A)-C(4)-H(4B)	109.4
C(6)-C(5)-C(6)#1	122.5(3)
C(6)-C(5)-N(1)	118.76(13)
C(6)#1-C(5)-N(1)	118.76(13)
C(5)-C(6)-C(7)	118.7(2)
C(5)-C(6)-H(6)	120.6
C(7)-C(6)-H(6)	120.6
C(8)-C(7)-C(6)	119.6(2)
C(8)-C(7)-H(7)	120.2
C(6)-C(7)-H(7)	120.2
C(7)#1-C(8)-C(7)	120.9(3)
C(7)#1-C(8)-C(9)	119.55(14)
C(7)-C(8)-C(9)	119.55(14)
N(4)-C(9)-C(8)	177.6(4)
Si(1)-C(10)-H(10A)	109.8
Si(1)-C(10)-H(10B)	109.3
H(10A)-C(10)-H(10B)	109.5
Si(1)-C(11)-H(11A)	109.5
Si(1)-C(11)-H(11B)	109.5
H(11A)-C(11)-H(11B)	109.5
Si(1)-C(11)-H(11C)	109.5
H(11A)-C(11)-H(11C)	109.5
H(11B)-C(11)-H(11C)	109.5

N(2)-N(1)-C(2)	110.3(2)
N(2)-N(1)-C(5)	118.7(2)
C(2)-N(1)-C(5)	131.0(2)
N(3)-N(2)-N(1)	107.3(2)
N(2)-N(3)-C(1)	110.2(2)

Symmetry transformations used to generate equivalent atoms:

#1 $x, -y+1/2, z$

Anisotropic displacement parameters ($\text{\AA}^2 \times 10^3$) for pnmm. The anisotropic displacement factor exponent takes the form: $-2\pi^2 [h^2 a^{*2} U^{11} + \dots + 2 h k a^* b^* U^{12}]$

	U^{11}	U^{22}	U^{33}	U^{23}	U^{13}	U^{12}
Si(1)	42(1)	38(1)	32(1)	0	-11(1)	0
C(1)	35(1)	31(2)	26(1)	0	-2(1)	0
C(2)	29(1)	30(2)	27(1)	0	-1(1)	0
C(3)	33(2)	34(2)	31(1)	0	3(1)	0
C(4)	39(2)	67(2)	30(2)	0	9(1)	0
C(5)	29(1)	46(2)	24(1)	0	-1(1)	0
C(6)	54(1)	46(1)	36(1)	1(1)	-12(1)	-1(1)
C(7)	58(1)	53(2)	41(1)	-7(1)	-16(1)	-5(1)
C(8)	35(2)	64(2)	31(2)	0	-8(1)	0
C(9)	49(2)	70(3)	41(2)	0	-12(2)	0
C(10)	72(2)	80(3)	32(2)	0	-14(2)	0
C(11)	59(2)	53(2)	69(2)	2(1)	-19(1)	16(1)
N(1)	30(1)	41(1)	22(1)	0	1(1)	0
N(2)	34(1)	64(2)	26(1)	0	4(1)	0
N(3)	37(1)	51(2)	24(1)	0	1(1)	0
N(4)	73(2)	85(3)	47(2)	0	-27(2)	0
O(1)	33(1)	75(2)	44(1)	0	4(1)	0

Hydrogen coordinates ($\times 10^4$) and isotropic displacement parameters ($\text{\AA}^2 \times 10^{-3}$)
for pnmam.

	x	y	z	U(eq)
H(4A)	5301	2500	4189	68
H(4B)	4466	1361	4415	68
H(6)	2952	-372	5254	55
H(7)	2236	-376	3769	61
H(10A)	5373	2500	9941	92
H(10B)	4582	3637	9549	92
H(11A)	6218	320	7352	91
H(11B)	5616	-809	8074	91
H(11C)	6425	227	8488	91

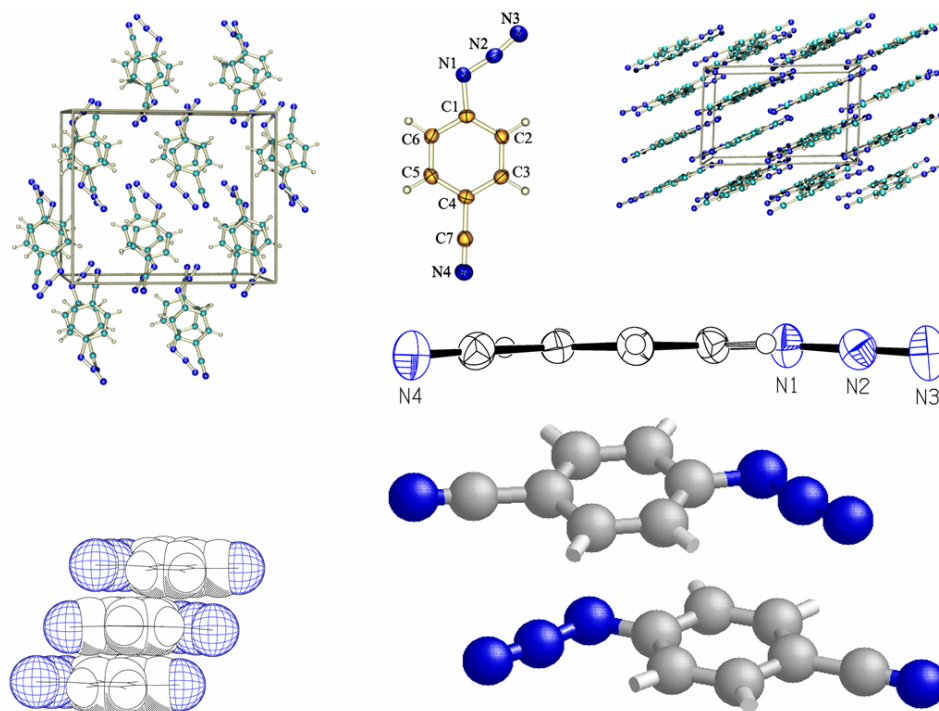
Torsion angles [°] for pnmam.

C(11)#1-Si(1)-C(1)-N(3)	-117.58(11)
C(11)-Si(1)-C(1)-N(3)	117.58(11)
C(10)-Si(1)-C(1)-N(3)	0.0
C(11)#1-Si(1)-C(1)-C(2)	62.42(11)
C(11)-Si(1)-C(1)-C(2)	-62.42(11)
C(10)-Si(1)-C(1)-C(2)	180.0
N(3)-C(1)-C(2)-N(1)	0.0
Si(1)-C(1)-C(2)-N(1)	180.0
N(3)-C(1)-C(2)-C(3)	180.0
Si(1)-C(1)-C(2)-C(3)	0.0
N(1)-C(2)-C(3)-O(1)	180.0
C(1)-C(2)-C(3)-O(1)	0.0
N(1)-C(2)-C(3)-C(4)	0.0
C(1)-C(2)-C(3)-C(4)	180.0
C(6)#1-C(5)-C(6)-C(7)	2.2(5)
N(1)-C(5)-C(6)-C(7)	-176.8(2)
C(5)-C(6)-C(7)-C(8)	0.2(4)
C(6)-C(7)-C(8)-C(7)#1	-2.5(5)
C(6)-C(7)-C(8)-C(9)	175.6(3)
C(7)#1-C(8)-C(9)-N(4)	89.0(3)
C(7)-C(8)-C(9)-N(4)	-89.0(3)
C(1)-C(2)-N(1)-N(2)	0.0
C(3)-C(2)-N(1)-N(2)	180.0
C(1)-C(2)-N(1)-C(5)	180.0
C(3)-C(2)-N(1)-C(5)	0.0
C(6)-C(5)-N(1)-N(2)	-90.5(2)
C(6)#1-C(5)-N(1)-N(2)	90.5(2)
C(6)-C(5)-N(1)-C(2)	89.5(2)
C(6)#1-C(5)-N(1)-C(2)	-89.5(2)
C(2)-N(1)-N(2)-N(3)	0.0
C(5)-N(1)-N(2)-N(3)	180.0
N(1)-N(2)-N(3)-C(1)	0.0
C(2)-C(1)-N(3)-N(2)	0.0
Si(1)-C(1)-N(3)-N(2)	180.0

Symmetry transformations used to generate equivalent atoms:

#1 $x, -y+1/2, z$

X-Ray Structure Determination, C₇H₄N₄



X-ray intensity data from a pale yellow parallelepiped were measured at 150(2) K on a Bruker SMART APEX CCD-based diffractometer (Mo K α radiation, $\lambda = 0.71073$ Å).¹ Raw data frame integration and Lp corrections were performed with SAINT+.¹ Final unit cell parameters were determined by least-squares refinement of 1840 reflections from the data set with $I > 5(\sigma)I$. Analysis of the data showed negligible crystal decay during collection. No correction for absorption was applied. Direct methods structure solution, difference Fourier calculations and full-matrix least-squares refinement against F^2 were performed with SHELXTL.²

C₇H₄N₄ crystallizes the space group C2/c as determined by the pattern of systematic absences in the intensity data and by the successful solution and refinement of the data. Non-hydrogen atoms were refined with anisotropic displacement parameters. Hydrogen atoms were located and freely refined with isotropic displacement parameters.

(1) SMART Version 5.625 and SAINT+ Version 6.22. Bruker Analytical X-ray Systems, Inc., Madison, Wisconsin, USA, 2001.

(2) Sheldrick, G. M. SHELXTL Version 6.1; Bruker Analytical X-ray Systems, Inc., Madison, Wisconsin, USA, 2000.

Table A12. Crystal data and structure refinement for sb1173m.

Identification code	sb1173m	
Empirical formula	C7 H4 N4	
Formula weight	144.14	
Temperature	150(2) K	
Wavelength	0.71073 Å	
Crystal system	Monoclinic	
Space group	C2/c	
Unit cell dimensions	a = 7.6716(7) Å	$\alpha = 90^\circ$.
	b = 14.8121(13) Å	$\beta = 92.753(2)^\circ$.
	c = 12.2933(11) Å	$\gamma = 90^\circ$.
Volume	1395.3(2) Å ³	
Z	8	
Density (calculated)	1.372 Mg/m ³	
Absorption coefficient	0.093 mm ⁻¹	
F(000)	592	
Crystal size	0.36 x 0.16 x 0.04 mm ³	
Theta range for data collection	2.75 to 25.02°.	
Index ranges	-9 ≤ h ≤ 9, -17 ≤ k ≤ 17, -14 ≤ l ≤ 14	
Reflections collected	5047	
Independent reflections	1234 [R(int) = 0.0562]	
Completeness to theta = 25.02°	99.9 %	
Absorption correction	None	
Refinement method	Full-matrix least-squares on F ²	
Data / restraints / parameters	1234 / 0 / 116	
Goodness-of-fit on F ²	0.952	
Final R indices [I > 2σ(I)]	R1 = 0.0387, wR2 = 0.0736	
R indices (all data)	R1 = 0.0572, wR2 = 0.0783	
Largest diff. peak and hole	0.136 and -0.179 e.Å ⁻³	

Atomic coordinates ($\times 10^4$) and equivalent isotropic displacement parameters ($\text{\AA}^2 \times 10^3$) for sb1173m. $U(\text{eq})$ is defined as one third of the trace of the orthogonalized U^{ij} tensor.

	x	y	z	U(eq)
C(1)	3057(2)	4217(1)	1644(1)	28(1)
C(2)	2930(2)	3322(1)	1968(1)	31(1)
C(3)	2255(2)	3124(1)	2957(1)	33(1)
C(4)	1707(2)	3813(1)	3629(1)	31(1)
C(5)	1850(2)	4707(1)	3298(1)	33(1)
C(6)	2534(2)	4906(1)	2314(1)	32(1)
C(7)	948(2)	3617(1)	4648(2)	35(1)
N(1)	3700(2)	4505(1)	642(1)	36(1)
N(2)	4123(2)	3910(1)	-12(1)	36(1)
N(3)	4557(2)	3470(1)	-703(1)	50(1)
N(4)	316(2)	3468(1)	5457(1)	45(1)

Bond lengths [Å] and angles [°] for sb1173m.

C(1)-C(6)	1.384(2)
C(1)-C(2)	1.390(2)
C(1)-N(1)	1.4138(19)
C(2)-C(3)	1.376(2)
C(2)-H(2)	0.942(15)
C(3)-C(4)	1.390(2)
C(3)-H(3)	0.947(16)
C(4)-C(5)	1.391(2)
C(4)-C(7)	1.436(2)
C(5)-C(6)	1.373(2)
C(5)-H(5)	0.950(15)
C(6)-H(6)	0.942(16)
C(7)-N(4)	1.1486(19)
N(1)-N(2)	1.2463(18)
N(2)-N(3)	1.1330(19)
C(6)-C(1)-C(2)	120.47(15)
C(6)-C(1)-N(1)	114.84(15)
C(2)-C(1)-N(1)	124.69(15)
C(3)-C(2)-C(1)	119.38(16)
C(3)-C(2)-H(2)	122.1(10)
C(1)-C(2)-H(2)	118.6(10)
C(2)-C(3)-C(4)	120.44(17)
C(2)-C(3)-H(3)	119.7(10)
C(4)-C(3)-H(3)	119.8(10)
C(3)-C(4)-C(5)	119.63(16)
C(3)-C(4)-C(7)	121.13(15)
C(5)-C(4)-C(7)	119.22(15)
C(6)-C(5)-C(4)	120.04(16)
C(6)-C(5)-H(5)	120.1(9)
C(4)-C(5)-H(5)	119.9(9)
C(5)-C(6)-C(1)	120.03(16)
C(5)-C(6)-H(6)	122.7(10)
C(1)-C(6)-H(6)	117.3(10)

N(4)-C(7)-C(4)	178.84(18)
N(2)-N(1)-C(1)	117.51(13)
N(3)-N(2)-N(1)	170.15(17)

Anisotropic displacement parameters ($\text{\AA}^2 \times 10^3$) for sb1173m. The anisotropic displacement factor exponent takes the form: $-2\pi^2 [h^2 a^{*2} U^{11} + \dots + 2 h k a^* b^* U^{12}]$

	U^{11}	U^{22}	U^{33}	U^{23}	U^{13}	U^{12}
C(1)	23(1)	35(1)	28(1)	2(1)	2(1)	-2(1)
C(2)	30(1)	30(1)	33(1)	-3(1)	5(1)	2(1)
C(3)	35(1)	30(1)	35(1)	5(1)	4(1)	0(1)
C(4)	27(1)	37(1)	27(1)	0(1)	0(1)	0(1)
C(5)	33(1)	33(1)	32(1)	-7(1)	1(1)	1(1)
C(6)	35(1)	28(1)	34(1)	2(1)	1(1)	-2(1)
C(7)	37(1)	33(1)	34(1)	-1(1)	0(1)	1(1)
N(1)	44(1)	31(1)	34(1)	-3(1)	10(1)	-2(1)
N(2)	38(1)	35(1)	35(1)	6(1)	7(1)	-3(1)
N(3)	66(1)	41(1)	45(1)	-2(1)	20(1)	1(1)
N(4)	57(1)	42(1)	38(1)	1(1)	11(1)	1(1)

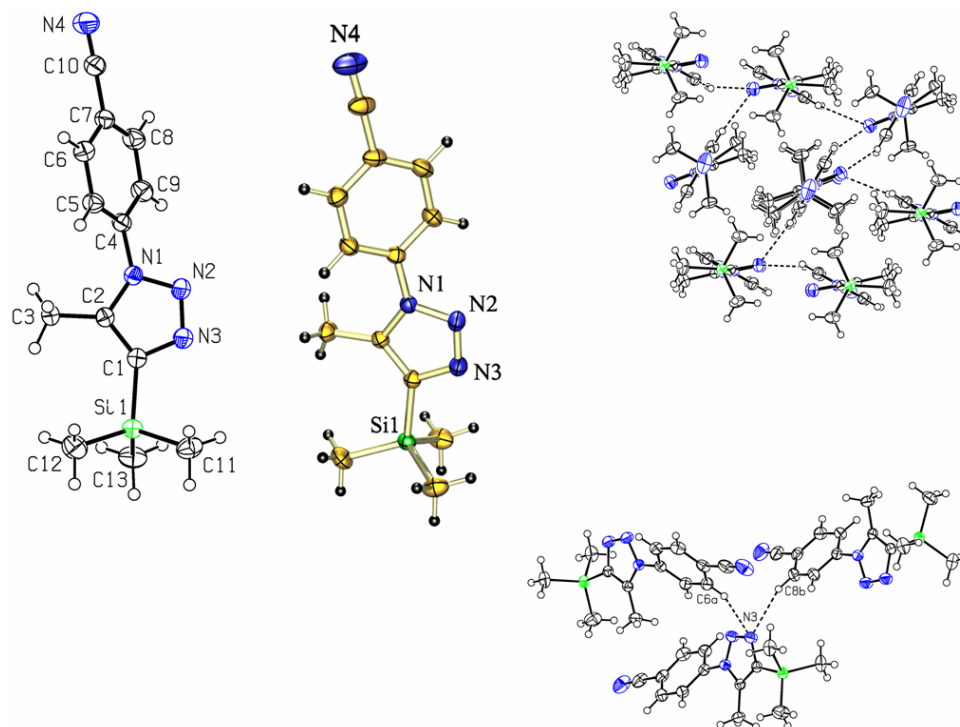
Hydrogen coordinates ($\times 10^4$) and isotropic displacement parameters ($\text{\AA}^2 \times 10^{-3}$)
for sb1173m.

	x	y	z	U(eq)
H(2)	3328(18)	2868(11)	1503(12)	33(5)
H(3)	2198(19)	2516(11)	3191(12)	41(5)
H(5)	1476(18)	5180(10)	3755(11)	32(4)
H(6)	2639(18)	5502(12)	2056(12)	39(5)

Torsion angles [°] for sb1173m.

C(6)-C(1)-C(2)-C(3)	0.9(2)
N(1)-C(1)-C(2)-C(3)	-178.99(14)
C(1)-C(2)-C(3)-C(4)	-0.1(2)
C(2)-C(3)-C(4)-C(5)	-0.2(2)
C(2)-C(3)-C(4)-C(7)	177.98(15)
C(3)-C(4)-C(5)-C(6)	-0.2(2)
C(7)-C(4)-C(5)-C(6)	-178.44(14)
C(4)-C(5)-C(6)-C(1)	1.0(2)
C(2)-C(1)-C(6)-C(5)	-1.3(2)
N(1)-C(1)-C(6)-C(5)	178.57(13)
C(6)-C(1)-N(1)-N(2)	-177.10(14)
C(2)-C(1)-N(1)-N(2)	2.8(2)

X-Ray Structure Determination, C₁₃H₁₆N₄Si



X-ray intensity data from a yellow plate were measured at 150(1) K on a Bruker SMART APEX CCD-based diffractometer (Mo K α radiation, $\lambda = 0.71073$ Å).¹ Raw data frame integration and Lp corrections were performed with SAINT+.¹ Final unit cell parameters were determined by least-squares refinement of 6098 reflections from the data set with $I > 5(\sigma)I$. Analysis of the data showed negligible crystal decay during collection. No absorption correction was applied. Direct methods structure solution, difference Fourier calculations and full-matrix least-squares refinement against F^2 were performed with SHELXTL.²

C₁₃H₁₆N₄Si crystallizes in the space group P2₁2₁2₁ as determined uniquely by the pattern of systematic absences in the intensity data. Non-hydrogen atoms were refined with anisotropic displacement parameters; hydrogen atoms were placed in idealized positions and included as riding atoms. Due to the lack of any atoms heavier than Si, Freidel opposites were merged and no attempt made to determine the absolute structure.

(1) SMART Version 5.628 and SAINT+ Version 6.22. Bruker Analytical X-ray Systems, Inc., Madison, Wisconsin, USA, 2001.

(2) Sheldrick, G. M. SHELXTL Version 6.1; Bruker Analytical X-ray Systems, Inc., Madison, Wisconsin, USA, 2000.

Table A13. Crystal data and structure refinement for merg4.

Identification code	sb188tm	
Empirical formula	C13 H16 N4 Si	
Formula weight	256.39	
Temperature	150(1) K	
Wavelength	0.71073 Å	
Crystal system	Orthorhombic	
Space group	P2 ₁ 2 ₁ 2 ₁	
Unit cell dimensions	a = 9.9546(6) Å	α = 90°.
	b = 14.5997(9) Å	β = 90°.
	c = 9.7103(6) Å	γ = 90°.
Volume	1411.24(15) Å ³	
Z	4	
Density (calculated)	1.207 Mg/m ³	
Absorption coefficient	0.155 mm ⁻¹	
F(000)	544	
Crystal size	0.46 x 0.40 x 0.28 mm ³	
Theta range for data collection	2.48 to 27.67°.	
Index ranges	-12 ≤ h ≤ 13, -19 ≤ k ≤ 17, -12 ≤ l ≤ 12	
Reflections collected	13990	
Independent reflections	1896 [R(int) = 0.0369]	
Completeness to theta = 27.67°	100.0 %	
Absorption correction	None	
Refinement method	Full-matrix least-squares on F ²	
Data / restraints / parameters	1896 / 0 / 167	
Goodness-of-fit on F ²	1.072	
Final R indices [I > 2σ(I)]	R1 = 0.0331, wR2 = 0.0869	
R indices (all data)	R1 = 0.0336, wR2 = 0.0873	
Absolute structure parameter	opposites merged	
Largest diff. peak and hole	0.203 and -0.310 e.Å ⁻³	

Atomic coordinates ($\times 10^4$) and equivalent isotropic displacement parameters ($\text{\AA}^2 \times 10^3$) for merg4. $U(\text{eq})$ is defined as one third of the trace of the orthogonalized U^{ij} tensor.

	x	y	z	U(eq)
Si(1)	3781(1)	1612(1)	4649(1)	26(1)
C(1)	3912(2)	2866(1)	5042(2)	25(1)
C(2)	3865(2)	3668(1)	4287(2)	24(1)
C(3)	3785(2)	3828(1)	2770(2)	34(1)
C(4)	3958(2)	5327(1)	5088(2)	26(1)
C(5)	3076(2)	5738(1)	4174(2)	30(1)
C(6)	3041(2)	6688(1)	4088(2)	34(1)
C(7)	3865(2)	7209(1)	4945(2)	33(1)
C(8)	4727(2)	6791(1)	5874(2)	36(1)
C(9)	4792(2)	5841(1)	5937(2)	33(1)
C(10)	3787(2)	8196(1)	4838(2)	41(1)
C(11)	2536(2)	1146(1)	5889(2)	40(1)
C(12)	3184(3)	1411(2)	2863(2)	49(1)
C(13)	5467(2)	1097(1)	4927(2)	39(1)
N(1)	3980(1)	4352(1)	5236(1)	25(1)
N(2)	4091(2)	4004(1)	6528(2)	32(1)
N(3)	4049(2)	3117(1)	6410(2)	32(1)
N(4)	3707(3)	8973(1)	4721(2)	60(1)

Bond lengths [Å] and angles [°] for merg4.

Si(1)-C(12)	1.857(2)
Si(1)-C(11)	1.857(2)
Si(1)-C(13)	1.8584(19)
Si(1)-C(1)	1.8743(17)
C(1)-C(2)	1.383(2)
C(1)-N(3)	1.385(2)
C(2)-N(1)	1.364(2)
C(2)-C(3)	1.494(2)
C(3)-H(3A)	0.9800
C(3)-H(3B)	0.9800
C(3)-H(3C)	0.9800
C(4)-C(5)	1.386(2)
C(4)-C(9)	1.390(2)
C(4)-N(1)	1.430(2)
C(5)-C(6)	1.390(2)
C(5)-H(5)	0.9500
C(6)-C(7)	1.394(3)
C(6)-H(6)	0.9500
C(7)-C(8)	1.387(3)
C(7)-C(10)	1.447(3)
C(8)-C(9)	1.390(3)
C(8)-H(8)	0.9500
C(9)-H(9)	0.9500
C(10)-N(4)	1.143(3)
C(11)-H(11A)	0.9800
C(11)-H(11B)	0.9800
C(11)-H(11C)	0.9800
C(12)-H(12A)	0.9800
C(12)-H(12B)	0.9800
C(12)-H(12C)	0.9800
C(13)-H(13A)	0.9800
C(13)-H(13B)	0.9800
C(13)-H(13C)	0.9800
N(1)-N(2)	1.357(2)

N(2)-N(3)	1.301(2)
C(12)-Si(1)-C(11)	109.53(11)
C(12)-Si(1)-C(13)	111.16(11)
C(11)-Si(1)-C(13)	111.11(10)
C(12)-Si(1)-C(1)	111.51(9)
C(11)-Si(1)-C(1)	105.76(9)
C(13)-Si(1)-C(1)	107.63(8)
C(2)-C(1)-N(3)	106.68(14)
C(2)-C(1)-Si(1)	135.81(12)
N(3)-C(1)-Si(1)	117.47(11)
N(1)-C(2)-C(1)	105.03(14)
N(1)-C(2)-C(3)	123.85(15)
C(1)-C(2)-C(3)	131.04(15)
C(2)-C(3)-H(3A)	109.5
C(2)-C(3)-H(3B)	109.5
H(3A)-C(3)-H(3B)	109.5
C(2)-C(3)-H(3C)	109.5
H(3A)-C(3)-H(3C)	109.5
H(3B)-C(3)-H(3C)	109.5
C(5)-C(4)-C(9)	121.63(16)
C(5)-C(4)-N(1)	120.34(15)
C(9)-C(4)-N(1)	117.95(15)
C(4)-C(5)-C(6)	119.14(16)
C(4)-C(5)-H(5)	120.4
C(6)-C(5)-H(5)	120.4
C(5)-C(6)-C(7)	119.57(16)
C(5)-C(6)-H(6)	120.2
C(7)-C(6)-H(6)	120.2
C(8)-C(7)-C(6)	120.85(15)
C(8)-C(7)-C(10)	121.19(17)
C(6)-C(7)-C(10)	117.96(18)
C(7)-C(8)-C(9)	119.75(16)
C(7)-C(8)-H(8)	120.1
C(9)-C(8)-H(8)	120.1
C(8)-C(9)-C(4)	119.03(17)

C(8)-C(9)-H(9)	120.5
C(4)-C(9)-H(9)	120.5
N(4)-C(10)-C(7)	178.2(3)
Si(1)-C(11)-H(11A)	109.5
Si(1)-C(11)-H(11B)	109.5
H(11A)-C(11)-H(11B)	109.5
Si(1)-C(11)-H(11C)	109.5
H(11A)-C(11)-H(11C)	109.5
H(11B)-C(11)-H(11C)	109.5
Si(1)-C(12)-H(12A)	109.5
Si(1)-C(12)-H(12B)	109.5
H(12A)-C(12)-H(12B)	109.5
Si(1)-C(12)-H(12C)	109.5
H(12A)-C(12)-H(12C)	109.5
H(12B)-C(12)-H(12C)	109.5
Si(1)-C(13)-H(13A)	109.5
Si(1)-C(13)-H(13B)	109.5
H(13A)-C(13)-H(13B)	109.5
Si(1)-C(13)-H(13C)	109.5
H(13A)-C(13)-H(13C)	109.5
H(13B)-C(13)-H(13C)	109.5
N(2)-N(1)-C(2)	110.92(13)
N(2)-N(1)-C(4)	117.81(13)
C(2)-N(1)-C(4)	131.24(14)
N(3)-N(2)-N(1)	106.82(13)
N(2)-N(3)-C(1)	110.56(14)

Symmetry transformations used to generate equivalent atoms:

Anisotropic displacement parameters ($\text{\AA}^2 \times 10^3$) for merg4. The anisotropic displacement factor exponent takes the form: $-2\pi^2 [h^2 a^{*2} U^{11} + \dots + 2 h k a^* b^* U^{12}]$

	U ¹¹	U ²²	U ³³	U ²³	U ¹³	U ¹²
Si(1)	23(1)	25(1)	30(1)	-1(1)	-1(1)	0(1)
C(1)	23(1)	27(1)	26(1)	0(1)	-1(1)	1(1)
C(2)	20(1)	27(1)	25(1)	-1(1)	1(1)	-1(1)
C(3)	46(1)	32(1)	23(1)	0(1)	3(1)	1(1)
C(4)	26(1)	24(1)	28(1)	-2(1)	3(1)	-1(1)
C(5)	31(1)	29(1)	31(1)	-3(1)	-3(1)	-1(1)
C(6)	38(1)	30(1)	33(1)	1(1)	0(1)	2(1)
C(7)	39(1)	26(1)	33(1)	-3(1)	12(1)	-4(1)
C(8)	39(1)	35(1)	36(1)	-8(1)	1(1)	-11(1)
C(9)	32(1)	34(1)	33(1)	-4(1)	-4(1)	-4(1)
C(10)	56(1)	30(1)	39(1)	-3(1)	17(1)	-6(1)
C(11)	33(1)	32(1)	55(1)	5(1)	8(1)	-3(1)
C(12)	63(1)	42(1)	40(1)	-7(1)	-13(1)	-9(1)
C(13)	27(1)	33(1)	58(1)	-5(1)	-1(1)	5(1)
N(1)	25(1)	26(1)	24(1)	1(1)	-1(1)	-1(1)
N(2)	41(1)	31(1)	25(1)	2(1)	-4(1)	1(1)
N(3)	41(1)	30(1)	26(1)	1(1)	-3(1)	0(1)
N(4)	85(2)	33(1)	61(1)	-3(1)	28(1)	-5(1)

Hydrogen coordinates ($\times 10^4$) and isotropic displacement parameters ($\text{\AA}^2 \times 10^{-3}$)
for merg4.

	x	y	z	U(eq)
H(3A)	2865	4000	2521	50
H(3B)	4036	3266	2281	50
H(3C)	4402	4322	2512	50
H(5)	2502	5375	3613	36
H(6)	2460	6980	3448	40
H(8)	5271	7153	6466	44
H(9)	5398	5547	6550	39
H(11A)	1662	1437	5733	60
H(11B)	2836	1273	6831	60
H(11C)	2453	483	5758	60
H(12A)	3075	752	2708	73
H(12B)	3842	1656	2209	73
H(12C)	2319	1720	2728	73
H(13A)	5405	429	4838	59
H(13B)	5788	1254	5851	59
H(13C)	6095	1335	4238	59

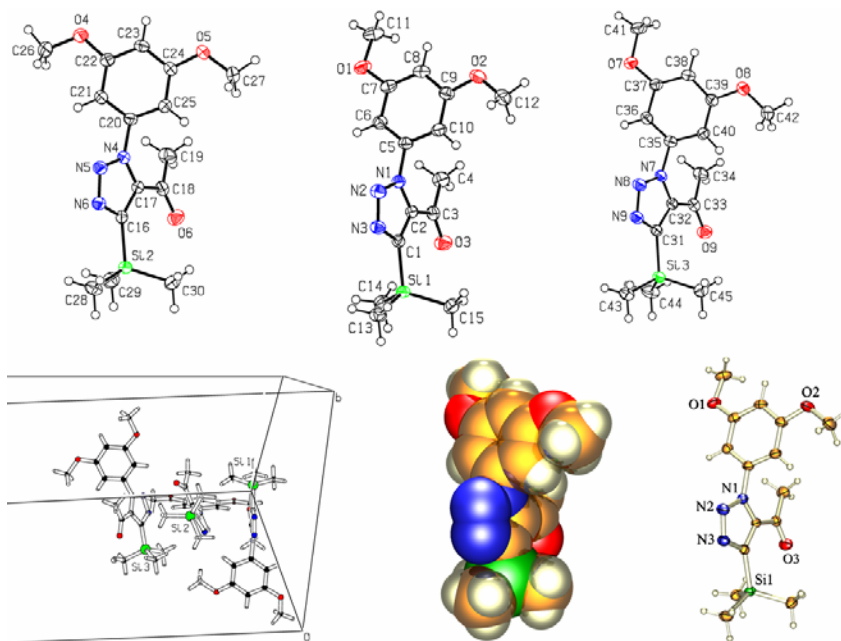
Torsion angles [°] for merg4.

C(12)-Si(1)-C(1)-C(2)	-11.6(2)
C(11)-Si(1)-C(1)-C(2)	-130.63(19)
C(13)-Si(1)-C(1)-C(2)	110.53(19)
C(12)-Si(1)-C(1)-N(3)	165.77(15)
C(11)-Si(1)-C(1)-N(3)	46.78(17)
C(13)-Si(1)-C(1)-N(3)	-72.06(16)
N(3)-C(1)-C(2)-N(1)	0.16(19)
Si(1)-C(1)-C(2)-N(1)	177.76(15)
N(3)-C(1)-C(2)-C(3)	177.07(19)
Si(1)-C(1)-C(2)-C(3)	-5.3(3)
C(9)-C(4)-C(5)-C(6)	1.1(3)
N(1)-C(4)-C(5)-C(6)	177.63(16)
C(4)-C(5)-C(6)-C(7)	-1.7(3)
C(5)-C(6)-C(7)-C(8)	0.6(3)
C(5)-C(6)-C(7)-C(10)	-179.20(17)
C(6)-C(7)-C(8)-C(9)	1.2(3)
C(10)-C(7)-C(8)-C(9)	-178.99(18)
C(7)-C(8)-C(9)-C(4)	-1.9(3)
C(5)-C(4)-C(9)-C(8)	0.7(3)
N(1)-C(4)-C(9)-C(8)	-175.91(16)
C(8)-C(7)-C(10)-N(4)	168(8)
C(6)-C(7)-C(10)-N(4)	-12(8)
C(1)-C(2)-N(1)-N(2)	-0.08(18)
C(3)-C(2)-N(1)-N(2)	-177.28(18)
C(1)-C(2)-N(1)-C(4)	-177.93(16)
C(3)-C(2)-N(1)-C(4)	4.9(3)
C(5)-C(4)-N(1)-N(2)	-138.32(17)
C(9)-C(4)-N(1)-N(2)	38.3(2)
C(5)-C(4)-N(1)-C(2)	39.4(3)
C(9)-C(4)-N(1)-C(2)	-143.94(18)
C(2)-N(1)-N(2)-N(3)	-0.03(19)
C(4)-N(1)-N(2)-N(3)	178.14(14)
N(1)-N(2)-N(3)-C(1)	0.1(2)
C(2)-C(1)-N(3)-N(2)	-0.2(2)

Si(1)-C(1)-N(3)-N(2)

-178.30(12)

X-Ray Structure Determination, C₁₅H₂₁N₃O₃Si



X-ray intensity data from a colorless plate were measured at 150(1) K on a Bruker SMART APEX CCD-based diffractometer (Mo K α radiation, $\lambda = 0.71073$ Å).¹ Raw data frame integration and Lp corrections were performed with SAINT+.¹ Final unit cell parameters were determined by least-squares refinement of 8872 reflections from the data set with $I > 5(\sigma)I$. Analysis of the data showed negligible crystal decay during collection. No absorption correction was applied. Direct methods structure solution, difference Fourier calculations and full-matrix least-squares refinement against F^2 were performed with SHELXTL.²

C₁₅H₂₁N₃O₃Si crystallizes in the space group *Pbca* as determined uniquely by the pattern of systematic absences in the intensity data. The asymmetric unit contains three crystallographically independent but chemically similar molecules. All non-hydrogen atoms were refined with anisotropic displacement parameters. Hydrogen atoms were placed in geometrically idealized positions and included as riding atoms.

(1) SMART Version 5.625 and SAINT+ Version 6.22. Bruker Analytical X-ray Systems, Inc., Madison, Wisconsin, USA, 2001.

(2) Sheldrick, G. M. SHELXTL Version 6.1; Bruker Analytical X-ray Systems, Inc., Madison, Wisconsin, USA, 2000.

Table A14. Crystal data and structure refinement for sb195t.

Identification code	sb195t	
Empirical formula	C ₁₅ H ₂₁ N ₃ O ₃ Si	
Formula weight	319.44	
Temperature	150(1) K	
Wavelength	0.71073 Å	
Crystal system	Orthorhombic	
Space group	Pbca	
Unit cell dimensions	a = 17.8594(10) Å	α = 90°.
	b = 21.5853(12) Å	β = 90°.
	c = 26.2129(15) Å	γ = 90°.
Volume	10105.1(10) Å ³	
Z	24	
Density (calculated)	1.260 Mg/m ³	
Absorption coefficient	0.155 mm ⁻¹	
F(000)	4080	
Crystal size	0.48 x 0.42 x 0.22 mm ³	
Theta range for data collection	1.55 to 26.42°.	
Index ranges	-22 ≤ h ≤ 22, -27 ≤ k ≤ 26, -30 ≤ l ≤ 32	
Reflections collected	95261	
Independent reflections	10375 [R(int) = 0.0544]	
Completeness to theta = 26.42°	99.8 %	
Absorption correction	None	
Refinement method	Full-matrix least-squares on F ²	
Data / restraints / parameters	10375 / 0 / 613	
Goodness-of-fit on F ²	1.057	
Final R indices [I > 2σ(I)]	R1 = 0.0401, wR2 = 0.1106	
R indices (all data)	R1 = 0.0490, wR2 = 0.1155	
Largest diff. peak and hole	0.452 and -0.273 e.Å ⁻³	

Atomic coordinates ($\times 10^4$) and equivalent isotropic displacement parameters ($\text{\AA}^2 \times 10^3$) for sb195t. U(eq) is defined as one third of the trace of the orthogonalized U^{ij} tensor.

	x	y	z	U(eq)
Si(1)	4058(1)	3785(1)	1172(1)	24(1)
C(1)	3614(1)	2990(1)	1174(1)	23(1)
C(2)	2893(1)	2804(1)	1290(1)	23(1)
C(3)	2258(1)	3212(1)	1430(1)	27(1)
C(4)	1474(1)	2971(1)	1468(1)	36(1)
C(5)	2299(1)	1727(1)	1298(1)	26(1)
C(6)	1886(1)	1508(1)	894(1)	27(1)
C(7)	1292(1)	1104(1)	999(1)	29(1)
C(8)	1146(1)	919(1)	1494(1)	30(1)
C(9)	1592(1)	1139(1)	1894(1)	31(1)
C(10)	2175(1)	1554(1)	1799(1)	29(1)
C(11)	161(1)	655(1)	677(1)	41(1)
C(12)	1889(1)	1107(1)	2778(1)	46(1)
C(13)	5047(1)	3678(1)	975(1)	35(1)
C(14)	3555(1)	4274(1)	698(1)	34(1)
C(15)	4040(1)	4136(1)	1820(1)	36(1)
N(1)	2878(1)	2180(1)	1204(1)	24(1)
N(2)	3557(1)	1983(1)	1048(1)	30(1)
N(3)	3999(1)	2470(1)	1025(1)	28(1)
O(1)	883(1)	924(1)	585(1)	35(1)
O(2)	1409(1)	930(1)	2366(1)	41(1)
O(3)	2401(1)	3754(1)	1508(1)	39(1)
Si(2)	4404(1)	2371(1)	2807(1)	26(1)
C(16)	3514(1)	2843(1)	2828(1)	24(1)
C(17)	3354(1)	3439(1)	2995(1)	24(1)
C(18)	3909(1)	3900(1)	3181(1)	28(1)
C(19)	3743(1)	4581(1)	3176(1)	38(1)
C(20)	2109(1)	4033(1)	3004(1)	25(1)
C(21)	1744(1)	4292(1)	2589(1)	31(1)
C(22)	1241(1)	4769(1)	2689(1)	33(1)
C(23)	1139(1)	4987(1)	3180(1)	31(1)

C(24)	1515(1)	4714(1)	3584(1)	25(1)
C(25)	2004(1)	4221(1)	3501(1)	26(1)
C(26)	949(1)	4854(1)	1805(1)	49(1)
C(27)	1752(1)	4689(1)	4476(1)	45(1)
C(28)	4139(1)	1618(1)	2509(1)	40(1)
C(29)	5124(1)	2752(1)	2405(1)	39(1)
C(30)	4734(1)	2229(1)	3468(1)	33(1)
N(4)	2608(1)	3521(1)	2901(1)	24(1)
N(5)	2315(1)	3005(1)	2691(1)	28(1)
N(6)	2859(1)	2600(1)	2644(1)	27(1)
O(4)	824(1)	5054(1)	2319(1)	48(1)
O(5)	1360(1)	4949(1)	4055(1)	32(1)
O(6)	4515(1)	3707(1)	3313(1)	39(1)
Si(3)	2507(1)	2164(1)	4364(1)	25(1)
C(31)	3204(1)	2814(1)	4446(1)	23(1)
C(32)	3924(1)	2851(1)	4640(1)	22(1)
C(33)	4415(1)	2324(1)	4787(1)	25(1)
C(34)	5247(1)	2411(1)	4839(1)	32(1)
C(35)	4749(1)	3801(1)	4816(1)	24(1)
C(36)	5165(1)	4147(1)	4482(1)	27(1)
C(37)	5751(1)	4504(1)	4683(1)	26(1)
C(38)	5901(1)	4503(1)	5201(1)	27(1)
C(39)	5462(1)	4139(1)	5526(1)	26(1)
C(40)	4877(1)	3783(1)	5339(1)	26(1)
C(41)	6754(1)	5203(1)	4502(1)	37(1)
C(42)	5202(1)	3812(1)	6375(1)	36(1)
C(43)	1699(1)	2515(1)	4022(1)	38(1)
C(44)	2870(1)	1502(1)	3984(1)	40(1)
C(45)	2212(1)	1910(1)	5012(1)	35(1)
N(7)	4111(1)	3464(1)	4621(1)	23(1)
N(8)	3539(1)	3796(1)	4428(1)	29(1)
N(9)	2995(1)	3405(1)	4321(1)	29(1)
O(7)	6137(1)	4840(1)	4331(1)	36(1)
O(8)	5648(1)	4168(1)	6031(1)	36(1)
O(9)	4122(1)	1822(1)	4841(1)	33(1)

Bond lengths [Å] and angles [°] for sb195t.

Si(1)-C(13)	1.8559(17)
Si(1)-C(15)	1.8597(17)
Si(1)-C(14)	1.8602(16)
Si(1)-C(1)	1.8920(14)
C(1)-N(3)	1.3718(19)
C(1)-C(2)	1.382(2)
C(2)-N(1)	1.3658(18)
C(2)-C(3)	1.483(2)
C(3)-O(3)	1.2138(18)
C(3)-C(4)	1.496(2)
C(4)-H(4A)	0.9800
C(4)-H(4B)	0.9800
C(4)-H(4C)	0.9800
C(5)-C(6)	1.374(2)
C(5)-C(10)	1.385(2)
C(5)-N(1)	1.4436(18)
C(6)-C(7)	1.401(2)
C(6)-H(6)	0.9500
C(7)-O(1)	1.3653(19)
C(7)-C(8)	1.382(2)
C(8)-C(9)	1.398(2)
C(8)-H(8)	0.9500
C(9)-O(2)	1.3574(19)
C(9)-C(10)	1.395(2)
C(10)-H(10)	0.9500
C(11)-O(1)	1.434(2)
C(11)-H(11A)	0.9800
C(11)-H(11B)	0.9800
C(11)-H(11C)	0.9800
C(12)-O(2)	1.431(2)
C(12)-H(12A)	0.9800
C(12)-H(12B)	0.9800
C(12)-H(12C)	0.9800
C(13)-H(13A)	0.9800

C(13)-H(13B)	0.9800
C(13)-H(13C)	0.9800
C(14)-H(14A)	0.9800
C(14)-H(14B)	0.9800
C(14)-H(14C)	0.9800
C(15)-H(15A)	0.9800
C(15)-H(15B)	0.9800
C(15)-H(15C)	0.9800
N(1)-N(2)	1.3479(17)
N(2)-N(3)	1.3161(17)
Si(2)-C(29)	1.8542(17)
Si(2)-C(30)	1.8574(17)
Si(2)-C(28)	1.8633(17)
Si(2)-C(16)	1.8887(15)
C(16)-N(6)	1.3692(19)
C(16)-C(17)	1.3887(19)
C(17)-N(4)	1.3662(19)
C(17)-C(18)	1.486(2)
C(18)-O(6)	1.2102(19)
C(18)-C(19)	1.501(2)
C(19)-H(19A)	0.9800
C(19)-H(19B)	0.9800
C(19)-H(19C)	0.9800
C(20)-C(25)	1.379(2)
C(20)-C(21)	1.384(2)
C(20)-N(4)	1.4448(18)
C(21)-C(22)	1.392(2)
C(21)-H(21)	0.9500
C(22)-O(4)	1.3690(19)
C(22)-C(23)	1.382(2)
C(23)-C(24)	1.385(2)
C(23)-H(23)	0.9500
C(24)-O(5)	1.3632(18)
C(24)-C(25)	1.395(2)
C(25)-H(25)	0.9500
C(26)-O(4)	1.430(2)

C(26)-H(26A)	0.9800
C(26)-H(26B)	0.9800
C(26)-H(26C)	0.9800
C(27)-O(5)	1.422(2)
C(27)-H(27A)	0.9800
C(27)-H(27B)	0.9800
C(27)-H(27C)	0.9800
C(28)-H(28A)	0.9800
C(28)-H(28B)	0.9800
C(28)-H(28C)	0.9800
C(29)-H(29A)	0.9800
C(29)-H(29B)	0.9800
C(29)-H(29C)	0.9800
C(30)-H(30A)	0.9800
C(30)-H(30B)	0.9800
C(30)-H(30C)	0.9800
N(4)-N(5)	1.3489(17)
N(5)-N(6)	1.3132(17)
Si(3)-C(45)	1.8589(17)
Si(3)-C(44)	1.8592(17)
Si(3)-C(43)	1.8602(17)
Si(3)-C(31)	1.8888(15)
C(31)-N(9)	1.3684(18)
C(31)-C(32)	1.386(2)
C(32)-N(7)	1.3649(18)
C(32)-C(33)	1.487(2)
C(33)-O(9)	1.2131(18)
C(33)-C(34)	1.503(2)
C(34)-H(34A)	0.9800
C(34)-H(34B)	0.9800
C(34)-H(34C)	0.9800
C(35)-C(36)	1.369(2)
C(35)-C(40)	1.390(2)
C(35)-N(7)	1.4454(18)
C(36)-C(37)	1.402(2)
C(36)-H(36)	0.9500

C(37)-O(7)	1.3622(18)
C(37)-C(38)	1.383(2)
C(38)-C(39)	1.398(2)
C(38)-H(38)	0.9500
C(39)-O(8)	1.3661(19)
C(39)-C(40)	1.388(2)
C(40)-H(40)	0.9500
C(41)-O(7)	1.4252(19)
C(41)-H(41A)	0.9800
C(41)-H(41B)	0.9800
C(41)-H(41C)	0.9800
C(42)-O(8)	1.4285(19)
C(42)-H(42A)	0.9800
C(42)-H(42B)	0.9800
C(42)-H(42C)	0.9800
C(43)-H(43A)	0.9800
C(43)-H(43B)	0.9800
C(43)-H(43C)	0.9800
C(44)-H(44A)	0.9800
C(44)-H(44B)	0.9800
C(44)-H(44C)	0.9800
C(45)-H(45A)	0.9800
C(45)-H(45B)	0.9800
C(45)-H(45C)	0.9800
N(7)-N(8)	1.3473(17)
N(8)-N(9)	1.3160(17)

C(13)-Si(1)-C(15)	108.73(8)
C(13)-Si(1)-C(14)	110.18(8)
C(15)-Si(1)-C(14)	111.76(8)
C(13)-Si(1)-C(1)	106.62(7)
C(15)-Si(1)-C(1)	111.08(7)
C(14)-Si(1)-C(1)	108.35(7)
N(3)-C(1)-C(2)	106.96(12)
N(3)-C(1)-Si(1)	122.08(11)
C(2)-C(1)-Si(1)	130.90(11)

N(1)-C(2)-C(1)	105.56(12)
N(1)-C(2)-C(3)	127.77(13)
C(1)-C(2)-C(3)	126.45(13)
O(3)-C(3)-C(2)	116.95(14)
O(3)-C(3)-C(4)	121.34(14)
C(2)-C(3)-C(4)	121.70(13)
C(3)-C(4)-H(4A)	109.5
C(3)-C(4)-H(4B)	109.5
H(4A)-C(4)-H(4B)	109.5
C(3)-C(4)-H(4C)	109.5
H(4A)-C(4)-H(4C)	109.5
H(4B)-C(4)-H(4C)	109.5
C(6)-C(5)-C(10)	123.54(14)
C(6)-C(5)-N(1)	119.08(14)
C(10)-C(5)-N(1)	117.34(14)
C(5)-C(6)-C(7)	117.89(15)
C(5)-C(6)-H(6)	121.1
C(7)-C(6)-H(6)	121.1
O(1)-C(7)-C(8)	124.35(14)
O(1)-C(7)-C(6)	115.09(15)
C(8)-C(7)-C(6)	120.55(15)
C(7)-C(8)-C(9)	119.86(14)
C(7)-C(8)-H(8)	120.1
C(9)-C(8)-H(8)	120.1
O(2)-C(9)-C(10)	123.73(15)
O(2)-C(9)-C(8)	115.65(14)
C(10)-C(9)-C(8)	120.61(15)
C(5)-C(10)-C(9)	117.50(15)
C(5)-C(10)-H(10)	121.2
C(9)-C(10)-H(10)	121.2
O(1)-C(11)-H(11A)	109.5
O(1)-C(11)-H(11B)	109.5
H(11A)-C(11)-H(11B)	109.5
O(1)-C(11)-H(11C)	109.5
H(11A)-C(11)-H(11C)	109.5
H(11B)-C(11)-H(11C)	109.5

O(2)-C(12)-H(12A)	109.5
O(2)-C(12)-H(12B)	109.5
H(12A)-C(12)-H(12B)	109.5
O(2)-C(12)-H(12C)	109.5
H(12A)-C(12)-H(12C)	109.5
H(12B)-C(12)-H(12C)	109.5
Si(1)-C(13)-H(13A)	109.5
Si(1)-C(13)-H(13B)	109.5
H(13A)-C(13)-H(13B)	109.5
Si(1)-C(13)-H(13C)	109.5
H(13A)-C(13)-H(13C)	109.5
H(13B)-C(13)-H(13C)	109.5
Si(1)-C(14)-H(14A)	109.5
Si(1)-C(14)-H(14B)	109.5
H(14A)-C(14)-H(14B)	109.5
Si(1)-C(14)-H(14C)	109.5
H(14A)-C(14)-H(14C)	109.5
H(14B)-C(14)-H(14C)	109.5
Si(1)-C(15)-H(15A)	109.5
Si(1)-C(15)-H(15B)	109.5
H(15A)-C(15)-H(15B)	109.5
Si(1)-C(15)-H(15C)	109.5
H(15A)-C(15)-H(15C)	109.5
H(15B)-C(15)-H(15C)	109.5
N(2)-N(1)-C(2)	110.06(11)
N(2)-N(1)-C(5)	118.91(12)
C(2)-N(1)-C(5)	130.75(12)
N(3)-N(2)-N(1)	107.55(12)
N(2)-N(3)-C(1)	109.85(12)
C(7)-O(1)-C(11)	117.49(14)
C(9)-O(2)-C(12)	117.04(13)
C(29)-Si(2)-C(30)	112.57(8)
C(29)-Si(2)-C(28)	109.01(9)
C(30)-Si(2)-C(28)	109.08(8)
C(29)-Si(2)-C(16)	111.13(7)
C(30)-Si(2)-C(16)	109.22(7)

C(28)-Si(2)-C(16)	105.58(7)
N(6)-C(16)-C(17)	106.85(12)
N(6)-C(16)-Si(2)	120.14(10)
C(17)-C(16)-Si(2)	133.01(11)
N(4)-C(17)-C(16)	105.34(13)
N(4)-C(17)-C(18)	128.43(13)
C(16)-C(17)-C(18)	125.91(13)
O(6)-C(18)-C(17)	117.35(13)
O(6)-C(18)-C(19)	121.11(14)
C(17)-C(18)-C(19)	121.43(14)
C(18)-C(19)-H(19A)	109.5
C(18)-C(19)-H(19B)	109.5
H(19A)-C(19)-H(19B)	109.5
C(18)-C(19)-H(19C)	109.5
H(19A)-C(19)-H(19C)	109.5
H(19B)-C(19)-H(19C)	109.5
C(25)-C(20)-C(21)	124.00(14)
C(25)-C(20)-N(4)	118.98(13)
C(21)-C(20)-N(4)	116.98(13)
C(20)-C(21)-C(22)	117.11(15)
C(20)-C(21)-H(21)	121.4
C(22)-C(21)-H(21)	121.4
O(4)-C(22)-C(23)	115.94(14)
O(4)-C(22)-C(21)	123.34(15)
C(23)-C(22)-C(21)	120.72(15)
C(22)-C(23)-C(24)	120.33(14)
C(22)-C(23)-H(23)	119.8
C(24)-C(23)-H(23)	119.8
O(5)-C(24)-C(23)	115.91(13)
O(5)-C(24)-C(25)	123.54(14)
C(23)-C(24)-C(25)	120.53(14)
C(20)-C(25)-C(24)	117.23(14)
C(20)-C(25)-H(25)	121.4
C(24)-C(25)-H(25)	121.4
O(4)-C(26)-H(26A)	109.5
O(4)-C(26)-H(26B)	109.5

H(26A)-C(26)-H(26B)	109.5
O(4)-C(26)-H(26C)	109.5
H(26A)-C(26)-H(26C)	109.5
H(26B)-C(26)-H(26C)	109.5
O(5)-C(27)-H(27A)	109.5
O(5)-C(27)-H(27B)	109.5
H(27A)-C(27)-H(27B)	109.5
O(5)-C(27)-H(27C)	109.5
H(27A)-C(27)-H(27C)	109.5
H(27B)-C(27)-H(27C)	109.5
Si(2)-C(28)-H(28A)	109.5
Si(2)-C(28)-H(28B)	109.5
H(28A)-C(28)-H(28B)	109.5
Si(2)-C(28)-H(28C)	109.5
H(28A)-C(28)-H(28C)	109.5
H(28B)-C(28)-H(28C)	109.5
Si(2)-C(29)-H(29A)	109.5
Si(2)-C(29)-H(29B)	109.5
H(29A)-C(29)-H(29B)	109.5
Si(2)-C(29)-H(29C)	109.5
H(29A)-C(29)-H(29C)	109.5
H(29B)-C(29)-H(29C)	109.5
Si(2)-C(30)-H(30A)	109.5
Si(2)-C(30)-H(30B)	109.5
H(30A)-C(30)-H(30B)	109.5
Si(2)-C(30)-H(30C)	109.5
H(30A)-C(30)-H(30C)	109.5
H(30B)-C(30)-H(30C)	109.5
N(5)-N(4)-C(17)	110.15(11)
N(5)-N(4)-C(20)	117.87(12)
C(17)-N(4)-C(20)	131.92(12)
N(6)-N(5)-N(4)	107.51(12)
N(5)-N(6)-C(16)	110.15(12)
C(22)-O(4)-C(26)	116.60(13)
C(24)-O(5)-C(27)	117.11(12)
C(45)-Si(3)-C(44)	111.26(8)

C(45)-Si(3)-C(43)	109.94(8)
C(44)-Si(3)-C(43)	108.96(9)
C(45)-Si(3)-C(31)	107.63(7)
C(44)-Si(3)-C(31)	113.67(7)
C(43)-Si(3)-C(31)	105.19(7)
N(9)-C(31)-C(32)	106.70(12)
N(9)-C(31)-Si(3)	119.14(11)
C(32)-C(31)-Si(3)	134.06(11)
N(7)-C(32)-C(31)	105.62(12)
N(7)-C(32)-C(33)	127.27(13)
C(31)-C(32)-C(33)	126.82(13)
O(9)-C(33)-C(32)	117.32(13)
O(9)-C(33)-C(34)	121.86(14)
C(32)-C(33)-C(34)	120.75(13)
C(33)-C(34)-H(34A)	109.5
C(33)-C(34)-H(34B)	109.5
H(34A)-C(34)-H(34B)	109.5
C(33)-C(34)-H(34C)	109.5
H(34A)-C(34)-H(34C)	109.5
H(34B)-C(34)-H(34C)	109.5
C(36)-C(35)-C(40)	123.84(14)
C(36)-C(35)-N(7)	118.50(14)
C(40)-C(35)-N(7)	117.56(13)
C(35)-C(36)-C(37)	117.66(14)
C(35)-C(36)-H(36)	121.2
C(37)-C(36)-H(36)	121.2
O(7)-C(37)-C(38)	124.64(13)
O(7)-C(37)-C(36)	114.51(14)
C(38)-C(37)-C(36)	120.84(14)
C(37)-C(38)-C(39)	119.33(14)
C(37)-C(38)-H(38)	120.3
C(39)-C(38)-H(38)	120.3
O(8)-C(39)-C(40)	123.44(14)
O(8)-C(39)-C(38)	115.35(13)
C(40)-C(39)-C(38)	121.20(14)
C(39)-C(40)-C(35)	117.13(14)

C(39)-C(40)-H(40)	121.4
C(35)-C(40)-H(40)	121.4
O(7)-C(41)-H(41A)	109.5
O(7)-C(41)-H(41B)	109.5
H(41A)-C(41)-H(41B)	109.5
O(7)-C(41)-H(41C)	109.5
H(41A)-C(41)-H(41C)	109.5
H(41B)-C(41)-H(41C)	109.5
O(8)-C(42)-H(42A)	109.5
O(8)-C(42)-H(42B)	109.5
H(42A)-C(42)-H(42B)	109.5
O(8)-C(42)-H(42C)	109.5
H(42A)-C(42)-H(42C)	109.5
H(42B)-C(42)-H(42C)	109.5
Si(3)-C(43)-H(43A)	109.5
Si(3)-C(43)-H(43B)	109.5
H(43A)-C(43)-H(43B)	109.5
Si(3)-C(43)-H(43C)	109.5
H(43A)-C(43)-H(43C)	109.5
H(43B)-C(43)-H(43C)	109.5
Si(3)-C(44)-H(44A)	109.5
Si(3)-C(44)-H(44B)	109.5
H(44A)-C(44)-H(44B)	109.5
Si(3)-C(44)-H(44C)	109.5
H(44A)-C(44)-H(44C)	109.5
H(44B)-C(44)-H(44C)	109.5
Si(3)-C(45)-H(45A)	109.5
Si(3)-C(45)-H(45B)	109.5
H(45A)-C(45)-H(45B)	109.5
Si(3)-C(45)-H(45C)	109.5
H(45A)-C(45)-H(45C)	109.5
H(45B)-C(45)-H(45C)	109.5
N(8)-N(7)-C(32)	110.07(11)
N(8)-N(7)-C(35)	117.52(11)
C(32)-N(7)-C(35)	131.99(12)
N(9)-N(8)-N(7)	107.42(11)

N(8)-N(9)-C(31)	110.18(12)
C(37)-O(7)-C(41)	118.05(13)
C(39)-O(8)-C(42)	116.82(12)

Symmetry transformations used to generate equivalent atoms:

Anisotropic displacement parameters ($\text{\AA}^2 \times 10^3$) for sb195t. The anisotropic displacement factor exponent takes the form: $-2\pi^2 [h^2 a^{*2} U^{11} + \dots + 2 h k a^* b^* U^{12}]$

	U ¹¹	U ²²	U ³³	U ²³	U ¹³	U ¹²
Si(1)	25(1)	21(1)	27(1)	2(1)	-1(1)	-3(1)
C(1)	23(1)	23(1)	22(1)	2(1)	0(1)	0(1)
C(2)	25(1)	22(1)	21(1)	1(1)	-1(1)	-2(1)
C(3)	26(1)	28(1)	27(1)	-1(1)	3(1)	0(1)
C(4)	25(1)	35(1)	48(1)	-7(1)	4(1)	1(1)
C(5)	24(1)	20(1)	33(1)	-1(1)	3(1)	-2(1)
C(6)	30(1)	21(1)	30(1)	-1(1)	2(1)	0(1)
C(7)	26(1)	21(1)	39(1)	-3(1)	-4(1)	1(1)
C(8)	26(1)	22(1)	42(1)	1(1)	0(1)	-5(1)
C(9)	33(1)	26(1)	34(1)	4(1)	2(1)	-4(1)
C(10)	29(1)	26(1)	32(1)	-1(1)	-2(1)	-5(1)
C(11)	30(1)	34(1)	59(1)	-1(1)	-13(1)	-6(1)
C(12)	53(1)	53(1)	32(1)	6(1)	-1(1)	-19(1)
C(13)	27(1)	34(1)	43(1)	0(1)	2(1)	-7(1)
C(14)	39(1)	27(1)	34(1)	4(1)	-5(1)	-3(1)
C(15)	47(1)	29(1)	31(1)	-2(1)	-3(1)	-4(1)
N(1)	23(1)	22(1)	27(1)	-1(1)	3(1)	-1(1)
N(2)	26(1)	25(1)	39(1)	0(1)	6(1)	1(1)
N(3)	25(1)	23(1)	36(1)	0(1)	4(1)	0(1)
O(1)	35(1)	33(1)	38(1)	-2(1)	-8(1)	-9(1)
O(2)	44(1)	46(1)	34(1)	7(1)	1(1)	-20(1)
O(3)	36(1)	26(1)	54(1)	-7(1)	11(1)	0(1)
Si(2)	25(1)	27(1)	26(1)	0(1)	0(1)	6(1)
C(16)	27(1)	25(1)	20(1)	-1(1)	-2(1)	1(1)
C(17)	26(1)	25(1)	21(1)	-1(1)	-2(1)	4(1)
C(18)	31(1)	28(1)	24(1)	-5(1)	0(1)	0(1)
C(19)	39(1)	25(1)	51(1)	-8(1)	-1(1)	-3(1)
C(20)	25(1)	23(1)	28(1)	-2(1)	0(1)	4(1)
C(21)	39(1)	29(1)	24(1)	-2(1)	-1(1)	9(1)
C(22)	41(1)	30(1)	29(1)	2(1)	-3(1)	12(1)
C(23)	35(1)	27(1)	33(1)	-2(1)	1(1)	11(1)

C(24)	27(1)	25(1)	24(1)	-3(1)	2(1)	0(1)
C(25)	25(1)	26(1)	25(1)	0(1)	-3(1)	2(1)
C(26)	69(1)	50(1)	28(1)	1(1)	-10(1)	25(1)
C(27)	49(1)	59(1)	26(1)	-11(1)	-5(1)	17(1)
C(28)	41(1)	32(1)	47(1)	-10(1)	0(1)	11(1)
C(29)	32(1)	48(1)	35(1)	7(1)	5(1)	5(1)
C(30)	29(1)	38(1)	33(1)	6(1)	-2(1)	5(1)
N(4)	25(1)	24(1)	23(1)	-3(1)	-2(1)	4(1)
N(5)	28(1)	24(1)	32(1)	-5(1)	-4(1)	3(1)
N(6)	26(1)	25(1)	30(1)	-4(1)	-4(1)	4(1)
O(4)	71(1)	44(1)	28(1)	-1(1)	-7(1)	33(1)
O(5)	35(1)	34(1)	26(1)	-7(1)	1(1)	7(1)
O(6)	32(1)	36(1)	49(1)	-6(1)	-14(1)	1(1)
Si(3)	22(1)	27(1)	26(1)	-2(1)	-3(1)	-3(1)
C(31)	21(1)	26(1)	22(1)	-1(1)	-1(1)	-1(1)
C(32)	23(1)	24(1)	20(1)	-2(1)	-1(1)	-3(1)
C(33)	25(1)	27(1)	22(1)	-2(1)	-3(1)	1(1)
C(34)	22(1)	33(1)	40(1)	-1(1)	-4(1)	3(1)
C(35)	22(1)	23(1)	29(1)	-4(1)	-3(1)	-1(1)
C(36)	28(1)	29(1)	24(1)	-2(1)	-3(1)	-2(1)
C(37)	24(1)	27(1)	28(1)	-2(1)	2(1)	-3(1)
C(38)	23(1)	27(1)	30(1)	-5(1)	-1(1)	-4(1)
C(39)	27(1)	27(1)	24(1)	-4(1)	-1(1)	0(1)
C(40)	26(1)	25(1)	25(1)	0(1)	1(1)	-2(1)
C(41)	31(1)	42(1)	39(1)	-5(1)	5(1)	-14(1)
C(42)	39(1)	44(1)	25(1)	-1(1)	1(1)	-7(1)
C(43)	27(1)	46(1)	42(1)	5(1)	-10(1)	-7(1)
C(44)	36(1)	39(1)	44(1)	-14(1)	0(1)	-7(1)
C(45)	32(1)	36(1)	36(1)	4(1)	0(1)	-4(1)
N(7)	23(1)	24(1)	23(1)	-1(1)	-4(1)	-1(1)
N(8)	27(1)	26(1)	34(1)	0(1)	-6(1)	-1(1)
N(9)	26(1)	29(1)	31(1)	1(1)	-6(1)	-2(1)
O(7)	37(1)	44(1)	28(1)	2(1)	1(1)	-18(1)
O(8)	38(1)	45(1)	23(1)	-2(1)	-4(1)	-14(1)
O(9)	32(1)	27(1)	41(1)	2(1)	-5(1)	-1(1)

Hydrogen coordinates ($\times 10^4$) and isotropic displacement parameters ($\text{\AA}^2 \times 10^{-3}$)
for sb195t.

	x	y	z	U(eq)
H(4A)	1421	2726	1781	54
H(4B)	1364	2710	1172	54
H(4C)	1123	3320	1477	54
H(6)	1999	1627	553	32
H(8)	745	643	1563	36
H(10)	2475	1711	2069	35
H(11A)	223	253	845	62
H(11B)	-101	598	352	62
H(11C)	-132	931	897	62
H(12A)	2398	959	2711	69
H(12B)	1705	924	3096	69
H(12C)	1893	1560	2809	69
H(13A)	5064	3516	625	52
H(13B)	5291	3383	1206	52
H(13C)	5309	4076	989	52
H(14A)	3723	4705	730	50
H(14B)	3015	4252	761	50
H(14C)	3663	4123	353	50
H(15A)	4145	3816	2075	53
H(15B)	3545	4316	1884	53
H(15C)	4421	4462	1841	53
H(19A)	3505	4700	3499	57
H(19B)	3404	4676	2892	57
H(19C)	4210	4813	3134	57
H(21)	1834	4151	2252	37
H(23)	810	5324	3241	38
H(25)	2254	4022	3776	31
H(26A)	1467	4943	1708	74
H(26B)	607	5075	1576	74
H(26C)	857	4407	1781	74

H(27A)	1619	4250	4510	67
H(27B)	1614	4910	4789	67
H(27C)	2292	4727	4419	67
H(28A)	4573	1341	2507	60
H(28B)	3971	1690	2158	60
H(28C)	3733	1428	2706	60
H(29A)	5236	3164	2543	58
H(29B)	4935	2794	2055	58
H(29C)	5581	2501	2403	58
H(30A)	5195	1983	3459	50
H(30B)	4349	2002	3658	50
H(30C)	4833	2625	3637	50
H(34A)	5364	2550	5186	47
H(34B)	5417	2723	4593	47
H(34C)	5501	2017	4771	47
H(36)	5061	4145	4127	32
H(38)	6297	4748	5334	32
H(40)	4576	3536	5558	31
H(41A)	6578	5513	4747	56
H(41B)	6986	5412	4210	56
H(41C)	7124	4933	4666	56
H(42A)	4674	3927	6334	54
H(42B)	5360	3896	6726	54
H(42C)	5264	3371	6300	54
H(43A)	1852	2629	3675	57
H(43B)	1533	2887	4205	57
H(43C)	1287	2216	4006	57
H(44A)	3309	1326	4154	59
H(44B)	3012	1648	3643	59
H(44C)	2480	1185	3953	59
H(45A)	1826	1590	4981	52
H(45B)	2010	2265	5200	52
H(45C)	2645	1742	5195	52

Torsion angles [°] for sb195t.

C(13)-Si(1)-C(1)-N(3)	-2.93(15)
C(15)-Si(1)-C(1)-N(3)	-121.24(13)
C(14)-Si(1)-C(1)-N(3)	115.64(13)
C(13)-Si(1)-C(1)-C(2)	-179.92(15)
C(15)-Si(1)-C(1)-C(2)	61.77(16)
C(14)-Si(1)-C(1)-C(2)	-61.35(16)
N(3)-C(1)-C(2)-N(1)	-0.10(16)
Si(1)-C(1)-C(2)-N(1)	177.23(12)
N(3)-C(1)-C(2)-C(3)	-174.99(14)
Si(1)-C(1)-C(2)-C(3)	2.3(2)
N(1)-C(2)-C(3)-O(3)	177.32(15)
C(1)-C(2)-C(3)-O(3)	-8.9(2)
N(1)-C(2)-C(3)-C(4)	-3.5(2)
C(1)-C(2)-C(3)-C(4)	170.26(16)
C(10)-C(5)-C(6)-C(7)	2.2(2)
N(1)-C(5)-C(6)-C(7)	-175.49(13)
C(5)-C(6)-C(7)-O(1)	177.24(13)
C(5)-C(6)-C(7)-C(8)	-2.0(2)
O(1)-C(7)-C(8)-C(9)	-178.78(14)
C(6)-C(7)-C(8)-C(9)	0.4(2)
C(7)-C(8)-C(9)-O(2)	-179.70(14)
C(7)-C(8)-C(9)-C(10)	1.1(2)
C(6)-C(5)-C(10)-C(9)	-0.7(2)
N(1)-C(5)-C(10)-C(9)	177.01(13)
O(2)-C(9)-C(10)-C(5)	179.93(15)
C(8)-C(9)-C(10)-C(5)	-1.0(2)
C(1)-C(2)-N(1)-N(2)	0.62(16)
C(3)-C(2)-N(1)-N(2)	175.41(15)
C(1)-C(2)-N(1)-C(5)	174.30(15)
C(3)-C(2)-N(1)-C(5)	-10.9(3)
C(6)-C(5)-N(1)-N(2)	-82.87(18)
C(10)-C(5)-N(1)-N(2)	99.29(17)
C(6)-C(5)-N(1)-C(2)	103.91(19)
C(10)-C(5)-N(1)-C(2)	-73.9(2)

C(2)-N(1)-N(2)-N(3)	-0.91(17)
C(5)-N(1)-N(2)-N(3)	-175.45(13)
N(1)-N(2)-N(3)-C(1)	0.84(17)
C(2)-C(1)-N(3)-N(2)	-0.46(17)
Si(1)-C(1)-N(3)-N(2)	-178.08(11)
C(8)-C(7)-O(1)-C(11)	15.8(2)
C(6)-C(7)-O(1)-C(11)	-163.40(13)
C(10)-C(9)-O(2)-C(12)	-5.7(2)
C(8)-C(9)-O(2)-C(12)	175.18(15)
C(29)-Si(2)-C(16)-N(6)	118.22(13)
C(30)-Si(2)-C(16)-N(6)	-116.99(13)
C(28)-Si(2)-C(16)-N(6)	0.17(15)
C(29)-Si(2)-C(16)-C(17)	-60.65(17)
C(30)-Si(2)-C(16)-C(17)	64.13(17)
C(28)-Si(2)-C(16)-C(17)	-178.71(16)
N(6)-C(16)-C(17)-N(4)	-0.16(16)
Si(2)-C(16)-C(17)-N(4)	178.82(12)
N(6)-C(16)-C(17)-C(18)	-174.07(14)
Si(2)-C(16)-C(17)-C(18)	4.9(3)
N(4)-C(17)-C(18)-O(6)	169.06(15)
C(16)-C(17)-C(18)-O(6)	-18.4(2)
N(4)-C(17)-C(18)-C(19)	-14.8(2)
C(16)-C(17)-C(18)-C(19)	157.74(16)
C(25)-C(20)-C(21)-C(22)	-0.3(2)
N(4)-C(20)-C(21)-C(22)	177.56(14)
C(20)-C(21)-C(22)-O(4)	-177.84(16)
C(20)-C(21)-C(22)-C(23)	2.7(3)
O(4)-C(22)-C(23)-C(24)	177.72(15)
C(21)-C(22)-C(23)-C(24)	-2.7(3)
C(22)-C(23)-C(24)-O(5)	-178.02(15)
C(22)-C(23)-C(24)-C(25)	0.4(2)
C(21)-C(20)-C(25)-C(24)	-1.9(2)
N(4)-C(20)-C(25)-C(24)	-179.75(13)
O(5)-C(24)-C(25)-C(20)	-179.84(14)
C(23)-C(24)-C(25)-C(20)	1.9(2)
C(16)-C(17)-N(4)-N(5)	0.52(17)

C(18)-C(17)-N(4)-N(5)	174.23(14)
C(16)-C(17)-N(4)-C(20)	177.81(15)
C(18)-C(17)-N(4)-C(20)	-8.5(3)
C(25)-C(20)-N(4)-N(5)	116.93(15)
C(21)-C(20)-N(4)-N(5)	-61.04(19)
C(25)-C(20)-N(4)-C(17)	-60.2(2)
C(21)-C(20)-N(4)-C(17)	121.84(18)
C(17)-N(4)-N(5)-N(6)	-0.69(17)
C(20)-N(4)-N(5)-N(6)	-178.41(12)
N(4)-N(5)-N(6)-C(16)	0.58(17)
C(17)-C(16)-N(6)-N(5)	-0.26(17)
Si(2)-C(16)-N(6)-N(5)	-179.40(11)
C(23)-C(22)-O(4)-C(26)	177.16(17)
C(21)-C(22)-O(4)-C(26)	-2.4(3)
C(23)-C(24)-O(5)-C(27)	-178.46(15)
C(25)-C(24)-O(5)-C(27)	3.2(2)
C(45)-Si(3)-C(31)-N(9)	-108.83(13)
C(44)-Si(3)-C(31)-N(9)	127.48(13)
C(43)-Si(3)-C(31)-N(9)	8.36(14)
C(45)-Si(3)-C(31)-C(32)	67.00(17)
C(44)-Si(3)-C(31)-C(32)	-56.69(18)
C(43)-Si(3)-C(31)-C(32)	-175.81(16)
N(9)-C(31)-C(32)-N(7)	-0.13(16)
Si(3)-C(31)-C(32)-N(7)	-176.33(12)
N(9)-C(31)-C(32)-C(33)	-174.26(14)
Si(3)-C(31)-C(32)-C(33)	9.5(3)
N(7)-C(32)-C(33)-O(9)	171.13(15)
C(31)-C(32)-C(33)-O(9)	-16.0(2)
N(7)-C(32)-C(33)-C(34)	-11.8(2)
C(31)-C(32)-C(33)-C(34)	161.07(15)
C(40)-C(35)-C(36)-C(37)	-0.4(2)
N(7)-C(35)-C(36)-C(37)	175.84(13)
C(35)-C(36)-C(37)-O(7)	-179.40(13)
C(35)-C(36)-C(37)-C(38)	0.2(2)
O(7)-C(37)-C(38)-C(39)	179.81(14)
C(36)-C(37)-C(38)-C(39)	0.3(2)

C(37)-C(38)-C(39)-O(8)	-179.83(14)
C(37)-C(38)-C(39)-C(40)	-0.6(2)
O(8)-C(39)-C(40)-C(35)	179.54(14)
C(38)-C(39)-C(40)-C(35)	0.3(2)
C(36)-C(35)-C(40)-C(39)	0.2(2)
N(7)-C(35)-C(40)-C(39)	-176.11(13)
C(31)-C(32)-N(7)-N(8)	0.39(16)
C(33)-C(32)-N(7)-N(8)	174.49(14)
C(31)-C(32)-N(7)-C(35)	172.59(15)
C(33)-C(32)-N(7)-C(35)	-13.3(3)
C(36)-C(35)-N(7)-N(8)	-64.28(18)
C(40)-C(35)-N(7)-N(8)	112.20(15)
C(36)-C(35)-N(7)-C(32)	123.99(17)
C(40)-C(35)-N(7)-C(32)	-59.5(2)
C(32)-N(7)-N(8)-N(9)	-0.51(16)
C(35)-N(7)-N(8)-N(9)	-173.98(13)
N(7)-N(8)-N(9)-C(31)	0.43(17)
C(32)-C(31)-N(9)-N(8)	-0.19(17)
Si(3)-C(31)-N(9)-N(8)	176.69(11)
C(38)-C(37)-O(7)-C(41)	2.1(2)
C(36)-C(37)-O(7)-C(41)	-178.34(13)
C(40)-C(39)-O(8)-C(42)	-0.6(2)
C(38)-C(39)-O(8)-C(42)	178.68(13)

X-Ray Structure Determination, C₅₄H₈₁N₉

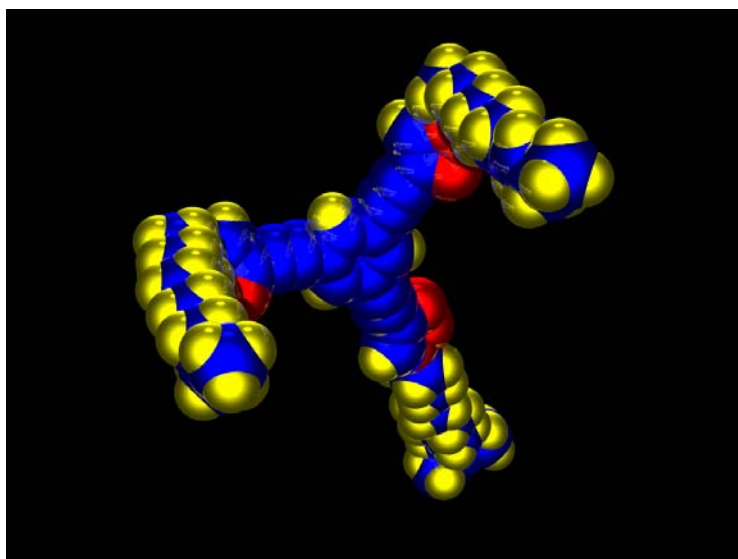


Table A15. Crystal data and structure refinement for ClickMom.

Identification code	BCEClickMom	
Empirical formula	C ₅₄ H ₈₁ N ₉	
Formula weight	856.28	
Temperature	105(2) K	
Wavelength	0.71073 Å	
Crystal system	Monoclinic	
Space group	P2(1)	
Unit cell dimensions	a = 5.4454(8) Å	α = 90°.
	b = 23.246(4) Å	β = 91.572(4)°.
	c = 20.351(3) Å	γ = 90°.
Volume	2575.2(7) Å ³	
Z	2	
Density (calculated)	1.104 Mg/m ³	
Absorption coefficient	0.066 mm ⁻¹	
F(000)	936	
Crystal size	0.40 x 0.09 x 0.04 mm ³	
Theta range for data collection	1.75 to 28.32°.	
Index ranges	-7 ≤ h ≤ 7, -30 ≤ k ≤ 31, -27 ≤ l ≤ 26	
Reflections collected	26675	
Independent reflections	12755 [R(int) = 0.1705]	
Completeness to theta = 28.32°	99.7 %	

Absorption correction	None
Refinement method	Full-matrix least-squares on F ²
Data / restraints / parameters	12755 / 1 / 255
Goodness-of-fit on F ²	1.133
Final R indices [I>2sigma(I)]	R1 = 0.2034, wR2 = 0.4180
R indices (all data)	R1 = 0.2798, wR2 = 0.4720
Absolute structure parameter	2(9)
Largest diff. peak and hole	0.852 and -0.676 e.Å ⁻³

Atomic coordinates ($\times 10^4$) and equivalent isotropic displacement parameters ($\text{\AA}^2 \times 10^3$) for ClickMom. $U(\text{eq})$ is defined as one third of the trace of the orthogonalized U^{ij} tensor.

	x	y	z	U(eq)
C(1)	-3930(14)	-9674(3)	-5055(4)	18(2)
C(2)	-5860(11)	-9706(3)	-4620(3)	3(1)
C(3)	-7026(10)	-9151(3)	-4402(3)	9(1)
C(4)	-6197(11)	-8656(3)	-4605(3)	4(1)
C(5)	-4029(12)	-8651(3)	-5008(3)	6(1)
C(6)	-2995(10)	-9239(3)	-5223(3)	4(1)
C(7)	-2911(12)	-10242(2)	-5267(3)	4(1)
C(8)	-2212(13)	-10702(3)	-5408(3)	11(1)
C(9)	-1628(14)	-11262(3)	-5641(4)	15(2)
C(10)	841(13)	-11449(3)	-5830(3)	10
C(11)	2103(13)	-12384(3)	-6350(3)	10
C(12)	2447(13)	-12243(3)	-7059(3)	13(1)
C(13)	77(13)	-12328(3)	-7473(3)	13(1)
C(14)	554(12)	-12321(3)	-8234(3)	6(1)
C(15)	-1792(19)	-12453(4)	-8665(5)	36(2)
C(16)	-1307(15)	-12483(3)	-9316(4)	22(2)
C(17)	-3856(15)	-12521(3)	-9715(4)	20(2)
C(18)	-3615(12)	-12505(3)	-10521(3)	7(1)
C(19)	-6194(17)	-12513(4)	-10768(4)	31(2)
C(20)	-5870(30)	-12534(7)	-11604(8)	87(5)
C(21)	-8450(20)	-12618(6)	-11941(6)	62(3)
C(22)	-8030(19)	-12395(4)	-12638(5)	36(2)
C(23)	-8999(11)	-9149(3)	-3962(3)	10(1)
C(24)	-10602(9)	-9174(3)	-3557(2)	2(1)
C(25)	-12445(11)	-9128(3)	-3080(3)	13(1)
C(26)	-14293(12)	-9416(3)	-2854(3)	7(1)
C(27)	-17569(10)	-9121(3)	-2015(3)	8(1)
C(28)	-16969(10)	-9201(3)	-1253(3)	7(1)
C(29)	-19398(12)	-9143(4)	-915(3)	18(1)
C(30)	-19052(12)	-9102(3)	-151(3)	14(1)
C(31)	-21572(11)	-9248(3)	189(3)	12(1)

C(32)	-21281(12)	-9252(3)	948(3)	14(1)
C(33)	-23663(11)	-9075(3)	1294(3)	9(1)
C(34)	-23380(15)	-9280(4)	2028(4)	27(2)
C(35)	-25838(12)	-9086(3)	2389(3)	13(1)
C(36)	-25552(13)	-9301(3)	3136(3)	17(2)
C(37)	-27915(12)	-9153(4)	3495(3)	15(1)
C(38)	-28660(20)	-9771(5)	3426(6)	10
C(38B)	-28140(30)	-8513(6)	3512(8)	11(3)
C(39)	-3127(15)	-8127(3)	-5233(4)	18(2)
C(40)	-2242(14)	-7678(3)	-5449(4)	14(2)
C(41)	-1367(13)	-7127(3)	-5659(3)	10
C(42)	735(13)	-6904(3)	-5795(3)	10
C(43)	2031(13)	-5925(3)	-6228(3)	11(1)
C(44)	2529(14)	-6011(3)	-6966(4)	16(2)
C(45)	448(15)	-5783(4)	-7404(4)	23(2)
C(46)	856(13)	-5824(3)	-8126(3)	15(2)
C(47)	-1576(15)	-5850(4)	-8550(4)	23(2)
C(48)	-1405(17)	-5894(4)	-9356(4)	32(2)
C(49)	-3769(16)	-5838(4)	-9723(4)	22(2)
C(50)	-3554(15)	-5843(3)	-10389(4)	20(2)
C(51)	-5901(11)	-5809(3)	-10866(3)	4(1)
C(52)	-5878(14)	-5832(3)	-11567(4)	15(2)
C(53)	-8256(17)	-5875(4)	-11927(4)	30(2)
C(54)	-8154(17)	-5641(4)	-12751(4)	32(2)
N(1)	-3190(11)	-11662(3)	-5750(3)	13(1)
N(2)	-2094(13)	-12118(3)	-5986(3)	24(2)
N(3)	454(11)	-12009(2)	-5986(3)	10
N(4)	-12427(12)	-8570(3)	-2725(3)	19(1)
N(5)	-14150(10)	-8606(2)	-2287(3)	10(1)
N(6)	-15328(9)	-9154(3)	-2381(2)	9(1)
N(7)	-3154(12)	-6690(3)	-5769(3)	16(1)
N(8)	-2001(11)	-6225(2)	-5981(3)	9(1)
N(9)	267(11)	-6378(2)	-6044(3)	10

Bond lengths [Å] and angles [°] for ClickMom.

C(1)-C(6)	1.187(9)	C(17)-C(18)	1.648(10)
C(1)-C(2)	1.395(10)	C(17)-H(17A)	0.9900
C(1)-C(7)	1.501(9)	C(17)-H(17B)	0.9900
C(2)-C(3)	1.510(9)	C(18)-C(19)	1.479(12)
C(2)-H(2)	0.9500	C(18)-H(18A)	0.9900
C(3)-C(4)	1.308(9)	C(18)-H(18B)	0.9900
C(3)-C(23)	1.416(8)	C(19)-C(20)	1.716(18)
C(4)-C(5)	1.456(9)	C(19)-H(19A)	0.9900
C(4)-H(4)	0.9500	C(19)-H(19B)	0.9900
C(5)-C(39)	1.395(10)	C(20)-C(21)	1.56(2)
C(5)-C(6)	1.547(8)	C(20)-H(20A)	0.9900
C(6)-H(6)	0.9500	C(20)-H(20B)	0.9900
C(7)-C(8)	1.172(9)	C(21)-C(22)	1.535(16)
C(8)-C(9)	1.424(10)	C(21)-H(21A)	0.9900
C(9)-N(1)	1.277(9)	C(21)-H(21B)	0.9900
C(9)-C(10)	1.475(10)	C(22)-H(22A)	0.9800
C(10)-N(3)	1.356(8)	C(22)-H(22B)	0.9800
C(10)-H(10)	0.9500	C(22)-H(22C)	0.9800
C(11)-N(3)	1.465(9)	C(23)-C(24)	1.218(8)
C(11)-C(12)	1.497(10)	C(24)-C(25)	1.420(8)
C(11)-H(11A)	0.9900	C(25)-C(26)	1.302(9)
C(11)-H(11B)	0.9900	C(25)-N(4)	1.484(10)
C(12)-C(13)	1.534(10)	C(26)-N(6)	1.283(8)
C(12)-H(12A)	0.9900	C(26)-H(26)	0.9500
C(12)-H(12B)	0.9900	C(27)-N(6)	1.449(7)
C(13)-C(14)	1.578(9)	C(27)-C(28)	1.586(8)
C(13)-H(13A)	0.9900	C(27)-H(27A)	0.9900
C(13)-H(13B)	0.9900	C(27)-H(27B)	0.9900
C(14)-C(15)	1.560(12)	C(28)-C(29)	1.514(9)
C(14)-H(14A)	0.9900	C(28)-H(28A)	0.9900
C(14)-H(14B)	0.9900	C(28)-H(28B)	0.9900
C(15)-C(16)	1.361(12)	C(29)-C(30)	1.564(9)
C(15)-H(15)	0.9500	C(29)-H(29A)	0.9900
C(16)-C(17)	1.591(12)	C(29)-H(29B)	0.9900
C(16)-H(16A)	0.9900	C(30)-C(31)	1.591(9)
C(16)-H(16B)	0.9900	C(30)-H(30A)	0.9900

C(30)-H(30B)	0.9900	C(43)-H(43B)	0.9900
C(31)-C(32)	1.548(9)	C(44)-C(45)	1.518(11)
C(31)-H(31A)	0.9900	C(44)-H(44A)	0.9900
C(31)-H(31B)	0.9900	C(44)-H(44B)	0.9900
C(32)-C(33)	1.549(9)	C(45)-C(46)	1.494(11)
C(32)-H(32A)	0.9900	C(45)-H(45A)	0.9900
C(32)-H(32B)	0.9900	C(45)-H(45B)	0.9900
C(33)-C(34)	1.570(10)	C(46)-C(47)	1.562(11)
C(33)-H(33A)	0.9900	C(46)-H(46A)	0.9900
C(33)-H(33B)	0.9900	C(46)-H(46B)	0.9900
C(34)-C(35)	1.608(10)	C(47)-C(48)	1.648(12)
C(34)-H(34A)	0.9900	C(47)-H(47A)	0.9900
C(34)-H(34B)	0.9900	C(47)-H(47B)	0.9900
C(35)-C(36)	1.605(9)	C(48)-C(49)	1.476(12)
C(35)-H(35A)	0.9900	C(48)-H(48A)	0.9900
C(35)-H(35B)	0.9900	C(48)-H(48B)	0.9900
C(36)-C(37)	1.535(10)	C(49)-C(50)	1.364(11)
C(36)-H(36A)	0.9900	C(49)-H(49)	0.9500
C(36)-H(36B)	0.9900	C(50)-C(51)	1.586(10)
C(37)-C(38)	1.496(14)	C(50)-H(50A)	0.9900
C(37)-C(38B)	1.493(17)	C(50)-H(50B)	0.9900
C(38)-H(38A)	0.9800	C(51)-C(52)	1.429(9)
C(38)-H(38B)	0.9800	C(51)-H(51A)	0.9900
C(38)-H(38C)	0.9800	C(51)-H(51B)	0.9900
C(38B)-H(38D)	0.9800	C(52)-C(53)	1.473(12)
C(38B)-H(38E)	0.9800	C(52)-H(52)	0.9500
C(38B)-H(38F)	0.9800	C(53)-C(54)	1.766(13)
C(39)-C(40)	1.235(10)	C(53)-H(53A)	0.9900
C(40)-C(41)	1.437(10)	C(53)-H(53B)	0.9900
C(41)-C(42)	1.293(10)	C(54)-H(54A)	0.9800
C(41)-N(7)	1.420(9)	C(54)-H(54B)	0.9800
C(42)-N(9)	1.347(8)	C(54)-H(54C)	0.9800
C(42)-H(42)	0.9500	N(1)-N(2)	1.313(9)
C(43)-N(9)	1.480(9)	N(2)-N(3)	1.410(9)
C(43)-C(44)	1.547(10)	N(4)-N(5)	1.314(8)
C(43)-H(43A)	0.9900	N(5)-N(6)	1.436(8)

N(7)-N(8)	1.328(9)	C(11)-C(12)-H(12A)	109.2
N(8)-N(9)	1.295(8)	C(13)-C(12)-H(12A)	109.2
		C(11)-C(12)-H(12B)	109.2
C(6)-C(1)-C(2)	124.5(7)	C(13)-C(12)-H(12B)	109.2
C(6)-C(1)-C(7)	120.1(7)	H(12A)-C(12)-H(12B)	107.9
C(2)-C(1)-C(7)	115.2(6)	C(12)-C(13)-C(14)	112.2(6)
C(1)-C(2)-C(3)	118.1(6)	C(12)-C(13)-H(13A)	109.2
C(1)-C(2)-H(2)	121.0	C(14)-C(13)-H(13A)	109.2
C(3)-C(2)-H(2)	121.0	C(12)-C(13)-H(13B)	109.1
C(4)-C(3)-C(23)	118.1(6)	C(14)-C(13)-H(13B)	109.1
C(4)-C(3)-C(2)	120.5(5)	H(13A)-C(13)-H(13B)	107.9
C(23)-C(3)-C(2)	121.4(6)	C(15)-C(14)-C(13)	113.3(6)
C(3)-C(4)-C(5)	118.5(6)	C(15)-C(14)-H(14A)	108.9
C(3)-C(4)-H(4)	120.7	C(13)-C(14)-H(14A)	108.9
C(5)-C(4)-H(4)	120.7	C(15)-C(14)-H(14B)	108.9
C(39)-C(5)-C(4)	119.4(6)	C(13)-C(14)-H(14B)	108.9
C(39)-C(5)-C(6)	122.9(6)	H(14A)-C(14)-H(14B)	107.7
C(4)-C(5)-C(6)	117.4(5)	C(16)-C(15)-C(14)	112.4(8)
C(1)-C(6)-C(5)	120.5(6)	C(16)-C(15)-H(15)	123.8
C(1)-C(6)-H(6)	119.7	C(14)-C(15)-H(15)	123.8
C(5)-C(6)-H(6)	119.7	C(15)-C(16)-C(17)	108.1(8)
C(8)-C(7)-C(1)	175.9(7)	C(15)-C(16)-H(16A)	110.1
C(7)-C(8)-C(9)	172.4(8)	C(17)-C(16)-H(16A)	110.1
N(1)-C(9)-C(8)	124.8(7)	C(15)-C(16)-H(16B)	110.0
N(1)-C(9)-C(10)	110.3(6)	C(17)-C(16)-H(16B)	110.0
C(8)-C(9)-C(10)	124.7(6)	H(16A)-C(16)-H(16B)	108.4
N(3)-C(10)-C(9)	102.0(6)	C(16)-C(17)-C(18)	114.5(6)
N(3)-C(10)-H(10)	129.0	C(16)-C(17)-H(17A)	108.7
C(9)-C(10)-H(10)	129.0	C(18)-C(17)-H(17A)	108.7
N(3)-C(11)-C(12)	116.9(6)	C(16)-C(17)-H(17B)	108.6
N(3)-C(11)-H(11A)	108.1	C(18)-C(17)-H(17B)	108.6
C(12)-C(11)-H(11A)	108.1	H(17A)-C(17)-H(17B)	107.6
N(3)-C(11)-H(11B)	108.1	C(19)-C(18)-C(17)	103.8(6)
C(12)-C(11)-H(11B)	108.1	C(19)-C(18)-H(18A)	111.0
H(11A)-C(11)-H(11B)	107.3	C(17)-C(18)-H(18A)	111.0
C(11)-C(12)-C(13)	112.0(6)	C(19)-C(18)-H(18B)	111.0

C(17)-C(18)-H(18B)	111.0	C(28)-C(27)-H(27A)	109.7
H(18A)-C(18)-H(18B)	109.0	N(6)-C(27)-H(27B)	109.7
C(18)-C(19)-C(20)	102.5(8)	C(28)-C(27)-H(27B)	109.6
C(18)-C(19)-H(19A)	111.3	H(27A)-C(27)-H(27B)	108.2
C(20)-C(19)-H(19A)	111.3	C(29)-C(28)-C(27)	106.0(5)
C(18)-C(19)-H(19B)	111.2	C(29)-C(28)-H(28A)	110.6
C(20)-C(19)-H(19B)	111.2	C(27)-C(28)-H(28A)	110.5
H(19A)-C(19)-H(19B)	109.2	C(29)-C(28)-H(28B)	110.5
C(21)-C(20)-C(19)	108.9(11)	C(27)-C(28)-H(28B)	110.5
C(21)-C(20)-H(20A)	109.9	H(28A)-C(28)-H(28B)	108.7
C(19)-C(20)-H(20A)	109.9	C(28)-C(29)-C(30)	112.0(5)
C(21)-C(20)-H(20B)	109.9	C(28)-C(29)-H(29A)	109.2
C(19)-C(20)-H(20B)	109.9	C(30)-C(29)-H(29A)	109.2
H(20A)-C(20)-H(20B)	108.3	C(28)-C(29)-H(29B)	109.2
C(22)-C(21)-C(20)	101.9(11)	C(30)-C(29)-H(29B)	109.2
C(22)-C(21)-H(21A)	111.4	H(29A)-C(29)-H(29B)	107.9
C(20)-C(21)-H(21A)	111.4	C(29)-C(30)-C(31)	109.7(5)
C(22)-C(21)-H(21B)	111.4	C(29)-C(30)-H(30A)	109.7
C(20)-C(21)-H(21B)	111.4	C(31)-C(30)-H(30A)	109.7
H(21A)-C(21)-H(21B)	109.3	C(29)-C(30)-H(30B)	109.8
C(21)-C(22)-H(22A)	109.5	C(31)-C(30)-H(30B)	109.7
C(21)-C(22)-H(22B)	109.4	H(30A)-C(30)-H(30B)	108.2
H(22A)-C(22)-H(22B)	109.5	C(32)-C(31)-C(30)	111.7(5)
C(21)-C(22)-H(22C)	109.5	C(32)-C(31)-H(31A)	109.3
H(22A)-C(22)-H(22C)	109.5	C(30)-C(31)-H(31A)	109.3
H(22B)-C(22)-H(22C)	109.5	C(32)-C(31)-H(31B)	109.3
C(24)-C(23)-C(3)	175.5(7)	C(30)-C(31)-H(31B)	109.3
C(23)-C(24)-C(25)	172.9(7)	H(31A)-C(31)-H(31B)	107.9
C(26)-C(25)-C(24)	140.4(7)	C(31)-C(32)-C(33)	112.8(5)
C(26)-C(25)-N(4)	105.7(6)	C(31)-C(32)-H(32A)	109.0
C(24)-C(25)-N(4)	113.8(6)	C(33)-C(32)-H(32A)	109.1
N(6)-C(26)-C(25)	112.4(6)	C(31)-C(32)-H(32B)	109.0
N(6)-C(26)-H(26)	123.8	C(33)-C(32)-H(32B)	109.0
C(25)-C(26)-H(26)	123.8	H(32A)-C(32)-H(32B)	107.8
N(6)-C(27)-C(28)	110.0(5)	C(32)-C(33)-C(34)	106.9(5)
N(6)-C(27)-H(27A)	109.6	C(32)-C(33)-H(33A)	110.4

C(34)-C(33)-H(33A)	110.4	C(42)-C(41)-N(7)	106.7(6)
C(32)-C(33)-H(33B)	110.3	C(42)-C(41)-C(40)	136.4(7)
C(34)-C(33)-H(33B)	110.3	N(7)-C(41)-C(40)	117.0(6)
H(33A)-C(33)-H(33B)	108.6	C(41)-C(42)-N(9)	106.5(6)
C(33)-C(34)-C(35)	106.8(6)	C(41)-C(42)-H(42)	126.7
C(33)-C(34)-H(34A)	110.4	N(9)-C(42)-H(42)	126.7
C(35)-C(34)-H(34A)	110.3	N(9)-C(43)-C(44)	106.6(5)
C(33)-C(34)-H(34B)	110.4	N(9)-C(43)-H(43A)	110.4
C(35)-C(34)-H(34B)	110.4	C(44)-C(43)-H(43A)	110.4
H(34A)-C(34)-H(34B)	108.6	N(9)-C(43)-H(43B)	110.4
C(36)-C(35)-C(34)	106.6(5)	C(44)-C(43)-H(43B)	110.4
C(36)-C(35)-H(35A)	110.4	H(43A)-C(43)-H(43B)	108.6
C(34)-C(35)-H(35A)	110.4	C(45)-C(44)-C(43)	112.1(6)
C(36)-C(35)-H(35B)	110.4	C(45)-C(44)-H(44A)	109.2
C(34)-C(35)-H(35B)	110.4	C(43)-C(44)-H(44A)	109.2
H(35A)-C(35)-H(35B)	108.6	C(45)-C(44)-H(44B)	109.2
C(37)-C(36)-C(35)	108.6(5)	C(43)-C(44)-H(44B)	109.2
C(37)-C(36)-H(36A)	110.0	H(44A)-C(44)-H(44B)	107.9
C(35)-C(36)-H(36A)	110.0	C(46)-C(45)-C(44)	115.2(7)
C(37)-C(36)-H(36B)	109.9	C(46)-C(45)-H(45A)	108.5
C(35)-C(36)-H(36B)	109.9	C(44)-C(45)-H(45A)	108.5
H(36A)-C(36)-H(36B)	108.3	C(46)-C(45)-H(45B)	108.5
C(38)-C(37)-C(38B)	159.4(9)	C(44)-C(45)-H(45B)	108.5
C(38)-C(37)-C(36)	88.2(7)	H(45A)-C(45)-H(45B)	107.5
C(38B)-C(37)-C(36)	107.7(8)	C(45)-C(46)-C(47)	113.5(6)
C(37)-C(38)-H(38A)	109.5	C(45)-C(46)-H(46A)	108.9
C(37)-C(38)-H(38B)	109.5	C(47)-C(46)-H(46A)	108.9
C(37)-C(38)-H(38C)	109.4	C(45)-C(46)-H(46B)	108.9
C(37)-C(38B)-H(38D)	109.4	C(47)-C(46)-H(46B)	108.9
C(37)-C(38B)-H(38E)	109.5	H(46A)-C(46)-H(46B)	107.7
H(38D)-C(38B)-H(38E)	109.5	C(46)-C(47)-C(48)	118.8(7)
C(37)-C(38B)-H(38F)	109.5	C(46)-C(47)-H(47A)	107.6
H(38D)-C(38B)-H(38F)	109.5	C(48)-C(47)-H(47A)	107.7
H(38E)-C(38B)-H(38F)	109.5	C(46)-C(47)-H(47B)	107.6
C(40)-C(39)-C(5)	176.9(8)	C(48)-C(47)-H(47B)	107.6
C(39)-C(40)-C(41)	174.5(8)	H(47A)-C(47)-H(47B)	107.0

C(49)-C(48)-C(47)	115.2(7)	C(9)-N(1)-N(2)	110.2(6)
C(49)-C(48)-H(48A)	108.4	N(1)-N(2)-N(3)	108.2(6)
C(47)-C(48)-H(48A)	108.4	C(10)-N(3)-N(2)	108.6(6)
C(49)-C(48)-H(48B)	108.5	C(10)-N(3)-C(11)	126.5(6)
C(47)-C(48)-H(48B)	108.5	N(2)-N(3)-C(11)	120.7(5)
H(48A)-C(48)-H(48B)	107.5	N(5)-N(4)-C(25)	106.2(5)
C(50)-C(49)-C(48)	113.9(8)	N(4)-N(5)-N(6)	106.9(5)
C(50)-C(49)-H(49)	123.0	C(26)-N(6)-N(5)	108.4(5)
C(48)-C(49)-H(49)	123.1	C(26)-N(6)-C(27)	143.6(6)
C(49)-C(50)-C(51)	121.2(7)	N(5)-N(6)-C(27)	105.4(5)
C(49)-C(50)-H(50A)	107.0	N(8)-N(7)-C(41)	107.8(6)
C(51)-C(50)-H(50A)	107.0	N(9)-N(8)-N(7)	105.7(5)
C(49)-C(50)-H(50B)	107.0	N(8)-N(9)-C(42)	112.5(6)
C(51)-C(50)-H(50B)	107.0	N(8)-N(9)-C(43)	117.2(5)
H(50A)-C(50)-H(50B)	106.8	C(42)-N(9)-C(43)	128.6(6)
C(52)-C(51)-C(50)	125.5(6)		
C(52)-C(51)-H(51A)	105.9		
C(50)-C(51)-H(51A)	105.9		
C(52)-C(51)-H(51B)	106.0		
C(50)-C(51)-H(51B)	106.0		
H(51A)-C(51)-H(51B)	106.3		
C(51)-C(52)-C(53)	117.9(7)		
C(51)-C(52)-H(52)	121.1		
C(53)-C(52)-H(52)	121.1		
C(52)-C(53)-C(54)	113.7(7)		
C(52)-C(53)-H(53A)	108.8		
C(54)-C(53)-H(53A)	108.8		
C(52)-C(53)-H(53B)	108.8		
C(54)-C(53)-H(53B)	108.8		
H(53A)-C(53)-H(53B)	107.7		
C(53)-C(54)-H(54A)	109.5		
C(53)-C(54)-H(54B)	109.5		
H(54A)-C(54)-H(54B)	109.5		
C(53)-C(54)-H(54C)	109.5		
H(54A)-C(54)-H(54C)	109.5		
H(54B)-C(54)-H(54C)	109.5		

Symmetry transformations used to generate equivalent atoms:

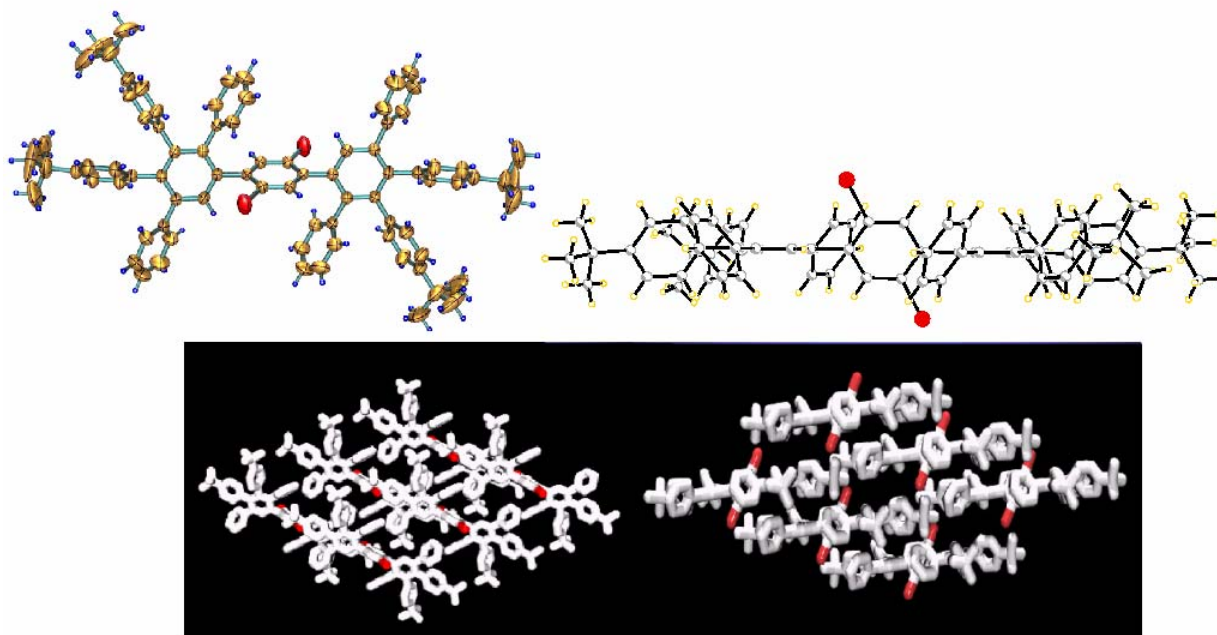
Hydrogen coordinates ($\times 10^4$) and isotropic displacement parameters ($\text{\AA}^2 \times 10^{-3}$)
for ClickMom.

	x	y	z	U(eq)
H(2)	-6425	-10067	-4465	3
H(4)	-6992	-8307	-4492	4
H(6)	-1599	-9252	-5493	5
H(10)	2320	-11232	-5840	12
H(11A)	1475	-12782	-6323	12
H(11B)	3736	-12376	-6124	12
H(12A)	3752	-12492	-7234	16
H(12B)	2992	-11839	-7098	16
H(13A)	-1100	-12019	-7368	15
H(13B)	-678	-12701	-7354	15
H(14A)	1194	-11938	-8356	7
H(14B)	1831	-12610	-8331	7
H(15)	-3379	-12506	-8492	44
H(16A)	-299	-12828	-9405	26
H(16B)	-385	-12138	-9452	26
H(17A)	-4906	-12196	-9581	25
H(17B)	-4695	-12881	-9593	25
H(18A)	-2765	-12151	-10662	9
H(18B)	-2706	-12844	-10678	9
H(19A)	-7084	-12162	-10633	37
H(19B)	-7074	-12856	-10610	37
H(20A)	-5130	-12171	-11757	104
H(20B)	-4778	-12856	-11722	104
H(21A)	-8945	-13028	-11945	75
H(21B)	-9724	-12390	-11719	75
H(22A)	-6510	-12560	-12803	54
H(22B)	-7894	-11974	-12629	54
H(22C)	-9415	-12507	-12928	54
H(26)	-14816	-9778	-3022	8
H(27A)	-18722	-9425	-2168	10

H(27B)	-18366	-8744	-2092	10
H(28A)	-16238	-9585	-1167	8
H(28B)	-15800	-8903	-1094	8
H(29A)	-20442	-9480	-1026	22
H(29B)	-20257	-8795	-1079	22
H(30A)	-18517	-8709	-26	17
H(30B)	-17765	-9375	2	17
H(31A)	-22823	-8959	55	15
H(31B)	-22159	-9630	37	15
H(32A)	-19945	-8984	1082	16
H(32B)	-20797	-9643	1095	16
H(33A)	-25109	-9260	1077	11
H(33B)	-23885	-8653	1274	11
H(34A)	-21921	-9099	2242	32
H(34B)	-23185	-9703	2048	32
H(35A)	-26026	-8663	2372	16
H(35B)	-27299	-9264	2172	16
H(36A)	-25270	-9722	3149	21
H(36B)	-24128	-9109	3356	21
H(38A)	-29593	-9824	3012	15
H(38B)	-29675	-9880	3795	15
H(38C)	-27183	-10013	3425	15
H(38D)	-27704	-8354	3084	17
H(38E)	-27022	-8358	3854	17
H(38F)	-29831	-8407	3608	17
H(42)	2303	-7078	-5731	12
H(43A)	3575	-5961	-5963	13
H(43B)	1327	-5539	-6152	13
H(44A)	4071	-5811	-7075	20
H(44B)	2755	-6426	-7054	20
H(45A)	-1067	-5997	-7305	27
H(45B)	168	-5374	-7292	27
H(46A)	1838	-6172	-8213	18
H(46B)	1822	-5486	-8264	18
H(47A)	-2546	-5502	-8449	28
H(47B)	-2527	-6186	-8400	28

H(48A)	-283	-5589	-9507	38
H(48B)	-665	-6269	-9467	38
H(49)	-5301	-5802	-9514	26
H(50A)	-2660	-6199	-10502	24
H(50B)	-2476	-5516	-10502	24
H(51A)	-6999	-6124	-10730	4
H(51B)	-6745	-5446	-10756	4
H(52)	-4378	-5820	-11794	18
H(53A)	-9484	-5641	-11695	36
H(53B)	-8813	-6280	-11920	36
H(54A)	-8382	-5972	-13046	48
H(54B)	-6558	-5462	-12828	48
H(54C)	-9466	-5360	-12838	48

X-Ray Structure Determination, $C_{82}H_{76}Br_2 \cdot 3CH_2Cl_2$



X-ray intensity data from a colorless prism were measured at 293(2) K on a Bruker SMART APEX CCD-based diffractometer (Mo $K\alpha$ radiation, $\lambda = 0.71073$ Å).¹ Raw data frame integration and Lp corrections were performed with SAINT+.¹ Final unit cell parameters were determined by least-squares refinement of 9082 reflections from the data set with $I > 5(\sigma)I$. Analysis of the data showed negligible crystal decay during collection. An empirical absorption correction was applied with SADABS.¹ Direct methods structure solution, difference Fourier calculations and full-matrix least-squares refinement against F^2 were performed with SHELXTL.²

$C_{82}H_{76}Br_2 \cdot 3CH_2Cl_2$ crystallizes with monoclinic symmetry in the space group C2/c. The asymmetric unit consists of half of the $C_{82}H_{76}Br_2$ molecule located on a center of symmetry, half a CH_2Cl_2 molecule of crystallization disordered about a two-fold rotational axis and another CH_2Cl_2 disordered over three orientations. Both independent *tert*-butyl groups of the $C_{82}H_{76}Br_2$ molecule are rotationally disordered over two orientations in a ca. 90/10 ratio. A total of 78 geometric restraints was used to model the solvent and *tert*-butyl disorder. Eventually all non-hydrogen atoms were refined with anisotropic displacement parameters except the carbon atoms of the minor *tert*-butyl disorder components (isotropic); hydrogen atoms of the $C_{82}H_{76}Br_2$ molecule were placed in geometrically idealized positions and included as riding atoms; CH_2Cl_2 hydrogens were not located or calculated.

(1) SMART Version 5.625, SAINT+ Version 6.22 and SADABS Version 2.05. Bruker Analytical X-ray Systems, Inc., Madison, Wisconsin, USA, 2001.

(2) Sheldrick, G. M. SHELXTL Version 6.1; Bruker Analytical X-ray Systems, Inc., Madison, Wisconsin, USA, 2000.

TableA16. Crystal data and structure refinement for bce02s.

Identification code	bce02s	
Empirical formula	C ₈₅ H ₈₂ Br ₂ Cl ₆	
Formula weight	1476.03	
Temperature	293(2) K	
Wavelength	0.71073 Å	
Crystal system	Monoclinic	
Space group	C2/c	
Unit cell dimensions	a = 18.0965(8) Å	α = 90°.
	b = 13.1459(6) Å	β = 97.9830(10)°.
	c = 34.1803(15) Å	γ = 90°.
Volume	8052.5(6) Å ³	
Z	4	
Density (calculated)	1.218 Mg/m ³	
Absorption coefficient	1.247 mm ⁻¹	
F(000)	3056	
Crystal size	0.42 x 0.28 x 0.22 mm ³	
Theta range for data collection	1.92 to 22.54°.	
Index ranges	-19 ≤ h ≤ 19, -14 ≤ k ≤ 14, -36 ≤ l ≤ 36	
Reflections collected	25999	
Independent reflections	5289 [R(int) = 0.0387]	
Completeness to theta = 22.54°	100.0 %	
Absorption correction	Semi-empirical from equivalents	
Max. and min. transmission	1.0000 and 0.8297	
Refinement method	Full-matrix least-squares on F ²	
Data / restraints / parameters	5289 / 78 / 504	
Goodness-of-fit on F ²	1.038	
Final R indices [I > 2σ(I)]	R1 = 0.0481, wR2 = 0.1326	
R indices (all data)	R1 = 0.0632, wR2 = 0.1433	
Largest diff. peak and hole	0.351 and -0.553 e.Å ⁻³	

Atomic coordinates ($\times 10^4$) and equivalent isotropic displacement parameters ($\text{\AA}^2 \times 10^3$) for bce02s. $U(\text{eq})$ is defined as one third of the trace of the orthogonalized U^{ij} tensor.

	x	y	z	$U(\text{eq})$
Br	5570(1)	2026(1)	4583(1)	95(1)
C(1)	5222(2)	855(2)	4828(1)	57(1)
C(2)	4938(2)	955(2)	5183(1)	52(1)
C(3)	4717(2)	74(2)	5352(1)	57(1)
C(4)	4867(2)	1960(2)	5380(1)	53(1)
C(5)	5306(2)	2197(2)	5740(1)	53(1)
C(6)	5211(2)	3146(2)	5917(1)	53(1)
C(7)	4695(2)	3852(2)	5735(1)	52(1)
C(8)	4249(2)	3598(2)	5380(1)	53(1)
C(9)	4348(2)	2659(2)	5212(1)	58(1)
C(10)	5866(2)	1448(2)	5925(1)	56(1)
C(11)	6451(2)	1156(3)	5734(1)	72(1)
C(12)	6974(3)	454(4)	5897(2)	98(2)
C(13)	6906(3)	39(4)	6253(2)	104(2)
C(14)	6336(3)	310(3)	6447(1)	93(1)
C(15)	5807(2)	1015(3)	6287(1)	73(1)
C(16)	5653(2)	3389(2)	6309(1)	54(1)
C(17)	6413(2)	3534(3)	6358(1)	68(1)
C(18)	6801(2)	3772(3)	6722(1)	80(1)
C(19)	6453(2)	3886(3)	7054(1)	75(1)
C(20)	5694(2)	3747(3)	7004(1)	76(1)
C(21)	5302(2)	3498(3)	6638(1)	67(1)
C(22A)	6894(3)	4175(4)	7455(1)	102(2)
C(23A)	7533(4)	3468(8)	7561(2)	174(5)
C(24A)	6410(4)	4181(8)	7784(2)	167(5)
C(25A)	7176(6)	5254(6)	7425(2)	188(5)
C(22B)	6894(3)	4175(4)	7455(1)	102(2)
C(23B)	6560(20)	5130(20)	7589(12)	111(16)
C(24B)	7699(10)	4310(30)	7419(14)	124(18)
C(25B)	6780(20)	3310(20)	7725(11)	113(17)
C(26)	4616(2)	4852(2)	5934(1)	54(1)

C(27)	5194(2)	5546(3)	5987(1)	64(1)
C(28)	5135(2)	6424(3)	6203(1)	70(1)
C(29)	4516(2)	6649(3)	6373(1)	68(1)
C(30)	3928(2)	5967(3)	6306(1)	75(1)
C(31)	3978(2)	5086(3)	6089(1)	69(1)
C(32A)	4448(3)	7599(3)	6628(1)	103(2)
C(33A)	4268(5)	7273(5)	7026(2)	160(4)
C(34A)	5129(5)	8245(6)	6654(3)	238(7)
C(35A)	3768(4)	8239(5)	6438(2)	158(4)
C(32B)	4448(3)	7599(3)	6628(1)	103(2)
C(33B)	4500(20)	8550(20)	6386(10)	45(14)
C(34B)	3770(17)	7650(40)	6840(14)	90(20)
C(35B)	5144(16)	7500(40)	6932(11)	66(18)
C(36)	3677(2)	4303(2)	5171(1)	58(1)
C(37)	3859(2)	5252(3)	5040(1)	75(1)
C(38)	3328(3)	5873(3)	4837(1)	98(2)
C(39)	2595(3)	5559(4)	4768(2)	109(2)
C(40)	2409(3)	4631(5)	4894(2)	110(2)
C(41)	2945(2)	3999(3)	5095(1)	80(1)
C(61)	7635(7)	-3591(13)	6054(5)	354(12)
Cl(4)	7048(7)	-2716(11)	5963(5)	216(7)
Cl(5)	7236(7)	-3220(19)	6389(5)	349(8)
Cl(6)	7310(11)	-2501(7)	6030(7)	279(12)
Cl(7)	8510(6)	-3690(20)	6128(5)	273(12)
Cl(8)	8292(11)	-3920(20)	6348(5)	327(10)
Cl(9)	8431(9)	-3055(17)	6099(7)	326(13)
C(51)	4917(13)	1388(18)	7540(13)	370(20)
Cl(1)	4378(8)	1151(12)	7138(4)	225(5)
Cl(2)	5718(9)	920(30)	7492(7)	351(13)
Cl(3)	4423(14)	472(16)	7339(9)	314(12)

Bond lengths [Å] and angles [°] for bce02s.

Br-C(1)	1.901(3)
C(1)-C(3)#1	1.378(4)
C(1)-C(2)	1.388(5)
C(2)-C(3)	1.378(5)
C(2)-C(4)	1.495(4)
C(3)-C(1)#1	1.378(4)
C(3)-H(3)	0.9300
C(4)-C(9)	1.381(4)
C(4)-C(5)	1.403(4)
C(5)-C(6)	1.407(4)
C(5)-C(10)	1.489(4)
C(6)-C(7)	1.400(4)
C(6)-C(16)	1.498(4)
C(7)-C(8)	1.399(4)
C(7)-C(26)	1.497(4)
C(8)-C(9)	1.384(4)
C(8)-C(36)	1.496(4)
C(9)-H(9)	0.9300
C(10)-C(11)	1.372(5)
C(10)-C(15)	1.382(5)
C(11)-C(12)	1.382(5)
C(11)-H(11)	0.9300
C(12)-C(13)	1.355(7)
C(12)-H(12)	0.9300
C(13)-C(14)	1.349(7)
C(13)-H(13)	0.9300
C(14)-C(15)	1.389(6)
C(14)-H(14)	0.9300
C(15)-H(15)	0.9300
C(16)-C(21)	1.373(5)
C(16)-C(17)	1.375(5)
C(17)-C(18)	1.378(5)
C(17)-H(17)	0.9300
C(18)-C(19)	1.381(5)

C(18)-H(18)	0.9300
C(19)-C(20)	1.371(5)
C(19)-C(22A)	1.536(5)
C(20)-C(21)	1.388(5)
C(20)-H(20)	0.9300
C(21)-H(21)	0.9300
C(22A)-C(23A)	1.489(7)
C(22A)-C(25A)	1.516(7)
C(22A)-C(24A)	1.517(7)
C(23A)-H(23A)	0.9600
C(23A)-H(23B)	0.9600
C(23A)-H(23C)	0.9600
C(24A)-H(24A)	0.9600
C(24A)-H(24B)	0.9600
C(24A)-H(24C)	0.9600
C(25A)-H(25A)	0.9600
C(25A)-H(25B)	0.9600
C(25A)-H(25C)	0.9600
C(23B)-H(23D)	0.9600
C(23B)-H(23E)	0.9600
C(23B)-H(23F)	0.9600
C(24B)-H(24D)	0.9600
C(24B)-H(24E)	0.9600
C(24B)-H(24F)	0.9600
C(25B)-H(25D)	0.9600
C(25B)-H(25E)	0.9600
C(25B)-H(25F)	0.9600
C(26)-C(31)	1.371(5)
C(26)-C(27)	1.380(5)
C(27)-C(28)	1.382(5)
C(27)-H(27)	0.9300
C(28)-C(29)	1.363(5)
C(28)-H(28)	0.9300
C(29)-C(30)	1.387(5)
C(29)-C(32A)	1.539(5)
C(30)-C(31)	1.384(5)

C(30)-H(30)	0.9300
C(31)-H(31)	0.9300
C(32A)-C(34A)	1.490(7)
C(32A)-C(33A)	1.504(7)
C(32A)-C(35A)	1.557(7)
C(33A)-H(33A)	0.9600
C(33A)-H(33B)	0.9600
C(33A)-H(33C)	0.9600
C(34A)-H(34A)	0.9600
C(34A)-H(34B)	0.9600
C(34A)-H(34C)	0.9600
C(35A)-H(35A)	0.9600
C(35A)-H(35B)	0.9600
C(35A)-H(35C)	0.9600
C(33B)-H(33D)	0.9600
C(33B)-H(33E)	0.9600
C(33B)-H(33F)	0.9600
C(34B)-H(34D)	0.9600
C(34B)-H(34E)	0.9600
C(34B)-H(34F)	0.9600
C(35B)-H(35D)	0.9600
C(35B)-H(35E)	0.9600
C(35B)-H(35F)	0.9600
C(36)-C(41)	1.373(5)
C(36)-C(37)	1.380(5)
C(37)-C(38)	1.375(6)
C(37)-H(37)	0.9300
C(38)-C(39)	1.376(7)
C(38)-H(38)	0.9300
C(39)-C(40)	1.353(7)
C(39)-H(39)	0.9300
C(40)-C(41)	1.386(6)
C(40)-H(40)	0.9300
C(41)-H(41)	0.9300
C(61)-Cl(8)	1.509(15)
C(61)-Cl(5)	1.515(13)

C(61)-Cl(6)	1.547(15)
C(61)-Cl(4)	1.568(14)
C(61)-Cl(7)	1.574(15)
C(61)-Cl(9)	1.591(16)
Cl(4)-Cl(6)	0.57(3)
Cl(4)-Cl(5)	1.59(2)
Cl(5)-Cl(6)	1.57(2)
Cl(5)-Cl(8)	2.14(3)
Cl(6)-Cl(9)	2.14(3)
Cl(7)-Cl(9)	0.84(3)
Cl(7)-Cl(8)	0.95(2)
Cl(8)-Cl(9)	1.46(3)
C(51)-C(51)#2	0.43(9)
C(51)-Cl(2)#2	1.29(4)
C(51)-Cl(1)#2	1.60(4)
C(51)-Cl(3)	1.60(2)
C(51)-Cl(1)	1.60(3)
C(51)-Cl(2)	1.60(2)
C(51)-Cl(3)#2	1.71(3)
Cl(1)-Cl(3)	1.12(3)
Cl(1)-Cl(2)#2	1.34(2)
Cl(1)-C(51)#2	1.60(4)
Cl(2)-Cl(3)#2	0.89(3)
Cl(2)-C(51)#2	1.29(4)
Cl(2)-Cl(1)#2	1.34(2)
Cl(2)-Cl(3)	2.40(2)
Cl(3)-Cl(2)#2	0.89(3)
Cl(3)-C(51)#2	1.71(3)
Cl(3)-Cl(3)#2	2.22(5)
C(3)#1-C(1)-C(2)	122.4(3)
C(3)#1-C(1)-Br	117.9(3)
C(2)-C(1)-Br	119.6(2)
C(3)-C(2)-C(1)	116.7(3)
C(3)-C(2)-C(4)	120.5(3)
C(1)-C(2)-C(4)	122.8(3)

C(2)-C(3)-C(1)#1	120.9(3)
C(2)-C(3)-H(3)	119.6
C(1)#1-C(3)-H(3)	119.6
C(9)-C(4)-C(5)	119.1(3)
C(9)-C(4)-C(2)	119.8(3)
C(5)-C(4)-C(2)	121.1(3)
C(4)-C(5)-C(6)	119.0(3)
C(4)-C(5)-C(10)	119.6(3)
C(6)-C(5)-C(10)	121.4(3)
C(7)-C(6)-C(5)	120.7(3)
C(7)-C(6)-C(16)	119.8(3)
C(5)-C(6)-C(16)	119.5(3)
C(8)-C(7)-C(6)	119.7(3)
C(8)-C(7)-C(26)	121.7(3)
C(6)-C(7)-C(26)	118.6(3)
C(9)-C(8)-C(7)	118.8(3)
C(9)-C(8)-C(36)	118.3(3)
C(7)-C(8)-C(36)	122.9(3)
C(4)-C(9)-C(8)	122.7(3)
C(4)-C(9)-H(9)	118.7
C(8)-C(9)-H(9)	118.7
C(11)-C(10)-C(15)	118.0(3)
C(11)-C(10)-C(5)	120.6(3)
C(15)-C(10)-C(5)	121.3(3)
C(10)-C(11)-C(12)	121.8(4)
C(10)-C(11)-H(11)	119.1
C(12)-C(11)-H(11)	119.1
C(13)-C(12)-C(11)	119.2(4)
C(13)-C(12)-H(12)	120.4
C(11)-C(12)-H(12)	120.4
C(14)-C(13)-C(12)	120.3(4)
C(14)-C(13)-H(13)	119.8
C(12)-C(13)-H(13)	119.8
C(13)-C(14)-C(15)	121.1(4)
C(13)-C(14)-H(14)	119.5
C(15)-C(14)-H(14)	119.5

C(10)-C(15)-C(14)	119.5(4)
C(10)-C(15)-H(15)	120.2
C(14)-C(15)-H(15)	120.2
C(21)-C(16)-C(17)	117.1(3)
C(21)-C(16)-C(6)	120.3(3)
C(17)-C(16)-C(6)	122.6(3)
C(16)-C(17)-C(18)	121.1(3)
C(16)-C(17)-H(17)	119.4
C(18)-C(17)-H(17)	119.4
C(17)-C(18)-C(19)	122.2(4)
C(17)-C(18)-H(18)	118.9
C(19)-C(18)-H(18)	118.9
C(20)-C(19)-C(18)	116.4(3)
C(20)-C(19)-C(22A)	122.2(4)
C(18)-C(19)-C(22A)	121.4(4)
C(19)-C(20)-C(21)	121.5(4)
C(19)-C(20)-H(20)	119.2
C(21)-C(20)-H(20)	119.2
C(16)-C(21)-C(20)	121.6(3)
C(16)-C(21)-H(21)	119.2
C(20)-C(21)-H(21)	119.2
C(23A)-C(22A)-C(25A)	110.1(5)
C(23A)-C(22A)-C(24A)	109.4(5)
C(25A)-C(22A)-C(24A)	106.3(5)
C(23A)-C(22A)-C(19)	110.7(4)
C(25A)-C(22A)-C(19)	107.9(4)
C(24A)-C(22A)-C(19)	112.3(4)
C(22A)-C(23A)-H(23A)	109.5
C(22A)-C(23A)-H(23B)	109.5
H(23A)-C(23A)-H(23B)	109.5
C(22A)-C(23A)-H(23C)	109.5
H(23A)-C(23A)-H(23C)	109.5
H(23B)-C(23A)-H(23C)	109.5
C(22A)-C(24A)-H(24A)	109.5
C(22A)-C(24A)-H(24B)	109.5
H(24A)-C(24A)-H(24B)	109.5

C(22A)-C(24A)-H(24C)	109.5
H(24A)-C(24A)-H(24C)	109.5
H(24B)-C(24A)-H(24C)	109.5
C(22A)-C(25A)-H(25A)	109.5
C(22A)-C(25A)-H(25B)	109.5
H(25A)-C(25A)-H(25B)	109.5
C(22A)-C(25A)-H(25C)	109.5
H(25A)-C(25A)-H(25C)	109.5
H(25B)-C(25A)-H(25C)	109.5
H(23D)-C(23B)-H(23E)	109.5
H(23D)-C(23B)-H(23F)	109.5
H(23E)-C(23B)-H(23F)	109.5
H(24D)-C(24B)-H(24E)	109.5
H(24D)-C(24B)-H(24F)	109.5
H(24E)-C(24B)-H(24F)	109.5
H(25D)-C(25B)-H(25E)	109.5
H(25D)-C(25B)-H(25F)	109.5
H(25E)-C(25B)-H(25F)	109.5
C(31)-C(26)-C(27)	117.7(3)
C(31)-C(26)-C(7)	120.8(3)
C(27)-C(26)-C(7)	121.4(3)
C(26)-C(27)-C(28)	120.6(3)
C(26)-C(27)-H(27)	119.7
C(28)-C(27)-H(27)	119.7
C(29)-C(28)-C(27)	122.4(4)
C(29)-C(28)-H(28)	118.8
C(27)-C(28)-H(28)	118.8
C(28)-C(29)-C(30)	116.6(3)
C(28)-C(29)-C(32A)	123.6(4)
C(30)-C(29)-C(32A)	119.8(4)
C(31)-C(30)-C(29)	121.6(4)
C(31)-C(30)-H(30)	119.2
C(29)-C(30)-H(30)	119.2
C(26)-C(31)-C(30)	121.0(4)
C(26)-C(31)-H(31)	119.5
C(30)-C(31)-H(31)	119.5

C(34A)-C(32A)-C(33A)	113.0(5)
C(34A)-C(32A)-C(29)	111.4(4)
C(33A)-C(32A)-C(29)	109.1(4)
C(34A)-C(32A)-C(35A)	108.4(5)
C(33A)-C(32A)-C(35A)	105.9(5)
C(29)-C(32A)-C(35A)	108.9(4)
C(32A)-C(33A)-H(33A)	109.5
C(32A)-C(33A)-H(33B)	109.5
H(33A)-C(33A)-H(33B)	109.5
C(32A)-C(33A)-H(33C)	109.5
H(33A)-C(33A)-H(33C)	109.5
H(33B)-C(33A)-H(33C)	109.5
C(32A)-C(34A)-H(34A)	109.5
C(32A)-C(34A)-H(34B)	109.5
H(34A)-C(34A)-H(34B)	109.5
C(32A)-C(34A)-H(34C)	109.5
H(34A)-C(34A)-H(34C)	109.5
H(34B)-C(34A)-H(34C)	109.5
C(32A)-C(35A)-H(35A)	109.5
C(32A)-C(35A)-H(35B)	109.5
H(35A)-C(35A)-H(35B)	109.5
C(32A)-C(35A)-H(35C)	109.5
H(35A)-C(35A)-H(35C)	109.5
H(35B)-C(35A)-H(35C)	109.5
H(33D)-C(33B)-H(33E)	109.5
H(33D)-C(33B)-H(33F)	109.5
H(33E)-C(33B)-H(33F)	109.5
H(34D)-C(34B)-H(34E)	109.5
H(34D)-C(34B)-H(34F)	109.5
H(34E)-C(34B)-H(34F)	109.5
H(35D)-C(35B)-H(35E)	109.5
H(35D)-C(35B)-H(35F)	109.5
H(35E)-C(35B)-H(35F)	109.5
C(41)-C(36)-C(37)	118.1(3)
C(41)-C(36)-C(8)	119.7(3)
C(37)-C(36)-C(8)	122.2(3)

C(38)-C(37)-C(36)	121.2(4)
C(38)-C(37)-H(37)	119.4
C(36)-C(37)-H(37)	119.4
C(37)-C(38)-C(39)	120.0(5)
C(37)-C(38)-H(38)	120.0
C(39)-C(38)-H(38)	120.0
C(40)-C(39)-C(38)	119.5(4)
C(40)-C(39)-H(39)	120.3
C(38)-C(39)-H(39)	120.3
C(39)-C(40)-C(41)	120.7(5)
C(39)-C(40)-H(40)	119.6
C(41)-C(40)-H(40)	119.6
C(36)-C(41)-C(40)	120.6(4)
C(36)-C(41)-H(41)	119.7
C(40)-C(41)-H(41)	119.7
Cl(8)-C(61)-Cl(5)	90.1(15)
Cl(8)-C(61)-Cl(6)	123.8(19)
Cl(5)-C(61)-Cl(6)	61.6(10)
Cl(8)-C(61)-Cl(4)	142.2(18)
Cl(5)-C(61)-Cl(4)	62.2(10)
Cl(6)-C(61)-Cl(4)	21.1(11)
Cl(8)-C(61)-Cl(7)	35.8(9)
Cl(5)-C(61)-Cl(7)	118.7(12)
Cl(6)-C(61)-Cl(7)	116.6(18)
Cl(4)-C(61)-Cl(7)	136.7(18)
Cl(8)-C(61)-Cl(9)	56.1(12)
Cl(5)-C(61)-Cl(9)	107.7(14)
Cl(6)-C(61)-Cl(9)	85.8(17)
Cl(4)-C(61)-Cl(9)	105.8(17)
Cl(7)-C(61)-Cl(9)	30.9(13)
Cl(6)-Cl(4)-C(61)	77.4(18)
Cl(6)-Cl(4)-Cl(5)	77(3)
C(61)-Cl(4)-Cl(5)	57.3(8)
C(61)-Cl(5)-Cl(6)	60.2(8)
C(61)-Cl(5)-Cl(4)	60.5(8)
Cl(6)-Cl(5)-Cl(4)	20.8(11)

C(61)-Cl(5)-Cl(8)	44.8(8)
Cl(6)-Cl(5)-Cl(8)	91.9(9)
Cl(4)-Cl(5)-Cl(8)	101.4(8)
Cl(4)-Cl(6)-C(61)	81.4(17)
Cl(4)-Cl(6)-Cl(5)	82(3)
C(61)-Cl(6)-Cl(5)	58.2(7)
Cl(4)-Cl(6)-Cl(9)	127(2)
C(61)-Cl(6)-Cl(9)	48.0(9)
Cl(5)-Cl(6)-Cl(9)	83.7(10)
Cl(9)-Cl(7)-Cl(8)	109(2)
Cl(9)-Cl(7)-C(61)	75.7(12)
Cl(8)-Cl(7)-C(61)	68.4(11)
Cl(7)-Cl(8)-Cl(9)	33.2(18)
Cl(7)-Cl(8)-C(61)	75.9(11)
Cl(9)-Cl(8)-C(61)	64.8(9)
Cl(7)-Cl(8)-Cl(5)	113(2)
Cl(9)-Cl(8)-Cl(5)	86.2(15)
C(61)-Cl(8)-Cl(5)	45.0(9)
Cl(7)-Cl(9)-Cl(8)	38.0(15)
Cl(7)-Cl(9)-C(61)	73.4(12)
Cl(8)-Cl(9)-C(61)	59.1(8)
Cl(7)-Cl(9)-Cl(6)	119.4(15)
Cl(8)-Cl(9)-Cl(6)	95.3(12)
C(61)-Cl(9)-Cl(6)	46.2(9)
C(51)#2-C(51)-Cl(2)#2	129(7)
C(51)#2-C(51)-Cl(1)#2	83(6)
Cl(2)#2-C(51)-Cl(1)#2	126(3)
C(51)#2-C(51)-Cl(3)	97(6)
Cl(2)#2-C(51)-Cl(3)	33.8(13)
Cl(1)#2-C(51)-Cl(3)	120(2)
C(51)#2-C(51)-Cl(1)	81(8)
Cl(2)#2-C(51)-Cl(1)	53.7(13)
Cl(1)#2-C(51)-Cl(1)	153(2)
Cl(3)-C(51)-Cl(1)	41.1(13)
C(51)#2-C(51)-Cl(2)	39(5)
Cl(2)#2-C(51)-Cl(2)	128(3)

Cl(1)#2-C(51)-Cl(2)	49.4(11)
Cl(3)-C(51)-Cl(2)	97(2)
Cl(1)-C(51)-Cl(2)	107(3)
C(51)#2-C(51)-Cl(3)#2	68(4)
Cl(2)#2-C(51)-Cl(3)#2	106(2)
Cl(1)#2-C(51)-Cl(3)#2	39.6(10)
Cl(3)-C(51)-Cl(3)#2	84(2)
Cl(1)-C(51)-Cl(3)#2	113(2)
Cl(2)-C(51)-Cl(3)#2	31.0(11)
Cl(3)-Cl(1)-Cl(2)#2	41.3(14)
Cl(3)-Cl(1)-C(51)#2	75.5(19)
Cl(2)#2-Cl(1)-C(51)#2	65.6(19)
Cl(3)-Cl(1)-C(51)	69.2(9)
Cl(2)#2-Cl(1)-C(51)	51.2(19)
C(51)#2-Cl(1)-C(51)	16(3)
Cl(3)#2-Cl(2)-C(51)#2	92(3)
Cl(3)#2-Cl(2)-Cl(1)#2	56(3)
C(51)#2-Cl(2)-Cl(1)#2	75(2)
Cl(3)#2-Cl(2)-C(51)	81(2)
C(51)#2-Cl(2)-C(51)	12(3)
Cl(1)#2-Cl(2)-C(51)	65(2)
Cl(3)#2-Cl(2)-Cl(3)	68(3)
C(51)#2-Cl(2)-Cl(3)	43.1(14)
Cl(1)#2-Cl(2)-Cl(3)	90.6(12)
C(51)-Cl(2)-Cl(3)	41.2(10)
Cl(2)#2-Cl(3)-Cl(1)	82(3)
Cl(2)#2-Cl(3)-C(51)	54(3)
Cl(1)-Cl(3)-C(51)	69.7(10)
Cl(2)#2-Cl(3)-C(51)#2	68.1(18)
Cl(1)-Cl(3)-C(51)#2	64.9(18)
C(51)-Cl(3)-C(51)#2	15(3)
Cl(2)#2-Cl(3)-Cl(3)#2	91(3)
Cl(1)-Cl(3)-Cl(3)#2	106.6(18)
C(51)-Cl(3)-Cl(3)#2	49.8(15)
C(51)#2-Cl(3)-Cl(3)#2	45.7(11)
Cl(2)#2-Cl(3)-Cl(2)	93(2)

Cl(1)-Cl(3)-Cl(2)	85.5(19)
C(51)-Cl(3)-Cl(2)	41.4(11)
C(51)#2-Cl(3)-Cl(2)	31.2(15)
Cl(3)#2-Cl(3)-Cl(2)	21.7(7)

Symmetry transformations used to generate equivalent atoms:

#1 $-x+1, -y, -z+1$ #2 $-x+1, y, -z+3/2$

Anisotropic displacement parameters ($\text{\AA}^2 \times 10^3$) for bce02s. The anisotropic displacement factor exponent takes the form: $-2\pi^2 [h^2 a^{*2} U^{11} + \dots + 2 h k a^* b^* U^{12}]$

	U^{11}	U^{22}	U^{33}	U^{23}	U^{13}	U^{12}
Br	155(1)	50(1)	85(1)	1(1)	38(1)	1(1)
C(1)	77(2)	41(2)	51(2)	-2(2)	-3(2)	8(2)
C(2)	63(2)	43(2)	46(2)	-8(2)	-11(2)	11(2)
C(3)	72(2)	51(2)	45(2)	-8(2)	-2(2)	9(2)
C(4)	66(2)	44(2)	48(2)	-8(1)	-3(2)	8(2)
C(5)	61(2)	45(2)	49(2)	-6(1)	-1(2)	7(2)
C(6)	59(2)	51(2)	46(2)	-10(2)	0(2)	5(2)
C(7)	57(2)	44(2)	53(2)	-11(2)	2(2)	4(2)
C(8)	60(2)	44(2)	53(2)	-6(2)	-2(2)	7(2)
C(9)	71(2)	49(2)	49(2)	-11(2)	-8(2)	5(2)
C(10)	63(2)	49(2)	51(2)	-13(2)	-10(2)	8(2)
C(11)	76(2)	74(2)	62(2)	-9(2)	-6(2)	21(2)
C(12)	92(3)	108(4)	85(3)	-9(3)	-16(3)	46(3)
C(13)	100(4)	92(3)	108(4)	5(3)	-24(3)	43(3)
C(14)	111(4)	82(3)	78(3)	23(2)	-21(3)	10(3)
C(15)	84(3)	68(2)	62(2)	2(2)	-7(2)	5(2)
C(16)	60(2)	48(2)	50(2)	-13(2)	-2(2)	8(2)
C(17)	70(3)	77(3)	56(2)	-22(2)	3(2)	7(2)
C(18)	66(2)	97(3)	74(3)	-28(2)	-5(2)	1(2)
C(19)	80(3)	82(3)	57(2)	-25(2)	-8(2)	11(2)
C(20)	82(3)	92(3)	54(2)	-17(2)	6(2)	5(2)
C(21)	63(2)	79(3)	56(2)	-13(2)	0(2)	5(2)
C(22A)	100(3)	131(4)	68(3)	-39(3)	-14(3)	6(3)
C(23A)	160(7)	245(11)	93(5)	-54(6)	-63(5)	88(7)
C(24A)	142(6)	289(13)	62(4)	-62(5)	-9(4)	-10(7)
C(25A)	253(12)	170(8)	120(6)	-45(5)	-49(7)	-83(8)
C(22B)	100(3)	131(4)	68(3)	-39(3)	-14(3)	6(3)
C(26)	61(2)	46(2)	53(2)	-9(2)	-2(2)	8(2)
C(27)	74(2)	52(2)	66(2)	-12(2)	9(2)	-1(2)
C(28)	84(3)	47(2)	77(2)	-12(2)	4(2)	-9(2)
C(29)	96(3)	49(2)	59(2)	-12(2)	13(2)	2(2)

C(30)	84(3)	64(2)	80(3)	-20(2)	21(2)	7(2)
C(31)	68(2)	57(2)	81(3)	-19(2)	8(2)	0(2)
C(32A)	170(5)	62(3)	83(3)	-28(2)	39(3)	-6(3)
C(33A)	283(11)	124(5)	81(4)	-50(4)	54(5)	-20(6)
C(34A)	233(10)	168(8)	345(15)	-203(10)	155(10)	-121(8)
C(35A)	235(9)	82(4)	174(7)	-32(4)	84(6)	43(5)
C(32B)	170(5)	62(3)	83(3)	-28(2)	39(3)	-6(3)
C(36)	67(2)	48(2)	55(2)	-13(2)	-4(2)	13(2)
C(37)	84(3)	56(2)	79(3)	0(2)	-7(2)	11(2)
C(38)	132(4)	58(3)	93(3)	7(2)	-18(3)	24(3)
C(39)	118(4)	97(4)	99(3)	-5(3)	-28(3)	50(3)
C(40)	79(3)	114(4)	126(4)	-4(3)	-27(3)	20(3)
C(41)	69(3)	69(3)	94(3)	0(2)	-17(2)	7(2)
C(61)	400(30)	370(30)	275(19)	-126(17)	10(20)	190(20)
Cl(4)	171(7)	286(18)	210(9)	-4(10)	88(7)	-26(8)
Cl(5)	182(9)	500(30)	370(20)	-10(20)	86(12)	-4(12)
Cl(6)	390(30)	87(5)	380(20)	3(7)	100(18)	32(9)
Cl(7)	197(11)	450(30)	174(10)	-85(14)	34(8)	123(16)
Cl(8)	380(20)	350(20)	265(17)	132(17)	74(15)	59(17)
Cl(9)	213(15)	400(20)	380(20)	-24(17)	94(14)	-176(18)
C(51)	210(30)	340(40)	540(60)	-270(50)	-40(40)	-40(40)
Cl(1)	256(11)	210(10)	218(11)	11(8)	71(8)	-8(9)
Cl(2)	206(12)	600(40)	270(20)	-30(20)	90(14)	20(20)
Cl(3)	430(30)	214(12)	290(20)	-124(15)	47(19)	-85(15)

Hydrogen coordinates ($\times 10^4$) and isotropic displacement parameters ($\text{\AA}^2 \times 10^{-3}$)
for bce02s.

	x	y	z	U(eq)
H(3)	4525	106	5590	68
H(9)	4053	2492	4975	69
H(11)	6497	1438	5489	87
H(12)	7367	269	5763	117
H(13)	7255	-436	6365	124
H(14)	6297	20	6691	112
H(15)	5416	1195	6424	88
H(17)	6669	3471	6141	82
H(18)	7315	3859	6745	96
H(20)	5437	3821	7219	91
H(21)	4788	3403	6615	80
H(23A)	7874	3527	7371	260
H(23B)	7352	2782	7563	260
H(23C)	7786	3638	7819	260
H(24A)	6222	3508	7817	250
H(24B)	5999	4641	7716	250
H(24C)	6701	4398	8025	250
H(25A)	7340	5514	7685	282
H(25B)	6781	5674	7296	282
H(25C)	7585	5257	7274	282
H(23D)	6839	5338	7836	167
H(23E)	6053	5004	7623	167
H(23F)	6584	5648	7395	167
H(24D)	7755	4846	7236	186
H(24E)	7891	3686	7324	186
H(24F)	7970	4472	7673	186
H(25D)	6996	3477	7990	170
H(25E)	7019	2710	7641	170
H(25F)	6257	3183	7718	170
H(27)	5626	5422	5876	77

H(28)	5533	6879	6234	84
H(30)	3489	6106	6408	90
H(31)	3572	4645	6049	83
H(33A)	4629	6784	7139	241
H(33B)	3779	6973	6996	241
H(33C)	4279	7855	7196	241
H(34A)	5045	8872	6785	356
H(34B)	5239	8388	6392	356
H(34C)	5542	7892	6800	356
H(35A)	3745	8861	6582	237
H(35B)	3317	7859	6444	237
H(35C)	3822	8392	6168	237
H(33D)	4221	8454	6128	68
H(33E)	5012	8681	6362	68
H(33F)	4297	9112	6514	68
H(34D)	3705	8334	6927	138
H(34E)	3838	7203	7064	138
H(34F)	3336	7446	6663	138
H(35D)	5055	7818	7175	99
H(35E)	5554	7837	6835	99
H(35F)	5261	6799	6978	99
H(37)	4351	5476	5091	90
H(38)	3462	6504	4747	117
H(39)	2232	5982	4635	131
H(40)	1915	4415	4845	132
H(41)	2807	3364	5181	96

Torsion angles [°] for bce02s.

C(3)#1-C(1)-C(2)-C(3)	0.1(5)
Br-C(1)-C(2)-C(3)	-178.0(2)
C(3)#1-C(1)-C(2)-C(4)	-179.8(3)
Br-C(1)-C(2)-C(4)	2.2(4)
C(1)-C(2)-C(3)-C(1)#1	-0.1(5)
C(4)-C(2)-C(3)-C(1)#1	179.8(3)
C(3)-C(2)-C(4)-C(9)	-110.5(4)
C(1)-C(2)-C(4)-C(9)	69.3(5)
C(3)-C(2)-C(4)-C(5)	67.7(4)
C(1)-C(2)-C(4)-C(5)	-112.5(4)
C(9)-C(4)-C(5)-C(6)	-0.8(5)
C(2)-C(4)-C(5)-C(6)	-179.0(3)
C(9)-C(4)-C(5)-C(10)	179.9(3)
C(2)-C(4)-C(5)-C(10)	1.6(5)
C(4)-C(5)-C(6)-C(7)	-0.9(5)
C(10)-C(5)-C(6)-C(7)	178.4(3)
C(4)-C(5)-C(6)-C(16)	177.4(3)
C(10)-C(5)-C(6)-C(16)	-3.3(5)
C(5)-C(6)-C(7)-C(8)	2.3(5)
C(16)-C(6)-C(7)-C(8)	-176.0(3)
C(5)-C(6)-C(7)-C(26)	-179.9(3)
C(16)-C(6)-C(7)-C(26)	1.8(5)
C(6)-C(7)-C(8)-C(9)	-1.9(5)
C(26)-C(7)-C(8)-C(9)	-179.7(3)
C(6)-C(7)-C(8)-C(36)	179.0(3)
C(26)-C(7)-C(8)-C(36)	1.2(5)
C(5)-C(4)-C(9)-C(8)	1.2(5)
C(2)-C(4)-C(9)-C(8)	179.4(3)
C(7)-C(8)-C(9)-C(4)	0.2(5)
C(36)-C(8)-C(9)-C(4)	179.4(3)
C(4)-C(5)-C(10)-C(11)	62.2(5)
C(6)-C(5)-C(10)-C(11)	-117.1(4)
C(4)-C(5)-C(10)-C(15)	-116.7(4)
C(6)-C(5)-C(10)-C(15)	64.0(5)

C(15)-C(10)-C(11)-C(12)	-0.3(6)
C(5)-C(10)-C(11)-C(12)	-179.3(4)
C(10)-C(11)-C(12)-C(13)	0.3(7)
C(11)-C(12)-C(13)-C(14)	-0.2(8)
C(12)-C(13)-C(14)-C(15)	0.1(8)
C(11)-C(10)-C(15)-C(14)	0.2(5)
C(5)-C(10)-C(15)-C(14)	179.2(3)
C(13)-C(14)-C(15)-C(10)	-0.1(7)
C(7)-C(6)-C(16)-C(21)	65.4(5)
C(5)-C(6)-C(16)-C(21)	-113.0(4)
C(7)-C(6)-C(16)-C(17)	-113.2(4)
C(5)-C(6)-C(16)-C(17)	68.4(5)
C(21)-C(16)-C(17)-C(18)	0.4(6)
C(6)-C(16)-C(17)-C(18)	179.0(3)
C(16)-C(17)-C(18)-C(19)	-0.6(6)
C(17)-C(18)-C(19)-C(20)	0.2(6)
C(17)-C(18)-C(19)-C(22A)	-178.6(4)
C(18)-C(19)-C(20)-C(21)	0.4(6)
C(22A)-C(19)-C(20)-C(21)	179.2(4)
C(17)-C(16)-C(21)-C(20)	0.2(6)
C(6)-C(16)-C(21)-C(20)	-178.5(3)
C(19)-C(20)-C(21)-C(16)	-0.6(6)
C(20)-C(19)-C(22A)-C(23A)	128.1(6)
C(18)-C(19)-C(22A)-C(23A)	-53.2(7)
C(20)-C(19)-C(22A)-C(25A)	-111.3(6)
C(18)-C(19)-C(22A)-C(25A)	67.4(7)
C(20)-C(19)-C(22A)-C(24A)	5.6(7)
C(18)-C(19)-C(22A)-C(24A)	-175.8(6)
C(8)-C(7)-C(26)-C(31)	66.2(5)
C(6)-C(7)-C(26)-C(31)	-111.6(4)
C(8)-C(7)-C(26)-C(27)	-117.2(4)
C(6)-C(7)-C(26)-C(27)	65.0(4)
C(31)-C(26)-C(27)-C(28)	2.5(5)
C(7)-C(26)-C(27)-C(28)	-174.2(3)
C(26)-C(27)-C(28)-C(29)	0.0(6)
C(27)-C(28)-C(29)-C(30)	-2.4(6)

C(27)-C(28)-C(29)-C(32A)	177.5(4)
C(28)-C(29)-C(30)-C(31)	2.2(6)
C(32A)-C(29)-C(30)-C(31)	-177.6(4)
C(27)-C(26)-C(31)-C(30)	-2.7(5)
C(7)-C(26)-C(31)-C(30)	174.1(3)
C(29)-C(30)-C(31)-C(26)	0.3(6)
C(28)-C(29)-C(32A)-C(34A)	1.8(7)
C(30)-C(29)-C(32A)-C(34A)	-178.3(6)
C(28)-C(29)-C(32A)-C(33A)	-123.6(5)
C(30)-C(29)-C(32A)-C(33A)	56.3(6)
C(28)-C(29)-C(32A)-C(35A)	121.3(5)
C(30)-C(29)-C(32A)-C(35A)	-58.8(5)
C(9)-C(8)-C(36)-C(41)	58.9(5)
C(7)-C(8)-C(36)-C(41)	-122.0(4)
C(9)-C(8)-C(36)-C(37)	-119.7(4)
C(7)-C(8)-C(36)-C(37)	59.4(5)
C(41)-C(36)-C(37)-C(38)	-0.8(6)
C(8)-C(36)-C(37)-C(38)	177.8(4)
C(36)-C(37)-C(38)-C(39)	1.4(7)
C(37)-C(38)-C(39)-C(40)	-1.3(8)
C(38)-C(39)-C(40)-C(41)	0.6(8)
C(37)-C(36)-C(41)-C(40)	0.2(6)
C(8)-C(36)-C(41)-C(40)	-178.5(4)
C(39)-C(40)-C(41)-C(36)	-0.1(8)
Cl(8)-C(61)-Cl(4)-Cl(6)	35(4)
Cl(5)-C(61)-Cl(4)-Cl(6)	83(3)
Cl(7)-C(61)-Cl(4)-Cl(6)	-21(4)
Cl(9)-C(61)-Cl(4)-Cl(6)	-19(3)
Cl(8)-C(61)-Cl(4)-Cl(5)	-48(2)
Cl(6)-C(61)-Cl(4)-Cl(5)	-83(3)
Cl(7)-C(61)-Cl(4)-Cl(5)	-103.3(18)
Cl(9)-C(61)-Cl(4)-Cl(5)	-102.0(14)
Cl(8)-C(61)-Cl(5)-Cl(6)	129.1(18)
Cl(4)-C(61)-Cl(5)-Cl(6)	-24.0(12)
Cl(7)-C(61)-Cl(5)-Cl(6)	107(2)
Cl(9)-C(61)-Cl(5)-Cl(6)	75.0(18)

Cl(8)-C(61)-Cl(5)-Cl(4)	153.1(17)
Cl(6)-C(61)-Cl(5)-Cl(4)	24.0(12)
Cl(7)-C(61)-Cl(5)-Cl(4)	131(2)
Cl(9)-C(61)-Cl(5)-Cl(4)	99.0(18)
Cl(6)-C(61)-Cl(5)-Cl(8)	-129.1(18)
Cl(4)-C(61)-Cl(5)-Cl(8)	-153.1(17)
Cl(7)-C(61)-Cl(5)-Cl(8)	-23(2)
Cl(9)-C(61)-Cl(5)-Cl(8)	-54.2(14)
Cl(6)-Cl(4)-Cl(5)-C(61)	-83(2)
C(61)-Cl(4)-Cl(5)-Cl(6)	83(2)
Cl(6)-Cl(4)-Cl(5)-Cl(8)	-64(2)
C(61)-Cl(4)-Cl(5)-Cl(8)	19.0(13)
Cl(5)-Cl(4)-Cl(6)-C(61)	58.8(6)
C(61)-Cl(4)-Cl(6)-Cl(5)	-58.8(6)
C(61)-Cl(4)-Cl(6)-Cl(9)	17(3)
Cl(5)-Cl(4)-Cl(6)-Cl(9)	76(3)
Cl(8)-C(61)-Cl(6)-Cl(4)	-155(3)
Cl(5)-C(61)-Cl(6)-Cl(4)	-86(3)
Cl(7)-C(61)-Cl(6)-Cl(4)	164(3)
Cl(9)-C(61)-Cl(6)-Cl(4)	162(3)
Cl(8)-C(61)-Cl(6)-Cl(5)	-69.0(18)
Cl(4)-C(61)-Cl(6)-Cl(5)	86(3)
Cl(7)-C(61)-Cl(6)-Cl(5)	-109.8(15)
Cl(9)-C(61)-Cl(6)-Cl(5)	-112.7(13)
Cl(8)-C(61)-Cl(6)-Cl(9)	43.7(16)
Cl(5)-C(61)-Cl(6)-Cl(9)	112.7(13)
Cl(4)-C(61)-Cl(6)-Cl(9)	-162(3)
Cl(7)-C(61)-Cl(6)-Cl(9)	2.9(15)
C(61)-Cl(5)-Cl(6)-Cl(4)	85(2)
Cl(8)-Cl(5)-Cl(6)-Cl(4)	118(2)
Cl(4)-Cl(5)-Cl(6)-C(61)	-85(2)
Cl(8)-Cl(5)-Cl(6)-C(61)	33.2(12)
C(61)-Cl(5)-Cl(6)-Cl(9)	-43.6(9)
Cl(4)-Cl(5)-Cl(6)-Cl(9)	-128(2)
Cl(8)-Cl(5)-Cl(6)-Cl(9)	-10.4(13)
Cl(8)-C(61)-Cl(7)-Cl(9)	-117(3)

Cl(5)-C(61)-Cl(7)-Cl(9)	-76(3)
Cl(6)-C(61)-Cl(7)-Cl(9)	-6(3)
Cl(4)-C(61)-Cl(7)-Cl(9)	3(3)
Cl(5)-C(61)-Cl(7)-Cl(8)	41(4)
Cl(6)-C(61)-Cl(7)-Cl(8)	112(3)
Cl(4)-C(61)-Cl(7)-Cl(8)	120(4)
Cl(9)-C(61)-Cl(7)-Cl(8)	117(3)
C(61)-Cl(7)-Cl(8)-Cl(9)	-65(2)
Cl(9)-Cl(7)-Cl(8)-C(61)	65(2)
Cl(9)-Cl(7)-Cl(8)-Cl(5)	39(3)
C(61)-Cl(7)-Cl(8)-Cl(5)	-26.3(16)
Cl(5)-C(61)-Cl(8)-Cl(7)	-145(3)
Cl(6)-C(61)-Cl(8)-Cl(7)	-90(3)
Cl(4)-C(61)-Cl(8)-Cl(7)	-104(4)
Cl(9)-C(61)-Cl(8)-Cl(7)	-33(2)
Cl(5)-C(61)-Cl(8)-Cl(9)	-111.4(19)
Cl(6)-C(61)-Cl(8)-Cl(9)	-56(2)
Cl(4)-C(61)-Cl(8)-Cl(9)	-71(3)
Cl(7)-C(61)-Cl(8)-Cl(9)	33(2)
Cl(6)-C(61)-Cl(8)-Cl(5)	55.2(14)
Cl(4)-C(61)-Cl(8)-Cl(5)	41(2)
Cl(7)-C(61)-Cl(8)-Cl(5)	145(3)
Cl(9)-C(61)-Cl(8)-Cl(5)	111.4(19)
C(61)-Cl(5)-Cl(8)-Cl(7)	37(3)
Cl(6)-Cl(5)-Cl(8)-Cl(7)	-5(3)
Cl(4)-Cl(5)-Cl(8)-Cl(7)	14(3)
C(61)-Cl(5)-Cl(8)-Cl(9)	57.6(15)
Cl(6)-Cl(5)-Cl(8)-Cl(9)	15.3(18)
Cl(4)-Cl(5)-Cl(8)-Cl(9)	34.0(19)
Cl(6)-Cl(5)-Cl(8)-C(61)	-42.3(15)
Cl(4)-Cl(5)-Cl(8)-C(61)	-23.7(15)
C(61)-Cl(7)-Cl(9)-Cl(8)	60.8(18)
Cl(8)-Cl(7)-Cl(9)-C(61)	-60.8(18)
Cl(8)-Cl(7)-Cl(9)-Cl(6)	-57(3)
C(61)-Cl(7)-Cl(9)-Cl(6)	4(2)
C(61)-Cl(8)-Cl(9)-Cl(7)	-103(2)

Cl(5)-Cl(8)-Cl(9)-Cl(7)	-144(2)
Cl(7)-Cl(8)-Cl(9)-C(61)	103(2)
Cl(5)-Cl(8)-Cl(9)-C(61)	-41.3(8)
Cl(7)-Cl(8)-Cl(9)-Cl(6)	133(2)
C(61)-Cl(8)-Cl(9)-Cl(6)	30.1(12)
Cl(5)-Cl(8)-Cl(9)-Cl(6)	-11.2(14)
Cl(8)-C(61)-Cl(9)-Cl(7)	38.8(17)
Cl(5)-C(61)-Cl(9)-Cl(7)	117(2)
Cl(6)-C(61)-Cl(9)-Cl(7)	175(2)
Cl(4)-C(61)-Cl(9)-Cl(7)	-178(2)
Cl(5)-C(61)-Cl(9)-Cl(8)	78(2)
Cl(6)-C(61)-Cl(9)-Cl(8)	136(2)
Cl(4)-C(61)-Cl(9)-Cl(8)	143(2)
Cl(7)-C(61)-Cl(9)-Cl(8)	-38.8(17)
Cl(8)-C(61)-Cl(9)-Cl(6)	-136(2)
Cl(5)-C(61)-Cl(9)-Cl(6)	-58.4(12)
Cl(4)-C(61)-Cl(9)-Cl(6)	6.8(13)
Cl(7)-C(61)-Cl(9)-Cl(6)	-175(2)
Cl(4)-Cl(6)-Cl(9)-Cl(7)	-29(6)
C(61)-Cl(6)-Cl(9)-Cl(7)	-6(3)
Cl(5)-Cl(6)-Cl(9)-Cl(7)	47(3)
Cl(4)-Cl(6)-Cl(9)-Cl(8)	-60(5)
C(61)-Cl(6)-Cl(9)-Cl(8)	-36.6(17)
Cl(5)-Cl(6)-Cl(9)-Cl(8)	15.5(19)
Cl(4)-Cl(6)-Cl(9)-C(61)	-23(4)
Cl(5)-Cl(6)-Cl(9)-C(61)	52.1(11)
C(51)#2-C(51)-Cl(1)-Cl(3)	111.3(18)
Cl(2)#2-C(51)-Cl(1)-Cl(3)	-43(2)
Cl(1)#2-C(51)-Cl(1)-Cl(3)	55(6)
Cl(2)-C(51)-Cl(1)-Cl(3)	82(3)
Cl(3)#2-C(51)-Cl(1)-Cl(3)	50(3)
C(51)#2-C(51)-Cl(1)-Cl(2)#2	155(2)
Cl(1)#2-C(51)-Cl(1)-Cl(2)#2	99(6)
Cl(3)-C(51)-Cl(1)-Cl(2)#2	43(2)
Cl(2)-C(51)-Cl(1)-Cl(2)#2	125(4)
Cl(3)#2-C(51)-Cl(1)-Cl(2)#2	93(3)

Cl(2)#2-C(51)-Cl(1)-C(51)#2	-155(2)
Cl(1)#2-C(51)-Cl(1)-C(51)#2	-56(5)
Cl(3)-C(51)-Cl(1)-C(51)#2	-111.3(18)
Cl(2)-C(51)-Cl(1)-C(51)#2	-29(2)
Cl(3)#2-C(51)-Cl(1)-C(51)#2	-62(2)
C(51)#2-C(51)-Cl(2)-Cl(3)#2	-158(7)
Cl(2)#2-C(51)-Cl(2)-Cl(3)#2	-51(5)
Cl(1)#2-C(51)-Cl(2)-Cl(3)#2	57(3)
Cl(3)-C(51)-Cl(2)-Cl(3)#2	-66(5)
Cl(1)-C(51)-Cl(2)-Cl(3)#2	-107(4)
Cl(2)#2-C(51)-Cl(2)-C(51)#2	108(10)
Cl(1)#2-C(51)-Cl(2)-C(51)#2	-145(6)
Cl(3)-C(51)-Cl(2)-C(51)#2	92(8)
Cl(1)-C(51)-Cl(2)-C(51)#2	51(8)
Cl(3)#2-C(51)-Cl(2)-C(51)#2	158(7)
C(51)#2-C(51)-Cl(2)-Cl(1)#2	145(6)
Cl(2)#2-C(51)-Cl(2)-Cl(1)#2	-108(4)
Cl(3)-C(51)-Cl(2)-Cl(1)#2	-123(3)
Cl(1)-C(51)-Cl(2)-Cl(1)#2	-164(3)
Cl(3)#2-C(51)-Cl(2)-Cl(1)#2	-57(3)
C(51)#2-C(51)-Cl(2)-Cl(3)	-92(8)
Cl(2)#2-C(51)-Cl(2)-Cl(3)	16(3)
Cl(1)#2-C(51)-Cl(2)-Cl(3)	123(3)
Cl(1)-C(51)-Cl(2)-Cl(3)	-41.0(16)
Cl(3)#2-C(51)-Cl(2)-Cl(3)	66(5)
C(51)#2-Cl(1)-Cl(3)-Cl(2)#2	69.3(19)
C(51)-Cl(1)-Cl(3)-Cl(2)#2	54(3)
Cl(2)#2-Cl(1)-Cl(3)-C(51)	-54(3)
C(51)#2-Cl(1)-Cl(3)-C(51)	15(3)
Cl(2)#2-Cl(1)-Cl(3)-C(51)#2	-69.3(19)
C(51)-Cl(1)-Cl(3)-C(51)#2	-15(3)
Cl(2)#2-Cl(1)-Cl(3)-Cl(3)#2	-88(2)
C(51)#2-Cl(1)-Cl(3)-Cl(3)#2	-19(2)
C(51)-Cl(1)-Cl(3)-Cl(3)#2	-34(2)
Cl(2)#2-Cl(1)-Cl(3)-Cl(2)	-94(2)
C(51)#2-Cl(1)-Cl(3)-Cl(2)	-24.3(18)

C(51)-Cl(1)-Cl(3)-Cl(2)	-39.3(14)
C(51)#2-C(51)-Cl(3)-Cl(2)#2	-163(7)
Cl(1)#2-C(51)-Cl(3)-Cl(2)#2	111(5)
Cl(1)-C(51)-Cl(3)-Cl(2)#2	-95(4)
Cl(2)-C(51)-Cl(3)-Cl(2)#2	158(4)
Cl(3)#2-C(51)-Cl(3)-Cl(2)#2	129(5)
C(51)#2-C(51)-Cl(3)-Cl(1)	-68(6)
Cl(2)#2-C(51)-Cl(3)-Cl(1)	95(4)
Cl(1)#2-C(51)-Cl(3)-Cl(1)	-154(4)
Cl(2)-C(51)-Cl(3)-Cl(1)	-107(3)
Cl(3)#2-C(51)-Cl(3)-Cl(1)	-135(3)
Cl(2)#2-C(51)-Cl(3)-C(51)#2	163(7)
Cl(1)#2-C(51)-Cl(3)-C(51)#2	-86(4)
Cl(1)-C(51)-Cl(3)-C(51)#2	68(6)
Cl(2)-C(51)-Cl(3)-C(51)#2	-39(4)
Cl(3)#2-C(51)-Cl(3)-C(51)#2	-67(5)
C(51)#2-C(51)-Cl(3)-Cl(3)#2	67(5)
Cl(2)#2-C(51)-Cl(3)-Cl(3)#2	-129(5)
Cl(1)#2-C(51)-Cl(3)-Cl(3)#2	-19(2)
Cl(1)-C(51)-Cl(3)-Cl(3)#2	135(3)
Cl(2)-C(51)-Cl(3)-Cl(3)#2	28.3(14)
C(51)#2-C(51)-Cl(3)-Cl(2)	39(4)
Cl(2)#2-C(51)-Cl(3)-Cl(2)	-158(4)
Cl(1)#2-C(51)-Cl(3)-Cl(2)	-47.0(17)
Cl(1)-C(51)-Cl(3)-Cl(2)	107(3)
Cl(3)#2-C(51)-Cl(3)-Cl(2)	-28.3(14)
Cl(3)#2-Cl(2)-Cl(3)-Cl(2)#2	84(8)
C(51)#2-Cl(2)-Cl(3)-Cl(2)#2	-36(4)
Cl(1)#2-Cl(2)-Cl(3)-Cl(2)#2	31(5)
C(51)-Cl(2)-Cl(3)-Cl(2)#2	-18(4)
Cl(3)#2-Cl(2)-Cl(3)-Cl(1)	166(5)
C(51)#2-Cl(2)-Cl(3)-Cl(1)	46(4)
Cl(1)#2-Cl(2)-Cl(3)-Cl(1)	113(3)
C(51)-Cl(2)-Cl(3)-Cl(1)	64(3)
Cl(3)#2-Cl(2)-Cl(3)-C(51)	102(5)
C(51)#2-Cl(2)-Cl(3)-C(51)	-18(5)

Cl(1)#2-Cl(2)-Cl(3)-C(51)	49(4)
Cl(3)#2-Cl(2)-Cl(3)-C(51)#2	120(6)
Cl(1)#2-Cl(2)-Cl(3)-C(51)#2	67(4)
C(51)-Cl(2)-Cl(3)-C(51)#2	18(5)
C(51)#2-Cl(2)-Cl(3)-Cl(3)#2	-120(6)
Cl(1)#2-Cl(2)-Cl(3)-Cl(3)#2	-53(2)
C(51)-Cl(2)-Cl(3)-Cl(3)#2	-102(5)

Symmetry transformations used to generate equivalent atoms:

#1 -x+1,-y,-z+1 #2 -x+1,y,-z+3/2

References:

- (1) SMART Version 5.625 and SAINT+ Version 6.22. Bruker Analytical X-ray Systems, Inc., Madison, Wisconsin, USA, 2001.
- (2) Sheldrick, G. M. SHELXTL Version 6.1; Bruker Analytical X-ray Systems, Inc., Madison, Wisconsin, USA, 2000.